12 B.S.

(18) AFML-TR-77-44

(19)

(6)

PROCEEDINGS OF THE ARPA/AFML REVIEW OF PROGRESS IN QUANTITATIVE (NDE).

Nondestructive Evaluation

SCIENCE CENTER, ROCKWELL INTERNATIONAL
1049 CAMINO DOS RIOS
THOUSAND OAKS, CALIFORNIA 91360

(11) SEP[illegible]77 (12) 265 p. (10) Donald O. Thompson

(14) SC595-16AR

TECHNICAL REPORT AFML-TR-77-44
Second Annual Report, 18 July [illegible]75 – 3 Sep[illegible]76.

(9) no. 2

(15) F33615-74-C-5184

Approved for public release; distribution unlimited.

(16) 7351

62102F

AIR FORCE MATERIALS LABORATORY
AIR FORCE WRIGHT AERONAUTICAL LABORATORIES
AIR FORCE SYSTEMS COMMAND
WRIGHT-PATTERSON AIR FORCE BASE, OHIO 45433

389 949

NOTICE

When Government drawings, specifications, or other data are used for any purpose other than in conjunction with a definitely related Government procurement operation, the United States Government thereby incurs no responsibility nor any obligation whatsoever; and the fact that the government may have formulated, furnished, or in any way supplied the said drawings, specifications, or other data, is not to be regarded by implication or otherwise as in any manner licensing the holder or any other person or corporation, or conveying any rights or permission to manufacture, use, or sell any patented invention that may in any way be related thereto.

This report has been reviewed by the Information Office (OI) and is releasable to the National Technical Information Service (NTIS). At NTIS, it will be available to the general public, including foreign nations.

This technical report has been reviewed and is approved for publication.

RODNEY M. PANOS
Project Monitor

DONALD M. FORNEY, Jr., Chief
Nondestructive Evaluation Branch
Metals and Ceramics Division

Copies of this report should not be returned unless return is required by security considerations, contractual obligations, or notice on a specific document.

AIR FORCE/56780/31 October 1977 — 550

UNCLASSIFIED

SECURITY CLASSIFICATION OF THIS PAGE (When Data Entered)

REPORT DOCUMENTATION PAGE		READ INSTRUCTIONS BEFORE COMPLETING FORM
1. REPORT NUMBER AFML-TR-77-44	2. GOVT ACCESSION NO.	3. RECIPIENT'S CATALOG NUMBER
4. TITLE (and Subtitle) PROCEEDINGS OF THE ARPA/AFML REVIEW OF PROGRESS IN QUANTITATIVE NONDESTRUCTIVE EVALUATION		5. TYPE OF REPORT & PERIOD COVERED Second Annual Report 07/18/75 through 09/03/76
		6. PERFORMING ORG. REPORT NUMBER SC595.16AR
7. AUTHOR(s) Donald O. Thompson, Program Manager		8. CONTRACT OR GRANT NUMBER(s) F33615-74-C-5180
9. PERFORMING ORGANIZATION NAME AND ADDRESS Science Center, Rockwell International 1049 Camino Dos Rios Thousand Oaks, Calif. 91360		10. PROGRAM ELEMENT, PROJECT, TASK AREA & WORK UNIT NUMBERS 7351
11. CONTROLLING OFFICE NAME AND ADDRESS Advanced Research Projects Agency 1400 Wilson Blvd. Arlington, Va. 22209		12. REPORT DATE Sept. 77 13. NUMBER OF PAGES 264
14. MONITORING AGENCY NAME & ADDRESS (if different from Controlling Office) Air Force Materials Laboratory Air Force Systems Command Wright-Patterson Air Force Base, Ohio		15. SECURITY CLASS. (of this report) UNCLASSIFIED 15a. DECLASSIFICATION/DOWNGRADING SCHEDULE

16. DISTRIBUTION STATEMENT (of this Report)

Approved for Public Release; Distribution Unlimited.

17. DISTRIBUTION STATEMENT (of the abstract entered in Block 20, if different from Report)

18. SUPPLEMENTARY NOTES

19. KEY WORDS (Continue on reverse side if necessary and identify by block number)

nondestructive evaluation; nondestructive testing; qualitative ultrasonics; signal processing; adhesive bonds; composites' residual stress; acoustic emission; reliability; quality;

20. ABSTRACT (Continue on reverse side if necessary and identify by block number)

The edited transcripts of the ARPA/AFML Review of Quantitative NDE held on August 31-September 3, 1976, at Asilomar Conference Facility, Pacific Grove State Beach, Calif., are presented in this document. Several key topics form the core of these presentations and discussions. They include quantitative ultrasonics, adhesives and composites, emissions related to failure prediction, residual stress. In addition a Mini-Symposium is presented related to Advances in Electromagnetic Transducers. It is believed that this document provides a reasonable summary of NDE research and development currently underway.

DD FORM 1 JAN 73 1473 EDITION OF 1 NOV 65 IS OBSOLETE

UNCLASSIFIED

SECURITY CLASSIFICATION OF THIS PAGE (When Data Entered)

PREFACE

This report contains the edited transcripts of the Review of Progress in Quantitative NDE held at the Asilomar Conference Grounds, Pacific Grove State Beach, California, August 31 - September 3, 1976. The Review was sponsored by the Advanced Research Projects Agency and the Air Force Materials Laboratory as a part of and at the conclusion of the second year of effort on the Interdisciplinary Program for Quantitative Flaw Definition, Contract No. F33615-74-C-5180. Arrangements for the Review were made by the Science Center, Rockwell International, host organization for the Interdisciplinary Program. Since an objective of this program is the provision of a forum for the exchange of information within the NDE professional community in areas of interest to the DoD, several papers related to the main technical interests of the ARPA/AFML program were included even though they were not sponsored directly by it. The Review clearly demonstrated that the interdisciplinary research interest in key NDE problem areas has grown at a rapid pace over the past two years and continues to accelerate. It is important to note, however, that this growth has been guided by strong interactions with the NDE user community so that the scientific base developed has a direct bearing on the solution of problems associated with the reliability and quality assurance of present and future materials and material systems. The guidance that the user community has provided is sincerely appreciated and has helped curb "false" research starts. It is thought that this series of ARPA/AFML sponsored Workshops and Reviews has played a key role in constructing a "bridge" between the technology generation and application areas of the NDE profession.

A format was adopted for the Review which was believed to be suitable for both the stimulation of interaction between participants and for the focusing of attention upon the needs and opportunities for technology transition. Two sessions were set aside for discussion of the latter. The Honorable Harold L. Brownman, Assistant Secretary of the Army for Installations and Logistics, highlighted the need for technology transition in his opening keynote address. In the final session of the Review other aspects of the same topic were presented. These included a presentation by Mr. Roy Sharpe, head of the NDT Centre at Harwell, England, of experiences in technology transfer at Harwell, and descriptions of the mechanisms for technology transfer within the Air Force. This discussion was timely, for a number of research efforts in the ARPA/AFML program have matured to the point where they are ready for application development. The intermediate sessions of the Review were dedicated to presentation of research results in the areas of adhesives and composites, measurements of internal stresses, theoretical fundamentals of acoustic emission, and quantitative ultrasonic defect characterization. As time permitted, the sessions were followed by discussion periods. These discussions are also presented, for it is believed that they contain important information and are indicative of the fruitful exchanges that took place at the Review.

The organizers of the Review wish to acknowledge the financial support and encouragement provided by the Advanced Research Projects Agency and the Air Force Materials Laboratory. Special thanks are due the Honorable Harold L. Brownman for his presentation of the keynote address and Mr. Roy Sharpe of the NDT Centre at Harwell for his review. In addition, they wish to thank the speakers, the session chairmen, and the participants who collaborated to provide a stimulating meeting. They also wish to acknowledge the assistance of Mrs. Diane Harris who managed the organizational matters of the meeting for the Science Center, Ms. Shirley Dutton who ably assisted her, Mr. Paul Ocorr who took care of the many details associated with the audio and visual presentations, and Mrs. Jo Mills who prepared the manuscript of the Proceedings. The cooperation received from Mrs. Roma Philbrook, Asilomar Manager, is appreciated as is the work of Mr. Charles Voitsberger who transcribed the Proceedings.

Donald O. Thompson

Donald O. Thompson
Director
Structural Materials
Rockwell International, Science Center

ADVANCED RESEARCH PROJECTS AGENCY/AIR FORCE MATERIALS LABORATORY

REVIEW OF PROGRESS
IN
QUANTITATIVE NDE

August 31-September 3, 1976
Asilomar Conference Grounds
Pacific Grove State Beach, California

TABLE OF CONTENTS

INTRODUCTORY REMARKS

D. O. Thompson
Science Center, Rockwell International
Thousand Oaks, California 91360

I'm Don Thompson, Director of the Structural Materials Department at the Rockwell International Science Center and Program Manager for the ARPA/AFML program. It's a pleasure to welcome you to our annual ARPA/AFML Review of Progress in Nondestructive Evaluation. It is the first time that this meeting has not been held at the Science Center; we are very pleased with the courtesies and hospitalities that the people at Asilomar have shown us.

This has been a busy summer for meetings in NDE. The schedule started with a meeting at the Bureau of Standards in April followed by an ASTM meeting in Florida on NDE; a special ARPA session was held in La Jolla in July and a meeting was held at Sagamore last week which was arranged by the AMMRC people;this review is to be followed by an internal DoD meeting on NDE and an international meeting in Cannes, France next week. Despite all these, we have a good crowd for which we're very pleased.

We're also pleased to have with us, and wish to welcome, two special guests. They are the Honorable Harold Brownman, Assistant Secretary of the Army for Installations and Logistics, and Mr. Roy Sharpe, Director of the NDT Centre at Harwell, England. Mr. Brownman will deliver the keynote address a little later this evening, and Roy has agreed to tell us of his experiences in technology transfer at Harwell on Friday morning. We look forward to both of these presentations.

I would like to make a couple of comments to try to place in perspective some of the work that you will hear during the course of this program. It may be worthwhile to take a step back and look at NDE in perspective. It is my opinion that if we look at it from this viewpoint, one can recognize that NDE is at the same time a general and a specific subject. It is general in the sense that there is a generic interdisciplinary "core" of phenomena and measurements that are applicable to many NDE problem areas. In a specific sense, one finds that each application may require a special configuration of transducers and/or sensors as dictated by the details of the part or the manufacturing process at which one is looking.

The work that you'll hear about during the course of this meeting falls mostly into the first category, i.e. the generic interdisciplinary "core" of research and development that forms the basis from which specific applications can be constructed.

We are very much interested in the ARPA/AFML program in seeking the opportunities for technology transition. You'll hear more about this on Friday morning. But we believe very strongly that one also needs to know something of the nature of the more fundamental mechanisms underlying the applications so that a feeling of confidence in the final NDE device can be developed and so that "oversell" of new technology may be prevented.

I'd like to say a few words now about the goals of the current ARPA/AFML program. They are:

- To pursue advanced research in quantitative techniques with NDE.
- To establish a focal point for NDE research.
- To enhance communication between the research community and the NDE user.
- To promote the image of NDE.

We believe these things are all very important.

The program content is divided into two projects. Project I is devoted to flaw characterization by ultrasonic techniques. About two-thirds of our activity is devoted to this area; it will be reported upon Thursday. Our motivation and goal in this area is to provide the capability for ultrasonic characterization of defects. The second project is concerned with the nondestructive evaluation of strength related properties of materials. Work is being done to develop measurement techniques and knowledge to the point where we can nondestructively determine the strength of an adhesively bonded structure and the strength of a composite as affected by moisture degradation. These are important measurements which will help relieve some of the limitations upon the application of these materials. Other work in this project is aimed at the development of ways to measure residual stress. We believe these are important measurements in the development of a capability to predict the remaining life of a part. Another area that we're looking at in this project is that of acoustic emission. The work in this area this year has been primarily associated with acoustic emission in composite materials and the discovery of emission characteristics that can be related to strength properties.

I'd like to say a few words about the program plan that we have followed. During the first year we recognized that, in order to develop these projects and because of the lack of fundamental activities in past years in some of these areas, it was necessary to focus individual capabilities into primary problem areas. This, I believe, was quite successful. During the second year several interdisciplinary teaming interactions occurred and a synergism began to develop both of which were essential to the solutions of some of the problems. Our efforts in the third year will be aimed primarily at further integration in order to achieve the desired ultrasonic and other material property capabilities. We have people working with us who have varied expertise in their own rights and in their own fields. Each of them has a role to play in developing a piece of the overall problem in order to achieve the composite goals of this program.

In conclusion, I would like to make two more comments. Perhaps by now many of you have become aware of the COSMAT report that was published a couple of years ago concerning the priorities given to the subject of nondestructive evaluation and it's importance in our society as a whole. This report, which was prepared after a rather exhaustive survey of technology, recognizes a high priority need for both basic and applied NDE research. Secondly, the report made the comment that routine uses of new methods requires more understanding of the physics of the phenomen involved, its quantitative relationship to the phsyical property to be monitored, and the limits of its applicability. These strike me as very important words. You can make many mistakes by not knowing at an early point the limits of applicability of a measurement technique. Such understanding is important to the development of confidence in a technique.

We are all also aware of the various concerns that have been voiced with regard to both energy and materials availability in the future. Regardless of how each of us views these various warnings, there is little doubt that more efficient useage of these commodities is important. A quantitative NDE capability is important to the achievement of those goals. As an example, over-design in structures can be reduced if increased capability and confidence in NDE technologies can be obtained. Reduced overdesign and weight conserves on both materials useage and fuel (energy). Concern for product safety is also increasing, both on the part of the consumer and on the part of the manufacturers. Quantitative NDE capabilities offer a potential trade-off option to ensure safety consistent with minimum materials and energy consumption.

Thus, I believe very strongly that the subject of NDE is large in scope. It relates to many aspects of immediate problems as well as being a key aid in the solutions of those that are going to be with us for many years.

COMMENTS FROM ARPA/AFML

E. C. van Reuth
Advanced Research Projects Agency
and
M. J. Buckley
Air Force Materials Laboratory

DR. ED VAN REUTH: I want to take a moment to give you a few reflections from the sponsoring agency. The Advanced Research Projects Agency has been set up to take chances on high risk R and D. I have a warm spot in my heart for this particular program because it's the first one that I was fortunate enough to pull together on an integrated basis. However, I have to admit that when it was first suggested by Mike Buckley that I should put a few chips in NDE, I felt kind of blah about it. I felt it was not a risky area, tnat it was not the colorful type of thing that ARPA should be getting into. The more I heard about it, however, the more I realized the importance of this area and that a good investment in some people that Don had pulled together would pay off handsomely. I want to compliment Don and the excellent team he has gotten together. I am particularly excited tonight to have the atteniton of people like Secretary Brownman who, I can appreciate, understands technology and understands that it needs diffusing out into the services. The program is still risky unless we can pull that off. Let's hope that getting the attention of people like Secretary Brownman and others will aid in a technology transfer so that new developments will not be lost for another decade or two, or until someone rediscovers it.

DR. MICHAEL J. BUCKLEY: Every year Don puts us on the agenda and I'm never quite sure what we should say. I will begin by saying that one of my favorite words is paradigm, as Keuhn uses it. It means the changing of the whole foundation upon which a technology rests. That is what people win a Nobel prize for--for changing the concept in which a technology is structured. And we set out in this program to really try to do that for NDE. That's what made it a blue chip area for Ed.

Let me give you a few observations made over the last few years. Two years ago when we first got the researchers together and they came to our meetings, one quickly got the feeling that they were there because the money was there. NDE was not really a respectable place to be doing research, but if that's where the money was, that was fine. Last year I think one saw more of a mixture of people getting into some discussions, not quite really ready to say that this is where the research is, but it looked a little bit better. And I think over the last year what has happened is that it has almost become respectable to some pretty good people. That is really important. This field, as those of you who have been in it for awhile will agree, has been one that has been neglected. We're now getting more first rate people involved, and that's exciting. It has become technically acceptable, and this is critical.

Much of the credit for this elevation is due ARPA and Ed van Reuth. The funding was raised to a level which would allow us to show some progress in a reasonable time period. And what's happened now is that it is not only accepted, it's expected, that we will produce things which will have a major impact. So that on the sponsoring side, the fundamental aspects of NDE are accepted now as being an area which will produce results and which will result in payoffs. I think, as you will hear in Friday's talk, a lot of work is going into transitioning this technology and trying to make a major impact on systems with what has happened already in this program.

But okay, that's enough of, "Gee whiz, we've done a lot of good stuff and isn't that nice", and we all pat ourselves on the back. A final observation is that in one way we've gotten off cheap so far. A lot of the things which we have been able to identify for transition have been things which were developed for other technologies and which we have borrowed; it was easy to move them over to NDE. Now, we're faced with some very difficult problems that other areas have not worked on, and hopefully, both the researchers and the sponsors will be patient enough and forceful enough to push along to really get to an analytical ability to predict failure. That's our real test. We've got some good marks in the beginning, but will we persevere enough to really get to the capability which we've all talked about? Will NDE really become the tool which most of us would like to see it become?

Thank you.

RELIABILITY, QUALITY, AND NDT - KEYS TO SOLDIER SATISFACTION

Hon. Harold L. Brownman
Assistant Secretary of the Army
(Installations and Logistics)

With Introduction
by

George Darcy
Army Materials & Mechanics Research Center

I have been following the ARPA/AFML program now for better than a year and have never been disappointed in the content and spirit of the meetings that have been held. It's truly a credit to Mike Buckley and the supervisors at AFML, to Ed Van Reuth at ARPA, and to the team of people at Rockwell and the support contractors who, with Dr. Thompson, are undertaking this far-looking program. It represents a well structured attack on some major problems in NDT; the results will allow the discipline better application in production and field testing, and this is really the nub of the whole thing. There is a tremendous chasm between the application in the factory and the techniques that are and can be available from the laboratory.

Now, this business of NDE is something in which the Army has great interest. While the Air Force has interest in aircraft and their propulsion systems, the Army has a very wide spectrum of products some of which are procured in enormous quantities -- rather staggering quantities -- about which we have a concern for requirements in quality. We thought it would be most appropriate to get an expression of Army material developments and trends since this project at Rockwell is also supported by DoD through ARPA. It is truly a DoD program. And we've had the support, of course, of Ed Van Reuth and the people at ARPA. We are thus most priviledged this evening to have a speaker from Army Headquarters, the Honorable Harold L. Brownman, Assistant Secretary of the Army for Installations and Logistics, who will speak to us on "Reliability, Quality and Nondestructive Testing - Keys to Soldier Satisfaction."

I'd like to take a minute to tell you some of his background. His current responsibilities for almost two years now as Assistant Secretary of the Army are extensive, and I'll note these in reverse order to that given in his vitae sheet. His duties include small business, family housing, construction, facilities and real property management, installations, planning and programming, industrial mobilization, nonfinancial aspects of the military assistance program, and last but certainly not least -- and really the reason we're here tonight -- material requirements. And that means weaponry and supplies. It means procurement and production; it is management--material management and logistic services -- the support, maintenance, and logistic services to weaponry.

You'll find that his background is tempered with experience in the electronics world. He began with electrical engineering degrees from Polytechnic Institute of Brooklyn; he's had experience at Fairchild Engine and Airplane Corporation, Servomechanisms Incorporated, American Bosch, and Fairchild Camera. He was Director of Systems Engineering at Airborne Instrument Labs. and Vice President of the Garland Division of LTV Electrosystems.

Just prior to his service with the Army, Mr. Brownman spent almost four years with the CIA as head of the Office of Special Projects and as Deputy Director for Management and Services, responsible in these positions for national intelligence surveys, gathering programs, and the solution of management issues.

Now, his technical experience in these prior mentioned positions is very wide indeed. It includes missile guidance, servosystems, computers, data processing, display devices, photographic and radar reconnaissance systems, electronic warfare and communications--a very wide spectrum.

He has been very active in IEEE. He is a member of Sigma Xi, AIAA, and last but not least, the National Association of Old Crows, but I'll say no more on that.

And so, ladies and gentlemen, I have the distinct pleasure of presenting the Honorable Harold L. Brownman, Assistant Secretary of the Army.

RELIABILITY, QUALITY, AND NDT - KEYS TO SOLDIER SATISFACTION

Hon. Harold L. Brownman
Assistant Secretary of the Army
(Installations and Logistics)

Thank you George Darcy. I must admit that it's rather strange to be here. In fact, I'm not quite sure why I was asked to be the keynote speaker; I'm not sure what a keynote speaker does. I formed one conclusion listening to the earlier comments. ARPA sends money, the Air Force sends money, the Army sends a keynote speaker, Harold Brownman. I suspect that somebody in the Army is trying to get even with me and that's how I got tagged for the chore.

Now, all good speakers start out with a couple of interesting little stories, and in all honesty, I had planned a couple of little stories and anecdotes, but all of them were off color, and seeing we have a mixed audience, I'm just going to have to pass them by tonight.

I have been asked to speak about reliability, quality engineering, quality assurance, and nondestructive testing. The nondestructive testing part has really gotten to me, and I'll address that at the end of the little talk. I get myself quite upset when I visit contractors, upset with myself when I was a contractor. You come in and you get a wiring diagram of the corporation. Here's a reliability organization and here's the quality assurance organization. Here's an R and D group, and here's the production engineering group, and it sort of sounds like everybody is running their own corporation. Being an old-fashioned engineer, I was brought up to believe and understand that you design reliability into the equipment in the first place. Of course, my experience was limited to vacuum tubes and discrete components and none of this sexy stuff of solid state physics and MOS and LSI devices. When you designed a circuit and you looked at the worst case power requirement and current flow and somebody said "you're going to have to deal with this kind of a range of ambient temperature," you derated a resistor. This meant that if it had to dissipate an eighth of a watt, you might decide to put a half watt resistor in there and you provide enough space so that it would fit in and some cooling air around it and maybe a little heat sink and the equipment worked very, very well.

It seems to me, from my own personal experiences, somewhere or another we lost this. You know, we have separate reliability organizations, we have separate quality engineering organizations, and by God they haven't joined the main stream of design and development of weapon systems. I don't know where or why we lost it, but frankly, it's a serious consequence and one that should not be given as the subject of talks, but by God we ought to do something about it.

Now, many people here in the audience are in management positions in their various companies, and I think this is a message that they have to bring back, that reliability is designed into the equipment from the first day, and after the design is complete, it's too late to go ahead and try and achieve reliability.

Now, we do have product improvement programs. Product improvement programs are a very cost effective way, as far as the Department of Defense are concerned and the Army specifically, to improve what we have. Principally, they are for the enhancement and the expansion of equipment capability and really not to re-engineer or re-do a lousy job in the first place. And all too often, it comes across my desk as a request for a million dollars here and ten millions dollars there for product improvement programs which are really to re-engineer a lousy job in the first place, and I think it has got to stop. Enough of a bawling out!

I have been asked to talk about Army requirements. I want to talk about Army requirements. I want to talk about the Army's needs in perhaps a way that you haven't been talked to in a long, long time- or maybe never. Every DOD speaker will come up and tell you, "We've got a budget crunch. Salaries and cost of services go up at anywheres from 5 to 12 percent a year; material costs go up so much and the DOD and the Army budgets stay fixed and where are we going?" We're going no place!

Well, all that's true, and that's a broken record. I want to talk about the Army, which is an all volunteer Army. Congress, as the spokesman of the people of this country, decided to do away with the draft. Well, I'm not going to discuss the merits of whether we should have done away with the draft or not, but the fact is that the young soldier in the field is there because he volunteered. Now, some people say, "Yes, he volunteered because he couldn't get a job in the civilian economy because we had a recession over the last two or three years." That may be, but he still volunteered. His continuing existence in the field doing this job is going to be based upon a voluntary expression on his part.

Now, frankly, you work in industry and you work for companies. If a company didn't give you a decent desk or a decent chair or an opportunity to use a telephone to carry on your normal day-to-day business, you would up and quit and find a company that would. Now, I didn't say you needed a sexy, air-conditioned office, a good secretary or a typewriter or what have you, but there are certain basic items that you need; otherwise, you go look for another job. Well, our young soldier is the same kind of person now, and unless we can give him in the field something that permits him to do his job efficiently, he's going to up and quit.

The other issue, and perhaps you people haven't been close to it, is the publicized-well publicized-Army position of improving the tooth to tail ratio. What this means is we want more people in uniform to be fighters, not lovers, and less people to be in the support and maintenance area. Now, this has got an immediate reflection in terms of the quality, life, and performance of our hardware in the field. Sometimes, I think that what we need in the Army is a one-horse shay. We need a tank

where everything that's perishable or vulnerable fails at one time. We can't stand one item failing one day and the next day another item. You know, it's continually in the maintenance shop. And if you look at those kinds of numbers, you will find that with very little problem, we can have about 30 percent of the Army inventory in what is very affectionately known as maintenance float. In other words, it's in the shop. If you people own two cars, and most families have two cars, you figure out what it would mean to you to have your two cars, in terms of 30 percent of their capability, in the shop at all times. Number one, the frustration of getting the kids to school, dancing lessons, yourself to work, your wife shopping, and all the other chores that you use your cars for, as well as, incidentally, the cost. It doesn't come cheap.

So, the name of the game is to clean out the maintenance facilities, keep the equipment out of the maintenance shops, and get going with it.

Now, we have perhaps a unique problem in the Army, compared to the other services. We run arsenals and depots. Arsenals and depots are part of the Army backbone for mobilization, but they are also for overhaul and maintaining our equipment. We have some depots overseas; we have most of them here in the United States. Incidentally, if you think it's cheap to transport a tank from Europe back to Anniston, Alabama, for overhaul, you try and pay the freight bill just one time. It's not easy. It's very frustrating to have a tank go into the Anniston Army Depot and be overhauled and go down the road 50 miles and have the alternator quit.

Well, you know, why didn't you put a new alternator in the damn thing in the first place? The answer is we can't afford it. Well, what do you mean you can't afford it? Well, we have to put out, and this is a standard answer, we have to put out what's known as DMWR. If you're not used to the alphabet soup of the Army in Washington, a DMWR is a Depot Maintenance Work Requirement. It sort of says a tank goes in for overhaul and you do certain things to it; you look at certain of the components; you inspect, repair and replace as necessary. And so somebody looked at the alternator and it looked perfectly fine; it spun, you ran it at the rated speed and the voltage was right and maybe you put a dummy load on it, and it even carried the dummy load, but 50 miles downstream it crapped out.

You know, before we had jets, for those who travelled in airplanes, we had reciprocating engines. The pilot used to go to the beginning of the runway and he would stop there and he'd rev his engines. What was he doing? He was doing a mag check. What he was really doing was stress testing. He was developing a level of confidence that those engines would continue to put out the power that they were supposed to during the period of critical flight, namely, takeoff. We don't do that with our jet engines anymore, although we have what's known as BITE or built-in test equipment, and presumably the little red lights and the dials and the knobs and what have you tell the pilot that the jet engines are working and they're going to supply the power on takeoff.

Now, I felt a lot more comfortable when they did the mag check, frankly. You know, I was able to see something, hear something. It was alive.

Well, one of the reasons why I'm being punished by giving the keynote speech here is somebody in the Army, I think, got upset with me and I said, "Goddamn it, why can't we have stress testing with equipment coming out of our depots? Why can't I get a howitzer that's been rebuilt and overhauled and tested so that I know it's going to last a certain period of time under normal usage?" Well, we're trying. I'll go into some details on that, and I'll go into a story that perhaps you've heard. It's been well publicized in the papers and press for about three years.

About three years ago or so, the Army found itself woefully in need of tanks. Its inventory was somewhat less than 50 percent of our authorized levels. Now, some of this was due to the Army's fault; some of it was due to circumstances beyond our control. We got involved in a series of programs to increase the inventory of combat-worthy tanks. And if you go to somebody in the Army today, a combat-worthy tank is the following kind of tank; it has a diesel engine; it has a 105 millimeter gun; and it's able to carry a minimum of 47 rounds of ammo. That's a combat-worthy tank. We were able to develop the industrial base to produce tanks known as an M60-A1 which had those characteristics. We also had, oh, something less than 5,000 rusty hulks known as M48-A1s and M48-A3 tanks which were at least 25 years old.

Well, in a desperate desire to build up this inventory, we said, "Hey, you know, our short supply is castings for M60 tanks. We have all these castings sitting around in various dump yards and PDO places rusting away, why can't we use those castings in some way?" So, we came across the concept of modifying the castings to install a diesel engine, put a 105 millimeter gun in it and carry 47 rounds of ammunition. We were able to do that very cheaply and very quickly and we thought, "Well, we have a combat-ready tank."

Well, some wise heads in the Army said, "Well, what kind of a tank have you got here?"

"Well, it's combat-worthy. It has all the characteristics you told me . Yeah, but is it as good as the M60-A1?"

I said, "Gee, I don't know." "I used all the M60-A1 parts; I used the engine, the transmission; I used the same breech block; I used the same gun tube; I even used the same little racks that held the ammo in the tanks. It's got to be, I even used the same track and the same suspension."

Well, the Army people, being people who work on the land and the ground, probably all come from Missouri, and they wouldn't believe that it was a combat-ready tank. So, after a great deal of fuss and fury and negotiations, we said, "All right, we'll take five tanks now known with the official name of M48-A5--what happened to M48-A4, I don't know, but it's somewheres--and we'll arbitrarily choose five of them and we'll take them over to a place called the Yuma Proving Grounds.

Now, the Yuma Proving Ground, if you want to envision it, is rough terrain, somewhat approximating the moon, and about a hundred degrees Fahrenheit hotter than the surface of the moon. This was considered the proper place to test our beloved new combat-ready tanks.

We ran those tanks with some soldiers who were experienced tanks crews up from, I believe, Fort Carson, and they were run by a very nice young lieutenant whose name was Mudd. So help me! From Buffalo, New York, a very bright young lad, and you know, he became the most popular lieutenant in the Pentagon as far as the Army was concerned for approximately three months.

After that he disappeared, not in defeat, but back to something that had less visibility, because it did worry his nerves to have the Assistant Secretary of the Army come out and visit him every six weeks to see how things were going on.

Some interesting statistics came out of that test. The Yuma test, you know, was really a milestone. It turned out that those five tanks had a mean miles between failure of 85 miles. Now, don't laugh, don't laugh. A tank in combat will travel approximately 50 miles a day. So, you know, I figured "Hell, that's not too bad. It's got 300 miles of fuel in its gas tank, so it doesn't have to be topped off too much." You've got a lot of ammo in the ammo racks, and you can fire a lot of rounds without being resupplied, and what we have to do is just take four guys that are in the crew and have them maintain the goddamn tanks. Every night!

That gets kind of tough. If you're fighting all day, it's kind of tough to maintain and repair the tank at night. And besides, those smart heads in the Army told me, "You know, that's a loser because the next war, the next ground battle is going to be fought at night." So, we're developing all these night sights and all these night fighting weapons for that."

And so, being a cilivan at heart, I said, "Well, we'll repair the tanks during the day." But that was no good.

But seriously, in looking at the data that came out and yielded that 85 miles, I detected that an awful lot of the subsystems that we borrowed, literally, from the production lines of the M50-A1 like the engine, the transmission, the tracks, the suspensions, the ammo racks and all that--the ammo racks didn't fail--that a lot of those things were failing. And I said, "Hey, why don't we segregate those failures into two piles; those failures in this pile that were M60 unique, and these that were M48-A5 unique. Maybe we'll have a difference.

Well, it really didn't pay off too much. And after a great deal of blood, sweat and tears, we decided that the M48-A5 was a combat-worthy tank, and that we would distribute it in accordance with a previously organized plan to the Army--well, not to the active Army-to the National Guard and reserve units.

But don't laugh. It's kind of important. There was a case made. You know, we'll give them valuable training on maintaining diesel engines, transmission, all those things that they will have in the M60.

Of course, in the course of this conversation, being a naive civilian, I said, "Hey, by the way, what's the mean miles between failure in M60-A1, that grand and glorious device that you're producing out of Detroit at so much a month?"

Well, somebody said, I thought it was 275 miles," and then somebody said, "No, it was 120 miles," and I got enough different answers that I was convinced that really nobody knew anything in terms of it.

So, after a lot of blood, sweat and tears, we ran, or we organized and planned and are running, today a test called BART. Now, I know this is Monterey and before anybody laughs, it's not intended to be a duplicate of BART in San Francisco. Believe me! It stands for Baseline Armor Reliability Test. We did what I consider a very interesting kind of experiment. We took five tanks, M60-A1, brand spanking new, arbitrarily chosen off the production line in Detroit. We took five M60-A1 tanks that had been turned into the Army Depot system for major overhaul--and I'll get to the characteristics of that major overhaul, we're not through with that yet--and we'll take five of my beloved M48-A5 tanks and we're going to put them down at Fort Hood, and we're going to test them simultaneously for three phases of 750 miles each, and we're going to have inspectors looking for failures and maintenance problems and see how the tanks work out.

It turns out all three tanks are about the same in terms of mean miles between failures. It also turns out that we have about tripled the mean miles between failure of the M48-A5 tanks as a result of the BART test. You know, a little thing like the change of the material that carries the gas from the gas tank to whatever the diesel engines use to distribute fuel around. It no longer snaps due to the vibration because we have a thicker material and a different material. We are learning from this test, and we hope to learn more. I think it really demonstrates in a serious way that the Army is fully cognizant and recognizes its problems in terms of reliability and in terms of deciding to give the man in the field an even break.

He needs more than an even break. If you look at the number of tanks that the Soviet Union and the Warsaw Pact nations can field, you will find that their inventories are about four times what ours is. I can only hope and pray that their maintenance float is ten times our's. If they're in the field, we're going to get clobbered, literally clobbered. By the way, don't think that their tanks are a poor quality, or less sophisticated than ours. They are every bit as good, every bit as sophisticated. Don't believe this stuff that you will read in the papers and the editorial pages about how the Russian soldier can't read a map and he's illiterate and he's stupid. Not so. He's pretty smart. Just as smart as our boys are. And, you know, there is no break on that battle field. That stuff has got to be there and it's got to work.

Incidentally, out of the BART test came another kind of interesting issue. The Army flies a lot of helicopters and we have the greatest, most sophisticated spectrum analysis capability for oil from engines, crankcases, and transmissions down in Corpus Christi, Texas, at the Corpus Christi Army Depot. Most people think that's a Navy base, but no , it isn't. It's really Army. The Navy is sort of a tenant of ours there. We find that we can determine that a helicopter engine is about to fail by looking at an oil sample of the engine or of the transmission.

Well, we finally got the armor people around to saying, "For the BART test we're going to take oil samples from those engines and from those transmissions." I think--I may be prejudging it--but I think that we're about to make a breakthrough that will permit us to say that an engine is going to fail in the next, perhaps 50 or 100 miles by just analyzing the oil sample with spectrum analysis.

The last part of the problem is if somebody can get me a little oil spectrum analyzer about the size of this pack of cigarettes that I could put in between the ammo in those ammo racks so that every day or every hour or every night the driver goes over and he drops a couple of drops of oil, just like you do with your swimming pool to determine if you have enough chlorine in the pool, and he looks at it and it's a red light or a color--and I'm colorblind, so I have no appreciation of these things--to tell him that, "Hey, that engine is about to crap out. Don't count on this tank for next day's battle," or, "Get back to some sort of a maintenance area and have it pulled."

Incidentally, it only takes about 15 or 20 minutes for an experienced crew to pull an engine and transmission and replace it with a new one. That's part of the RAM activity that we do.

Okay. I've said some bad things about the Army. I could have said some things that were even worse, but I really don't want to scare you and I don't want to embarrass some of the people in the audience. We had a pre-dinner session on one or two little problems. We are trying to right what I consider about 201 years of ills and head in the sand attitude. The Army is 201 years old; we're older than the nation, and so we are doing things. For example, in FY-77 the materials testing technology budget is about $4 million of which $3 million is devoted to nondestructive testing, NDT. I'm confused as to the difference between NDT and NDE, but we'll get to that later.

By the way, of the $3 million, about $1 million is going to be devoted to the automation of nondestructive testing, looking for critical defects. That's, by the way, a high payoff area, let's not kid ourselves. You take that 105 millimeter gun on a tank and you fill up all those tanks with those rounds, it turns out that we produce 105 millimeter ammo at anywhere from 20,000 to 50,000 rounds a month, and nondestructive testing of those rounds has got to be a very serious matter.

First of all, the warlords--those are the people who know how to fight--they say, and the Israelis back it up with their experience in 1973 that in order to win a ground battle, a tank must have what is known as the first round kill. Now that goddamn shell has got to work, and don't let anybody kid you. If it doesn't work, your tank crew is finished, because somebody else is going to get that first round kill.

It's pretty easy to do with all the sophisticated fire control and gunsights and infrared and night fighting sights. You just can't hardly fool a man, even with smoke.

I find it kind of embarrassing to stand in front of you and say, "Hey, the Army had --I don't know--$18 billion a year budget, which includes everything: pay of soliders, shipping of tanks back from Europe to be overhauled, and what have you, and all we can find is $4 million for materials testing technology."

My only excuse for that is that by God it falls under the aegis of the Assistant Secretary for R and D and not for I and L. So, I'm not responsible for it. Now, maybe I wasn't invited here as punishment, maybe this is a backhanded way of saying, "Hey, could you lend us a little money?" My reaction is that, "Yes, I think we could."

Now, I talked about our budget, let me talk a little bit about the things that we are attempting to do. We're attempting to have automated radiography to inspect explosives. You know, that's nondestructive testing right off the bat. We're spending money in optical laster techniques for service defects.

By the way, my ignorance in this field of what the Army is doing, because it really doesn't come under me, is proven because I have to read these from cards. It's no joke; it's serious.

We're using ultrasonic devices to examine billets and bar stock and castings for integrity in terms of locating blow holes, impurities, and things of that sort. When you think of tanks and think of 105 millimeter shells hitting tanks, weaknesses in tanks are kind of important, and to find them is equally important in terms of the survivability of the crew.

I find the next one absolutely fascinating. We're going to use a scanning densiometer for automated handling of data of spectrographic plates and films which are made during chemical analysis of engine oils and steels. You know, that's in the technology program. I want to tell you a little secret. You heard a tad of my resume background. I have been involved in reconnaissance and intelligence business for a hell of a long time. You know, we used scanning densitometers to locate targets on reconnaissance film when Hector was a pup, and the Army today is spending technology money to use this in its testing and reliability business. I don't understand. What happened to that technology? Did it go down the drain? Did somebody lose it? Or do we have to re-invent it? I told you I wasn't going to be pleasant to the Army people.

The next one boggles my mind. We're going to use a holographic fringe quantification system for use in interpreting holographs. I have a feeling that I read some material on that awhile back, and I think that's also a do-over, and it's probably getting ourselves into trouble.

Okay. Enough for the theory, and I call that theory. I did talk about the fact that we are concerned at Corpus Christi about crankcases and transmission oils from helicopters and prediction of failures and life extension.

We overhaul helicopters at Corpus Christi Army Depot, but we also have a very interesting activity there, which is very closely tied with helicopters, and that is, we have a complete bearing facility. We do have techniques which are in hand; using magnetic leakage field techniques and other techniques to determine what the stress patterns are on components of bearings. Also, to identify the infant bearing failures. These are failures of bearings in helicopter engines that fail before or occur before the helicopter and engine is due to go in for overhaul. In other words, you overhaul an engine, a helicopter and you say, "Okay, fellow, you've got 250 hours of flying time. When you get that, come back and see me and I'll overhaul it again." Which is great, if that's the right number. But then, the bearing fails after 75 hours and all of a sudden he's back for an overhaul because he has got a bearing failure and you have got to redo the whole engine and it costs us--I guess it adds about 25 percent to Corpus Christi's budget just to keep track of the infant failures on bearings. So, we have, not only sophisticated techniques in evaluating bearings, but we also have a rather elegant--and being a rather cynical chap, I consider it elegant--bearing reclamation facility whereby we are reclaiming these big, expensive bearings that cost a thousand, two thousand dollars a shot, for very little money.

Now, the nondestructive testing people in the Army do many things, and I do want to add a personal note about Mr. Paul Vogel, who is very heavily involved in our nondestructive testing program, and he, in his program, had been using some infrared mapping equipment as part of a research project.

Well, looking for additional challenges besides his job, it turns out that Paul Vogel drives around Army installations at night, preferably in the wintertime when the temperature is below the freezing level in a 1969 Cadillac which reportedly has 236,000 miles on its odometer. This is not non-destructive testing. He's required to use the Cadillac because of the equipment he hauls around.

Now, what he does is take this infrared mapping equipment and maps the heat losses from buildings in the Army facilities as part of the Army Energy conservation program.

Now, maybe that's also nondestructive testing. It's kind of an interesting application and perhaps it's a little vignette that says, "All our people aren't that bad; they're pretty smart people and they know what they're doing." I'd like to develop that kind of confidence, and I have. I have been cynical perhaps a bit, but that's to prove a point, and I don't think the Army is the worst there is. I think maybe there are some other people around who might not be able to face up to their problems in an honest way.

Okay. Back to being a keynote speaker. I think we have to provide you with a challenge. I can't hope to debate and discuss sophisticated physics and mathematics with you on a toe-to-toe basis, because I'm sort of an old, worn out engineer, and I really haven't kept up with the technology all that much. But let me refresh your memories. It wasn't more than a couple, three or four years ago that the automobile industry recognized they had an obligation to the consumer and out of that obligation came warranties of 50,000 miles and five years; 10,000 miles and two years; or 10,000 miles and 12 months, and we warranty certain major parts of your automobile.

Now, some of that initiative has been dissipated and lost because of the recession and depressions and other pressures that have been put on the automobile industry, and I think they've had other fish to fry. But it's kind of interesting. The automobile industry can go ahead and provide those kinds of guarantees and warranties to their customer, and our soldier in the field is our customer. Why can't we provide the same kind of guarantees and warranties to him?

Now, you say, "Well, maybe we do." Well, not so; not so. Let me give you some numbers that will boggle your mind.

A tank is considered to have a useful life of 30 years. That's not bad. Your tin Lizzie at home -if you get 10 years out of it, you're probably doing all right. Well, not quite the same. It's sort of apples to oranges.

In peacetime, for training and other activities, a tank averages about 1200 miles a year. That's 36,000 miles of tank life. Depending upon the location of the tank, if it's here in the continental limits of the United States, the number is 6,000 miles; if it's overseas, the number if 5,000 miles. When it reaches that mileage it goes back to an Army Depot for a major overhaul. When I say "major overhaul," it is disassembled and all the paint is removed down to bare metal. Every subassembly, every black box is inspected, repaired, replaced, reassembled and given a little cursory test and, bing, off it goes.

Well, the argument is,a tank takes a hell of a lot of beating compared to your car. You know, if I had a car like that,I'd junk it. I just couldn't afford to keep it. Well, yeah, a tank does take a hell of a lot of beating compared to my car, but you know what? I don't know what you pay for a car nowadays, I haven't bought one in a couple of years. I probably can't afford one, but let's assume that an automobile for family use runs $10,000. Do you know what a tank costs? Fifty times that! $500,000 for a tank. Well, I wonder if we beat it around 50 times as much as my teenage sons beat around my family car, but I'll tell you, that tank isn't performing anywhere near what the automobile industry is providing me. I think there's got to be something wrong.

Now, I listened to a few of the preliminary remarks this evening. We had some exciting discussions at dinner and prior to dinner, and you know, about the physicist really getting into this thing and nondestructive testing and evaluation is multidisciplinary and by God, there are physicists and mathematicians all over the place. Well, god-

damn it, let's get it out of the laboratory and out of the cloistered halls of theory, and let's get it into the field. Let's get it into the depot where it belongs!

The program that was discussed is two years old. I'd like to see a practical result. I'm not a young man; I haven't got much more to live. Please help me!

Now, I have another problem. I was given a speech. You know, when the Assistant Secretary gets a request to speak, he doesn't really look at the subject or why, he looks at the location. Monterey, California, obviously is a nondestructive environment, and I have to compliment everybody on the choice. So, it looked like this was a fun thing to do, and then as time went by I spoke to one of my execs and I said, "Hey, we've got to do something about that speech in Monterey. Why don't you get some bright fellow to write a speech that's appropriate for the location and the people and the subject at hand." I got a speech. It's sitting back there in my room. It's about this thick. I didn't use it really, because I thought it kind of missed the point, but it just added to my confusion to no end. Nondestructive testing- you know if I examine that and try to figure out "what the hell does it mean?" it tells me what it isn't, but it doesn't tell me what it is.

Well, I'm not the smartest guy in the world, believe me, but I sort of divined out the other night on the airplane that maybe what people mean by nondestructive testing is a confidence building test. Huh? I don't want to change your nomenclature, but just think about these things, do something about them. Maybe even more than a confidence building test. Maybe it's a life expectancy test. You know, that's not bad.

As a matter of fact, if I look at us as people--the good book says, and I don't know why it says it, that once a year I've got to have an annual physical. And after going through all the treadmills and all the poking and what have you, the doctor sits down with me and says, "Well, Harold, old boy, I think you're good for another year." That's a life expectancy test. Isn't that what we're looking for?

I really would like to take an APC or a howitzer or a tank or a truck or a jeep and I'd like to be able to put it into something that simulates a carwash--everybody knows what that is--and when it comes out the other end, there's a tag that says, "Good for 750 more miles." That's the challenge that the Army has, and that's the challenge that I think I have to lay on you people.

You know, you don't have many chances in this life. That sounds like an ad for Miller's beer, but I think in all seriousness, you don't have many chances to do this kind of a job, and if you're not going to take it out of the laboratory, if you're not going to provide for an impact on today's world today, we might as well forget it.

Thank you.

DISCUSSION

MR. JOSEPH JOHN (IFT Corporation, San Diego): This has got to do with the topic of liability. Don Thompson, in his opening remarks, identified NDE as being related to the concept of liability in the commercial world. I'm aware of two court decisions in which the Government has been found to be liable for products, particularly with respect to 105 millimeter shells. Would you care to speculate if that is going to be a continuing process where the Government is going to be found liable for the product?

MR. BROWNMAN: I suspect so, but let me tell you something, if you don't know it already. The greatest game in the country is to sue the Government, no matter what. So, to be liable for performance of equipment, yeah, I guess we can be liable, and I think contractors can be liable.

Fair enough?

DR. ELLIS FOSTER (Institute for Defense Analysis): What is the time between breakdowns in World War II tanks?

MR. BROWNMAN: We don't have those numbers. You've got to be kidding. We didn't worry about that. We were too busy fighting, really. There are no statistics. In fact, you raise an interesting point, and that is that the Army seems to be totally devoid of statistical data, real live statistical data, not simulated stuff from a mickey mouse computer where somebody can change the ground rules on you so you don't really know what's going on. I'm talking about real live statistical data. It's nonexistent.

DR. GEORGE MAYER (Army Research Office): First of all, the $4 million that you mentioned in MTT will have a bit of supplement from $200 million additional in a very large MT program, which is manufacturing technology, part of which will be devoted to things like inspectability. The other thing that we really haven't talked about is the human factor in inspection, and I call your attention to things like the sinking of the submarine THRESHER a few years back. Well, we had quite adequate inspection techniques, but these were human failures, and I think that with some of these new techniques that are automated, these human failures will be circumvented. But the human element is still going to be a very major element in this product reliability business. And you have to consider ways of motivating people to make them more responsible and knowledgeable about what they're doing and to become conscientious in their everyday jobs.

MR. BROWNMAN: Well, you're right. Let me address that second point, which I think is interesting, and the reason why I'm glad you asked it is it does identify initiative that I am very, very familiar with, because somebody suggested it and I hopped on the bandwagon. I wish it was mine, and we are doing it, and maybe you are aware of it. We found out in a moment of frustration in building up our inventory of tanks that we were getting a lot of M60-A1 tanks, brand new tanks, brand spanking new tanks out of Detroit Army tank plant, which were heaps of garbage, deficiencies all over the place, and we hadn't had a chance to put a soldier in it to louse it up yet. So, one bright general who is now retired, unfortunately, but he's still bright and deserves the credit, by the name of Joe Pieklik, who was then Commanding General of the Tank Army Automotive Command, did a little analysis--not a study. He didn't study, he went out and analyzed what was going on, and it turned out that about 90 percent of the people who were inspecting tanks, both Chrysler employees and U.S. Government employees, didn't know what the hell they were inspecting.

So, the first thing he instituted was a training program and a method whereby he certified inspectors so they really understood what they were inspecting. If a guy was certified to inspect engines, he wasn't permitted to inspect fire control unless he was specifically certified on that piece of equipment.

Then he instituted a deficiency advertisement reporting system on the tank line using the concept of peer pressure where certain groups at certain work stations were competing against others in terms of the number of deficiencies, and that worked out very well.

Then he went further and he looked at jigs and fixtures in the Army tank plant, which, by the way, has been producing these things for 25, 30 years, something like that, and he found out that they were either in poor shape or nonexistent.

For example, certain nuts or bolts had to be torqued down to a certain torque specification, and there were not torque wrenches on the line. It's not funny.

So, he gave them the torque wrenches and then the mechanics didn't know how to use them. I've gone into plants and I've looked at torque wrenches on the production line and found that they were calibrated 17 years ago.

So, you're right. There is an awful lot of that. Incidentally, you walk into depots and arsenals, and you will find alignment jigs and fixtures not so tapped and you will find that nobody ever checked them to see if they ever got out of alignment themselves for years and years and years. Sometimes they use jigs and fixtures as stepping stools, you know, to get up on the top bin over there, and God knows what they do to the calibration on it. So, the inspection process is a very important one.

Now, there are ladies here, so I'll temper the next one. Chrysler, who runs the Detroit Army tank plant with their people and has been the contractor for many years and is very comfortable in that role, and it's a profit-making venture for them, had a session with me once right after we uncovered all these problems with tanks and the quality of tanks coming out of Detroit, and I said to one of the key executives, "Hey, O.J" --Ollie, his name was. Not O. J. Simpson, Ollie White-- I said, "Hey, Ollie, last night before I went to sleep I couldn't fall asleep because things were troubling me. So I needed a diversion, so I invented a new game and I wonder if you'd play with me." He says, "Well, what is it?" "Well, I guess I'll call it 'You Bet Your Life'" -- to him I used another word, but "You Bet Your Life." I said, "How would you like to make a deal with me on the next contract, for every tank that has five defects or more out of this line, you give me $1,000 of your fee back." Incidentally, they make about $16,000 worth of fee in the course of a tank. You know what? He refused to do it. That tells you the quality of people that are involved in these things.

Also--I'll carry on, I have a couple of points here to make--it turns out that if people on the production line in Detroit goof up--and you can identify now because of this autotrail who goofed up and put the wrong part with the right part and that kind of thing -and they're all unionized, I asked Chrysler, I said, "Do you think your union would stand for a man who has made three errors, three assembly errors in one week to be sent back to a training program for two weeks, at the salary of a trainee?" The answer was, "Unh-uh, no way."

The last item about quality doesn't involve tanks. I am involved in other things besides tanks. I went out to a Army airbase in Stuart, Florida. There was a Grumman facility on that airfield, and there is a Grumman airplane known as the Mohawk, and the Army has a little reconnaissance program in which we install various modular equipment in Mohawks to do reconnaissance chores that would be necessary to the Army. There were some things of issue in the program and that's why I visited the place, and they went through a big rain dance about how we are going to get you in this Mohawk and we're going to fly the infrared and the side-looking radar and we're going to show you the readout and the air-to-ground link and how it works.

This was all very interesting to me because reconnaissance and that sort of thing has been sort of a second hobby of living. But catastrophy befell that day and the infrared equipment wasn't working. It had a bad bearing. Of course, it's just a scanner-type device and I said, "Gee, how many flying hours does that piece of equipment have that it's worn out at this point? The guy looks it up in his records and he says, "Well, we just got that from the depot last week and we put it in the bonded warehouse waiting for your arrival so we could show you how well it works." It was, incidentally, overhauled at the Sacramento Army Depto.

Well, after a little bit of pushing and shoving, it turned out that the great guy who inspected it in the Sacramento Army Depot didn't know what the hell he was inspecting, and so he really never did inspect it, and it was just a piece of garbage.

Okay, next question. That was a long answer to not even a question, but a couple of statements.

You had one?

PROF. GORDON KINO (Stanford University): Yes. I was wondering if there had been any examination of whether there was a tendency to make things too sophisticated that they can never work?

MR. BROWNMAN: I think that's fair and there is an aspect of that. You know, we like to enjoy the elegant sophisticated things, and we play with it and play with it and play with it and it never gets to real life, and I think there is a facet of this. We do reliability studies and analyses and very sophisticated calculations and we bring in high powered computers and we come out with printouts that nobody reads, and certainly nothing gets to the field. You're right.

DR. ROBB THOMSON (National Bureau of Standards): Just a comment on that vignette you mentioned. If the Army learns to use this oil spectrum analysis technique for their new diesel you may be interested to know that this technique was invented back in the 30's by the railroads for guess what? the diesel engines.

MR. BROWNMAN: Yes, that doesn't shock me at all.

CAPT. JIM ANDERSON (Naval Research, Pasadena): I liked your car wash analog and that's something that all the services need for their equipment. But what we need that to do is not to give us a tag saying the equipment is good for so many miles or years but to tell us what to do so it will be good. What that's going to tell us on some of those tanks that come through is that the paint is okay, don't strip it and don't repaint it, but you better replace the number 2 diode in the alternator because that's about to fail.

MR. BROWNMAN: I think there's something to that. By the way, let me take issue with something you said. I think the Army has got a problem that is not shared by the Air Force and the Navy. The Navy carries it's maintenance facility on its back. You go to those capital ships, even destroyers and they've got machine shops and they've got facilities and they're right there, right Johnny-on-the-spot.

The Air Force traditionally flies out of a well-instrumented, well-organized airfield with lots of maintenance facilities and they fly back to the same one or to an equivalent one. But that Army tank, that Army APC and that Army howitzer, they never know where they're going to end up that night when they're going to have their eight hours of rest, and they don't know what maintenance facilities they're going to have. Only what tools and jigs and fixtures and a little know-how that the fighting crew-emphasis on the word "fighting crew" - knows about their vehicle, that's their maintenance facility, and boy, that's vastly different than what the Air Force or the Navy live with. Very different.

PROF. JOHN TIEN (Columbia University): One of the most important points you made, of course, is to shorten the time constant between the theory and getting something into the field. Now, if you look at statistics, we're not very good at doing this unless there is a very strong motivation like a war or something. Do you have anything concrete to suggest on how we can improve on this lacking of ours, any incentive, perhaps, you have in your back pocket?

MR. BROWNMAN: You know, John, you've just given me an oportunity to be the hero of the symposium, but unfortunately, I'll have to decline. Because if I had such a scheme or thought or technique, I probably would patent it and end up as a rich man rather than a worn out, old engineer.

I don't know the answer to it, and that's just the tip of the iceberg. The Army's tank program XM-1 has got some stalls due to NATO politics and Congress and what have you, but let's ignore that facet for a minute, and I don't think it's appropriate to talk about. I don't think you people would be interested anyway. But you look at the XM-1 tank, and it's a good example. We started that about four years ago, and the plan was that it would be in the Army inventory. It has been a few years from concept to operational capability of something known as a tank, which we have been building for, what, 50 years, of that generic type? We can't even get a tank into the field in a

hurry! We're worse than the traffic engineers who build roads. The big cry is the day they cut the ribbon on the freeway, the super-highway, it's overcrowded. Well, the day we give the man in the field the weapon, it's outdated. I don't know the answer to it; it goes beyond me. But how do you get the theory, how do you get the concept into the field, gee, if I knew that I'd tell you, but I don't.

DR. ROMAN WASILEWSKI (National Science Foundation): Just a quicky on some statistics. In the last year of the war, the operative actual lifetime mileage of a Sherman tank in our unit was 430 miles. You said 30 years is lifetime for a desirable tank. The two are somewhat disparate.

MR. BROWNMAN: I'm surprised. The Sherman tank?

DR. WASILEWSKI: Yes.

MR. BROWNMAN: That had a gasoline engine?

DR. WASILEWSKI: We had a selection from diesels to gasoline, five different types per each squadron--

MR. BROWNMAN: I'm frankly amazed. We've gone backwards.

MR. JACK NICHOLAS (Navy): I don't know the answer to John Tien's question either, but I think part of it has to do with getting the people who are going to use the test instrumentation or technique involved in its development very early in the stage of its development. What I have been finding is that I come across very interesting techniques which can be used in the field by one Ph.D. and three people with Masters Degrees, which ultimately is going to be used by somebody who has a high school education if you're lucky and who has to apply a great deal of subjectivity to the interpretation of the results that he's getting out of the instrument. When you can see objectivity, what the end result of the test is, you're much further along towards the solution of the problem of application of a nondestructive examination technique or instrument in the field.

MR. BROWNMAN: That's true. User involvement early on is certainly valuable and can shorten the concept of field time of test equipment or anything. Only one word of caution. The user quite often vacillates. First of all, the planned turbulence in the service means the man in uniform, who represents and speaks for the user in the field, every two years changes, and so you've got somebody with a new idea coming in.

Also, the user tends to want more than he should want, because everything has got to be gold-plated, got to be the latest, newest bauble, and the latest and newest technology, and some of that motivation is good, but I think you've got to be very careful that he doesn't put you into a situation where you can never climb out of it, but your point is well taken.

DR. DON THOMPSON: We have time for one more question.

DR. PETE CANNON (Rockwell International, Science Center): Mr. Secretary, isn't part of the answer to the Columbia University charge that we in industry should not take on scientists and engineers who don't know how things work and don't care, and that the universities shouldn't graduate scientists and engineers who don't know how things work and don't care?

MR. BROWNMAN: Yes, I think so, but that's a subject for another night. Here's a rebuttal. I think we're going to hold the rebuttal until we have the mixer or hospitality hour. I can hardly wait for that.

Thank you.

DR. DON THOMPSON. Thank you.

INTRODUCTORY OVERVIEW

George A. Alers
Science Center, Rockwell International
Thousand Oaks, California 91360

As previously mentioned, the ARPA program is divided into three parts. The major part devoted to defect characterization will be discussed tomorrow. The other parts are the subject of today's program and involve some major NDT problems that are not directly associated with defect characterization in a solid. They have to do with the problem of adhesive bonds, the problem of measuring residual stress and some new techniques that show great promise for failure prediction. The solution of these problems not only requires improvements in our understanding of the physical phenomena involved but they also require translation into a device for use in the field. During today's program, we will cover the four distinct areas of: 1) adhesives and composites, 2) new measurements and techniques, 3) internal stress, and 4) acoustic emission. I will begin by going over the program, pointing out the connections between each of the talks and introducing some of the ideas that tie the subjects together.

The first several talks are concerned with the very important problem of adhesives and composites. Polymers are steadily moving into more and more structural applications, especially in the aerospace industry, because weight and ease of fabrication are assuming greater importance. The adhesive bond is a method of joining metals that is very efficient because it provides the maximum amount of strength for the least amount of weight. Composites, of course, are the ultimate in structural efficiency because the strong fibers can be put in the direction of the loads thereby taking strength away from where it is not needed and putting it where it is needed. Unfortunately, these very efficient materials have not seen broad acceptance because we do not have nondestructive test techniques that will show that the completed part is reliable. We do not have a way of non-destructively testing an adhesively bonded part to assure that the bulk adhesive is at the strength level that it is supposed to have, and that it is properly stuck to the metal. Without these kinds of tests, the part has to be terribly overdesigned. In fact, standard practice appears to involve making an adhesive joint to the best of our ability and then boring a hole in it to bolt the members together.

Later in the meeting we will discuss the inspection of new materials. Not only are the composite and the polymer on the horizon as new structural materials, but ceramic materials with their high temperature capabilities will certainly need to be inspected for flaws. Here, the minute size of the critical defect will tax all of the tools that we are developing today and we shall see how important it will be to provide defect characterization capabilities at unusually high frequencies and their application to some old problems such as the measurement of internal stress. There are a lot of black magic and witchcraft methods of processing that extend the fatigue life of a part by putting compressive internal stresses into the surface. Shot peaning is the most common, but one must use the right size shot, driven at the right speed for the right length of time before the fatigue life of a metal part is extended. The only available method to insure that the processing has been done correctly is to use x-ray techniques for measuring the stresses in the surface. Unfortunately, the measurement technique is very subtle to use and very easily misinterpreted. There are many other places where residual stresses play an important role on an atomic level; the internal stresses between dislocations and between precipitates control deformation on a microscopic scale. These, in turn, determine the yield strength and the ultimate strength of a metal part. There has always been a dream among nondestructive testing workers to invent a little black box that could be used to give a meter reading of the ultimate strength or the yield strength of a metal. It is my opinion that this ultimate aim will be achieved by some of the work that is being done with nonlinear acoustics as we will hear about later.

Then, there is the field of acoustic emission. Everywhere in nondestructive testing we hear about acoustic emission as the greatest technique now being developed. It's main use so far has been in the testing of very large objects where it is economically impossible to go over every cubic inch of the structure looking for flaws. Acoustic emission has the very powerful capability of locating the flaw by detecting the direction from which the noises come. Once located, some of the defect characterization techniques can be used to assess it's criticality and a decision can be made concerning the safety of the entire structure. Unfortunately, after acoustic emission has been used for awhile, a lot of the chief engineers who were in charge of building giant structures began to view the technique with skepticism and used a line from Macbeth to describe their feelings that acoustic emission "is a tale told by an idiot; full of sound and fury but signifying nothing." It is our objective in the advanced NDE field to give some respectability to acoustic emission by learning to understand how it is that the noises are made and how to interpret them so that we can recognize the true flaws and be able to predict better how to use the technique.

Now that I have summarized the problems and payoffs that face us, I would like to go back and go over each area to tell you about our authors and how their work ties together in today's session.

In composites, the basic geometry is either a sandwich structure consisting of metal plates glued together with an adhesive, or fibers embedded in an epoxy matrix. There are always likely to be gross defects, such as disbonded areas, bubbles and porosity and there may be a subtle lack of adhesion at

the joint between the polymer and the metal or between the epoxy and the fiber that ruins the adhesive strength of the interface and thus deprives the whole part of its strength. These adhesion effects may be on a very small scale, perhaps even on an atomic scale, and thus they will be very difficult to see. There may also be a chemical deficiency in the bulk of the epoxy or adhesive that causes a reduction in its cohesive strength. Our work today is to understand not only how these large defects that are relatively easily seen by x-rays and ultrasonics affect the strength of the part, but also to look at the subtle defects at the interface or in the chemistry of the adhesive itself to see how they play a role in the strength of the part.

Our first speaker, Bill Bascom, from the Naval Research Lab, will set the stage by talking about the role of gross defects as deduced from the fracture mechanics of this kind of layered structure. Then we will turn to one of the main problems with adhesive bonds and polymeric materials, which is their susceptibility to moisture. Currently, the designer can only use a fraction of the strength potential of composites and adhesives because he is not sure how water degrades strength and he doesn't have any kind of a nondestructive test tool to tell him if the water is there or if it has been there. Since this moisture problem is particularly difficult in the composite materials, Dave Kaelble and Lloyd Graham from the Rockwell Labs. will tell us about how the water gets into the graphite-epoxy composites, what it does when it gets there, how it affects the strength, and what nondestructive tests we can hope to use to detect it.

Following this discussion of fiber reinforced materials we will turn to the structure where layers of aluminum or metal are joined by an adhesive. Dr. Scott from the Naval Air Development Center will tell us about how the layered nature of the structure influences the sound waves, both for acoustic emission and for ultrasonic pulses. Then, Paul Flynn from General Dynamics and Mike Buckley of the Air Force will describe the standing wave effects that occur with a transducer in a water bath sending sound waves through the layered structure perpendicular to the interfaces. The frequencies at which the standing wave conditions arise can be used to deduce the quality and properties of the joint. I will then appear back on the podium to describe some new results obtained by sending the sound waves parallel to the adhesive layer in an attempt to allow the sound more time to interact with the defects that may be at the interface. Tom Wolfram from the University of Missouri will then tell us about the use of electron tunneling from superconductors to get an atom's eye view of what happens at that interface between the metal and the adhesive.

After we have spent the morning on adhesives and composites, the afternoon will be spent on some new NDE techniques and the NDE of new materials. Tony Evans of the Science Center is going to tell us about the problems we face with ceramics and we will get a glimpse of defect characterization. George Matzkanin of Southwest Research is going to tell us about how nuclear resonance can be used for nondestructive testing. Then Otto Buck from our Laboratories and Mr. James from Northwestern University will cover the NDE problem of measuring internal stresses.

Late in the afternoon we will get down to the fundamentals of acoustic emission with two speakers, Bill Pardee and R. Clough, who will describe theoretical approaches to the question of how to interpret emission signals and derive the most information we can from them.

I think it is important during this overview to look back over the program to see where we were two years ago, where are we now, and what we have accomplished thus far by taking a rather fundamental view of nondestructive testing and trying to get at the basic mechanisms. In the area of adhesive bonds, today's program should show that we are on the verge of having field-applicable techniques for measuring the cohesive strength of a bond. Also, we have got some pretty promising leads for measuring the adhesive strength of that interface between the polymer and the metal. It will take another year's work to provide the statistical basis to prove that these statements are true, but I think we have come from no tests at all to some very specific tests for some specific features of the adhesive bonds.

In the composites area, it was only a few years ago that it was said, "water ruins composites" and everybody had a different idea of how and why this happened. Over the past two years, we and other laboratories have figured out where the water goes, why it does what it does when it gets there and have even found some physical properties that can be used to measure, in a nondestructive way, that the water has been there or is still there or that the strength has been degraded.

In the area of ceramics, our program is very new and we are using some of the output of the defect characterization studies that you will hear about tomorrow in this type of new material where the critical defects are a few microns in size and are way outside the range of conventional ultrasonic equipment. In residual stresses, we have some new methods that utilize some unexpected techniques involving the magnetostrictive interaction to reflect the stresses that may be in a ferromagnetic material.

I am really most excited about the area of acoustic emission, which has been around for years. During the last two years, there has been a major thrust in the theoretical aspects of what generates the noise and what are its characteristics. We have coupled experimental and theoretical investigations that are already giving us information about what to look for in the frequency spectrum to tell the difference between a crack and a broken precipitate. It won't be too long into the future when we can tell the difference between a crack and the dropping of a wrench on top of a pressure vessel.

DISCUSSION

MR. MAX WILLIAMS (University of Pittsburgh): Thank you very much. The chair here is very encouraged by the fact that we also have a mechanical device in case the electronics fall apart.

Thank you very much, George Alers. As the next item on the program, we have Bill Bascom from the Navy who will discuss the Durability of Composites and Adhesives.

DURABILITY OF COMPOSITES AND ADHESIVE BONDS

Williard D. Bascom
Naval Research Laboratory
Washington, D.C. 20375

Any consideration of the durability of the high performance composite materials and structural adhesives used in aerospace construction must recognize that these are brittle materials and that their failure mode is characterized by flaw growth and propagation. One can easily anticipate a variety of flaws and defects; surface cuts, internal cracks due to stress relief and deliberate holes cut for fasteners. In this presentation we wish to discuss yet another type of flaw in fibrous composites and adhesive bonds that is inherently present because of the processing methods used to fabricate composites or bonded joints. These flaws are microvoids created by air entrapment that usually occurs when a viscous liquid is forcibly spread over a solid surface. Such forced spreading is characteristic of both adhesive bonding and composite fabrication.

The static wetting behavior of a liquid on a solid surface is characterized by the equilibrium contact angle (θ) illustrated in Fig. 1. However, even if this equilibrium contact angle is zero, the dynamic angle (θ_D) is not. The situation is illustrated in Fig. 2 showing a film of liquid initially having $\theta = 0$ but, because of high viscous resistance at the solid/liquid boundary, the dynamic angle is nonzero. As a result the advancing liquid traps a thin air film which is unstable against surface tension forces and forms a bubble trapped at the interface.

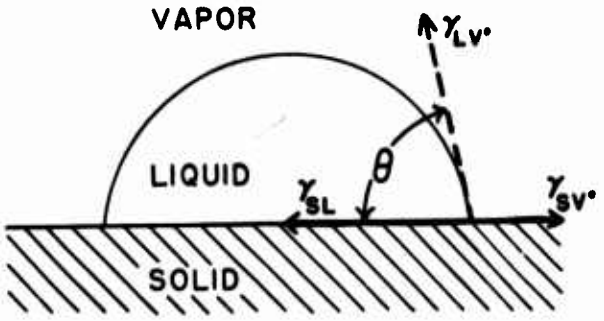

Figure 1. Equilibrium contact angle, θ. γ_{LV} = liquid surface energy, γ_{SV} = solid surface energy and γ_{SV} = solid/liquid surface energy.

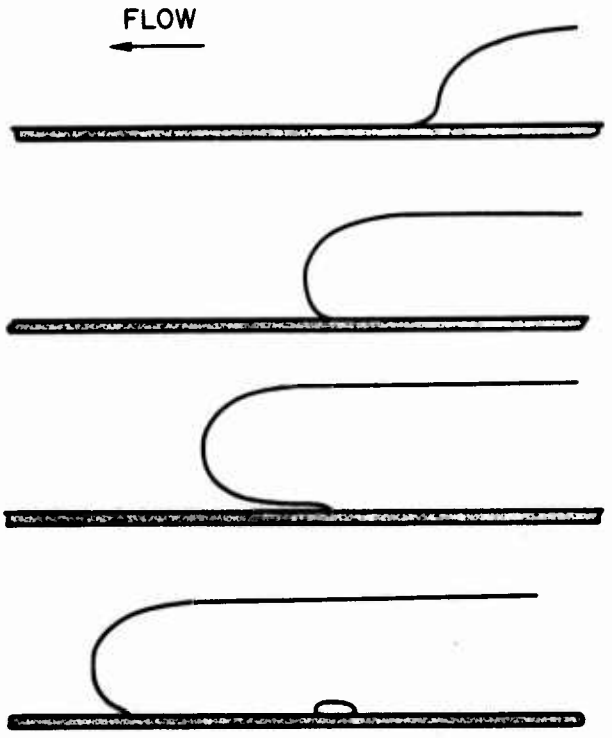

Figure 2. Schematic of a liquid film ($\theta = 0$) being forcibly spread over a smooth surface and trapping air.

There have been a number of analytical relationships developed for θ_D in terms of the viscous and surface chemical forces involved. Typical of these is the Friz equation (1,2),

$$\text{Tan } \theta_D = a \left(\frac{\eta v}{\gamma_{LV}}\right)^b \qquad (1)$$

where η is the liquid viscosity, v the average flow rate of the liquid film, i.e., spreading rate, γ_{LV} is the surface tension of the liquid and a and b are constants. Consider a typical case of an epoxy liquid resin ($\gamma_{LV} \approx$ 30 dynes/cm) and a spreading rate of 10 cm/sec. Even if the equilibrium contact angle is zero, Fig. 3 indicates that the dynamic contact angle approaches 90° even for moderately viscous liquids.

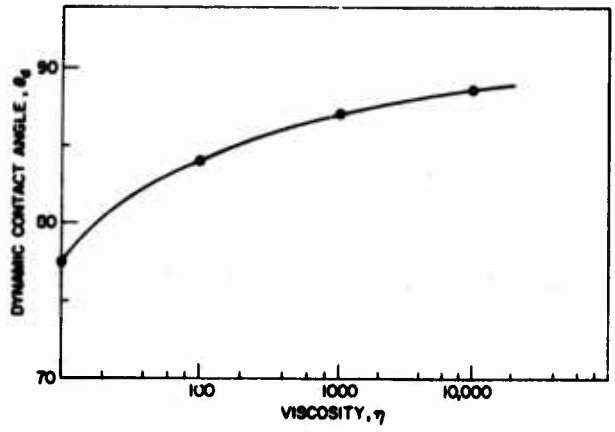

Figure 3. Plot of equation 1 for a liquid having γ_{LV} = 30 dynes/cm and a spreading rate of $10^{}$ cm/sec.

Air entrapment under conditions of forced spreading is by no means limited to flat surfaces. The situation of a rod being forced or pulled through a liquid surface is illustrated in Fig. 4. The air/liquid surface around the rod is forced down and the cylinder of air so formed may actually be carried on the rod into the liquid bath.

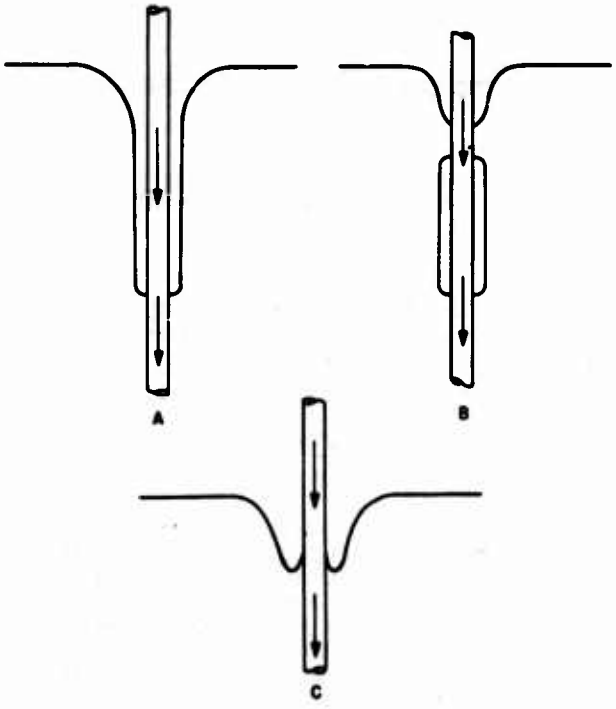

Figure 4. Schematic of air entrapment around a rod entering a liquid bath.

Resin/Fiber Composite Materials

A similar albiet more complex situation exists in wet winding of continuous filament composite. This technology involves strands of exceedingly thin (9μm) glass or graphite fiber being rapidly drawn through a bath of liquid resin. One need only observe the froth of air bubbles that accumulate in the resin bath to suspect that a process of air entrapment and release is occurring.

A study was made [3,4] of this air entrapment in filament winding by simulating the process so it could be observed microscopically. Figure 5 shows the experimental arrangement in which a strand (∿ 200 filaments) of glass fibers is pulled through a glass optical cell containing transparent resins and other liquids and onto a wind-up drum. Tension on the strand was maintained by a friction brake. The strand was observed as it entered the liquid bath and just before it emerged.

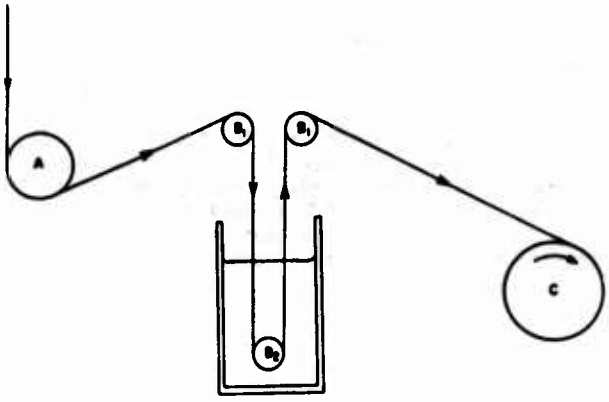

Figure 5. Experimental arrangement for observing air entrapment in filament winding. The strand is pulled from a spool (not shown) by the wind-up drum (C) and tension is maintained by a friction brake (A).

A photograph of the moving strand entering a bath of epoxy resin is presented in Fig. 6. The dark areas represent air surrounding the strand and being drawn into the bath. At typical winding rates not all of the air could be displaced by the liquid. Observed near the point of emergence from the liquid the trapped air has been rearranged into elongated voids as shown in Fig. 7. The voids are held in the strand in this elongated configuration because of the lateral constraint resulting from the tension on the filaments. Similar elongated voids can be seen in cured glass fiber-resin matrix composites.

Figure 6. Photograph of strand entering a liquid bath. Dark areas are air.

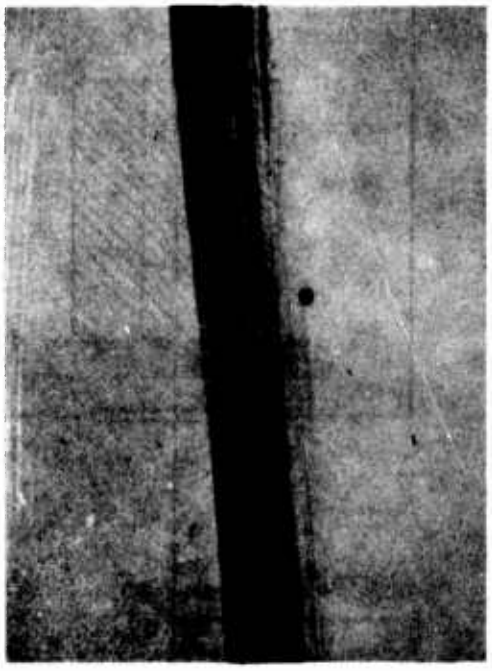

Figure 7. Photograph of strand just before emerging from the bath. Elongated features within the strand are trapped air bubbles.

A

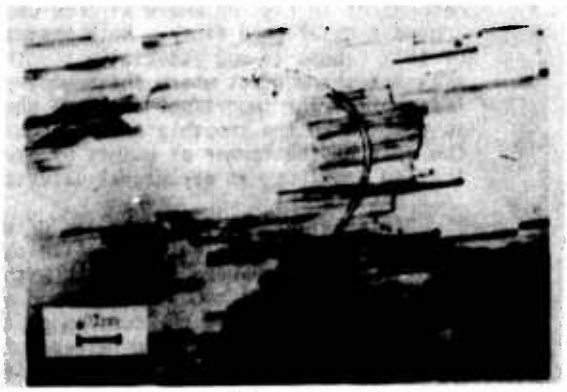

B

Figure 8. Air voids in commercially prepared wetwound composites.

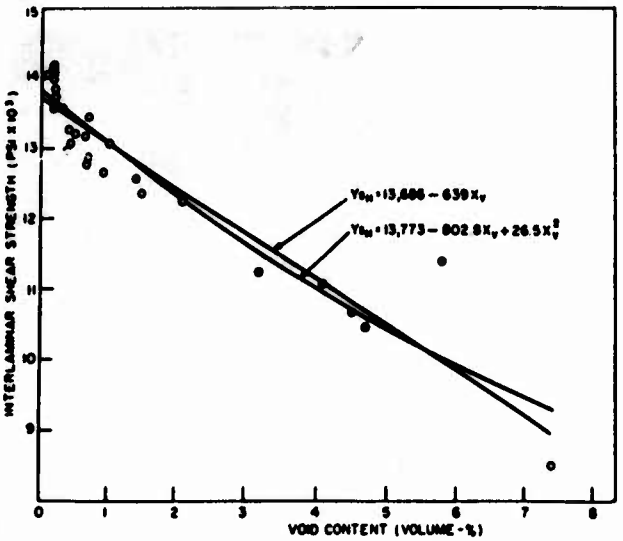

Figure 9. Effect of void content on NOL-ring interlaminar shear strength

There are two specific features of special interest in these photographs. First, that some of the air voids have sharp edges, notably where they intersect a filament (Fig. 8A). Secondly, that individual voids can collect into wide area debonds as in Fig. 8B where air has collected around a misaligned fiber. Note that the periphery of this debond is not especially smooth in that it presents sharp edges where the boundary intersects fi..ments. The importance of these sharp defects as opposed to the smoothly contoured air voids is the role of the former as points of stress concentration and thus, as structural defects.

In an effort to determine the extent to which this entrapped air affects composite strength, NOL-ring specimens (5) were fabricated with various void contents. The amount of trapped air was controlled by oscillating the tension on the strand during winding which allowed release of air when the filaments were relaxed. Fully void free specimens were prepared using a "vacuum release" technique[3] which simulates the effect of fabricating under pressure (autoclave) to reduce or collapse the air voids.

The effect of void content on interlaminar shear strength (ILSS) is shown in Fig. 9. This is essentially a resin dependent property and it is quite clear that reduction of void content to at least 1% significantly improves the shear strength.

Structural Adhesives

The opportunity for air entrapment is far greater in the case of adhesive bonding with structural adhesives than it is in filament winding. Commercial structural adhesives are supplied as slightly tacky films of resin supported on an open weave cloth of glass, polyester or nylon fiber. Their principal use is in aerospace construction to bond aluminum or composite skins to each other or to spars or honeycomb. In application these adhesive films, which are essentially semi-rigid solids, are pressed between rigid metal plates. The opportunity for air entrapment is exceedingly great because of the very high viscosity of the resin.

An experiment was devised to simulate this air entrapment process and to observe microscopically the fate of the trapped air as the resin film is softened by heat and then cured into a rigid solid[6]. The experimental arrangement is shown in Fig. 10 and consisted of a vacuum chamber with windors at top and bottom. The specimen consisted of a film of commercial adhesive sandwiched between microscope slides and supported on a ring-shaped heater from an oil diffusion vacuum pump. Weight was applied to the sandwich by a brass cylinder bored through the center to pass a light beam. The events occurring within the film could be observed by viewing the lower glass/adhesive boundary with reflected-light microscopy or by viewing through the sandwich with transmitted light.

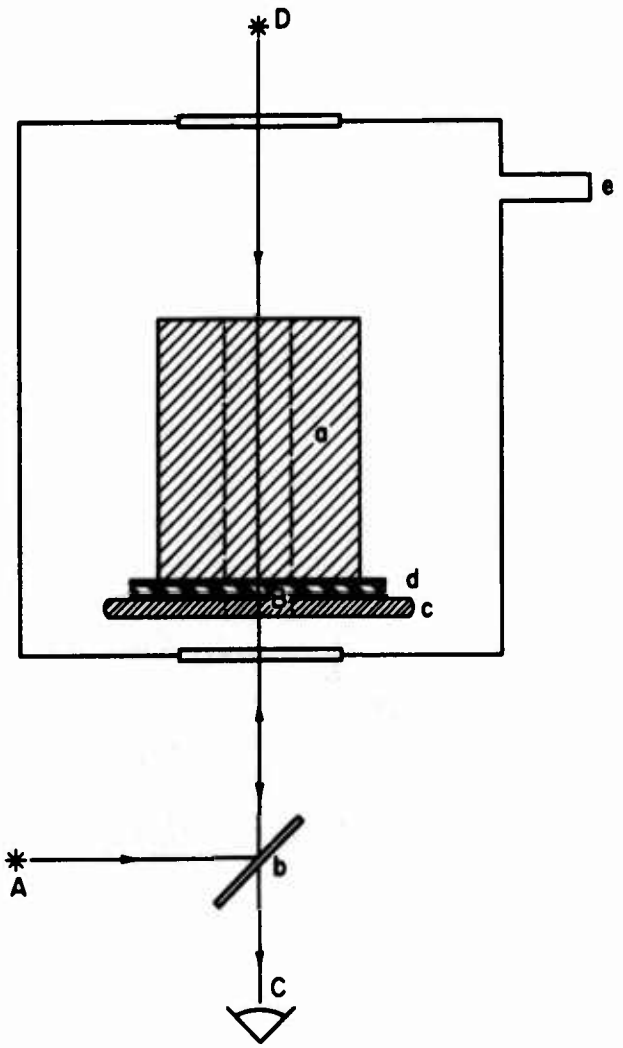

Figure 10. Experimental arrangement for viewing entrapped air at the adhesive/glass interface.

The photomicrographs presented in Fig.'s 11-15 demonstrate that considerable air is initially caught at the glass/adhesive interface but as the resin viscosity is reduced by heating it flows (under pressure from the brass weight) and the air is displaced from the interface and into the adhesive. The process is illustrated schematically in Fig. 16.

In photograph 11A the light areas represent trapped films of air and cover at least 50% of the interfacial area. Viewed in transmitted light (Fig. 11B) the trapped air film is too thin to be observed but the dark regions are believed to be air trapped at the intersection of filaments of the support cloth during manufacture of the adhesive film itself. As the resin softens the air is displaced and the regions of resin contact increase in area (Fig. 11C and 11D) and the air accumulates into bubbles thick enough to be observed in transmitted light (Fig. 12).

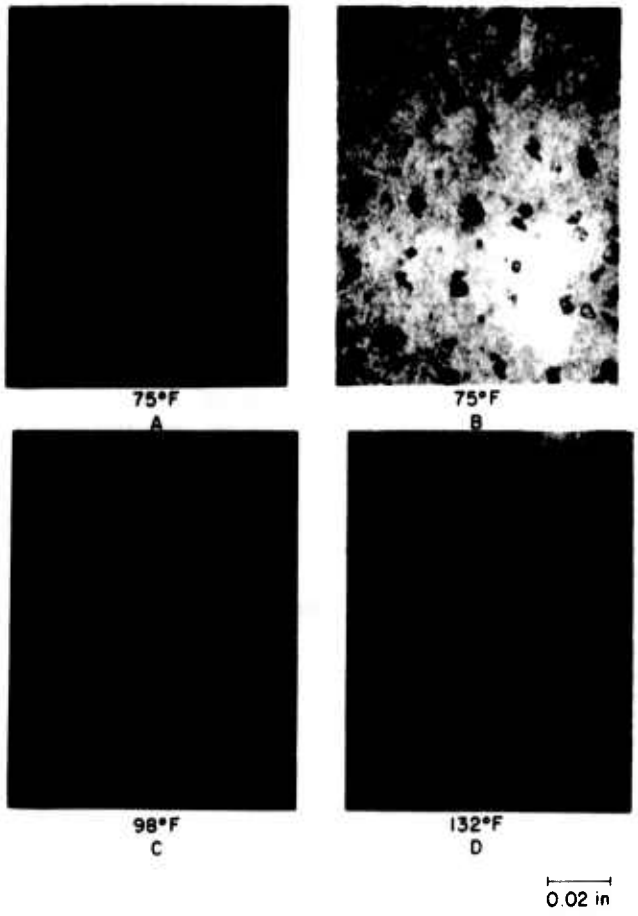

Figure 11. Photomicrographs of trapped air during resin cure (θ = 0)

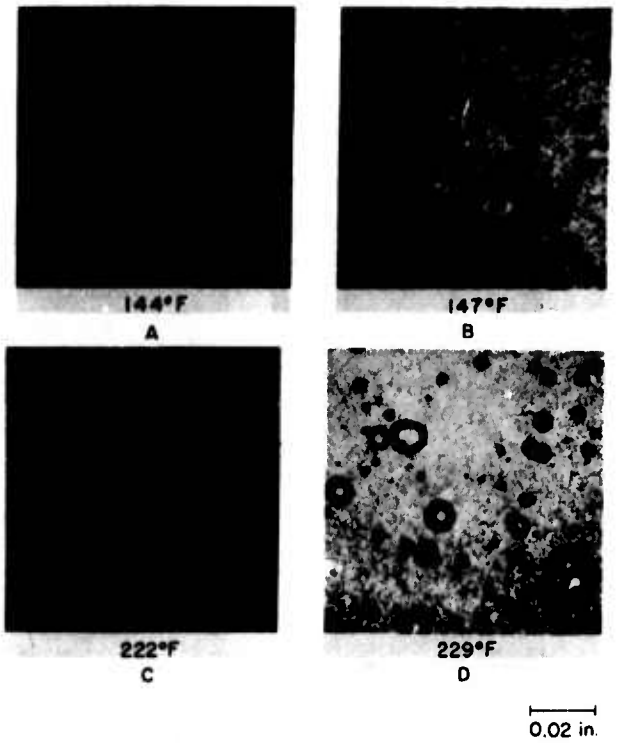

Figure 12. Photomicrographs of trapped air during resin cure (θ = 0)

Eventually, the air is fully displaced into the adhesive layer and tends to accumulate as elongated bubbles aligned along the fabric of the support cloth. At the end of the resin cure the adhesive film has thinned by flow-out along the edge of the specimen. This thinning is limited by the thickness of the support cloth. However, the process presses the trapped air bubbles against the glass surface so that they are again visible in reflected light (Fig. 13).

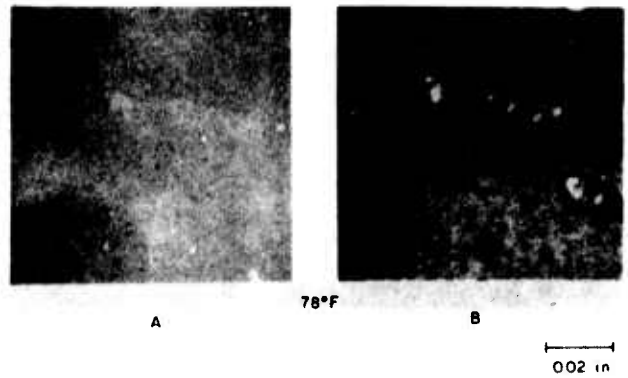

Figure 13. Final appearance of cured bond in reflected (A) and transmitted (B) light (θ = 0)

The air displacement process is truncated if the resin does not "wet" the adherend, i.e., exhibits a finite contact angle on the glass surface. In this situation displacement does not progress beyond step B in Fig. 16 as illustrated by the sequence of photographs in Fig. 14 and 15 from an experiment where the glass had been deliberately contaminated with a very thin film of silicone oil to make the glass oleophobic.[6]

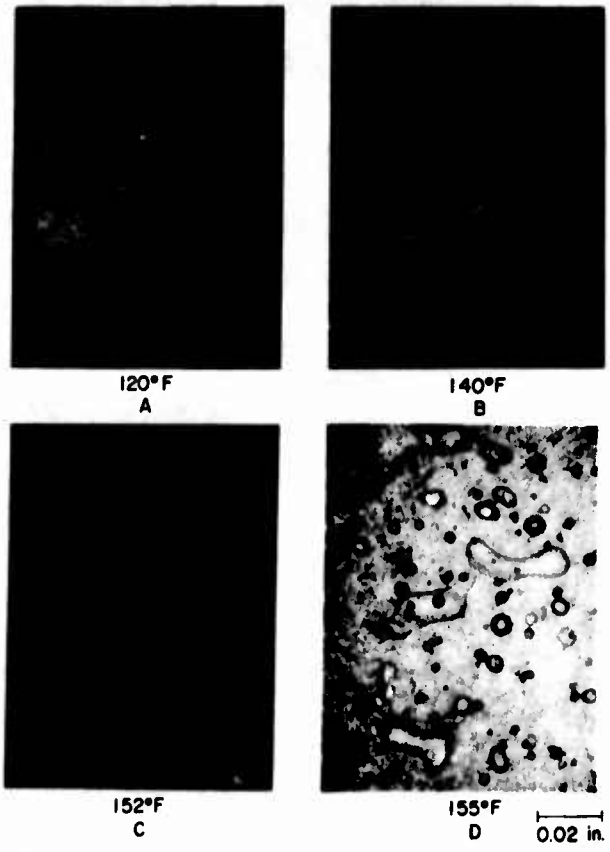

Figure 14. Photomicrographs of trapped air during resin cure. No further air displacement occurred upon continued heating (glass surface treated so that $\theta \neq 0$)

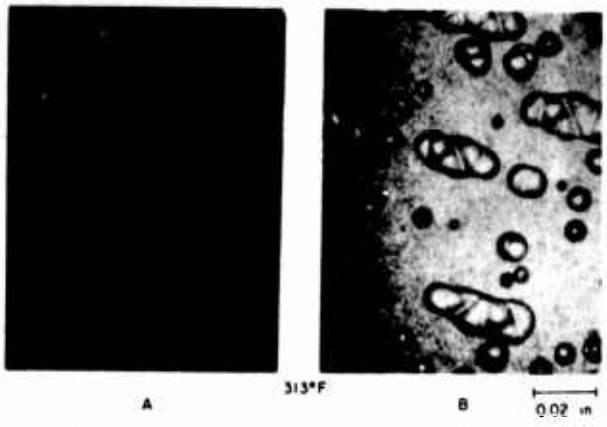

Figure 15. Photomicrographs of cured bond in reflected (A) and transmitted (B) light (glass surface treated so that $\theta = 0$)

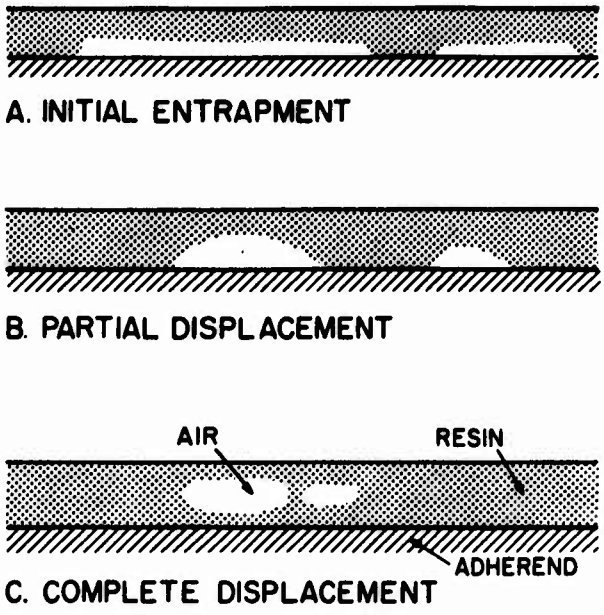

Figure 16. Air displacement process

Air entrapment in structural adhesive bonding is not prevented by curing under vacuum. All that occurs is that the initially trapped air film is evacuated along with the surrounding chamber. During the subsequent curing operation air is displaced either partially or fully into the resin layer. The only difference from what occurs at atmospheric pressure is that the air in the trapped voids is at a reduced pressure. In Fig. 17 the same array of bubbles is evident in specimens cured at 5 mm Hg and at 760 mm Hg. However, a vacuum release procedure can produce a void free bond (Fig. 17A). This technique involves evacuating ($\sim$ 5 mm Hg) the chamber initially but then returning to 760 mm Hg during the heat cure when the resin is most fluid. The hydrostatic pressure imposed on the resin causes the entrapped air bubbles to collapse to a size undetectable at 500X and higher. The actual volume reduction is of course $\sim$ 760/5.

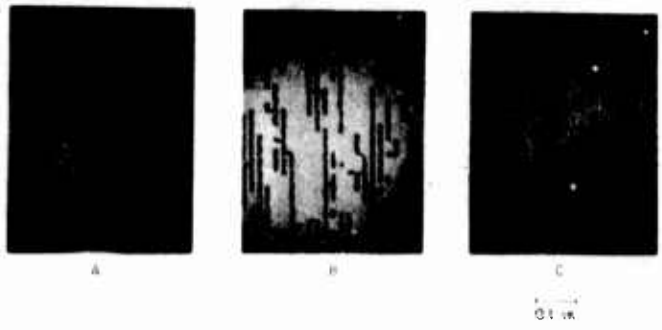

Figure 17. Low magnification views of glass-adhesive sandwiches bonded using the vacuum-release technique (A), vacuum through entire cure cycle (B) and no vacuum (C)

A point to be kept in mind is that the extent of air displacement and the effectiveness of the vacuum release technique (or autoclave pressurizing) depend on the resin becoming sufficiently fluid so that surface and hydrostatic forces can overcome the viscous resistance of the resin. Many adhesives are so highly loaded with inorganic fillers that they never attain this necessary degree of fluidity.

To test whether this entrapped air actually affects bond strength, adhesive specimens were prepared using aluminum sheet bonded with the same adhesive (modified epoxy) used in the microscopy studies. Peel test results are presented in Fig. 18. The top curve is for the adhesive without a support cloth and without any attempt to prevent air entrapment. Failure in this case was of a brittle, slip-stick nature and at a low peel strength. The slip-stick failure mode is considerably reduced and the peel strength improved with the inclusion of the scrim cloth (Fig. 18B) and still further improvements are attained in the absence of air voids (Fig. 18C). The recorder trace in Figure 18D is for another structural adhesive (nitrile-epoxy) and although there was as much as 30% air space in the bond, failure did not occur in the brittle slip-stick mode.

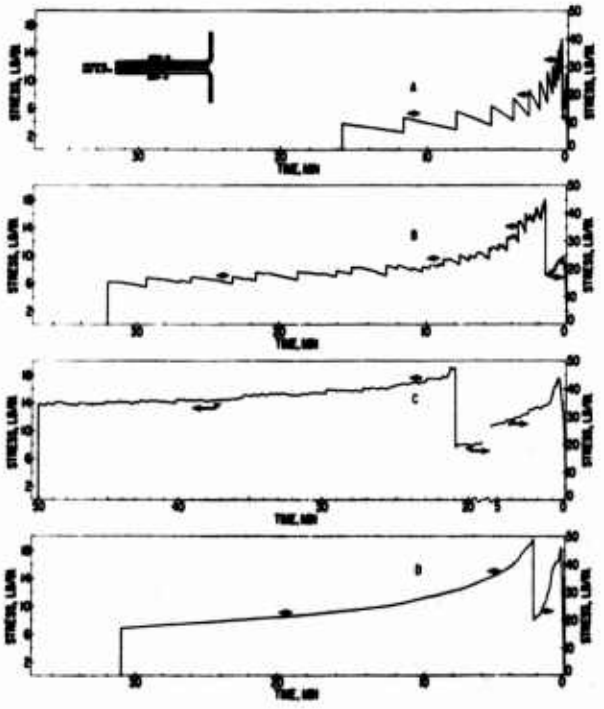

Figure 18. Stress-time curves for peel strength. A, modified epoxy with no cloth; B, modified epoxy with cloth; C, modified epoxy with cloth and void free; D, nitrile-epoxy with cloth.

Critical Flaw Size

It is quite evident from these two studies that these flaws inherent to the fabrication processing do in fact reduce material strengths - at least those dependent on resin properties. It is fair to ask if we could reasonably predict that these are serious flaws and worth removing or avoiding. The answer, at least to a crude approximation, comes from linear elastic fracture mechanics which relates the critical flaw size, r_c to the yield strength, σ_y, modulus E and fracture energy $\mathcal{G}_c$ (strain energy release rate (7));

$$r_c = Z \frac{\mathcal{G}_c E}{\sigma_c^2} \qquad (2)$$

where Z is a geometric factor dependent on the specimen shape and the loading conditions. The fracture energy, $\mathcal{G}_c$, is characteristic of the material and in Fig. 19 values of $\mathcal{G}_{Ic}$ for pure opening-mode (cleavage) fracture are compared. Note the relatively low toughness of the matrix resins but which, when formulated with elastomers, become high toughness (peel strength) adhesives. Unfortunately, the same micro-failure mechanisms which give rise to tough adhesives do not carry over into composites[8].

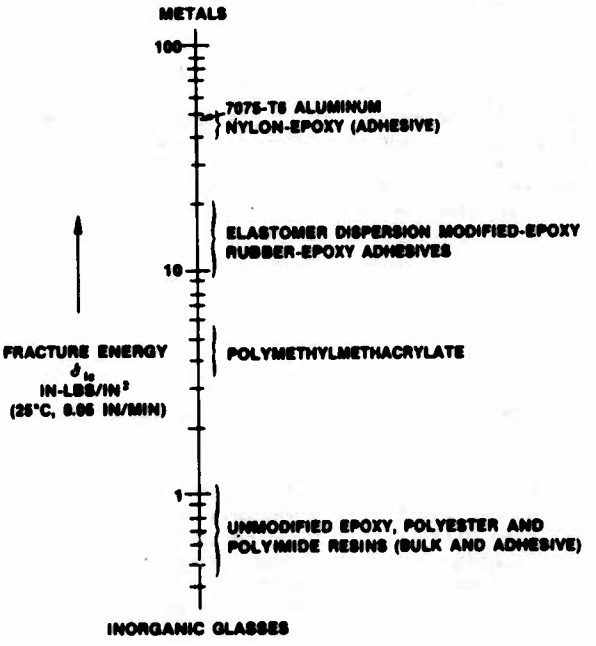

Figure 19. Ranking of $\mathcal{G}_{Ic}$ (1 in-lb/in^2 = 175.3 J/m^2).

In Table I the critical flaw size for matrix resins and the structural adhesives are listed along with the corresponding void size as determined in the microscopy studies. This elementary analysis clearly predicts that the air voids in the composite will cause matrix fracture.

TABLE I

	$\mathcal{G}_{Ic}$, J/m^2	r_c, μm	Microvoid Dimension, μm
Matrix Resin[a]	100	4	5
Structural Adhesive[b]	1700-3500	70-140	100-250

[a] bisphenol A diglycidyl ether/anhydride or amine systems

[b] "modified" epoxy systems

The $\mathcal{G}_{Ic}$ and critical flaw size for structural adhesive vary depending on resin formulation and so for a very tough (high peel strength) adhesive the void dimension may be less than r_c. This situation might explain why the nitrile-epoxy adhesive (Fig. 18D) appeared to be insensitive to the presence of trapped air voids. When the flaw size is less than r_c failure occurs by resin yielding rather than fracture.

The use of equations such as (2) assumes an "infinitely sharp" edge at the flaw tip. More precisely, a crack tip radius, ρ, also characteristic of the material. It is for this reason that the point was made that at least some of the air voids have sharp edges. Notably, in Fig. 8 and when voids are not completely displaced from the adhesive/adherend interface (Fig. 16B). Smoothly contoured air bubbles do not meet the sharp tip criteria although fatigue loading, internal stress relief or other sources of microcracks which themselves would not be critical could provide the necessary sharp radius to make an air void a critical flaw.

Certainly there are other factors to be considered in any sophisticated analysis of critical flaw size. Hopefully, this elementary discussion has illustrated how flaws produced in materials processing and fracture failure analysis with NDE in predicting material strength.

References

1. Friz, G., Z. fur. Angw. Physik 19, 374 (1965).
2. Schwartz, A.M. and Tegada, S.B., J. Colloid and interface Science 38, 359 (1972).
3. Bascom, W.D. and Romans, J.B., I and EC Prod. Res. and Dev. 7, 172 (1968).
4. Kohn, E.J., Sands, A.G. and Clark, R.C., I and EC Prod. Res. and Dev. 7, 179 (1968).
5. ASTM Standard Designation D2291-67 (reapproved 1974) and D2344-72, Amer. Soc. Testing Materials, Annual Standards, Part 35, April 1975.
6. Bascom, W.D. and Cottington, R.L., J. Adhesion 4, 193 (1972).
7. Tetelman, A.S. and McEvily, A.J., Fracture of Structural Materials, Wiley, N.Y., 1967, p.51.
8. Bascom, W.D., 30th Anniv. Techn. Conf. Reinforced Plastics/Composites Inst., Soc. Plastics Ind. Inc., Washington, D.C., Feb. 1975.

DISCUSSIONS

PROF. MAX WILLIAMS (Univ. of Pittsburgh): Do we have some questions for Bill Bascom?

I would like to stress the obvious in case you missed the point, that he's working with his early experiments with a transparent material where it's easy to see the flaw. In the fracture community, this is extremely important, as Bill and I have discussed before, because there are some rare cases, including the modified toothpick test, as I call it, that he showed first whereby pushing the rod down and entrapping the air just happens to be one of the problems that the mechanics in the community can solve. So it does have the extra added advantage of permitting a comparison between the NDE efforts and the fracture community efforts, and it's this bridge that I'm particularly interested in.

A question here?

DR. SAM K. NASH (Frankford Arsenal): Is there any reason for thinking that the initial air entrapment that you referred to is a manifestation of a lack of wetting, in other words, dirty interfaces?

DR. BASCOM: One of the main points I tried to make was that even with a perfectly smooth surface and a perfectly clean surface so that I have a zero contact angle, there are a number of equations that predict that the dynamic contact angle approaches 90 degrees in any real system - real in the sense of real flow velocities and viscosities and surface tensions. So the answer to your question is no, you can have a thoroughly clean surface and you still have the fundamental fact that the dynamic contact angle is greater than zero and would lead to air entrapment.

PROF. WILLIAMS: Bill, would you take your own questions until the time runs out? There's one in the back.

DR. BASCOM: Yes.

DR. ROBB THOMSON (National Bureau of Standards): What would happen and would it be successful if you wet the fiber with some kind of spray before you put it into the liquid to build up the layer? Then can you keep the air away from the fiber surface so that you get into the bubble situation instead of the crack situation?

DR. BASCOM: Yes, that is certainly feasible. In fact, it is possible to apply a coating so that the viscous resistance of the spreading resin at the boundary is reduced and θ_D is lower. However, it doesn't take much viscous resistance to overwhelm the thermodynamic surface forces.

DR. JERRY TIEMANN (General Electric): Has there been any recent progress in developing resins that have lower viscosities that also have good adhesive and strength properties?

DR. BASCOM: The trend seems to be to higher and higher viscosities-to melt forming for the high temperature resin. The high temperature polyimides, for example, are sometimes applied as melts with viscosities much higher than the conventional resins.

MR. ROBERT IRWIN (Northrop): It appeared in your commercial adherence interface versus wetting (or improved wetting properties) that you had a higher stress riser condition than usual.

DR. BASCOM: Yes.

MR. IRWIN: All right. What kind of NDT system did you utilize to prove that out or did you?

DR. BASCOM: To prove what out? That I--

MR. IRWIN: That you had a higher stress riser condition and--

DR. BASCOM: I am just presuming. If I have a sharp edge as opposed to a natural curvature, I assume I have a higher stress concentration.

MR. DAVE KAELBLE (Rockwell Science Center): I have a brief comment and then a question really for both Bill and Max.

The comment is this: that work that Bill has shown us this morning has not been lost in the wash. People concerned with prepreg and composite manufacture spend a lot of money and a lot of time attempting to use the curing cycle itself and at a certain stage of the cure, by following it by valid telemmetry, for example, to pinpoint a certain point in cure where pressure is applied. High pressure is applied in conjunction with the use of vacuum bagging at the early stages of curing, and these two things together seem to provide an approach to minimize this problem. So, in that sense you're early work has been very good.

DR. BASCOM: I'm glad to hear that.

MR. KAELBLE: The question that I have in my mind is: we know these flaws exist, and in your peel slide, you showed the slipstick type failure with the bubble specimen. Does that relate to a critical spacing between the flaws because throughout each flaw I note there's a stress field, and there is a sort of an idea that if the stress field overlapped, then you have this type of an interlinking or zipper effect. Maybe Max or Bill would have some comments on that.

DR. BASCOM: My only comment is that it certainly looked that way when we ran the test.

PROF. WILLIAMS: And theoretically your answer is yes, Dave.

DR. BASCOM: Are we out of time?

PROF. WILLIAMS: We have time for one or two more.

DR.JOSEPH JOHN (IFT): If I interpret what you have on the screen, is it fair to say that the idea here is to move the air bubble from the interface into the adhesive to increase the strength of the bond?

DR. BASCOM: This is the first improvement that you can make, yes.

DR. JOHN: Are there any data which indicate what the effect of the location of the air bubble; i.e., its distance from the interface, has upon the strength of the bond?

DR. BASCOM: Yes, there are. We have shown that failure tends to occur along the support cloth (especially glass). Voids have less effect if they are kept out of the cloth.

MR. DAVE KAELBLE: It appears that if you can displace the bubble two effective radii away from the surface, then the localization effects of the interface and the surface stress of the bubble tend to be diminished; in the bond line, generally, there is not that type of space available.

DR. RICHARD CHANCE (Grumman Aerospace): On the specimens where you showed a loss of strength due to the void condition in the prepreg specimens, were those specimens prepared using the standard method of vacuum bag, or was there vacuum used in making them at all?

DR. BASCOM: All our specimens were wet wound. We found we could shake the air out of single strands by slipsticking the tension. To reduce voids to 4 to 2 volume precent, we used a vacuum release technique to get to <|001.%.

DR. CHANCE: I was referring to the specimens that had the voids. How were they prepared?

DR. BASCOM: We oscillated the tension on the strand. In effect, shaking the air out of the strand before it came out of the bath.

PROF. WILLIAMS: I think that's fine. Thank you very much for your presentation, Bill.

WAVE PROPAGATION AND ACOUSTIC EMISSION IN LAYERED COMPOSITED

W. R. SCOTT
Naval Air Development Center
Warminster, Pennsylvania 18974

I will be presenting two different phases of our NDT composites program. The first of these, an in-house effort, is on the use of ultrasonic techniques, including spectrum analysis, for the nondestructive testing of composite materials. The second part of the presentation will be on characterization of acoustic emissions for boron/aluminum. This latter program is a joint effort between NADC and the University of Delaware. By way of background, Fig. 1 shows a diagram of an apparatus used for ultrasonic detection and mapping of flaws in composites. This is quite a conventional apparatus with the possible exception of the incorporation of the spectrum analysis capability.

SCHEMATIC DIAGRAM OF ULTRASONIC TESTING APPARATUS

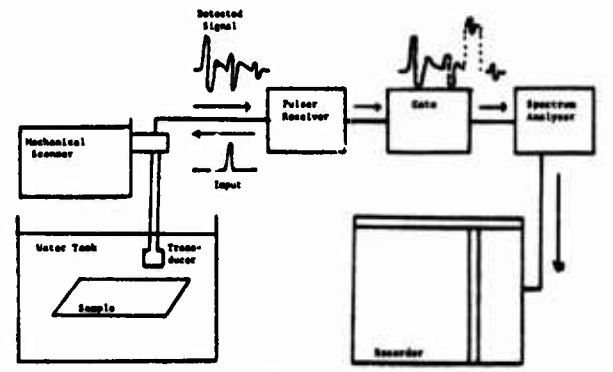

Figure 1. Schematic of Ultrasonic Testing Apparatus

An ultrasonic transducer projects a short duration pulse of broadband ultrasound onto a sample, which returns a decaying transient response due to the multiple echoes and reflections within the sample. The returning stress wave is detected, amplified, and a given time slice from the returning echo is gated and put through a spectrum analyzer. The resulting signal can be used to drive the intensity of a C-scan recorder, thereby producing flaw maps like the one shown in Fig. 2a.

There are several ways in which the effect of gating on flaw detection can be seen. One of these is to look at the displaced superposition of all the A-scans formed by scanning linearly once through a given region. The multiple A-scan of Fig. 2b was taken over a region containing a tight delamination. Between the interface and back echoes there is very little change in the ehco due to the presence of the defect. However, the second multiple echo and the third multiple echo show perturbations of the pulse which give more sensitivity for detecting the flaw than could be obtained with just a first echo.

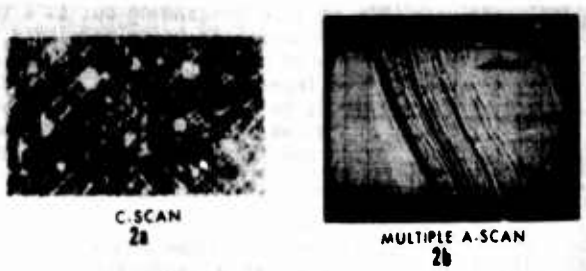

Figure 2. Presentations of Flaws in Graphite Epoxy Panel. White circles are prefabricated flaws.

Figure 3 illustrates another application of multiple echoes for detecting flaws in boron/aluminum. For these C-scans, 10th and higher order multiple echoes were needed to provide the sensitivity necessary to find very small strength-limiting flaws. Clearly the light areas in the C-scans correspond to the areas where the samples failed in the tensile tests.

Figure 3. C-Scan detection of strength limiting flaws (fiber density variations) for B/Al composite. Detected flaws correspond to less than 10% reduction in theoretical strength.

Figure 4 illustrates the use of spectrum analysis for C-scan mapping of particular material properties such as thickness. For example, the scan in Fig. 4 used a frequency filter set at the half power point frequency of a transmission thickness resonance. Such resonances are frequencies for which multiple echoes passing through a sample, constructively reinforce each other producing a peak in transmission.

These resonances have been utilized by a number of investigators for making accurate thickness and velocity measurements. In this case, variations in sample thickness effect a motion of the resonance peak, which causes darkening in thicker areas of the sample and lightening in thinner areas of the sample, producing a thickness map of the sample.

In addition, the sensitivity of this technique can be changed by using either a narrow gate or a wide gate, the wide gate yielding a sharper peak and high sensitivity; the narrow gate yielding a broader peak and less sensitivity.

Because of the potential utility of spectrum analysis, not only in C-scanning but as a tool for flaw detection, a model is being developed to mathematically predict or characterize the nature of spectra from layered composites. One reason for doing this is to avoid cataloging different spectra ad infinitum for all of the different possible layups and flaws in a composite sample.

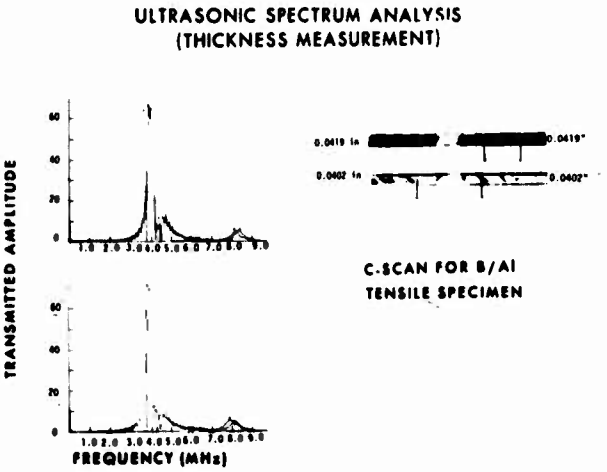

Figure 4. Ultrasonic Thickness Mapping

In Fig. 5 it is shown that the spectrum of a composite material differs somewhat from that of a monolithic plate in that the features corresponding to thickness resonances are not evenly spaced and vary somewhat in sharpness. In addition, the spectral features are found empirically to vary with fatigue, composite layup and environmental exposure.

In an attempt to understand composite spectra, we have been investigating a simple linear model in which the transmission and reflection coefficients of layered media are built up from the known responses of individual layers.

Equations (1a) and (1b) give the expression used to compute the Fourier transform for the transmission (T') and reflection (R') response functions for a layered medium when an additional monolithic medium is joined.

$$T'(w) = \frac{t\,T(w)\exp(-iwd/c)}{1 + r\,R(w)\exp(-2iwd/c)} \qquad (1a)$$

$$R'(w) = \frac{r + R(w)\exp(-2iwd/c)}{1 + r\,R(w)\exp(-2iwd/c)} \qquad (1b)$$

The lower case t and r can be either computed reflection and transmission coefficients or tabulated experimental data. d and c are respectively the thickness and velocity of sound in the appended medium and T (w) and R (w) are transmission and reflection coefficients before adding on the additional medium. By making d/c complex, damping may be introduced into the model.

To describe non-normal incidence, a matrix quantity may be used for these variables, and in that way the effects of coupling between shear and longitudinal waves may be introduced.

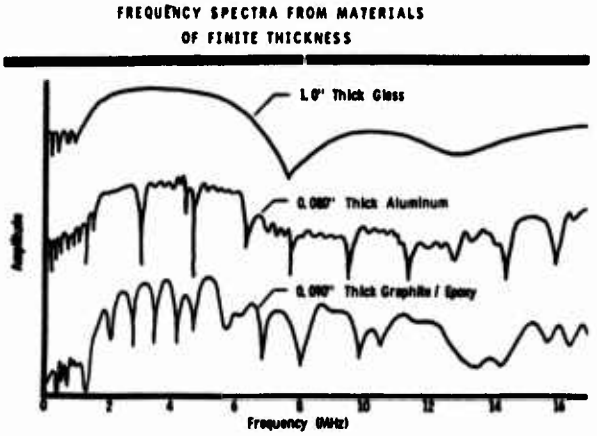

Figure 5. Ultrasonic Frequency Spectra

Figure 6 is a comparison between a frequency spectrum calculated from equation 1 and a measured spectrum. Clearly, all the essential features are predicted. The difference in the peak magnitudes is due to the fact that there was not a perfectly flat frequency envelope in the pulses of ultrasound that were used.

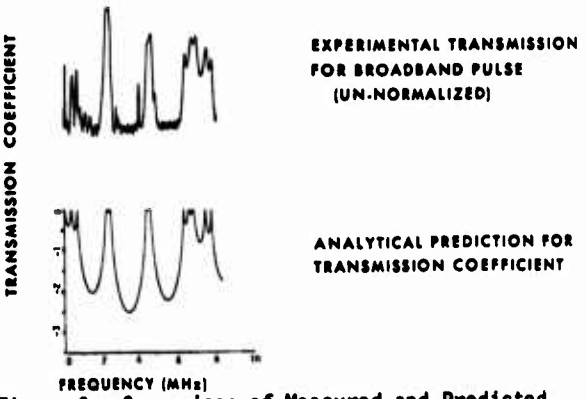

Figure 6. Comparison of Measured and Predicted Frequency Spectra

Figure 7 shows the predicted effect on spectra of adding increasing numbers of layers to a laminate starting with a two-layer laminate and going to a five-layer one. These laminates have very strong reflection coefficients at interfaces thereby emphasizing the effects of the interface.

The closely spaced thickness resonances clustered at low frequencies correspond roughly to thickness resonances for the entire laminate. Between the clusters of thickness resonances are broad minima. These minima deepen rapidly with increasing thickness and in the limit of an infinitely thick laminate, they form bands of frequencies for which traveling waves will not propagate.

The locations of these bands for infinitely thick laminates have been verified independently by utilizing Floquet's theorem which predicts that in such forbidden regions there will be no wave propagation in the infinite laminate limit. An additional prediction is that in the vicinity of these forbidden regions discontinuities in phase velocity occur. In a limit of very weak interface reflections these regions of forbidden transmission get narrow and the whole spectrum merges into the spectrum of a monolithic laminate.

It follows that if, by analogy, with monolithic materials the phase velocities are computed from the positions of thickness resonances, a measure of reflection strength at interfaces can be related to discontinuities in phase velocity.

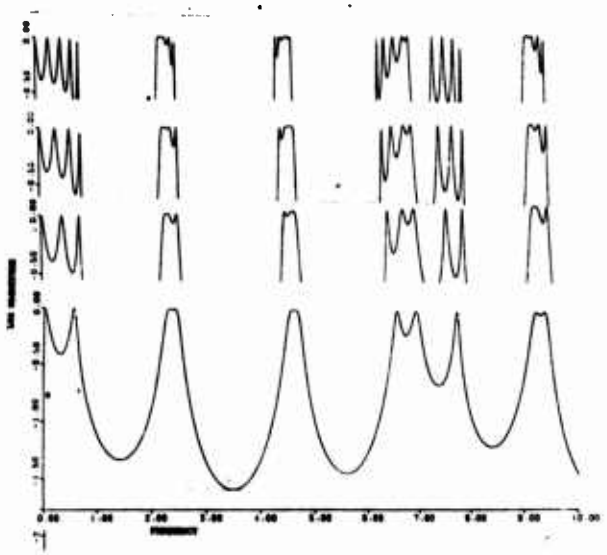

Figure 7. The Effect of Layering on Frequency Spectra

Figure 8 shows dispersion relations obtained from a graphite epoxy laminate having considerable interface porosity, and this material shows considerable variation in velocity of sound and sizeable discontinuities in phase velocity near the predicted forbidden transmission regions.

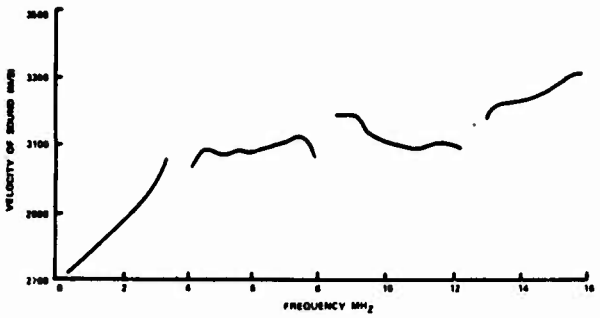

Figure 8. Measured Dispersion Curve for Graphite Epoxy with Porous Interfaces

Figure 9 shows dispersion relations of somewhat higher quality laminates. The T300/5208 material exhibits almost no dispersion below 10 MHz. And all the 0° material, which in theory would be most like monolithic material, shows almost no velocity discontinuity at the predicted forbidden frequency. However, there probably would be a sizeable discontinuity in the group velocity for waves around that frequency.

Dispersion has been observed qualitatively conforming to our model in a number of graphite reinforced resin systems, and variations in this dispersion have been correlated with fatigue, changes in layup, and environmental exposure. The model is less useful for describing materials such as boron/aluminum, since their fiber size gives them a two-dimensional periodic structure which cannot be approximated very accurately by monolithic layers.

Our future work will be directed towards improving quantitative predictions for real laminates, qualitatively and quantitatively correlating dispersion with material degradation and predicting spectra for waves obliquely incident upon laminates. Initial indications are that the oblique incidence results will give much more sensitivity than normal incidence measurements.

The second part of this presentation deals with the work that was done on acoustic emission from boron/aluminum carried out jointly by the University of Delaware and the Naval Air Development Center.

The objective of this research is to characterize acoustic emission signatures from boron/aluminum under various conditions of biaxial loading which might be present in a laminate, in particular, the loading conditions of in-plane shear, fiber tension and transverse tension. The conditions were produced experimentally through the use of off-axis unidirectionaly tensile specimens in which the fibers for different specimens presented different angles to the applied load.

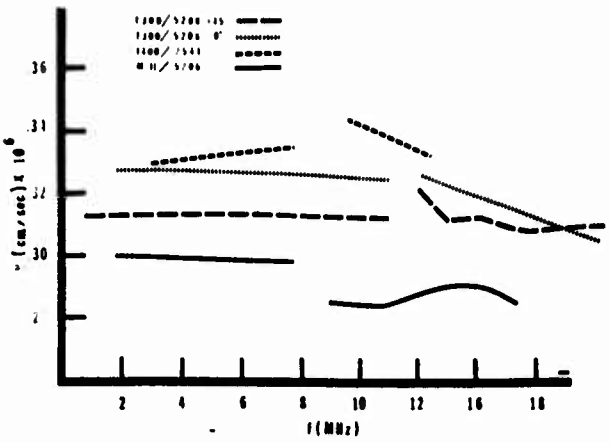

Figure 9. Dispersion Curves for Graphite Epoxy Laminates

Figures 10a and 10b show acoustic emission rate versus strain curves taken for two different frequency regions for a 0° tensile specimen. Figure 10a was taken with peak sensitivity in the frequency region from 0.1 to 0.3 MHz. Figure 10b was taken with maximum sensitivity in the region 0.3 MHz to 1.5 MHz. For the 0° mode of loading the fibers are by far the dominant load bearers and the sample ultimately fails due to fiber breakage.

The rapid peaking of the emission rate at low frequencies (Figure 10a) accompanied by a low emission rate at high frequencies (Figure 10b) is characteristic of this mode of loading.

Preliminary results of spectrum analysis done on tape recordings of these acoustic emissions seem to reveal two kinds of events: a low frequency event at high amplitude and somewhat higher frequency event at a lower amplitude.

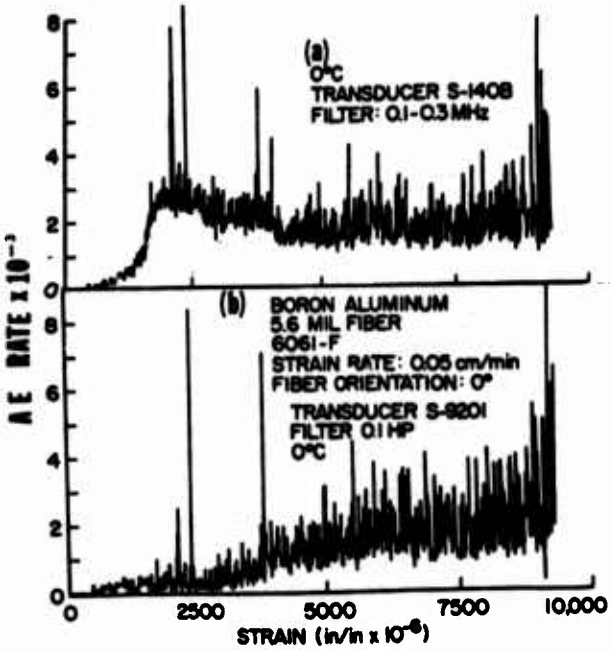

Figure 10. Acoustic Emission from 0° Boron/ Aluminum Tensile Specimen, (a) low frequency, (b) high frequency

For off-axis tensile specimens with fiber to load angles greater than 0° and less than 60°, in-plane shear becomes a dominant load bearing mechanism and the sample fails when its in-plane shear strength is exceeded. However, there still exists a large component of fiber tension for angles up to 45°, and the emissions from this fiber tension loading, dominate those emissions resulting from the much quieter in-plane shear mode (see Figure 11).

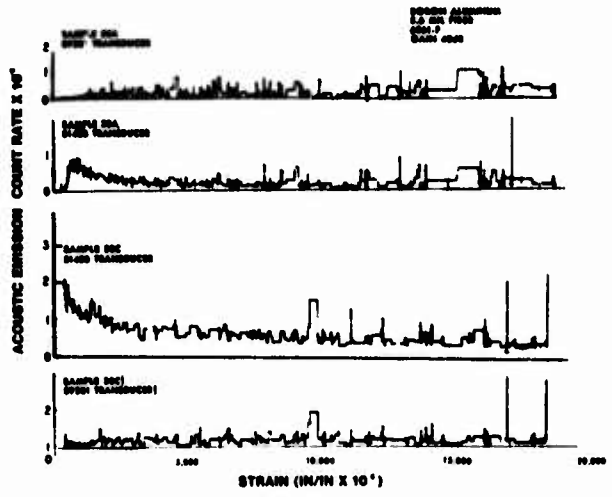

Figure 11. Acoustic Emission from 30° Boron/ Aluminum Tensile Specimens

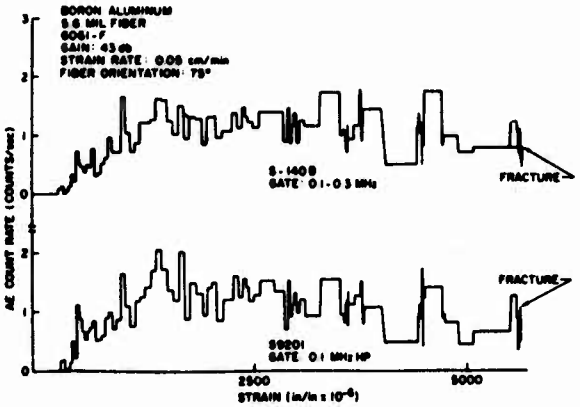

Figure 12. Acoustic Emission Spectra from 75° Boron/Aluminum Tensile Specimen (upper curve-low frequency), (lower curve-high frequency

The 60° specimen (Fig. 13) has a mixed mode of failure (i.e. it is not clear whether we have failure due to transverse tension or in-plane shear) and since the in-plane mode of acoustic emission is very weak, we have the 60° specimen acoustic emissions dominated by the same type of signature seen in transverse tension.

The signature for the in-plane shear mode was measured in separate rail shear tests and was found to be of a low level, peaking only near failure.

For samples with fiber angles greater than 60° the primary load applied is transverse tension, which is also the failure mode of the specimen. And the AE signatures for this mode of loading are essentially identical at high and low frequencies, differentiating them from fiber tension signatures which are different at high and low frequencies (see Fig. 12).

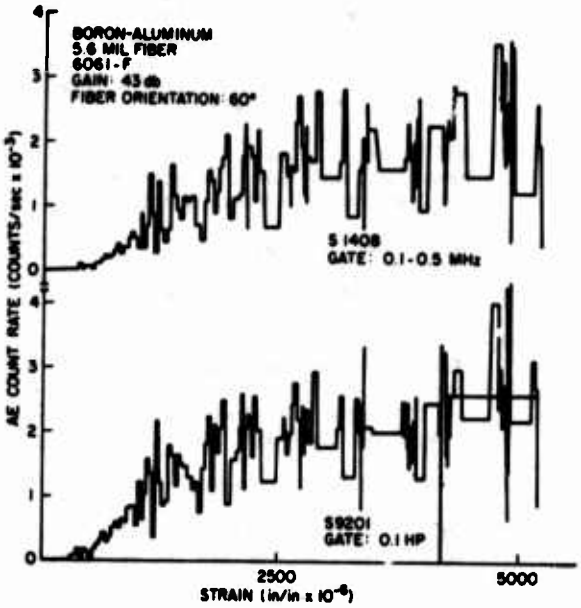

Figure 13. Acoustic Emission from 60° Boron/Aluminum Tensile Specimen

DISCUSSION

PROF. JOHN TIEN (Columbia University): I must have missed the punch line to your first part. Is that a feasible technique for determining defects or not? I mean all the spectrum analysis.

DR. SCOTT: Yes, it definitely is sensitive to defects. Now we are trying to do more than just say something changed; we're trying to find out what changed. As I said, we have empirical measurements of changes in the spectra due to fatigue and environmental exposure of specimens, and also we can to some extent recognize a layup which is very often important because many times after someone makes a layup, he is not sure what he put in it.

DR. JIM DOHERTY (Pratt Whitney Aircraft): On a system like this with the spectrum analysis you showed us, (the scanning system), what kind of scanning rates in the sense of lines per square foot can you use to get reasonably small spatial resolution for these kinds of defects you're looking at?

DR. SCOTT: The work that I've reported here has been done mostly in the laboratory and I haven't tried to push the speed. So I really don't know.

DR. EMMANUEL PAPADAKIS (Ford Motor Company): In the same vein, were the transmission pictures obtained with two transducers or one, or is it just a multiple echo?

DR. SCOTT: Instead of using two transducers I just used a reflector plate, which essentially gives you very much the same sort of thing as transmissions.

MR. DAVE CARVER (Lockheed): In the first section do you do repetitive scans with transducers of different frequencies?

DR. SCOTT: No. I use a transducer that puts out a very narrow pulse and therefore has a broad frequency spectrum, and then I select the frequencies that I want. You can even pick out combinations of frequencies to enhance particular features.

DR. PAUL FLYNN (General Dynamics): You said that the lower frequency resonances correspond to the thickness resonances. Would the higher frequency resonances be due to ply thicknesses or interply adhesive thicknesses, or what?

DR. SCOTT: Well, they really are all thickness resonances. It's just that you get that big discontinuity due to the periodicity of the laminate, and you get so much dispersion at the higher frequencies, and it's really difficult to recognize that what you are seeing are thickness resonances, at least in the example I showed you. However, in something like graphite epoxy, for example, where the interface isn't all that strong, they are really all thickness resonances.

DR. FLYNN: Do both 0° and 45° plies show resonances?

DR. SCOTT: Yes. In that first slide I showed for graphite epoxy, (Fig. 2) some discontinuities were due to the fact that we had two periodicities: one layer to layer and the other from one 0°/45° pair to the next.

MR. B. G. MARTIN (Douglas Aircraft): I understand that in your calculations you took into account attenuation. I was wondering what value you used.

DR. SCOTT: In the particular calculations which I showed, which were just examples of the model, I did not take attenuation into account. If you wanted to take attenuation into account, you would have to measure it.

MR. MARTIN: That was exactly my question. Thank you.

PROF. MAX WILLIAMS (University of Pittsburgh): Let me conclude, then, by one question for clarification. Do I understand that you get very distinct and recognizable signals that permit you to distinguish in-plane shear from direct stress? And that there is no question in your mind about the product mix and the content of the signals for those two loadings; is that correct?

DR. SCOTT: Well, this seems to be the case when we're just using unidirectional material. Now, I don't know what's going to happen when we start getting into laminated material. For example, in the transverse tension mode, there was some localized yielding and when the material is laminated that localized yielding seems to be arrested somewhat: that may change the signature of the material and this is something we are currently trying to determine.

PROF. WILLIAMS: You've recognized that you can distinguish between in-plane shear and direct tension. Can you separate out the energy content, for example, as well?

DR. SCOTT: It may be possible, but I'm not sure. This was our ultimate goal of approaching research in this way, to break the response up into components. We haven't done it yet.

PROF. WILLIAMS: I understand that you must tolerate impatient engineers.

METHODS FOR DETECTING MOISTURE DEGRADATION IN GRAPHITE-EPOXY COMPOSITES

D. H. Kaelble
Science Center, Rockwell International
Thousand Oaks, California 91360

This presentation reports on the second year of our participation in this NDE program (Ref. 1). The purpose of this work is two-fold and this talk divides itself naturally into two segments which relate to the following objectives:

1) To determine the effects of moisture degradation on the mechanical properties of a graphite-epoxy composite under study for use on B-1.

2) To apply promising techniques found in last year's program to detect moisture degradation nondestructively.

The uniaxial reinforced composite chosen for study is described by constituents, lay up, and cure cycle in Table 1 and represents a standard 350°F (177°C) service ceiling composite. Following cure and post cure as described in Table I, this composite was maintained in a dry state by storage over anhydrous K_2SO_4 until initiation of moisture degradation studies.

TABLE I. Fabrication and Curing Cycles for Hercules 3501/AS-5 Epoxy Matrix/Uniaxial Graphite Fiber Reinforced Composite SC4 (Volume fraction fiber V_f=0.60, Void Volume fraction < 0.01)

A. Layup Procedure

Ply Number	Tape Width (cm)
1	30.5 + 15.3
2	15.3 + 30.5
3	7.6 + 30.5 + 7.6
4	22.9 + 22.9
5-48	repeat patterns for 1-4

B. Cure Cycle

Step No.	Procedure
1	Bleeder cloth in 3 plies 120 GL plus 14 plies 181 GL and vacuum bag.
2	Vacuum on part plus 5.98 Kg/cm^2 external pressure to bag during heat up from 23°C to 177° (heating rate 1.1 to 1.7°C/min with 15 min. dwell at 121°C).
3	Dwell at 177 ± 5°C for 1 hour then lower temperature to 23°C
4	Cool down under pressure and vacuum to below 65°C before removing pad.
5	Debag and oven post cure for 3 hours at 188°C.

The experiments used for study of moisture degradation (Part 1) and nondestructive detection (Part 2) are summarized in Table II. In Part 1, the study of moisture degradation interposed measurements of the kinetics of water up-take, interlaminar shear strength, and failure surface analysis. This study was somewhat simplified from last year, based upon a more complete knowledge of the potential degradation mechanisms.

TABLE II. Experimental Methods for Study of Moisture Effects

Part 1: Moisture Degradation

- Moisture take up
- Interlaminar shear strength
- SEM failure surface

Part 2: Nondestructive Detection

- Infrared spectroscopy
- Dynamic mechanical spectroscopy (3.5-110 Hz)
- Specific heat
- Ultrasonics (2.25 MHz)
- NMR pulse relaxation spectroscopy
- Microwave spectroscopy
- Micro Hardness

The curves of Fig. 1 show that simple Fickian diffusion kinetics operates. The fraction of maximum moisture, ϕ (H_2O), is proportional to the square root of exposure time $t^{1/2}$ at both 23° and 100° C under water immersion. Independent study of the pure matrix showed similar Fickian controlled diffusion mechanisms as shown in Fig. 1 for the composite.

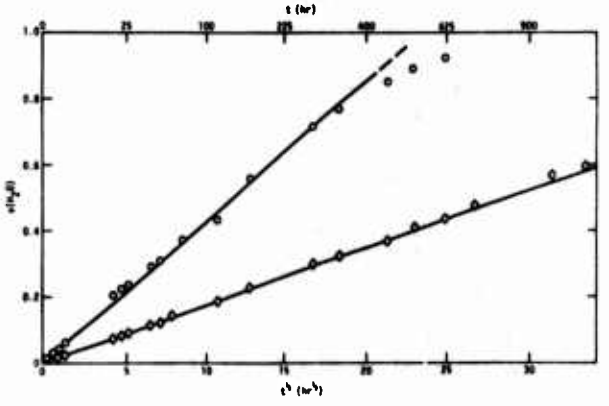

Figure 1. Fractional amount ϕ of water uptake versus exposure time t for composite SC4 (O=100° C, ◇ = 23° C).

The numeric analysis of water up-take studies in both composite and pure epoxy matrix are summarized in Table III. Inspection of Table III shows the equilibrium moisture uptake $f_\infty(H_2O)$ is constant for 23°C and 100°C. Table III shows that the moisture uptake in the pure matrix and the matrix phase of the composite agree within 10%. The data of Table III also indicate substantial equivalence for diffusion coefficients D and activation energies of diffusion E_0 for composite and pure matrix. These results show that the bulk diffusion through the matrix is the rate limiting step and that the moisture resides in the matrix phase of the graphite-epoxy composite of this study. The fact that the matrix phase of the composite will absorb up to 6.7 wt. % of water at 23°C when the composite weight increase is 2.3% suggests substantial changes in internal stresses and mechanical responses.

TABLE III. Water diffusion kinetics for composite SR4 and cured epoxy 3501 matrix

Parameter	SC4 composite (V_f = 0.60 unitape)		Pure Matrix	
$L_1 \times L_2 \times L_3$ (cm)	0.50 × 1.50 × 1.50	0.50 × 1.50 × 1.50	0.22 × 1.50 × 1.50	0.22 × 1.62 × 1.52
m_0 (gm)	1.77643	1.76205	0.65767	0.68931
T(°C)	23	100	23	100
$f_\infty(H_2O)$ wt%	2.30	2.30	6.70	6.70
D(cm²/sec.)	$7.67 \cdot 10^{-10}$	$2.58 \cdot 10^{-8}$	$8.65 \cdot 10^{-10}$	$6.42 \cdot 10^{-8}$
E_0(kcal/mol)	10.0		12.2	

Interesting additional information was generated by SEM studies of sectioned composites and of the failure surfaces from interlaminar shear testing. Two notable types of manufacturing defects, as shown in Fig. 2, were found in sectioned composite. The long needle-like defect in the left view of Fig. 2 appears related to fiber misalignment in the prepreg tape. The elliptically shaped cavity shown in the right view of Fig. 2 appears related to deficiencies in interply bonding. Both types of defects, as indicated by the 10 μm bench marks, are of large dimensions relative to the fiber diameter. Further studies showed that these large defects were sparsely distributed in the composite and the overall void content is less than 1% by volume.

The combined effects of matrix controlled diffusion kinetics and the noted distribution of large defects and cavities is displayed in the interlaminar shear strength data shown in Fig. 3. The degradation in average shear strength λ_b appears to decrease linearly with increased moisture content at both 23° C and 100°C aging conditions. The effect of 100°C aging is to accelerate the rate of moisture uptake by a factor of 23.

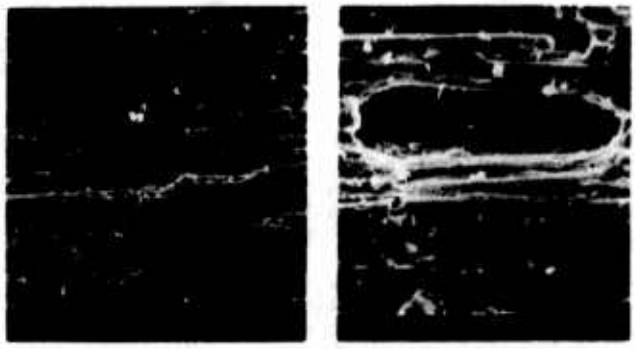

Figure 2. SEM view of external cut surface of shear test specimen (λ_b = 920 Kg/cm²) for dry unaged SC4 composite showing two types of macroscopic defects (size larger than 10 μm).

The large scatter of interlaminar shear data in Fig. 3 are indicated by the vertical bars which enclose the extreme high and low values of λ_b based on five or more tests at each test condition. This large data scatter is a striking feature of the composite response which appears related to the manufacturing defects shown by SEM studies. The dry unaged composite has a mean shear strength λ_b = 779 kg/cm² (= 11000 psi) with extreme high and low values of 1000 kg/cm² (14000 psi) and 528 kg/cm² (7500 psi) in a group of 20 test specimens. The mean strength degradation of 22% in λ_b shown by the linear least square fit curve of Fig. 3 is clearly overshadowed by the data scatter.

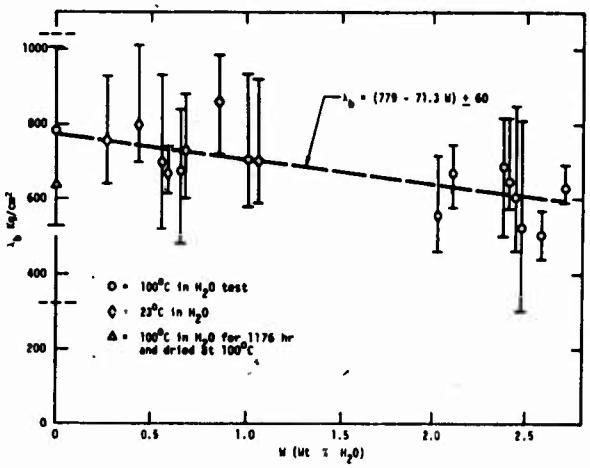

Figure 3. Variation in interlaminar shear strength λ_b with moisture content (Wt % H_2O) in composite SC4. Bars on data points indicate extreme λ_b values for test group.

The results of analysis of three test conditions using the Weibull (or extreme value method is shown in the curves of Fig. 4. The ordinate of Fig. 4 is a linear scale of survival probability

(Ref. 2):

$$S = 1 - \frac{j-0.50}{N}$$

where the test results are arranged serially j = 1, 2, 3, ...N in increasing order of λ_b and N is the number of test specimens. The solid curves in Fig. 4 are fit to the experimental data by use of the relation (Ref. 2):

$$S = \exp\ (-\lambda/\lambda_o)^m$$

where λ_o is the mode of the distribution, and m defines the breadth of the distribution. The right curve of Fig. 4 for unaged composite displays λ_o=837 kg/cm^2 and m = 7.6. .Both the aged - wet and aged-dried data fall on a second curve with λ_o = 636 kg/cm^2 and m = 3.9. These results indicate that the effects of moisture aging are not reversed by subsequent removal of water for this composite. Secondly, the significant lowering of the Weibull shape factor m due to moisture aging shows an appreciable strength degradation of 50% at high survival probability of S = 0.95.

A simple physical interpretation of the data of Fig. 4 suggests that samples with larger internal defects and therefore lower intrinsic strength are more severly damaged by hydrothermal aging than samples of higher intrinsic strength. For the aged and dried material, only a few data points representing samples with small defects indicate the possibility of strength recovery after aging. These latter samples appear to suggest that a composite intrinsically free of large defects should show a larger degree of reversibility in moisture damage effects. These are early results; further study of these interesting results are required.

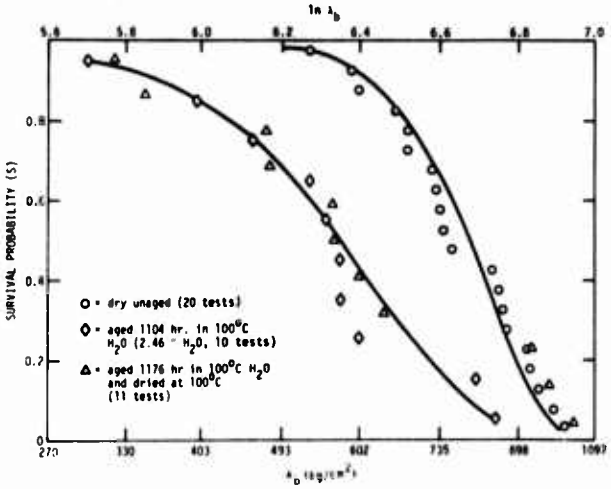

Figure 4. Probability of survival (S) versus interlaminar shear strength λ_b measured at 23°C.

The nondestructive characterization which constitutes part II of this study utilized infrared spectroscopy, NMR, and other techniques that are very familiar to the analytical chemist. From this characterization, one obtains the chemical composition of the uncured material and chemical structure of the cross-linked epoxy matrix. The results of this study, shown in Table IV, show that the tetrafunctional epoxy is cured by diaminodiphenyl sulfone (DDS) to produce the cross-link network shown in the chemical structure in the lower portion of Table IV. This chemical structure is indicative of a higher glass temperature T_g and more brittle epoxy than the epoxy matrix studied in the previous year. In particular, this resin system does not contain the flexible glycidyl ether segment which characterized the 250°F (122°C) service ceiling epoxy matrix of last year.

These differences in chemical structure between the two resin systems studied last year and this year appear very clearly in the mechanical spectroscopy response, using thermal scans of dynamic mechanical damping at fixed frequency of 110 Hz on the Rheovibron instrument. The test specimen is a thin axially reinforced cylinder of composite subject to cyclic flexure deformation.

TABLE IV. Suggested Curing Mechanism for Epoxy 3501 Resin

Epoxy (E): tetraglycidyl 4,4' diaminodiphenyl methane: M.W. = 422 gm/mole

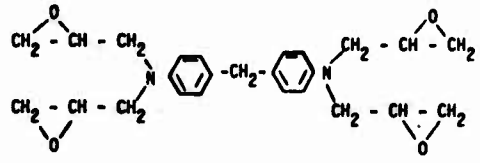

Curative (C) : diaminodiphenylsulfone; M.W. = 251.5 gm/mole

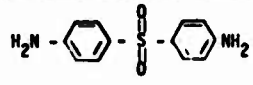

Crosslink Reaction (62.7% by weight E + 37.3% by weight C)

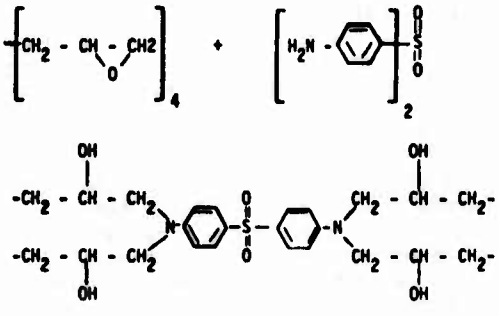

As shown in Fig. 5, the curve of loss tangent (tan δ) versus temperature for the unaged composite shows no detectable damping maximum below 200°C indicative of the lack of segment motion as revealed by chemical analysis. Above 200°C the rise in tan δ to a maximum at 260°C is characteristic of the glass transition Tg and onset of rubbery response of the epoxy matrix.

Testing this same material aged and wet is shown as a second curve in Fig. 5 where tan δ values begin to increase at T = 130°C. Water is lost as heating progresses so that this second curve represents a wet sample at low temperature T < 100°C and dried during measurement at T ≥250°C. A third thermal scan shows that the tan δ curve for aged and dried composite generally resembles the unaged material. These data show the water reversibly plasticizes high temperature molecular motions above 130°C but has little effect upon 23°C rheological properties.

The expectation from chemical analysis and mechanical spectroscopy was that ultrasonic properties such as sound velocity and matrix attenuation in the composite of this year's should be only slightly affected by moisture. In contrast the 250°F composite of last year's study showed substantial changes in ultrasonic response with moisture uptake at ambient 23°C test temperatures.

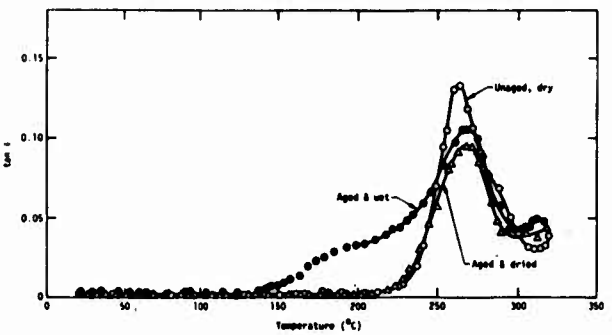

Figure 5. Flexural damping tan σ properties of composite SC4 measured by increasing temperature scans at f = 110 Hz

Based upon this knowledge we designed a hybrid experiment. We machined a bar of composite of shape L x W x T = 30 x 2.5 x 0.5 cm dimensions with fibers parallel to the length. This bar looks like a ruler which is very black and very opaque. The moisture aging produced four zones of hydrothermal exposure which are boiling water, water vapor at 100°C, seal area, ambient 23°C, and 50% RH exposure along the length of the bar. This aging was carried on for 1128 hr. to fully hydrate the 6.3 cm (2.5 in) length immersed in boiling water.

This sample was then removed and ultrasonically scanned along its length using 2.25 MHz and 23°C as test conditions and C-scan through the sample thickness. Details of the method follow methods discussed in the first year effort. This procedure profiles in one dimension the influence of variable hydrothermal aging on ultrasonic response.

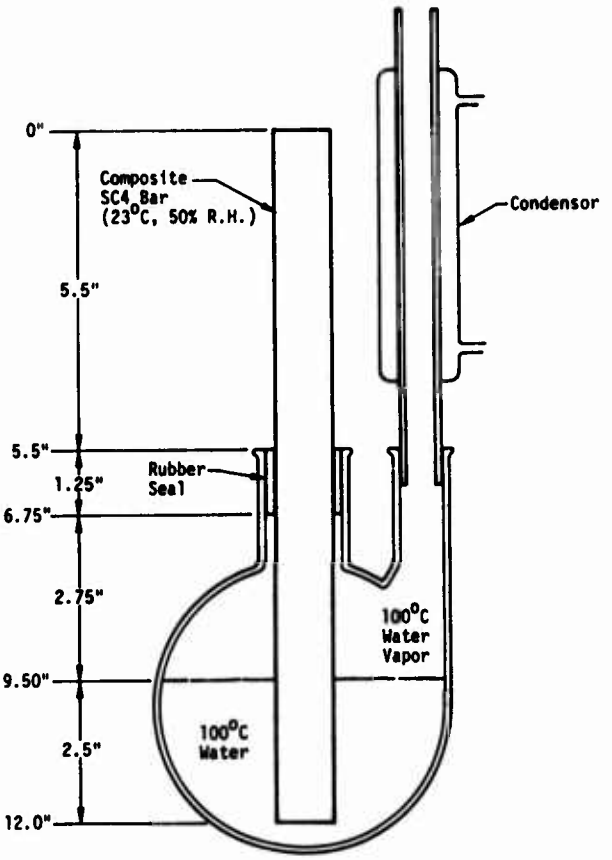

Figure 6. Schematic of variable moisture exposure of composite SR4 aged for 1128 hours.

The lower curves of Fig. 7 show that spatial attenuation α_L does not vary with moisture aging or moisture content along the bar length. The lower curve of Fig. 8 shows that sound velocity C_L is dependent upon prior moisture aging and moisture content along the bar length.

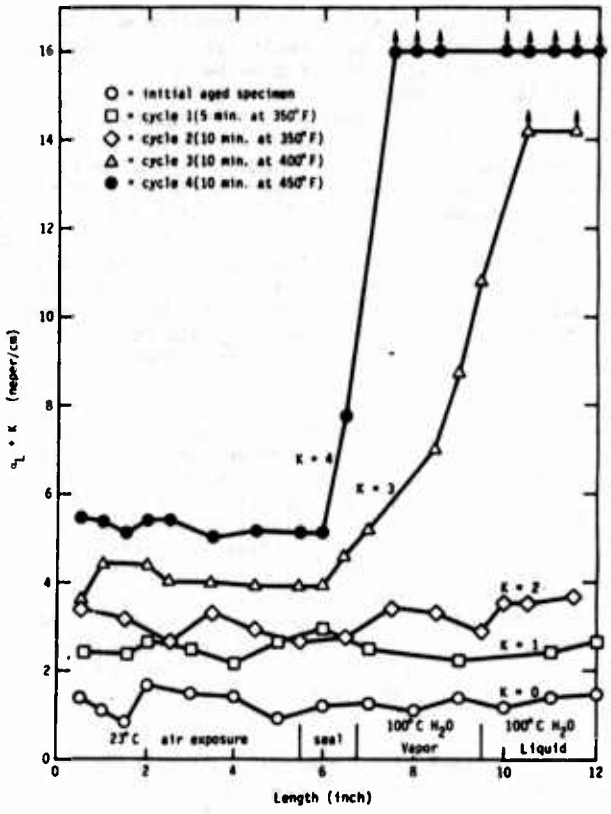

Figure 7. Effects of varied moisture exposure and subsequent thermal cycles on the acoustic attenuation α_L of composite SC4.

Having established the base line shown by the lowest curves of Figs. 7 and 8 the bar was then subjected to a series of thermal shock cycles between 23°C and the ceiling temperature shown in upper Fig. 7. Cycle 1 and Cyle 2(to the 350°F service ceiling recommended for this composite) show only minor effects on either α_L or C_L. These curves are vertically shifted by the indicated factors K along the ordinate to provide separation of the curves. A subsequent thermal shock cycle to 400°F produces a large increase in α_L in the length exposed to high moisture and unchanged α_L in the ambient aged low moisture section. A final cycle to 450°F effectively raises α_L out of the region of available measurement in the high moisture exposed region and shows α_L unchanged for the ambient aged section.

Inspection of Fig. 8 shows that the sound velocity change along the bar length decreases slightly with thermal shock cycling due to thermal cycling. Thermal cycles 3 and 4 which produce the high attenuation lead to signal loss and prevent velocity measurements on the hydrated end of the bar.

In the above measurement it appears that velocity profiles as shown in Fig. 8 correlate with moisture content. Sound velocity transverse to the fibers is matrix dominated. With increasing moisture content the lower sound velocity of water C_L = 1.49 km/s operates through the rule of mixtures to lower the average sound velocity from C_L = 3.6 km/s for the dry composite.

In addition to the above acoustic measurements, accurate measures of thickness confirm the opening of microcracks in the high moisture length by a relative thickening or dilation of this damaged section.

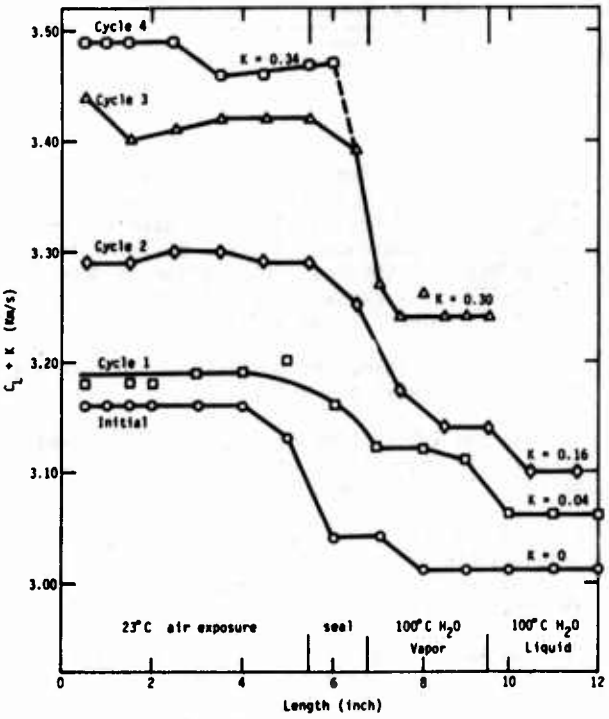

Figure 8. Effects of varied moisture exposure and subsequent thermal cycles on the ultrasonic velocity C_L of composite SC4.

As a result of both the work reported for this year and the previously reported study of last year, we have developed a systematic outline for composite durability and NDE anlaysis as detailed in Table V. This outline calls for first analyzing the composite in terms of its separated components. This physiochemical study of the fiber and matrix constituents isolates their discrete interactions to moisture and temperature.

In this outline of study the fiber-matrix interface stands out as an independent subject of study in terms of surface energetics.

The composite is evaluated in terms of system response with a large variety of relevant measuring tools and interacting information.

Finally, in Part 3 of Table 5 is outlined a data analysis task to correlate constituents,

TABLE V. Outline for Composite Durability Characterization

Part 1:	Analysis of Separated Fiber and Matrix
	1a. Obtain and separate uncured prepreg components,
	1b. Analyze fiber and matrix surface energies,
	1c. Analyze resin chemistry and curing mechanism,
	1d. Define curing kinetics and network structure,
	1e. Analyze hydrothermal aging effects on network structure.
Part 2:	Analysis of Composite Laminate Aging
	2a. Obtain composite laminates for aging studies,
	2b. Measure kinetics of water diffusion into composite,
	2c. Determine interlaminar shear strength versus moisture content,
	2d. Determine fracture energy versus moisture content,
	2e. Measure dynamic mechanical (NDT) response versus moisture content.
Part 3:	Data Analysis and NDT Methodology
	3a. Determine relation between strength degradation mechanisms and NDT methodology,
	3b. Design NDT experiments and statistical analysis for tracking strength degradation,
	3c. Define improved matrix and interface chemistries.

interface, and system responses in terms of analytic models. Quantitative NDE tracking methodology and statistical analysis of data are resultant from this approach. A final dividend is that enough detailed chemical information is developed to intelligently pursue material substitutions or changes in interfaces by surface treatments.

In brief, then, the conclusions that come from this phase of work are as follows for Part I.

1. In the 3501-5/type AS composite the kinetics of moisture degradation are controlled by the matrix bulk properties.

2. The interlaminar shear strength degradation is irreversible and the Weibull analysis shows that degradation is greatest in samples with larger intrinsic flaws.

In Part II for NDE response the following conclusions appear justified.

1. In the 3501-5/type AS composite ultrasonic sound velocity at 23°C varies with moisture content but not with strength.

2. Alternatively, attenuation transverse to the fiber axis is principally sensitive to internal defects and microcracks which influence matrix and interface dominated measures of strength.

These results differ from the composite system studied last year where both sound velocity and attenuation changed complimentary with strength and were related by chemical changes in matrix rheology and molecular motion.

This year's study in conjunction with last year's shows that each resin type can be expected to display a singular physio-chemical response to moisture and require a specific NDE tracking methodology. Consistent with this result for the B-1 composite we can now undertake NDE black box development for moisture degradation effects. Two parallel developments appear warranted. We have used a number of NDE tools including NMR and microwave dielectric spectroscopy this year in addition to the ordinary measurements but we find that, for field surveillance, precision ultrasonics stand out as a well verified technique. Using ultrasonics to assess changes in physical state response as well as physical flaws is the present extension of this methodology.

The second measurement to be recommended is a direct reading moisture content meter for composites. It appears quite necessary to know the current moisture state of the composite, and if the moisture content can be spatially resolved by mapping all the better. We have plans and activity in progress on this latter subject in which moisture effusion measurements are utilized. By placing a surface cell on the composite and lowering the relative humidity to zero one can accomplish a kinetic analysis of moisture effusion which is the reverse of the moisture uptake analysis discussed earlier in this presentation.

In conclusion, precision ultrasonics combined with direct moisture content analyses appear applicable to field surveillance of B-1 composites studied in this program.

References

1. D. H. Kaelble, in Proceedings of the ARPA/AFML Review of Quantitative NDE, AFML TR-75-212, pp 549-562.

2. E. Y. Robinson, in Proc. of Colloquium on Structural Reliability (Editors: J. L. Swedlow, T. A. Cruse, and J. C. Halpin), Carnegie-Mellon University, Pittsburgh (1972), pp 463-526.

DISCUSSION

PROF. MAX WILLIAMS (University of Pittsburgh): I can't believe that you have beat the bell. Just, perhaps one question to start our discussion, Dave, to make sure I understand, the wave velocity through the specimens decreased with increased moisture. Do you have a qualitative feeling that that change with moisture is a density effect or a chemical structure effect like backbone binding energy?

DR. KAELBLE: First of all, the wave velocity in the dry composite is definitely assignable to the matrix. It looks like the matrix is interacting with fibers in a series fashion. The dry matrix sound velocity is C_L = 2.92 km/cm and water is C_L = 1.49 km/s at 23°C and 2.25 MHz. In a rule of mixtures a 7% water uptake would reduce the sound velocity by about 3% as is shown in Figure 6B.

PROF. WILLIAMS: You know, a simple engineering approach would be that if the wave velocity is proportional to the square root of modulus over the density and if you're adding water, that would increase the density in the denominator which would drop the wave velocity which is consistent with your observation. My question is whether that is entirely too simplified an approach or whether it is actually tied up in the binding energy dropping along the backbone chain.

DR. KAELBLE: Yes, if water is entering only void and pores, its density would act as you suggest. This effect is taken into account because we do a precise thickness measurement so the water that goes in, actually its volume effect, is taken up in the path length measurement. You see, we do a time delay measurement. Calculations show that density changes accounts for about 20 percent of the velocity change.

DR. WILLIAMS: Any other questions? Dave, would you call your own questions, please.

DR. KAELBLE: Bill?

DR. BILL BASCOM (Naval Research Laboratory): In your damping curve for your NARMCO 5208--were you using the Narco or some other resin?

DR. KAELBLE: Hercules 3501-5 was the resin used in this study.

DR. BASCOM: They're essentially the same. You did not get a peak until you got to the glass transition phase for the dry material; is that correct?

DR. KAELBLE: That s true.

DR. BASCOM: We see one at about 75°centigrade on supposedly dry material.

DR. KAELBLE: That's right.

DR. BASCOM: Is this saying that the specimens are taking up water, or are yours intentionally dry?

DR. KAELBLE: Yes, ours are dry. They're dry from the point of manufacture. They're held dessicated. We have gotten a lot more careful about that since we came across the fact that the effects, damage effects, are irreversible and if you let these materials sit at room temperature you can have an unknown history of change from point of manufacture. So, we hold these dessicated up until either the time of controlled exposure or time of test. I have seen that transition, and actually, on another scale of sensitivity, even on these curves, it might show up. But I might mention these measurements are made on the composite by transverse bending of longitudinal reinforced.

DR. JOSEPH HEYMAN (NASA, Langley): Is the temperature dependence of the velocity of sound in the epoxy sufficiently well known so that you could monitor the water content by looking at the temperature dependent change in velocity of water?

DR. KAELBLE: Yes. We haven't done that. I presume that would be a useful extension on the reported velocity measurements.

PROF. WILLIAMS: One more question, please.

DR. PAUL FLYNN (General Dynamics): Did you see any mechanical properties and other possible changes other than strength that were relatable to the velocity of sound? Did you do modulus effect on the property?

DR. KAELBLE: In this program we limited our measurements to interlaminar shear strength. This built up enough data base to say something significant about a matrix or interface controlled system response property. This same material is being looked at concurrently in an IR&D program where much more extensive results will be reported separately.

PROF. WILLIAMS: Thank you very much, Dr. Kaelble.

CHARACTERIZATION OF ACOUSTIC EMISSION SIGNALS AND APPLICATION TO COMPOSITE STRUCTURES MONITORING

L. J. Graham
Science Center, Rockwell International
Thousand Oaks, California 91360

The objectives of this study were first, to identify characteristics of the acoustic emission signals from graphite-epoxy composites which could be related to the various fracture mechanisms, and second, to determine how these are related to the history of the flaw growth and to the degree of degradation of the strength of the composites due to moisture.

The fracture behavior of the composite specimens was very erratic as was the acoustic emission behavior. There were a great number of emissions covering a very wide range of amplitudes, estimated from the shape factors to vary by 14 orders of magnitude. As a result, it was very difficult to perform a systematic study to relate acoustic emission characteristics with any specific fracture mechanism such as fiber fracture, matrix fracture, or fiber pullout.

Another difficulty was that there were only very subtle differences in the acoustic emission characteristics between the unaged material and the fully aged or moisture degraded material, although there were big differences in the mechanical properties of the composites due to aging.

We have made some progress, however, and I would like to present some of the results now in the context of how they might apply to monitoring a structure in a proof loading situation.

We looked at three materials. These are the same materials that Dave Kaelble and Paul Dynes looked at during last year's and this year's program. They were all unidirectional graphite-epoxy fiber composites made into laminate sheets about a quarter of an inch thick, and were chosen to have different degrees of moisture susceptibility.

We tried quite a few different specimen geometries; however, most of the work was done with three-point bend specimens. These bend specimens were two and a half inch long bars having about a quarter inch square cross section. Side grooves were cut into each side of the bar at the mid-length, leaving about a 90 mil wide web down which the crack propagated.

With this geometrical orientation in mind, the left-hand picture of Fig. 1 shows the fracture surface of one of these bend specimens. Cracks started at the top at the maximum tensile stress position on the specimen and proceeded down through the 90 mil wide web.

On the right of Fig. 1 is an artist's drawing of that fracture surface. The main features are that there are very smooth regions and very rough regions of fracture. Through the load diagrams we have established that fast fracture produces a smooth surface and very slow, semi-stable crack growth produces a very rough surface.

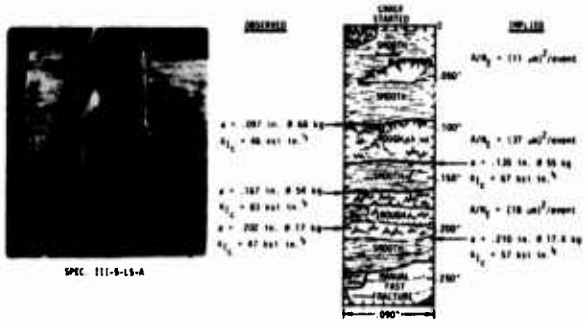

Figure 1. Combination of observed load and acoustic emission data with implications of the appearance of the fracture surface to arrive at crack growth parameters.

From this observation, we can make correlations with the acoustic emission data and can calculate certain parameters. For example, after abrupt load drops or certain other key features on the loading curve, and knowing what the crack length is at that time, we can calculate the approximate stress intensity factor. Some of these values are indicated on Fig. 1 where you can see a range of values at different times in the load history. I must emphasize that these are only approximate because of the complex geometry of the specimen, but are sufficient for the purpose of comparison between specimens of identical geometry at various times in the specimen loading history.

At the left of the drawing in Fig. 1, we show the optical observations of the crack front at certain load levels during the loading. On the right, we have implied the values of the load at certain crack front positions by correlating the appearance of the fracture surface with the loading history. The values of K_{1c} calculated from these observed and implied data fall within the same range. The spread in these values could well represent the inhomogeneity in the strength of this material.

A second parameter that we can get out of these observations is a measure of the average fracture surface area per detectable acoustic emission event. Some of these numbers are shown in Fig. 1 for different regions during the slow fracture. We determined the area of a slow fracture region which was formed between two well-defined points in the loading history and divided it by the number of events which occurred during that time. This ratio is a measure of the average fracture surface area per event which for this specimen was an area of 11-37 microns squared. Comparing this to the fiber diameters of about 8 microns, you can see that these areas for the individual fracture units are small, of the order of a few fiber diameters on the average. But then again, because of the wide range in the amplitudes of the emissions that we see, we get some feeling for the wide range in the fracture surface areas, too.

We looked at various orientations of the specimens. This happens to be an LS specimen, that is, the maximum stress axis was along the fiber direction and the crack propagation direction was in the S orientation or through the thickness of the plate normal to the plies. Other orientations were the LT, TS and TL. We used these different orientations to change the dominant fracture modes in order to identify the characteristics of the acoustic emission signals generated by the various modes. Although different types of emission signals were seen, we were not able to correlate them with specific fracture processes, because the individual variations between supposedly identical specimens overshadowed any of the changes that we were able to produce.

Loading was done on an Instron machine using a constant crosshead speed, and loading was carried to failure in most instances. In Fig. 2 are shown some examples of the loading history. The solid line in each figure is the load-time curve. In the top two figures, the dotted curve is the cumulative acoustic emission event count and the dashed curve is the cumulative acoustic emission count. The difference here is that the event curve is obtained by taking each of the acoustic emission bursts and counting it as one event. The count curve is obtained by counting each cycle in the oscillatory bursts and accumulating that number. Larger amplitude events will give more counts per burst. The ratio of the slopes of these two curves, the number of counts to the number of events during a given time interval, is plotted in the bottom figures. This gives a measure of the average amplitude of the emissions at any time during the test. Also, at the bottom is plotted the event rate. You can see that this is a widely fluctuating quantity and was found to be widely erratic between identical specimens, presumably very dependent upon the exact nature of the pre-existing flaws and the exact nature of the fracture process.

The curves shown in Fig. 2 are only examples for the unaged and the aged materials. There was no typical curve for the two conditions. Sometimes the unaged material would load up and fracture all the way through, and in this example, the biggest crack step was in the aged material, but that wasn't necessarily typical.

At the normal 60 dB gain settings of the detection amplifiers, a great many of the emission bursts would saturate the amplifiers. At various times in the loading history, for example, where the crack was growing stably, we reduced the gain to increase the dynamic range of the amplitude measurements. This is indicated by the 60 dB and 40 dB notations during some time periods in Fig. 2. During tests on other specimens, 20 dB gain was sometimes also used.

So, that's kind of an overview of what is shown in Fig. 2. It shows the erratic nature of the fracture and some of the types of data that we can get from these tests.

Now, looking at this in a little more detail, we performed some tests by loading and unloading in the elastic region. Early in the loading history, we get a few events on loading, none on unloading. Loading it back up again, no emission events occurred until the previous high load had been reached and exceeded, then more emission events would start coming out. This would continue until the specimen was loaded up to a point such as indicated by a small inflection or load drop on the loading curve. Upon unloading from that point, emission events occurred during the unloading part of the cycle. I interpret that as being interference of the fibers coming back together in the fracture region. If the load is cycled to that load level two or three times, all the emission activity goes away. The point of all this is that any characterization of the fracture behavior or the state of the specimen, based upon just the number of emission events alone, is going to be very dependent upon past loading history, and it will be very hard to interpret.

Another effect is seen on the bottom curves of Fig. 2. The average amplitude of the emission events with time during the loading history, as measured by the ratio N/N_E, goes through a maximum and then levels off at some lower value. This was typical of all specimens. We interpret the maximum as being due to the growth and stabilization of the pre-existing flaws, growing out from localized weaker regions into the stronger matrix. The constant amplitude region is then the growth from that point on, through the presumably stronger composite material. A second point is that the average value for the unaged specimens was always greater than the average value for the aged specimens.

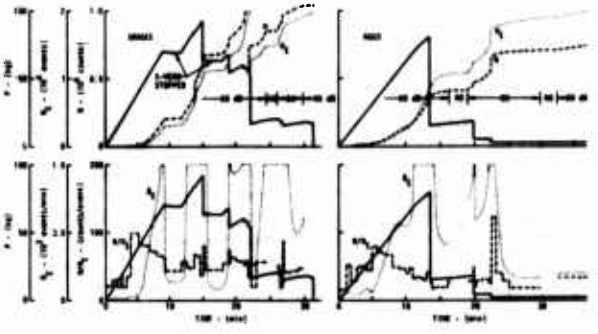

Figure 2. Typical load and acoustic emission vs. time histories for SC-2-3 three-point bend specimen in the LS-orientation illustrating erratic behavior of crack propagation.

We have now discussed two rough measures of the amplitudes of the emissions and the amplitudes of the fracture steps, first in the average fracture surface area per emission and then in the measure

of the average amplitudes of the emissions at various times during the history. In Table I, these data are summarized along with the strength data for the three classes of materials tested, shown in order of increasing moisture resistance from left to right. The least resistant material, designated SC-2-2, had the graphite fibers treated during manufacture of the composite to substantially reduce the strength between the fibers and the epoxy matrix. One result of this was that all of the bend specimens failed in compression on the bottom side of the specimen, so we can't really compare that material to the results of the others. You can see there's a big difference in the strength of that material between the unaged and the aged condition, but no consistent difference in the average amplitude of the emissions. In the other two materials, there was consistent difference in the strength properties and in the acoustic emission amplitudes, between the unaged and the aged materials.

Table I.
Summary of Comparative Strength and Average Crack Step Size for the Various Test Conditions

Figure 3 shows a more quantitative description of the amplitudes of the acoustic emissions. This is a conventional cumulative amplitude distribution, plotted on logarithmic scales, showing the number of emission events which were greater in peak amplitude than a certain value on the abscissa. Normally, this type of data is interpreted in terms of a power law, a theoretical relation borrowed from seismology which is represented by a straight line on this type of plot. The slope of the curve gives the exponent of the power law relation and physically represents the spread of the distribution in amplitude of the emission events.

Tony Evans of our laboratory was first to point out that the power law relation does not really describe the real world very well and suggested, perhaps, that a statistical extreme value distribution function represents a better model of acoustic emission generation, particularly in the low amplitude region. The extreme value function also agrees better with some previous experimental data, and in this case, where the power law obviously doesn't apply, we have tried to fit three of these extreme value distributions, just as an exercise, to one of the experimental curves. The three dashed lines are these theoretical extreme value distributions. The sum of the three are shown as the open circles superimposed upon the experimental data which is the solid curve. So, it can be done. In this case, it's only an exercise because I'm not all that confident of the accuracy of these data, for one thing, because of the method we had to use to obtain it, and also because we would like to see a wider dynamic range in the amplitudes in order to provide a less ambiguous fit with the theory. The fit is good enough to at least suggest that there are three different fracture mechanisms going on with their own amplitude distributions, and that these change, particularly down in the low amplitude end, between the aged material and the unaged material with confirmation. This might be used as a tool in determining the degree of environmental degradation in a proof test of a structure.

Considerable effort went into identifying the different fracture mechanisms by frequency spectral analysis of the acoustic emissions. I don't want to spend any time describing the methods used today, since we have reported them to you before and they are well documented in the literature. We did identify several distinct spectral types. Again, correlation with particular fracture mechanisms was not possible. Also, one other observation was that the variability between the frequency spectrum of individual acoustic emission events within a given spectral type was much greater in this material than in any previous material that we have studied. That could possibly be due to the greater variation in the geometries of the emission sites in this very complex composite material, or it could be due to the dispersion in the acoustic path between the source and the detection transducer.

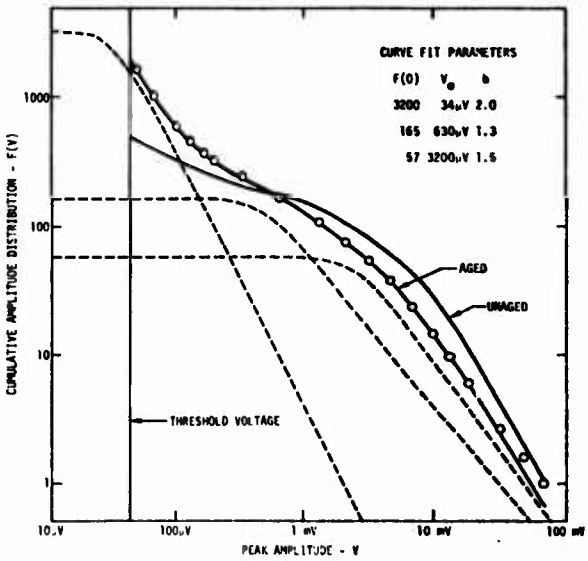

Figure 3. Cumulative amplitude distribution - F(V)

Frequency spectral data for one specimen is shown in Fig. 4. Again, the load-time curve showing the acoustic emission record is shown. Above it, different frequency spectral types and when they were observed to occur during the loading are indic ..ed for several time periods during the test for which the recorded signals were analyzed. Most of the acoustic emissions were white noise (WN), i.e., having a very broad frequency content, but tending to have either of two rather distinctive spectral shapes as indicated at the top of Fig. 4. At any given time the relative numbers of the other different types are indicated by the density of the lines shown. For example, most of them were white noise during the first analysis period, while quite a few of them were Type III near the end of the period. That's how this display was intended to read.

You can see some correlations between the occurrence of the different spectral types and the loading history; for example, at the first deviation from linear loading, the first occurrence of the Type III emission was noted. Also, the first occurrence of the Type I emissions was immediately preceding and during a major catastrophic crack growth step, and these occurred throughout the rest of the history of the specimen. I don't want to make any more of that than is indicated here, but for each specimen analyzed, there was some indication that the frequency spectral information can be used as an indication of where you are in the crack growth history. Also, comparing these data for the unaged specimen with those of the aged specimen, there are some differences. They are subtle and, at this point, it is not possible to sort out the exact mechanisms operating. The fact that differences can be seen is encouraging, however.

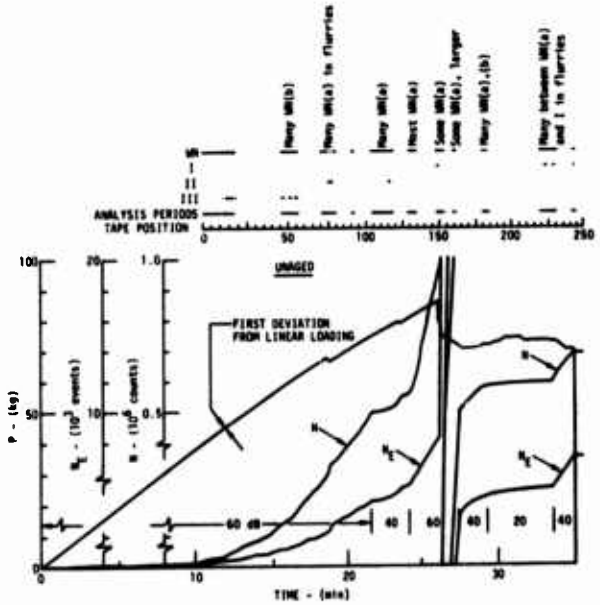

Figure 4. Correlation of frequency spectral types of emissions with the load and event vs. time histories for an LT-orientation specimen of B-1 material in the unaged condition. Note that the event and count curves are folded back at increments of N_E=20x10^3 events and N=1x10^6 counts.

In order to apply signal characterization to the test of a large component structure, attention must be paid to the highly attenuating and dispersive nature of wave propagation in these material. Figure 5 shows the velocity and the attenuation vs. frequency in the B-1 material. Both plate specimens and bar specimens were used to obtain these data. You can see it is very attenuating at higher frequencies and very dispersive at lower frequencies. This must be taken into account in a test on a structure. Of course, crossply laminates would have different characteristics than this, so in each case these properties of the material would have to be measured.

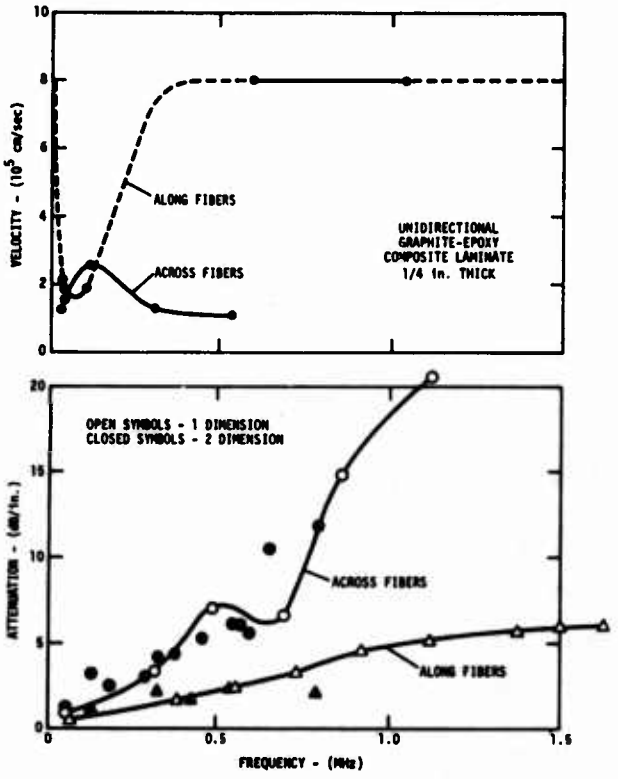

Figure 5. Directional dependence of the velocity and amplitude of acoustic pulses in a 1/4 inch thick unidirectional graphite-epoxy composite laminate.

In a proof test situation, acoustically active areas would be located in a conventional manner by triangulation and then a single broadband transducer would be attached to the structure in close proximity to the source. Characterization could then be done on the amplitudes, frequency spectra, and so on, much as in a laboratory test specimen.

In summary, where are we? Although there is no guarantee from this study that acoustic emission signal characterization will help in defining flaw severity or the degree of moisture degradation, some of the results suggest that this capability is possible. The number of emission events alone is ambiguous, particularly in the early flaw growth history, being strongly dependent upon the past loading history. However, the amplitude distribution

and the spectral information may provide the information required.

Now, where are we going? We would like more accurate data taken over a wider dynamic range, and we are building equipment now to do this. It will collect in real time several characteristics of the emission events and display these characteristics as they change during a test.

Also, Dick Elsley of our laboratory has developed computer software to sort out and cross-correlate these characteristics, making this chore less tedious and more quantitative.

Finally, Bill Pardee has developed a theoretical description of the contributions of the acoustic emission source, the wave propagation path between the source and the detector, and the detector response to the characteristics of the emission signal. In this formalism, these three components are separable and their effect on the received emission signal can be analyzed independently, as you will hear more about this afternoon. This theoretical work has helped in interpreting the experimental observations already, and further source modelling is expected to provide an important contribution in this area.

DISCUSSION

PROF. MAX WILLIAMS (University of Pittsburgh): Thank you very much, Mr. Graham. We have a couple of minutes left. Are there any questions?

DR. SAM NASH (Frankford Arsenal): You gave us some data on the number of events per unit area. What kind of an area are you measuring: projected area or actual area?

MR. GRAHAM: Projected area.

DR. NASH: That would be quite different from the real area.

MR. GRAHAM: You have to make up your own model for just what it means in terms of actual area according to the details of what's going on. And also, you have to phase into this the very wide dynamic range of the areas and the emission amplitudes. So, this is just a very gross number which provides a starting point for these considerations.

DR. STEVE CARPENTER (University of Denver): Where you start to get the emission and throughout the deflection, do you correlate that with a plastic strain rather than time? It looks like that begins where you begin to have some plastic strain.

MR. GRAHAM: Right. It starts building up about that point, although there are some emissions before then. I'm not sure how you would sort out the difference between plastic strain and actual irreversible microfracture processes that are going on around the pre-existing defects. No, I haven't tried to analyze it.

PROF. WILLIAMS: I have a general question to the speaker, perhaps to some of the audience. It has bothered me for a considerable length of time on acoustic measurements, and I'm going to focus on the unloading mechanisms, that the acoustic bursts, the acoustic emission energies that are indicated perhaps might be used in reverse. When one unloads the specimen, if you had a perfect crystal, presumably the burst energy could, through recombination of the atomic structure, absorb some of the energy and then lead to absorption of energy instead of the outburst of energy. The question is: has anyone measured or attempted to measure this kind of energy absorption under the unloading or recombination of energies even during the loading? The first question is the primary one that concerns me. Has anyone in the acoustic business attempted to measure the absorption of energy as a specimen is unloaded or loaded?

First crack at it to you, I suppose, Mr. Graham.

MR. GRAHAM: I'm not aware of it.

PROF. WILLIAMS: Anybody in general?

DR. CARPENTER: If you consider the absorption of energy in measuring the damping as you unload it, yes, we have measured the dislocation damping along with the acoustic emission both in loading and unloading.

PROF. WILLIAMS: With simultaneous measurements?

DR. CARPENTER: Simultaneous measurements.

PROF. WILLIAMS: That's very good. And the material, please.

DR. CARPENTER: We're working now in very pure iron with four levels of carbon concentration and also doing some hexagonal close-packed materials.

PROF. WILLIAMS: And that is a metal structure we note for the record. There has been some work in the rubbers - thermo-elastic materials - that I have been aware of which sparked my question.

Thank you very much, Mr. Graham.

APPLICATION OF INELASTIC ELECTRON TUNNELING TO THE STUDY OF ADHESION

T. Wolfram and H. White
Department of Physics
University of Missouri 65201

The problem of devising meaningful and reliable methods for nondestructive evaluation of adhesively bonded joints has been the subject of considerable effort for many years. It remains an important and unsolved problem. The use of conventional NDT methods involving ultrasonics is not entirely satisfactory because the thickness of a bond line is small compared with typical acoustic wavelengths and, perhaps more importantly, because the strength and service life of an adhesive bond is dependent on its chemical as well as mechanical properties. That is, an adhesive bond that is mechanically perfect may fail because of chemical degradation initiated at the adhesive/adhered interface.

Figure 1 is a schematic of a typical metal/adhesive bond. Any metal employed in a practical situation will have a thin oxide layer on its surface and consequently any adhesively bonded metal joint will involve an oxide/polymeric interface.

The dashed line in Fig. 1 represents a typical fracture line (or fracture surface) which occurs in failure. It is well known that the fracture line is very rarely limited to the glue line[1,2] (adhesive/oxide interface). The final morphology of a fracture line and the position of the initial crack may be only weakly related if at all. Once a critical sized crack is formed the development of the line is usually determined by the mechanical properties of the component materials.

In addition to mechanical mechanisms of failure such as large stress concentrations associated with voids and residual stress, chemical and physicochemical mechanisms associated with interface phenomena are frequently involved in the initiation of bond failure.

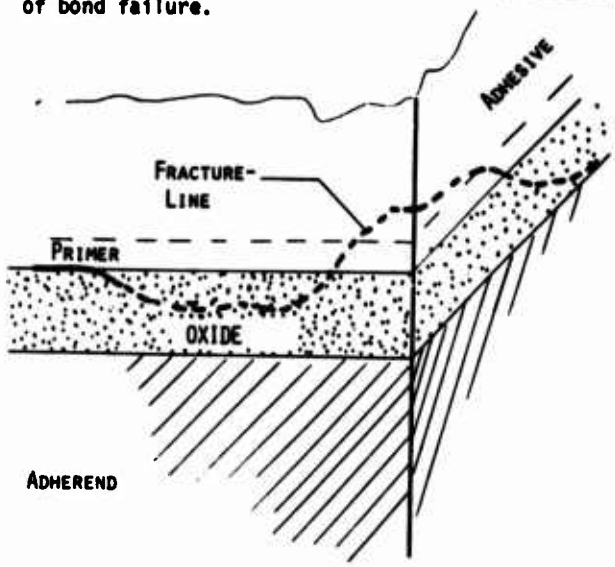

Figure 1. Schematic of adhesive bond joint

An interface consists of an organic or polymeric substance in intimate contact with a non-stoicheometric metal oxide. Many of the metal oxides are excellent catalysts. The oxides of many common metals such as Al, Mn, Cr, Fe, Ni or Zn are well known for their ability to catalyze reactions in organics. TiO_2 is an excellent catalyst and its action in oxidizing a polymeric binder is well known to be the cause of "chalking" of paints[3]. Black and Blomquist[4] reported that adhesive joints employing phenolic and epoxy resins were critically degraded by the metal adherend when heated in air due to catalytic oxidation of the adhesive. Such effects were observed for numerous common metals. The results of Black and Blomquist are illustrated in Table 1:

TABLE 1

EFFECT OF HEATING IN AIR ON PHENOLIC/EPOXY BONDS BETWEEN DIFFERENT METALS

Metal	Shear Strength (bars) before heating	after
Al	122	65
Mn	118	72
Cr	112	63
Fe	99	38
Ni	111	47
Zn	127	78
Cu	96	0
Ag	146	80
Ce	130	82

The role of H_2O in degrading an adhesive bond is not understood in detail but its action in accelerating detrimental chemical reactions is well documented[2].

The initiation of chemical degradation of an adhesive bond takes place at the microscopic interface between the metal oxide and the adhesive (or primer). We are concerned in our project with possible new measurement techniques for detecting and monitoring the chemical state of this microscopic interface. The technique of inelastic electron tunneling spectroscopy (or IETS) offers a potential tool of incredible sensitivity and great versatility for investigating, in situ, the chemical state of a metal oxide/adhesive interface. It should be made clear that at the present time it is not obvious how IETS can be employed as a

practical, "on-line", NDE tool. However, it seems clear that knowledge of the oxide/adhesive interface chemistry would be extremely valuable in developing new types of NDE measurements.

With this point of view we initiated, in January of this year, a small exploratory project to assess the feasibility of utilizing IETS to monitor the properties of an aluminum oxide/adhesive interface.

Inelastic Electron Tunneling Spectroscopy

In order to describe our progress a brief review of inelastic electron tunneling spectroscopy[5,6] is needed. We are concerned with a metal/insulator/metal thin film junction as illustrated in Fig. 2. A typical tunnel-junction is fabricated by evaporation of a thin Al film onto a glass substrate. The film is oxidized to form an aluminum oxide layer 30 to 100 A° in thickness; similar to the natural oxide on any aluminum surface. A molecular substance such as an adhesive is then deposited on the oxide by a variety of "doping" techniques[6]. In most cases the molecular layer is 5 to 20 A° in thickness. Finally, a second metallic film (often Pb) is deposited over the molecular layer forming a four terminal thin film MIM junction as shown in Fig. 2.

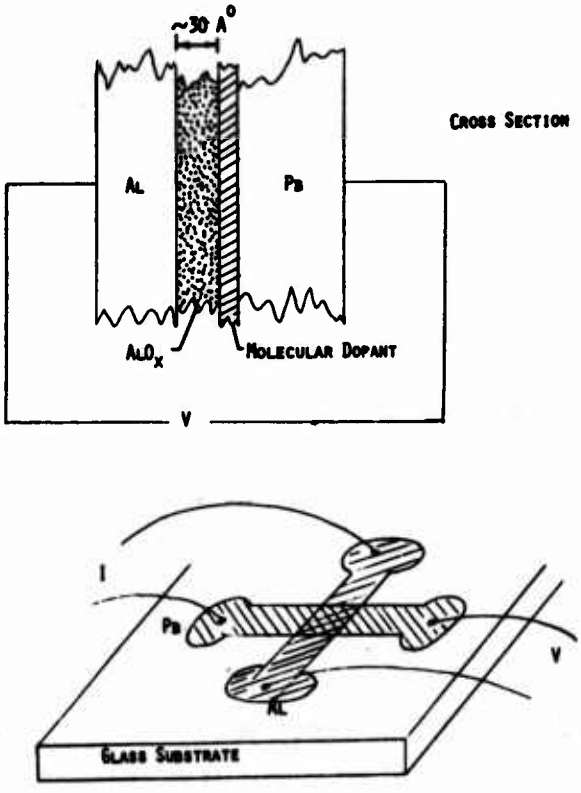

Figure 2. Schematic diagram of metal/insulator/metal junction.

A variable bias is applied across two of the junction terminals and the current is measured across the second two terminals. Since the oxide is a good insulator only a small current of the order of 5×10^{-3} amperes flows across the junction. This current is due principally to electrons which, in the quantum mechanical sense, tunnel through the oxide barrier. A schematic of the tunneling process is shown in Fig. 3. Fig. 3a illustrates the elastic electron tunneling process in which an electron tunnels through the insulating barrier from below the Fermi level of the Al film to an empty state above the Fermi level in the Pb film with no loss of energy. Fig. 3b illustrates the inelastic process. In this case the tunneling electron collides with one of the molecules on the oxide and excites one of the vibrational modes of the molecule having a characteristic energy $h\nu_m$ where ν_m is the vibrational frequency.

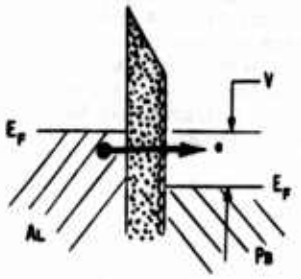

Figure 3a. Elastic tunneling

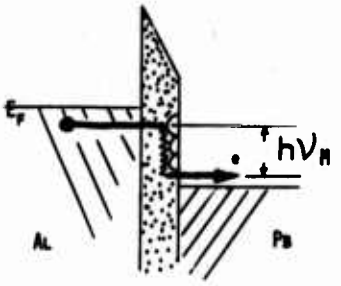

Figure 3b. Inelastic tunneling

An inelastic tunneling process produces an abrupt change in the slope of the current-voltage characteristic at an applied voltage equal to the vibrational frequency $h\nu_m$. The effect is shown schematically in Fig. 4a. The effect can be greatly enhanced in two ways. First, by making measurements at very low temperatures thermal smearing effects can be greatly reduced. Usually measurements are made at liquid helium temperatures so that the Pb film is superconducting. Second, by using electronic modulation methods the junction conductance $G = dI/dV$ and the second derivative $\frac{d^2I}{dV^2}$ can be recorded. Structure due to excitation of molecular vibrational modes of the molecular layer are easily observed in d^2I/dV^2 versus V curves. The characteristic shapes of these curves are illustrated in Fig. 4b and c. The structure due to inelastic tunneling processes as seen in d^2I/dV^2 curves is remarkably similar to infrared absorption by the molecular substance. However, the tunneling method is different in several respects. First, the sensitivity to small quantities of material is fantastic: A monolayer of material on a junction with an area of 10^{-2} cm^2 is very easily detected. Second, all vibrational modes are detected by tunneling. That is, there are no selection rules and both infrared and Raman modes are seen in the same spectrum.

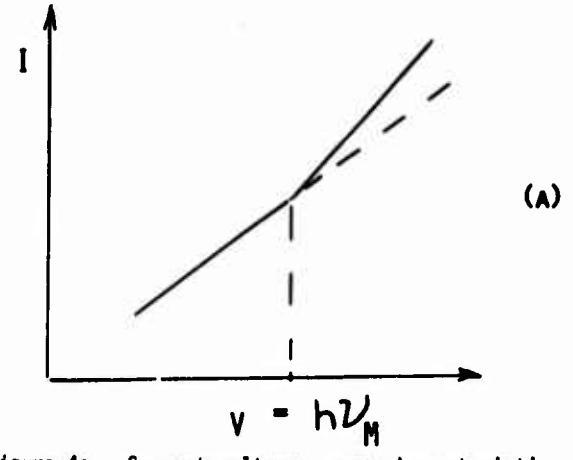

Figure 4a. Current-voltage curve characteristic of inelastic tunneling Process

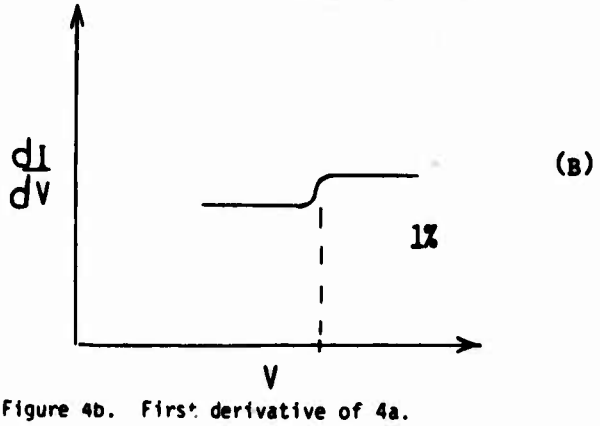

Figure 4b. First derivative of 4a.

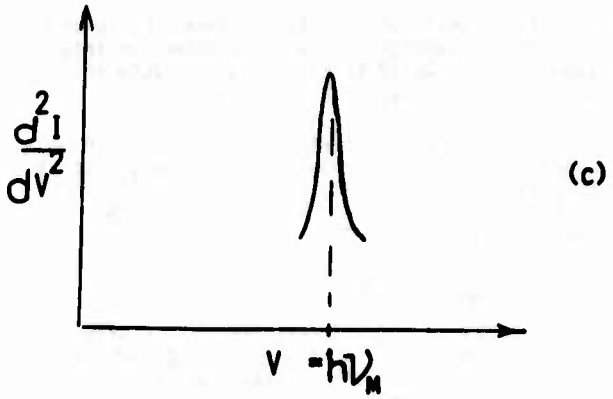

Figure 4c. Second derivative of 4b.

As an example of IETS we show in Fig. 5 the tunneling spectrum of the organic compound phenylalanine. The upper panel is the tunneling spectrum obtained by Simonsen and Coleman[6] and the lower panel is the infrared transmittance reported by Nugol Mull.[7] A large number of characteristic vibrational modes are easily identified and the IETS spectrum is quite similar to the IR spectrum. The IETS spectrum can be used to monitor the chemical state of the molecular layer. It is this property that is the basis of employing IETS for the study of an oxide/adhesive interface.

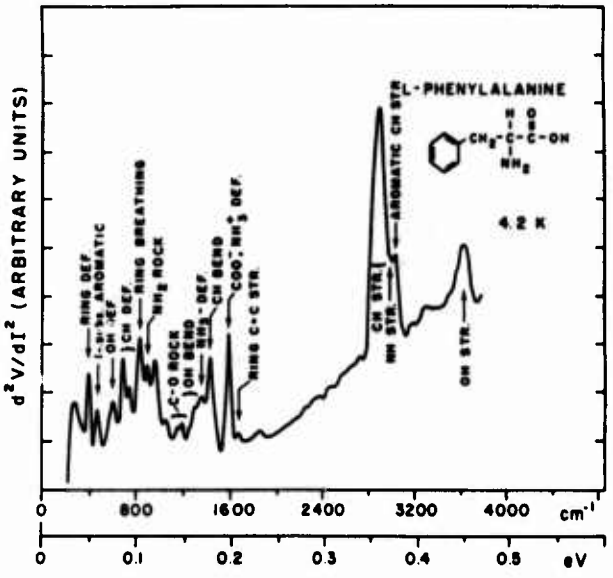

Figure 5. Tunneling spectrum of organic compound phenylalanine.

Application of IETS to Adhesives

The purpose of our project is to assess the feasibility of utilizing IETS as a tool for the study of the chemical state of a metal oxide/adhesive interface. Our immediate objectives are to determine if measurable changes in the tunneling spectrum can be correlated with processes involved in adhesive setting, curing, and degradation.

Setting of a typical adhesive involves cross-linking polymerization, chemical addition or condensation. In the cross-linking process for example, c = c bonds may be replaced by C-C bonds as illustrated in Fig. 6. This cross-linking can be accelerated by heating of the joint. It may be possible to monitor the cross-linking process by recording the IETS spectrum before and after heat treatment of the junction. The question of interest here is whether the dimunition of the intensity of the vibrational stretching mode of the carbon-carbon double bond and the change in the distribution of vibrational modes can be observed as the cross-linking increases.

In the setting of epoxy resins such as illustrated by the addition reaction in Fig. 6 three molecules are joined in the curing process. Many epoxy adhesives cure slowly and at elevated temperatures. It may be possible to monitor the curing process by recording the IETS as a function of time or by performing isochronal heating of the tunnel junction.

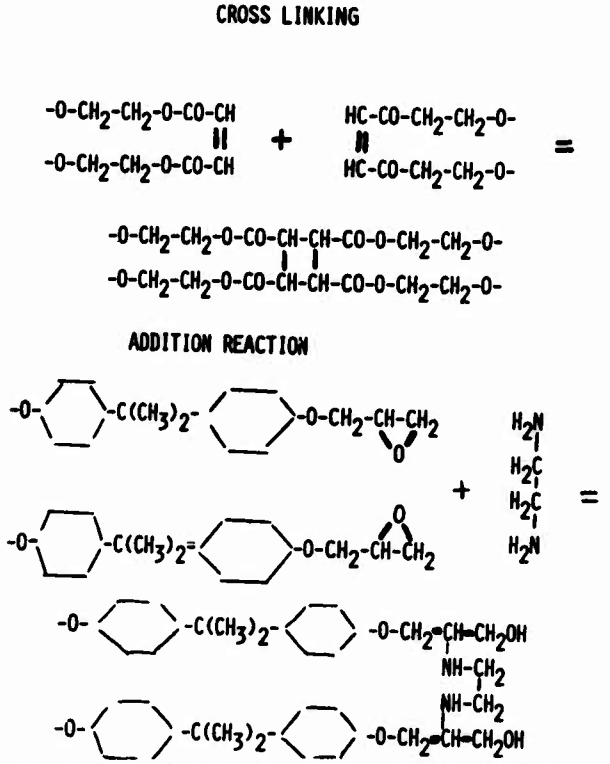

Figure 6. Schematic bonding configurations that may be observed with IETS.

By heating junctions in oxygen or in a high humidity environment, it may be possible to observe the catalytic oxidation of the adhesives at the interface. Catalytic interface reactions may produce chemisorption bonds between the adhesive and the oxide and intermediate chemical species such as O_2^- and excited O_2 which are known to be reactive. It may be possible to detect and identify these species with IETS. Excited state (singlet) oxygen is known to accelerate the degradation of polymeric material. New vibration modes associated with the formation of chemisorption bonds may also be observable using IETS.

The penetration of water into the interface will be easily detected by inelastic tunneling since both the O-H bending and stretching modes are known to be quite intense. On the investigation of water permeation, D_2O may be used so that water entering from the environment may be easily distinguished from residual water contained in or on the oxide film.

We may also investigate the catalytic properties of the interface by looking for the appearance of C-D stretching and bending modes. If H atoms are exchanged with the D atoms of the permeating water it would be suspected that such an exchange reaction would require the action of a catalyst. In this case the oxide would be the catalytic agent.

Progress

In the remainder of this report we review our progress towards investigating adhesive properties using IETS.

Equipment

A large oil diffusion pumping system was modified for use in preparing tunneling junction. This system together with suitable cold traps was utilized in obtaining the data presented below. The system must be replaced by an oil-less "vac-ion" system in order to reduce junction contamination. The components of a vac-ion system are now available and after suitable modification will be assembled and utilized in future work.

An electronic (lock-in) modulation system capable of measuring and recording I-V, dI/dV-V and d^2I/dV^2-V curves was built and employed in our experiments. The D.C. sweep unit was designed to provide voltage sweeps from 10 sec to 24 hours. Long sweep times are necessary to obtain good spectral resolution. Noise in the system with 10^{-3} V modulation was reduced to within 3 Db of the Johnson noise limit.

Two dewar systems were constructed. One allowed the junction to be immersed directly into a storage dewar for measurements made at 4.2 K. The second is a He^4 glass dewar which can be pumped to 1.3 K and can accept several junctions. A special holder with leads and shielding and grounding was constructed.

Results

$Al/AlO_x/Pb$ junctions were fabricated and data taken at 4.2 K. Measurements of I-V, dI/dV and d^2I/dV^2 recorded. Initial measurements were made on "clean" (undoped) junctions. A typical dI/dV-V curve is shown in Fig. 7 with V in the range from $\pm 40 \times 10^{-3}$ ev. The sharp peaks near zero bias are due to the super-conducting density of states of the Pb film at 4.2 K. This response is characteristic of elastic tunneling and serves to document that the current flow is due to tunneling and not to small electrical shorts in the oxide. The energy gap of Pb, 2Δ, corresponds to the separation between the peaks.

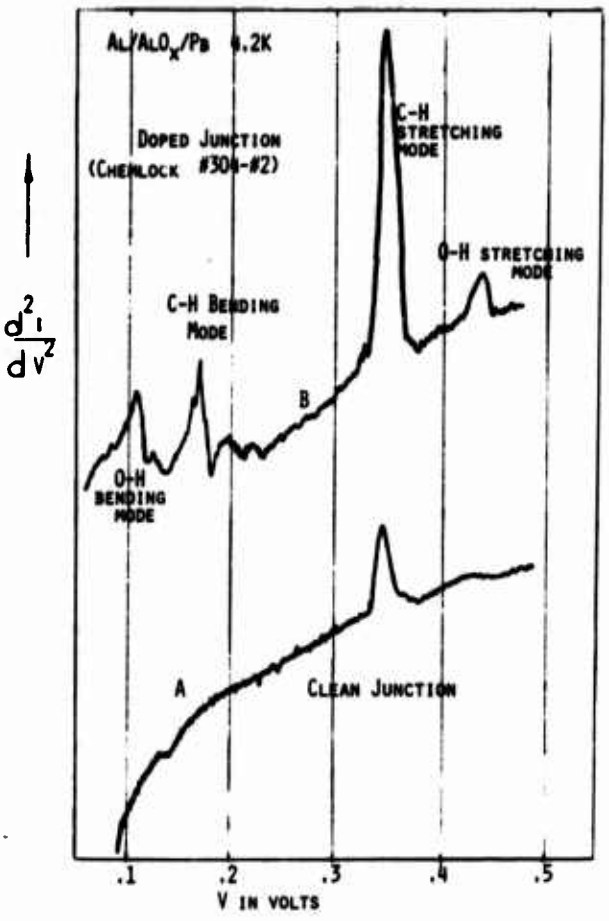

Figure 7. Inelastic tunneling spectra for (A) a clean junction and (B) a junction with epoxy contamination.

In Fig. 7 we show inelastic tunneling spectra obtained on two different junctions. Curve A is for a "clean" junction which was not doped with a molecular material. There is very little structure in the d^2I/dV^2 curve. The shoulder at about .15 V is due to the O-H stretching mode. These structures are associated with residual contamination on the junction acquired during the formation of the oxide in the vacuum system. Curve B is for a junction doped with one component of a commercial epoxy adhesive, "Chemlock 304." Several vibrational modes associated with the adhesive component are clearly evident. The most intense modes are the C-H stretching and bending modes. The O-H stretching and bending modes are also very intense.

The data presented in Fig. 8 is our first attempt to observe inelastic tunneling with the adhesive dopant. There are many other vibrational modes evident in the data but considerable improvement in the signal to noise must be accomplished before the data can be used quantitatively. A number of improvements in the fabrication and signal processing are currently being implemented.

Experiments are underway to look at the spectrum of the other component of Chemlock and at the mixed epoxy itself. Following this we shall attempt to monitor changes in the epoxy due to thermal setting and degradation of the adhesive due to water and/or heating in a gaseous environment. An assessment of the feasibility of using IETS to study the chemical state at an aluminum oxide/adhesive interface should be completed in the next few months.

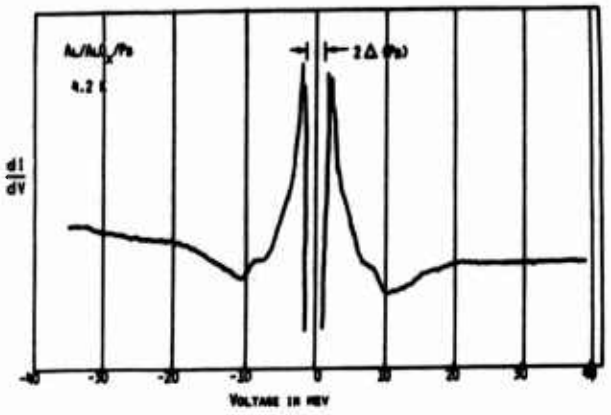

Figure 8. First attempt to observe inelastic tunneling spectra with an added dopant in the junction.

REFERENCES

1. J.J. Bikerman, The Science of Adhesive Joins Academic Press (1961).
2. T. Smith, Proc. ARPA/AFML Review of Quantitative NDE (AFML-TR-75-212) Jan. 1976; page 565.
3. S.P. Pappas and R.M. Fischer, J. Points 46, 65 (1974).
4. J.M. Black and R. F. Blomquist, Ind. Eng. Chem. 50, 918 (1958).
5. R.C. Jaklevic and J. Lambe, Phys. Rev. Lett. 17, 1139 (1966); Phys. Rev. 165, 821 (1968).
6. M.G. Simonsen and R.G. Coleman, Phys. Rev. B8 5875 (1973). Nature, 244, 1218 (1973).
7. see Charles J. Pouchert, The Aldrich Library of Infrared Spectra. (Aldrich Chemical Co., Cedar Knolls, N.J., 1970).

PROF. MAX WILLIAMS (University of Pittsburgh): We have time for any questions of points of fact. We won't have time for discussion of the paper, but are there any questions as points of fact?

DR. BILL BASCOM (Naval Research Laboratory): Can you distinguish between a hydroxl of water and hydroxl bonded to aluminum?

PROF. WILLIAMS: I think I must ask you to just reply either yes or no or maybe.

PROF. WOLFRAM: I suspect the answer is maybe.

PROF. WILLIAMS: I saw one other question of fact back here.

DR. G. GARDNER (Southwest Research Institute): At what temperature are these measurements?

PROF. WOLFRAM: Pardon?

DR. GARDNER: At what temperature are these measurements?

PROF. WOLFRAM: These measurements that you saw were performed at liquid helium temperatures. The technique itself does not require superconductivity. You increase your sensitivity or your resolution by going to low temperature. It also impedes any further chemical processes, so you can take a picture of it, then warm it back up, and then go back down and freeze in your particular chemical state. It doesn't really require superconductivity; it does require low temperatures to get resolution.

PROF. WILLIAMS: Thank you very much, Dr. Wolfram, particularly for meeting your shortened time for presentation.

TRAPPED ACOUSTIC MODES FOR ADHESIVE STRENGTH DETERMINATION

G. A. Alers
Science Center, Rockwell International
Thousand Oaks, California 91360

The most important aspect of measuring the strength of adhesion at an adhesive to metal interface is to understand the chemistry of the interface and to know what makes a good interface. The existence of a strong interface will make the joint less susceptible to fabrication defects that are going to be there no matter how carefully the joint is prepared.

It is also pretty obvious that we cannot use very sophisticated laboratory tools such as superconducting tunneling that we have just heard about on an airplane wing in the field. Our problem is to relate the kind of measurements made on the microscopic scale in the laboratory to the kind of measurements that can be made in the field. This paper is an attempt to bridge the gap between current ultrasonic techniques, which we have heard a little bit about already and some newer more sophisticated and sensitive ultrasonic techniques that may open up an avenue for bringing the microscopic chemistry of the interface out into a nondestructive test performed on macroscopic parts.

Our problem then is to find an ultrasonic test that is going to look at that tiny molecular dimension at the joint between the metal, its oxide, and the adhesive. It is obviously a difficult problem because we're working with a layer that is many times smaller than the wave length of our probing sound wave. Last year we tried some experiments directed at the interaction of very thin layers with sound waves, and the results were not too encouraging for the simple geometry of sending the sound waves perpendicular to the interface as many of the conventional experiments are done nowadays. That is probably to be expected because the sound wave does not have much time or distance in which to interact with the interface. Therefore, the idea in this year's program was to send the sound wave parallel to the interface so that it could run along for some distance and interact with the defects at the interface and accumulate an effect that could be measured. This immediately became a complicated problem because it involved mathematical analysis of the modes of propagation in a sandwich structure. It involved developing the experimental techniques to observe these modes and it also involved the preparation of specimens that would have variable adhesive strength at the joint between the adhesive and the metal while maintaining a constant cohesive strength.

In order to attack these many problems cooperative work with a lot of people was demanded. Dick Elsley and his computer helped immeasurably when it became apparent that we wanted to observe some special modes of vibration of the total panel and his computer was there waiting to go and answer those questions and to guide the experiments along a very easy path. Chris Fortunko, who has just recently joined our laboratory, provided electromagnetic non-contact transducers for exciting the surface waves of high purity. These new devices were already assembled and easy to use so they greatly simplified our experiments in exciting sound waves in the adhesive layer. Of course, Tennison Smith, working from the very beginning of the program, prepared some specimens that had poor adhesion between the adhesive and the metal and strong cohesive strength so we could test our modes to see if they would, indeed, tell the difference between high and low quality of adhesion.

Our basic experiment is to excite propagating modes of vibration that travel in the adhesive between the two pieces of metal being bonded together. Since the wave velocity is slow in the adhesive, one can imagine that when these trapped waves try to get out of the adhesive they are refracted back in by the higher wave speed in the metal. Thus, the energy is trapped in the adhesive layer. We shall seek to measure some property of the acoustic wave such as the velocity of propagation, although it would pay us to keep track of the attenuation of the wave also. It would appear to be a simple project to make some adhesive-metal sandwiches and then excite some trapped waves in the adhesive. However, there are a great many modes, and conventional transducers readily excite all of them. Therefore, our first task was to attack the problem of calculating the trapped modes and then to look for regions in the mode spectrum that might be particularly sensitive to the boundary conditions.

The first figure shows the experimental configuration we used. It is a simple lap shear specimen onto which we attached electromagnetic, noncontact surface wave transducers to excite and detect a surface wave on the metal that sticks out from the adhesive. By launching a surface wave into the adhesive from the metal tab, it was possible to excite one of the trapped modes in the adhesive layer which came out on the right-hand side where a receiver transducer detected it. It is a simple experiment also because the geometry of specimen allows one to test the strength of the bond in shear by pulling on the tabs. The electromagnetic transducer was important because conventional surface wave transducers are wedge type transducers which allow a lot of other modes to get excited, making a mess out of the signals that emerge from the bond line.

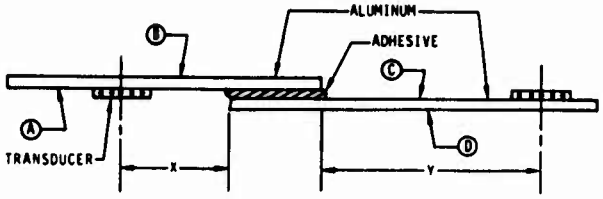

Figure 1. Typical lap shear specimen for mechanical testing of adhesive bond strength with electromagnetic transducers in place for exciting and detecting surface waves on surfaces A and C.

We were able to excite very nice clean surface waves at postion A and to pick them up with another transducer on the right side near the Letter D after going through the adhesive bond. Figure 2 shows the kind of signal we detected and is a photograph of the oscilloscope trace from the receiving transducer. That little triangular pulse labeled A is the signal that was excited as a surface wave on the left-hand side of our sample, went through the adhesive and came out the other side. By plotting the arrival time of this signal as a function of the separation between the two transducers, a straight line is obtained whose intercept corresponds to the time that the sound waves spent in the adhesive. From this amount of time and a knowledge of how long the adhesive is, it is easy to deduce the velocity of sound in the adhesive. Unfortunately, there are a lot of problems with this kind of measurement. First, it is not that accurate a technique and we had to use a different transducer every time we wanted to change the frequency. Thus, in order to measure velocity as a function of frequency and thereby examine some different modes, we had to use a series of specially built transducers. Furthermore, when we probed around the surface of the entire sample, we found acoustic energy all over the place. The adhesive bond not only converted the incident surface wave into a trapped mode, but it produced bulk modes in the aluminum that transferred energy to the other surfaces. It would be interesting to measure this mode conversion process since it might be a way of looking at the adhesive bond, but our objective was to look at the adhesive layer with trapped modes so we discontinued these experiments.

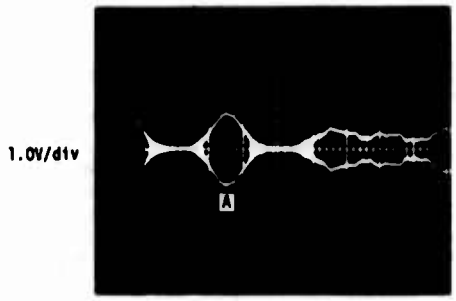

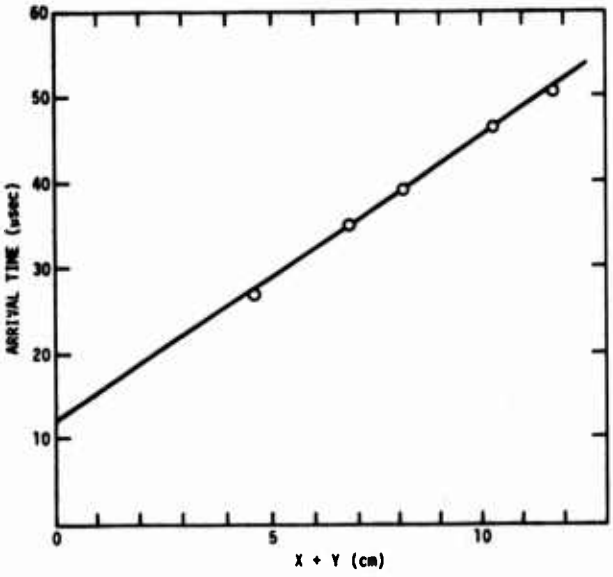

Figure 2. Oscilloscope trace photograph showing the surface wave signal A detected on surface C of the adhesively bonded structure shown in Fig. 1. The time of arrival of this signal varies as a function of transducer separation distance X + Y in Fig. 1.

Because so many modes are possible, it is important to consider the problem theoretically by asking which modes of motion can propagate along the adhesive layer parallel to the metal plates and which are most sensitive to the boundary conditions at the metal to adhesive interface. The method that we had available at the Science Center was a computer program that Bruce Thompson had prepared with the help of Dick Cohen for calculating the properties of acoustic waves in layered media. This program was modified by putting in different boundary conditions at the adhesive to metal interface and recalculating the propagation velocity of the modes of a simple three-layered sandwich consisting of two aluminum layers separated by an adhesive layer. Of course the conventional boundary condition of continuous stress and continuous displacement across the interface was used as a standard of comparison. There are a lot of different kinds of boundary conditions one could choose. The one we chose was to put a step in displacement at the boundary whose magnitude was proportional to the local stress. You can rationalize this choice of boundary condition if you imagine that there is a very thin layer of very compliant material at the interface.

By inserting a value for the compliance of the thin layer and recalculating all the propagating modes, we were able to locate modes and frequencies where there were big effects in the velocity of propagation due to the boundary conditions. For the delight of the physicists present in the audience, Fig. 3 is the ωk diagram (the frequency versus wave number graph) for the modes of motion in which the energy is confined to the adhesive. As you can see, it is complicated and shows many possible modes. Thus, it is not surprising that our surface wave experiments showed the excitation of other modes all over our sample. I would like to call your attention to k=0 where a lot of those curves come in and hit the frequency axis at a finite value of frequency. These frequencies correspond to the standing wave modes in the thickness dimension of the total sandwich. They are not propagating modes parallel to the direction of the adhesive layer because they have infinite wave lengths. They actually correspond to the standing wave modes propagating normal to the surface and are the resonances that we saw in Scott's paper this morning and we will see more this afternoon. By recalculating this whole set of curves for a different set of boundary conditions, we looked to see where the curves were shifted the most; that is, frequencies and k vectors that were more sensitive to the boundaries.

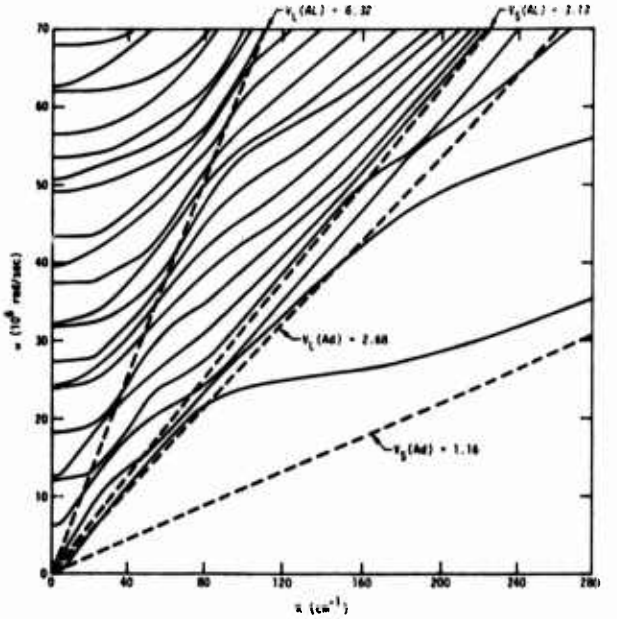

Figure 3. Curves of the angular frequency versus wave number for the acoustic wave modes that are trapped in the adhesive layer between aluminum plates.

Figure 4 is a graph of the percentage change in phase velocity of that first antisymmetric mode produced by a fixed change in boundary conditions. It shows that for a particular change in boundary conditions, there is a big effect in phase velocity right around 4 megacycles. By calculating the phase velocity versus frequency curve for this mode, as is shown in Fig. 5, along with some of the other modes, we found that the first antisymmetric mode starts at zero velocity at zero frequency, goes up over a peak and falls back down to a low velocity at high frequency.

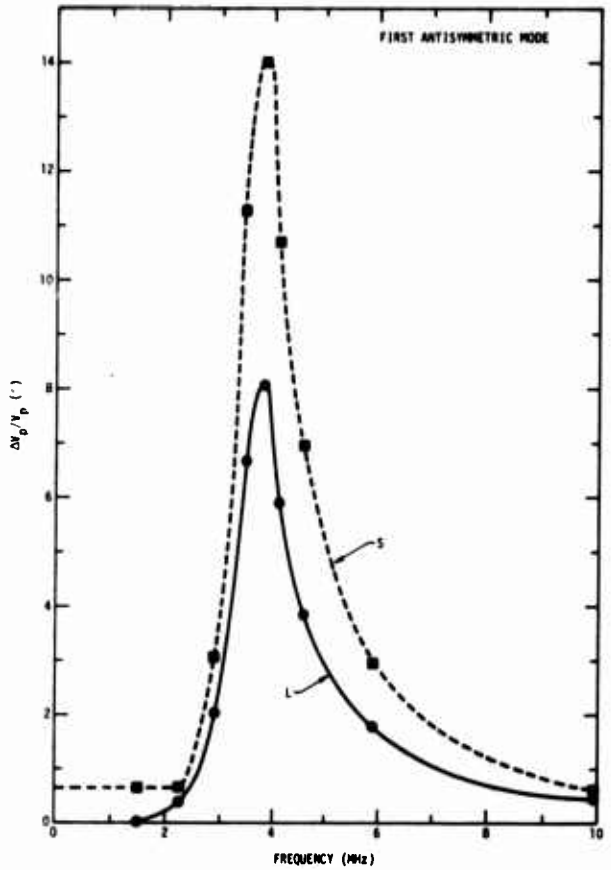

Figure 4. Percentage change in propagation velocity of the first antisymmetric trapped mode produced by insertion of a very thin layer of material at the interface having a small shear stiffness (curve S) or a small compressional stiffness (curve L).

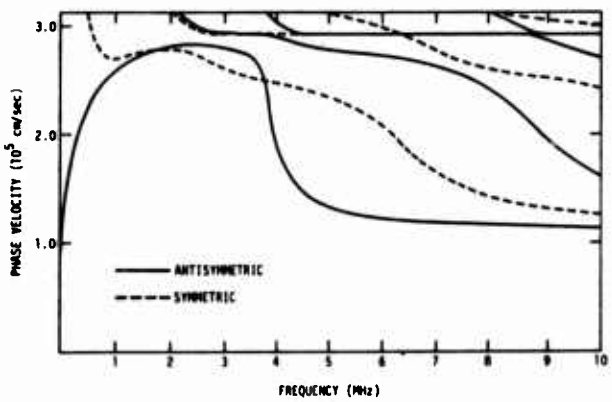

Figure 5. Curves of the phase velocity versus frequency for the trapped modes that propagate along the adhesive in an aluminum-adhesive aluminum sandwich.

At very low frequencies it is the flexure mode of the total sandwich. At intermediate frequencies where the wave length becomes comparable to the sandwich thickness, the velocity approaches the wave velocity of a surface wave on aluminum. Near 3 or 4 megacycles the velocity plunges downward to describe a shear wave confined to the adhesive and propagating with the shear wave velocity in the adhesive independent of the presence of the aluminum boundaries. Note that the transition from a wave that feels the effects of aluminum to one dominated by the adhesive occurs near 4 megacycles and that is where we have shown unusual sensitivity to the interface.

Based on these theoretical arguments, it is obvious that our experiment must be to try and excite this particular first antisymmetric mode where the curve is changing rapidly near 3 1/2 or 4 megahertz. This would require the design of special transducers for each frequency and probably imbedding them in the adhesive to avoid mode conversion at the edges of the adhesive layer when exciting the mode by external surface waves. At this point, Bruce Thompson suggested that by imbedding a single wire in the adhesive and by driving it with an alternating current in the presence of a strong magnetic field, we would have a broad band transducer imbedded in the adhesive and could excite it to any frequency we chose. Three wires were placed in the adhesive as shown in Fig. 6, and the whole thing was put in a magnetic field. When an alternating current was driven through the wire farthest on the left, it mechanically vibrated and excited mechanical waves in the adhesive. When these waves arrived at the wire farther down the sandwich, they moved it in the static magnetic field and thus generated an electrical signal which could be observed on an oscilloscope. Since only a single wire is involved, there is no particular frequency associated with it and one should be able to tune the frequency to any desired value. This concept worked just beautifully, as is shown in the oscilloscope signal photographs in Fig. 6. These pictures show the received, pulse signals at receiver 1 and at receiver 2. It can easily be seen that when the wave pulse is close to the transmitter, it is one burst, but after it has run a short distance the effects of dispersion and different modes appear, to split that burst up into three separate, broader signals. Thus it is clear that the broad band, single wire transducers have excited three modes in this experiment, and we could measure their velocities of propagation from a knowledge of the distance between the wires and the time delay. Unfortunately, the clean, large amplitude signals shown in Fig. 6 could only be obtained at one particular frequency. It turned out that our wire was acting as a little resonator consisting of the wire mass imbedded in a compliant adhesive with the adhesive acting as a spring. Good sensitivity was observed only when the vibrational resonance of that wire was excited. Thus when we tried to operate at the 4 megahertz that we wanted to use, all we saw was the tail end of the 2 megahertz resonant vibrations of the wires.

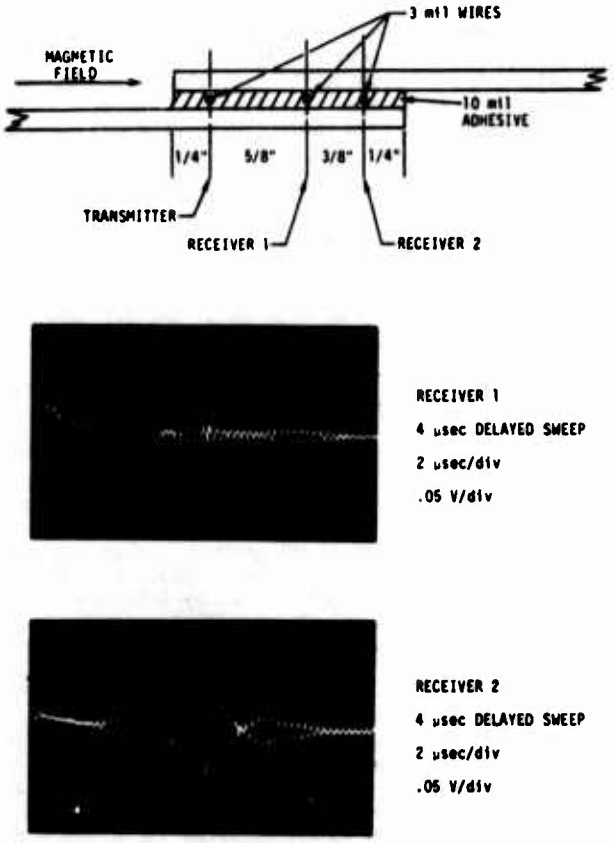

Figure 6. Geometrical configuration used to excite the trapped modes of the adhesive layer by a current carrying wire embedded in the adhesive in a magnetic field. The photographs show tone bursts picked up at the two receiver wires after launching a tone burst acoustic signal from the transmitter wire.

By adjusting the mass of the wires it should be possible to put the resonant frequency near 4 megahertz, but searching for the correct wire would be time consuming and could easily go beyond the scope of the current phase of the program. Instead, it was decided to return to the theory and look for other modes which would be seasitive to the boundary conditions. This examination of the theory showed that whenever the stress distribution of the waves within the adhesive put a maximum stress on the interface, then a maximum in sensitivity to the boundary conditions occurred. In particular, the thickness vibration of the whole sandwich (the lowest frequency k=0 intercept on Fig. 3) was found to be stressing the interface the most. This mode represents the two pieces of aluminum moving as rigid bodies with the adhesive acting as a spring, and occurs for usual bond geometries around 1/2 a megahertz to 1/4 of a megahertz. For the kind of specimens we were working with, it was actually down at 1/3 of a megahertz, which was somewhat lower than our available transducers. By making the aluminum sheets 1/16 inch thick instead of 1/8 inch, the standing wave frequency could be moved up to a half a megahertz where we had a transducer. Pulse-echo measurements of the reflectivity of the specimen in a water bath with this transducer directing waves at normal incidence on the bonded sandwich showed a minimum in reflectivity at the frequency of this mode. Such measurements were easily performed by Dick Elsley and his computer who took the Fourier transform of the echo signal. Figure 7 shows the dip in reflectivity associated with the thickness resonance as it is observed superimposed on the response curve of the transducer.

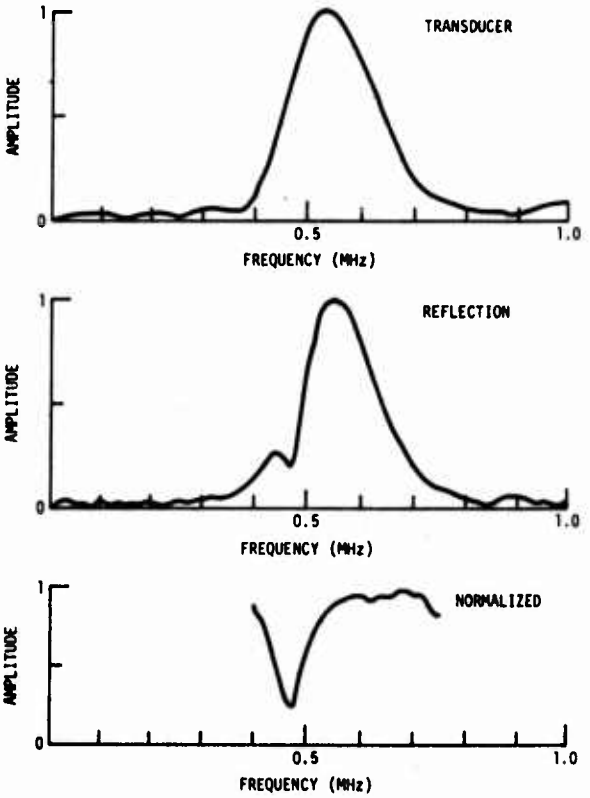

Figure 7. Fourier transform of the pulse signal reflected from a block of aluminum to define the transducer band pass response and from the adhesive bond sandwich to define its frequency of minimum reflectivity. The bottom curve is the ratio of the top two curves.

In order to observe a correlation with strength, eight lap shear specimens were prepared to have different adhesive strengths but a constant cohesive strength. These samples were constructed by Dr. Tennison Smith who used four different surface preparations on the aluminum to reduce the strength of adhesion. Wires were also imbedded in the adhesive so that data on the wave velocities of the propagating modes and the Q of the wire resonances could be recorded for possible correlation with the specimen strength.

Tables I and II show the results of the correlation obtained between the strengths of the eight lap shear specimens having different surface preparations, and the various measurable quantities that can be obtained from the standing wave resonances and the imbedded wire transducers. Table I shows the strengths and the measurements from the imbedded

wires which are the velocities of propagation of the different waves as deduced from the time of arrival of the pulses; the frequencies of the wires vibrating inside the adhesive; and the Q of that resonance of the wire. The subscripts ∥ and ⊥ denote the orientation of the external magnetic field relative to the adhesive bond plane. The resonant frequency of the thickness mode is shown in Table II along with the depth of the minimum in reflectivity. Since this resonant frequency depends upon the "spring constant" of the adhesive which in turn depends on the thickness of the bond, all frequencies have been normalized to a uniform bond line thickness, and this is shown in the column labeled corrected. Examination of the observed strengths of the eight specimens showed that we succeeded in producing two distinct groups of different strength in spite of our attempt to achieve four different levels of strength. Four specimens exhibited strengths in the 2400 to 2500 psi range, and four of them were very weak having strengths in the 1500 to 1800 psi strengths. The weak samples showed a completely adhesive failure because they broke nicely right along the interface.

Table I. Mechanical and ultrasonic properties of adhesive bond specimens deduced from embedded wires. The subscripts ∥ and ⊥ refer to the direction of the magnetic field relative to the bond plane.
V is the group velocity of a trapped mode pulse,
f is the resonant frequency of the transmitter wire,
Q is the mechanical quality factor of the wire resonance.

Specimen	Surface Treatment	Bond Line Thickness mils	Failure Stress psi	$V_{\parallel}$ 10^5 cm/sec	$V_{\perp}$ 10^5 cm/sec	$f_{\parallel}$ MHz	$f_{\perp}$ MHz	$f_{\parallel}/f_{\perp}$	$Q_{\parallel}$	$Q_{\perp}$
G-2	Degrease	10.1	1550	1.4	1.7	2.61	1.59	1.64	3.3	3.9
AR-1	As Rec'd.	10.1	1783	2.2	2.2	2.48	1.53	1.62	3.8	3.4
G-1	Degrease	10.8	1790	1.7	2.0	2.53	1.52	1.66	3.5	4.0
AR-2	As Rec'd.	9.8	1843	2.2	2.0	2.51	1.52	1.65	3.5	3.4
FM2	Monolayer	9.3	2440	2.0	2.3	2.5	1.69	1.50	3.4	3.7
FM1	Monolayer	9.5	2460	1.4	1.8	2.55	1.69	1.51	3.4	3.8
F2	FPL Etch	9.5	2476	1.9	3.0	2.46	1.75	1.40	3.7	4.5
F1	FPL Etch	10.3	2533	3.0	2.4	2.50	1.58	1.58	3.8	4.4

Table II. Mechanical and ultrasonic properties of adhesive bond specimens deduced from fundamental thickness vibration mode.

Specimen	Surface Treatment	Bond Line Thickness mils	Failure Stress psi	Resonant Frequency Measured KHz	Resonant Frequency Corrected KHz	Depth of Minimum %
G-2	Degrease	10.1	1550	449	467	27
AR-1	As Rec'd.	10.1	1783	449	467	28
G-1	Degrease	10.8	1790	429	458	15
AR-2	As Rec'd.	9.8	1843	439	451	0.6
FM2	Monolayer	9.3	2440	469	469	17
FM1	Monolayer	9.5	2460	454	474	4
F2	FPL Etch	9.5	2476	454	472	27
F1	FPL Etch	10.3	2533	468	474	13

The tables show that the resonant frequency of the thickness mode correlated with the strength in that for the weak bonds the resonant frequencies ran between 469 and 475. Thus there was a good 10 KHz difference between the groupings of the two resonant frequencies measured, and the resonant frequencies separated nicely according to whether it was a good bond or a bad bond. The resonant frequencies of the wires imbedded in the epoxy also correlated or fell into groups that corresponded to the actual strength measurements. Again, the differences were rather small, but there was a systematic trend in the data that was clear. The other quantities, the Q values and the wave velocities, did not seem to show any correlation.

Our tentative conclusion, based on two sets of four specimens having different strengths, is that the low frequency resonance which vibrates the total sandwich seems to reflect the quality of the interface. This quantity is a property that could be easily measured with conventional ultrasonic techniques. We do not rule out the use of propagating waves, and we will proceed to try some more sophisticated methods of exciting these waves. Hopefully, next year we will be able to report some better statistical correlation between the propagating mode and the strength of the bond.

DISCUSSION

PROF. MAX WILLIAMS: There is not time for discussion, but the chair will entertain any questions of fact for Dr. Alers as far as the details or questions that were not clear. Are there any questions of fact?

DR. JOSEPH HEYMAN (NASA, Langley): What was the thickness of the adhesives in this?

DR. ALERS: 10 mils.

COHESIVE STRENGTH PREDICTION OF ADHESIVE JOINTS

P. L. Flynn
Material Research Laboratory
General Dynamics
Fort Worth, Texas 76101

My part of this program was to investigate a nondestructive method for measuring the cohesive strength properties of adhesively bonded joints.

I started this problem by viewing a reasonably fundamental study in modeling the adhesive as a layer between two infinite aluminum adherends. You can set up wave potentials in these different regions in terms of reflected and transmitted waves, as is seen in Fig. 1. If you set up your wave number in a very classical manner, where everything is elastic and there is no damping, you just get a regular Rayleigh-type solution. If you desire to include the damping of the adhesive layer, then you must have a complex wave number. The appropriate relationship was derived by Brekhovshikh.[2] We took his relationships and did parametric studies on the bond line in terms of the acoustic properties of the adhesive.

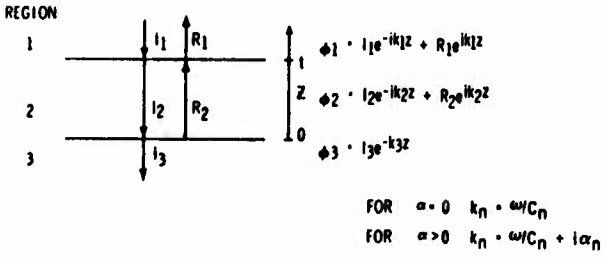

Figure 1. Model of Three-Region Laminate Treated in Analytical Calculation

Figure 2 shows the type of theoretical spectrum you get when reflected intensity is plotted against frequency in megahertz. The top curve is for the case where you don't have any attenuation in the adhesive layer. It is a simple Rayleigh solution. Then we have successive plots of bond lines with attenuation coefficients of 10, 20, and 30 Neper/cm. You will notice that as the attenuation coefficient is increased, the resonances tend to become both broader and shallower for this .0254 cm thick bondline.

We set up our code so it would scan the information that it produced and give the magnitudes of the depths of the resonances, the separations, and the quality factors of the resonances.

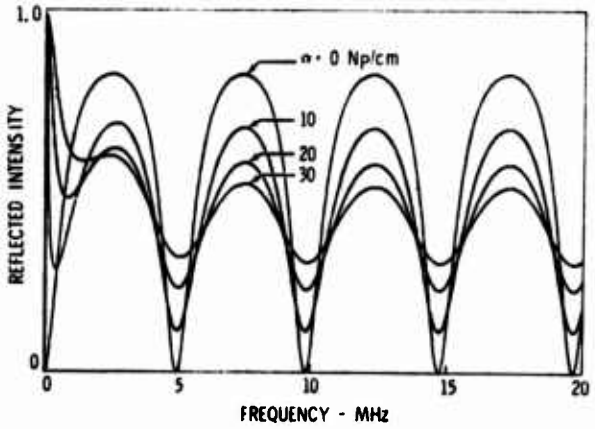

Figure 2. Theoretical Spectra for a 0.0254 on Adhesive Layer Between Aluminum Adherends

One of the terms that can be measured using Fourier transform spectroscopy is the resonance quality, or Q, which is defined as the resonance frequency divided by the half-power bandwidth. It's an easily measured term to characterize the shape of the resonance. However, in our parametric study we saw that with reasonable attenuations in the bond line, such as you get at the higher frequencies where the resonances occur, you end up really flattening out these curves as seen in Fig. 3. So, you don't really have very much sensitivity.

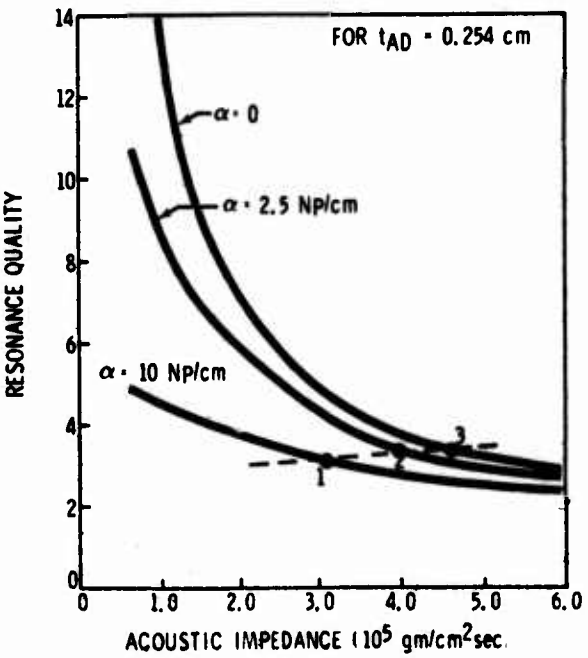

Figure 3. Theoretical Relationship Found Between Resonance Quality and Acoustic Impedance as a Function of Attenuation

In order to look at other types of measurables you can get from an adhesive bond line, we looked at the returned signal from the top aluminum-adhesive interface, seen in Fig. 4 as R_2, which is inverted because of the impedance mismatch, and the return signal from the bottom of the adhesive layer, R_3. We took these amplitudes in the time base signal and extracted one measurable, R_3/R_2, which will be referred to as the Amplitude Ratio of the bondline.

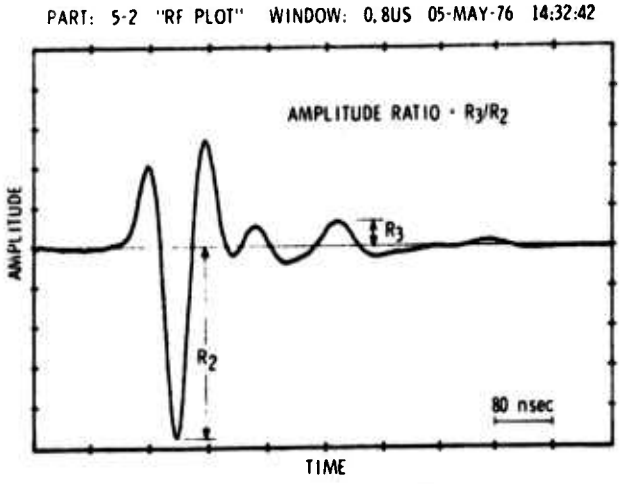

Figure 4. Reflected Signal from Adhesive Bondline

From very simple energy partitioning relationships with a superimposed attenuation term, you can make a plot of how amplitude ratio varies with acoustic impedance and then plot this for different amounts of attenuation in the bond line, as seen in Fig. 5. Again, the zero attenuation case returns the highest signals and increasing attenuation drives the ratio to lower values.

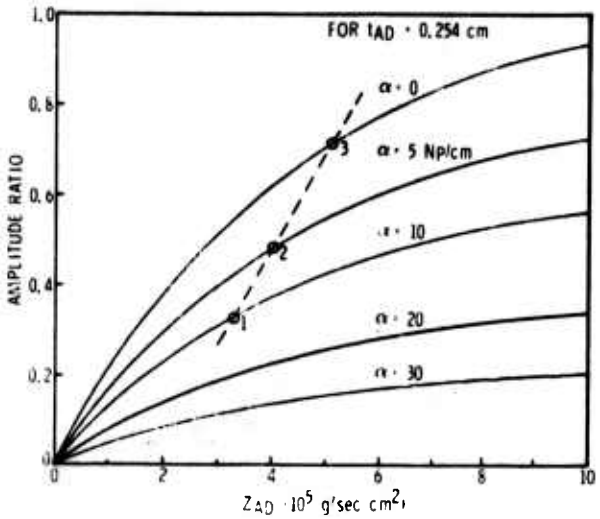

Figure 5. Analytical Relationship Between Amplitude Ratio and Z_{AD} as a Function of Attenuation

You will also note that in this case things start flattening out for higher attenuations, but the trend is in the opposite direction than with resonance quality. So when you are working with a reasonable physical property relationship that says that when the sound velocity increases, the attenuation will go down, you can again trace the response of the measureable with the expected material property changes in the numerical order of the points. You can see that the expected relationship between attenuation and velocity increases the sensitivity of the amplitude ratio to property changes. It was thought that this would give us a better chance of making measurements that would truly reflect what was going on, in a material property sense, in our adhesive.

Tennison Smith made some specimens for us that were one eighth of an inch thick aluminum adherends with a one-inch overlap. These specimens were made with Chemlok 304 adhesive, and the surfaces were properly prepared. The only variation between the specimens was the mixture of the two components of the Chemlok 304 adhesive. Mixing was done over the range of 2 parts A to 3 parts B, to 3 parts A to 1 part B. These were cured under the proper cure cycle to give different cohesive properties.

We investigated these from an ultrasonic standpoint with a pulse that is seen in Fig. 6. This was a 15 MHz highly damped pulse. We examined the laminates with a normal incidence compressional wave in the pulse echo made. We had the capability of digitizing the signal that was returned from the bond line Fourier transforming it to get its bond line spectrum, Fig. 7. These resonances correspond to standing waves in the adhesive layer, with the resonance separation given by the velocity of sound divided by twice the thickness. On these curves, you can look at the resonance quality, the resonance separation and the resonance depth.

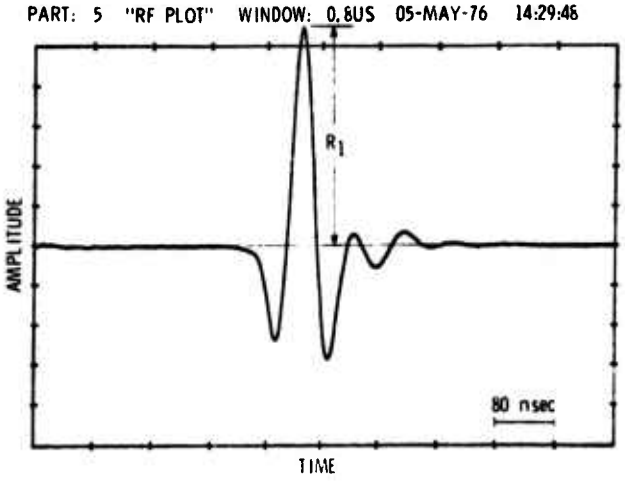

Figure 6. Reflected Signal from Top of Aluminum Plate Used as Reference Waveform

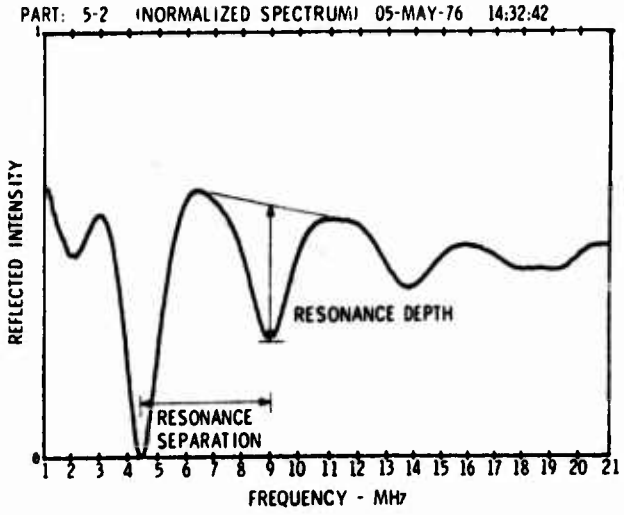

Figure 7. Reflected Spectrum of Adhesive Bondline

You notice that as you increase in frequency you have a higher and higher damping which gives you less intense resonances and also broadens them. So, in order to compensate for this factor, I used the tangents to the maximas in measuring the resonance depths.

Using the resonance separation, we were able to extract the velocity of sound by measuring the thickness of the adhesive layer. Figure 8 shows how the amplitude ratio varied with the velocity of sound. The first set of specimens all fell inside the dark lines. These received a cure at 93° centigrade for an hour. The second set of specimens received another cure, 121°C for 20 minutes, a higher temperature cure for a shorter amount of time. They fell above the data of the first set. This separation in data according to cure will follow on through the rest of the correlations, but will be rectified at the end.

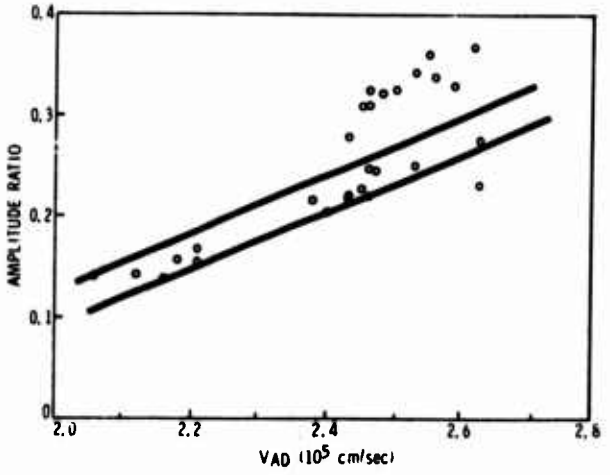

Figure 8. Experimental Relationship Between Amplitude Ratio and Adhesive Sound Velocity for Chemlok 304 Adhesive Specimens

From the amplitude ratio data we were also able to extract the attenuation coefficient of the bond line at the frequency of the transducer, which was 15 MHz. The calculated attenuation coefficients were reasonably high, in the range of about 10 nepers per centimeter to about 30 nepers per centimeter. For those of you who aren't used to looking at things in terms of nepers, a neper is about 8.6 db. So, these adhesives are relatively highly attenuating polymers.

When the attenuation coefficient was plotted against sound velocity, Fig. 9, we had a very nice relationship among the first set of specimens, but the specimens cured at the higher temperature fell below the trend.

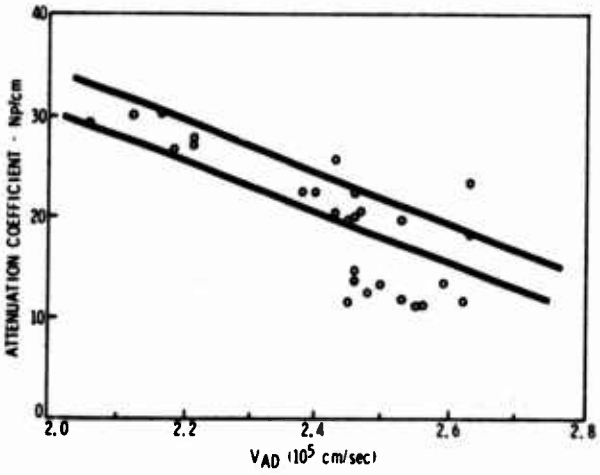

Figure 9. Experimental Relationship between attenuation coefficient and sound velocity for Chemlok 304 Adhesive

When we finished nondestructively inspecting these specimens, we strength tested them, and we got a very nice correlation between ultrasonic amplitude ratio and the maximum load sustained by the specimens before failure as seen in Fig. 10. You notice by comparing Figs. 10 and 11 that the ultrasonic amplitude ratio was largely determined by the attenuation coefficient. The alternately cured specimens did not deviate from the correlation that was set up by the rest of the specimens.

We also saw a correlation between attenuation coefficient and strength, where the two sets of points in the upper left are the alternately cured material which had much lower attenuation than the initial material.

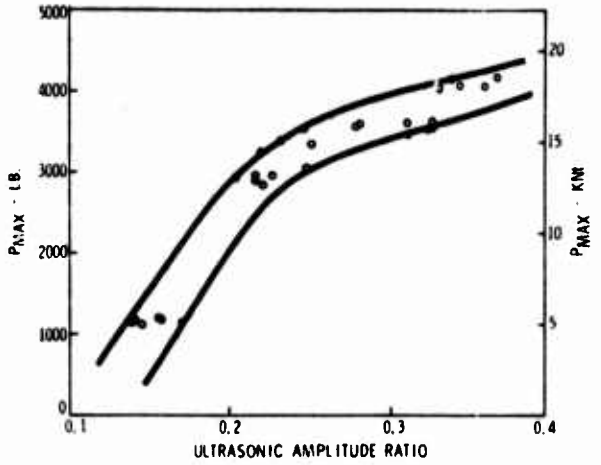

Figure 10. Experimental Relationship Between Ultrasonic Amplitude Ratio and Bond Strength in Chemlok 304 Adhesive

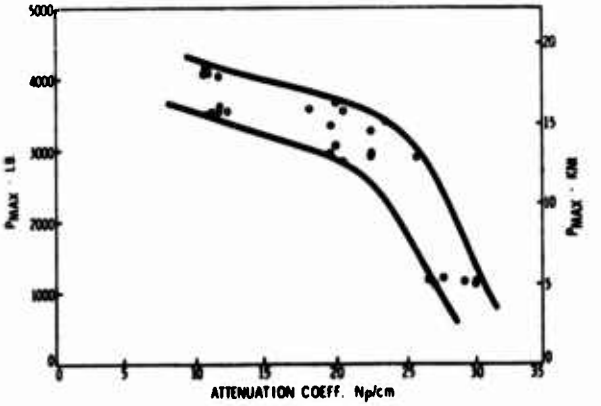

Figure 11. Experimental Realtionship Between Attenuation Coefficient and Bond Strength for Chemlok 304 Adhesive

In Fig. 12, we see the relationship that was found between the strength of the adhesive joints and the velocity of sound that was measured, and here the alternate cure ones do fall a little bit above the spread of the other data.

Considering the strength correlations seen in the time domain, we tried to look at the quality of the resonances that we measured experimentally. We did not see a correlation, and that was as originally thought from the type of relationship we had found between the velocity of sound and the attenuation coefficient.

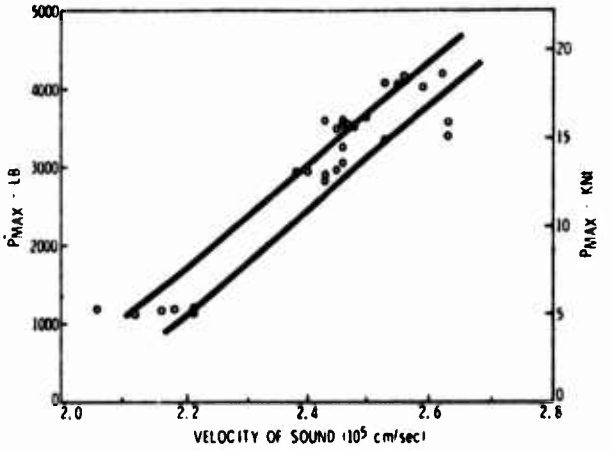

Figure 12. Experimental Relationship Between Adhesive Velocity of Sound and Bond Strength for Chemlok 304 Adhesive

To search for a meaningful parameter in the frequency domain, I took my analytically prepared code and substituted into it the experimentally derived acoustic parameters of the different adhesive mixtures. The results of this study are seen in Fig. 13. You notice that the widths of the resonances don't vary appreciably. The only thing that really is very striking is the depth of the resonances. The top curve in each box is the total amount of energy emanating from the adhesive layer, the center curve is the reflected spectrum and the bottom curve is the transmitted spectrum. The upper left box is the 2 to 3 mixture which was very soft and compliant and highly attenuating. The lower right box is the 2 to 1 mixture which was hard and had a low attenuation coefficient.

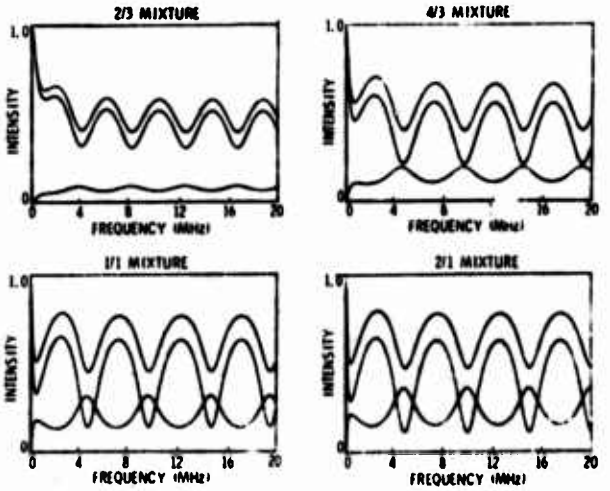

Figure 13. Theoretical Spectra Obtained Using Experimentally Determined Adhesive Properties

Seeing this relationship in the analytical work, we went back and took a closer look at some of the spectra we had experimentally generated on

these specimens. I measured the resonance depth and it correlated very nicely with the strengths of the specimens. Figure 14 shows the specimen strength plotted against the depth of the first standing wave resonance in the bondlines. Some of this scatter is due to the fact that the thickness of the specimens varied a little and the velocity of sound varied a little, so you end up having the resonances at different frequencies. And the attenuation, which is largely responsible for the resonance depth, varies quite strongly with frequency. We also looked at the depth of the second resonance, and we got a pronounced knee in the curve, as seen in Fig. 15.

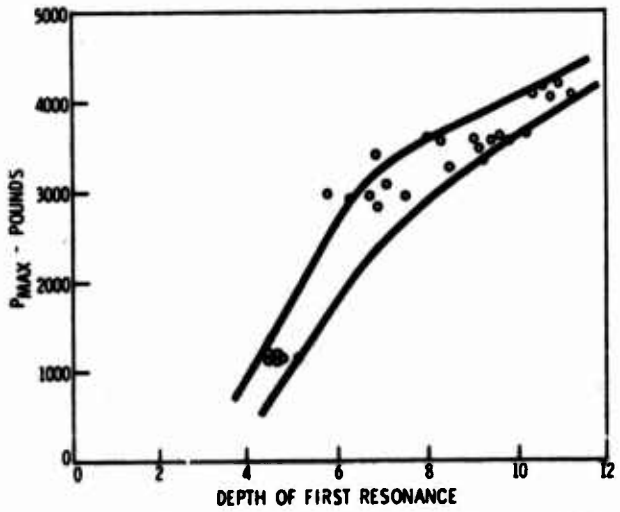

Figure 14. Experimental Relationship Between Joint Strength and First Resonance Depth for Chemlok 304 Adhesive Specimens

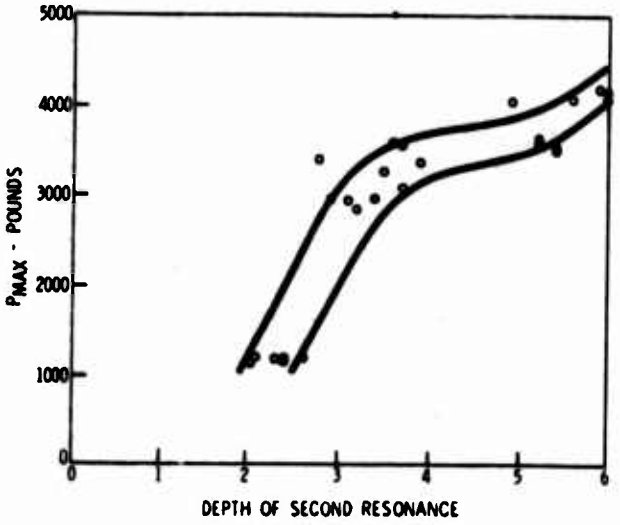

Figure 15. Experimental Relationship Between Joint Strength and Second Resonance Depth for Chemlok 304 Adhesive Specimens

In order to rectify the disparity seen between the strength and velocity of sound, we went back and looked at the stress/strain curves (actually, load/displacement curves) of the adhesively bonded joints, as seen in Fig. 16. We looked at the slope of the curves as being an indication of the stiffness of the adhesive material. Because you can draw a valid relationship between velocity of sound and stiffness, we made the correlation shown in Fig. 17. In this case, the alternately cured specimens did not vary from the scatter band set up by the initial specimen set. And if you plot the joint strength versus joint stiffness, Fig. 18, you see that the alternately cured specimen did separate out very nicely under those terms.

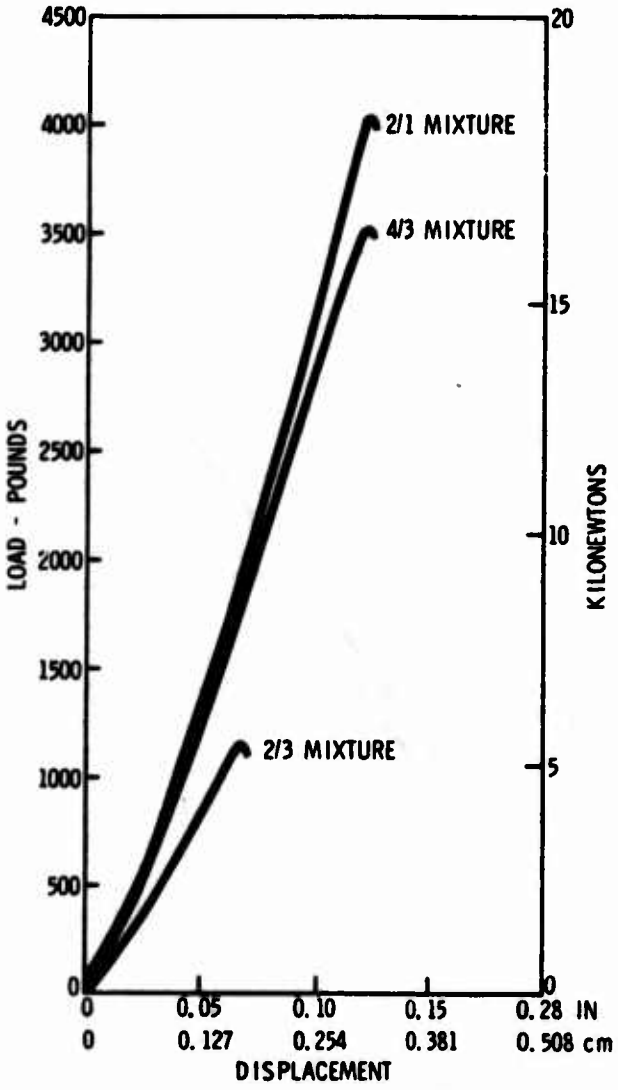

Figure 16. Typical Load-Displacement Curves for Chemlok 304 Adhesive Specimens Showing Strength-Stiffness Trend

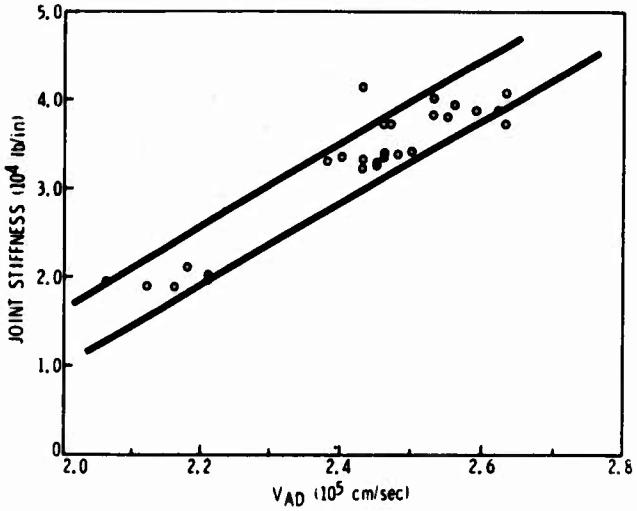

Figure 17. Experimental Relationship Between Joint Stiffness and Adhesive Sound Velocity for Chemlok 304 Adhesive Specimens

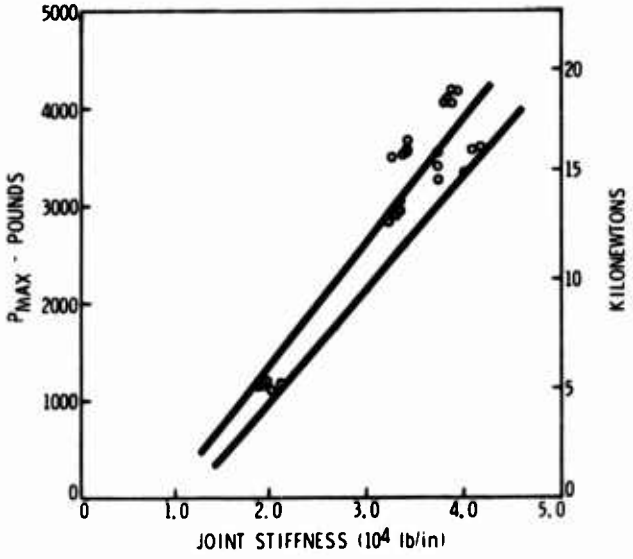

Figure 18. Experimental Relationship Between Joint Strength and Stiffness for Chemlok 304 Adhesive Specimens

I also looked at the failure surfaces generating by these specimens. The initial specimen set is represented by the three fracture surfaces on the left, and the higher temperature-shorter time cure specimens are represented by the two on the right in Fig. 19. The fracture surfaces are arranged, one side above the other, to show both sides of the fracture surface.

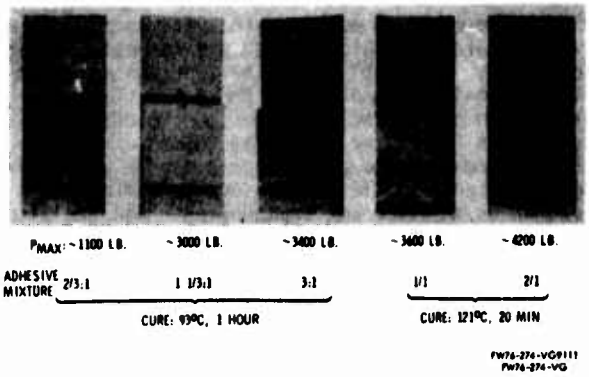

Figure 19. Fracture Surfaces of Single Overlap Specimens

The 2/3:1 mixture was a very soft, compliant, highly attenuating adhesive, and had a definite interfacial type of failure, even though the surfaces were properly prepared. We had an interfacial failure just because the adhesive was not mixed properly and thus did not have the right chemistry to enable it to cure properly and set up the right interfacial strength. The intermediate specimens, 1 1/3:1 and 1/1 in each cure set showed almost a purely cohesive failure. The adhesive ended up stuck to both of the adherends and the fracture path was directly down the center. In the higher strength materials they were not much stiffer but were stronger and had lower attenuation coefficients. The fracture started at the leading edge of the overlap in a cohesive manner as indicated by the light color, and the final fracture event was an adhesive failure as marked by the dark area in the center for both these specimens.

So, in conclusion, I would have to say that the basic finding was that the strength was most directly correlated to the attenuation coefficient of the adhesive layer, and the stiffness was most directly related to the velocity of sound.

And finally, the only thing that really keeps this analysis from practical application is the necessity of measuring the bondline thickness to extract the velocity of sound and the attenuation coefficient. This is because the sound velocity and attenuation coefficient are paired with the bondline thickness. This is true even in the analytical analysis, as was seen in Fig. 1. One hope lies in the very nice correlation seen between the attenuation coefficient and the velocity of sound in this adhesive material. If you can fully characterize this relationship and use it in your analysis, then that provides you with the extra known that relieves you from the necessity of measuring the bondline thickness in order to be able to extract the material properties of the adhesive layer and predict the strength of the adhesive bond.

Thank you.

REFERENCES

1. Lord Rayleigh, "Theory of Sound", Vols. I and II, 2nd Ed., (John W. Strutt), Dover Publications, New York (1945).

2. Brekhovskikh, L.M., Waves in Layered Media, Academic Press, New York, 1960, page 53.

3. Yee, B. G. W., Chang, F.H., Couchman, J.C., "Applications of Ultrasonic Interference Spectroscopy to Materials and Flaw Characterization,: Materials Evaluation, August 1975.

DISCUSSION

PROF. MAX WILLIAMS (Pittsburgh University): Dr. Flynn has succeeded in finishing before the bell.

DR. TENNISON SMITH (Science Center): I just wondered if in your analysis you take into consideration roughness effects?

DR. PAUL FLYNN (General Dynamics): No, I don't. You mean roughness of the---

DR. SMITH: The metal surface.

DR. FLYNN: No, I don't. I modeled the interfaces between the adhesive and the aluminum in a classical sense in that the pressures matched their displacements matched. They're much the same as most of the routine wave mechanics analysis.

MR. DAVE KAELBLE (Science Center): Paul, in your model studies, do you take into account the fact that the attenuation actually varies with frequency?

DR. FLYNN: No, I didn't. I can, but I didn't in this case.

MR. KAELBLE: It's not difficult to do.

DR. FLYNN: No, it's not at all. The way those curves were generated, you set up your reflection coefficient in terms of frequency and then iterate the frequency to plot out a spectrum, and while you're iterating, you can also change the attenuation coefficient with frequency. It plots out and draws an enevelope depending on the relationship between the frequency and the attenuation coefficient just like the experimental analysis I did.

DR. BILL BASCOM (Naval Research Laboratory): Since Tennison Smith's lap shear joints have become a standard for this conference, I wonder if he could tell us what the general composition of the adhesive is which might explain something about the heavy damping that you saw.

DR. FLYNN: I can answer part of that question. The adhesive used was the same adhesive that was used in the other part of the program. It's Chemlok 304 adhesive. Do you know what the generic makeup of that is, Tennison?

DR. SMITH: I'm going to turn to Dave.

MR. KAELBLE: I think it's an epoxy polyamyline.

DR. SMITH: We tried to pick something that didn't have any glass scrim in it, didn't have carriers and fillers and things in it, and we put three little wires in between to keep a constant bond line thickness which came out fairly close to 10 mils, plus or minus half a mil.

DR. BASCOM: It does not have dispersed rubber?

DR. SMITH: No, I don't think so.

DR. BASCOM: What happens to all of this if there is a scrim cloth?

DR. FLYNN: I can't give you any answer on the basis of the work that was done here, but in some other work that is going on in our department at General Dynamics on commercial aircraft adhesive we always have nylon or dacron scrim. You don't see the scrim in AF-147 or the filler in FM-400 for example. I'm not sure what the definite size of that glass would be, but I think the fiber would be pretty small; probably smaller than the wave length you are working with. You would have to go to pretty high wave frequencies to see it.

PROF. WILLIAMS: I want to thank Dr. Flynn for his presentation.

THE USE OF CONTINUOUS WAVE ULTRASONIC SPECTROSCOPY FOR ADHESIVE-BOND EVALUATION

M. J. Buckley
Air Force Materials Laboratory
Wright Patterson Air Force Base
Ohio 45433

and

J. M. Raney
Systems Research Laboratories, Inc.
2800 Indian Ripple Road
Dayton, Ohio 45440

The program to be described here was initiated during the past year at the Air Force Materials Laboratory. The problem of determining adhesive bond strength was undertaken with a rather brute-force approach of simply collecting the best possible data, utilizing existing ultrasonic plane-wave theory for layed structures to calculate ultrasonic spectra, and then attempting the inversion of the data to obtain the acoustic properties of the material or structure. An empirical correlation of these acoustic properties with the destructively measured bond strength is planned.

This research was initiated to determine whether, in general, continuous-wave ultrasonic techniques would provide more accurate data than conventional pulse techniques. Adhesively bonded structures were examined because they are representative of a class of inspection problems for which this technique appears particularly well suited. With this technique, the sample is considered to be a black box, just as it is in the performance of a network analysis on an electronic device. Data were collected by establishing standing waves and measuring the amplitude and phase of the transmitted or reflected ultrasound at each frequency point. The sample spectra were deconvolved with the transducer spectra to reduce the influence of the particular ultrasonic transducers on the spectra.

The experimental system is very straightforward and, in principal, much simpler than a pulse system, although this particular system is more sophisticated than absolutely necessary. As shown in Fig. 1, a signal averager is used to step a synthesizer which drives a broad-band transducer (Panametrics Model V111-HD, 1/4-in. diam.). The through transmission is measured with a Hewlett-Packard gain/phase meter. The analog output of the gain/phase meter is recorded by the signal averager and then is recorded on magnetic tape for further off-line processing. The gain/phase-meter output is the log of the signal amplitude which compresses the spectra and increases the dynamic range.

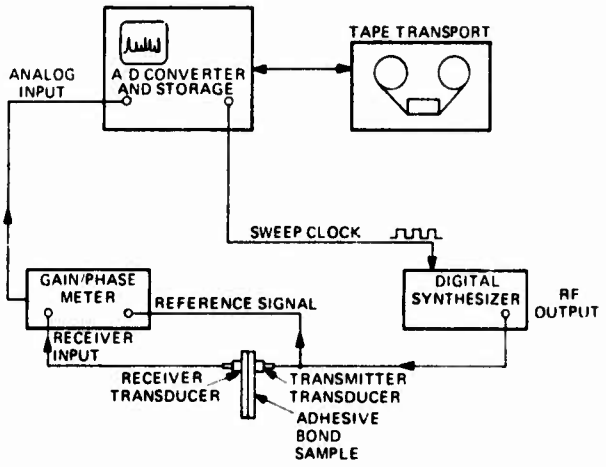

Figure 1. Continuous wave acoustic spectroscopy system diagram.

In summary, the primary advantage of this technique is that the data are taken directly in the frequency domain--the same domain in which the theoretical calculations are performed. The significant improvement in signal-to-noise ratio over that possible with pulse techniques is based upon the same premise as Vernon Newhouse's work with random signal noise methods (i.e., improvement in the on-off ratio through the use of CW versus pulse techniques may, in turn, improve the signal-to-noise ratio by as much as a factor of 1000.)[1] In addition, the frequency resolution is basically unlimited since with a synthesizer any part of the spectra can be expanded easily. Finally, the system utilizes very low power levels to excite the transducer (~ 1 V RMS), and as a result the transducer is not shock excited; therefore, less nonlinear behavior is expected.

Figure 2 shows some preliminary data taken with a solid bond. This sample, which has been used for several months, is composed of two aluminum plates, about 1/16 in. thick, bonded together with an adhesive utilizing a cloth carrier. The bond-line thickness is roughly 0.008 in. The bond-line thickness varies considerably resulting in significant changes in the spectra across the sample as the bond thickness varies. As indicated by the arrows in Fig. 2, the bond resonance occurs periodically. This spectrum has already been corrected for the transducer response by deconvolution with the transducer spectra.

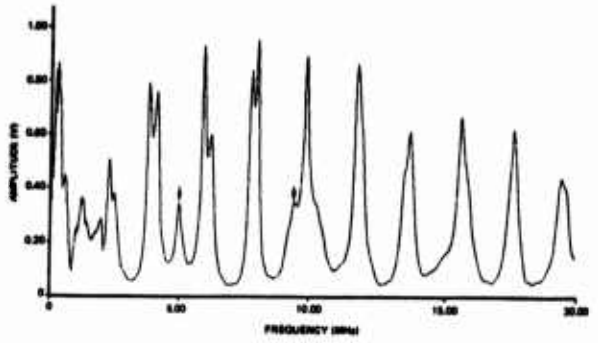

Figure 2. Deconvolved amplitude spectrum for an adhesive bond sample--data taken using oil couplant.

Figure 3 is a phase spectrum of the same sample, which by itself is not very interesting. However, the measurement of amplitude and phase response allows calculation of the real and imaginary spectra as shown in Fig. 4a and 4b.

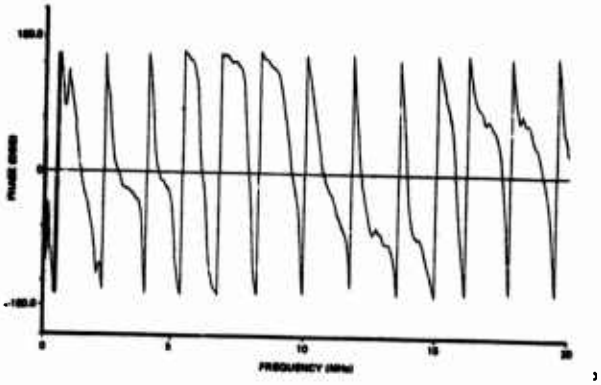

Figure 3. Deconvolved phase spectrum for an adhesive bond sample--data taken using oil couplant.

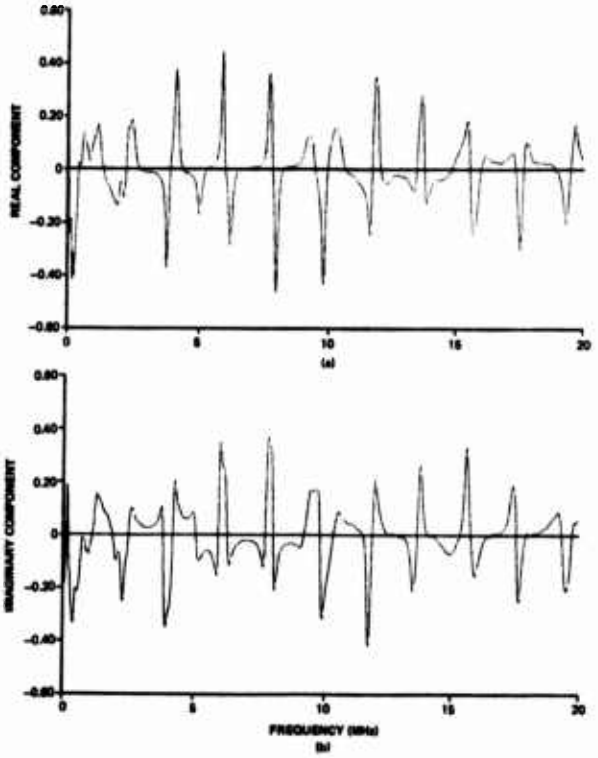

Figure 4. (a) Real component and (b) imaginary component of the complex transmitted amplitude--computed from amp/phase data.

In order to demonstrate that frequency-domain data is equivalent to time data, an inverse Fourier transform was performed, and Fig. 5 shows the type of time data obtained. These spectra actually extend to 50μsec; however, only the first 10μsec are plotted in this figure. This time spectrum has better resolution than that obtainable with the same transducers and a commercial pulse echo system.

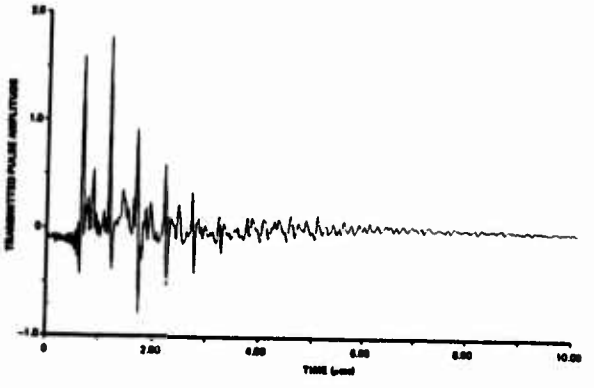

Figure 5. Inverse Fourier transform of deconvolved amp/phase data.

After a water tank was obtained, additional data were taken. Figure 6a is a nondeconvolved spectrum of an aluminum plate in water. The standing waves in the water (on the order of 3-4 kHz) were small compared to the synthesizer step size of 20 kHz and, therefore, appeared to be noise. After

FM modulation of the synthesizer signal, with a maximum frequency excursion which was less than the step size, the water peaks averaged out, leaving only the aluminum resonances, as shown in Fig. 6b.

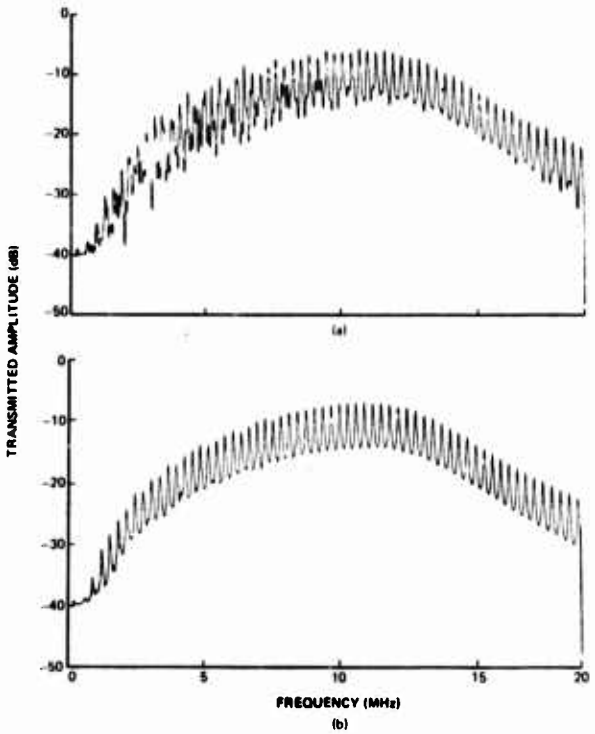

Figure 6. Logarithm (dB) of nondeconvolved transmitted amplitude spectrum for a 3/8 in. aluminum plate in water, without FM modulation (a) and with FM modulation (b).

Figure 7a shows an adhesive-bond water spectrum without deconvolution. With a correction for transducer response the spectra shown in Fig. 7b resulted. One peak goes off scale, and at first there seems to be no reason for that one line to have a transmission coefficient greater than 1. Since, in general, the aluminum plate should attenuate the sound, there should be a gain of less than one. Apparently very good impedance matching exists at this frequency, and the sound is transmitted at that frequency better than through the water bath only.

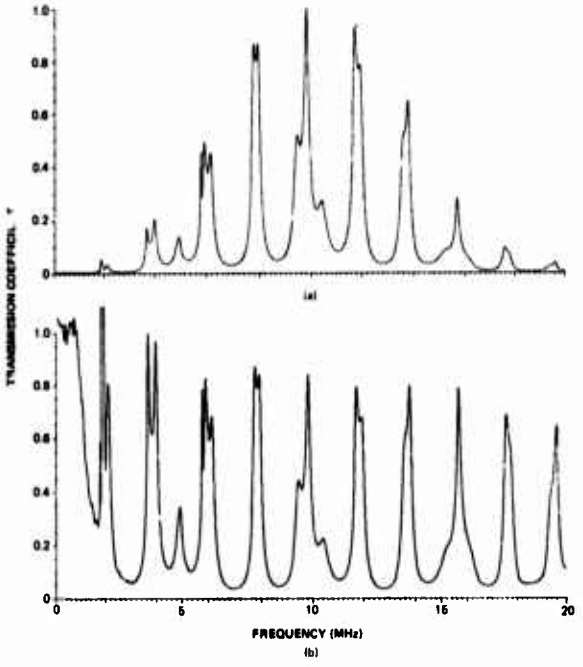

Figure 7. Transmitted amplitude spectrum at normal incidence for an adhesive bond sample in water with FM modulation, without deconvolution (a) and with deconvolution (b).

In general, although some instrumentation should be improved, we are quite satisfied with the quality of the data being obtained with the techniques. Brekhovshikh's n-layered model[2] was used for interpreting the data. Frequency-dependent attenuation terms were added to this model and necessary programming accomplished to calculate and plot the theoretical spectra. The transmission and the reflection coefficients could then be calculated for an n-layered solid in water for any frequency and angle of incidence. Each layer was characterized by seven parameters: thickness, density, longitudinal and transverse phase velocity, and three terms for attenuation--quadratic (α_2) and linear (α_1) frequency dependence as well as a constant term (α_0).

The type of transmission spectra calculated are shown in Figs. 8a through 8d. When compared with the experimental spectra in Figs. 2 through 4b, it is clear that the general features of the data have been obtained. Reflection coefficients were calculated, and the results are shown in Figs. 8e through 8h. The reflection data are theoretically "cleaner" than transmission data. Modification of the experimental system is planned in order to obtain reflection data.

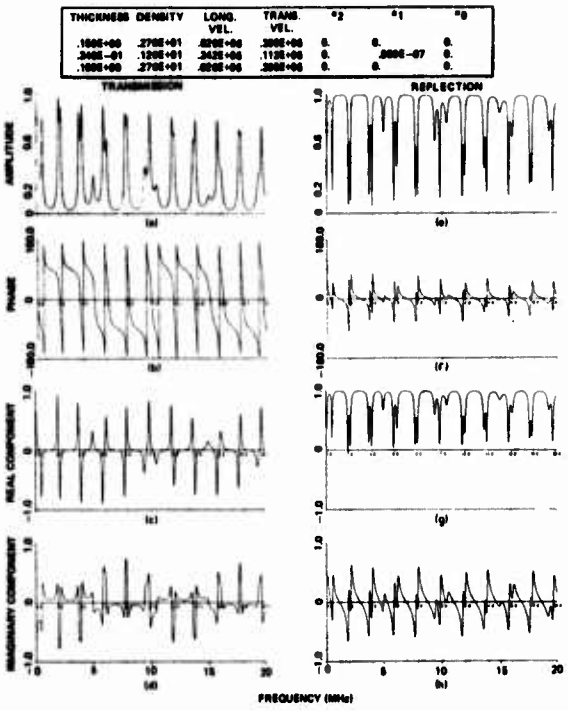

Figure 8. Theoretical spectra for a three-layer system in water. The table shows the acoustic parameters for each layer with thickness in cm, velocities in cm/sec., and linear attenuation in nepers/cm/ 2π Hz. Figures (a) through (d) are a transmission series and (e) through (h) are a reflection series.

Another interesting theoretical result can be seen in Fig. 9, which is a plot of the sum of the energy-reflection and transmission coefficients. This calculation indicates where energy is lost through attenuation. This theoretical plot includes losses in the adhesive bond only. The variation in the spectrum due to attenuation in the aluminum was very small compared to that due to the attenuation in the adhesive. The bond line peak, being a major source of loss, is accentuated significantly.

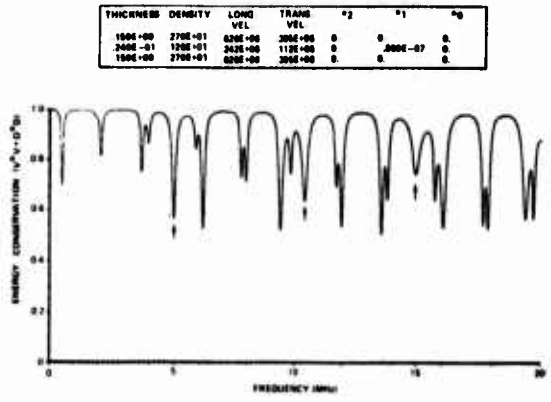

Figure 9. V*V and D*D are the energy reflection and transmission coefficients, respectively. For a conservative system the sum of V*V and D*D would be identically one, but for a lossy system this is not the case. The arrows indicate the bond line resonances.

Figure 10b is the inverse Fourier transform of the theoretical spectrum shown in Fig. 10a. Here again, the same type of time response was obtained theoretically and experimentally.

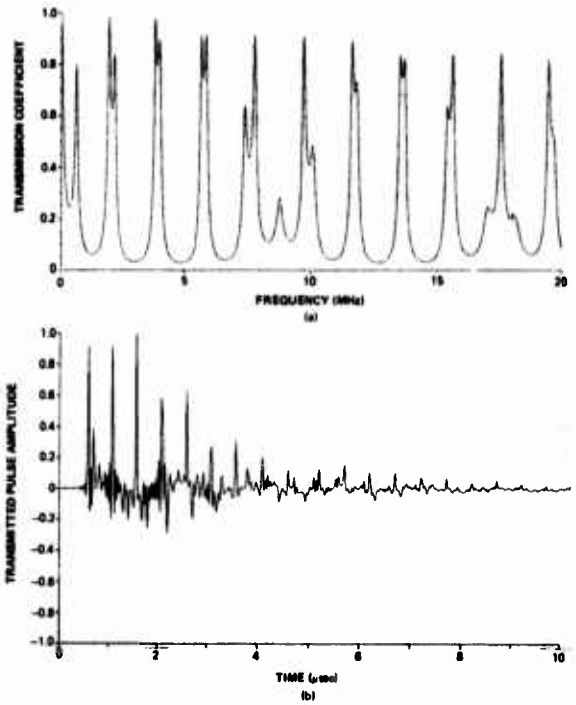

Figure 10. (a) Theoretical transmitted amplitude spectrum. (b) Time domain response resulting from the inverse Fourier transform of the theoretical frequency domain spectrum shown in (a).

Figure 11 is a sequence of transmission spectra where the bond-line thickness was the only parameter varied. Figure 11a has a bond-line thickness of ~ 0.009 in. or 0.0216 cm. The first bond-line standing-wave peak should occur at 5.4 MHz. As the bond thickness is decreased as in Fig. 11b to 0.004 in., the first resonance should occur at ~ 11.5 MHz; as can be seen additional fine structure is also calculated. A further reduction in bond-line thickness to 0.001 in., as in Fig. 11c, shifts the resonance to 23 MHz which is outside the bandwidth of this spectrum. However, at low frequency a portion of the spectra begins to resemble the spectra that would be obtained for a single plate twice as thick. Therefore, twice as many peaks are observed. Figure 11d is an extreme case for a 0.0005-in. bond line. For this bond-line thickness the first bond-line resonance would be at 92 MHz. As can be seen, it resembles a continuous structure with no bond-line resonance. Although the resonance is occurring at 92 MHz, it appears that the bond-line resonance frequency could be extracted from these data based on the trends in the spectra. The critical problem of inverting the experimental data to obtain the physical acoustic properties of the structure remains.

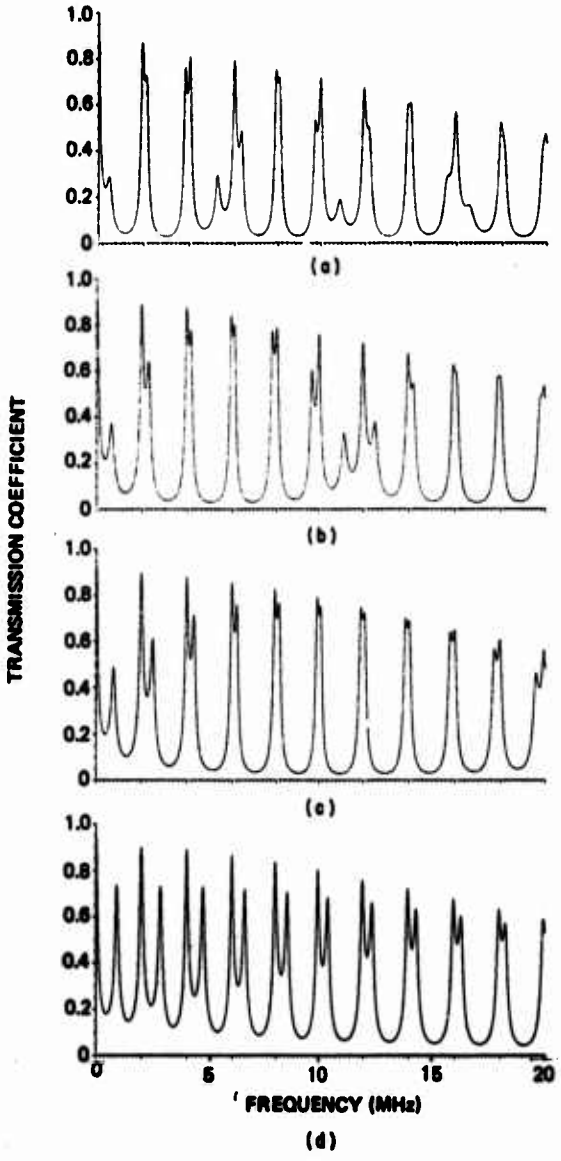

Figure 11. A sequence of theoretical spectra where only the bond line thickness is being varied. The thickness in (a) is .009 in., (b) .004 in., (c) .001 in., and (d) .0005 in.

The result of attempts to make a rough fit to experimental data is shown in Fig. 12. This bit was obtained by trial and error; however, a non-linear least-squares program is being written to accomplish this more accurately. If the least-squares inversion is successful, the result will be a system which will allow the physical acoustic parameters for an entire layered structure to be obtained. This reduced set of acoustic properties of the structure will then be empirically correlated with bond strength, a residual life, or some other engineering parameters of interest. Appropriate destructive tests for bond strength will also be performed.

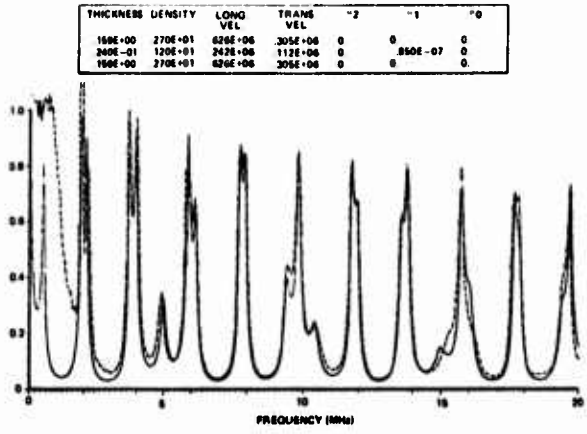

Figure 12. The dotted line indicates an experimentally obtained amplitude spectrum for a bond line sample in water. The solid line is a theoretical plot of a hand estimated fit to the data.

REFERENCES

1. V. L. Newhouse, N. M. Bilgutay, and E. S. Furgason, "Random Noise Signal Processing," in Proceedings of the ARPA/AFML Review of Quantitative NDE, AFML-TR-75-212 (Air Force Materials Laboratory, WPAFB, OH, Jan 1976), p. 343.

2. L.M. Brekhovskikh, Waves in Layered Media (Academic Press, New York, 1960), p. 61.

DISCUSSION

PROF. MAX WILLIAMS (Univ. of Pittsburgh): That was perfect. May I ask if Dr. Raney has any comments to add? Are there any questions from the audience?

DR. PAUL FLYNN (General Dynamics): You talked about that first resonance. I think that is what George called the dumbbell mode, because we have a code that deals with 6 layers. It doesn't include the attenuation but the same peaks end up in the same place; they're just in different shapes.

DR. BUCKLEY: Right.

DR. FLYNN: We have done a parametric study to look at that particular mode, and you can approximate that with spring and mass type stuff and it follows the same type of relationship. And if you bring your bond line down to zero, then you end up with just a sort of organ-type resonance-type thing.

PROF. WILLIAMS: Mike, will you handle your own questions while there is time, please.

DR. FRANCIS CHANG (General Dynamics): About the first peak, the value we calculated is different from the dumbbell model that George had, and we did those studies similar to what you did there. In other words, we changed the density of the material, changed the bond line thickness, and changed the combination of layers of bond line thickness, and we actually plot our curves showing how all those parameter changes affect that frequency of the curve peak.

DR. BUCKLEY: Well, the first peak I don't think is the dumbbell mode; I think the splitting is a function of the dumbbell mode. The first peak is a standing wave I'm talking about. And George isn't talking about the normal standing wave.

DR. GEORGE ALERS (Science Center): Yes.

DR. BUCKLEY: You are? At 300 KHz?

DR. ALERS: Right.

DR. BUCKLEY: That's a thick bond, then. Okay.

DR. CHANG: That sort of describes the difference between the dumbbell model and the layered wave calculations.

DR. BUCKLEY: I'm impressed.

DR. GEORGE ALERS: Bruce Thompson and Dick Elsley attacked this problem which we called the dumbbell mode, and Bruce calculated the stress distributions throughout the whole sandwich structure, and it's an approximation to say that the aluminum moves as a rigid body. And if you do the back of the envelope calculations for the masses and springs, you only get close to the right answer. But Dick and Bruce's programs, two different programs, predicted what that mode was and I think they came right on. Now maybe we weren't very critical about what we meant by agreement, but it is a standing wave in the total thickness, and the stress distribution in that standing wave- all the stretch-is in the adhesive and very little in the bonds, and it is the first mode you run into as you come up from zero.

DR. BUCKLEY: Okay.

DR. ALERS: I might ask Dick if he wanted to add any comments on that splitting and stuff. He has looked into that a lot more than any of us.

DR. RICHARD ELSLEY (Science Center): The usual adhesively bonded structure can be viewed as a simple harmonic oscillator at the lowest frequency with the metal adherends acting as masses and the adhesive layer as a spring. At higher frequencies, each individual layer can be viewed as an individual standing wave resonator, generating harmonically related "lines" in any graph of frequency dependent properties. However, because the layers are mechanically joined, these resonators represent coupled oscillators and each resonance then appears as a split pair of "lines". We have found it to be very instructive to graph the frequencies of all the resonant "lines" as a function of the adhesive layer parameters to display what happens when the adhesive resonances cross or interfere with the aluminum plate resonance. The result is like an energy level diagram in solid state physics complete with not-allowed level crossings and the resulting distortion of the mode frequencies in the vicinity of the crossings.

DR. BUCKLEY: Empirically you can see that and you're giving a simple explanation for a spectra that sometimes seems fairly complicated.

DR. JERRY TIEMANN (General Electric): It seems to me that when you're doing this inversion operation you should consider doing it in the time domain rather than the frequency domain, because in the time domain you don't have these subtle questions of what's causing a splitting or what mode is this or what mode is that. Each reflection comes from one well-defined surface that you can really relate to what you know about the physical shape of the object you're looking at. And if you go one layer at a time down through there, you can actually separate the problem into a whole sequence of small dimensional fits instead of one great big N dimensional fit all at once as you would have to do if you did it in the frequency domain.

DR. BUCKLEY: That's what I don't agree with. At least from our work if you take that layer and try to separate it out from the rest of the structure, i.e. make it an infinitely thick aluminum structure, that affects the time spectra, too, theoretically. It is coupled, and I don't know to what degree of subtlety we have to go in this spectra to extract the information of interest. So, again, we did take a brute force approach because it does affect it. It isn't completely separated, it does traverse the other material in going through the bond line. So, we decided okay, it does do that, we'll just handle it and avoid that problem or that question. Additionally, the question of how you set a window in the time domain and the subtleties of that to avoid any disturbances of the frequency spectra are kind of involved, at least to me they were kind of involved. So, we just said we'll just avoid that problem, also.

PROF. WILLIAMS: Thank you very much, Mike.

In concluding the Session II here, as an interloper, it's very pleasant for me to listen to the path of progress presented by you all this morning and this afternoon. However, I would like to compliment the members of the NDE community for what is a tremendous amount of progress since the last time I had an occasion to participate, like three or four years ago. Perhaps there are a few new members, and I would like to warn that there are a few alligators in the swamp. If I may be permitted the chairman's prerogative for just a few minutes, I would like to remind you of a few of these, and I don't mean to imply that there are too many and we cannot live with them.

The first goes back to a comment made last night, relating to human factors. These human factors relate to such things as we've heard recently in the Alaskan pipeline where, for one reason or another, various measurements that were thought to have been made were not made. The economic difficulty has been rather large.

A second area in human factors is more or less an apocryphal story that was told to me when I had my first baptism to the NDE fire. Measurements using ultrasonics were made on flat plates by men in the laboratory running the gauges across the flat plates watching for the perturbation of the needle. And it was told to me at that time that they had a human factor difficulty because at the time this was first introduced, the ladies in the plant were still walking through in dresses and skirts. It was quite frequent, it is alleged, that sometimes the inspectors reading the needle took their eyes off the needle giving omissions at sometimes critical points.

Now, in a serious aspect of that, that same kind of steel plate was put into a 260 inch rocket motor case at Newport News for a very large rocket motor. When it finally failed due to hydrostatic testing there was a crack one and one half inches long in a plate of MAR 18 steel over an inch thick. There was human error involved, partly due to specifications, partly due to plain missing the crack because of its orientation with respect to the ultrasonic device used. Now, these are the human factors.

The second comment I would like to make concerns the importance of the interpretation of the end result, fracture and structural integrity, the purpose for much of the work being done. I think it's extremely important that the members of the NDE community recognize that there are some alligators in the fracture mechanics swamp, too. I'll mention one. There has been much glib comment about the use of, say, Griffith's theory to determine critical flaw size. There is a dicotomy with respect to measurements and understanding of fracture in metals and to some extent polymers using the Griffith energy theory, which is supposedly straightforward.

It occurs to relatively few people that, in the ceramics business (of which we are going to hear in the next talk) the ceramics community generally speaking does not use Griffith energy theory for failure; they use vital statistics. And there's not a priori fundamental reason why fracture is fracture and a rose is a rose. Why should one not be able to interchange fracture theory energy and fracture theory statistics? But if the members of the NDE community do not appreciate that there are different interpretations and different reasons for those interpretations, you could, perhaps, get bitten by one of these alligators.

The third and last comment I would like to make is that I don't disagree with the present interpretations and procedures at all. But I would like to stress very strongly the importance that you all and we all attach to and utilize in the premise of linearity in the interpretations that we make. It's important in understanding the material behavior which most of the time is assumed to be linear and elastic. It is not linear and elastic and that affects many of the estimates that are made. It affects whether you are, perhaps, concerned with a resin, which is, first, linearly viscoelastic if you're lucky, and perhaps, if you're somewhat lucky, subject to a time and temperature shift so the temperature and frequency effects can be interchanged in an ad hoc but reasonably satisfactory region, or if you're very unlucky, a completely nonlinear material where the effects are felt most at the lower frequencies or at the higher temperature.

So, from first material aspects there are nonlinearities that bite you. There are nonlinearities that I don't know how to handle when we deal with Fourier transforms and other transforms that are bandied about in making the calculations to interpret the experimental data that will then be used as a judge on the engineering results.

So, in times of this type of difficulty, or this alligator in my analogy, I would summarize by suggesting serious consideration be given to human factors, to the proper incorporation of fracture analysis by the NDE community and third, the very proper use of linearity where justified, but to consider as a possible difficulty that introduced by nonlinearities of material and geometric types.

ULTRASONIC FLAW DETECTION IN CERAMICS

A. G. Evans
Science Center, Rockwell International
Thousand Oaks, California 91360

The work I shall be describing this afternoon is a recently initiated joint study between Stanford University and the Science Center to determine the viability of ultrasonics as a failure prediction technique for structural ceramic materials.

To put this work in perspective, I thought it would be worthwhile spending a few moments at the start of the talk describing failure prediction techniques in ceramics, in general. In many ways they are similar to those employed for metals, but there are three or four key differences, and I think that these should be emphasized.

The first point to realize is that the critical flaws are typically rather small. The reason they are small is that ceramics have a much lower toughness than comparable metallic systems. Specifically, fracture mechanics data for structural ceramic materials can be used to compute the size of the initial flaw that would lead to a failure (as a function of the stress level) assuming that 10,000 hours is the requisite component lifetime (Fig. 1). If the maximum tensile stress is assumed to be 300 MPa, then the critical flaws at room temperature range from 80 microns to about 30 microns. At higher temperatures, the critical flaws are even smaller, e.g., 10 microns for the best commercially available silica nitride at 1400°C.

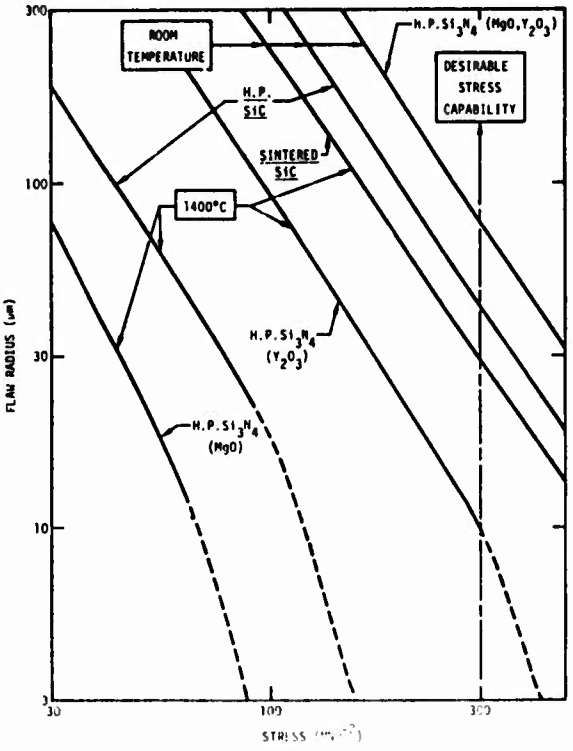

Figure 1. Maximum allowable flaw sizes in several structural ceramics, as a function of the maximum tensile stress, derived assuming a lifetime of~10,000 hrs.

The high temperature curve is dotted in the high stress regime because it has been calculated on the premise that the propagation of a pre-existing defect is analagous to that of the large crack used to obtain fracture mechanics data. However, when the flaws are on the same scale as the grains, microstructurally related slow crack can occur. In the extreme case, if the flaw is smaller than the grain size, the requisite toughness is the single crystal toughness; whereas, when the flaw is large, the toughness is given by the polycrystalline value.

The next problem arises because the slow crack growth exponents in ceramics are fairly large, which means that 90 percent of the time to failure is spent while the flaw is growing from its initial size to a size approximately 10 percent larger. There, it is indeed required to detect flaws essentially as small as indicated on Fig. 1.

The third feature is illustrated by Fig. 2; not all flaws are equally deleterious. For example, an inclusion with a lower elastic modulus and a lower thermal expansion coefficient than the matrix can be extremely deleterious; whereas an inclusion with a similar modulus and expansion coefficient to the matrix would be quite innocuous. Hence, it is not sufficient to determine the size of the defect; it is also required to determine something about its character. Otherwise, satisfactory components would be eliminated.

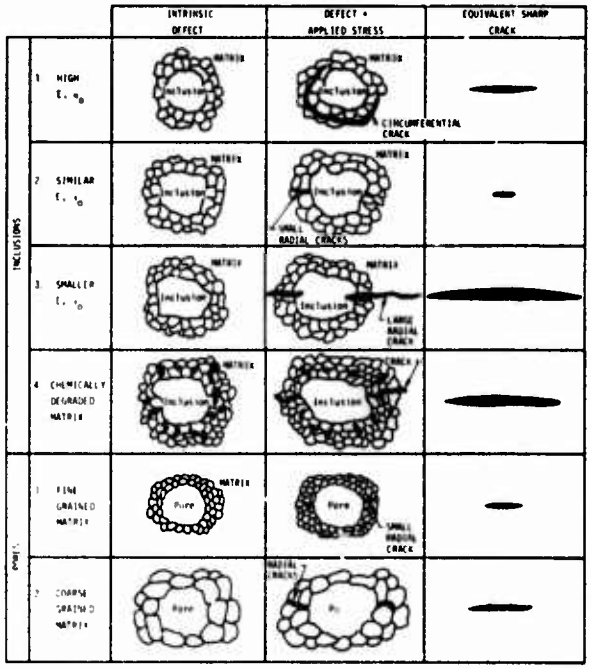

Figure 2. A schematic indicating the relative severities of typical defect types in ceramic systems.

These problems have, in the past, limited the application of ultrasonics to failure prediction, and alternate failure prediction methods have been tried first. The first technique is a statistical technique, which attempts to characterize the fracture statistics; recently a first principles theory has been developed for this purpose. The problem with fracture statistics for failure prediction derives from the large number of samples that have to be used to achieve a high confidence and a low failure probability. Also, the flaw population must be invariant from batch to batch; this is often an invalid assumption. The statistical method thus has major shortcomings.

Another approach which has been tried with much greater success is that of overload proof testing. With this approach, the component is subjected to a stress state that simulates the inservice stress state, but at a larger level than that to be experienced in service. Then, provided that it is unloaded under conditions where no additional crack growth can occur, there is an unequivocal assurance that the component will last for a specified time during service. But proof testing is limited to fairly simple geometries, and the approach cannot easily be applied to many real components. So, there is still a requirement to develop a direct flaw detection technique that is capable of detecting flaws in the pertinent size range. Of all the techniques that are available, we believe that ultrasonics has the greatest promise.

Back scattering calculations from spherical cavities in silicon nitride (Fig. 3) indicate that useful information about the size of the defect is obtained in the range $ka \approx 1$, suggesting that frequencies in the range of 100 to 200 MHz are required. Having established that high frequencies are important, it is firstly required that transducers be available for this frequency range. A pertinent transducer configuration consists of zinc oxide chemically vapor deposited onto a sapphire buffer, (Fig. 4). These transducers have center frequencies of the order of 250 MHz and a band width of 150 MHz. A short pulse is also required and the pulsing and the protection circuitry for this purpose have been developed.

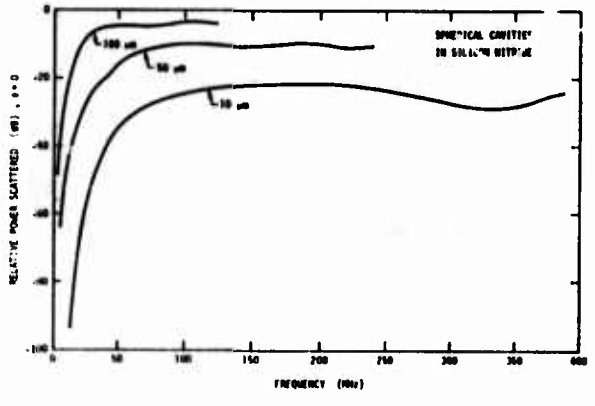

Figure 3. The backscatter cross section for spherical cavities in silicon nitride.

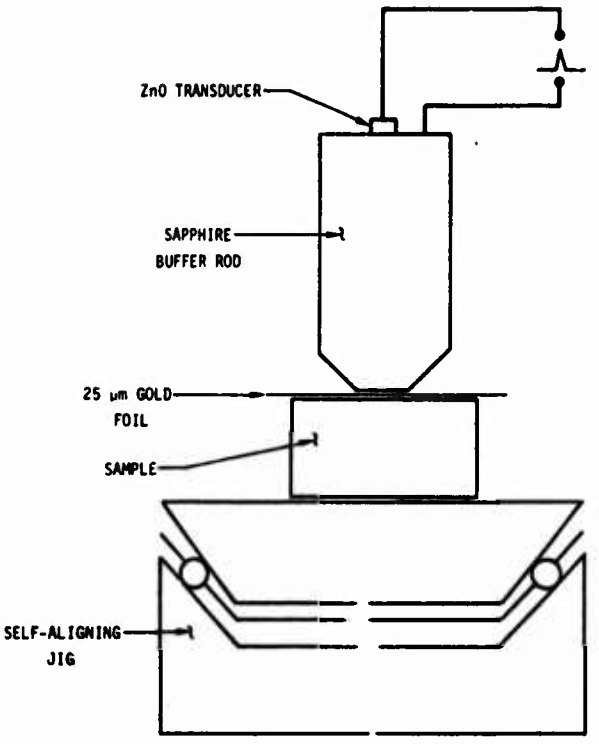

Figure 4. A schematic of the high frequency transducer system.

The next question is whether these materials are too attenuating at these frequencies. A sampling of some data (Fig. 5) indicates that in the fine grain nearly fully dense structural ceramics, the attenuation seems to be fairly reasonable up to at least 200 MHz and probably up to even 400 MHz.

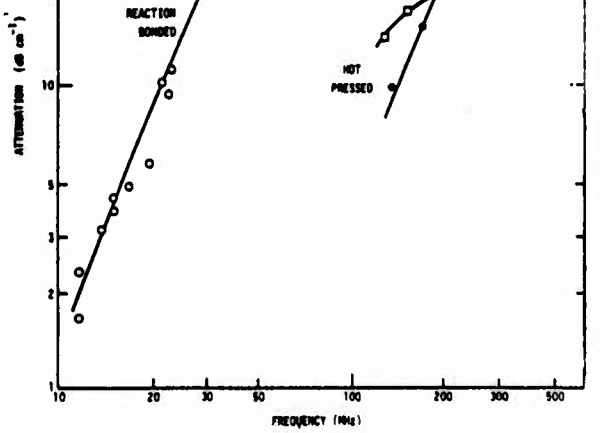

Figure 5. Attenuation data obtained for three silicon nitrides.

Having established that attenuation is reasonable, some calculations have been performed of the relative amplitude received at the transducer, as a function of frequency for typical defects in structural ceramics. From these it appears that, with the particular transducer developed in this study, it should be able to detect defects at least as small as 50 microns at frequencies at least as large as 100 MHz. These are approaching the important range.

These are just initial calculations, and experiments are needed to confirm these expectations. Initially, the depth resolution at high frequencies has been demonstrated for a 135 micron thick glass slide (Fig. 6). This indicates that resolutions at least as small as 30 microns could be possible with this technique. Next, defect studies have been performed on optically transparent magnesium oxide and on a silicon nitride block. Figure 7 shows a typical example of the reflection from small defects in silicon nitride. Note that they are well above the background. Hence, at this stage, the method looks promising, and we might indeed be able to use ultrasonics as a failure prediction technique in fine grained, fully dense ceramics; but, of course, there are two or three key steps to be explored before we can determine the range of applicability of this method.

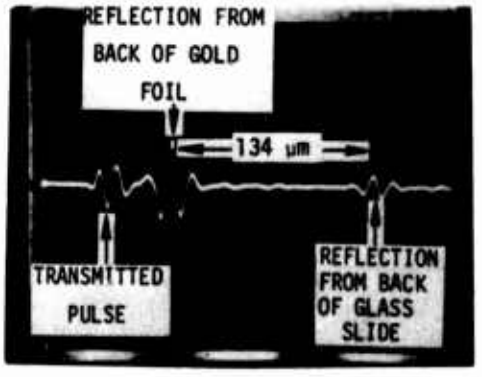

Figure 6. A demonstration of the depth reduction at 200 MHz obtained on a glass slide.

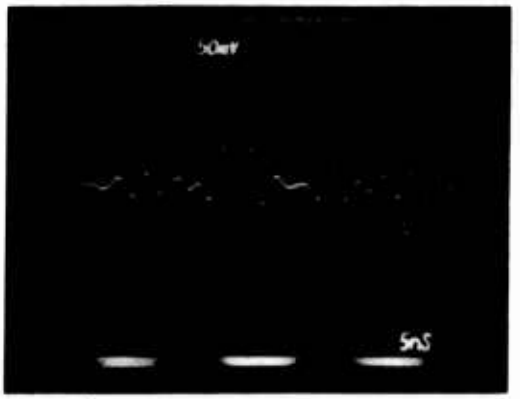

a) 125 μm Silicon Inclusion

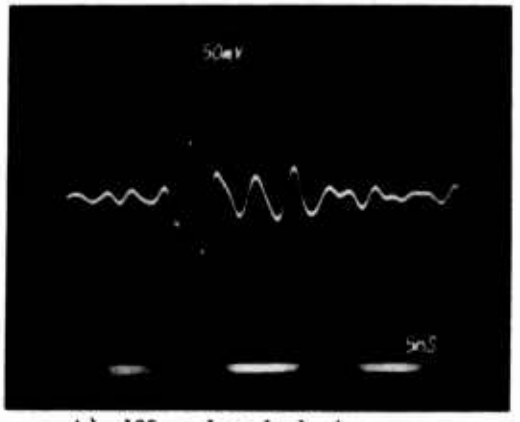

b) 125 μm Iron Inclusion

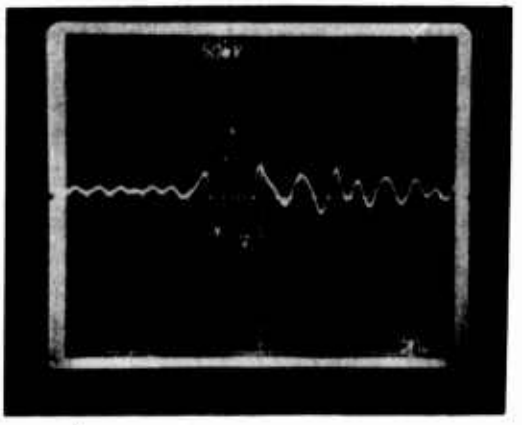

c) 25 μm Boron Nitride Inclusion

Figure 7. The scattering obtained from several defect types in silicon nitride.

DISCUSSION

PROF. JOHN TIEN (Columbia University): One of the problems with structural ceramics is that they are not pure materials; additives must be used to enhance sintering ability and, unfortunately, these become segregated at grain boundaries and the thickness of these materials may control the creep properties or strength at high temperatures. Is there any hope for ultrasound to interrogate grain boundary films?

DR. EVANS: I do not believe that existing theory tells us anything about this interaction of ultrasound with grain boundary films. However, we are preparing a series of model systems based on PZT to look at attenuation effects.

DR. PAUL FLYNN (General Dynamics): Do you anticipate any problem in detecting flaw sizes of the size you are looking at here near or on the surfaces?

DR. EVANS: Gordon Kino and Lazlo Adler have some ideas on the use of surface waves to detect surface or near surface defects, and we will incorporate these in our program.

DR. OTTO BUCK (Rockwell Science Center): Do you have a homogeneous distribution of defects within your materials?

DR. EVANS: It depends very much on the materials. For the materials of greatest interest, the defects are large inclusions and large pores, and they are randomly distributed throughout the material. But their separation is many orders of magnitude larger than their diameter. So they should be identified on an individual basis.

MR. ROY SHARPE (Harwell Labs): It may be a bit heretical in an acoustic meeting like this, but isn't it possible to detect these flaws by something like radiography? It's possible to get resolutions of that order right now, quite easily.

DR. EVANS: Radiography was one of the first techniques tried for these materials because it was a well established technique that was capable, certainly, of detecting fairly dense inclusions (such as tungsten carbide) in the 100 micron range; but it was quite incapable of detecting many other inclusions (such as silicon and silicon carbide) smaller than a few millimeters. With microfocus x-rays, the resolution is superior and defects as small as 25 microns can be resolved, but again, many of the important inclusions do not produce a detectable contrast in the appropriate (10-100 micron) size range.

PROF. GORDON KINO (Stanford University): I think the other problem with radiography is that when you get down to the root of the turbine blade, access is difficult, and I think the use of surface waves might be much easier.

PROF. TIEN: Thank you, Tony.

NUCLEAR RESONANCE FOR THE NONDESTRUCTIVE EVALUATION OF STRUCTURAL MATERIALS*

G. A. Matzkanin
Southwest Research Institute
San Antonio, Texas

It is appropriate that this presentation is in a session on new techniques because the program I will discuss this afternoon is sufficiently new that few concrete results are available to report. The program I will discuss was recently funded at Southwest Research Institute by AFOSR and involves examining the possibility of developing nuclear resonance techniques for the nondestructive evaluation of structural materials. What I hope to do this afternoon is to fill you in a bit with regard to the background involved in this program and bring you up to date regarding our research plans. I will discuss some of the experiments we hope to perform, and briefly describe a few results that were obtained in some related preliminary experiments. [1]

As I have said, the intention of this research program is to examine various NMR techniques with regard to their possibility for nondestructive evaluation of structural materials. The program will be primarily directed toward nonmagnetic materials, with interest initially centering on aluminum and aluminum alloys. It is intended that later in the program titanium and titanium alloys will also be investigated. In addition, we are expecting to look primarily at the residual stress problem in these materials. So, at least in the initial stage of the program we will be investigating the effects of internal strain and residual stress on NMR signals in aluminum specimens.

During the course of the program, we intend to pursue both conventional electromagnetic NMR approaches and acoustic NMR approaches. Participating in this program, especially with regard to the acoustic NMR aspects, is Professor Robert Leisure from Colorado State University. Besides utilizing his expertise in acoustic NMR, I believe having Professor Leisure involved in this program is important from the standpoint of increasing the participation of the university community in NDE research activities. Professor Leisure has been involved in recent years in a variety of acoustic nuclear resonance studies and is expected to contribute in this general area to this research program.

I don't want to belabor the fundamentals of NMR because most of you, I am sure, are familiar with nuclear magnetic resonance, but it might be worthwhile to take a few minutes to remind those of you who have not been exposed to this area for awhile just what is involved. In nuclear resonance we are interested in the resonant excitation of nuclear magnetic dipole moments. Figure 1 shows a semi-classical picture of a precessing magnetic moment in an applied magnetic field, H_o, where the precessional frequency, called the Larmor frequency, is proportional to the magnetic field. For most materials of interest, these precessional frequencies are in the neighborhood of 10 MHz for magnetic fields of 10 kilogauss. One achieves nuclear resonance by introducing radio frequency energy into the system at the appropriate frequency, namely, the Larmor frequency, so that there is a resonant interaction that takes place with the nuclear spin system. [2]

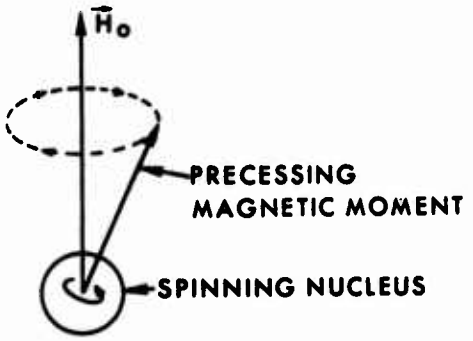

Figure 1 Precession of a Nuclear Magnetic Moment in a Static Magnetic Field.

In Fig. 2 are shown two basic experimental approaches that can be utilized for NMR, namely, the electromagnetic NMR approach whereby the energy is introduced into the specimen by means of an inductive coil which encircles the specimen, and the acoustic approach whereby the rf energy is introduced into the specimen by means of a transducer mechanically coupled to the specimen. By several possible mechanisms, the acoustic energy can couple to the nuclear spin system, and if at the appropriate frequency, can bring about a resonant interaction. [3]

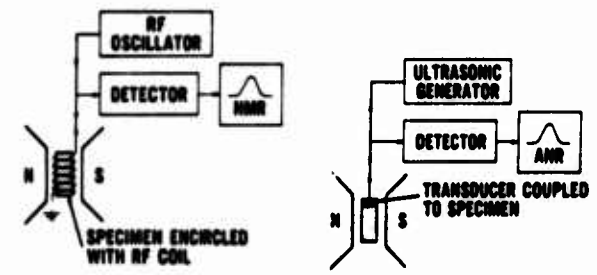

Figure 2 Experimental Methods for Nuclear Magnetic Resonance.

The electromagnetic NMR approach, while it is older and much better understood than the acoustic approach, has a fundamental limitation with regard to metals. That is, the radiofrequency fields can

*Research supported by the Air Force Office of Scientific Research (AGSC) under Contract F44620-76-C-0114.

only penetrate into the skin depth of the metal and at the frequencies normally employed, this is nominally 10 to 100 microns. So from the practical standpoint of nondestructive evaluation of metals and alloys, the electromagnetic NMR approach is limited to the surface. The skin depth problem in metals can be circumvented by the acoustic NMR approach in which the energy penetrates into the bulk of the metal. In our research program, we are intending to investigate both methods. Although the electromagnetic method is limited to the skin depth in metals, it is much better understood than the acoustic method and there are theoretical models available for the effects of strain and internal stress that can be readily applied to the results. Also from the practical standpoint, there are many instances where surface residual stresses are of interest.[4]

Figure 3 is a schematic diagram of the nuclear magnetic resonance process. Energy, either acoustically or inductively, is introduced into the nuclear spin system. If the corresponding frequency is appropriate to cause transitions between the magnetic energy levels of the system, a resonant interaction takes place and energy is absorbed by the nuclei. If the applied magnetic field, H, is varied, one observes a typical bell-shaped signal. As we shall see in a moment, it is in the characteristics of this signal where the information regarding residual stress and strain lies. So the investigation centers around a study of the effect of stress and strain on the various parameters of this signal, such as amplitude, width, shape, and frequency.

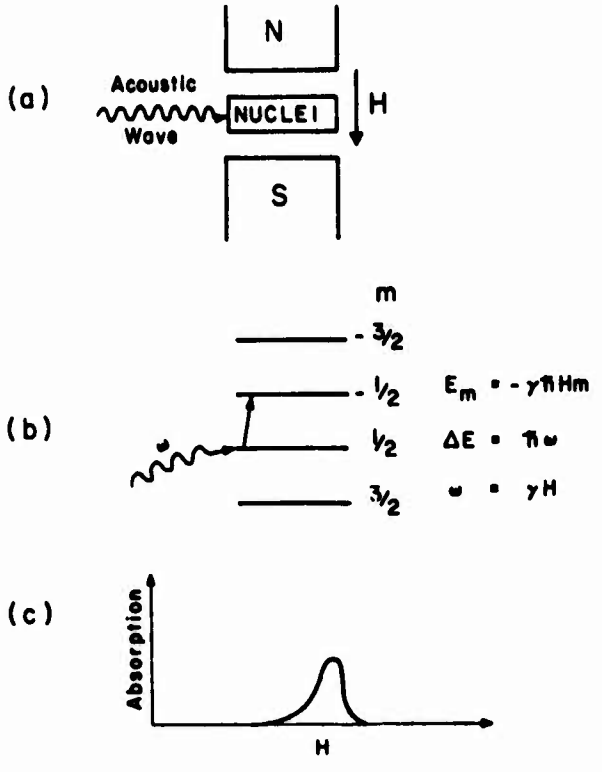

Figure 3. Schematic Diagram of a Nuclear Magnetic Resonance

The dominant physical mechanism by which residual stress and strain enter the picture, is the nuclear quadrupole interaction, shown schematically in Fig. 4. Many nuclei, in addition to a magnetic moment, also possess a nuclear quadrupole gradient set up by other ions and electrons in the material. It is by means of this interaction that information regarding stress and strain is manifested in the NMR signal. In general, the quadrupole interaction vanishes for cubic symmetry. However, even in cubic crystals, several perturbations may exist so that electric field gradients are produced. Three of these possibilities are listed in Fig. 4: (1) stress/strain fields produced by external loads or lattice defects; (2) charge difference between point defects and the host ions; and (3) redistribution of conduction electrons around a defect in the case of metals.

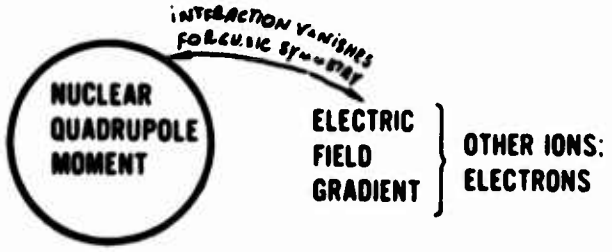

Figure 4. Schematic Illustration of Nuclear Quadrupole Interaction

Figure 5 illustrates schematically how the energy levels for a magnetic system are perturbed by the presence of an electric field gradient. The case illustrated is for a nuclear spin of five-halves which would be the case appropriate to aluminum. For a magnetic field only, the energy levels are all equidistant; however, with a quadrupole interaction present, the energy levels are shifted so that the NMR signal which would be observed in the case of no quadrupole effects is affected in various ways depending on the circumstances. The result is that the quadrupolar perturbations that are present generally have an observable effect on the various parameters of the net nuclear resonant signal.

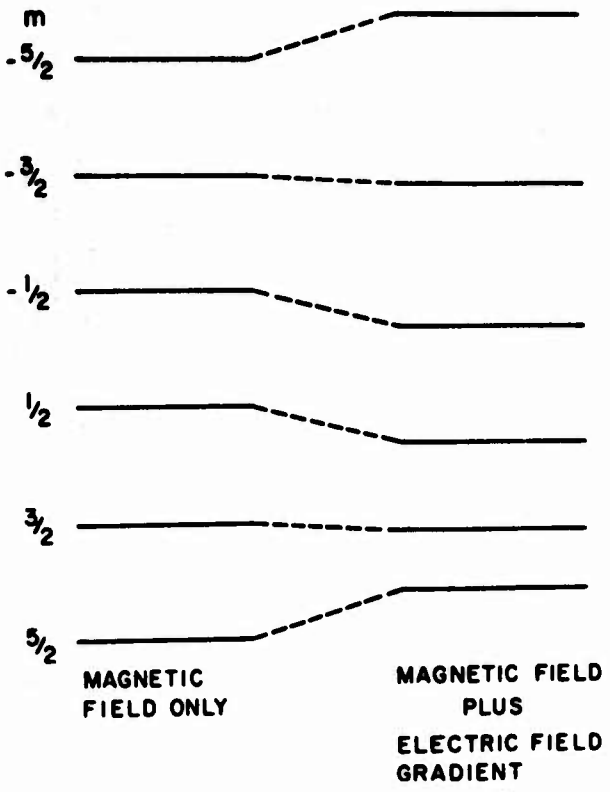

Figure 5 Energy Level Diagram of a Spin 5/2 System, Showing Electric Quadrupole Effects.

Some theoretical work has been performed by Kanert and his co-workers in Germany where they have calculated the electric field gradients due to various kinds of defects. Specifically, they have calculated the electric field gradients for point defects including both strain and valence effects; for dislocations, both screw and edge types; and for dislocation dipoles and tilt boundaries. They calculated the electric field gradient appropriate to these various kinds of defects and analyzed the way in which these electric field gradients affect a nuclear magnetic resonance signal for the case of cubic symmetry. [5]

We have performed some experiments to investigate these theoretical approaches. Figure 6 shows some of the results obtained on bulk aluminum specimens. These experiments were performed with the conventional electromagnetic NMR techniques where, as was indicated earlier, only the skin depth layer of the bulk metal specimens is sensed. The specimens were polycrystalline aluminum cylinders that were deformed in compression to various amounts. The continuous wave approach was utilized and the intensity variation in the signal was compared to the theoretical analysis provided by Kanert's approach. As is seen in Fig. 6 the agreement is quite good. These data can be examined in another way whereby the dislocation density is obtained from the measured changes in the NMR signal intensity using the theoretical development of Kanert. These results can be plotted against the flow stress for this specimen, and, as is shown in Fig. 7, the expected linear relationship is obtained.

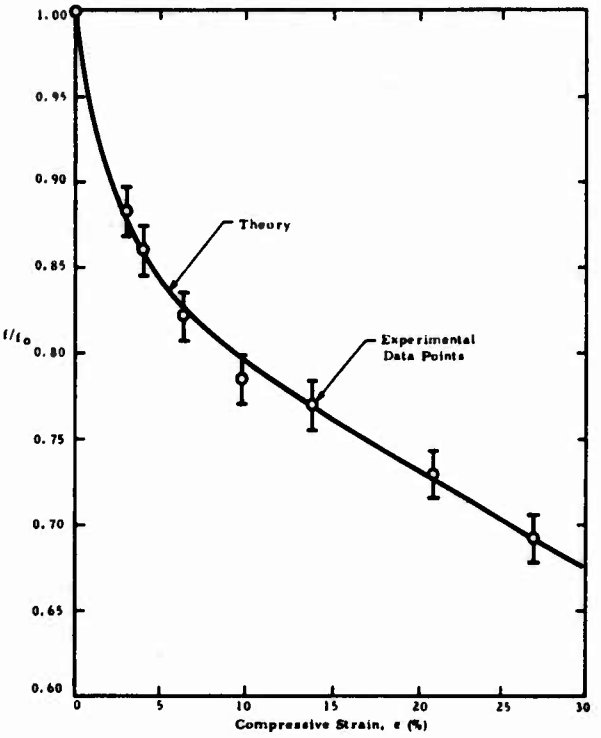

Figure 6. ^{27}Al Normalized Peak-to-Peak NMR Signal Intensity in Bulk Polycrystalline Aluminum versus Compressive Strain

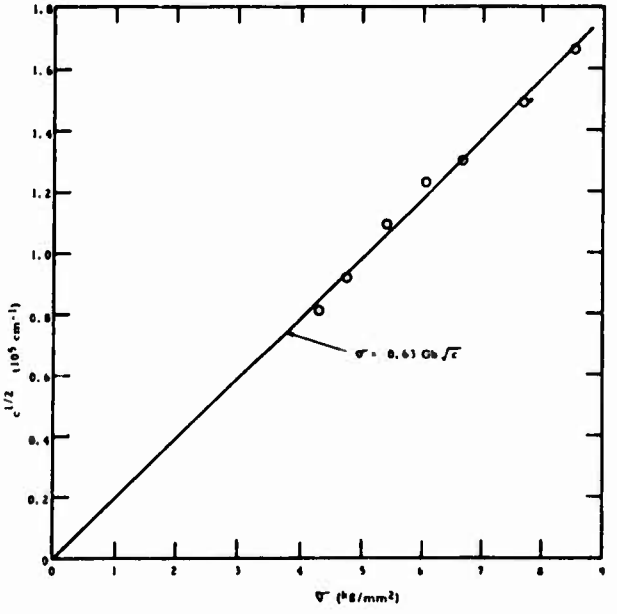

Figure 7. Square Root of the Mean Dislocation Density c in Polycrystalline Aluminum as Determined from NMR Signal Intensity Measurements versus Compressive Stress

As far as acoustic nuclear resonance goes, no studies of the effects of strain have been performed yet, but some recent work by Prof. Leisure and his co-workers illustrates acoustic NMR signals that have been observed from aluminum. [6] In Fig. 8, at the top, is shown an acoustic nuclear resonance absorption signal which was observed in a single crystal of aluminum. At the bottom of Fig. 8 is shown an acoustic NMR signal which was obtained in an aluminum-zinc alloy. The specimen was a dilute alloy of about 1 percent zinc. The observed signal was a dispersion signal, as opposed to an absorption signal, and is associated with the change in the acoustic velocity.

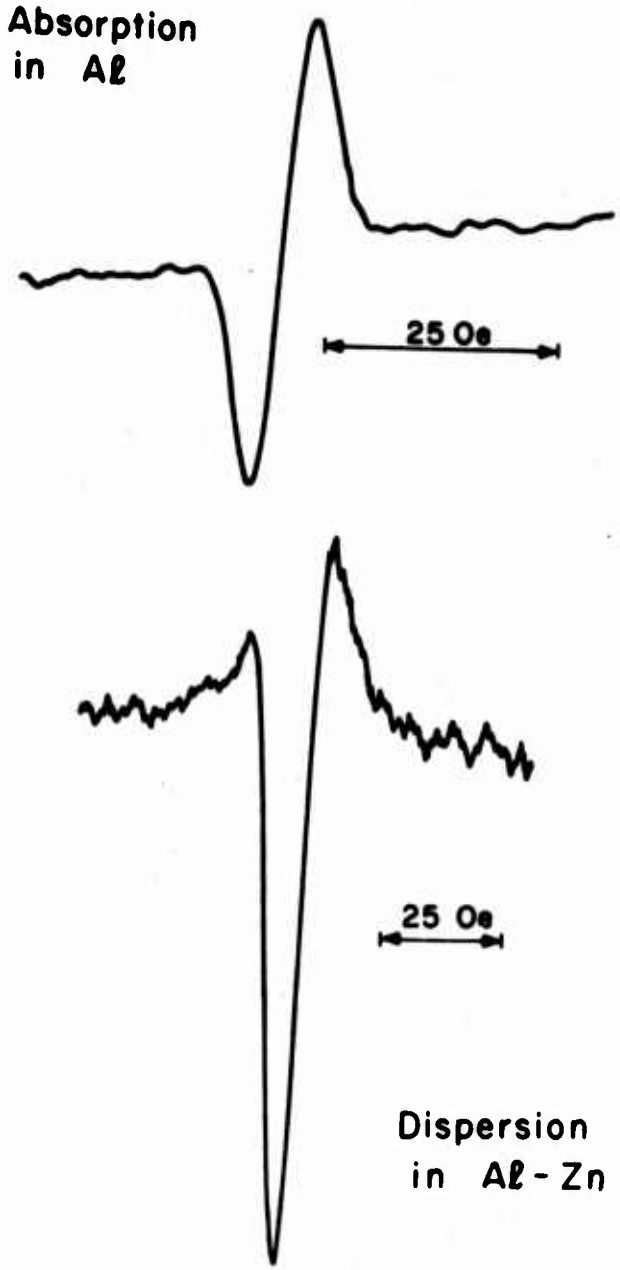

Figure 8. Representative Acoustic Nuclear Resonance Signals

Prof. Leisure has also investigated the satellite signals that appear in dilute alloys by the acoustic nuclear resonance approach. In the case of a material like aluminum, which is normally a cubic crystal structure, if an impurity such as zinc is introduced, then the aluminum atoms which are close to the zinc nuclei will feel the effects of the quadrupolar interactions and the electric field gradients which are produced in the specimen by the presence of the zinc impurities. Thus, those aluminum atoms which are close to zinc atoms will have a resonance signal separated from the main resonance which is observed for the majority of aluminum nuclei not near zinc atoms. This gives rise to the so-called satellite signals as shown in Fig. 9 (only one side of the signal is shown). These satellite signals can be associated with aluminum atoms which are surrounding the zinc atoms -- first neighbor, second neighbor, or whatever the case may be -- and thus affords a mechanism for studying the quadrupole effects introduced by the zinc atoms.

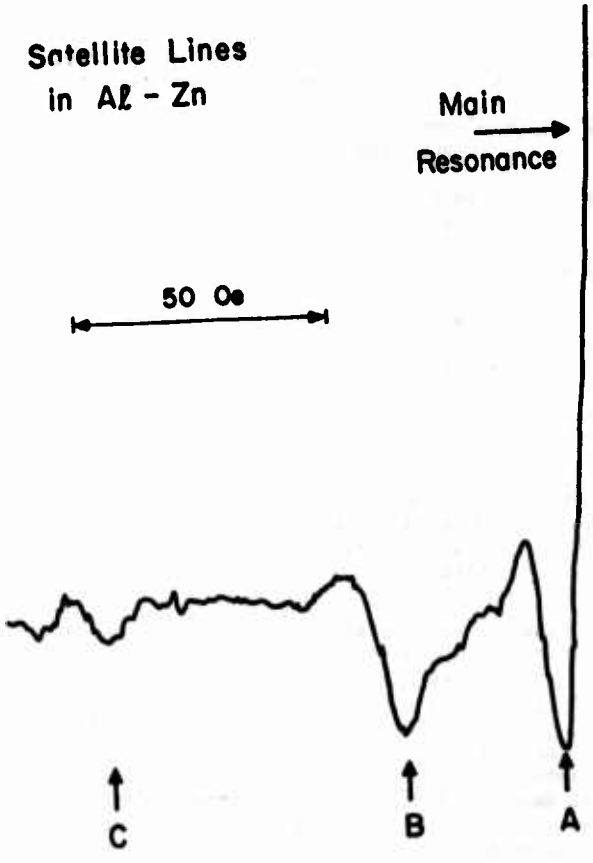

Figure 9. Acoustic Nuclear Resonance Signal from an Aluminum-Zinc Alloy

Although it will take much work to realize the potential of NMR for nondestructive evaluation, a summary of what we are hoping to accomplish in this particular program is shown in Fig. 10. The first thing we hope to do is to investigate the effects of strain using encircling coils and homogeneous fields. These will be relatively straightforward conventional NMR experiments where we will take specimens of aluminum and, using the usual encircling coil techniques, we will investigate specimens which have been strained in various ways with both applied and residual stress. We will compare the results of these experiments to the theoretical results that are available primarily from the work of Kanert and his co-workers. Within the context of this task, we will investigate the effects of strain fields on the parameters that one measures in a nuclear resonance experiment. We expect to use primarily pulsed NMR approaches where the relaxation times and nuclear spin echoes can be interpreted in terms of the electric field gradients which exist in the specimen and thus be related to strain fields.

TASKS

Task 1. Investigation of Effects of Strain Using Encircling Coils and Homogeneous Fields

Task 2. Development of Non-encircling Coil Techniques and One-Sided Magnet Techniques

Task 3. Preliminary Investigation of Effects of Lattice Strain by the ANR Technique

Task 4. Extension of Non-encircling Coil and One-Sided Magnet Techniques to Lattice Strain Measurements

Task 5. Extension of ANR Techniques

Task 6. Parametric Study for Prototype Practical Instrumentation

Figure 10. Outline of Program to Investigate and Develop NMR Methods for the Nondestructive Evaluation of Residual Stress in Structural Materials

Task 2 involves an investigation of nonencircling coil and one-sided magnet techniques. Eventually, of course, we are interested in practical application of these techniques, and therefore, one would like to be able to perform NMR experiments using nonencircling coils, where the specimen is removed from the coil, and also using magnetic fields that are somewhat less homogeneous than those available in the laboratory. So within the context of Task 2, we expect to begin looking at these possibilities. We have already done some work along these lines in another program underway at our laboratory. Although the situation is somewhat simpler, namely, detecting proton NMR signals, the success achieved using pancake-shaped rf coils and one-sided magnets indicates that these approaches are, at least, feasible.

Task 3 involves an investigation of the effects of strain by the acoustic NMR technique. Here, we will essentially be extending Task No. 2 in that some of the work performed in that task will be applied to using acoustic NMR to investigate signals obtained from strained specimens. In this task, we will initially work with relatively well understood specimens such as alkalide-halides. There has been a good deal of acoustic NMR work performed on these materials so they present a good starting point for investigating strain effects. After understanding the effect of strain on acoustic NMR in alkalide-halides, we will extend the investigation to aluminum.

Task 4 involves investigations of extensions of acoustic NMR techniques. There are several things that it would be useful to pursue with regard to the potential application of acoustic NMR for NDE purposes. Some of these we expect to pursue in this task. For example, the acoustic NMR work that has been performed so far has been on single-crystal materials. Also, we plan to pursue the possibility of utilizing pulsed techniques in acoustic NMR.

Task 5 involves incorporation of nonencircling coil and one-sided magnet techniques into the work that was done in Task 1 and 2, namely, the investigation of strain.

Finally, Task 6, a little further down the line, involves what will eventually be needed in order to bring this work to practical realization. In this task we would hope to perform a parametric study of the parameters that are needed in order to breadboard stress-measuring instrumentation for practical implementation.

REFERENCES

1. Matzkanin, G.A., "Nuclear Magnetic and Quadrupole Resonance", Proceedings of a Workshop on Nondestructive Evaluation of Residual Stress, NTIAC-76-2, San Antonio, Texas (August 1975), pp. 275-283.

2. Slichter, C.P., Principles of Magnetic Resonance, Harper and Row, New York, 1963.

3. Bolef, D.I., "Interaction of Acoustic Waves with Nuclear Spins in Solids", in Physical Acoustics, Ed. by Mason, W.P., Volume IV-Part A, Academic Press, New York, 1966, pp. 113-182.

4. Proceedings of a Workshop on Nondestructive Evaluation of Residual Stress, NTIAC-76-2, San Antonio, Texas (August 1975).

5. Kanert, O. and Mehring, M., "Static Quadrupole Effects in Disordered Cubic Solids", in NMR-Basic Principles and Progress, Ed. by Hiehl, P., Fluck, E., and Kosfeld, R., Vol. 3, Springer-Verlag, New York, 1971, pp. 1-83.

6. Seiber, F.A., Leisure, R.G., and Hsu, D.K., "Nuclear-Acoustic-Resonance Study of Electric Quadrupole Interactions and Spin-Phonon Coupling in an Aluminum-Zinc Alloy", Phys. Rev. B, 12, 4702 (1975).

PROF. JOHN TIEN (Columbia University): Thank you. We have time for a couple of questions before coffee.

DR. BRUCE MAXFIELD (Livermore Labs): Were the line widths that you showed typical line widths of the order of 10 to 15 kHz?

DR. MATZKANIN: Do you mean the acoustic NMR line widths?

DR. MAXFIELD: Yes.

DR. MATZKANIN: Yes. For aluminum that would be a typical line width. The specimen was a crystal, by the way.

PROF. TIEN: Would you put some time frame on those tasks? Are they a month apiece?

DR. MATZKANIN: I was afraid you would ask that. We are thinking in terms of about a three-year program for what you see there, for those six tasks. That, of course, is assuming that everything goes as planned and things fall together as we would like.

PROF. TIEN: Also, you keep mentioning aluminum,and I hope I didn't hear right, alkali-halides?

DR. MATZKANIN: That's right. Do you mean why did I say that?

PROF. TIEN: No. Does this NMR not like titanium or anything else?

DR. MATZKANIN: That's a good question. Titanium, of course, is something that we are interested in and, yes, you can perform nuclear resonance on titanium and it has been done. However, there are some difficulties involved, primarily the fact that the NMR frequency in titanium is very low and somewhat weaker than aluminum. For example, in a magnetic field of 10 kilogauss, the resonance frequency for titanium is only about 2 MHz. So it is very low, and it is a difficult signal to observe. There may be ways to get around this, for example, by using signal averaging techniques and pulsed approaches. It's not out of the picture. We hope to look at titanium within the context of the program.

PROF. TIEN: How about things like nickel and higher temperature alloys? Are there any material restrictions?

DR. MATZKANIN: One of the slides I didn't get to since we ran out of time listed other things that one might think of doing within the context of nuclear resonance, and one of these is ferromagnetic resonance. This is an approach that one can use in magnetic materials where the internal magnetic fields are set up internally to the materials. It would certainly be of interest to pursue these investigations for application to steels, nickel and so forth. NMR experiments have been performed on these materials; however, we have not included them within the context of this program since we have to limit the scope.

PROF. TIEN: All right, one more question.

DR. R. CLOUGH (National Bureau of Standards): Would you care to make any speculations about using X-ray or neutron excitation?

DR. MATZKANIN: In what way now? I'm not sure I understand --

DR. CLOUGH: Instead of phonons.

DR. MATZKANIN: Instead of phonons? I don't know. As far as coupling to the nuclear spin system goes, I'm not sure what mechanisms would be available to do this. I don't know of any work in that area currently going on.

PROF. TIEN: Thank you.

ACOUSTIC INTERACTIONS WITH INTERNAL STRESSES IN METALS

O. Buck and R. B. Thompson
Science Center, Rockwell International
Thousand Oaks, California 91360

It became evident at the residual stress meeting in San Antonio last year[1] that it is necessary to restate the definitions for internal stresses.[2] In general, we are talking about three kinds of residual stresses as shown in Table I. The one that's called the first kind of internal stress ranges over millimeters or centimeters (or long range internal stress) and can be identified by x-rays through a line shift. The second kind ranges over dimensions of microns and with the x-ray method gives rise to a shift as well as a line broadening. This type is usually due to particles within the material or particles of a different phase or something similar. The third kind, which ranges over 100 to 1,000 Angstroms, is a microscopic internal stress in a true sense and is indicated by x-ray line broadening only. In the following, we will be talking about the internal stresses of the third kind, due to dislocations, and later about the first kind of internal stresses.

Kind	Range	X-Ray	Examples
1st	Macroscopic (Order μm to cm)	Line shift	Elastic deformation of a cut and rewelded toroid. Thermal stresses.
2nd	(Order μm) Microscopic	Line shift and line broadening.	Particles of different phases in a matrix.
3rd	(Order 100-1000Å)	Line broadening.	Edge and screw dislocations (plastic deformation).

Table I. Classification of internal stresses.

Why do we talk about the third kind of internal stresses in connection with dislocations? I will use the elastic model of a dislocation, and for simplicity, let's just use the model of a screw dislocation, which is the simplest case that you can have. This model is a cylinder cut along the axis as shown in Fig. 1. A displacement of one of the surfaces against the other parallel to the axis (a Burgers vector) and a rewelding of these surfaces, yields a stress field that will drop off as 1/R over a range of 100 to 1,000 Å. The third kind of internal stresses is of practical importance since these are the stresses which determine the flow stress of a material during deformation and during fatigue. They also determine fatigue softening or hardening effects depending on how the dislocation structure is altered. As was pointed out before in this meeting, one would like to have a nondestructive method for determining these kinds of internal stresses since it would allow the measurement of such parameters as yield stress and perhaps even fracture toughness without destroying the material.

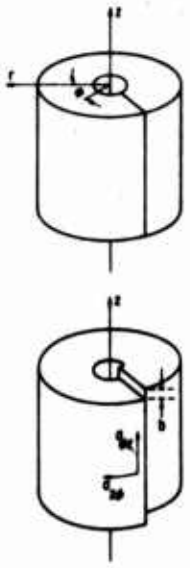

Figure 1. Model of a "screw" dislocation. The cylinder in the top part of the figure is cut along a radial direction. An offset b, as shown in the bottom part of the figure, and rewelding generates an internal stress field, given by Equation (1).

Let us define the internal stresses due to dislocations and their meaning in more detail. The model, defined in Fig. 1, yields a stress field given by

$$\sigma_G = \frac{bG}{2\pi R} \qquad (1)$$

with b = Burgers vector and G the shear modulus. R will be of the order of the loop length L of the dislocations. As has been established before,[3] one of the methods that can be used to determine the internal stresses due to dislocations is that of acoustic harmonic generation. As will be discussed later, the harmonic amplitude is a function of L and thus, the internal stress. Basically, an ultrasonic wave launched at one side of a crystal will become distorted as it travels through the crystal due to nonlinearities within the crystal. There are two nonlinear contributions to this distortion. The first one is due to the anharmonicity of the lattice. This is a very well known contribution since it is the same one which gives rise to the thermal expansion coefficient. Almost all lattices contain dislocations which bow out under stress and give rise to a nonlinearity. Both types of nonlinearities contribute to second harmonic generation [4] as shown in the next equation.

$$U_2 = U_1^2 \omega^2 a \,(\text{Lattice} + KL^2) \qquad (2)$$

The second harmonic amplitude U_2 increases with the square of the fundamental amplitude U_1 as well as ω^2 (ω being 2π times the frequency of the acoustic wave). As you can see, the higher the frequency the better the sensitivity of the measurement (our equipment operates close to 30 MHz). Furthermore, the term a is the propagation distance of the wave. The terms in the brackets are the lattice part, determined by second and third order elastic constants and the dislocation part KL^2 with L being the dislocation loop length, and K a proportionality constant.

Using Eqn. 1, and replacing R by L, we can calculate the second harmonic amplitude due to dislocations, U_{2d}. In other words, $U_{2d} = U_2 - U_{2\text{lattice}}$ is the second harmonic in terms of the internal stresses of the third kind. We find that U_{2d} is proportional to σ_G^{-2}, going back to Eqn. 1 again, or also that U_{2d} is proportional to $(\sigma - \sigma_0)^{-2}$, since[3] $\sigma_G \approx \sigma - \sigma_0$ (σ= flow stress, σ_0 = yield stress.)

Each crystal contains a certain dislocation arrangement typical of the crystal's state of deformation. In the above terms, there is a certain stress distribution (third kind of internal stresses) which is symbolized in Fig. 2. The arrangement may contain dislocation pile-ups of both negative as well as positive dislocations (determined by the sign of the Burgers vector), which gives rise to an oscillating internal stress. As you see, this stress field averages out to zero. The wavelength of these oscillations is in the neighborhood of 100 to 1,000 Å.

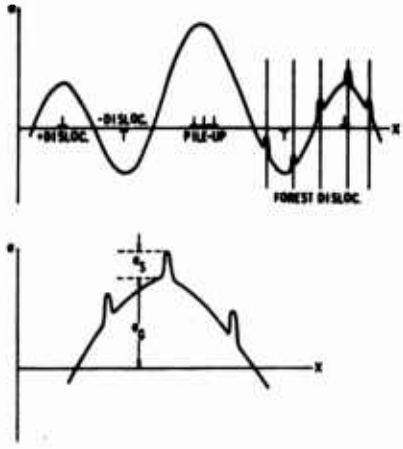

Figure 2. A dislocation arrangement, consisting of + and - dislocations as well as a dislocation pile-up generates a sinusoidally varying stress field, the amplitude of which depends on the number of dislocations in the group. "Forest" dislocations give rise to additional stress-spikes (top of the figure). A dislocation pressed against this stress field has to overcome a total stress $\sigma = \sigma_G + \sigma_s$ (bottom of the figure).

In the following, I will discuss measurements of these internal stresses by second harmonic generation. I talked about the technique last year[5] so let us just concentrate on the results. Using a virgin aluminum single crystal we expect the second harmonic amplitude to be high since the loop length L in Eqn. 2 is large (dislocation density about 10^6 cm^{-2}). As we apply a compressive stress σ which exceeds the yield stress σ_0 of the material, one expects a change in the observed second harmonic amplitude. Since the dislocation density goes up during plastic deformation, the loop length goes down. From the above discussion, we expect that with increasing deformation the dislocations will see an increasing internal stress field, indicated by a decreasing second harmonic amplitude. As shown in Fig. 3, harmonic generation indeed decreases with increasing applied stress for stresses above σ_0. Below σ_0 the situation is reversed since in the elastic range the dislocation loop length becomes larger due to dislocation bowing out under the applied stress[4]. Harmonic generation is defined in Fig. 3 as the ratio of the total received second harmonic amplitude U_2 over the fundamental amplitude U_1. U_2 is the sum of the harmonic amplitude due to a lattice contribution (U_{2e}) and the amplitude produced by dislocations (U_{2d}), as given by Eqn (2). The lattice contribution to U_2/U_1 should be independent of applied stress and has been drawn as the horizontal dashed line in Fig 3. Qualitative verification of the dislocation contribution U_{2d} to harmonic generation above σ_0 in agreement with Eqn (2) is the major point made here.

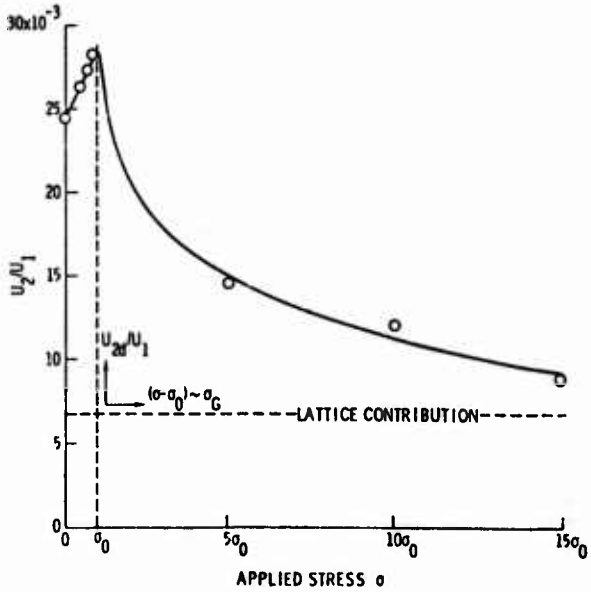

Figure 3. Normalized second harmonic displacement versus compressive stress (in multiples of the yield stress σ_0) for 30 MHz longitudinal waves along the [100] direction of aluminum. A second coordinate system has been introduced to show these data.

After the compression tests, shown in Fig. 3, the crystal was fatigued at a maximum stress level of 7.5 σ_0 and the harmonic generation was determined as a function of fatigue cycles applied to the aluminum. Since it was impossible to determine the flow stress of the material after different degrees of fatigue directly, the surface hardness was measured using a Knoop hardness indenter. Basically, the harmonic generation increased and Knoop hardness decreased as fatigue proceeded. These results are shown in Fig. 4 in the form U_2/U_1 versus Knoop hardness to demonstrate the qualitative features expected from Eqn. (2). In terms of the dislocation parameters, the result can be interpreted in the following way. The dislocation loop length in the present case is quite short prior to fatigue. Long loops develop during fatigue and yield an increased contribution to the second harmonic; thus harmonic generation reflects the internal stresses (at least within the "dislocation cells") as fatigue proceeds.

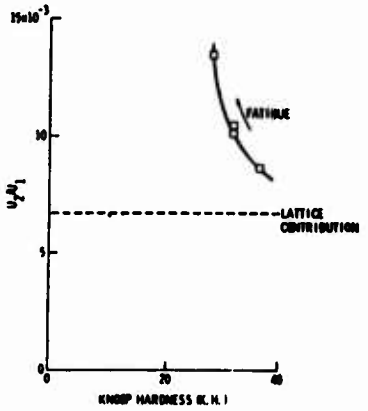

Figure 4. Normalized second harmonic displacement versus Knoop hardness during fatigue of a deformed Al single crystal ($\sigma_{max} = 7.5\sigma_0$, $\sigma_{min} = 0.8\ \sigma_0$).

Effects of fatigue on harmonic generation in the high strength alloy Al 2219-T851 were studied over a relatively wide range of maximum stress levels ($0.8\sigma_y \leq \sigma_{max} \leq 1.1\sigma_y$ with σ_y being the yield stress). The results, shown in Fig. 5, indicate that within the accuracy of the measurements fatigue of a high strength aluminum produces no systematic change in the second harmonic amplitude. To be sure that the absence of an effect was not caused by (the somewhat unusual) compression-compression type fatigue, similar experiments were performed on Al 6061-T6 fatigued in tension-compression at 20 KHz with an ultrasonic horn arrangement. Again, within the accuracy of our measurements, no change in the second harmonic was observed.

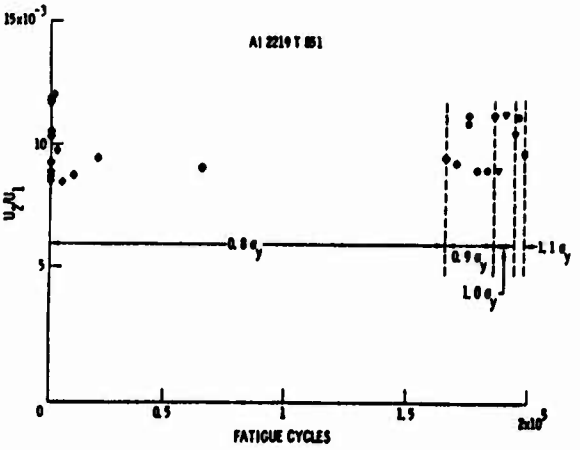

Figure 5. The effect of fatigue on second harmonic generation in Al 2219 T851 at various maximum load levels.

These results demonstrate the limitations of our present method: it is speculated that in this type of material the diffusion of interstitals at room temperature causes repinning of dislocations in aluminum, thus effectively preventing changes in acoustic harmonic generation. In materials like Ti-alloys and steels, such immediate repinning may not be expected. As can be clearly seen from the results[6] on Ti-alloys and steel replotted in Fig. 6, the generation of a second harmonic seems to be a useful quantity to determine the remaining life of the specimen. Experiments using these materials are presently underway and are aimed at understanding the responsible mechanisms of second harmonic generation of Ti-alloys and steels.

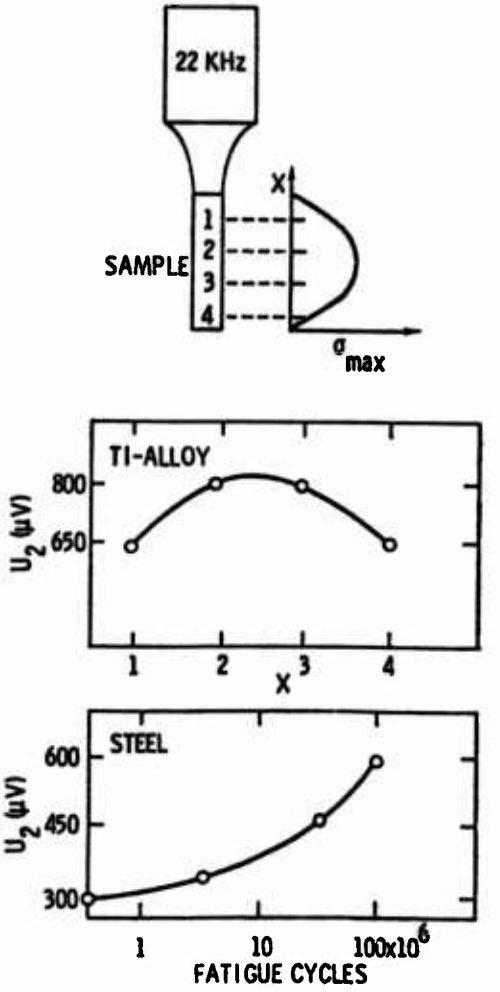

Figure 6. Top: Experimental 20 KHz arrangement to generate fatigue.

Middle: Amplitude of second harmonic (U_2) as a function of extent of fatigue (positions 1 and 4 - low stress amplitudes, positions 2 and 3 - high stress amplitudes).

Bottom: U_2 as a function of fatigue at maximum stress amplitude [after Ref. (6)].

The present results on second harmonic generation in Al and Al alloys can be summarized as follows:

(1) Theory and experiments demonstrate that acoustic harmonic generation in bulk waves could be a useful tool to nondestructively test the flow stress and the state of fatigue as long as processes are involved in which the free dislocation loop is changed. Using an Al single crystal as a model system, theoretical semiquantitative correlations have been verified. Limitations on the applicability of the method in the case of Al alloys have been studied. Alloy additions apparently repin the dislocations immediately, due to a low activation energy of motion, and no effect can be observed.

(2) In materials where acoustic harmonic generation is sensitive to fatigue, the major part of the change occurs in the very early part of the fatigue life concomitant with a fatigue hardening or softening effect. In the latter part of the fatigue life where microcrack initiation and propagation takes place (saturation stage of fatigue), changes of the bulk properties are minor so that harmonic generation is affected very little.

I'd like to describe a second way in which we are using ultrasonic waves to detect residual stresses. I'll primarily be concerned with the longer range stresses associated with bending, shot peening, drawing, or other macroscopic effects, rather than the short range microscopic stresses just discussed. My comments will be directed specifically at ferromagnetic materials. For these materials, there are a number of magnetic parameters which have already been studied as possible indicators of stress.[1] However, one set of parameters that are rather sensitive to stress, but which have not been utilized before, are the magnetostrictive properties of a ferromagnetic material. Figure 7 shows static magnetostriction data for Armco iron.[7] For zero stress, a sample first lengthens and then shortens during magnetization. However, for a relatively modest tension of 10 ksi, the initial lengthening is suppressed, and the material only shortens during magnetization. On the other hand, for a compressive stress of the same magnitude, lengthening is enhanced.

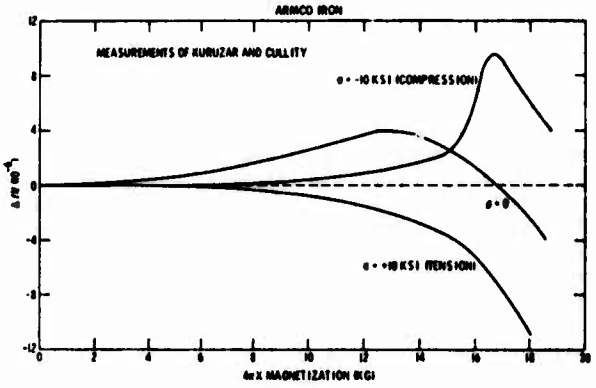

Figure 7. Changes in the magnetostriction of iron induced by tensile and compressive stress.

The differences between the three cases are striking. We have found that electromagnetic transducers for generating ultrasonic waves can be used to nondestructively measure this stress-sensitive magnetostrictive response. The detailed experimental configuration is illustrated in Fig. 8. An electromagnetic transducer consists of a meander coil carrying a dynamic current, which establishes dynamic magnetic fields in the sample, and

an electromagnet which produces a variable bias magnetic field. Such a transducer, through the magnetostrictive effect, launches an ultrasonic surface wave which is detected by any means convenient, for example, a piezoelectric wedge transducer. The amplitude of the detected wave is proportional to the differential magnetostrictive coefficients of the material and thereby is related to the stress through the physical effect that was illustrated in Fig. 7.

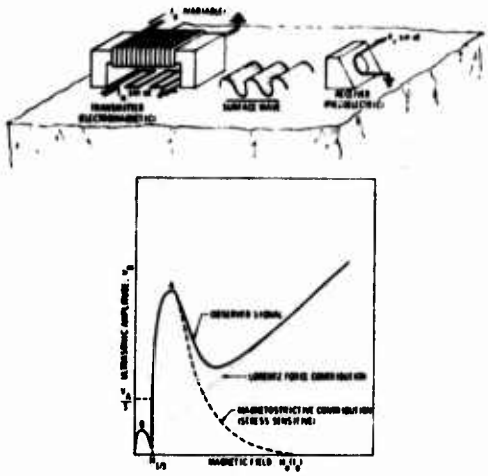

Figure 8. Experimental apparatus for determining efficiency of electromagnetic generation of surface waves as a function of magnetic field. The major features observed in ferrous materials are shown in the schematic efficiency plot below.

The bottom of Fig. 8 illustrates a typical magnetic field dependence of transducer efficiency. At high fields, there is a linear relation between the applied field and the received signal strength. This is caused by the Lorentz force generation process, which is dominant when the material is magnetically saturated. It occurs in all metals and is not of use in the detection of stress.

At lower fields there is considerable structure in the efficiency plot. The two peaks shown are typical for iron. Their origin can be explained by referring to models for transducer efficiency[8] which demonstrate that the amplitude of the generated wave is proportional to the differential magnetostriction of the material. From Fig. 7 it will be noted that there are two regions of large differential megnetostriction, one when the material is rapidly lengthening, and another while the material is shortening. These produce the two peaks in efficiency. The stress-induced changes in these features in Fig. 7 produce changes in transduction efficiency, which can be measured by an apparatus such as the one shown in Fig. 8.

Figure 9 summarizes the physics of the stress sensitivity. Recall that the orientation of the magnetic moments in a ferromagnetic body are determined, among other things, by the magnetic anisotropy energy. A three-dimensional plot of this energy for iron is shown at the top of the figure.[9] The energy is minimum when the magnetization is aligned along the cube axis, the so-called easy axes of magnetization. The energy is maximum when the magnetization is aligned along the body diagonals. The lower figure shows the anisotropy energy for particular planar cuts of this surface. The solid line shows the energy when there is no applied stress. The dotted line shows the energy when a tensile stress of 30 ksi is applied along the [100] axis. It can be seen that the magnetic energy is changed appreciably.

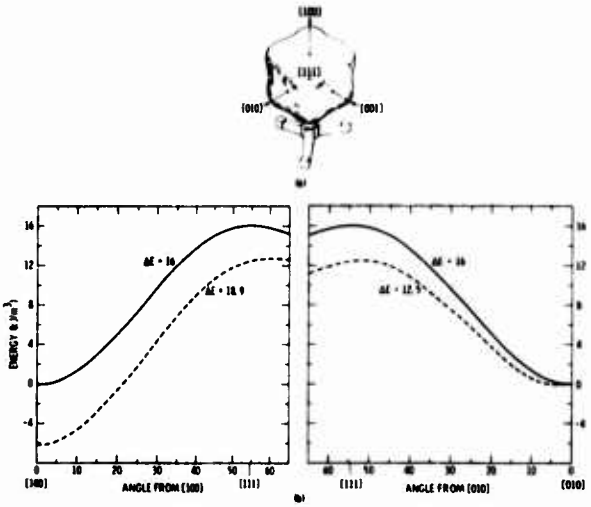

Figure 9. Anisotropy energy of iron; (a) three dimensional plot of energy versus angle, (b) planar cuts of energy surface with zero stress (solid line) and a tensile stress of 200MN/m^2 (29 KSI) along the [100] axis (broken line).

Two aspects should be emphasized. With no stress the energy minima along the [100] and [010] axes are of equal depth. This is not the case in the presence of stress, and there will be a preferential tendency for the magnetic moment to orient along the [100] axis, rather than the [010] or [001] axes. This influences the detailed distribution of domains and hence influences the magnetostrictive as well as other magnetic responses at low fields.

There is also a change in the effective magnetic anisotropy, i.e., the difference between the maximum and minimum energy points. This will influence the magnetic response at high fields, since changes are produced by field induced rotations of the magnetization against this anisotropy.

We have measured the stress dependence of the transducer efficiency in a number of materials. We have looked at three iron-nickel alloys: iron, nickel, invar. A detailed discussion is beyond the scope of this talk. However, it should be noted that the stress effects in invar and nickel are actually much larger than those in iron and carbon steel, which I am going to deal with today. Figure 10 shows the stress dependence of the transduction efficiency in Armco iron. For no stress, there is a large efficiency and a small peak B, as indicated by the solid line. When a tensile stress is applied, peak B is depressed and the rapid change in efficiency between peaks A and B moves to lower fields, as indicated by the dashed line. Conversely, the presence of a compressive stress enhances peak B, moves the rapid change in efficiency to higher fields, and changes some of the features at high fields.

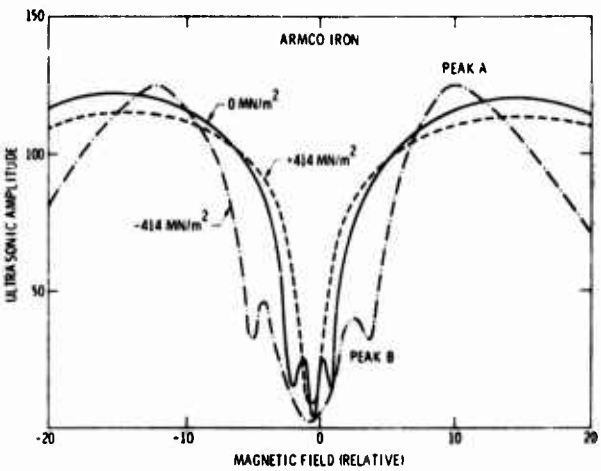

Figure 10. Efficiency plot in Armco iron for zero applied stress and calculated stresses of + 414 MN/m² (±60 KSI). The absolute magnetic field is approximately 300 Oesteds at peak A.

In order to quantitatively study the stress effects, we have defined some phenomenological parameters from the efficiency plot, as shown in Fig. 11. Here the efficiency data has been normalized so that the value at peak A is unity. The magnetic field necessary to produce an efficiency that is a certain fraction of this maximum value B is then taken as the stress sensitive parameter. For example, $H_{4/5}^{\pm}$ is defined as the magnetic field necessary to produce an efficiency that is 4/5 or 80% of the efficiency at peak A. By choosing normalized parameters in this way, the efficiency measurement is made independent of propagation losses that would lead to errors in an absolute measurement.

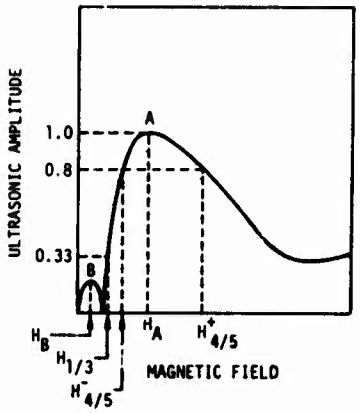

Figure 11. Definition of stress sensitive parameters.

These are rather ad hoc definitions, but they have yielded some very useful results. The variations of each of the parameters shown in Fig. 11 as a function of stress have been measured in several materials. The two most useful have been $H_{4/5}^{\pm}$ and $H_{1/3}$.

Figure 12 shows the value of $H_{1/3}$ as a function of stress for two materials: Armco iron and 1018 steel.[10] The stress was applied by bending the sample, so the tension data weretaken on a different side of the sample than the compression data. The offset in the data was caused by the presence of different residual stresses produced in the two sides of the sample by the forming process.

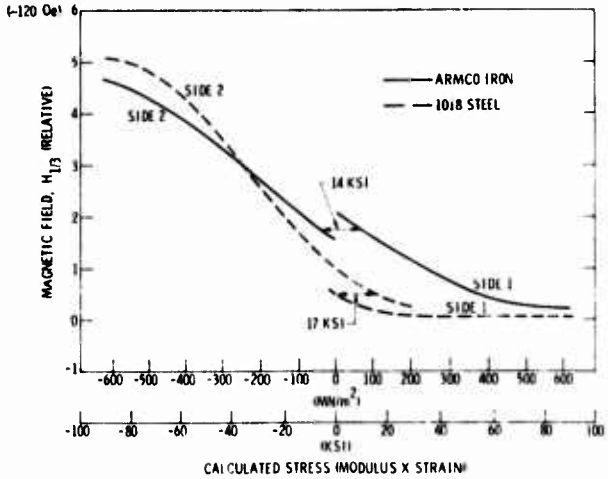

Figure 12. $H_{1/3}$ versus stress for Armco iron and 1018 steel.

The 1018 steel data here was reported at this meeting last year.[11] At that time, it was reported that the difference in stress implied by the offset in the data on the two sides was confirmed by independent x-ray measurements. Since that time, we have measured the Armco iron sample. The same basic phenomena were observed with slightly different details. In this case, however, x-ray measurements of stress were not consistent with the offset in the efficiency data. However, the x-ray data varied dramatically from point to point, and there was very heavy machining damage visible on the sample surface. It appears likely that there were rapid fluctuations of stress near the surface that were picked up by the x-rays, but not detected by the efficiency measurement which averages over a greater volume of material. (The efficiency technique senses the average stress under the transducer down to a depth equal to the electromagnetic skin depth.)

Inspection of Fig. 12 reveals that, although $H_{1/3}$ is quite sensitive to compressive stresses, it tends to be insensitive to tensile stresses. A second parameter, $H_{4/5}^{+}$, has just the opposite behavior. Figure 13 shows the variation of $H_{4/5}^{+}$ as a function of stress in two materials, A-366 steel, which is a cold rolled plate of low carbon steel, and A-569 steel, which is a hot rolled plate of the same nominal composition. In each case there is very little variation of $H_{4/5}^{+}$ for compressive stresses, but a very strong variation under tension. Two sets of experimental data are shown for each material. In one set, the stress and measurement axes were both parallel to the rolling direction, and in the second they were both perpendicular. The results for the two cases in A-569 steel were virtually identical, indicating that the effect is independent of texture in this material. This was not the case in the A-366 steel. However, one of the samples was inadvertently bent beyond the elastic limit during fabrication and hence had a built-in stress before the measurement was made. The differences between the responses of the two samples may be due to this history.

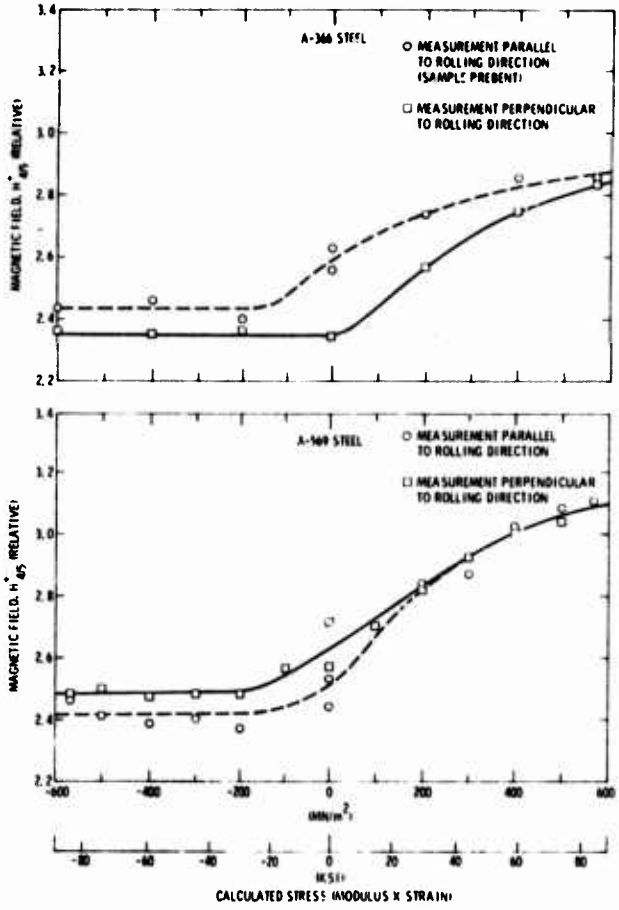

Figure 13. $H_{4/5}^{+}$ versus stress for A-366 and A-569 steel sheet cut both parallel and perpendicular to rolling direction.

Figure 14 shows the effect of rotating the direction of measurement with respect to the stress axis. For the A-569 steel, we see that both the $H_{1/3}$ and $H_{4/5}^{+}$ parameters exhibit large changes with stress when measurements are made parallel to the stress axis. However, the effect is very small when measurements are made perpendicular to the applied stress. This result should be useful in determining the axis as well as magnitude of an unknown stress.

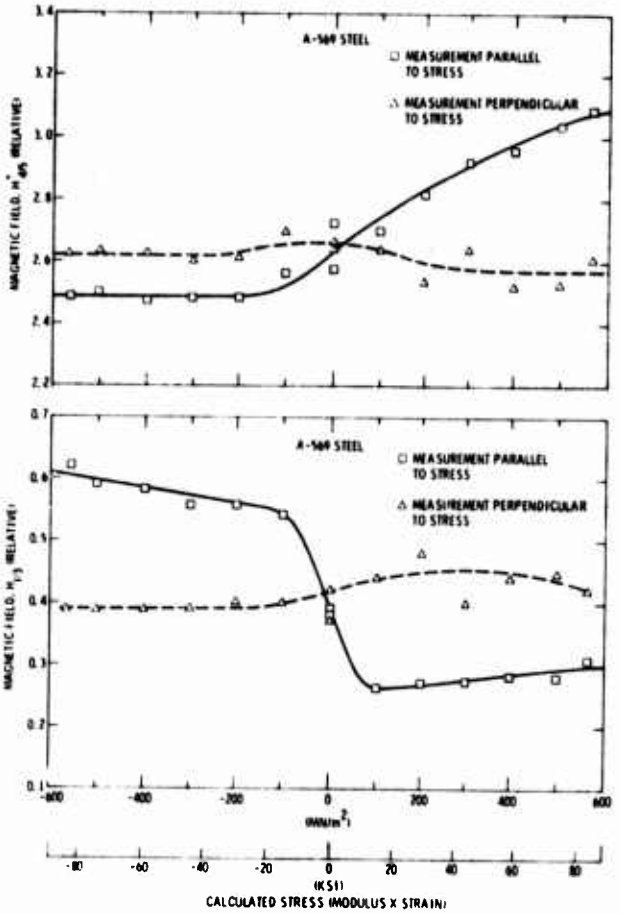

Figure 14. Effect of stress direction upon $H_{1/3}$ and $H_{4/5}^{+}$.

We have also made a number of qualitative observations which can not be reported within this brief paper. For example, the $H_{4/5}$+ parameter appears to be relatively insensitive to variations in microstructure, dislocation densities, and so forth of the material. This is presumably because the material is biassed to a point near saturation and consequently magnetic changes are essentially reversible and not strongly influenced by defects that tend to restrict Block wall motion at lower fields. Hence, this may be a very useful regime in which to measure an unknown material whose complete history and structure is not known. On the other hand, $H_{1/3}$ is quite sensitive to these effects. This appears to be somewhat of a disadvantage in the detection of stress, but may be quite useful in the detection of other important mechanical properties such as fatigue.

In summary, we have increased our understanding of the physics of the stress sensitivity of transducer efficiency; we have surveyed several materials; we have found a new parameter that we had not reported before, and we have looked at some orientation effects. Much more fundamental work is needed before we have a full understanding of this phenomena. However, the technique appears ready for development in specific applications where the material variations are well controlled.

REFERENCES

1. Proceedings of a Workshop on Nondestructive Evaluation of Residual Stress, San Antonio, Texas, August 1975, NTIAC-76-2.
2. A. Kochendorfer, Plastische Eigenschaften von Kristallen und metallischen Werkstoffen, Springer Verlag, Berlin, 1941.
3. O. Buck, IEEE Transactions on Sonics and Ultrasonics SU-23, 346 (1976)
4. A. Hikata, B. B. Chick, and C. Elbaum, Appl. Phys. Letters 3, 195 (1963)
5. R. B. Thompson, O. Buck, and D. O. Thompson, J. Acoust. Soc. Amer. 59, 1087 (1976)
6. J. V. Yermilin, L. K. Zarembo, V.A. Krasil'nikov, Ye. D. Mezintsev, V. M. Prokhorov, and K. V. Khilkov, Phys. Met. Metallogr. 36, No. 3, 1974(1973).
7. Michael E. Kuruzar and B.D. Cullity, Int. J. Magn. 1, 323 (1971).
8. R. Bruce Thompson, 1975 Ultrasonics Symposium Proceedings (IEEE, N.Y., 1975) p. 633.
9. R.M. Bozorth, Ferromagnetism (P. Van Nostrand, Inc., Princeton, 1951).
10. R. Bruce Thompson, Appl. Phys. Letters, 28. 483 (1975).
11. R. B. Thompson, Proceedings of the ARPA/AFML Review of Quantitative NDE, AFML-TR-75-212, p. 813.

PROF. JOHN TIEN: Thank you, Bruce. Would you please address your questions to either Bruce or Otto.

MR. ROY SHARPE (Harwell Labs): Did I understand you to say that your method will distinguish between stress and preferred orientation, because this obviously is the major problem in other ultrasonic methods.

DR. BRUCE THOMPSON: The experiments which I reported demonstrated little effect of preferred orientation on the data. We have to do more work to quantify this, since these experiments were performed on a single alloy. We have not constructed the pole figure as yet to say in detail what the texture was, but I think we can assume there was some significant preferred orientation in that material. The results are quite encouraging.

PROF. TIEN: Otto, I have a question on your aluminum data. I guess you are saying what messed it up is the fact that diffusion was too fast?

DR. BUCK: Yes, that's what I believe has happened.

PROF. TIEN: So, you still see success if you went lower in temperature?

DR. BUCK: That is quite possible.

PROF. TIEN: So, consequently for any other material, if you go high in temperature, it might show up again.

DR. BUCK: That's right. The results should depend on the diffusion energy.

PROF. TIEN: That is interesting.

RECENT ADVANCES IN THE MEASUREMENT OF RESIDUAL STRESS BY X-RAY DIFFRACTION

M. R. James
Northwestern University
Evanston, Illinois 60201

I was asked to come here and give an educational overview talk on the recent work that has been done in the x-ray residual stress area and some of the reasons why it is not always accepted as a valid technique. The main problem that we have to look at is that when anyone measures macroscopic residual stresses, by whatever method - mechanical techniques, x-ray techniques, ultrasonic techniques- one is always measuring a different property of the material and trying to relate that to the macroscopic residual stress. There is no reason that residual stress must be the same for all these particular techniques. People get upset when the x-ray technique does not coincide with mechanically measured values, but there are definite reasons why it doesn't, and I want to go through some of those reasons. Measurements of residual stress by x-ray is a diffraction technique - it's not a radiography technique. I want to go through the principles very quickly and then emphasize some of the recent instrumentation advances developed in the last couple of years. Then I want to use the remaining time to discuss the situations where the validity of the x-ray technique is sometimes questioned.

Metallic materials in industrial use are in general aggregates of polycrystalline materials with different orientations. The x-ray diffraction technique obtains information only from those crystallite lattice planes which are oriented to satisfy the Bragg condition of diffraction. The first thing this means is that it is a selective technique. We're only measuring information from certain lattice planes in the crystal, and we're trying to relate the strain from those lattice planes to a bulk residual stress on the surface of the sample.

In Fig. 1 we see that the incident radiation diffracts from more than one set of grains, but the same crystallographic lattice planes, because the grains are oriented differently within the polycrystalline material. Now, what this allows us to do is change the orientation of the incident radiation, as in Fig. 1b, and examine the same hkl planes now oriented differently with respect to the stress direction. Using Bragg's law, given in Fig. 1, we can correlate this angle of diffraction with the interplanar spacing, and because we have a change in the interplanar spacing between the two inclinations of the sample due to the resultant stress component on each of the lattice planes, we have a resultant shift in the diffraction angle.

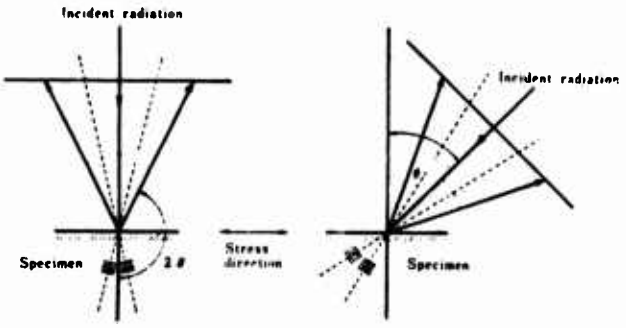

$$\lambda = 2d\sin\theta$$

$$\frac{\Delta d}{d} = -\cot\theta\,\Delta\theta$$

Figure 1. Principles of x-ray residual stress measurement

To show exactly what is done in the x-ray technique we normally measure the interplanar spacing, usually signified by d, which is parallel to the surface. Then we can either rotate the sample or we can rotate the x-ray beam and measure the planes at an angle, ψ, with respect to the surface. From the change in interplanar spacing we have a strain which can be related to the stress.

Because the x-rays only penetrate the surface of the material to a shallow depth of, say, 25μm or so, we're only going to get a surface residual stress. Also, because of the selective nature of the x-ray diffraction technique, the gauge length we're talking about here is just the interplanar spacing of the crystallographic planes.

In order to get the stress component from the strain, we have to make various assumptions. The first is that on the surface of the specimen we have a biaxial stress, which is reasonable, because we can't have a stress normal to the surface of the material and we're only looking at a shallow depth. The second assumption we make is that it is a homogeneous material, or at least if we're looking at one phase, that it is uniform. The third assumption, and this is the one that gets us into trouble, of course, is that isotropic elasticity applies. It's really not a bad assumption, because we are looking at a lot of grains in the surface of the sample. However, when preferred orientation is present, the anisotropic nature of the grains complicates the situation, but we will deal with this later.

Figure 2 shows the coordinate system we're talking about. ψ is the angle between the normal to the diffraction plane and the normal to the sample surface. We want to determine the stress, σ_ϕ, in the direction given by ϕ. Stress is a tensor and dependent on direction, so we arbitrarily define ϕ as an angle from one of the principal axes. Normally, we don't know what ϕ is; we just say we're looking at the longitudinal stress or the tangential stress or so forth.

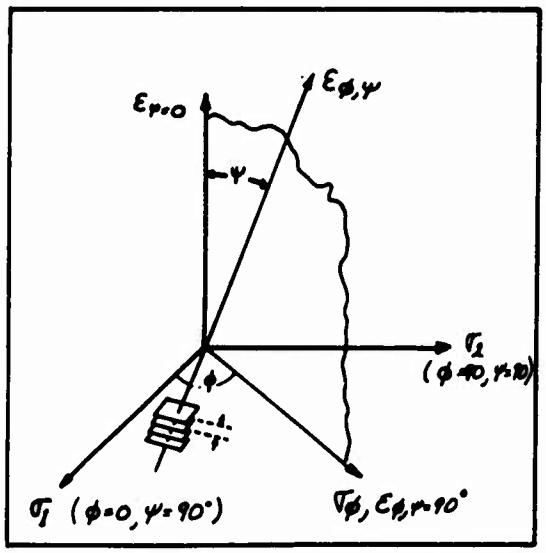

Figure 2. Illustration of symbols used in x-ray stress measurement.

I don't want to spend any time on the derivation of the equations used in residual stress techniques, they are found in numerous textbooks, but I do want to emphasize some of the points the equations imply. The relation between the stress and strain is given in Fig. 3. The first equation forms the basis for the so-called 'sin $^2\psi$' method of x-ray residual stress analysis. The terms $s_2/2$ and s_1 are the x-ray elastic constants. Now, if isotropic theory really applies, then it can be shown that these x-ray elastic constants are functions of the bulk mechanically measured values. This isn't always true because the isotropic theory doesn't always apply, so a lot of times we actually measure these values.

$$1)\quad \varepsilon_{\varphi,\psi} = \frac{s_2}{2}\sigma_\varphi \sin^2\psi + s_1(\sigma_1+\sigma_2) = \frac{d_{\varphi,\psi}-d_o}{d_o}$$

$$2)\quad \frac{S_2}{2} = \frac{1+\nu}{E} \qquad S_1 = -\frac{\nu}{E}$$

$$3)\quad m^* = \frac{\partial \varepsilon_{\varphi,\psi}}{\partial \sin^2\psi} = \frac{1}{d_o}\frac{\partial (d_{\varphi,\psi})}{\partial \sin^2\psi} = \frac{S_2}{2}\sigma_\varphi$$

FROM 3 $\qquad \sigma_\varphi = m^* / \frac{S_2}{2}$

Figure 3. Relations between stress and strain.

The important feature of this equation is that if we plot the strain versus $\sin^2\psi$ at a number of inclinations, then that line will be linear, it will be straight, and we can get the surface stress, σ_ϕ, just from calculating the slope and knowing the elastic constants.

Now, the fact that there is a linear relationship between $\sin^2\psi$ and the strain allows us to use what is normally called a two-tilt technique. We assume a straight line; therefore, we only need to measure the interplanar spacing at two particilar ψ inclinations. We can go even further and make another simple trigonometric substitution and we get the peak shift, the change in the Bragg angle related to the surface stress σ_ϕ, as given in Fig. 4.

TWO TILT METHOD

$$\sigma_\varphi = \frac{E}{1+\nu}\frac{1}{\sin^2\psi}\frac{\cot\theta}{2}(2\theta_o - 2\theta_\psi)$$

$$= K\,\Delta 2\theta$$

$$\text{where } K = \frac{E}{1+\nu}\frac{1}{\sin^2\psi}\frac{\cot\theta}{2}$$

Figure 4. Expression for σ_ϕ

In this case, the cotangent θ is a slowly varying function of θ so we can lump all of this into one term and call it the stress constant, K. This stress constant can be measured for the particular material that one is looking at. The two-tilt method is easy, especially when doing the measurement by hand, but the $\sin^2\psi$ method is more accurate.

Now, how is this measurement accomplished? Years ago it used to be done with film techniques; now it is normally done on a diffractometer in the back reflection region so that instrumental errors and systematic aberrations are minimized. We determine the profile of the diffraction curve and use curve fitting procedures to determine the actual peak location. By hand, this measurement now, normally, takes from a half an hour to an hour and is rather tedious, a very boring type of measurement, so computer applications have come in very handy. At Northwestern we've developed a completely automated package allowing for complete optimization of data collection. The measurements now take anywhere from five minutes to, say, half an hour depending on the statistical accuracy that the operator desires. The program includes sample alignment and either the two-tilt or $\sin^2\psi$ methods. However, the real instrumental improvements in the past few years have tended towards dedicated x-ray stress analysis devices, such as the fast stress system manufactured here in the United States,[1] and the Strain Flex[2] unit manufactured in Japan. These types of units enable stress measurements to be done in 1 to 5 minutes, but only at an accuracy, at best, of plus or minus 3,000 psi, probably more like 6,000 or 7,000 psi. They are reasonably expensive, the initial cost is $60-$65,000 and they suffer from the fact that they are not very flexible and are definitely not portable.

At Northwestern, we are completing work on the feasibility of applying a position sensitive detector to the measurement to improve the speed many times over[3]. The detector simultaneously records the entire diffraction profile without any movement. Figure 5 depicts a typical profile obtained from a mild steel sample in 60 seconds. The spatial resolution, that is, the resolution along the length of the detector, is about 180μm.

Figure 5. 211 diffraction peak from SAE 1045 sample.

We simultaneously collect data across the entire diffraction profile, therefore not wasting time collecting data point by point over the profile. The data is stored in a multichannel analyzer and then the profile is dumped to a computer. Curve fitting techniques are used to define the peak position, and while the computer is typing a report, we're accumulating data from the next ψ tilt, and so on. This is a commercial detector, by the way, and can be bought on the market right now. The packaging arrangement isn't very good and we're trying to get the commercial manufacturer to repackage it in a different form so it's about the size of a pocket dictionary so that the pre-amplifiers are actually in back of the detector. We're combining this detector with a new light-weight air cooled portable x-ray tube. The unit is 6 inches long, 2 inches in diameter and only weighs about 5 pounds. With the PSD and such an x-ray source, one can build a nice small device that one man can carry with a remote package for the power supply and detector electronics which is about the size of an attache case and weighs about 50 pounds. The actual detector assembly will be about 20 pounds.

What kind of times are we talking about? Well, on mild steel samples we can determine the residual stress to an accuracy of plus or minus 5,000 psi in 10 seconds - no problem. Hardened steel samples have a very broad peak profile, usually about 15° to 20° from background to background. To do the analysis on such a sample to plus or minus 10,000 psi takes about thirty seconds. So, this is considerably faster than existing techniques, and we hope to demonstrate such a unit to manufacturers in the next month and a half or so, and maybe someone will actually get one of these things out on the market within a reasonable amount of time.

For the remainder of the talk, I would like to discuss some of the problems with the x-ray residual stress technique. We're talking about measuring a residual macrostress, a stress that is long range, and it would be nice to be able to correlate this with mechanical measured values, but what is more important is to correlate it with fatigue life predictions, quality control, and so forth, and thereby know when the technique is useful.

There are problems which arise from the selective nature of x-ray diffraction in the peak shift measurement. Residual stresses are associated with both macrostrains and microstrains. Elastic deformation gives rise to uniform macrostrains which cause a shift in the position of the x-ray peak; this peak shift is then related to a macroscopic stress system. When a metal is plastically deformed, microstrains or variations in the interplanar spacing of the order of the subgrain size are introduced. They arise due to the energy or strain field produced by faulting, segregation of solute atoms, or dislocations. On the subgrain level this produces a distribution in the average interplanar spacing which gives rise to broadening of the diffraction profile and unfortunately a peak shift. It is this dependence of the peak shift on microstrains that is considered to be a problem in the residual macrostress analysis, because instead of measuring a pure macrostress, the quantity determined by the x-ray technique may be both a macrostress and a microstress superimposed upon each other.

The first evidence for the contribution of microstrain came from the existence of oscillations in d vs $\sin^2\psi$. Classical theory of x-ray residual stress analysis predicts that the relation between the interplanar spacing or strain and $\sin^2\psi$ should be linear. Experimental evidence has shown that this is not always the case. As shown in Fig. 6, oscillations can exist which not only prohibit the use of the 'two-tilt' method, but lead one to question the basic formulae in the x-ray technique.

Recently, Marion and Cohen[4] have derived a model to account for this effect based on the theory of Weidemann[5] which describes an orientation dependent relief of the elastic stresses present in a polycrystalline aggregate. During deformation texturing develops because some crystallite regions will have a tendency to rotate to a more energetically favorable position so that multiple slip or some dynamic recovery process takes place. The elastic stresses are relieved by the local plastic deformation. A microscopic distribution of strains will be present which is directly related to the texture developed during deformation. The distribution of the microstrains is non-random and produces oscillations in d vs $\sin^2\psi$. Marion and Cohen showed that the oscillations do indeed correspond to the developed texture, as shown in Fig. 6.

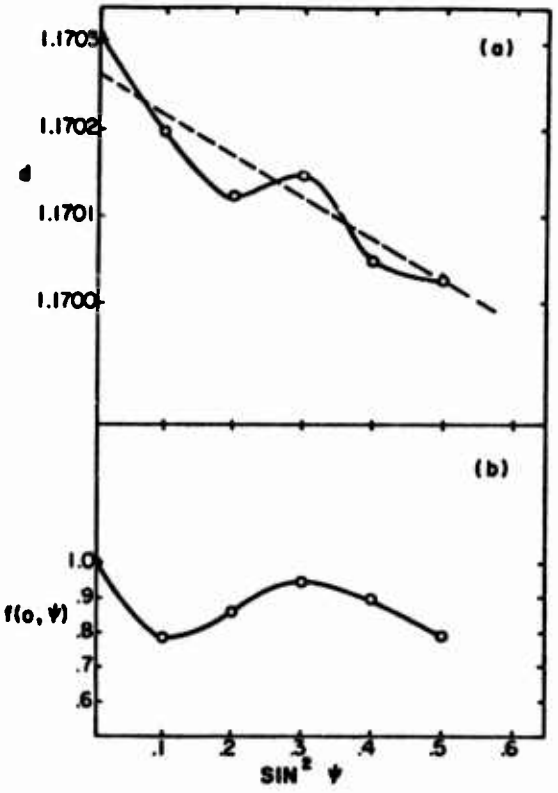

Figure 6 (a) d vs $\sin^2\psi$ for ARMCO iron specimen deformed in tension to a true strain of 18.4 pct. 211 peak with $Cr_{K\alpha}$. σ_φ = -10,148 psi.

(b) Texture distribution function for sample described in (a).

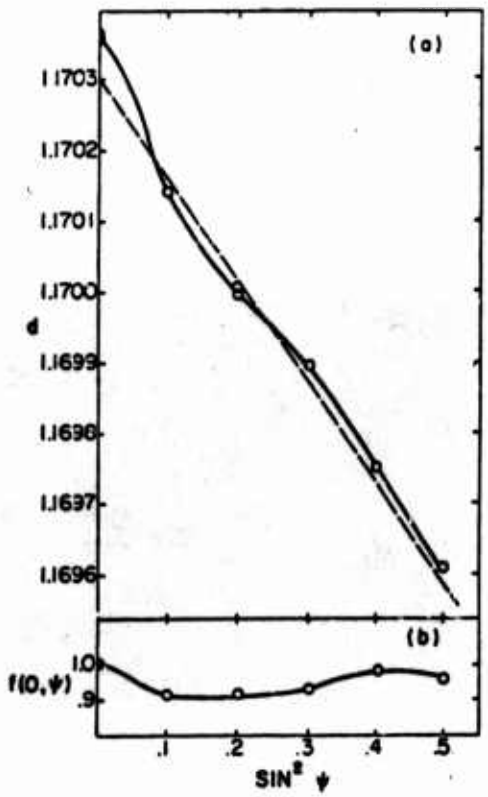

Figure 7 (a) d vs $\sin^2\psi$ for SAE 1045 steel deformed in tension to a true strain of 13 pct. 211 peak with $Cr_{K\alpha}$. σ_φ = -30,745 psi.

(b) Texture for sample described in (a).

They showed that a simple texture function can be obtained from the intensity of the diffraction peak and developed formulae to include the distribution of microstrains. Figure 6 depicts the oscillations found in an Armco iron sample. This has about .01 weight % C and is a reasonably homogeneous alloy. Figure 7, a 1010 steel, shows that the oscillations still exist but are very much diminished. Marion and Cohen showed that the effect is much more pronounced in homogeneous metals and their technique enables one to obtain the macrostress in the presence of oscillations in d vs $\sin^2\psi$. This technique is also automated in our residual stress package at Northwestern and adds maybe 10 minutes when using a diffractometer.

Another problem occurring when plastic deformation has taken place is that the microstrains may show a linear dependence of d vs $\sin^2\psi$, not just the oscillations accounted for by the Marion-Cohen method. As I said before, a linear dependence of d on $\sin^2\psi$ is usually associated with a macrostress. If it is possible to have microstresses existing which also yield a linear dependence, then the measured quantity is ambiguous because it is the superposition of the two types of stresses. This effect has been termed a 'fictitious' or 'baseline' stress by the Japanese and a 'pseudo-macrostress' by the Americans. It is an anomally in the x-ray technique which leads to an error in the measured macrostress.

An experimental technique to distinguish between residual macrostress and microstress concerns measuring the residual lattice strain on new surfaces as the specimen is progressively thinned. One expects that the microstress will remain sufficiently constant throughout the cross section while macrostresses must change to obey equilibrium. Characteristic results[5] on cylindrical specimens undergoing tensile plastic deformation are shown in Fig. 8. The stress measured in the direction of deformation through the cross section of the specimen shows that the stresses are in equilibrium in

the copper sample indicating a true macrostress. In the high carbon steel on the right, however, equilibrium is not obtained indicating that an anomalous stress is being measured and superimposed on a real macrostress. From these types of experiments it has been shown that this anomalous macrostress is measured only when axisymmetric plastic deformation takes place, that is, only when plastic deformation in one direction occurs such as in uniaxial tension or when rolling takes place.

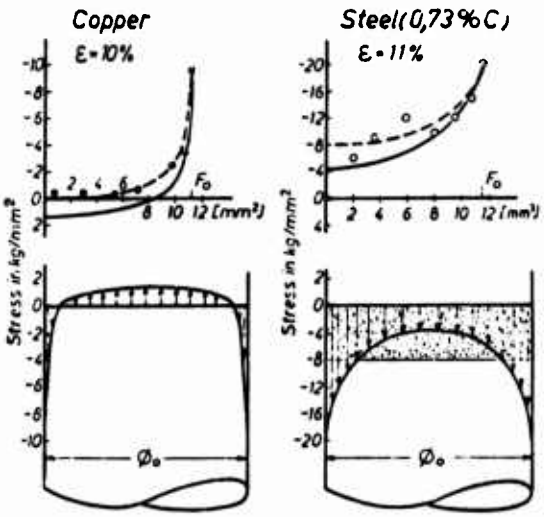

Figure 8. Distribution of residual stress in deformed specimens of Cu and plain steel from Ref. 5.

There are a number of reasons why this occurs. The most obvious is that the residual stress is being determined in only one phase of the material whereas other phases may have balancing residual stresses. Also back stress and work hardening occur differently between phases setting up the microstrain system which we are selectively sampling. Other mechanisms have been proposed (a good summary is given in Refs. 6 and 7) but only one method has been proposed to accurately obtain the true macrostress in the presence of this phenomena. Taira et al[8] have shown that in steel, the 'baseline' stress is dependent on the carbon content and have proposed a method, valid only for steel, whereby one can determine the 'fictitious' component of the peak shift and thereby obtain the macrostress. Their procedure is purely empirical and does not shed much light on the mechanism or mechanisms responsible for the anomally.

What is clear from experimental results is where one might expect the two anomalies discussed (the oscillations in d vs $\sin^2\psi$ and the pseudo-macrostress) to become important. Oscillations in d vs $\sin^2\psi$ are found most often in homogeneous materials whereas the pseudo-macrostress problem is found in heterogeneous alloys. In both cases, the anomally takes place only after axisymmetric plastic deformation such as that caused by uniaxial tension or rolling. Residual stress caused by heat treating, shot peening or grinding yields corresponding values when measured by x-ray diffraction and mechanical methods[9].

Thank you.

REFERENCES

1. E. W. Weiman, J.E. Hunter, and D.D. McCormack, Meta Progress, 96, No. 1, 88 (1969).
2. Y. Sakamoto, Adv. in X-Ray Analysis, Vol. 20, in press.
3. M.R. James and J.B. Cohen, Adv. in X-Ray Analysis, Vol. 18, 466 (1974).
4. R.H. Marion and J.B. Cohen, Adv. in X-Ray Analysis, Vol. 18, 466 (1974).
5. W. Widemann, Ph. D. Thesis, Techische Hochsule, Aachen, Germany (1966).
6. E. Macherauch, Exp. Mech., 6, 140 (1966).
7. R. I. Garrod and G. A. Harohes, Brit. Jrl. Apply. Phys., 14, 433 (1963).
8. S. Taira, K. Hayashi, and S. Ozawa, Mechanical Behavior of Materials, The Society of Materials Science, Japan, 287 (1974).
9. H. R. Letner, Trans. ASME, 77, 1089 (1955).

DISCUSSION

PROF. JOHN TIEN (Columbia University): Are there any questions?

DR. ROY SHARPE (Nondestructive Testing Centre, Harwell Labs): Is this an exercise in scientific stimulation or is there a real need for this? It seems that every ten years or so there is an interest in stress measurements, and then it dies away and people sort of learn to live with stress.

DR. JAMES: I think that's one of the problems with the field. It hasn't gotten out of the laboratory stage and to the field to be used for a fatigue life prediction, or for quality control. But a country like Japan, for instance, which is much smaller than us, smaller population and so forth, they have five times the number of residual stress devices out in industry and they're using it as a real in-field use tool. Apparently they feel it is a worthwhile tool.

DR. BOB ERWIN (Northrop Aircraft Div.): How do you introduce your material stress constant in this new equipment in such a rapid manner?

DR. JAMES: I beg your pardon? I didn't understand.

DR. ERWIN: How do you introduce your material stress constant in such a rapid manner? You said ten seconds in this new equipment.

DR. JAMES: Oh, well, that assumes you already know what your x-ray elastic constants are. You are determining the stresses only to plus or minus 10,000 psi, so the use of an average stress constant is satisfactory. For bulk mechanical values you are within 20 percent of the actual x-ray elastic constants, unless heavy plastic deformation has occurred. What is important is that the sample is in a compressive mode and not tensile mode or it's 10,000 and not 50,000 psi. It's those kinds of gross changes that are used as life prediction type of changes and not just changes on the order of 1 or 2 psi.

DR. DWAYNE JOHNSON (Failure Analysis Associates): What total weight is the package?

DR. JAMES: Well, I think we can get the part that is actually carried by hand to be about 20 pounds. You hold it by two hands and you do the measurement at one angle and then you actually move the tube and detector to the 45° tilt and take the data at the other angle. I suppose one could put on two of these detectors and two x-ray tubes, but you tend to make it very heavy, although you are saving half the time. Then you have the power supply and a micro-computer to analyze the data which can be 10 or 20 feet away. With an air cooled x-ray tube and solid state power supply, you don't have to worry about cooling water, etc. and everything plugs into a 110 line.

DR. SEYMOUR FRIEDMAN (Naval Ship Systems): In the use of a position detector, do you give the actual position of the diffraction peak----

DR. JAMES: What we do first of all is to calibrate the detector using a known standard so we can obtain the peak 2θ value along the relative position of the detector. All data is transformed into $^\circ 2\theta$ because in residual stress measurement you have to do Lorentz-polarization and absorption corrections to the intensity with subsequent curve fitting procedures to determine the peak position.

DR. FRIEDMAN: The actual determination of where the value of 2θ is, that's not that drastic?

DR. JAMES: We're using a least square parabolic curve fitted to the upper region of the peak profile. We're using as many of the data points as we can and still remain in the parabolic region to improve the statistics and so forth. We determine the actual peak position in degrees two theta ($^\circ 2\theta$) for each ψ tilt.

DR. FRIEDMAN: Can you get enough counts in 30 seconds to get a reading?

DR. JAMES: Oh, yes, when you're talking about a hardened steel sample and separating the detector into, say, 256 channels, I get usable information over about 120 of those channels. Using the theory of random counting statistics and propagating it through the curve fitting and stress formulae give us what I'm calling the precision of plus or minus 10,000 psi. That is the counting statistical precision, and we have shown that it indeed corresponds to the observed precision over many repeated runs.

DR. FRIEDMAN: I see. If you waited longer you would get a better sample?

DR. JAMES: Yes. If you wait longer, say the order of 200 seconds on a hardened steel sample, you can get statistical counting errors of plus or minus 2,000 psi.

PROF. TIEN: You don't happen to have one of these on you, do you?

DR. JAMES: No, but as I said, we hope to demonstrate the hand held unit within two months.

PROF. TIEN: One more question.

DR. ERWIN: Will this equipment handle titanium?

DR. JAMES: There's no reason why not, except that the proper characteristic radiation should be $Co_{K\alpha}$ or, preferrably $Cu_{K\alpha}$ which would mean changing x-ray tubes. One has a large flourescence problem when using $Co_{K\alpha}$, a lot of $Ti_{K\alpha}$ is produced, but this doesn't prohibit the use of the position sensitive detector.

PROF. TIEN: Thank you.

CONCEPT AND MATHEMATICAL MODELING OF ACOUSTIC EMISSION SOURCE

W. J. Pardee
Science Center, Rockwell International
Thousand Oaks, California 91360

Presently, most acoustic emission applications in nondestructive testing involve placing transducers on a large structure, a bridge or hydrocarbon cracking pressure vessel, then loading the structure and listening for the burst-type acoustic emissions that ensue, and finally using triangulation to locate the flaws whence came those bursts. This technique is very effective at locating defects, and that means that the typical, most studied acoustic emission parameters are just the number of events, the event rate, and to a somewhat lesser extent, the maximum amplitude . It might be the root mean square amplitude, or some other amplitude that characterizes the acoustic emission, or an amplitude distribution, that is, the number greater than some threshold V. These are typical, widely used acoustic emission parameters, and they have been very successful in locating defects. In fact, if they hadn't been, I don't think I would be here today talking about fancier things in acoustic emission.

However, they generally don't tell you all you can hope to find out. For example, you would like to use acoustic emission not only as a nondestructive testing tool to locate defects, but as a monitoring tool with which to warn you when something significant is happening. "Significant" is the key word, because many things going on in that structure generate acoustic waves which may be important. A very important example is crack growth under cyclic loading conditions. The rubbing of two cracked surfaces together generates acoustic emissions copiously, more so than crack propagation, and the crack surface friction generates a very significant signal. It has nothing to do with the length or width of the crack, and you would like to be able to distinguish it from crack growth; presently we can't do that.

To try to do that we must look at more detail in the signals. Instead of looking at what are largely statistical properties of large numbers of signals, we are trying to gain additional information by looking at the individual wave forms, in other words, the shape of a single acoustic emission. You can look at three components of displacement. You can look at them for all time or equivalently, Fourier transform and look at them in frequency space. I might add we don't have infinite media; so this means you look at it on the surface, so that gives you two dimensional wave vectors or a two dimensional distribution in space.

Both Roger Clough and I are talking about the same thing. What we look at is the Fourier transform or perhaps the time domain signal at a particular point in space averaged over a smaller region that is about the size of the detector.

Let me give you a specific example. The largest source of acoustic emission in most aluminum alloys is the fracture of brittle second phase inclusions. These are quite small, perhaps 20 microns or so. Before they fracture they almost certainly vibrate in one of their lowest normal modes. Of course, these modes are damped by their interaction with the medium, but the spatial dependence is determined by the size of the intermetallic particles, and the frequency is determined roughly by the elastic constants of the brittle intermetallic particles. So, if you could Fourier transform and measure both variables, one would expect a peak in ω k space corresponding (in k space) to the size of the particle and something (in frequency space) roughly characterizing its elastic properties. This is something which will give a great deal of fundamental information.

I described our acoustic emission theory in its heuristic and embryonic form a year ago at this meeting; I'm still talking about the same theory, more or less, with some refinements. We have learned a great deal more since then. But I want to review the elements of it and bring you up to date on our progress with it.

The basic picture that we started from is that there are really three important things that determine the frequency spectrum, and these can be varied independently. These are the source, the medium, and the detector. We have absolutely incontrovertible experimental evidence that each of these has a nontrivial influence, under some circumstances, on the spectrum you observe. I'm almost belaboring the obvious, but, of course, the actual details of the source process influences the frequency spectra. Not so obviously, the wave propagation characteristics of the medium affect the frequency spectrum. And, of course, the transducer response affects the frequency spectrum. Because I happened to be challenged about that recently, I brought along a slide (Fig. 1) to show you the difference between a piezoelectric transducer and a capacitor microphone when detecting the same source, which happened to be a fracture of a small silicon carbide grain. Because the piezoelectric transducer gives you a bigger signal, they are very commonly used for a great many acoustic emissions. When you first look at it, the dominant structure you see in a broad band analysis like this is going to be just that due to the response of the transducer.

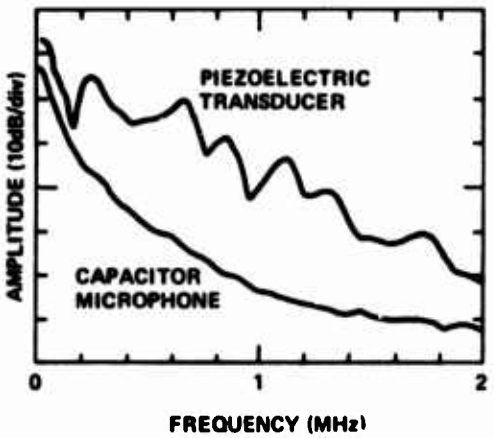

Figure 1. Amplitude responses for a piezoelectric transducer and a capacitor microphone pickup.

To take advantage of these three effects which are conceptually separate--we wrote our mathematics that way--we developed a transfer function formalism which includes all the properties in the medium --the boundary conditions in addition to attenuation and dispersion. We separately describe the source and we have to match that source to the transfer function of the medium and then later put on the transfer function of the transducer. Capacitor microphones, although they are not very sensitive, show a predictable frequency dependence; so, that doesn't complicate things too much. I might add that in the time domain the overall signal is a double convolution integral of these three things, while in the frequency domain it's just a product of these three factors. I think that that is probably the best reason for working in the frequency domain. It's not the only reason, however.

Now, I'm going to describe the theoretical principles of our acoustic emission wave form analysis. These are actually a set of conclusions we have come to by trial and error and, although they are conclusions, they are rather subjective, which is why I call them theoretical principles. They're not so much statements about the way nature works as about the way we work.

The first principle is to observe AE in the far field region. The applications, as I said, are typically to large structures--bridges, pressure vessels, things like that--but the experiments, because of the obvious size limitations, are done on small specimens where you are rather close to the crack. In fact, you are very frequently in the near field region and with complicated geometries. This is an intolerable situation for a theorist, and leads to the second principle, which is to avoid, as much as possible, spurious geometry dependent effects.

As an example, I want to particularly mention the complications concomitant to trying to do detailed model calculations for compact tension specimens. There are two things that come to mind. One is that the actual acoustic emission source with a compact tension specimen is going to be small--not the whole crack, but just a small segment of it--and the actual place where that occurs can be anyplace along the whole crack front. The position varies with crack propagation on a scale which is large compared to both the wave length and the distance of the transducer. Actually, I think that's not an intolerable problem. A greater consequence is the presence of all those boundaries which bias the frequency spectrum.

Let me show you the next slide, (Fig. 2), a very nice experiment done by Lloyd Graham, where a silicon carbide grain is fractured on a plate, which for our purposes may be regarded as infinite. In fact, it was about 6 inches square. The upper curve was obtained at the center of the bottom of the plate. The lower curve was obtained at a remote location on the top surface. That means 4 or 5 cm away, and the place was a half inch thick. As you can see, they are qualitatively the same. There is a significant difference (notice the log scale). The dashed curve is the electronic noise level. I wanted to make this point clear, because if you try to compare with a model calculation or if you try to look at the details and assume that they are valid when extrapolated to a large system, you will err, I believe. I do not want to overemphasize this point, but what one usually looks for is gross qualitative changes. I certainly don't suggest that those gross qualitative changes are going to be affected by these phenomena I just described.

The second point is to avoid spurious geometrical effects like very complicated geometries. But concomitant to that is an obligation not to neglect fundamental geometrical effects. For example, we have to make the measurements on the surface. What we find for the plate is that if you neglect the first surface, you get the wrong answer, an infinite medium does not give the right frequency falloff at high frequencies. You get roughly the right falloff at high frequencies if you include the first surface.

To get quantitative agreement, what we find is that you have to include the second surface. However, the calculations are for an infinite plate and I believe that's reasonable; we seem to be able to get quantitative results, although it's too soon to tell for sure. I think that a system with two parallel surfaces is a pretty good starting place; it's probably a good approximation to many nondestructive testing applications.

The third principle, and this is also even more subjective, is to avoid if possible, explicit normal mode decompositions. There are several reasons: first, it takes a whole lot of them to go to high frequencies. Second, you have to worry about mode conversions and reflections of these modes at the surface. The normal modes are very geometry dependent; they're very sensitive to the details and geometry of your system. I don't believe that the acoustic emission overall wave packet is that sensitive, and to illustrate that point in a very simple system, I considered a vibrating string.

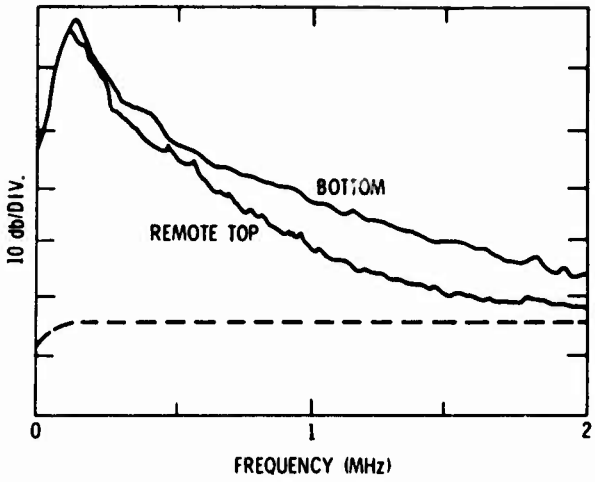

Figure 2. Emission from fracture of silicon carbide grain on a flat plate.

The vibrating string is picked up at t = 0 at each end and released. The exact solution is a square wave propagating between each end. I graphed the first six normal modes (Fig. 3) from the Fourier transform or the Fourier series analysis of this problem; the dotted curve is the sum of those first six. You can see the sum of the first six is not a very good approximation to the actual square wave. This is at a time t = L/4C later where L is the length of the string and C is a velocity. And more importantly, none of the individual normal modes looks at all like the solution. The exact solution, incidentally, is most easily obtained by using the solution for the one dimensional wave equation in the form F(x+vt) + F(x-vt), although both approaches are mathematically rigorously correct. We get far more physical intuition by avoiding the normal modes, if we can do it, but sometimes that's not possible. We were successful for the plate problem, however.

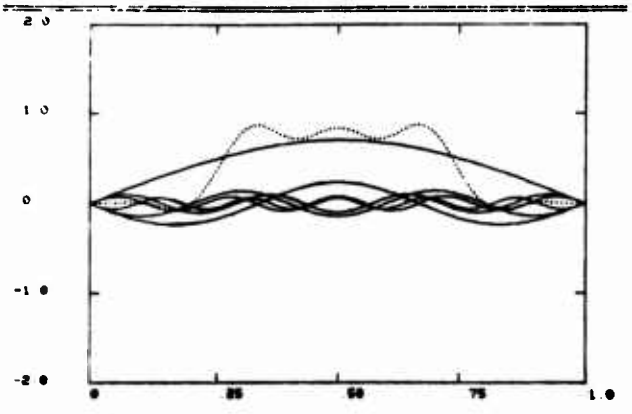

Figure 3. Normal modes of plucked string.

Let me get a little bit more mathematical. Now, the fourth principle is that--and you will see that I have to qualify this a bit later--acoustic emission arises from a sudden change in internal stresses. That certainly is a source of acoustic emission, a major source, and I want to distinguish it from body forces. You don't have real body forces creating these acoustic emissions. So, we try to describe this by nonlinear continuum mechanics, that is

$$\rho\omega^2 U_n + \frac{\partial P_{nm}}{\partial a_n} = 0. \qquad (1)$$

P is the mass density, ω the frequency, a_n the Euler variable, U_n is the n component of displacement U; Pnm is the Piola-Kirchhoff stress tensor; the stress tensor modified to include the effects of finite strain and the change in the mass density associated with the finite strain, but it can include a very complicated constitutive relation. It can include a real model for the details of what's happening physically. An example of a physical system described by this equation is a chemical reaction, precipitation of hydrogen out of solution to form a titanium hydride with concomitant expansion of the lattice and excitation of a stress wave. But we have to understand that the waves that we are observing are classical waves and they should be describable by continuum mechanics.

The next point is how can I make this horrible nonlinear equation tractable? As I said, let us work in the far field. I should say that my solution is, in fact, valid in the near field region as long as the near field region is linear. In the far field region it satisfies the same equation except instead of the complicated stress tensor, it's just a linear stress tensor, that is, the linear infinitesimal stress, in which the stress is proportional to the usual infinitesimal strain.

$$\rho\omega^2 U_n + \frac{\partial \sigma_{nm}}{\partial a_m} = 0 \qquad (2)$$

So, what I do is add and subtract the linear stress tensor

$$\rho\omega^2 U_n + \frac{\partial \sigma_{nm}}{\partial a_m} - \frac{\partial \sigma_{nm}}{\partial a_m} + \frac{\partial P_{nm}}{\partial a_m} = 0 \qquad (3)$$

The first two terms are purely linear and can be treated in a complicated but mathematically tractable fashion. The second two terms include very complicated nonlinear phenomena: plasticity, for example, but they are at least localized. We expect when we get far from the source that it will be a linear problem. The nonlinear effects are concentrated around the source, and for them we neglect the effect of the boundaries on the source itself as a reasonable, although not a universally true assumption. So, we gain a lot of things by this separation.

Last year I presented approximate calculations using substantially this approach for a couple of very simple acoustic emissions. At that time I calculated a transfer function H as an infinite but inadequate sum of some of the normal modes, and we found that at the center of the bottom of the slab

we had nearly quantitative agreement: elsewhere, the calculations had only qualitative significance. Our principal mathematical accomplishment this year was to find an exact solution for the plate transfer function which is not a normal mode decomposition. It's an exact treatment of the stress free boundaries on the two surfaces of the slab.

The exact solution of Eqn. 3 in terms of the transfer function H is given by

$$U_n(\omega,\underset{\sim}{r}) = \int dA' \frac{\partial H_{mnab}(\omega,\underset{\sim}{r},\underset{\sim}{r}')}{\partial r_m} n_b(\underset{\sim}{r}') U_a(\omega,\underset{\sim}{r}') \qquad (4)$$

$$- \frac{1}{\rho\omega^2} \int d^3r' \frac{\partial^3 H_{mnab}(\omega,\underset{\sim}{r},\underset{\sim}{r}')}{\partial r_m \partial r'_b \partial r'_k} (P_{ak}(\omega,\underset{\sim}{r}') - \sigma_{ak}(\omega,\underset{\sim}{r}'))$$

The surface integral is over the crack surface, an additional term arising because it does not include the stress free boundary conditions on the surface of the crack. But it still satisfies the same differential equation, and this is an exact statement. U_n is the n component of the displacement field, and that's what will be observed on the surface of the slab. This surface integral is an integral over the freshly created fracture surface of a certain derivative of H multiplied by a unit vector, and U_a is the displacement of the fracture surface. So, we have to understand the displacement of the fracture surface. The second term includes all the nonlinear effects, and what you have to do is solve that problem in the time domain, then Fourier transform it. But that's an infinite medium problem, so you don't have to worry about the boundary conditions. For brittle materials, I think it's a reasonable guess that only the first term contributes. My argument is simply that we probably can neglect nonlinear effects in plastic deformation in very brittle materials: ceramics, for example. It's linear until it fractures, and when it fractures, it's broken.

So, the dominant contribution is just a creation of fresh fracture surface. In fact, you see by looking at the expression that the amplitude you get out is going to be roughly proportional to the fracture surface area created, and it's also proportional to the displacement of that fracture surface area. And if you think about it in more detail and you want to know the instantaneous crack velocity, you realize that you have to look at the details of the way the frequency spectrum falls off.

In practice, the average crack velocity is probably more important than the instantaneous crack velocity, and you would get that with some suitable calibration from the amplitude and the event rate, representing an aposteriori justification for traditional acoustic emission techniques.

I will stop there with a brief comment. As I said, this is a series of conclusions about our approach to acoustic emission. Our plans for the near term are to explore this picture I just described for crack propagation in brittle materials and to do some careful experiments; that is, in geometries which are mathematically tractable and in an effort to quantitatively test this as carefully as possible. And I think we're going to have to iterate a couple of times until the model is good enough to describe quantitatively the experimental spectra. The second thing I want to do is to explore the extent of these near field phenomena so I can tell you something more quantitative about the problems you encounter in the near field region. And the third thing is to explore the polarization dependence; that is, whether it is desirable to look, for example, at transverse displacements or strains and to make--if the theory is reasonably successful--estimates about how high you have to go in frequency to really see the significant features.

DISCUSSION

PROF. JOHN TIEN (Columbia University): Thank you, Bill. Are there any comments?

PROF. GORDON KINO (Stanford University): I have had discussions before, any my viewpoint has changed entirely since I last talked to you, but one of the things I can't get clear in my mind and I wonder about is that when you've got something like a crack developing, it is a very small object. After all, as the crack develops it's a very small area, very small change of length. And typically, say, a piston radiator or any kind of radiator in acoustics tends to get more efficient as the frequency increases. Now, on that basis I would think you would get the noise emission increasing with frequency rather than decreasing with frequency. What is the catch in that argument?

DR. PARDEE: The decrease with frequency that we're seeing here is essentially a kinematic effect due to the fact that a differential equation is second order in time. I think you will see a peak when you get up to the frequency where things are really happening, which I think is perhaps 25 MHz instead of the 2 or 3 MHz that we're looking at. So, we're looking at a kinematic effect in the low frequency end, and you have to look very hard in order to pick out what's happening at much higher frequencies without going up there.

DR. ROBB THOMSON (National Bureau of Standards): Did I hear you say that you did not satisfy the boundary conditions on the crack surface as the crack moves? It seems to me that that would be very important.

DR. PARDEE: It is. I do satisfy all boundary conditions completely. It's just a question of how it's incorporated into the mathematical formalism. It's incorporated aposteriori instead of being built into the Green's function because when I built the Green's function, I don't know where the crack is going to be. The purpose of separation is to avoid the detailed description of the source. So, you have to satisfy them on the crack surface as a separate problem; it's not part of the medium description problem.

PROF. TIEN: Bill, you picked a very simple geometry, silicon carbide grain cracking. I guess the purpose of this entire work of yours is not so much a description of the multifaceted experimental spectra, which people observe, but basically to come up with a physical understanding so they could suggest--suggest what?

DR. PARDEE: Suggest where to look for more sensitive measures, more sensitive diagnostic tools, and how to recognize microscopic characteristics of the source.

PROF. TIEN: So, it's bigger than just some modeling curves?

DR. PARDEE: Certainly!

PROF. MAX WILLIAMS (University of Pittsburgh): What condition do you use to make the crack move?

DR. PARDEE: Presently I have very ad hoc descriptions of the crack propagation. It's not a fundamental theory in the sense that the other is a fundamental theory; it's a phenomenological description of the crack moving. I just say it does move for a certain length of time at a constant velocity.

PROF. WILLIAMS: So, basically--

DR. PARDEE: A very naive picture.

PROF. WILLIAMS: You are prescribing a priori the velocity versus the time of the crack gowth?

PROF. TIEN: You disregard the medium is what you do.

DR. PARDEE: That's right. Then from having prescribed that, one hopes, if one fits the acoustic emission to determine what that velocity is.

PROF. WILLIAMS: There is a difference in the character of the singularities of the crack growth as to whether the crack is running or it initiates and it's tied up with the initial radiation from the crack point; I think you might be leaving out a significant physical factor if you have the crack running a priori to the prescribed velocity.

DR. PARDEE: The correct description--I'm not sure exactly I understand the point you're getting at--but the correct description does require a detailed description of the stresses around the crack tip and their dynamics. So, you need the dynamic stresses around a moving crack which, of course, is a difficult problem by itself.

PROF. WILLIAMS: It's almost impossible.

DR. PARDEE: That's correct. However, I think it's possible to make progress with simpler models. In particular I reaffirm my suggestion that for brittle materials this may not be very important.

PROF. TIEN: One more question, Bill.

DR. WILLIAM A. ELLINGSON (Argonne National Lab): You threw a slide up there rather quickly about a calibration of your transducer. Would you just briefly say how you obtained that curve?

DR. PARDEE: I'm not sure exactly what slide you're talking about. Is it the slide showing the difference between the behavior on the top surface and the bottom surface?

DR. ELLINGSON: Right.

PROF. TIEN: The capacitor one.

DR. ELLINGSON: Yes, the capacitance microphone and apparently the pzt unit.

DR. PARDEE: Well, those were experiments done by Lloyd Graham. I can describe how they were done. You have a plate with a small amount of silicon carbide power on the surface and you have the detector, either the capacitor microphone or the pzt transducer at a remote point on the surface. You grind the silicon carbide powder and use the Hewlett-Packard spectrum analyzer to obtain the resulting spectrum. In fact, it's a composite of many events in that case.

PROF. TIEN: Thank you, Bill.

THEORETICAL ELEMENTS OF ACOUSTIC EMISSION SPECTRA

J. A. Simmons and R. B. Clough
National Bureau of Standards
Washington, D. C. 20234

I will be describing an acoustic emission program at the National Bureau of Standards sponsored jointly by NBS and the Electric Power Research Institute. This is part of a larger comprehensive NDE program at NBS. The acoustic emission program uses the spectral analysis approach for the characterization of moving defects and, as I will point out, includes the development of an acoustic emission transducer calibration facility as well as the experimental study of crack motion in glass and pressure vessel steels. These require a quantitative theory which serves to guide the experimental design as well as to interpret the results.

I will be speaking about progress in this theory of acoustic emission today. Rather than give you a verbal transcript which is lacking in details, I'd like to submit the text of a paper prepared last March which has been presented by Dr. Simmons at the Eighth World Conference on Nondestructive Testing at Cannes, France:

Frequency spectrum analysis of acoustic emission signals shows great promise as a nondestructive test method. It has potential for discriminating between harmful moving defects and system noise as well as for revealing more of defect characteristics than are currently revealed with threshold counting techniques. However, such an analysis requires a systematic examination of the entire acoustic emission process.

To address this problem, NBS expanded its acoustic emission program last fall through joint sponsorship by the Electric Power Research Institute. This AE spectrum analysis program has the following objectives: (1) develop calibration capability for acoustic emission transducers (2) develop theory of acoustic emission spectra from moving defects (3) measure crack velocities optically and acoustically and correlate with above theory, and (4) explore test methods for measuring crack velocity spectra in structural metals.

In this paper, we will be describing progress in the second task, the theory of acoustic emission. More specifically, we will examine acoustic emission from planar, straight line dislocation segments moving in bursts. For simplicity, we will for the present treat the ideal case of an infinite isotropic body. This case should, however, provide an illustration of the general nature of the acoustic emission spectrum and how it is produced.

Transfer Functions

An acoustic emission system is represented in Fig. 1. Stress waves are emitted from the defect as it moves from A to B. Although we shall discuss a particular type of defect, namely a straight line dislocation, the defect shown in Fig. 1 may in general be a dislocation, a crack, a twin, or any other defect which grows by relieving internal strain energy. The stress waves, following emission, propagate through the body and pass through a coupling interface, where they are detected as acoustic emission by a transducer with associated signal processing equipment. The original acoustic emission signal will be changed by the elasticity and geometry of the body as well as by the transducer and signal processing equipment.

These modifications of the stress wave as it passes through the system are conveniently described by transfer functions [1]. For example, if the input to a system is $\tilde{X}(\omega)$, where "~" represents the Fourier frequency (ω) transform, then the output is $\tilde{Y}(\omega) = \tilde{T}(\omega)\tilde{X}(\omega)$, where $\tilde{T}(\omega)$ is the transfer function for this input/output set. The transfer function for the entire acoustic emission system can often be separated into the product of the subsystem transfer functions. Then the specimen transfer function and the transducer and signal processing transfer function can be treated separately.

Acoustic Emission from a Moving Dislocation

We shall consider an infinite isotropic body containing a dislocation on a slip plane (Fig. 1). When this defect moves, it emits stress waves which are monitored at some point by a transducer which converts local field conditions into voltages.

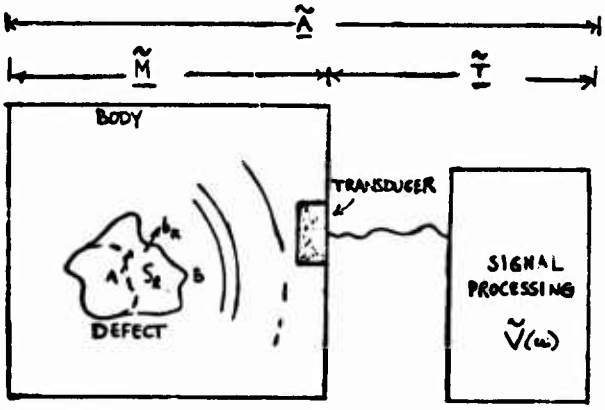

Figure 1. Schematic (not to scale) of acoustic emission system

In this paper, we employ what we shall call a non-disturbing transducer, that is, one whose interaction with the body does not substantially affect the dynamic elastic equilibrium of the body. The most common types of such transducers are "soft" surface transducers which are essentially strain or displacement sensitive. Another conceivable type of such transducer is an internally embedded unit (Fig. 1) whose elastic constants approximate those of the matrix, and it is this latter type of internally embedded transducer which we shall treat in this paper. To simplify some of the expressions, we shall also assume that the transducer response depends on the displacement u. Similar expressions can be obtained for stress and velocity components [3].

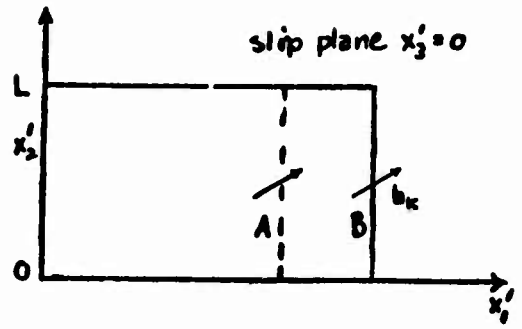

Figure 2. Slip plane with dislocation segment motion (A to B).

We shall derive the expression for acoustic emission from a moving dislocation by using the simplified configuration shown in Fig. 2. As shown, the slip plane ($x_3'=0$) contains a rectangular dislocation loop of Burgers vector $\underline{b}$. A line segment of length L of the loop moves along the x_1 axis so that its position at time t is given by $x_1'(t)$. Following Mura [2], the dynamic displacement components produced by the moving dislocation segment are given by:

(1)

$$u_m(\underline{r},t) = -C_{ijk\ell}\iint G^H_{mi,j}(\underline{r}-\underline{r}';t-t')\dot{\beta}^*_{k\ell}(\underline{r}';t')\,d\underline{r}'dt'$$

where $u_m(\underline{r},t)$ could be taken as the displacement at the transducer inside the body at point $\underline{r}$ and time t due to a prior plastic distortion rate $\dot{\beta}^*_{k\ell}(\underline{r}',t')$ at point $\underline{r}'$ and time t'. G^H_{mi} is the dynamic Heaviside Green's tensor for the infinite elastic body (called "H" by Mura [2]); $G^H_{mi}(\underline{r}-\underline{r}', t-t')$ represents the x_m components of displacement at point $\underline{r}$ and time t due to a concentrated force in the x_i' direction applied at point $\underline{r}'$ and time t' and maintained for all times after t'. $C_{ijk\ell}$ in Eqn. (1) are the elastic coefficients. With reference to Fig. 2, one can define the plastic distortion rate tensor

(2)

$$\dot{\beta}^*_{k\ell}(\underline{r}',t') = b_k\delta_{\ell 3}v_1(t')\delta(x_1'-x_1'(t'))\,H_{2,}(0,L)\delta(x_3')$$

Here, b_k are the components of the Burgers vector of the dislocation, $\delta_{\ell 3}$ are the components (in this example) of the slip plane normal, $v_1(t')$ is the dislocation velocity at time t', $\delta(x_1'-x_1'(t'))$ is the Dirac delta function expression for the position of the dislocation segment, $H_{2,}(0,L)$ is the characteristic function for the dislocation line segment:

(3)

$$H_{2,}(0,L) = 1 \text{ if } 0 \le x_2' \le L$$

$$= 0 \text{ otherwise,}$$

and $\delta(x_3')$ is the Dirac delta function identifying the slip plane $x_3'=0$.

Substituting equation (2) into equation (1) gives

(4)

$$u_m(\underline{r},t) = -C_{ijk\ell}b_k\delta_{\ell 3}$$

$$\times \int_0^L dx_2' \int_{-\infty}^{\infty} G^H_{mi,j}(\underline{r}-\langle x_1'(t'),x_2',0\rangle,t-t')\,v_1(t')dt'.$$

For many applications, it can be shown that the size of the moving dislocation segment and the distance it moves (i.e., the change in the position of $\underline{r}'$) are both sufficiently small relative to the distance of the transducer from the approximate position of the radiating dislocation segment (i.e., $\underline{r}-\underline{r}'$) that their effect on $\underline{G}^H$ is negligible (i.e., $\underline{G}^H$ depends only on $\underline{r}$ and t). In that case, $\underline{G}^H$ becomes independent of $\underline{r}'$ and equation (4) may be rewritten as:

(5)

$$u_m(\underline{r},t) = -C_{ijk\ell}b_k\delta_{\ell 3}L\int_{-\infty}^{\infty} G^H_{mi,j}(\underline{r},t-t')v_1(t')dt'.$$

Equation (5) contains a convolution integral in time, which Fourier transforms to a product in frequency (ω)space. If "~" represents the Fourier transform, then

(6)

$$\tilde{u}_m(\underline{r},\omega) = -b_k\delta_{\ell 3}LC_{ijk\ell}\tilde{G}^H_{mi,j}(\underline{r},\omega)\tilde{v}_1(\omega)$$

where L is the segment length and $\tilde{v}_1(\omega)$ is the velocity. Equation (6) can be recognized as a special case of a transfer function formula for the transmission of acoustic emission by a moving dislocation in an infinite isotropic elastic body:

(7)

$$\tilde{u}_m(\underline{r},\omega) = \tilde{M}_{mk\ell}(\underline{r},\omega)b_k\tilde{S}_\ell(\omega)$$

where

(8a)

$$\tilde{M}_{mk\ell}(\underline{r},\omega) = -C_{ijk\ell}\tilde{G}^H_{mi,j}(\underline{r},\omega)$$

is the medium transfer tensor, whose components are generally complex numbers, corresponding to the emission source tensor

(8b)

$$M_{mk\ell}(\underline{r},t) = -C_{jk1\ell}\,G^H_{mi,j}(\underline{r},t)\ ,$$

and $S_\ell(t)$ is the amount of non-recoverable (i.e., plastic) area swept out by the moving dislocation per unit time on the plane with normal in the "ℓ" direction (e.g., in Eqn. (6), $\delta_{\ell 3}L\tilde{v}_1(\omega) = \tilde{S}_\ell(\omega)$).

It is evident from the above equations that acoustic emission has a tensor nature. This is an important characteristic in that the magnitude of the total signal is not merely the sum of the magnitudes from two dislocation segments near a given point, one with a Burgers vector b_j on a plane with normal n_j and the second with Burgers vector b_k on a plane with normal n_ℓ. Let their respective velocity histories be $S_j(t)$ and $S_\ell(t)$. The total acoustic emission field spectrum at the transducer is the superposition of two separate signals whose magnitude is

(8c)

$$|\tilde{u}_m(r,\omega)| = |\tilde{M}_{mk\ell}(r,\omega)b_k\tilde{S}_\ell(\omega) + \tilde{M}_{mij}(r,\omega)b_i\tilde{S}_j(\omega)|.$$

This is not in general the sum of the individual emission spectrum magnitudes:

(9)

$$|\tilde{u}_m(r,\omega)| \neq |\tilde{M}_{mk\ell}(r,\omega)b_k\tilde{S}_\ell(\omega)| + |\tilde{M}_{mij}(r,\omega)b_i\tilde{S}_j(\omega)|.$$

Therefore, a precise analysis of acoustic emission due to plastic deformation, which is usually a multislip process, requires careful consideration.

In addition, it is evident from Eqn (7) that acoustic emission due to dislocation segment motion (Fig. 2) is a function only of the Burgers vector and the rate of area change on a given plane. It does not matter what direction the dislocation moves. Thus, dislocation acoustic emission is a function only of the rate of plastic strain volume generated.

Measurement of the Defect Velocity Spectrum

In considering applications of this theory, we must examine the voltage output from the transducer. Recall that, for simplicity, the transducer is assumed to be small enough relative to wave lengths in a bandwidth that it may be considered infinitesimal in extent and located at the point $\underline{r}_T$. The voltage output from the acoustic emission system can then be written as

(10a)

$$\tilde{v}(t) = \int_{-\infty}^{\infty}\int_{-\infty}^{\infty} T_m(t-t')M_{mk\ell}(\underline{r}_T, t'-t'')b_k S_\ell(t'')dt'dt''$$

with the corresponding voltage spectrum

(10b)

$$\tilde{v}(\omega) = \tilde{T}_m(\omega)\tilde{M}_{mk\ell}(\underline{r}_T,\omega)b_k\tilde{S}_\ell(\omega).$$

$\tilde{T}_m(\omega)$ is here the transducer and electronics transtransfer vector for the acoustic emission signal.

Note that the output of the system is the scalar voltage $\tilde{V}(\omega)$ while the input is the dislocation motion tensor $b_k S_\ell(\omega)$. It is therefore generally not possible to infer the complete nature of the emitting defect signal from a single acoustic emission signal. In order to completely characterize the source signal, a sufficient number of independent observations must be made, for example, by using strain gage type transducers and/or multiple positioned transducers. To be more specific, the transfer function formalism can be contracted to $\tilde{A}_a^{(\gamma)}(\omega) \equiv \tilde{A}_{k\ell}^{(\gamma)}(\omega) \equiv \tilde{T}_m(\omega)\tilde{M}_{mk\ell}(\underline{r}_T,\omega)$, where "a" is a convenient index representing "kℓ" and "(γ)" refers to an independent measurement using a transducer of a given type at a given location. Similarly, we refer to $D_{k\ell}(\omega)$ as $\tilde{D}_a(\omega) \equiv b_k\tilde{S}_\ell(\omega)$. This gives the voltage from the γth measurement as

(10c)

$$\tilde{V}^{(\gamma)}(\omega) = \tilde{A}_a^{(\gamma)}(\omega)\,\tilde{D}_a(\omega)$$

In order to solve for the components of $\tilde{D}_a$ one must have at least as many measurements (γ) as there are degrees of freedom in a. This requires one γ for each a, that is to say, one γ for each kℓ, and since $M_{mk\ell}$ is symmetric in kℓ, there are six possible a components. Thus, unless there are special restrictions on D_a, such as predetermined slip planes, at least 6 independent measurements are required a priori to find $\underline{D}$. In that case, Eqn. (10c) can be solved for $\underline{D}$:

(10d)

$$\tilde{D}_a(\omega) = [\tilde{A}^{(\gamma)}(\omega)]^{-1}\,\tilde{V}_a(\omega).$$

Convolution Smoothing and Stochastic Processes

Once the defect velocity spectrum $\tilde{V}_\ell(\omega) = \tilde{S}_\ell(\omega)/L$ is obtained by the above method, its inverse Fourier transform yields the defect velocity history $v_\ell(t)$. It may be recalled, however, that in deriving Eqn (5), the frequency range was in effect restricted to frequencies sufficiently low that the finite size of the defect could be removed. We will now be more precise about the maximum frequency cutoff and discuss the effects of such low-pass filtering on smoothing the corresponding time domain signal. This will be applied in particular to dislocation motion treated as a stochastic process.

Introducing a low-pass filter is equivalent to multiplying the "infinite" velocity spectrum $\tilde{v}_\infty(\omega)$ which extends over all frequencies by a function $\tilde{B}_m(\omega)$ which transmits signals only over a restricted frequency range $|\omega| \leq \omega_m$. The time history after filtering at ω_m is (11)

$$v_m(t) = \frac{1}{2\pi}\int_{-\infty}^{+\infty} \tilde{B}_m(\omega)\tilde{v}_\infty(\omega)e^{i\omega t}d\omega$$

and since a product in frequency space corresponds to a convolution in the time domain [4], we have

(12)

$$v_m(t) = \int_{-\infty}^{+\infty} R_m(\gamma)v_\infty(t-\gamma)d\gamma.$$

The high frequency components, distorted due to interference effects from the finite size of the moving defect, are filtered out. The equivalent

operation in the time domain is a convolution which, as we shall see, is the same as smoothing. In the context of our theory, this convolution smoothed integral represents the only meaningful information about the time history of a burst of motion.

In real materials one may expect that dislocation motion is generally irregular and dislocation segments may stop and start many times (Fig. 3a) during the course of an emission burst (what may be called the "chitty-chitty-bang-bang" effect). Segment velocity during such a burst may then be thought of as a probabilistic or stochastic process.

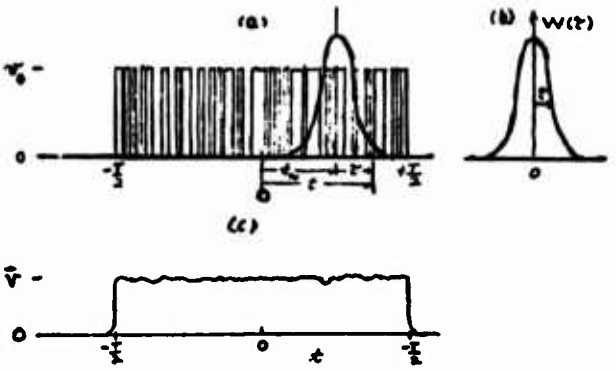

Figure 3. Dislocation segment velocity burst.

Suppose that, as an example of this, the dislocation segment shown in Fig. 2 moves in a burst of motion given by th velocity history in Fig. 3a, where the velocity alternates between v_0 and 0. Then, as we have discussed, the signal is (a) recorded, (b) Fourier transformed to frequency space, (c) the system transfer function is eliminated to yield the "infinite" velocity spectrum $\tilde{v}_\infty(\omega)$, and finally (d) and (e) this spectrum is passed through the low-pass filter at $|\omega| \leq \omega_m$ and the inverse Fourier transform is taken to the time domain. We wish to know the effects of the low-pass filter or the stochastic characteristics of velocity v(t).

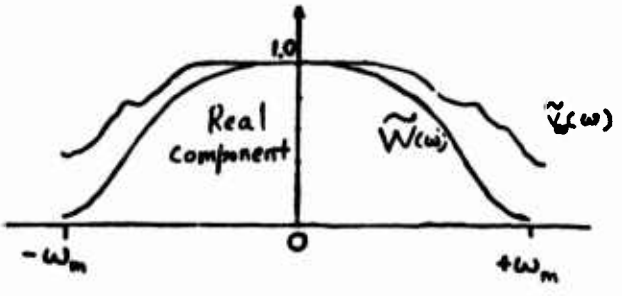

Figure 4. Spectrum of velocity for burst motion of segment.

The unfiltered velocity spectrum might appear as shown in Fig. 4, where the real part is plotted (the imaginary component can be treated by a similar procedure). A filter is used, as shown in Fig. 4, that has a Gaussian shape to simplify the example (since the Fourier transform of a Gaussian is also a Gaussian). Let the window function be given by $W(\omega) = W(-\omega)$ and which is chosen so that transmission is "insignificant" for $|\omega| \geq \omega_m$. This window is symmetric and real so that its time transform is also symmetric and real [4] as shown in Fig. 3b. These transform window pairs correspond to multiplication in frequency space (Eqn. 11) and convolution in time (Eqn. 12). The convolved signal is

$$v^c(t_w) = \int_{-\infty}^{+\infty} v_\infty(t_w - \gamma)\, W(\gamma)\, d\gamma \,. \tag{13}$$

Let us imagine, on the other hand, an averaging operation as depicted in Fig. 3a, where the signal is averaged over the unit area element $W(\gamma)$. This produces a smoothing as shown in Fig. 3c, where the relative magnitudes and details of the ripples will depend on the signal and the smoothing operation. The smoothed velocity is given by

$$v^s(t_w) = \int_{-\infty}^{+\infty} v_\infty(t_w + \gamma)\, W(\gamma)\, d\gamma = \tag{14}$$

$$v^s(t_w) = \int_{-\infty}^{+\infty} v_\infty(t_w - \gamma)\, W(-\gamma)\, d\gamma \,,$$

which, owing to the symmetry of W, is the same as the convolution in Eqn. (13). Therefore, we may write that $v^s(t_w)$, that is, time averaging and filtering are equivalent smoothing operations. The exact nature of the smoothing will depend on the signal and filter. We may expect, however, that a smaller defect size will permit the use of a higher cut-off frequency. A broader spectral window, to be somewhat imprecise, will generally correspond to a more narrow smoothing element, permitting greater resolution of the undistorted velocity signal as a function of time. One can generally expect, therefore, (other things being equal) to obtain more details of motion for finer sized defects.

Conclusions

We have attempted to set down a conceptual framework for some of the essential principles needed to make quantitative defect characterizations using acoustic emission spectrum analysis. The simplest possible system was therefore selected - an infinite isotropic body with an essentially one-dimensional moving dislocation segment. We formulated its transfer function and discussed some of the characteristics of the signal and its measurement. There are a number of important problems remaining to be solved: the analysis for cracks and inhomogeneities, the characterization of multiple and/or complex sources, the effects of geometrical boundaries and microstructure, as well as possible non-linear or anharmonic effects.

REFERENCES

1. J. Spanner, Acoustic Emission Techniques and Applications, Intex Publ. Co., Evanston, Ill. (1974)

2. T. Mura, Method of Continuously Distributed Dislocations in Mathematical Theory of Dislocations, T. Mura, Ed., American Society for Mechanical Engineers, N.Y. (1969)

3. J. A. Simmons and R. B. Clough, to be published.

4. R. Bracewell, The Fourier Transform and Its Applications, McGraw-Hill, Princeton, N.J. (1965).

DISCUSSION

PROF. JOHN TIEN (Columbia University): Thank you. I guess the obvious question is whether you and Bill Pardee have any large quantum disagreements?

DR. CLOUGH: I haven't had time to examine his work in detail, but it appears that so far he has concentrated on the geometrical effects of the medium, whereas we have more clearly examined the acoustic emission source.

PROF. TIEN: Any comments?

PROF. STEVE CARPENTER (University of Denver): It's interesting that in a lot of materials well into plastic flow where you're making dislocation loops, very great numbers of them, you see no acoustic emission.

DR. CLOUGH: I don't quite understand that. Could you---

PROF. CARPENTER: Well, what I'm saying : in a sample in which you're loading and you get well into plastic flow and the dislocation density is increasing with the plastic strain and you're generating dislocation loops - those loops are moving - you see no acoustic emissions.

DR. CLOUGH: This is not directly concerned with our theory, but let me make a comment. You're getting attenuation with increased total density of the loops. Also, the mobile (emitting) density actually decreases with strain so that one tends to get a maximum emission right at the yield point, right? Then it begins to decrease.

PROF. CARPENTER: Right at the yield point, but is that a motion that you're describing or is that a motion in breaking away from precipitates and that type of thing? I think it's a much different system.

DR. CLOUGH: Oh, yes. I'm not describing such a complex system. As I said, for a multiple dislocation system it's not immediately obvious just how one would obtain the total signal. What I'm talking about is the motion of a single defect in an infinite body.

PROF. TIEN: Otto?

DR. BUCK (Science Center): You distinguished between climb and regular motion of dislocations. Can you speculate what would happen in the case of cross slip?

DR. CLOUGH: Well, yes, we'd be talking about slip and you would have a change in slip systems. Now what I have shown is that the signal is very sensitive to the orientation of the Burgers vector and slip plane normal, so that if there is cross slip, you're going to change the slip plane normal, and the emission field will be correspondingly altered. If you're in a very sensitive position, you might just suddenly get a signal or not get a signal.

I might comment here that those signals that I showed were only along the principal directions and in off-axis directions. There may be other nodes and other maxima and so forth.

DR. BUCK: Does that mean that if you could pick up the dislocation motion, then, that would be a nice method to try to determine the stacking fault energy for the τ_{III} method?

DR. CLOUGH: That's a very interesting idea. I don't think that one could get sufficient signal from a single dislocation. If you had a large number of dislocations, moving in a shear band, let's say, you might be able to make something of that.

PROF. TIEN: Thank you.

OVERVIEW

R. B. Thompson
Science Center, Rockwell International
Thousand Oaks, California 91360

Today I would like to give an overview, both of the meeting program in general and, more specifically, on the work that is being done in the ARPA/AFML Program for Quantitative Flaw Definition. I will first briefly define the philosophy of quantitative flaw definition. I will then discuss, in a general way, some different approaches that are being used to obtain the necessary information. Finally, I will present a specific outline of the technical structure of the ARPA/AFML program. This will provide a framework to which the talks presented during the day can be related.

The type of situation that has pointed out the need for quantitative flaw definition is illustrated in Fig. 1. Consider the ultrasonic inspection of a part that is to be loaded by an in-plane stress. If a crack is oriented favorably with respect to a transducer on the surface, it will produce a very large ultrasonic reflection as shown in part a. However, if the crack is oriented at 90° it will produce a small reflection. The problem is that the crack which produces a small signal is much more likely to fail since it is perpendicular to the applied load. Thus, the ultrasonic indication is inversely related to the severity of the defect.

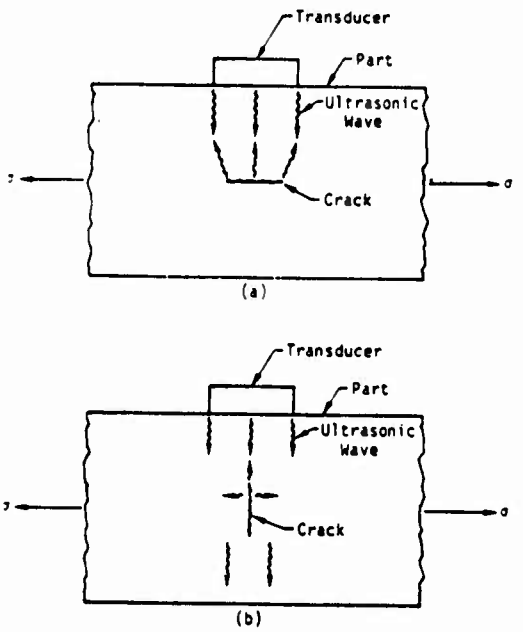

Figure 1. Comparison of ultrasonic reflections from two crack orientations. (a) crack favorably oriented. (b) crack unfavorably oriented.

This is only one example of a more general problem that is illustrated in Fig. 2. In any procedure in which the ultrasonic amplitude is chosen as the flaw indicator, a plot of detection probability versus flaw size will be quite broad. When an instrumental threshold is adjusted so that all flaws above a given size are detected with high probability, then quite a few of the flaws which are smaller will also be detected. Many parts will be unnecessarily reworked or rejected with the associated economic loss. This can only be avoided if quantitative techniques are developed so that this broad detection distribution approaches a step function.

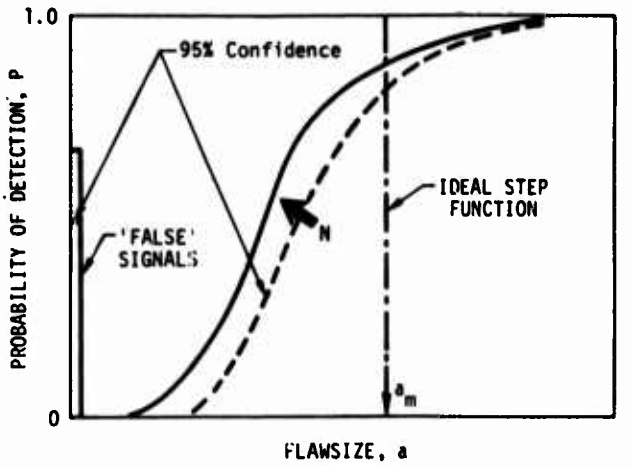

Figure 2. Probability of flaw detection for specific sensitivity setting, as function of flaw size, showing "false" signals and indicating 95 percent confidence level. Quantitative techniques will sharpen the distribution so that it approaches the ideal case of a step function.

The payoff of precisely measuring the size of a flaw is to be able to use this information in fracture mechanics models for failure prediction. By way of example, the relationship used in certain materials to predict the remaining lifetime t_r under static loading conditions when failure is controlled by crack propagation[1] is shown below.

$$t_r = \frac{2}{\nu_o(n-2)} \left(\frac{K_o}{\sigma_a Y}\right)^n \left[\frac{1}{a^{(n-2)/2}} - \left(\frac{\sigma_a Y}{K_c}\right)^{n-2}\right] \quad (1)$$

where 2a is the diameter of the flaw in the plane of propagation; ν_o, n, K_o, and K_c are parameters that define the crack propagation resistance of the material; and Y is a parameter that depends on the flaw profile along the prospective fracture

plane. It is the flaw diameter a which must be determined nondestructively. A specific example of the more general goal of quantitative NDE: to predetermine the in-service failure probability of a structural component with the best possible confidence.

There are many viable approaches for obtaining the necessary information about defect structure. In the ARPA/AFML program we have emphasized ultrasonics for a number of reasons. First, ultrasonics is a form of radiation which will penetrate structural parts so that interior defects can be interrogated. Secondly, the ultrasonic fields scattered by defects inherently contains much information about the defect structure. Finally, although other techniques are also recognized to be quite useful, it is felt that the most progress can be made by concentrating the available resources in a critical mass effort in one area.

Figure 3 further illustrates the technical goal of ultrasonic flaw definition. Ideally, we would like to find an operator, θ, which functionally relates scattered ultrasonic fields and some independently known material parameters to the failure probability of a part. One approach is to measure the size, shape, and orientation of defects and then use relationships such as the one shown in Eqn. 1 predict lifetime. In classes of materials with different failure modes, alternate but similar approaches will be needed.

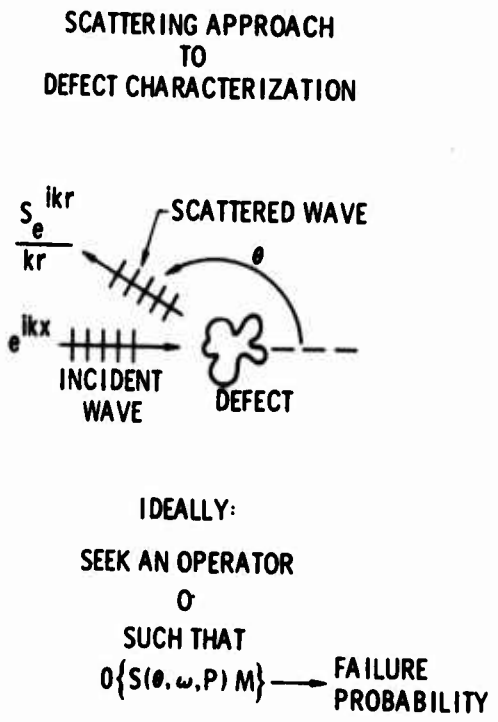

Figure 3. Ideal Goal of Quantitative Ultrasonic Non-Destructive Evaluation.

Let us now become more specific. Table I shows some critical flaw sizes that would be expected for a wide variety of materials under typical design loads. The striking feature is the range of flaw sizes with which NDE is forced to deal. These range from 25 millimeters for a particular aluminum alloy down to 20 microns for some of the high density ceramics and even less for the more brittle glasses. We have also included the frequency for which the ultrasonic wave length is equal to the diameter of these flaws. These range from 200 KHz on up to 250 MHz and into the gigantic range.

TABLE I

CRITICAL FLAW SIZE:

$$a_c \approx \left(\frac{K_c}{\sqrt{\sigma_a}}\right)^2$$

Order of magnitude estimates of critical flaw sizes in some metal and ceramic systems.

Materials		Flaw Size (mm)	Frequency for $\lambda_t = 2a_c$ (MHz)
Steels	4340	1.5	2.0
	D6AC	1.0	3.0
	Marage 250	5.0	0.59
	9NI4Co 20C	18.0	0.16
Aluminum Alloys	2014-T6S1	4.5	0.71
	2024-T3511	25.0	0.26
Titanium Alloys	6A1-4V	2.5	1.2
	8A1-1Mo-IV(a)	14.5	0.21
Silicon Nitrides	Hot Pressed	0.05	100
	Reaction Sintered	0.02	250
Glasses	Soda Lime	0.001	2,500
	Silica	0.003	830

This table illustrates two points which were made by Don Thompson[2] in an earlier paper in which he discussed the generic and specific aspects of NDE. From the range of defect sizes, it is quite clear that there are many special cases which are going to require their own individual solutions; it is necessary to develop some basic fundamentals which can then be applied to particular cases.

Table II defines the two classifications into which approaches for defect characterization can be divided. Imaging systems are designed to process the ultrasonic fields in such a way that a geometric outline of a defect is produced. This is very appealing since a visual display of the defect is easily interpreted by an operator. For good performance, a number of conditions must be satisfied. The wave length should be considerably less than the dimensions of the defect in order to obtain the resolution necessary to specify detailed shape. Results are best when the defect has a relatively rough surface with respect to the ultrasonic wave length so that the scattering is diffuse. Ideally, the object should have no elastic resonance.

Table II

FLAW CHARACTERIZATION CONCEPTS

TYPE OF MEASUREMENT	GOAL	CONDITIONS FOR BEST PERFORMANCE
IMAGING	DIRECTLY DEFINE GEOMETRIC OUTLINE	· WAVELENGTH < DIMENSIONS · SURFACE ULTRASONICALLY DIFFUSE · OBJECT HAS NO MAJOR ELASTIC RESONANCES
SCATTERING	DEDUCE KEY GEOMETRIC FEATURES FROM PARTICULAR DETAILS OF SCATTERED FIELDS	· DIMENSIONS <WAVELENGTH · SPECULAR OBJECTS · RESONANCE OBJECTS OR ANISOTROPIC MEDIA

The philosophy of scattering techniques is somewhat different. These are designed to enable one to deduce key geometric features of defects from particular details of the scattered field. They can be applied over a wider range of wave lengths. They can be used when the object is a specular reflector, and the presence of elastic resonances within the defect may give useful information about its structure.

Imaging and scattering approaches share a common foundation as illustrated in Fig. 4. Consider for simplicity a situation in which an ultrasonic wave is being scattered by an object consisting of two points. A pair of spherically spreading wave fronts will leave the object and, in the far field will be superimposed to form an interference pattern. Various defect characterization techniques are simply particular ways of processing this scattered field. For example, in an imaging system one inserts a lens or some electronic equivalent thereof to focus all of the rays leaving one point on the object to a single point in the image plane. Mathematically speaking, this is equivalent to taking a Fourier transform of the far field scattering pattern. However, as will be presented in later papers, other operations on the scattered fields can yield useful information. For example, defect sizes can be inferred directly from the spatial frequencies of the farfield scattering. Also, certain adaptive, nonlinear processing techniques are showing considerable promise.

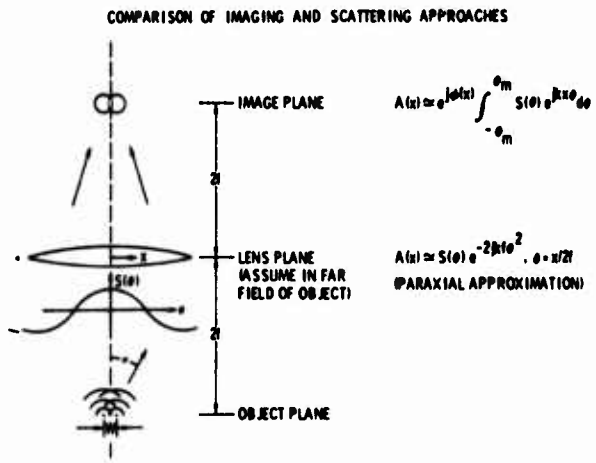

Figure 4. Comparison of Imaging and Scattering Approaches. A(x) is the field amplitude that would be measured in a given plane.

Let us now turn to some of the specifics of the ARPA/AFML program on quantitative NDE. This discussion is aided by reference to a model defect characterization system as shown in Fig. 5. Here, a transducer array is shown illuminating a part placed in a water bath with longitudinal waves. Both longitudinal mode converted shear waves will be scattered by a defect within the part as these waves reach the part surface. The longitudinal wave will be refracted and the shear wave will be mode converted into longitudinal waves in the water. Hence, the array will pick up signals arising from both the direct L → T scattering. Some signal processing is then often necessary to improve signal-to-noise ratios and to compensate for transducer frequency response and geometrical effects. Finally, signal interpretation is needed so that a decision can be made to determine whether the part is to be accepted or rejected.

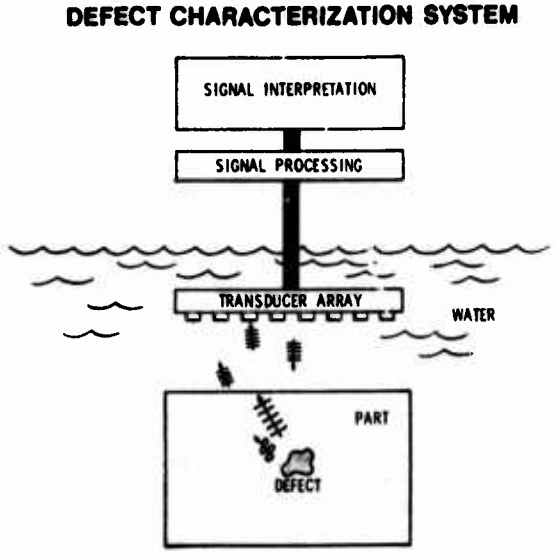

Figure 5. Model system for quantitative flaw characterization showing key components needed.

I would now like to briefly describe the research tasks going on in each of these areas and indicate their interrelationships. We have used the diffusion bonding technology to produce a set of samples with well characterized defects in their interior. Figure 6 shows the particular set that we have chosen. Included are spherical cavities, oblate (pancake-like) spheroidal cavities of two aspect ratios, 2 to 1 and 4 to 1, prolate (cigar-like) spheroidal cavities again with 2 to 1 and 4 to 1 aspect ratios. We have also reported previously some work on flat bottom holes. In addition, we have recently made some circular and elliptical cylindrical cavities of large diameter to height ratios similating cracks.

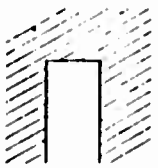

FLAT BOTTOM HOLE
TYPE 1 DEFECT
400, 800, 1200 μ DIA

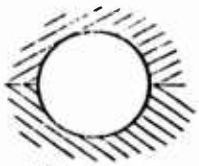

SPHERICAL CAVITY
TYPE 2 DEFECT
400, 800, 1200 μ DIA

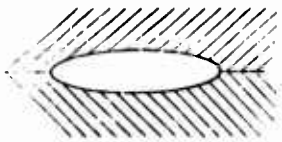

OBLATE SPHEROID
TYPE 3 DEFECT
800 μ DIA.
200, 400 μ HIGH

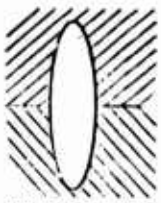

PROLATE SPHEROID
TYPE 4 DEFECT
1600 μ HIGH
400, 800 μ DIA

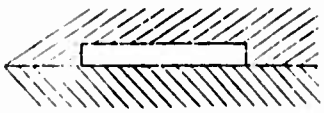

PENNY SHAPED CRACK
TYPE 5 DEFECT
1200, 2400 μ DIA.

Figure 6. Cavities placed on the interior of a titanium block by diffusion bonding techniques.

A few words should be said about the philosophy of the choice of the defect types. We have chosen these simple shapes because they are amenable to theoretical analysis. We feel that a firm theoretical foundation is a very important prerequisite of a quantitative NDE capability. Although these cavities have simple shapes, it should be noted that the limiting case of the oblate spheroid is a thin crack. Hence, we can project what will happen for that technologically important case from the solutions that are presently developing.

Due to time limitations, there will be no paper on the preparation of samples using diffusion bonding. However, in addition to preparing samples in titanium 6Al-4V alloy, new techniques have been developed for bonding certain steel alloys (as reported last year[3]), and also, more recently, aluminum.

Figure 7 illustrates the importance of developing a sound theoretical basis with which to interpret ultrasonic scattering experiments. This compares the solutions for scattering by spheres[4] for several cases that might initially be imagined to be quite similar. In the lower left-hand figure, the angular dependence of the scattering from a rigid sphere in a fluid is shown. This is obtained from the solution of a scalar wave equation with clamped boundary conditions at the sphere surface. The lower right-hand shows the scattering from a cavity in a fluid as obtained from a solution of a scalar wave equation with pressure-free boundary conditions on the surface of the sphere. The upper right-hand shows the solution that applies to a cavity in a solid. This requires solution of a vector wave equation.

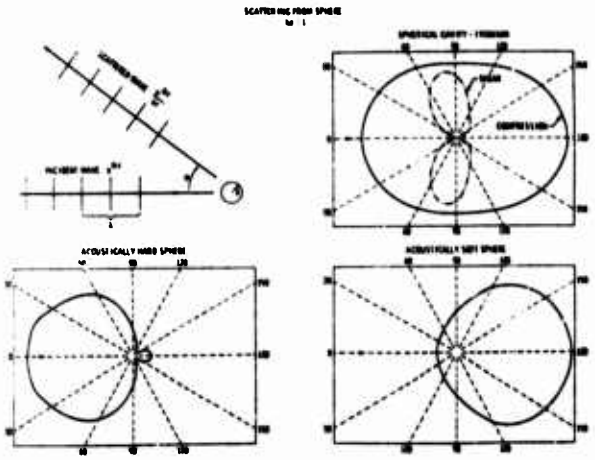

Figure 7. Comparison of the scattering from spherical obstacles in fluids and solids when ka=1.

It is immediately evident that there are tremendous differences between the three cases. If one wishes to develop quantitative systems for interpreting scattered fields, then the appropriate solutions must be available.

Figure 8 shows some of the scattering solutions that have been obtained and illustrates how these might be used to design a defect characterization system. These are the results of the theoretical efforts of Krumhansl, Gubernatis, Domany, et al at Cornell University[5]. The basic scattering geometry and coordinates of the plot are shown at the top of the figure.

The plots are projections of the scattered fields. The center of each plot corresponds to direct backscattering while the periphery shows the scattering at 90°. The information is presented in a contour representation, with regions of constant scattered amplitude shaded in like fashion. The left hand column illustrates the scattering by a spherical cavity. The upper plot shows the longitudinal to longitudinal (L→L) scattering, while the lower plot shows the longitudinal to transverse scattering (L→T). As would be expected, the results are symmetric. The L→ L scattering is strongest in the back scattered direction and becomes progressively weaker as 90° is approaches. The L→T scattering has just the opposite behavior. The right hand column shows similar results for an oblate spheroid inclined at 45° with respect to the incident wave. Here, the L→L scattering is greatest in the downward direction, but not exactly at 90° as would be predicted by specular reflection. Likewise, the L→T scattering follows intuition. These plots provide a quantitative template

which can be used in designing experimental systems, for example, in selecting the frequency and aperture required to distinguish between certain classes and orientation of defects.

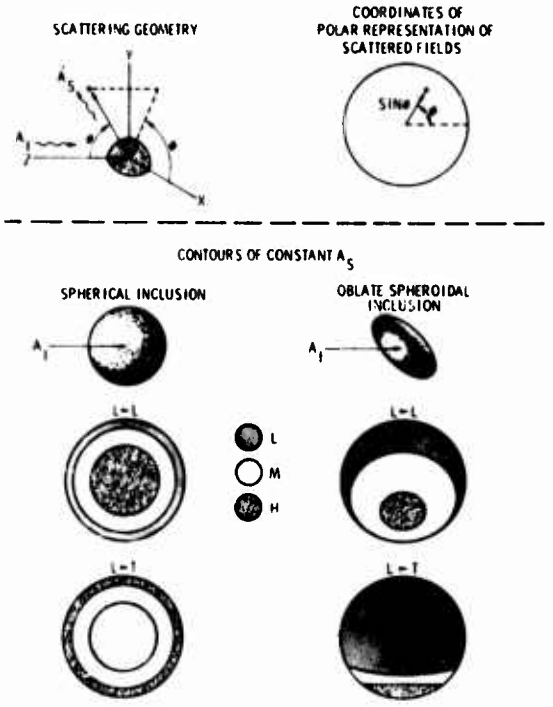

Figure 8. A contour representation of the elastic fields scattered by a spherical cavity and an oblate spheroid. The shadings designated as L, M, and H indicate low, medium, and high scattering amplitudes.

The remainder of the tasks can best be described with reference to Fig. 5. The importance of theoretical understanding of the scattering of the ultrasound by the flaw has already been discussed. In addition, it is important to develop the experimental techniques necessary to both test the theories in ideal samples and to apply the test techniques to real parts. Tittmann[6] and Adler[7] will present such results.

Transducers form an important element of any defect characterization system. It is at this point that much information can be lost. The ultimate transducer may well be the array along with appropriate electronic components to steer and shape the resulting beam. Array transducers developed as parts of other programs will be mentioned in the papers by Kino[8] and Posakony[9]. However, most present work is performed using single element transducers. Lakin[10] discusses the development of apparatus and analytical techniques to quantify their performance. Tiemann[11] also describes some advanced transducer development that has taken place at General Electric.

Once the ultrasonic information has been converted into electrical signals, signal processing is necessary to optimize bandwidth, signal-to-noise ratios and other parameters. White[12] describes the use of surface acoustic wave filters to increase resolution and Newhouse[13] presents his most recent results in the processing of random noise signals.

The final step, and one of the most critical ones, in a defect characterization system is the interpretation of the data. Kino[8] and Posakony[9] describe imaging systems designed for this purpose. In their studies of scattering, Tittmann[6], Adler[7], and Krumhansl[15] have also developed some preliminary interpretive schemes. Finally, Mucciardi presents some exciting results demonstrating the power of adaptive nonlinear learning procedures in measuring the size of fatigue cracks.

One of the problems with the system shown in Fig. 5 is the water bath. Making measurements in a tank is a slow and cumbersome procedure which is particularly difficult for components in service. Szabo[15], Moran[16], Maxfield[17], and Thompson[18], join to present a mini-symposium on alternate transducer, the transducer which operates with no contact and hence, avoids this problem.

The concepts just outlined are new, but they are already finding application. In a previous paper, Evans[19] described how they are being used in the development of inspection techniques for ceramic materials. In addition, Tittmann[20] will describe the development of new ultrasonic standards and calibration techniques based on these principles.

As Don Thompson said previously, the first year of our ARPA/AFML program was characterized by the individual efforts by a number of investigators to establish basic capabilities. A number of these people had not previously been a part of the NDE community but had expertises that were directly applicable. During last year, and as described in the following papers, these people have now joined together in many group efforts. Krumhansl, Adler and Tittmann have had strong interactions in the development of quantitative measurement techniques. Other interactions will also become evident. The second year has thus been characterized by a joining together to form teams directed towards the solution of common problems. During the next year we will be continuing and consolidating this effort to demonstrate the ability to nondestructively measure fracture critical parameters of certain classes of defects based on a firm fundamental understanding of the basic measurement phenomena. More work will be needed to develop a comprehensive system, but the basic procedures will have been demonstrated. As shown in Fig. 9, what is ultimately needed is the development of quantitative accept/reject criteria based on the combination of results such as these with appropriate fracture mechanics or other failure prediction analyses. This marriage can take place in a future program based on the foundation now being developed.

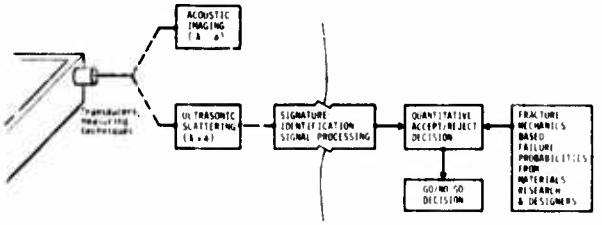

Figure 9. Steps required to incorporate quantitative accept/reject criteria with ultrasonic NDE to make Go/No Go decisions.

References

1. R. Bruce Thompson and Anthony G. Evans, "Goals and Objectives of Quantitative Ultrasonics," IEEE Trans. on Sonics and Ultrasonics, SU-23, 292 (1976).

2. D. O. Thompson, "Introduction Remarks", this proceeedings.

3. N. E. Paton, "Ultrasonic Samples Using Diffusion Bonding Techniques," Proceedings of the ARPA/AFML Review of Quantitative NDE, AFML-TR-75-212, p. 89 (1976).

4. E. R. Cohen, private communication.

5. J. Krumhansl, E. Domany, P. Muzilcar, S. Teitel, D. Wood, and J. E. Gubernatis, "Interpretation of Ultrasonic Scattering Measurements by Various Flaws From Theoretical Studies", this proceedings.

6. B. R. Tittmann, "Measurements of Scattering of Ultrasound by Ellipsoidal Cavities", this proceedings.

7. L. Adler and D. K. Lewis "Models For The Frequency Dependence of Ultrasonic Scattering From Real Flaws", this proceedings.

8. G. S. Kino, "The NDT Program at Stanford University", this proceedings.

9. G. J. Posakony, "Near Real Time Ultrasonic Pulse Echo and Holographic Imaging System", this proceedings.

10. K. M. Lakin, "Characterization of Piezoelectric Transducers", this proceedings.

11. J. J. Tiemann, "A Practical Approach to Fabricating Ideal Transducers", this proceedings.

12. R. M. White, "Signal Processing With SAW Devices", this proceedings.

13. V. Newhouse, "Adaptive Deconvolution To Improve Resolution Independence of Bond Width", this proceedings.

14. A. N. Mucciardi, "Measurement of Sub-Surface Fatigue Crack Size Using Nonlinear Adaptive Learning", this proceedings.

15. T. L. Szabo, "Surface Acoustic Wave Electromagnetic Transducer Modeling and Design for NDE Applications", this proceedings.

16. T. J. Moran, "Characteristics and Applications of Electromagnetic Surface Wave Transducers", this proceedings.

17. B. W. Maxfield and J. K. Hulbert, "Optimization and Application of Electrodynamic Acoustic Wave Transducers", this proceedings.

18. R. B. Thompson and C. M. Fortunko, "Optimization of Electromagnetic Transducer Systems", this proceedings.

19. A. G. Evans, B. R. Tittmann, G. S. Kino, and P. T. Khuri-Yakub, "Ultrasonic Flaw Detection in Ceramics", this proceedings.

20. B. R. Tittmann, "New Procedures for Calibrating Ultrasonic Systems for Quantitative NDE", this proceedings.

PROF. VERNON NEWHOUSE (Purdue University): Well, that certainly raised a lot of thoughts in my mind about the philosophy of approach. This talk suggests that we should try to characterize individual defects. It seems to me that this is a very interesting program. The risk is: will we be able to characterize a defect that is in a real environment with lots of multiple reflections? And will different defects have enough differences in their spectra so that one can separate them? And, of course, I'm sure you will keep in mind that there is the other approach, which I suppose will be talked about this afternoon, of actually trying to image things with very small wave lengths. We're faced with an interesting situation since in the next few years we won't know which of these techniques will be most successful where.

Now, I understand there are a few people who have some questions or comments.

DR. ARDEN BEMENT (ARPA): There are a couple of caveats I'd like to comment on, which probably don't need to be made in this audience. Referring to your table of critical flaw sizes, I think it's obvious that what you really have, if you can measure that flaw size, is a prediction for zero remaining life. So, one has to do, perhaps, an order of magnitude better than that in order to measure a size that will have a remaining in-service life of practical importance.

Also, in many cases the real problem is the opening up of a tight flaw with interconnected ductile ligaments during service and also the interconnection of co-planar, closed porosity to form an interconnected flaw. So, the problem gets much more difficult than just measuring a single isolated definable flaw.

DR. THOMPSON: We certainly agree with both those comments. Those are extremely difficult problems. We feel the successful solution of those problems is only going to be obtained after we have developed the fundamentals for the much simpler cases which we are presently addressing.

DR. NELSON HSU (University of Kentucky): I have a very long question. The philosophy of using the scattering field measurements to replace the pulse echo technique is right. But the reason is that if the flaw has a specific orientation, the use of a one directional measurement cannot always detect the defect. However, if you use the scattering technique you have to place the transducer at different angles to measure the scattered field. If the geometry is such that you can do that, then at the same time you could place a single transducer at different angles and actually just measure the pulse-echo back scattering. I don't know which technique gives more.

DR. THOMPSON: The basic point I want to make is we do have to gather a lot more information than is presently used. I think the approach you describe is one particular example of what I would call a scattering approach. I think we're in basic agreement. One has to make more than one single measurement and in addition needs a systematic way of interpreting the information.

PROF. NEWHOUSE: I think I would also like to make two comments on that last question. One is you can look at the scattered waves over a range of angles or you can vary the frequency and look at one angle. These are two dual techniques in a sense. By varying the frequency and seeing what spectral peaks you get, you should get the same information as is contained in these diagrams of radiation scattered over many directions. I see somebody shaking their head, so perhaps the information isn't quite pure.

Also, getting information about the scattering of one particle or one defect ought to be helpful in trying to tackle the problem of getting the spectra that comes from a series of grains so as to get more information about grain structure. And I think we ought to keep in mind there that the x-ray crystallographers, as we all learned shortly after high school, have been successful mainly in interpreting the spectra from periodic arrays or quasi-periodic arrays. So that here in the ultrasound, we are tackling a problem that has not yet been successfully solved by the x-ray people.

At this point I would like to call on the next speaker, Professor Lakin of the University of Southern California to talk about transducer characterization.

CHARACTERIZATION OF NDE TRANSDUCERS

K. M. Lakin
University of Southern California
Los Angeles, California 90007

Characterization of NDE transducers is an important part of current and future programs in quantative flaw detection. In the work reported here, emphasis has been placed on beam pattern measurements or profiling and circuit modeling of the transducer using electrical network scattering parameters, or S-parameters. The latter topic is relatively new and was developed in the last six to eight months in order to handle the problems of existing commercial transducers whose internal details are unknown. A subset of this goal is to: (a) explore single crystal or very high quality ceramic materials as the piezoelectric element, (b) examine the single disk in water as a transducer or reference element, and (c) look into electrical loading as an alternative to mechanical loading.

Shown in Fig. 1 is a schematic diagram of the setup for measuring or calculating the field pattern of a transducer. The transducer is located in the (x,y) plane and has an assumed extent of 2a for the purposes of field reconstruction. The measurement plane (u,v) is located at distance R from the source plane in the Fresnel zone or even in the far field. To first order the planes are parallel although a slight non-parallelism is easily detected and accounted for in the analysis. The sampling points are taken as Δu and Δv where usually $\Delta u = \Delta v$. As described in last year's meeting, the measurement plane is scanned by a computer controlled stepping motor driven table and the measured amplitude and phase are fed to the computer for analysis.

The information used for the field reconstruction is given below.

$$U(u,v) = \frac{2\pi}{jk} \iint U(x,y)\, \frac{e^{ikr}}{r}\, dxdy$$

u,v	field coordinates
x,y	source coordinates
r	source to field distance
U(x,y)	source field, magnitude and phase
kr	rapidly varying phase

Here the field amplitude is given by U(u,v) in the Huygens formulation so that the inverse equation can be simply cast in the Fourier transform regime for computer manipulation. The phase term kr is rapidly varying as a function of coordinates and must be expanded into terms which yield more tractible integrals. First r is expanded into the form,

$$r = R + \frac{1}{2R}\left[(x-u)^2 + (y-v)^2\right]$$

where R is the average distance from source to field position. From this substitution into the Huygens equation we obtain,

$$U(u,v) = C \iint U(x,y)\, e^{ik\left[(x-u)^2 + (y-v)^2\right]/2R}\, dxdy .$$

Letting $\theta = KR$,

$$R = \frac{U}{2\pi}\,\frac{d\theta}{df} \text{ , and}$$

$$d\theta = \theta\left[\, df/f + dR/R - dV/V \,\right].$$

The average distance R may be determined by measuring the variation of average phase θ with frequency. In addition the phase may be measured at several points and the parabolic phase cap evaluated to determine the apparent source-to-field distance. The phase measurement is sensitive to the changes in frequency, average distance, and velocity of sound in water.

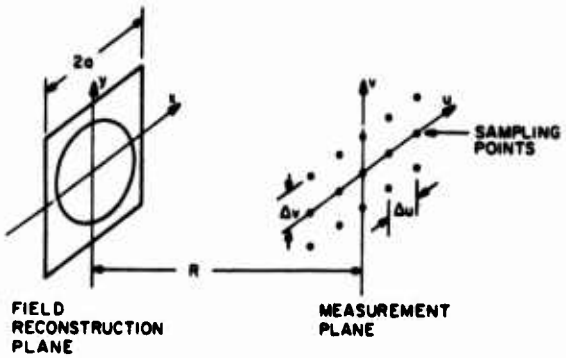

Figure 1. Coordinate system used to analyze direct and inverse scattering problem.

The average phase was held fixed by controlling frequency in a phased locked loop synthesizer. The natural building vibrations produced dR variations in the micron range at frequencies up to 100 Hz and resulted in phase fluctuations which could only be eliminated by signal averaging. The velocity of sound in water is quite temperature dependent and the measurement was complicated by the fact that the building air conditioner is shut down at night and turned on again in the morning, causing a long-term gradual shift in phase as the water bath slowly heated during the course of the measurement. More recently, the velocity and distance sensitivity has been circumvented by passing the reference signal of the network analyzer through the water bath as well, and thus greatly reducing the phase fluctuations.

The Fourier transform format is obtained by a normalization by expanding the parabolic phase factor. The results are given below.

$$\bar{U}(c',v') = C\iint_{-\infty}^{\infty} \bar{U}(x',y')\, e^{ik'(u'x'+v'y')}\, dx'\, dy'$$

where

$$\bar{U}(u',v') = U(u',v')\, e^{-ik'(u'^2+v'^2)/2}$$

$$\bar{U}(x',y') = U(x',y')\, e^{ik(x'^2+y'^2)/2}$$

$$C = 2\pi \frac{e^{ikR}}{ikR}$$

$$x' = x/a,\ y' = y/a,\ u' = u/a,\ v' = v/a$$

$$k' = ka^2/2R.$$

Once in the Fourier transform format, the inverse fields are readily defined and calculated. One of the research problems was to examine the nature of the field distribution and determine the minimum number of sampling points required to reproduce the field to a given degree of accuracy consistent with experimental accuracy.

Experimental results with computer reconstruction are shown in Figs. 2, 3, and 4. Figure 2 gives the field amplitude and phase of a transducer, at the transducer face, as reconstructed from measurements made in the Fresnel Zone. There is a tilt in the phase due to a slight non-parallelism between the average phase plane of the transducer and the scan plane. The shift in the plots to the right of the assumed origin accounts for the uncertainty in locating the axis of the transducer relative to the scan plane.

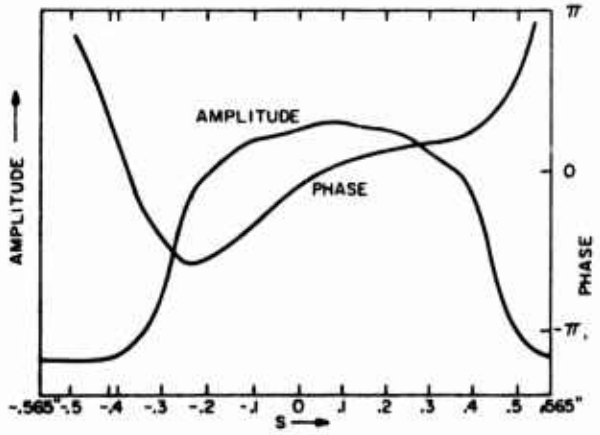

Figure 2. Amplitude and phase of the reproduced field of a 1.7 inch diameter transducer. The linear phase contribution is due to axis tilt during the measurement.

Figures 3 and 4 are reconstructions of a transducer whose front face was covered in a small area with a partially absorbing film of rubber cement. The reconstruction is based upon a 17x17 sampling grid taken at intervals of 0.5 inch. The contour plots in Fig. 3 are of the linearly smoothed amplitude at the transducer with the amplitude at the center of the defect normalized to unity. Figure 4 is a grey-scale reconstruction of the same case as in Fig. 3, except that no smoothing has been done to the 17x17 sampling grid. Both power and amplitude are shown in a graphic manner that corresponds to an image of the transducer field.

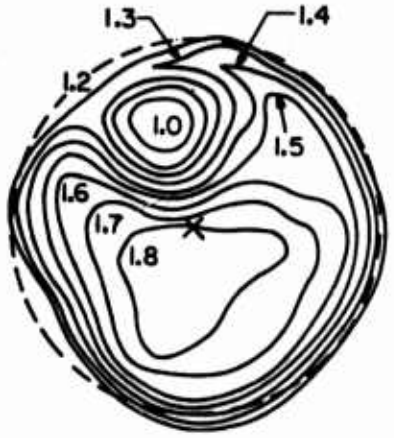

Figure 3. Amplitude contours on a 0.7 inch diameter transducer with defect. Dashed circle represents the assumed edge of the transducer.

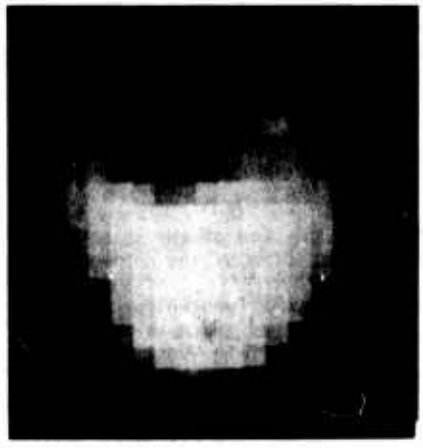

(a)

Figure 4 Grey-scale image of the acoustic field at the transducer surface. Black represents the lowest levels and white the highest levels. (a) Field intensity (amplitude squared).

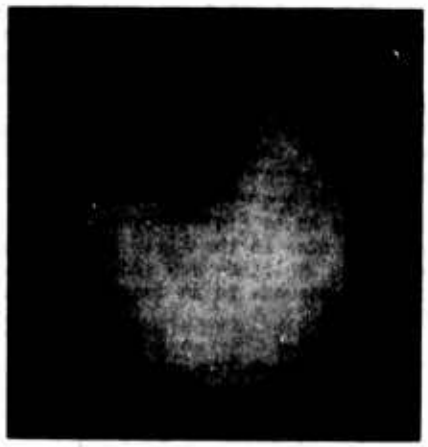

(b)

Figure 4. Grey-scale image of the acoustic field at the transducer surface. Black represents the lowest levels and white the highest levels.
(b) Field amplitude.

The methods used to image the transducer as a source can also be used to image a reflecting surface by treating the surface as an apparent source and using the reconstructions described above.

To review briefly, the experimental procedure for beam pattern measurements is to:

1. Locate the apparent beam axis by measuring the "phase cap"
2. Measure $d\theta/df$ and calculate R, the average distance between source and receiver
3. Assume a value for the source size and scan the grid accordingly
4. At each measurement point in the field plane, normalize the parabolic phase factor
5. At the end of the scan, calculate the transform of the normalized field, and,
6. Un-normalize the result if both amplitude and phase are desired, and display the source field.

Once having the amplitude distribution at the face of the transducer the acoustic field may be determined at any other location by the transform method. It is of interest in quantitative NDE to relate this acoustic pressure field to the electrical signals at the transducer terminals.

The inverse scattering results reviewed above were used to determine the amplitude and phase variations at the transducer surface based upon measurements made in the Fresnel zone. To complete the transducer characterization, it is necessary to determine the electrical to acoustical transduction efficiency as well. There are numerous procedures which may be used to accomplish this task involving calibrated sources of acousto-optic interactions. The method outlined here involves wave reflections from a known reference surface and can be accomplished with the usual ultrasonic equipment with the slight addition of a coaxial directional coupler. The S-parameters are then derived from measurements taken only at the electrical terminals.

The S-parameters, or scattering parameters, are a convenient means of describing devices involving transmission line type behavior. This concept may be adapted to the NDE transducer through the following set of equations,

$$V_r = S_{ee}V_i + S_{ea}T_i \qquad (1a)$$

$$T_r = S_{ae}V_i + S_{aa}T_i \qquad (1b)$$

In (1) V_i is the voltage of the wave incident upon the transducer, such as from a generator, V_r is the voltage of the wave reflected from or leaving the electrical terminals, T_i is the acoustic pressure field of a wave incident upon the transducer, and T_r is the acoustic pressure field of the wave reflected or radiated from the transducer. The four subscripted S constants are referred to as the S-parameters.

If the transducer radiates into an empty half space, containing no other sources, then T_i is zero since no acoustic waves can be incident upon the transducer. In this case (1) reduces to

$$V_r = S_{ee}V_i \qquad (2a)$$

$$T_r = S_{ae}V_i \qquad (2b)$$

Thus S_{ee} is just the electrical reflection coefficient due to an impedance mismatch between the electrical cable and the transducer, and is a readily measured parameter. The parameter S_{ae} relates to the conversion of electrical volts to acoustic stress or pressure and is of direct interest, as will be discussed later here in detail. If the transducer is excited only by an acoustic wave, then $V_i=0$ provided there are no reflections from the receiver input. In this case (1) reduces to

$$V_r = S_{ea}T_i \qquad (3a)$$

$$T_r = S_{aa}T_i \qquad (3b)$$

For this case S_{ea} is readily identified as the acoustic to electrical conversion factor and S_{aa} as the acoustic reflection coefficient when $V_i=0$.

Before reviewing the techniques that were developed to measure the S-parameters it is useful to first go back and re-evaluate the nature of the parameters S_{ea} and S_{ae} of (1). First of all, note that the parameters are really a hybrid mixture of acoustic and electrical quantities and not dimensionless as might be desired. Essentially S_{ea} and S_{ae} contain a factor which relates the conversion of units that is inherent to the transduction process. To see this in more detail, refer to the Mason equivalent circuit model of a piezoelectric disk, Fig. 5.

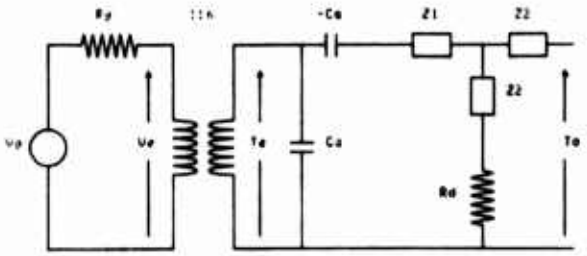

Figure 5. Equivalent circuit of piezoelectric disk including a backing load, R_g.

The lumped element parameters have the usual definitions,

$$n = 2fok\ C_t Z_o \quad (4a)$$

$$Z1 = -jZ_o \csc(p) \quad (4b)$$

$$Z2 = jZ_o \tan(p/2) \quad (4c)$$

$$C_a = C_t/n \quad (4d)$$

C_t = disk capacitance (4e)

$p = kd$, phase (4f)

k = wave number (4g)

d = disk thickness (4h)

Z_o = disk mechanical impedance (4i)

f_o = disk parallel resonant frequency (4j)

An important concept to be used in the analysis is that the transformer may be "drifted" across the network so long as the circuit elements take on appropriate units. For example, the normal circuit model is drawn with the capacitors on the electrical side of the transformer but are shown here on the acoustic side.

From the network in Fig. 5, it is apparent that the stress T_e is the mechanical equivalent of voltage V_e and is simply related to V_e by the relation,

$$T_e = nV_e$$

Likewise, T_o is related to T_e through a simple network relation,

$$T_o = ST_e$$

The stress T_o may be used to represent either T_i or T_r of (1). Thus the parameter equations may be written as,

$$V_r = S_{ee}V_i + S/n\ T_i \quad (5a)$$

$$T_r = nS\ V_i + S_{aa}\ T_i \quad (5b)$$

Now the S-parameters are in a dimensionless form.

A real transducer usually contains an electrical matching network and an acoustical matching network as well, Fig. 6a. However, since the transformer may be "drifted" to the left, the electrical network may now be included with the two acoustical networks to form one single network, Fig. 6b.

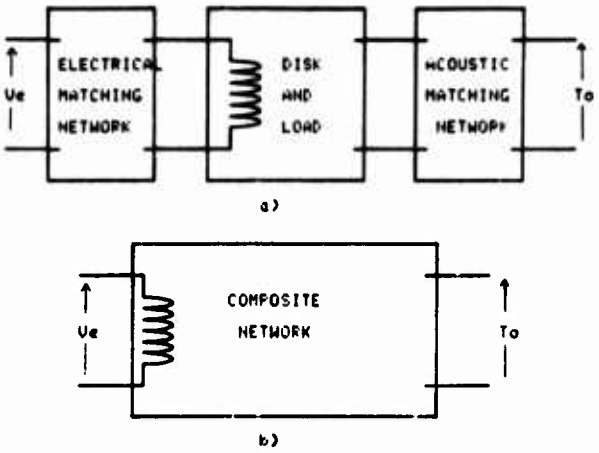

Figure 6. General network representation of a NDE transducer. (a) Back loaded disk having electrical and acoustic matching networks. The acoustic network may include external bonds. (b) The resultant acoustic composite network when all electrical networks are taken to the acoustic side of the transformer and when acoustic matching networks are lumped in with the disk and backing load.

In order to characterize the transducer within the scope of this model, it is necessary to establish a measurement procedure. Two kinds of procedures have been adopted and implemented experimentally. The basis for the procedures rests upon establishing a known relationship between T_i and T_r, since it is assumed that the acoustic stresses are not to be measured directly. One way to relate T_i and T_r is to use the transducer to scatter sound off of a known target such as a planar surface, Figs. 7 and 8. The relation is then,

$$T_i = R\ T_r \quad (8)$$

where R is the reflection coefficient of the surface including the phase factor. Using this relation in (7) an electrical reflection coefficient can be derived.

$$R_e = V_r/V_i = S_{ee} + RS/(1 - RS_{aa}) \quad (9)$$

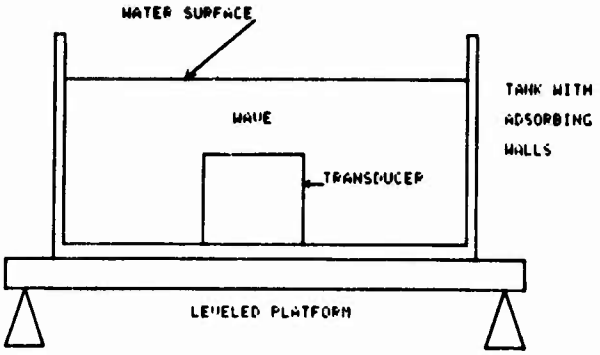

Figure 7 Mechanical setup for measuring the S-parameters using air liquid as the reference scattering surface. In the water bath system the water surface is adjusted for parallelism with the transducer surface. The water level may also be adjusted to move the "short-circuit".

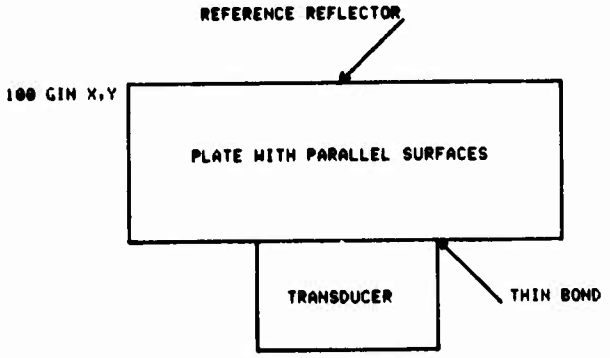

Figure 8 Measuring setup for air-solid reference using a block with parallel surfaces. The bond region is considered part of the transducer network.

By using a directional coupler or bridge in the electrical line, as shown in Fig. 9, R_e may be measured quite easily. If the measurement is in the pulse-echo mode, then the first and second terms may be resolved by time separation,

$R_e(t) = S_{ee}\, u(t)$ electrical reflection

$+ S^2\, u(t-t_a)$ first echo

$+ (S^2)S_{aa}\, u(t-2t_a)$ second echo

$+ (S^2)(S_{aa})^2\, u(t-3t_a)$ third echo

$+ \ldots\ldots\ldots$ etc.

where u(t) is the unit step function. Thus RS is measured directly if the time resolution is sufficient. The reflection coefficient, R, is assumed to be known and thus S is determined.

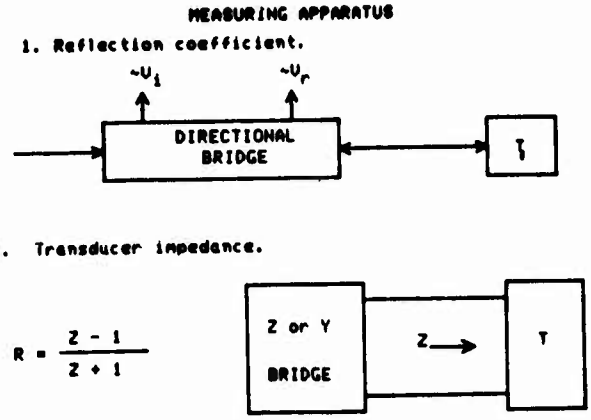

Figure 9. S-parameter measurement system.

In the steady state mode of operation, all the terms of (9) are determined using well known microwave network measuring techniques. The most simple method is to use a high frequency voltmeter or oscilloscope to measure the magnitude variations of R_e. If the phase of the acoustic reflection coefficient, R, is changed over several 360 degree intervals, the magnitude of S_a is seen to go through several maxima and minima, S+ and S- respectively, corresponding to the interference phenomena taking place between transducer and reflector. From these, S^2 and S_{aa} are given by,

$$S^2 = 2/\frac{S_a^+ S_a^-}{S_a^+ + S_a^-} \qquad S_{aa} = 1/\frac{S_a^+ + S_a^-}{S_a^+ - S_a^-}$$

The phase may be changed either by sweeping the input frequency or by moving the physical position of the reflector. The latter technique was implemented by reflecting off the top surface of a water bath and then raising or lowering the water level to change the distance between the transducer and reflecting surface, Fig. 7. The water level could be lowered to within several wavelengths of the transducer surface before surface tension distorted the reflecting surface. If a solid-air reference is used, then the system shown in Fig. 8 may be used in the swept frequency of pulse-echo mode and the bond considered part of the transducer. Using these techniques S_{ee}, S_{aa}, and S were measured for several NDE transducers.

The turns ratio n was not measured and cannot be measured without some absolute measure of stress such as by using a transducer or simple disk having a known turns ratio. It should be made clear that the turns ratio need not be known if the same transducer is used for both sending and receiving. Also note that n is a property of the piezoelectric disk itself and not dependent upon electrical or acoustical matching or damping elements.

Two transducers exhibit a composite S'given by

$$S' = S_1\, S_2\, (n_2/n_1)$$

where S_1, n_1 belong to the receiving transducer and S_2, n_2 belong to the sending transducer. If the two transducers are aimed nearby at each other and S' measured via transmission then the ratio of n's is now determined since S_1 and S_2 may be found separately.

Clearly, if the two transducers have identical disk elements, neither n need be determined since only the S's are required. Generally all that is needed is knowledge of what kind of material is used for the piezoelectric disk since the diameter and disk thickness are usually obvious.

DISCUSSION

PROF. VERNON NEWHOUSE (Purdue University): Are there any questions?

PROF. GORDON KINO (Stanford University): If the term on the S-parameter is, as you say, analagous to the wave guide case which postulates no loss, can the theory be extended over into the lossy case?

DR. LAKIN: Oh, yes.

PROF. KINO: Particularly, when you do measure these S-parameters, what sort of loss do you see?

DR. LAKIN: Well, the S-parameter essentially turns out to be what you would normally think of as the conversion loss of the transducer. The theory is a little more general in that it tells you how to put two transducers together. Say you're doing scattering with two transducers; it tells you how to use two sets of parameters together because you can use the S-parameter model for both transducers. I didn't show it.

You can also convert S-parameters over to other parameters such as the impedance parameters, the hybrid impedance parameters, the admittance parameters, which ever you like.

MR. ROY SHARPE (Harwell Labs): How in the world do you see this characterization being done? We find that a firm that buys a transducer for, say, $50, is not going to spend $200 to get it characterized.

DR. LAKIN: I'm not sure whether you can buy one for $50, but I understand the point. I think it's not really a matter of what the transducer costs. If it costs you $10, you still may have need to know what it's characteristics are. So, unfortunately, you may have to spend an hour or so of a man's time and some investment. Equipment investment here is about zero, because if you use your standard pulse echo system, all you have to do is just set up that reflector system and make your measurements right there. Your capital investment is very small, I would say.

DR. EMANUEL PAPADAKIS (Ford Motor Company): I have a comment and a question. In Settig's analysis, he put in a transducer that had two acoustic ports, the front and the back. And you always get losses from the back when you're generating the wave, and when you have an incoming wave, part of it goes out into the electrical system and part of it goes out into the backing system.

DR. LAKIN: That's right.

DR. PAPADAKIS: How are you getting away from that? That's the first question. The second part is how does the entire analysis relate to Settig's work in 1969 in the Microwave Transactions on sonics and ultrasonics?

DR. LAKIN: Okay, the first question. The backing load is included in the formulation. Settig did that, including it as part of the transducer network to make it a two port. As long as there is no active source there in the backing load, then the formulation handles everything. Now, let's say, for example, that your backing load was imperfect and it didn't completely absorb because some sound was reflected back into the transducer. Well, instead of putting the real impedance there you have to put in a second lossy transmission line. So, you will get something coming back from that rear interface. Now, so far as the electrical port is concerned, that's taken into account in the n^2 term.

DR. PAPADAKIS: Is the impedance of the backing taken into account in the turns ratio or something--so that you have less power out electrically than you would have because some of the power has gone into the backing?

DR. LAKIN: That is accounted for, but not in the turns ratio. The nice thing about the turns ratio is that it is intrinsic to the piezoelectric disk itself.

DR. PAPADAKIS: Okay.

DR. LAKIN: Not how it's bonded. It's intrinsic to the disk.

DR. PAPADAKIS: Is it some other impedance?

DR. LAKIN: Yes. There was a branch in the circuit called "backing loads." I put it in as a resistor because that's how you would like to have it unless you're trying to do something fancy with the frequency response. You would like to have that as a real absorbing element. If it's not, then it's a section of the transmission line, nevertheless well characterized.

PROF. NEWHOUSE: We're getting short of time. We have time only for one more short question.

PROF. R. E. GREEN (John Hopkins University): With respect to the single disk transducer, I think you'll find, and maybe you already know, that many people who are not in the NDE business or in the medical ultrasonic business use single disk transducers, and to the best of my knowledge, the only reason they use the commercially made transducer in a box is because the average NDE guy throws it around in the tool box. It is for protection. The main comment I want to make is why did you ever think of water anyway? I suggest that you could do some optical imaging of the sample, especially with a CW technique, and you can be sure you get the transducer parallel to the surface or whatever, because it's fairly critical in setting up a standing wave in a tank of water and pretty easy to do like the Stearn's technique. If you want to do a more quantative measurement you can do laser beam probing or something like that. I'm not saying you should do that every day in the shop, but for setting up standards I would suggest some optical technique be used.

DR. LAKIN: Yes. Well, in terms of measuring the S-parameters, you can very easily align the surface of the water parallel with the phase front of the transducer. I don't know whether it's going to be parallel with the geometric surface of the transducer, chances are it won't be. But you can do that just by watching the manifestation of the standing wave, mainly, the fluctuations in the electrical reflection coefficient and then adjust the table for parallelism. In the process of doing that it's hard to keep the slowly varying ripples from going across the surface of the water. It turns out to be a benefit because you know whether you're at the maximum or not.

PROF. NEWHOUSE: Thank you.

A PRACTICAL APPROACH TO FABRICATING IDEAL TRANSDUCERS

J. J. Tiemann
General Electric Corporate Research and Development
Schenectady, New York 12301

A 20 minute talk is something like the well known definition of an expert. One can choose a very narrow subject and say all there is to say about it, or choose a broad one and say very little about any one part. And there is presumably an optimum choice of material and treatment somewhere between these extremes. But I'm going to try a new approach this morning. I'm going to take an extremely narrow subject and say essentially nothing about it. Part of this is a prejudice on my part that it's not very easy to communicate technical details in a meeting like this, and the other part is that I noticed just last night that I left about two-thirds of my figures at home. And so, I'm going to fill up most of the time that would otherwise be my speech with some comments. Since some of these may be controversial, I plan to have substantial time at the end, or even during my talk, if you wish, to pursue whatever questions come up.

I was invited here to come to talk about transducers, and I'd like to tell you how that came about. It came about because the General Electric Jet Engine Dept. has been trying to perform water immersion ultrasonic inspection of engine forgings with commercially available inspection equipment and has found that this equipment is ill suited to the task. I would guess that most of these instruments were designed 5 or 10 years ago for applications in the steel industry. In any case, they do not have enough dynamic range to accommodate the large acoustic attenuation encountered in Jet Engine alloys, and they do not have adequate resolution. But above all, it seems to be impossible to purchase reliable transducers whose characteristics are reproducible and well specified.

This brings me to what I'd like to call the "Frequency Domain Delusion". In part, this is the idea that the transducers used for pulse echo inspection can be meaningfully characterized in the frequency domain. Pulse echo inspection is basically and inherently a time domain phenomenon. There is a one-to-one relationship between the physical location of a scattering center (defect) and the time when the echo returns to the transducer. In the inspection process, the peak amplitude of this highly localized energy pulse is measured, and the part is rejected if it is larger than a predetermined minimum. In the frequency domain, the basis vectors are continuous sine waves, and the descriptors are the amplitude and phase. This basis is inappropriate for describing pulses localized in time because time delay is a global property of the entire frequency domain representation rather than a property of a specific component. What the frequency domain describes is the resonant frequencies and damping factors of the normal modes of vibration of the transducer.

As we shall see, the characterization of a transducer by its resonance and Q factor presumes a structural simplicity that is not true. The implicit assumption of structural simplicity that hides within a frequency characterization can lead to grief.

Since the pulse echo inspection technique is a time domain problem, the entire system should be characterized, specified and analyzed in the time domain. The time domain characterization of a transducer is, of course, its impulse response, and many of us are used to seeing a scope trace of the impulse response of a transducer pasted onto the purchase sheet that comes with it. But this scope trace is not really an adequate document, because it hides a fatal problem that is often encountered when inspecting for flaws near the surface. Furthermore, I'm going to talk only about the longitudinal mode inspection problem which comes about because the reflection of the sound beam from the front surface comes right back into the transducer again. (Top of Fig. 1). Thus, unless the impulse response of that transducer is extremely clean the reflection from that front surface masks the echoes from the subsurface defects. There are two reasons for this. One of them is that the entire beam hits the front surface, and since it's flat, it's all coherently reflected back to the transducer. The defect, on the other hand, is very small so it intercepts less energy, and this energy is scattered in all directions. This accounts for a factor of about 100 (or 40 dB). The other reason is that the defect material is often very similar in acoustic impedance to the matrix, whereas the impedance mismatch at the front surface is very large. (Center of Fig. 1.). So, we're generally trying to look for things that are anywhere from 60 dB to 100 dB down from the reflection of the front surface, and we'd like to see them right under the surface. So, there's a big problem. In fact, if you look at the impulse response of a transducer such as the previous speaker showed in the frequency domain, it looks sort of like what I've shown in the lower part of Fig. 1 labeled "Front Reflection". It has sort of an ideal 3 1/2 cycle response followed by some junk; and this junk, which doesn't show up very well on the purchase sheet scope trace, is what does you in. Note that the relative amplitude of the "junk" will swamp out the defect indications close to the surface as shown in Fig. 1. If you turn the gain up high enough to be able to see the defects you are looking for, the actual ringing time of commercial transducers is typically 1 μsec before the defects can be reliably perceived. This 1 μsec ringing time is essentially independent of the center frequency of the transducer and independent of its Q factor. This delayed emission never shows up in the frequency specification or on the purchase sheet scope trace because, first of all, the frequency content of this delayed emission is the same as the main pulse and second, because the total energy is usually less than 1 percent of the energy in the main pulse.

Thus, the fact that there is a problem here would show up in the frequency domain only as an extremely subtle change in the phase characteristic (which is never presented), and is totally beyond the ability of any present spectrum analyzer to detect anyway. Nonetheless, this delayed energy makes the detection of near surface defects impossible.

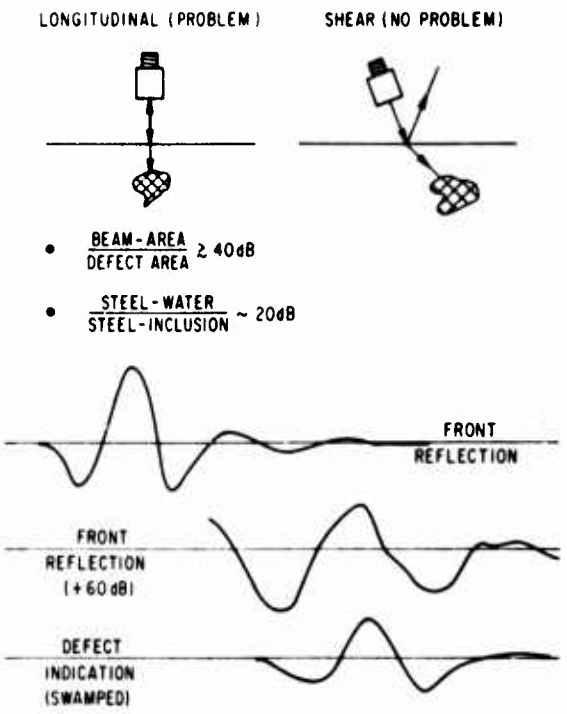

Figure 1. Near surface inspection.

Well, its one thing to argue about how transducers should be measured, and it's admittedly frustrating that commercial transducers aren't the best, but from a physicist's viewpoint, it should be possible to make transducers that do not have a delayed output, and there must be some specific reasons as to why transducers are bad. So, we took some of them apart; I could spend the whole morning on the chamber of horrors we found: things like being glued together with Eastman 910 cement, which is fine for a half a year, but this material continues cross linking and gets more and more brittle as time goes on. It's not surprising, then, that Q factors change with time: after a year or so, the transducers fall off the backing material! We also found electrode films that had completely flaked off and in many cases we found that the material used for the backing simply did not match the acoustic impedance of the transducer slab. In short, we found that the transducer manufacturers do not have the same perceptions as we do concerning the necessary attributes of a pulse echo transducer.

At this point we decided to make some transducers. We would use well characterized materials with uniform properties and well controlled dimensions, and we would use reliable bonding agents, and we would simply insist that they perform the way they were supposed to.

First, we studied some computer models. We took slabs of different materials-with different densities, sound velocities, piezo-electric coupling constants, etc., and predicted transducer parameters such as insertion loss, Q factor, impulse response, etc. (These were some of the figures I left home). And we looked into other design considerations such as the optimum focal length. For deep penetration it's desirable to have a transducer that focuses two or three inches within the material, and since there's a 4 to 1 speed change compared to water, there's actually a foreshortening of the focus. So, the transducer should have a focal length of about 12 inches in order to focus 2 or 3 inches below the surface. This is shown at the top of Fig. 2. Now, such a transducer will enable you to see a defect a couple of inches in, but a defect that is near the surface will have a time dispersion shown by Δt in Fig. 2, due to the fact that the defect is not equidistant from all points on the transducer surface. Thus, the round-trip time is not unique and you get a time dispersion which corresponds to a loss of resolution. There is no way to make a high resolution, near surface transducer that also has deep penetration. Conversely, if you focus on the front surface, as shown at the bottom of Fig. 2, then the time dispersion at the surface goes away, but the beam diverges and you don't get good penetration. So, you have to optimize the focus of the transducer depending on what the application is.

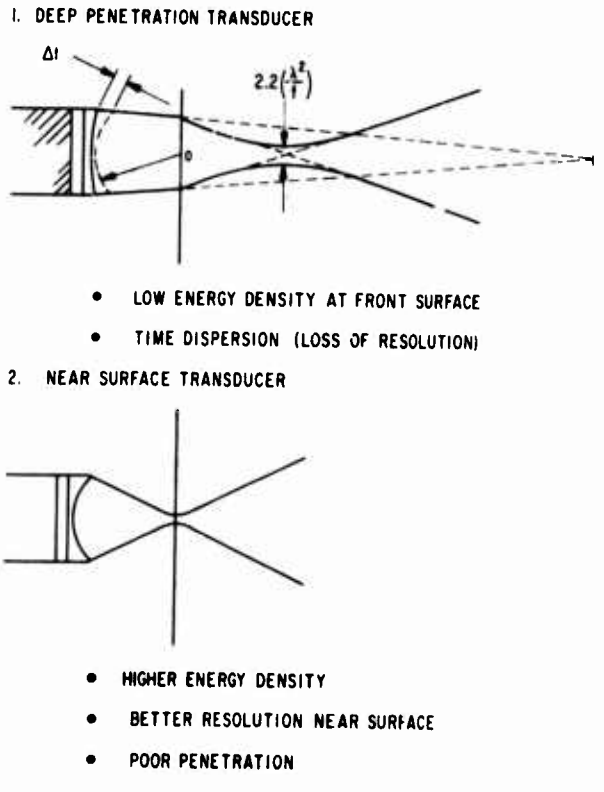

Figure 2. Transducer focal length.

On the other hand, if you put a lens in front, you blow it. There is no way you can put a lens in front of a transducer without destroying the impulse response. The problem is that the lens is usually plastic and has a different impedance from both the transducer and the water. Since both of the lens surfaces have reflections, the acoustic energy bounces back and forth several times as shown at the top of Fig. 3, and this represents a cause of delayed energy emission.

LENS PROBLEM

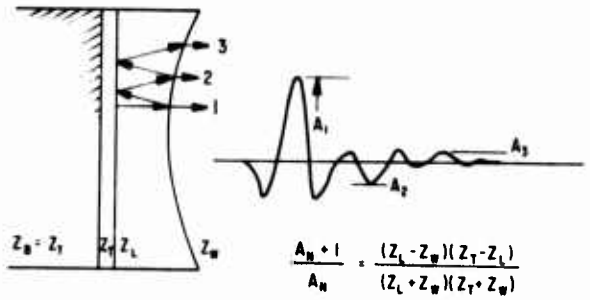

SOLUTION

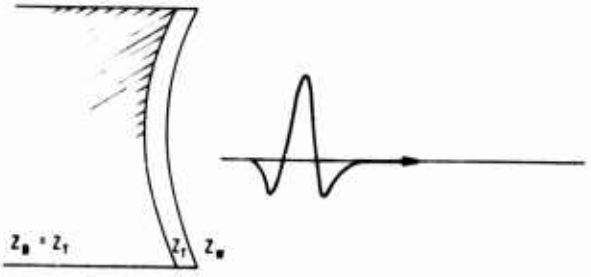

Figure 3. Lens Problem.

The problem is shown quantitatively in Fig. 4 which is a plot of round trip reflection loss and insertion loss as a function of lens impedance. Note that there is less than 10 dB round trip loss for the impedance range corresponding to most plastics. Thus, if you want to have an attenuation of 60 dB, (as is required to see a near surface defect), something like 6 round trips are needed. The time delay for these 6 round trips is unacceptable for near surface inspection.

We have investigated another approach as an alternative to a lens, namely to make the transducer in the form of a thin spherical shell instead of a plane slab. This approach, which is shown at the bottom of Fig 3, is actually quite practical, since spherical lapping tools are available with almost any radius of curvature (thanks to the optical industry). So, it's actually no more difficult to grind a spherical shell of material than it is to grind a flat slab.

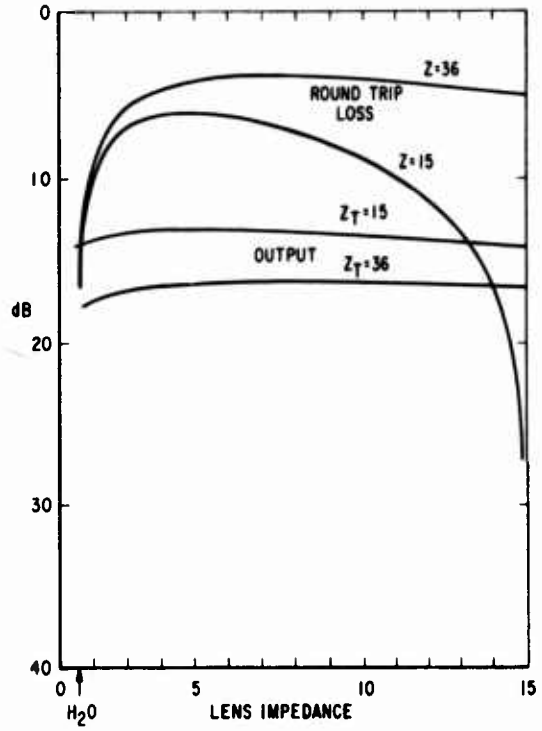

Figure 4. Plot of round trip reflection loss and insertion loss as a function of lens impedance.

We identified another problem which is a sneak path caused by the Poisson's ratio coupling of the transducer, namely, when the transducer squeezes in longitudinally, (indicated by horizontal arrows at the top of Fig. 5) it squeezes out laterally, (indicated by vertical arrows). The way commercially available transducers are made, the laterally directed energy just goes right out into the case and comes out about an eighth of an inch later at the edges of the case. (Shown by dotted path.) This was the source, by the way, of the delayed energy from the commercial transducers to be shown later. We identified that by putting a ring of plasticine clay (shown as dotted material) around the case and around the front of the transducer so as to hide the end of the case, and sure enough, the delayed energy went away. (That didn't completely solve the problem for that transducer because that particular transducer also had a lens on it.) Our approach to the sneak path problem was to not let the transducer edge have any contact with the case. Instead of continuing laterally, we want any energy that is emitted laterally to be converted into a backward motion which then enters the backing. The construction shown at the bottom of Fig. 5 apparently does work. It does cut down the delayed energy, and eliminates the sneak path to the transducer case.

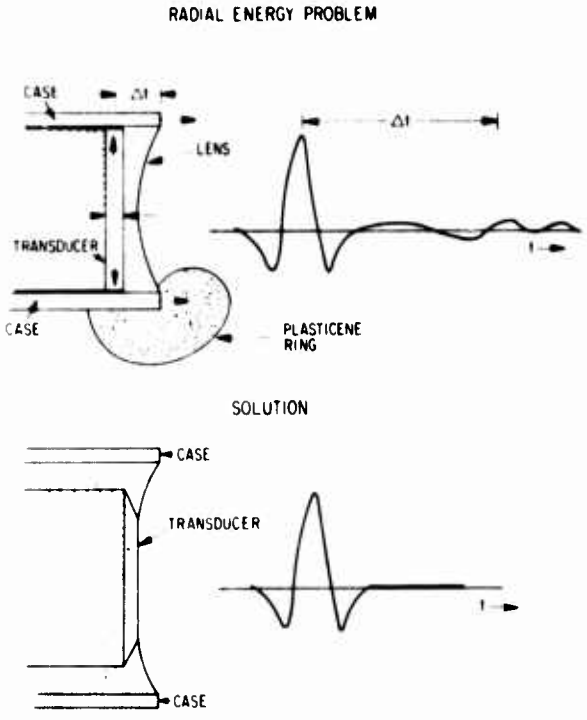

Figure 5. Radial energy problem.

There are other questions, such as the choice of transducer material. There is a figure of merit, for example, which is essentially the output voltage ratio. In other words, let's say I put one volt on the transducer; it emits some sound which then reflects back, and I measure the output pulse amplitude. The combination of material properties that gives the output voltage ratio is the acoustic impedance times the sound velocity times the dielectric constant times k^2, divided by an acoustic mismatch factor to take into account the mismatch between the front surface of the transducer and the water. Figures of merit for some commonly used transducer materials are shown in Table 1.

Table I

TRANSDUCER MATERIALS

FIGURE OF MERIT

- FIXED EXCITATION VOLTAGE
- UMATCHED AMPLIFIER

MATERIAL	k^2	ϵ^S_{33}	V	ζ	Z	$\frac{Z V \epsilon k^2}{\left(\frac{Z}{Z_w}+1\right)}$
PZT-2	26	260	441	76	335	184
PZT-4	26	635	46	75	345	455
PZT-5A	24	830	435	775	337	530
PZT-5H	26	1470	456	75	342	1052
PZT-6A	15	730	456	745	341	303
PZT-7A	25	235	48	76	365	160
$BaTiO_3$	14	1260	547	57	312	634
$Li_2SO_4H_2O$	09	9	547	206	113	07
$PbNb_2O_6$ LM278	16	225	254	58	147	115
K-81	14	300	325	60	195	136
K-83	14	175	533	43	229	113
K-85	18	800	330	55	182	502
$NaKNbO_3$	28	450	62	445	276	573

Finally, I'll make a few comments about anti-reflection coatings. We put an anti-reflection coating on a transducer under the delusion that we were going to improve the output voltage, but it turns out that the best you can do with an anti-reflection coating is about 2 or 3 dB; that's when the impedance of the anti-reflector equals the square root of the product of water impedance and transducer impedance. The improvement in insertion loss achieved by an anti-reflection layer is shown quantitatively in Fig. 4 for two values of transducer impedance. The impedance values shown correspond to lead metaniobate (z = 15) and PZT (z = 35). But what you pay for that is the round trip loss problem of the energy trapped in the anti-reflection layer. It's absolutely clear that you're better off with 2 or 3 dB more insertion loss than to fight with this delayed energy emission.

DISCUSSION

PROF. VERNON NEWHOUSE (Purdue University): Well, I'll take the first stab.

DR. TIEMANN: Great.

PROF. NEWHOUSE: Stab is the wrong word. Jerry and I have known each other for 20 years.

A few years ago, unfortunately, I don't remember the name of the contributor, maybe he's here in the audience, but somebody published a very impressive paper on being able to detect the coating on teeth, which is only a few microns thick using very long bursts of waves. And we this afternoon—if there is time, if Dr. Papadakis gives us the time—hope to present some preliminary results on the use of computer processing to get very high resolution results even from low band width systems. So, I don't think that it's an open and shut case that you need that ideal simple δ function to get high resolution.

DR. TIEMMANN: I agree with that, but let me put this in the context of the Jet Engine Department trying to inspect parts on the factory floor with a pulse echo technique. And in that context there's only one way I can see to be helpful, and that's to make better tools.

MR. DICK BUCKROP (Alcoa): Were you successful in coming up with transducers which have measurably better resolution at equal penetration to those commercially available?

DR. TIEMANN: I have to answer that with a waffle, and the problem is that we're just making these now and the answer is sort of yes or no. I will say that the transducers that we have made do behave the way they're supposed to. When we get the impedance of the backing to equal the impedance of the transducer, there will be no reflection from the backing, and they will either have the ideal impulse response, or we'll have to figure out the reason why. From the mathematics and the physics of it we must get three half cycles and nothing else.

DR. PAPADAKIS: Are you going to generate durable transducers with no wear plates?

DR. TIEMANN: I can't answer that right now, but I feel that there is no possibility of putting a wear plate on unless it matches the impedance of the transducer, in which case it's essentially not there. So there could be a wear plate, but you should not put an immediate impedance in. It should be the impedance of water or it should be the impedance of the transducer. There must be only one reflecting surface. There can be one reflection off the front surface provided it's never heard from again. The fatal problem comes when you have two surfaces that reflect.

PROF. J. SHAW (Stanford University): There's a relatively new material in the transducer art, poly (vinylidene) fluoride, a piezoelectric plastic, and if one makes a simple transducer using films of this material bonded onto backing rods, you can very easily realize a clean impulse response. It consists of a single bipolar pulse form. And also, being flexible, it perhaps--well, it's easy to think of making lenses and perhaps even variable focus lenses.

DR. TIEMANN: The comment is that there's a piezoelectric plastic which can be used to fabricate a very good looking transducer. I consider that kind of research to be extremely valuable potentially for use on the factory floor. I would encourage further work on that.

PROF. NEWHOUSE: One last question.

PROF. R. E. GREEN (Johns Hopkins): I happen to be working with some of this material myself, and I think it's hopeful that something will come out of it, but at the present time the melting point of poly(vinylidene) fluoride and the other type polymers that are piezoelectric, is not optimum for working around jet engines.

DR. TIEMANN: Oh, no, we do these inspections in water at the factory.

PROF. GREEN: But the response is very weak. I would say it's comparable to the EMAT. So, I don't know what its order of magnitude is, but it's two or three times from the common piezoelectric material; but these developments are going on all the time. So, it is interesting.

DR. TIEMANN: Yes. You can see from this figure of merit that unless you have a high impedance, a high velocity and a high dielectric constant, it's very hard to get a good figure of merit.

PROF. NEWHOUSE: One last question from Professor Shaw, then we'll go for coffee.

PROF. SHAW: Well, one advantage of poly(vinylidene) fluoride is in radiating into water it matches very well into water, and that goes a long way to compensating for the relatively lower piezoelectric constant.

DR. TIEMANN: It also has a relatively high velocity, and both of these factors help.

PROF. NEWHOUSE: Thank you.

SURFACE ACOUSTIC WAVE ELECTROMAGNETIC TRANSDUCER MODELING AND DESIGN FOR NDE APPLICATIONS

T. L. Szabo
Deputy for Electronic Technology (RADC/AFSC)
Hanscom Air Force Base, Massachusetts 01731

I'll be talking mainly about surface acoustic wave electromagnetic transducers, EMT's. These are useful for examining near surface flaws, defects or stress gradients, and they are also very useful for examining rough or painted, or dirty, or hot, or curved surfaces, not necessarily in that order. Recently, this technology has developed to the point where it's possible to fabricate identical transducers. What I'd like to show this morning is that it's also very straightforward to design them. There is quite a large flexibility in the design of these transducers, and they give very clean, reproducible and predictable characteristics, which are, of course, what you need for reproducible quantitative NDE measurements. I'll be describing the work we did last year, the development of a model for these transducers. This work[1,2,3,4] was done by myself, Harold Frost, and Jim Sethares.

Now, I assume that you know how electromagnetic transducers work. The kind I'll be talking about is shown in Fig. 1; it's basically a meander geometry. A large current flows through the meander geometry and produces eddy currents in the surface which produce the periodic stresses that generate surface acoustic waves in both directions. Other modified geometries are possible, including modifications obtained by varying the periodicity of the conductors and also by changing their length.

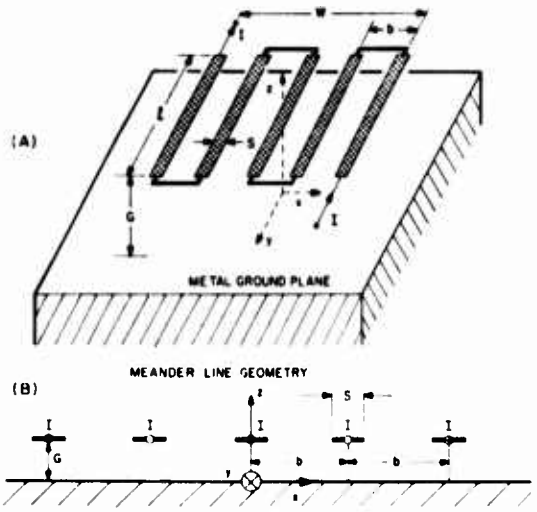

Figure 1. Schematic diagram for meander coil surface wave Transducer

The type of conductors I'll be talking about are flat conductors because they are very easy-to fabricate reproducibly and uniformly in production[1,3] as Fig. 2 shows. These are different kinds of electromagnetic transducers.[4] On the upper left is a five period wire transducer of the type that has been made in the past. On the right are three 10 MHz printed circuit board transducers. This kind of fabrication technique was developed by Moran and Thomas.[6] On the top we have a multiconductor flat cable EMT, in which the conductor length varies along with the direction of propagation, and I'll be describing that in more detail later.

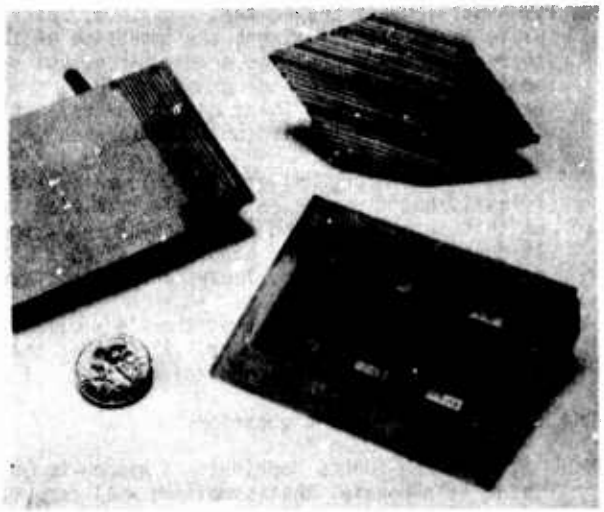

Figure 2. Various forms of surface wave Transducers

Figure 3 shows the EMT equivalent circuit model[1,4,5] Basically, what we've done is to completely characterize the electrical and acoustical properties of the transducer. This circuit is very useful for design and also, knowing the electrical properties, you can develop better matching techniques. For example, we found theoretically and experimentally that shunt capacitance matching is the best kind to use here because electrically the EMT is mainly an inductor and a resistor. Here R_E is just the normal resistance of the fingers. L_E is the inductance of the transducer. R_{EC} is the new loss mechanism that we identified as eddy current resistance, X_A is the acoustic reactance, and R_A is the acoustic radiation resistance.

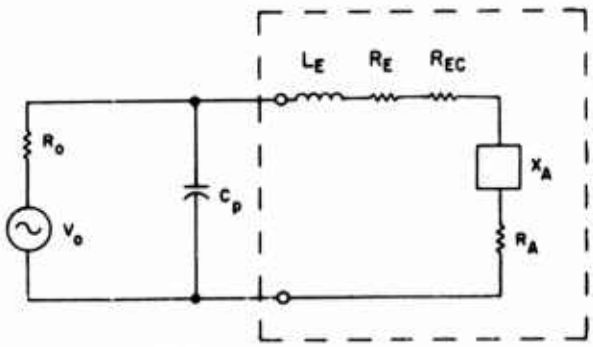

Figure 3. EMT Equivalent Circuit

In Fig. 4 we see that both the inductance and the eddy current resistance are functions of the gap.[5] These are some measurements we took at 10 MHz. We can see that the inductance is almost zero when the transducer is very close to the ground plane, and then when the transducer is removed from the surface, it assumes its free space value; whereas, the eddy current resistance (which is proportional to the square root of the frequency) is largest for small gaps and then decreases as you move the transducer away from the surface.

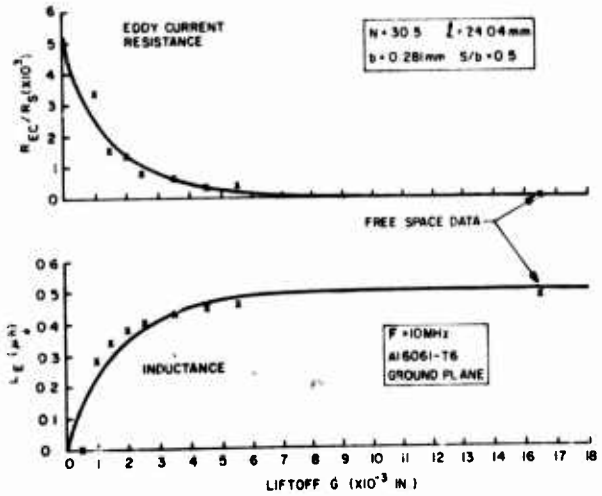

Figure 4. Eddy current resistance and inductance of EMT as function of liftoff.

Now, we will go to the acoustic properties in Fig. 5. This is the acoustic radiation resistance for a four period transducer plotted versus normalized frequency.

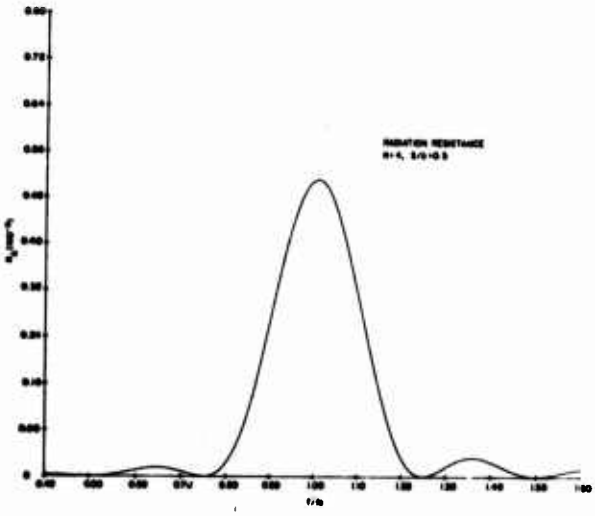

Figure 5. Acoustic radiation resistance as function of normalized frequency.

Now, in developing this model we started out from scratch-from first principles-and worked our way to this result.[4,5] This response has a $(\frac{\sin x}{x})^2$ shape which will seem familiar to those of you that know about interdigital transducers, because both transducers have the same type of response. In developing this model, we found that, in addition to the $(\frac{\sin x}{x})^2$ dependence, there is also a skewing term, so that, as you see here, the left side lobe is lower than the right one. We can show simply the similarity between the radiation conductance of an interdigital transducer (IDT) including the skewing term and the radiation resistance for an electromagnetic transducer.

If we define a parameter,

$$X = \pi N \left(\frac{\omega - \omega_0}{\omega_0}\right) \qquad (1)$$

in which N is the number of periods in the transducer, ω is the angular frequency and ω_0 is the angular center frequency of the transducer, then for the IDT radiation conductance we have

$$G_A(\omega) = \omega/\omega_0 \, G_A(\omega_0) \left(\frac{\sin x}{x}\right)^2. \qquad (2)$$

Similarly, for the EMT radiation resistance, we get

$$R_A(\omega) = \omega/\omega_0 \, R_A(\omega_0) \left(\frac{\sin x}{x}\right)^2. \qquad (3)$$

And now I'll show some experimental results. In Fig. 6 the insertion loss for two 15 period electromagnetic transducers is plotted as a function of normalized frequency.[5] The insertion loss is 90 dB with a modest input signal of 1 amp peak. We have quite a large range of sensitivity which is adequate for many applications, and you can see that in the pass band there's excellent agreement with the theory. The bandwidth here is simply related to one over the number of periods, so it's very easy to change your bandwidth.

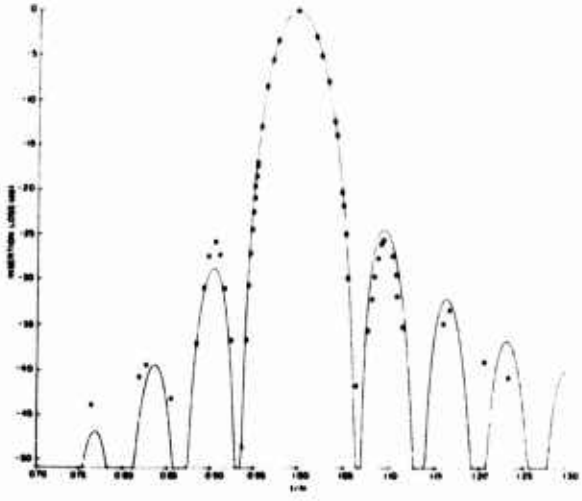

Figure 6. Insertion loss as a function of normalized frequency.

Figure 7 shows the insertion loss for one four period electromagnetic transducer.[5] In this case the experimental data were plotted against a theory in which the radiation resistance was just $(\frac{\sin x}{x})^2$. You can see that within the pass band some of the data points fall below the theory on the left side and above on the right side.

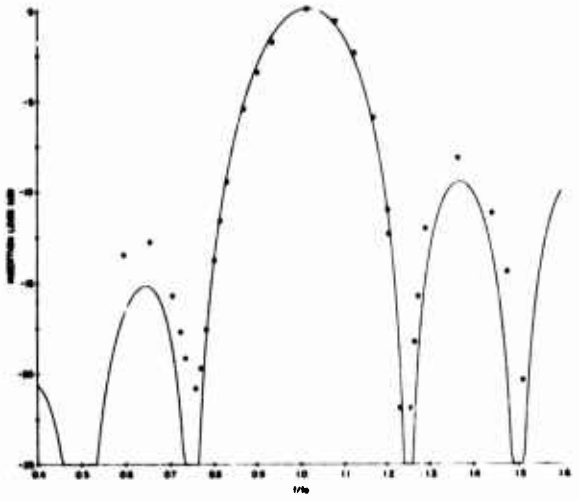

Figure 7. Insertion loss for four period EMT as a function of normalized frequency.

Figure 8 shows that better agreement is obtained with the skewing term included in the theory especially for the passband and on the right sidelobe.

Now, since there is a similarity between the interdigital transducer and the electromagnetic surface wave transducer, naturally, we can draw on the wealth of information on IDT design. We can try some of the same tricks with electromagnetic transducers to obtain not only transduction capability but also a signal processing capability.

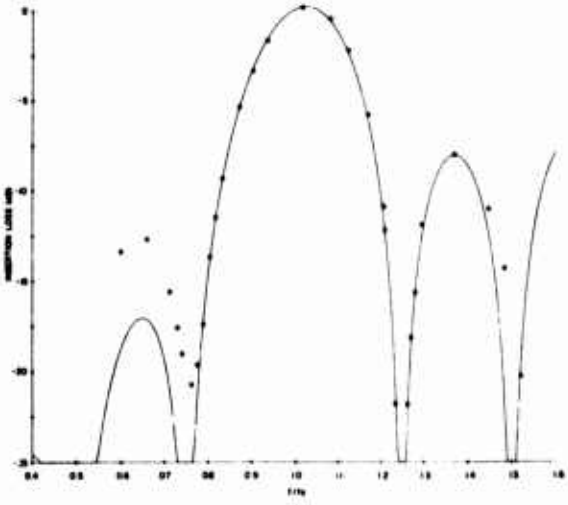

Figure 8. Comparison of experimental and theoretical insertion losses with skewing term included.

I will now describe the frequency response of an apodized transducer, which is the one on the upper right of Fig. 2, in which the length of the fingers varies linearly towards the center of the transducer.[4] Shown in the left side of Fig. 9 is the insertion loss of two uniform length transducers, one with 7 periods and one with 15 periods, and on the right we have, again, the insertion loss of the same 7 period transducer in conjunction with the apodized transducer. And you see that good agreement is obtained with the theory. The effect of apodization is to widen the passband and to lower the sidelobes.

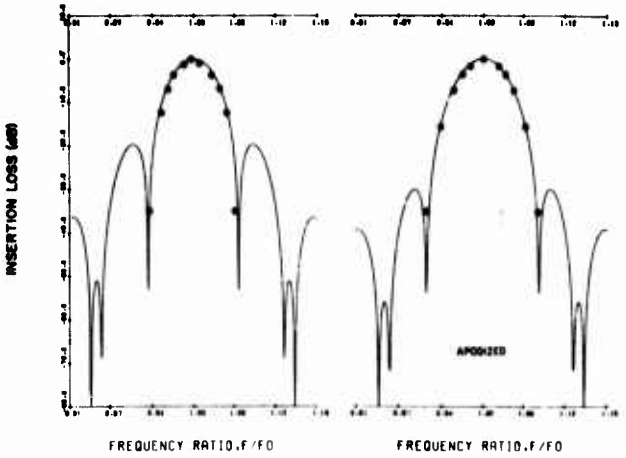

Figure 9. Insertion loss of apodized transducer as function of normalized frequency

Later, Tom Moran[7] will be talking about another way you can change the frequency response of the transducer by varying the periodicity. So, you can see now that you have a tremendous capability here in design flexibility for NDE applications.

And now I'll go into an application that uses a transducer we reported on last year.[8] The transducer shown in Fig. 10 is made out of multi-conductor flat cable bonded onto a samarium cobalt magnet which all results in a very compact package.

Figure 10. Photograph of EMT using multi-conductor flat cable configuration.

Figure 11 shows this transducer being applied. Here is an aerospace part, and on the right side a wedge transducer is used to launch a surface wave which travels up around the curvature of the part. The surface wave is picked up by the electromagnetic transducer shown in Fig. 10. On the top surface there is a scratch which could be either a forging lap or a deep crack. We want to discriminate between these defect types quantitatively. We designed the next experiment shown in Fig. 12 to simulate a forging lap. This is an aluminum downstep made very precisely with a step height of h. On the left we have a wedge transducer launching the surface wave, and the same type of electromagnetic transducer receiving the incident and reflected waves.[2,4] In Fig. 13 we show the theoretical curve for the reflection coefficient from a downstep and our data. This is the reflection coefficient versus the step height divided by wave length; alternatively, you may consider this curve to be the spectrum of the downstep. Here you see that the significant features of this curve are a maximum at .5 and a minimum at around .8. We were able to discriminate between these features using the single transducer for each step shown.[4]

Figure 11. Application of EMT to complex shaped part

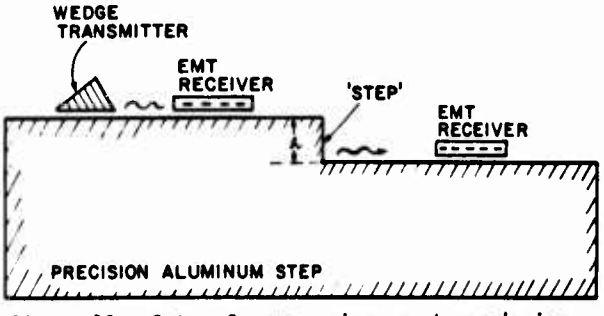

Figure 12. Setup for measuring saw transmission and reflection coefficients for a step

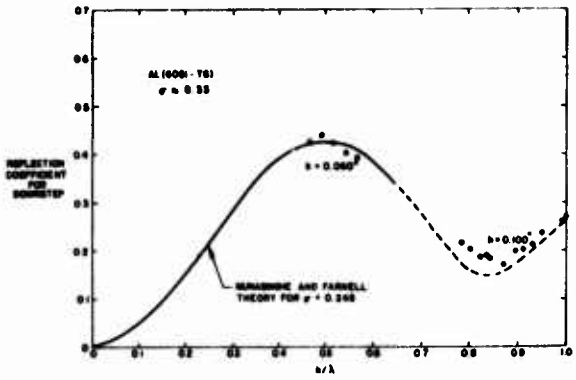

Figure 13. Comparison of theory and experiment for reflection coefficient for downstep

You might consider this problem an ideal case. These transducers may be designed to either filter out defects of certain sizes or, since their responses are very clean and well described, it's easy to remove their response from the defect spectra that you are examining.

Other work that we've done includes the successful generation of surface waves on insulators in a non-contact configuration by using these transducers and placing metal tape on the insulator.[4] We've also designed a very sensitive rotation rate sensor using curved electromagnetic transducers.[2,9]

So, in summary, these transducers are easy to design; they have very reproducible and predictable responses, and there's a lot of design flexibility for NDE applications.

REFERENCES

1. H. Frost, T.L. Szabo, and J.C. Sethares, "The Flat Conductor Electromagnetic SAW Transducer: Theory and Experiment," 1975 Ultrasonics Symp. Proc., pp 601-603

2. H.M. Frost, J.C. Sethares and T.L. Szabo, "Applications for New Electromagnetic SAW Transducers," 1975 Ultrasonics Symp. Proc., pp 604-606.

3. H.M. Frost and T.L. Szabo, "Surface Acoustic Wave Electromagnetic Transducers from Multiconductors Flat Cable," Appl. Phys. Lett. 29, pp 73-75 (1976).

4. T.L. Szabo and H.M. Frost, "SAW Electromagnetic Transducer Design for Nondestructive Evaluation Applications," IEEE Trans. SU-23, pp 323-328 (1976).

5. T.L. Szabo, H.M. Frost and J.C. Sethares, "Periodic Surface Acoustic Wave Electromagnetic Transducers," to be published in IEEE Trans. Sonics and Ultrasonics (1977).

6. T.J. Moran, M.J. Lin, F. Bucholtz and R.L. Thomas, "Electromagnetic Generation of Rayleigh Waves at MHz Frequencies," Rev. Sci. Instrum. 46, pp 931-932 (1975).

7. T. J. Moran, this proceedings.

8. H. M. Frost and T. L. Szabo, "Transducers Applied to Measurements of Velocity Dispersion of Acoustic Surface Waves," Proc. of ARPA/AFML Review of Quantitative NDE, (AFML-TR-75-212), Jan. 1976, pp 426-450.

9. H. M. Frost, J. C. Sethares and T. L. Szabo, "Rotation Sensing through Electromagnetic Surface-Acoustic-Wave Transduction, J. Appl. Phys., to be published in Jan. 1977.

10. T. L. Szabo, "Acoustic Beamshaping and Diffraction from Tapered Amplitude Distributions," 1975 Ultrasonics Symp. Proc., pp 116-119.

DISCUSSION

PROF. VERNON NEWHOUSE (Purdue University): Are there any questions or comments? Would you announce your name and organization, please, and I have been asked by our reporter that the speakers speak up. Otherwise, not only will their remarks be anonymous but there won't even be any remarks.

PROF. MACK BREAZEALE (University of Tennessee): I'm curious to know the reason for stopping with the apodized transducer in the configuration that you used. It seems to me that you can make the additional step of going to a Gaussian function and get rid of the sidelobes completely. Was there a fabrication reason for that?

DR. SZABO: We had considered that and Tom Moran has actually made transducers which do give a Gaussian acoustic beam. In this talk I described how we apodized the transducer to give a certain frequency response. You can also apodize the transducer to give a certain beam shape,[4] and this has been done. And you're right, the Gaussian beam you've described is the best sort of a shape to use for NDE applications rather than a rectangular shape.[10]

PROF. JOHN SHAW (Stanford University): In acoustic IDTs there is an optimum number of fingers. Is that true also for these?

DR. SZABO: It is, that's right. And our model will give you that result, but it's not as straightforward as it is for IDTs. It usually has to be done numerically.

MR. BOB IRWIN (Northrop): In comparative analysis of conventional systems with your EMT device, do you have any data on that as far as sensitivity and resolution?

DR. SZABO: What do you mean by sensitivity and resolution?

MR. IRWIN: Is it more sensitive and does it provide more resolution for near surface defects than immersion systems?

DR. SZABO: Well, this talk has been about surface waves. In an immersion system, you can launch a beam so it will mode convert to a surface wave, but most people just use wedge transducers. An EMT has slightly less sensitivity than a wedge transducer, but it has many other advantages because you are able to place the transducer very precisely and you are able to define its characteristics very well. Does that answer your question?

MR. IRWIN: Somewhat.

PROF. NEWHOUSE: Well, thank you.

OPTIMIZATION AND APPLICATION OF ELECTRODYNAMIC ACOUSTIC WAVE TRANSDUCERS

B. W. Maxfield*
Cornell University
Ithaca, New York

First, I would like to say that my affiliation as of Monday is with Lawrence Livermore Laboratories, but this work was all done at Cornell University.

I'm going to talk about the use of electromagnetic acoustic wave transducers, or EMATS as I call them, as they are being used for bulk wave generation. They have been applied specifically to the problem of measuring the intensity distribution of acoustic waves that are scattered by defects of known geometries. Related studies have been done elsewhere for some time and have formed an integral part of this general program.

Our measurements involve the use of a fixed transmitting element and a movable receiving element so that the intensity distribution can be mapped over a surface. Prior to our measurements, most work has involved compressional waves, although some work has been done using a combination of incident shear waves and the mode converted compressional waves scattered from the defect.

There is substantial interest in being able to generate incident shear waves and then detect the shear waves scattered by the defect. By setting the orientation of the induced current and the magnetic field, you can determine whether EMATS have sensitivity to either shear or compressional disturbances. If you pick your geometry correctly, you can both generate and detect shear waves. We have extended some of our earlier work, done during the first year of this program, to study the intensity distribution of waves scattered by defects of known geometry.

In the first part of this program, we developed a system which uses a small scanned EMAT to map the displacement field or beam profile of a larger EMAT and showed that one could obtain very good quantitative measurements of the displacement, that is, of the beam profile. With this experience, we designed a system which was the first step in being able to utilize scanned EMATS for quantitative intensity distribution measurements.

After a few preliminary measurements, we settled upon what I will refer to as a single surface access method where you have a fixed transmitter and a movable receiver coil near a single surface. The excitation coil is about 1 cm square and the receiver coil is about 1/2 mm thick and 1 1/2 mm square. This geometry has the advantage that scattering back from a defect is not measured against any background level. If the through transmission geometry were used, then there would be a large background signal produced by the unscattered acoustic energy. For the small defects of interest here, the unscattered energy would greatly exceed the scattered signals. The single surface geometry is also convenient for use within an electromagnet since the overall thickness can be made small, 5 cm is easily realized, so that quite reasonable magnetic fields of the proper orientation can be achieved.

It is probably clear that this geometry presents some problems. First, let us consider the receiver coil as a conducting element which sits in the electromagnetic field produced by the transmitter coil, thereby distorting this field.

To give you an idea of how significant this distortion can be, the skin depth in copper at 5 MHz is about 30 microns, or 1 mil. Any practical receiver coil is going to be made of wire of 1 mil or greater in size (unless you have an elf to wind it for you), and hence will produce some distortion of the drive field. I'll return to this problem of drive field distortion a little later but there are other problems that one should consider first.

One of these is overload of the receiver circuitry. This is easily realized by noting that the electric field outside the transmitter coil is the order of 1 V/mm, whereas the electric field that the receiver coil must sense in order to detect the reflection from a 1 mm void is the order of 1 μV/mm. This means that the current passing through the transmitter coil must drop to very low values before the voltages that they induce in the receiver coil are down to an acceptably low level. This oscillator ring-down was troublesome in the apparatus that we used, but there was no difficulty in circumventing this problem by using longer transit times. We had a dead time of about 6 microseconds which corresponds to 18 mm of total transit distance in aluminum.

A much more serious problem is outlined in Fig. 1 which shows portions of the pulse echo pattern for the scattering of a shear wave (wavelength - 0.6 mm) incident on a 1 mm diameter cylindrical flaw. The shear wave polarization is parallel to the flaw axis. If the receiver coil is placed directly over the flaw, you get the reflection as shown in Fig. 1a. With the receiver coil moved 5 mm normal to the flaw axis, you get the echo pattern in Fig. 1b. The expected decrease in response is clearly observed.

Because we are scanning across a flat surface, the signal from the displaced coil should also be displaced in time; for the conditions in Fig. 1b, it should be about .2 μs later but there is no apparent shift. This is even more evident when the receiver coil position is shifted to 10 mm which should then produce a 0.8 μs shift.

Figure 1c does show a response about .8 μs later, which is, in fact, due to scattering from the cylindrical flaw. However, there is also a response corresponding to the unshifted coil position. This is not due to a real scattered signal received by the coil when it is displaced 10 mm from the axis. Instead, this signal appears at the surface

*Now at Lawrence Livermore Labs, Livermore, Ca. Mail Code L415

directly above the flaw, that is, the pickup coil, and is coupled essentially instantaneously through the vacuum into the coil. This illustrates one of the major difficulties in using EMATs, namely, when trying to detect a small response adjacent to a much larger one, you must take account of possible coupling through the vacuum. Such spurious responses can be minimized by shielding the receiver coil. This works well in the through transmission geometry, but clearly introduces distortion into the drive field for single surface access.

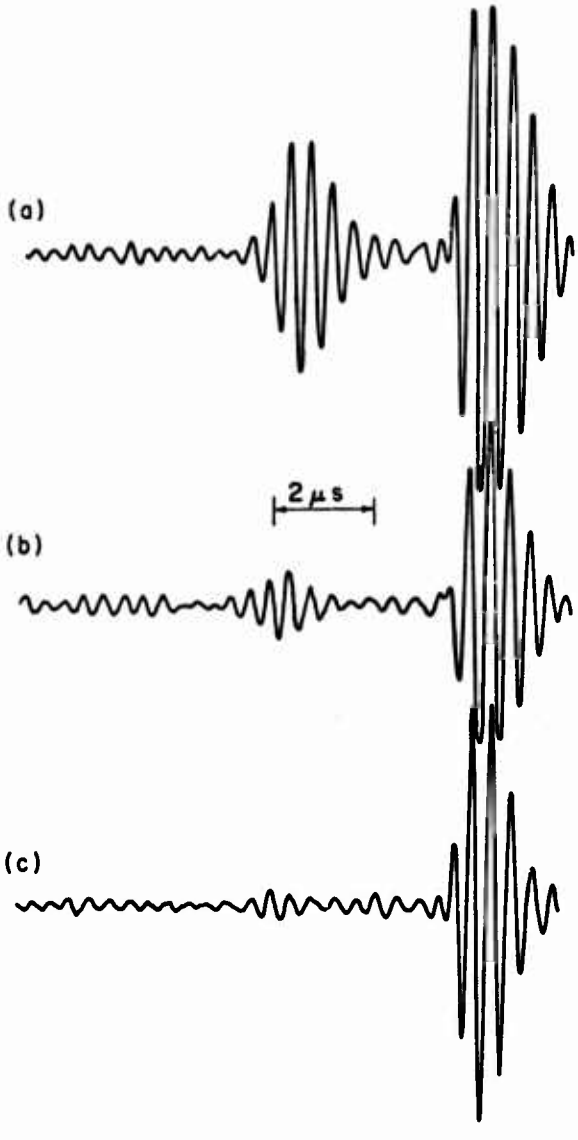

Figure 1. A portion of pulse-echo pattern showing scattering from a 1mm cylindrical flaw and the back surface (largest response) with the receiver coil. (1a) Directly above the flaw (1b) Displaced 5mm normal to the flaw axis (1c) Displaced 10mm

Another way around this coupling problem is to use shorter pulses of larger current which increases sensitivity and allows you to take full advantage of the differences in arrival time. For example, in the sequence shown in Fig. 1, if the pulses were very short, then even the vacuum-coupled signal would not distort much of the scattered signal. Thus, using shorter pulses would be a very significant advantage in this work.

One can also change the geometry to illuminate the void from the side and then scan along the top surface. In this case, the magnetic field would be parallel to one side of the specimen. An angular range of ± 30 degrees or more about 90 degrees could be studied and this would also give very significant information about the defect.

Lastly, I would like to show the type of resolution that can be obtained. Figure 2 shows the profile for vertically polarized shear waves back scattered from a 1.2mm diameter flat bottom hole. You get very good signals. These responses are very reproducible and have good signal-to-noise ratio, but because of the vacuum-field coupling that I referred to earlier, one could not take this as a quantitative measure of the scattering but only as a qualitative measure of the intensity distribution.

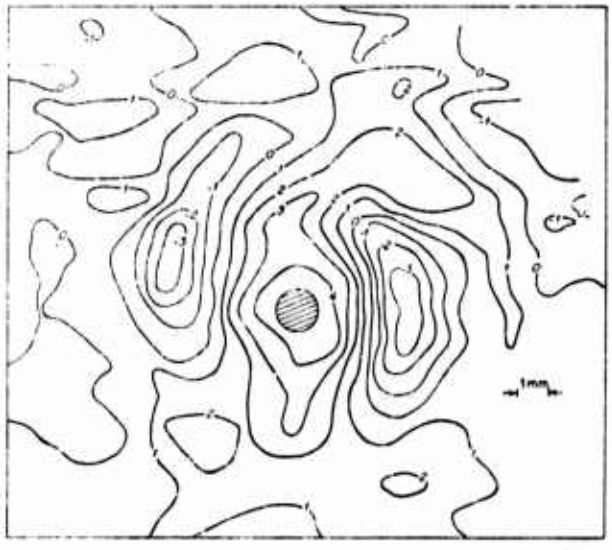

Figure 2. Equal amplitude contours for scattering back from a 1.2mm diameter flat-bottomed hole

This summarizes where we are at the moment in using the electromagnetic acoustic wave transducers for scattering studies. Some changes in the instrumentation and setup should allow quantitative results to be obtained.

I would also like to mention that we have done some work on making compact permanent magnet transducers weighing in the 200 to 250 gram range and having insertion losses of about 95 to 105 db that

have turned out to be quite useful. It may be possible to use these in scattering studies. Further information on our permanent magnet EMAT work is available in an NBS Report.

Thank you.

DISCUSSION

DR. SY FRIEDMAN (Naval R and D Center): I have a relatively elementary question. Those shear waves that you are studying are propagating normal to the surface--

DR. MAXFIELD: This is correct.

DR. FRIEDMAN: There is no simple way to get them to come in at an angle of a conventional acoustic shear wave transducer?

DR. MAXFIELD: Oh yes, you can get angle waves. I believe Tom Moran will be describing some of this.

MR. FRIEDMAN: Okay, fine, I'll wait.

DR. JERRY TIEMANN (General Electric Co.): About how many amperes or watts do you use in your oscillator or coils, transmitter coils?

DR. MAXFIELD: We use, in these measurements, 5 or 6 amperes peak rf current. It's relatively easy to increase this, and I think that Fortunko and Thompson are going to describe some work up to maybe 100 amps of peak current in essentially a pulse excitation instead of an rf envelope type of excitation. Pulse currents up to about 2,000 ameres have been used, and this given back surface received signals of the order of 30 millivolts. Large currents produce large signals even with permanent magnets which give you maybe 3 or 4 kilogauss fields.

CHARACTERISTICS AND APPLICATIONS OF ELECTPOMAGNETIC SURFACE WAVE TRANSDUCERS

T. J. MORAN
Air Force Materials Laboratory (AFML/LLP)
Wright-Patterson AFB, Ohio 45433

Tom Szabo mentioned during his presentation that there is a great deal of similiarity between the response of a meander line surface wave EMT and that of an interdigital transducer.[1] We have been investigating their common properties to see if they can be exploited for NDE applications.

The generation of bulk waves in delay lines is considered a problem for interdigital transducers,[2] but for NDE it might provide a convenient means of generating bulk waves propagating at an angle to the surface.[3]

The normal meander line transducer (Fig. 1) phase matches the wire spacing to the wavelength of the surface wave being generated. Surface waves are generated when the conditions shown in Fig. 2A are fulfilled. Here N is an odd integer. If the frequency is increased slightly, it is possible to phase match to a bulk wave propagating at an angle to the surface as is shown in Fig. 2B. At the lowest frequency of bulk wave generation the shear wave will propagate very close to the surface. It should be noted that this frequency is greater than the Rayleigh wave fundamental since $V_S > V_R$. As the frequency is increased, θ decreases from 90° and the shear waves sweep toward the normal to the surface. So you have a steerable bulk wave transducer.

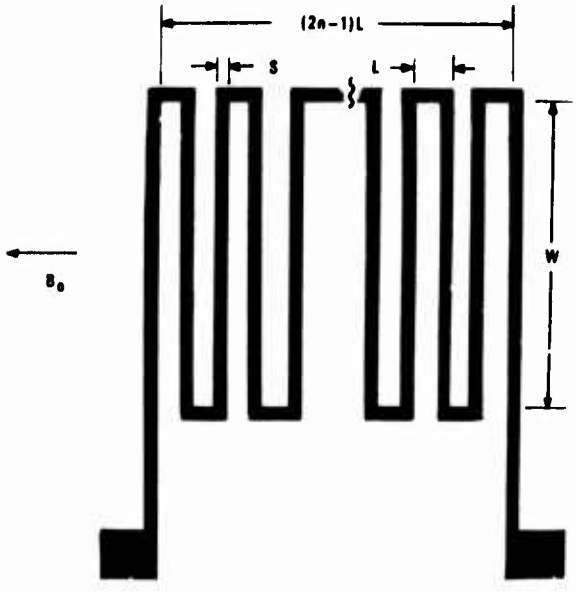

Figure 1. Meander Line EM Transducer

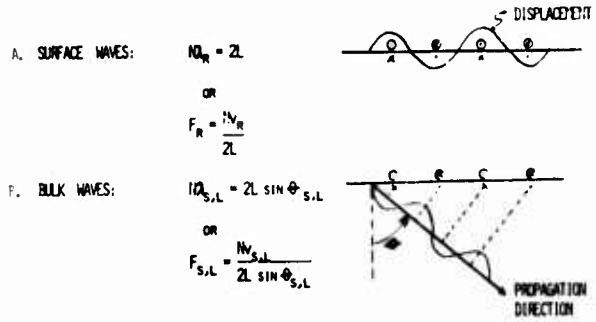

Figure 2. Meander line sound generation conditions
A) Surface waves
B) Bulk waves

The longitudinal wave velocity is approximately double the shear wave velocity. Thus, no longitudinal waves are generated until you reach double the onset frequency of the shear wave case. Therefore, it is possible to generate shear waves by themselves for frequencies up to twice the shear onset frequency and both longitudinal and shear waves above that frequency.

Now, let us look at one problem with these devices which is found when the bulk waves are propagated near the surface. In this case, the effective cross sectional area of the transducer is very small and the device looks essentially like a line source. A line source would emit a cylindrical wavefront instead of the desired narrow plane wave. Therefore, an enormous amount of beam spread near the surface is expected. The angle θ has to be less than 60° before you can get anything like a plane wave front out of the device.

We set up an experiment to determine if the transducer operated in the predicted manner. A 6" aluminum disk was cut in half (Fig. 3) with a meander line EMT in the middle and piezoelectric transducers on sliding mounts on the periphery. The first thing found was that when operated at the Rayleigh wave fundamental frequency bulk waves coming off normal to the surface were generated in addition to Rayleigh waves. We believe that the non-uniform magnetic field produced by the permanent magnet contributed to this bulk wave generation. Ordinarily with a uniform field, there would be almost complete cancellation of acoustic waves

propagating normal to the surface at the Rayleigh wave generation frequency due to the geometry of the transducer. In the permanent magnet case, there is a field gradient near the edges, so each region under the transducer sees a different field and the levels of excitation vary. Thus, there is an increase in the bulk wave generation from the edges. However, the level is still quite far down from the su face wave or phase-matched bulk wave levels.

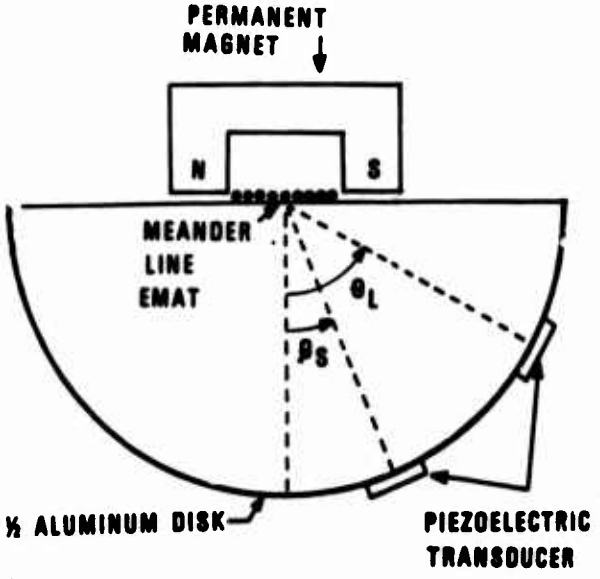

Figure 3. Experimental set-up for bulk wave propagation.

When the frequency was increased to look for the phase matched generation of bulk waves, they occurred at the predicted angles. This is shown in Fig. 4 for the shear waves, where the solid line is the theoretical prediction and the dots are experimental results. Note that the onset frequency is just above the Rayleigh wave fundamental as expected. The efficiency was also quite good in this case. For a single conversion, approximately 4dB was lost for angles down to 30° when the transducer was tuned correctly. It should be emphasized that this result only holds for the transducer used and with other devices there might be some variation in the efficiency.

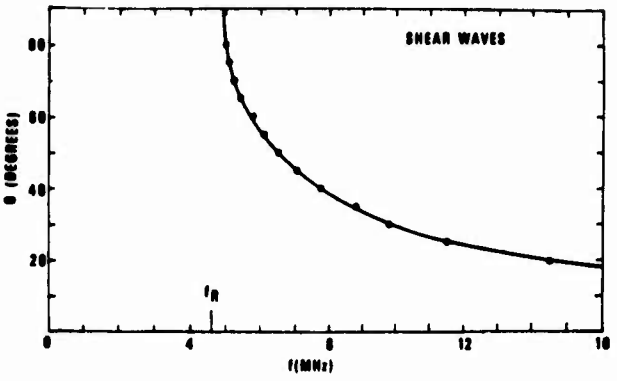

Figure 4. Dependence of bulk wave propagation direction on excitation frequency. The sited line is the theoretical prediction.

The longitudinal wave case gave equally good results (Fig. 5). The onset frequency is approximately double the Rayleigh wave frequency and again, there is an excellent agreement with theory. The efficiency decreased an additional 6dB per conversion from the shear wave efficiency due to the fact that the energy was split between the shear and longitudinal bulk waves at frequencies above the onset frequency for longitudinal waves.

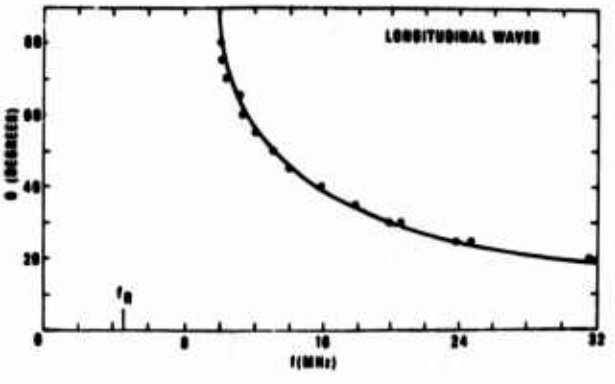

Figure 5. Dependence of longitudinal wave propagation direction or excitation frequency. The solid line is the theoretical prediction.

A second part of our work consisted of an attempt to use the signal processing capabilities of IDT's[4] with EMT's. Our initial venture into this area was to design the chirp transducer coil shown in Fig. 6. The transducer output consists of an rf burst with a linear frequency modulation from 2 to 6 MHz. The reason for looking at such a device is to improve the range resolution of EMT's. Normally, with a multiturn EMT, the shortest possible pulse has a duration equal to the acoustic transit time across the device, because N transducers are excited in series. For the devices we have been using, this time is on the order of 3 μsec. If a second identical transducer is used to receive the 3 μsec pulse, there is an additional pulse stretching of 3 μsec due to the finite size of the receiver. This stretching is illustrated in Fig. 7 for a pair of 32 line, 5 MHz coils where the transmitter was driven by a 50 nsec voltage spike. Note that the output is greater than 6 μsec in duration. Thus, the range resolution of these devices is rather poor. The chirp transducer should improve the resolution dramatically due to the fact that such a device produces a significant output only when there is a spatial phase matching of the complete acoustic waveform and the coil.

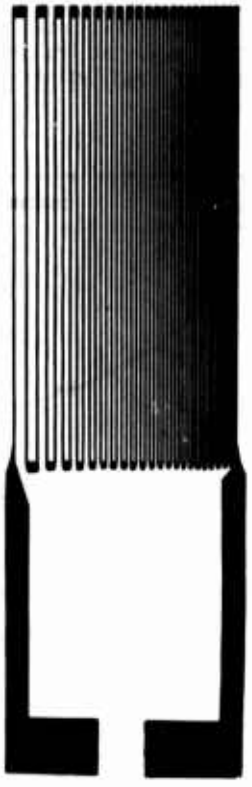

Figure 6. Linear F M Chirp E M Transducer

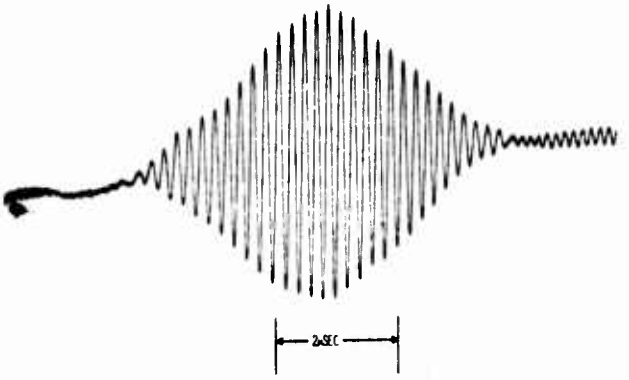

Figure 7. Response of a pair of 5 MHz EMT's to a 50 nsec input pulse.

Now, let us look at the actual operation of these devices. Figure 8 shows the output of the 2 to 6 MHz chirp transducer when it is driven by a 50 nsec pulse. Note that the duration of the output is of the order of 3.5 μsec. Figure 9 shows the compressed output pulse when the acoustic waveform shown in Fig. 7 is received by an identical chirp transducer. In this case, the duration is of the order of 0.25 μsec. To test the operation of these devices in a more realistic manner, a 1.09 mm notch was cut into the end of an aluminum plate and the pulse excited chirp transducer was used in a pitch-catch mode. Figure 10 shows the output waveforms and the signal from the notch is very easily distinguished from the end face reflection. From this figure, it may be estimated that signals from reflectors of the order of 0.5 mm apart would be resolvable provided the signals are of the same order of magnitude.

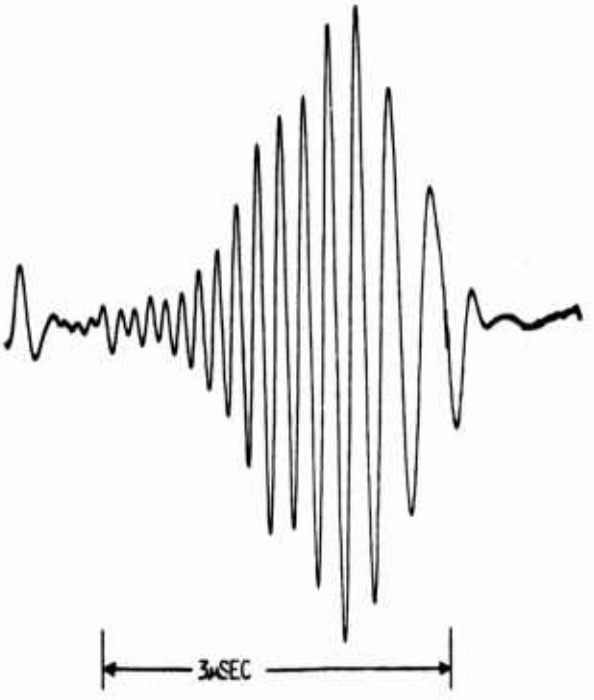

Figure 8. Output of Chirp Transducer driven by a 50 nsec pulse input.

Figure 9. Response of Chirp Transducer to pulse shown in Fig. 8.

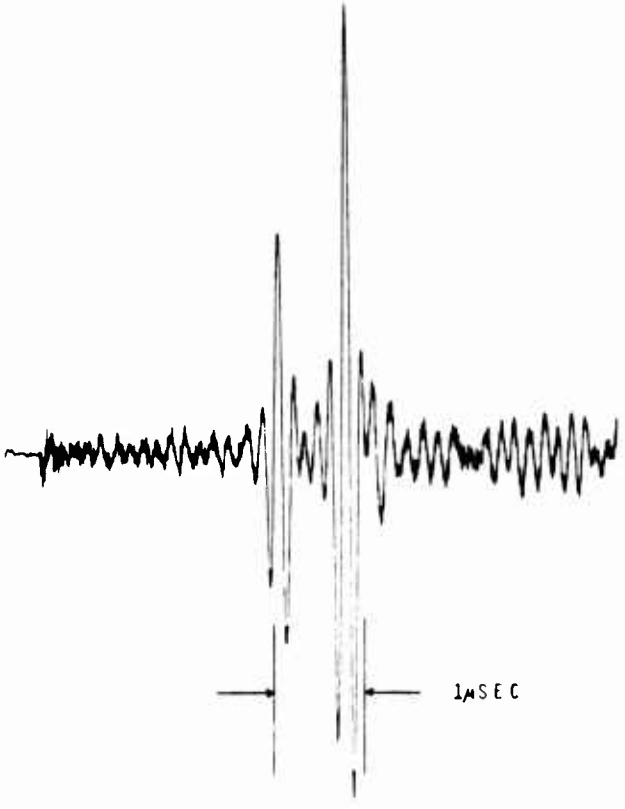

Figure 10. Resolution of signals from reflectors spaced 1.09 mm apart.

Some attempt has also been made to produce Gaussian waveforms with EMT's by tapering the lengths of the lines in the coil[5]. We have been able to reduce the near field amplitude fluctuations considerably, but a true Gaussian waveform has not been achieved. Work is still in progress in this area.

We also have put together a prototype NDE EMT transducer as shown in Fig. 11. The magnet consists of a pair of 0.5" x 0.5" x 1" Sm-Co bar magnets connected by a mild steel back plate with a 0.125" plastic spacer between them to form a quasi-horseshoe type magnet. The peak field is of the order of 5.5 kiloguass. A 1 mil thick mylar wear plate is used to cover the rf coil and protect it. If the surfaces being inspected are not too rough, this is quite adequate. If more protection is needed, 3 mils of mylar will only cause a 30% decrease in signal level at 5 MHz compared to the level using the 1 mil spacer.

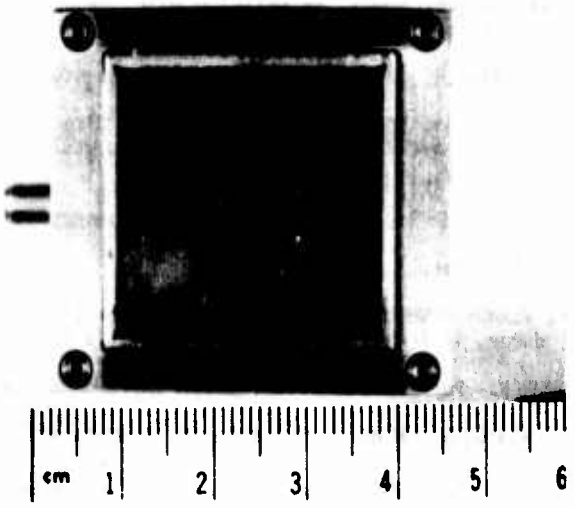

Figure 11. Photo of a prototype NDE EMT transducer.

In summary, we have been able to show that the bulk waves produced by a meander line EMT can be steered in a predictable fashion by varying the frequency. In addition, we have found that it is possible to obtain short pulses which give good range resolution using an EMT designed to produce a chirp output waveform. These advances in conjunction with the new small physical size have brought EMT technology close to the point where it can be applied to practical NDE problems.

References

1. T. L. Szabo and H. M. Frost, IEEE Trans. Sonics and Ultrasonics, SU-23, 323 (1976).
2. P. H. Carr, IEEE Trans. Microwave Theory Tech., MTT-17, 845 (1969).
3. T. J. Moran and R. M. Panos, J. Appl. Phys., 47, 2225 (1976).
4. J. D. Maines and E.G.S. Paige, Proc. IEEE, 64, 639 (1976).
5. T. L. Szabo, 1975 Ultrasonics Symp. Proc., IEEE Cat. #75, CHO 994-4SU, 116 (1975).

DISCUSSION

PROF. MACK BREAZEALE (University of Tennessee): The question I have is with regard to the chirp transducer. Is the idea that by utilization of a sweeping frequency one effectively sweeps a beam through the material?

DR. MORAN: No, that is not the chirp. We found that the single frequency Rayleigh wave devices could also be used to produce steerable bulk waves.

PROF. BREAZEALE: Single frequency?

DR. MORAN: Yes, the Rayleigh waves are single frequency. However, when such a device is operated at frequencies above the Rayleigh wave frequency, then bulk waves are produced and they can be steered by varying the frequency.

PROF. BREAZEALE: You choose a specific transducer for a specific frequency?

DR. MORAN: Yes, if you have a particular direction chosen for the wave. If you are interested in sweeping over a large angle, then you would have to sweep any transducer through a wide range in frequency.

PROF. BREAZEALE: So, you sweep through frequency and angle at the same time?

DR. MORAN: Yes.

PROF. VERNON NEWHOUSE (Purdue University): I'd like to follow up on that question. The chirp transducer, if I understand it correctly, is intended to give you better resolution.

DR. MORAN: For surface waves, yes. There should also be bulk waves generated, however.

PROF. NEWHOUSE: Right. And those bulk waves will go over a range of angles.

DR. MORAN: Yes, they should. However, since there is a staggered spacing to the lines, each pair of lines will generate bulk waves at a different angle at each frequency. Most of the directed energy will be concentrated in the Rayleigh wave.

PROF. K. LAKIN (University of Southern California-Los Angeles): I have a comment regarding bulk wave generation. The surface wave transducer, if you have a small number of interdigital electrodes as lines, will always phase match to the bulk modes.

DR. MORAN: Yes.

PROF. LAKIN: It's not necessarily an anomaly on the edge of the surface wave transducer.

DR. MORAN: This is a 32-line transducer I was looking at. Also, the anomalous bulk waves were generated at the edge were rather broadband, and were not phase matched. They were in addition to the phase matched waves.

PROF. NEWHOUSE: Last question.

DR. SY FRIEDMAN (Naval R&D Center): Is it possible by design to lower the threshold frequency for shear waves?

DR. MORAN: Yes, you just increase the spacing between the lines in the coil.

PROF. NEWHOUSE: Have you ever thought of producing focussing effects by trying to mess around with your magnetic field?

DR. MORAN: It's easier to change the coil. A coil with curved lines will produce a focussed beam.

DR. NEWHOUSE: You might even be able to produce dynamic focussing if you start changing your magnetic field.

DR. MORAN: We are using permanent magnets right now. To get a varying field you would need an electromagnet which would be bulkier and also would give a smaller field in most cases.

OPTIMIZATION OF ELECTROMAGNETIC TRANSDUCER SYSTEMS

R. B. Thompson and C. M. Fortunko
Science Center, Rockwell International
Thousand Oaks, Calif. 91360

Electromagnetic transducers have a number of inherent advantages, some of which have been touched on by other speakers. Historically, their major disadvantage has been their high insertion loss. We have undertaken a project which has been designed to explore techniques for optimizing transducer efficiencies and increasing the dynamic response of ultrasonic systems which use electromagnetic transducers. Today, we would like to report the results of that project.

Figure 1 reviews different electromagnetic transducer (EMAT) configurations. On the right-hand side is shown the surface wave transducer configuration, which has been discussed in previous papers.[1,2] Here we have shown a transducer configuration which uses a normally polarized permanent magnet. The meander coil is placed directly beneath the magnet. When this transducer is placed near a metal part and the coil is driven at the desired frequency, ultrasonic waves are launched in the metal through the reaction of the eddy currents induced in the metal and the static magnetic bias field. Maximum conversion efficiency is obtained when the spatial distribution of the driving stresses corresponds to the spatial period of the propagating ultrasonic signals.

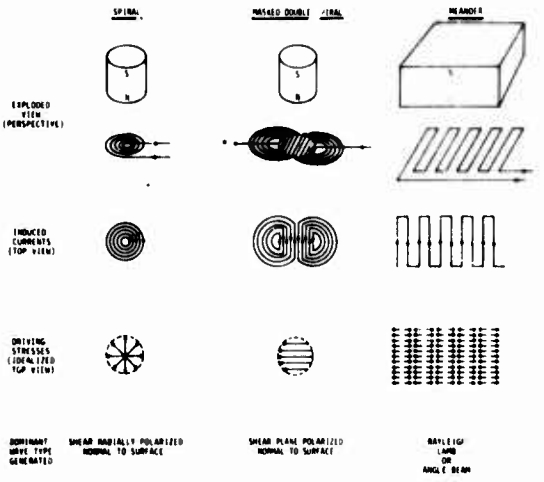

Figure 1. Electromagnetic Transducer configurations.

Bulk wave transducers are shown in the center and the left-hand side of Fig. 1. These are configured differently than surface wave transducers.[3] The induced eddy currents result in time harmonic stress distributions which are essentially spatially uniform so that ultrasonic waves are propagated away normal to the surface. The left-hand side shows a spiral coil transducer configuration. This transducer produces a radial distribution of stresses in the metal surface which generates a radially polarized shear wave having an on-axis null in the radiation pattern. This is an unusual and sometimes undesirable feature of this type of a transducer. For flaw detection, one would prefer to excite an ultrasonic signal with an unambiguous direction of polarization and uniform beam profile. A modified bulk wave transducer for exciting a linearly polarized, normally directed shear wave is shown in the center of Fig. 1. This transducer is made up of two co-planar, counterwound spiral coils and a conductive shield to mask the outer portions of the coils and to reduce transducer inductance. The resultant time harmonic stress distribution is essentially spatially uniform and possesses only one direction of polarization, perpendicular to the windings in the center of the transducer and parallel to the surface of the metal part. An essential feature of this transducer configuration is the permanent magnet which concentrates the magnetic field in the region where the currents are flowing in a uniform direction. The magnetic field is quite weak in other regions where the fringing currents deviate from the desired direction, and hence, generation of signals of unwanted polarizations is minimized.

One of the important common features of EMATS is that they can be packaged for hand-held use. Figure 2 shows both a bulk wave transducer and a surface wave transducer. These units were designed primarily for H.V. operation, but they could easily be adapted for hand-held use by insulating the H.V. terminals. The bulk wave transducer, shown at the left of the slide, uses a spiral transducer coil and a cylindrically shaped samarium-cobalt magnet. The unit at the right of the slide is a surface wave transducer, which under certain conditions can also be used to generate angled shear waves. The magnet is shown slightly offset with respect to the meander line coil. Both transducers have been used to launch ultrasonic waves on aluminum and other metals.

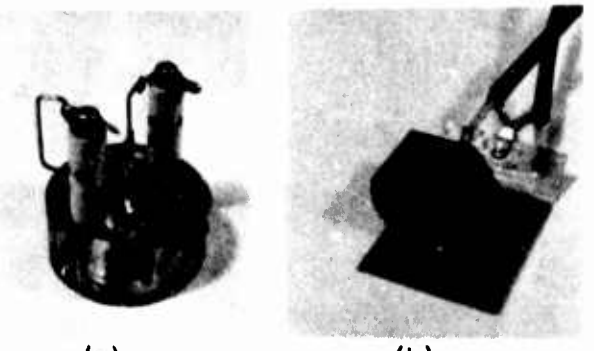

(a) (b)

Figure 2. Photograph of lightweight transducers. (a) spiral (b) meander

Our primary concern has been to optimize the signal-to-noise performance of actual systems which use transducers such as these. The effort has been primarily concentrated on the design of electronic assemblies optimized for maximum transmission and detection efficiency when operated in conjunction with electromagnetic transducers. This was done because commercial NDE instrumentation is, in general, designed for operation with piezoelectric transducer loads. Because electromagnetic transducers exhibit different electrical characteristics than piezoelectric transducers, the performance of commercial NDE receiver and transmitter can be severely degraded.

Figure 3 shows a schematic diagram of a "double-ended" ultrasonic inspection system which uses electromagnetic transducers. The dynamic response of such systems has been greatly increased under this program by constructing special purpose electronic equipment for transmission and reception of ultrasonic signals. Because the amplitude of ultrasonic waves generated by electromagnetic transducers is directly proportional to the input current, it is desirable to increase the current drive to the transducer to as high a value as possible. We have done this with high voltage pulse generation using spark gaps for switching. Pulse forming has been accomplished with distributed (coaxial) and lumped (LC) elements. Using such equipment, we have generated short current pulses similar in shape to output pulses of many commercial NDE instruments. The difference is in the magnitude of the pulses. Using our instrumentation, critically damped pulses in excess of several hundred amperes have been observed compared to several amperes available from commercial NDE instrumentation operating under the same loading conditions. Tone burst operation has also been demonstrated with highly dampened electromagnetic transducer systems. We found no difficulty in passing these high current pulses through coils such as those shown in Fig. 2.

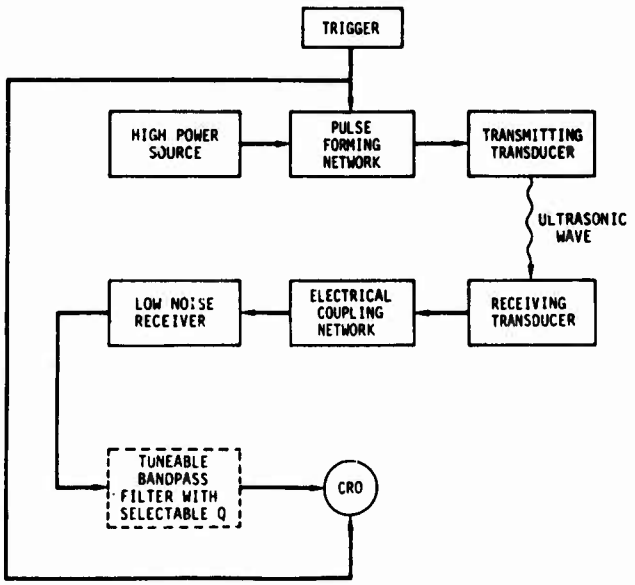

Figure 3. Block diagram of electromagnetic transducer system.

On the receiver side of the system we have been able to achieve significant improvements in sensitivity by proper electrical design of new impedance matching networks for coupling the electromagnetic transducers to amplifiers. This was done in order to transform the generally low impedance of electromagnetic transducers to the optimum source resistance of the amplifier. As a part of this effort, we have constructed special purpose, high input impedance receivers for sensing the open circuit voltage of the output transducer and novel broadband impedance transformers in order to transform the 1 to 2 ohm impedance levels of typical transducers up to impedances of approximately 200 ohms, which are necessary for low-noise operation of the amplifier. For surface wave transducers, we have also used a tunable bandpass filter in order to limit the bandwidth of the received signal to the actual bandwidth of the transmitted signal. In this way we were able to further increase our sensitivity by eliminating unneeded bandwidth. The filter is placed directly before the cathode ray oscilloscope used for display of the bandlimited but unrectified signal.

We would next like to compare the results we have obtained when standard NDE instrumentation was used with the electromagnetic transducers to those obtained with our new instrumentation. The signals shown in Fig. 4 were transmitted through 2 inches (5 cm) of aluminum. The signal shown at the top was obtained with an Immerscope 725 connected directly to the transducer. It is not a very clean signal. At the bottom of this slide we show the same signal when the transmitter transducer was connected directly to the high voltage pulse forming circuit. This photo clearly demonstrates the rather significant improvement in the signal-to-noise performance of the system.

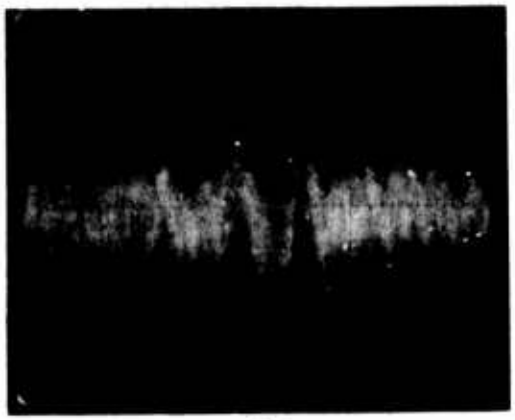

(a)

(b)

Figure 4. Broadband transmission of shear wave between two spiral coils through 5 cm of aluminum (0.2μsec/DIV)
(a) commercially available search unit
(b) newly designed electronics

We have also considered signal averaging techniques, since it is always possible to use such techniques in order to improve the signal-to-noise ratios of signals such as those shown at the top of Fig. 4. In this program we have used rather simple techniques; the analog waveform is digitized and several successive signals are digitally added together. Figure 5 shows the result when the same ultrasonic signal is averaged 10, 100 and 1,000 times. We have recently achieved essentially real time operation in this mode. By limiting our processing time to approximately 10msec per signal we are able to average over about 100 successive signals in one second.

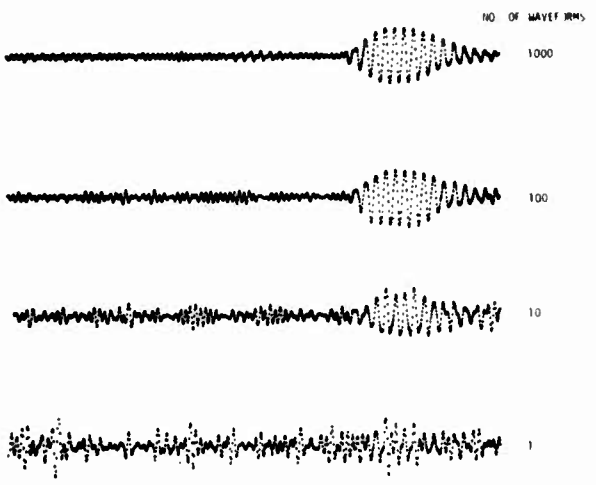

Figure 5. Signal-to-noise improvement of a 5 MHz burst by signal averaging.

As mentioned before, the spiral coils generate radially polarized shear waves which have some disadvantage for flaw detection. However, they do have one intriguing feature. In acoustic media with some shear wave birefringence, the radial distribution of stresses will couple to both polarizations of the shear wave. Part (a) of Fig. 6 shows the input current waveform used to excite one such transducer. Part (b) is a display of the received echo train on a 3/4 in. thick piece of rolled aluminum. One can see that each echo is broken up into two distinct signals. This is caused by the birefringence effect induced by the rolling texture. This effect is better illustrated in part (c), where the expanded time scale makes it easier to see the time separation between the arrival of the slow and fast shear wave signals. One present application of the shear wave birefringence effect is in the measurement of residual stresses. The ability of the spiral coil to couple to both polarizations with no contact may make these tests more easy to apply.

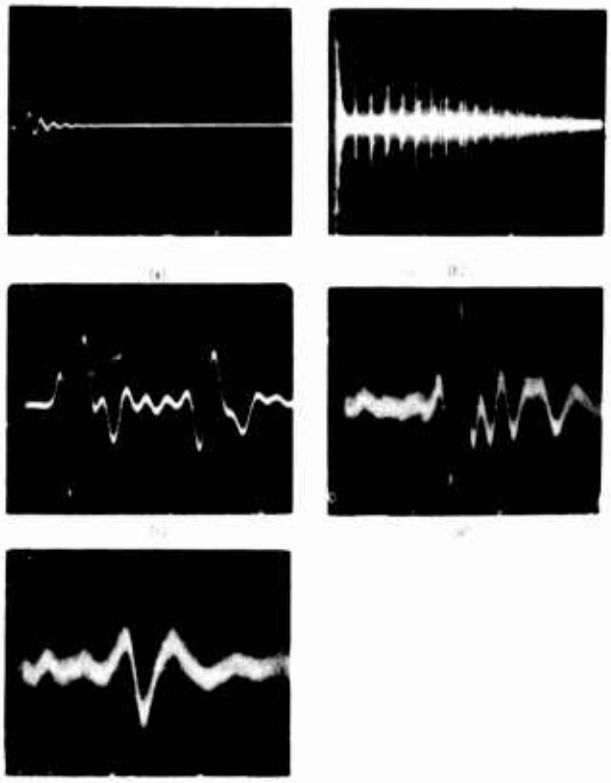

Figure 6. Transmission echoes through 3/4 in. aluminum plate.
(a) drive current (2 amp/div., 2μsec/DIV)
(b) echoes (0.1V/DIV, 20μsec/DIV)
(c) expanded view of echoes after 5 transits (0.1V/DIV, 0.2μsec/DIV)
(d) expanded view of faster shear wave after 19 transits (0.02μV/DIV, 0.2μsec/DIV)
(e) expanded view of slower shear wave after 19 transits (0.02 V/DIV, 0.2μsec/DIV)

Parts (d) and (e) of Fig. 6 reveal another interesting phenomenon observed in this rolled aluminum sample. These show separately the individual fast and slow shear wave signals which have each passed through the sample 19 times. Although the difference in their velocities is only 4%, they have propagated a sufficient distance that the pulses are well separated in time. It will be noted that the two signals do not have the same shape as they did in part (c) of this figure. Instead, the slow shear wave has been distorted and decreased in amplitude indicating a strong preferential attenuation of its high frequency components. This is clearly indicative of the microstructure of the material. Since shear waves propagating normal to surfaces are rather difficult to excite with piezoelectric transducers, such effects have not yet been explored for possible NDE application. The electromagnetic transducer removes this limitation and may open a new area of study.

Let us now turn to systems for generating surface waves, with which we have obtained by far the best signals. One reason for this is that the meander coil surface wave transducers exhibit very low inductances due to effective magnetic field cancellation by the adjacent, oppositely flowing currents. The low inductance inherent in these configurations makes it easy to drive large amounts of current through the transducers. The top trace of Fig. 7 shows the input current tone burst at 2.25 MHz with peak amplitude exceeding 150 amperes. Trace b shows the received ultrasonic signal transmitted over 7 inches of aluminum between a pair of 2.25 MHz transducers such as were shown in Fig. 2, and having dimensions 2.54 cm by 2.54 cm. The thickness of the trace does not indicate the electronic noise of the system. In fact, the dynamic range obtained in this experiment was in excess of 80 dB as demonstrated in the bottom trace, which shows the received signal on an expanded scale when 60 dB of attenuation has been inserted between the transducer and the receiver. This clearly demonstrates the potential of these transducers with permanent magnet biasing for hand-held ultrasonic applications.

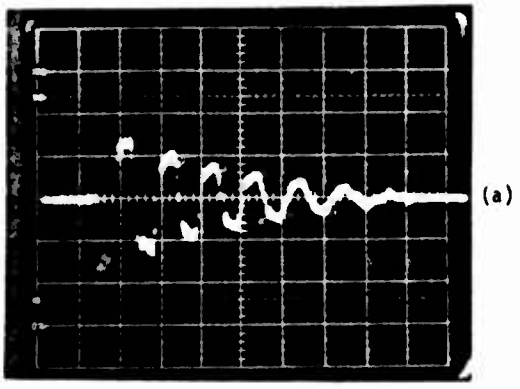

Figure 7a.

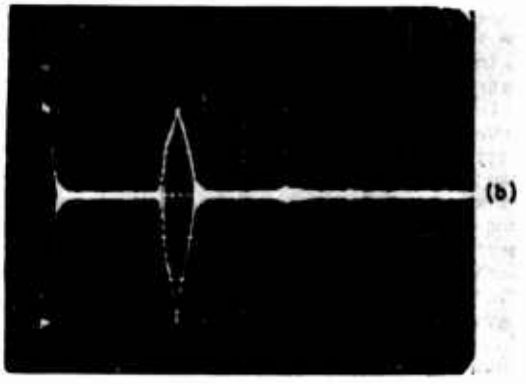

Figure 7b.

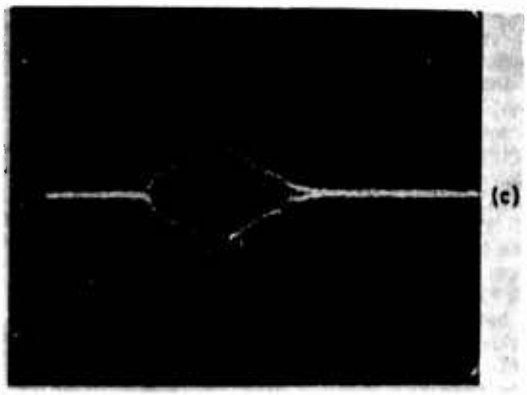

Figure 7c.

Figure 7. 2.25 MHz surface wave transmission over 7 inches of aluminum.
(a) drive current (100 amp/DIV, 0.5μsec/DIV)
(b) ultrasonic signal (2V/DIV,20μsec/DIV)
(c) expanded view of ultrasonic signal with 60 dB of attention inserted between transducer and receiver (5mV/DIV, 5μsec/DIV)

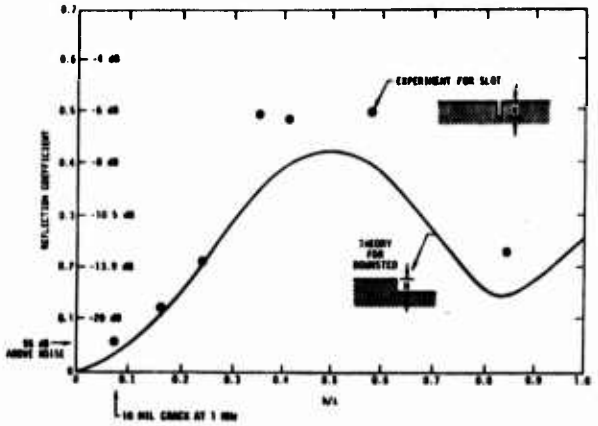

Figure 8. Reflection coefficient of surface waves from EDM slots in steel plate. No theory is available for the slot reflection so the data is compared to theory for a single downstep.

The high dynamic range of these signals suggests that the EMAT's might be useful for the detection of flaws by using surface waves. Szabo has recently used EMAT's to measure the ultrasonic reflection from a step in a surface.[4] We have recently carried out some similar reflection experiments. In our work, the reflections were saw slits used to simulate cracks. These data are presented in Fig. 8 and are compared to a theoretical curve for step reflectors due to Munasinghe and Farnell.[5] The reason for making this comparison was that the reflection from slits should be quantitatively similar to that from a step discontinuity, and this was, in fact, observed. The surface wave reflection coefficient is plotted as a function of the ratio of the depth of the slot to the ultrasonic wavelength. The most striking feature of this plot is the relatively large reflection coefficient obtained from a discontinuity whose depth is only 1/10th that of the ultrasonic wavelength. In fact, the reflected signal from this slot is only -26 dB. So, if we have a system with an 80 dB dynamic range, the reflected signal has a 55 dB signal-to-noise ratio. At a frequency of 1 MHz the slit depth is only 0.100 in. (0.025 cm). We are very encouraged by these results.

The saw slits used in these experiments were much wider than the elastic beam. Of course, real cracks would be much less wide and would have a non-uniform cross section. We are presently in the process of fabricating a set of such defects for further experiments. We have also seen reflected signals from slots 0.029 inch deep with a 1/2 inch surface length fabricated in steel projectiles. The signals from such defects were well above the noise level. We have not yet performed a full set of experiments necessary to completely define the system sensitivity.

We are now working at the Science Center on two applications programs which I do not have time to describe in detail at this meeting. One of these is a feasibility study of a system for rapid inspection of 155 inch artillery projectiles.[6] Let me just mention that this project involves magnetizing the whole projectile with an external electromagnet in order to take advantage of magnetostrictive effects which enhance transduction efficiency, and using moveable transducers to accomplish the inspection as shown in Fig. 9. We are also involved in a program for the Electric Power Research Institute.[7] This is intended to develop techniques for inspecting the interior of nuclear reactor steam generator tubes. The major difficulty here is that these tubes are very small in diameter, about 7/8 inch wide. However, preliminary experiments indicate that useable signal levels can be obtained here too, making it possible to design a successful inspection system.

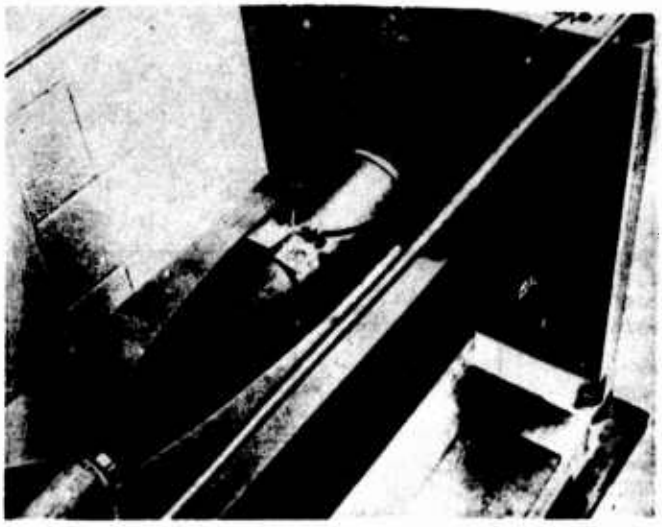

Figure 9. Inspection of 155mm artillery projectiles using EMAT's. The entire projectile is magnetized to the proper bias point by the electromagnet mounted underneath it, and the small surface wave coils are then rapidly scanned over the surface.

References

1. T. L. Szabo, this proceedings.
2. T. J. Moran, this proceedings.
3. B. W. Maxfield, "Electromagnetic Acoustic-Wave Transducers (EMATS): Design Considerations, Experimental Evaluations, and Potential Uses", IEEE Trans. on Sonics and Ultrasonics (in press).
4. T. L. Szabo, Proc. 1975 Ultrasonics Symposium. (N. Y., IEEE, 1975), p. 604.
5. M. Munasinghe and G. W. Farnell, J. Geophys. Res. 78, 2454 (1973).
6. Rapid Ultrasonic Inspection of Artillery Projectiles, Contract DAAA25-76-C-0381, U.S. Army Frankford Arsenal, Philadelphia, Pennsylvania.
7. Evaluation of Electromagnetic-Acoustic Concepts for Inspection of Steam Generator Tubing, Contract EPRI RP698-1, Electric Power Research Institute, Palo Alto, California.

DISCUSSION

PROF. VERNON NEWHOUSE (Purdue University): Are there any questions?

DR. JIM DOHERTY (Pratt/Whitney Aircraft): A simple comment. Slots do not behave like cracks.

DR. THOMPSON: Agreed.

DR. DOHERTY: They really do not. There is a very significant difference. What you see with cracks and what you see with your slots probably won't be similar.

DR. THOMPSON: I agree with that. This is just the first step. There is a question of closure and there's a question of the roughness of the surface, both of which clearly are going to influence the ultrasonic response. I don't know whether you'd like to comment further.

DR. DOHERTY: I think the closure is probably the most significant one. It's been our experience that cracks tend to be rather invisible to the surface waves unless they're very large.

DR. THOMPSON: I think that might be controversial. We certainly have to start somewhere in characterizing EMAT sensitivity, and the slot is a logical point. The next thing to do is look at some real cracks and see what the ultrasonic levels are. I certainly agree with that 100 percent.

PROF. NEWHOUSE: One more question.

DR. P. J. MCKINLEY (University of California): A question about why would you use a surface wave as opposed to an eddy current inspection?

DR. THOMPSON: There are a number of answers to that. In an eddy current inspection, of course, you have to scan your eddy current probe point by point over the surface of the part. In a surface wave inspection you can let the ultrasonic beam propagate over a large area and it will reflect from any defect within this region. Hence, one achieves higher scanning speeds using the surface waves because of the high speed of sound.

Secondly, the surface wave will interrogate the material to a depth equal to the wavelength of the ultrasound, which is, in general, much greater than the electromagnetic skin depth which governs the depth of eddy current inspection. So, you're going to get a much deeper look at the material for subsurface defects using the surface wave. I think those are two good reasons.

SIGNAL PROCESSING WITH SURFACE ACOUSTIC WAVE DEVICES

R. M. White
University of California
Berkeley, California

Our interest is in analog signal processing as it might be applied to NDE, carrying out some sophisticated signal processing using an inexpensive, real-time analog system based on the surface acoustic-wave technology, or perhaps the CCD technology.

To date we have considered an inverse filter for correcting for the frequency response of an NDT transducer: we have shown the feasibility of making such a device and will show some experimental results here. We are making and testing some filters that have been designed to go with a commercial NDT transducer that we have purchased. We are also looking at the possibility of realizing the same sort of filter with a charge-coupled device.

In the next year we should like to look at a more complicated analog signal processor - the convolver or correlator - to see how it can be realized and applied to defect signature recognition. At the end of my talk I'd like just to mention some work being done by another faculty member at Berkeley on an interesting receiving transducer which I don't think has come to the attention of this particular audience.

NDE Inverse Filter

As outlined last year, we are using as a test object a block having regions of different acoustic impedance (Fig. 1). When we send in a pulse it would be nice if our system produced nearly delta-function waveforms indicative of the presence of planar discontinuities of impedance. In our actual system (5 MHz PZT transducer bonded to an aluminum block), ringing of the transducer results in a distorted output which is not easy to interpret. So the idea is that we might design a simple filter for the system to correct for the frequency response of the NDT transducer and give us, in this case, a delta-function like output.

Initially, we followed the work of Seydel and Frederick[1] who have shown that you can make a digital inverse filter that will do this. Instead, we're using a surface wave filter. The output SAW transducer is designed to have a response which is inverse to the response of our NDT sending and receiving transducer; ideally, we should get some output that looks something like that sketched in the figure.

The design of this filter is based on the impulse response of the NDT transducer. In our case we get this by driving the transducer, letting the acoustic pulse reflect from the reflector, photographing the waveform of the reflection and then scanning that into a computer system.

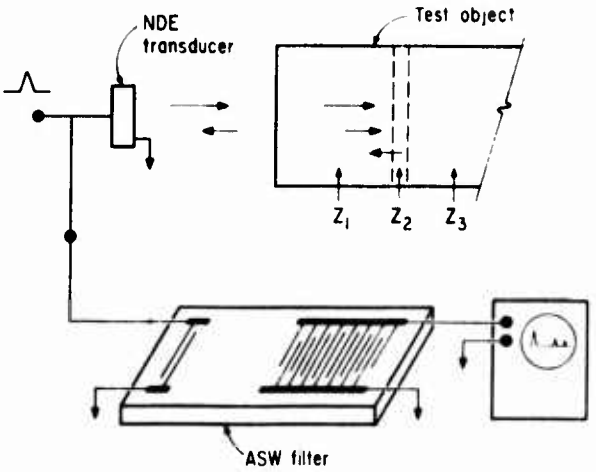

Figure 1. Schematic illustration of simulated NDE system with transducer, test block, filter, and indication of desired output on oscilloscope screen.

We take the impulse response as our reference function, the starting point for the design. We Fourier transform that to get the true inverse filter characteristic that we would like to have. We also do some weighting on the edges of that response so it doesn't go to infinity where our NDT transducer has no output. We then take an inverse Fourier transform to get the impulse response of our filter. It's the impulse response of the device we're trying to make.

In order to make the device easier to build, we would like to truncate that response somewhat, but not truncate it so much that it ruins the results. We have used both a mean square error criterion and a visual comparison of full and truncated impulse responses in order to determine how much truncation was permissible.

For design of the output transducer of our filter, we have recently implemented the Parks-McClellan finite impulse response (FIR) computer programs to tell us what the tap weights for our filter transducer electrodes should be. I think this is important because we can use that information in the design of either a charge-coupled or surface-wave filter, and we're building some actual filters so as to compare the results of these two designs and see which is best.

The other point here is that in principle, as I think I said last year, the artwork could be produced on a digital computer system. This is a fact now: we are cutting rubyliths for our filter on a digitized (Gerber) plotter (in our Mechanical Engineering Department) and find that this is a great improvement over doing it by hand.

Figure 2 shows a layout of one of the filters with its input transducer and output transducer designed to have the desired inverse response, and a multi-strip coupler to take care of incidental bulk waves. Our first filter had a rather simple input with only one set of fingers for broadbandedness. Later filters have more input electrodes for more efficient transduction.

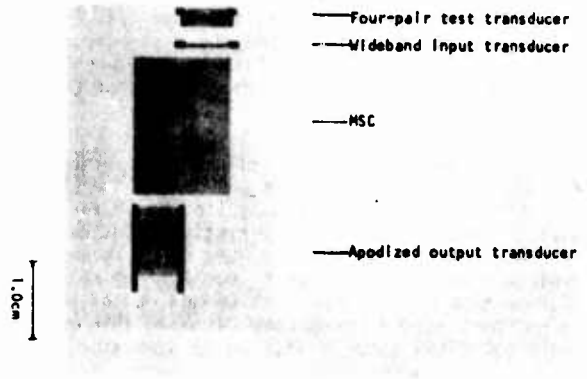

Figure 2. Layout of SAW inverse filter with input transducer(s) at left side and output transducer at right, separated by multistrip coupler for suppression of bulk waves.

In our test setup a PZT transducer is mounted on an aluminum block which is oil-coupled to a thin glass slide: the bottom surface of that glass slide is coupled by an oil film to another aluminum block, making a sandwich structure which produces reflections. On the oscilloscope trace (Fig. 3) are the unprocessed responses from the back of the test block and the output of our inverse filter. Comparing the responses, one sees that it is possible to resolve the separate peaks in the filtered output only.

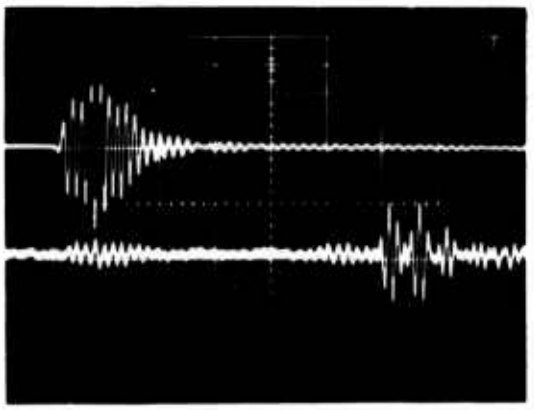

Figure 3. Reflections from test block. (a) Unfiltered return. (b) Return filtered with SAW inverse filter, showing resolved separate reflections from different layers at end of test block.

We made other measurements, trying to correlate the amplitudes of the peaks in the output with the magnitude of the impedance discontinuity, and found that the properties of the oil film dominate in the reflections. Since we didn't know how thick the film was, we set up instead a water bath system (Fig. 4) to permit measurement of resolution. The bottom end of the aluminum block is in a water bath; a (water-filled) gap between the bottom end of that block and another aluminum block in the water bath forms our impedance discontinuity. We can move the test block up and down (measuring the distance with a dial indicator) and measure the spatial resolution. We have shown that inverse filtering can improve the spatial resolution of our test transducer, which has lots of ringing. Now we are seeing to what extent it can improve the response of a purchased commercial transducer.

Figure 4. Photograph of test block in resolution test setup. Block can be moved known amounts vertically to vary width of gap in water bath between it and a second metal cylinder located in the bath.

As mentioned earlier, the starting point in the filter design is the impulse response of the NDE transducer. The impulse response of one purchased commercial transducer, driven by a rectangular pulse (from a commercial pulser that is nominally identical to the one used by the manufacturer of this transducer), is shown in Fig. 5. One realizes that if one were making an inverse filter to go with a particular transducer, one would not like to have the impulse response of the system (composed of pulser and NDE transducer) change; if the pulse duration of the drive pulser changes, then the impulse response of the system changes and the filter isn't as good. For this reason, it is advantageous to drive the transducer rather with a single step that then very gradually decays away to zero voltage sometime later. When our commercial transducer is driven with a single step, we get what most people would agree is a more nearly ideal response (Fig. 6). It is also interesting to note that with the same step voltage one obtains about 3.5 times the acoustic output amplitude as when one drives with a rectangular pulse.

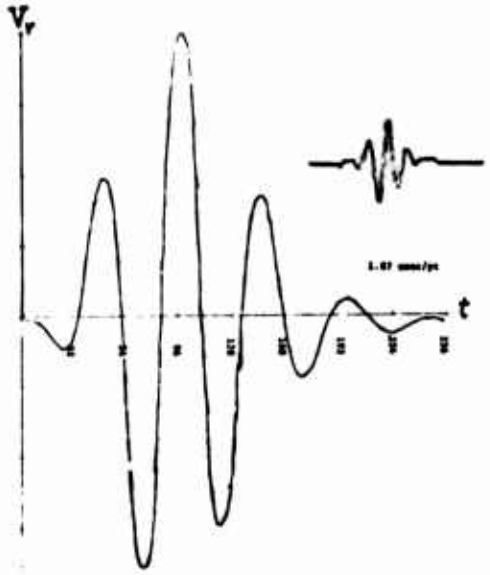

Figure 5. Impulse response (output voltage V_r versus time t when acoustic pulse reflects from a plane reflector in water bath) of commercial NDT transducer driven by rectangular pulse supplied by pulser made by same manufacturer. Inset shows tracing of impulse response as supplied by manufacturer with transducer.

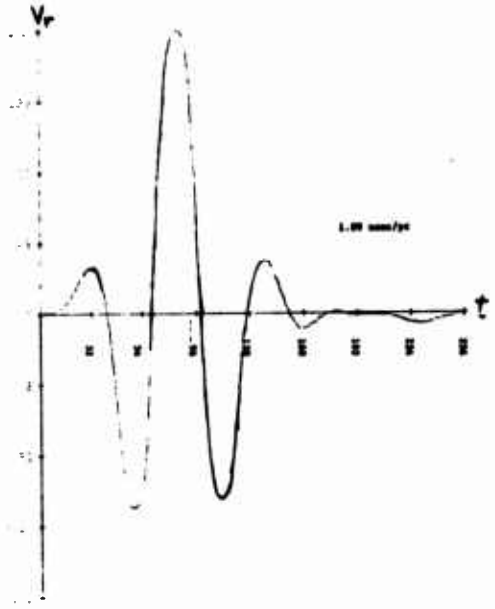

Figure 6. Transducer of Fig. 5 driven with single step to obtain impulse response. Note that response is more nearly symmetrical and of somewhat shorter duration.

Of course, one could generate such a step drive with solid-state circuitry, but we did it with a commercial (SKL) delay line pulse generator which is normally used for the generation of short duration rectangular pulses. The device operates by slowly charging a coaxial cable to a constant potential and then discharging it suddenly upon closure of a relay having mercury-wetted contacts. When the relay closes, disturbances travel in both directions along the coaxial line; the load sees, first of all, a rise in voltage when the disturbance reaches it, and then a fall back to zero when the disturbance reflecting from the open end of the coaxial line reaches the load.

All we want is the fast voltage rise at our load (NDT transducer). So we terminated the charging cable in a DC-blocking capacitor and a resistor equal in value to the characteristic impedance of the cable. Although this may seem crude because it involves a mechanical element, namely, the relay, the rise time of the step that we get out of this was as short as 0.4 nanosecond, showing this to be a very practical type of step pulse generator.

Piezoelectric field-effect Transducer

I would like to change now to a different topic--a receiving transducer being developed by Prof. Muller and his students at Berkeley. The transducer is a combination of a standard silicon device, a field effect transistor, with a piezoelectric film.[3] The important characteristics of the transducer are that it's a very sensitive transducer having a large bandwidth and a very small active area; that it makes a very natural interface between acoustics and signal processing because one obtains an electrical signal in a silicon integrated circuit ready for additional processing as needed.

Figure 7 is a cross-section through the device showing a silicon wafer and the conventional source and drain electrodes. Normally the current which flows from the source to the drain electrode depends only upon the potential applied to the gate electrode. To this standard field effect transistor has been added a thin rf sputtered layer of piezoelectric zinc oxide. When this film is strained, it produces an additional potential in the gate region which has a large effect on the current that flows from the source to drain. Because this film is very close to the flowing carriers, it has a very large effect, making a very sensitive device. (In the devices that have been made, the gate width is only one micron, so, one has a very well localized transducer also.)

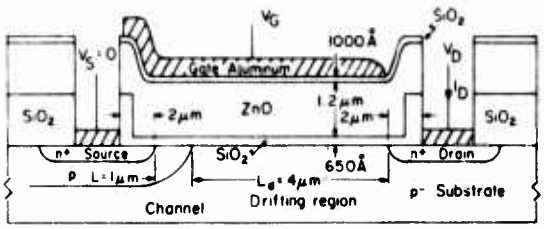

Figure 7. Schematic cross-section of piezoelectric field-effect transistor transducer, showing conventional source, drain, and gate electrodes of aluminum, together with film of piezoelectric zinc oxide (ZnO) underneath gate electrode. (From Yeh and Muller, Ref. 3)

The sensitivity is indicated by static measurements, shown in Fig. 8, where source-to-drain current is plotted against source-to-drain voltage, with gate bias as parameter. The amount of source-to-drain current flowing depends upon the magnitude of the strain. One can define something equivalent to a conventional gauge factor as the fractional change in this source-drain current divided by the strain. Static gauge factors as high as 160,000 have been measured, showing this is indeed a very sensitive device. More measurements of dynamic properties are probably needed, but the transducer has been shown to respond to bulk compressional waves up to about 20 MHz, to surface waves as high as 15 MHz, and there is no apparent reason for these to be upper limits; thus the transducer is expected to respond from DC up to many hundreds of megahertz.

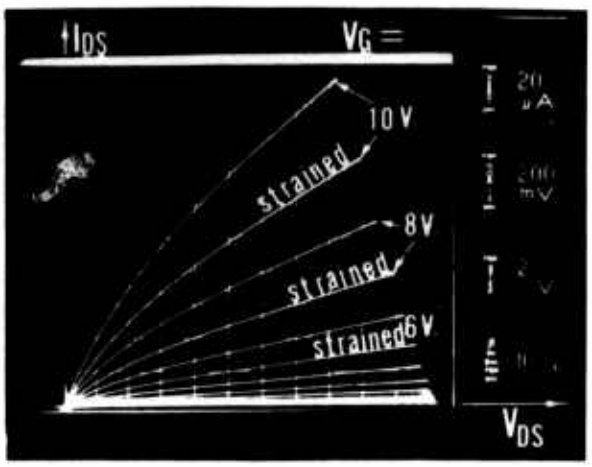

Figure 8. Source-drain current vs. source-drain voltage of transducer in unstrained and strained conditions (strain is 1.8×10^{-6}). (From Yeh and Muller, Ref. 3)

At this conference yesterday, somebody mentioned the need, in the field of acoustic emission, for a wideband transducer that can be located close to the sources of sound. Figure 9 suggests how this field-effect transducer might meet this need. The figure shows a mockup including a conventional transistor header on which the field effect transducer can be mounted. Small coaxial cables connect to the transducer. Some standard transistor headers have a ceramic post coming out of the bottom which can be used to couple sound into the transducer very conveniently. So one can obtain a very small receiving transducer which is well shielded and which has a nice coupling port for sound waves. Incidentally, we have compared the response of one of these FET transducers with the response of a 5 MHz PZT transducer, using a breaking glass capillary as sound source, and find we observe about the same output voltage from both transducers.

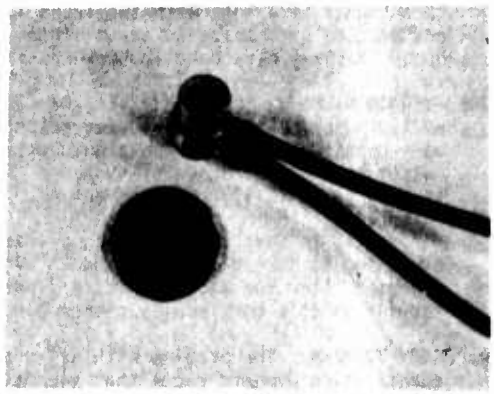

Figure 9. Mockup of piezoelectric field-effect transistor transducer in slightly modified transistor header package. Flexible miniature coaxial cables shown are for bias and output.

I will conclude by saying that I think we have demonstrated the feasibility of making an analog signal processor, namely, the inverse filter using acoustic surface wave technology. We are characterizing these filters, and have designed and are testing one for use with a commercial NDT transducer.

REFERENCES

1. J.A. Seydel, "Computerized Enhancement of Ultrasonic Non-destructive Testing Data," Doctoral Dissertation, University of Michigan, 1973.

2. E.G. Cook, "Transient and Steady-state Response of Ultrasonic Piezoelectric Transducers," Convention Record, IR.E., Pt. 9, pp. 61-69, 1956; H.E. Van Valkenburg, "Note on 'Sources of Sound in Piezoelectric Crystals'," J. Acoust. Soc. Am., 32, No. 11, p. 1468, 1960.

3. K.W. Yeh and R.S. Muller, "Piezoelectric DMOS Strain Transducers," Appl. Phys. Letters 29, No. 9, 521-522, 1 Nov., 1976.

DISCUSSION

DR. PAUL FLYNN (General Dynamics): Your SAW filter application that you showed might be of interest in an adhesive bar problem. I would like you to comment on possible applications of this inverse filter to signal processing to resolve out adhesive bond-type signals. Do you think it would be applicable?

PROF. WHITE: Possibly so. When people were talking yesterday about the adhesive bond problems and the difficulty of knowing the properties and the thickness, I was thinking about oil films where we had essentially the same problem.

DR. JERRY TIEMANN (General Electric): What is the order of magnitude of the output impedance relative to PZTs?

PROF. WHITE: The output impedance is typically around 15 kilohms, but good electrical response into the very high megahertz region can be observed, if that's what you were worried about.

DR. CHRIS FORTUNKO (Rockwell Science Center): I wanted to point out that it's possible to synthesize this signal like this with two transmission lines. We changed the amplitude and the pulse length and you can synthesize an input signal which will drive the transducer so as to minimize the ring out. This has been done in Berkeley in the 50s, around 55 or so.

PROF. VERNON NEWHOUSE (Purdue): Yes, Dr. Fortunko has pointed out that you can synthesize signals which will produce an ideal transducer response, and we've heard a talk by Dick White which has given some very beautiful results on designing surface acoustic wave devices to essentially deconvolve the outputs of these transducer systems. Would anybody who represents the computer area perhaps like to comment on this? (No comment.)

Well, in that case, I'll jump into the breech and point out that, as Dr. White pointed out, you are going to have different signals with different transducers, so you would have to design a different inverse filter for each transducer, and the computer or microprocessor might have an advantage there insofar as it's more easily changeable.

DR. JERRY TIEMANN: The problem with using a computer to do all of this is one of the digitization or quantization dynamic range that you have available. In order to preserve the accuracy you need to actually perform these deconvolutions, you require something like 14 to 16 bytes accuracy in the A to D conversion. Furthermore, to preserve the band widths, you have to have sampling rates up into the 20 or 30 megasamples per second range. And the expense and problems of getting these extremely accurate, very high speed A to D conversions, is beyond the state of the art.

PROF. NEWHOUSE: We are going to talk about that this afternoon using a correlation-type system which produces nice slow outputs which overcome the sampling rate problem and also refer to computer processing techniques which smear things out so as to overcome that other problem you mentioned.

DR. KEN LAKIN (USC): I have a comment regarding the inverse filter. There has been considerable work done on adaptive transversal filters wherein you are allowed to change the response of the filter. So, even if you have a transducer that is drifting with time conceivably recorrect on the adaptive basis, an electrical adjustment. There was a paper given at the '74 Sonics-Ultrasonics symposium on that and Tom Bristol of Hughes Aircraft might be able to comment on current work done on adaptive transverse filters. Do you care to comment, Tom?

DR. THOMAS BRISTOL (Hughes Aircraft): We're working on a surface wave tap delay line implementation of an adaptive filter, but it has to be a closed loop type of algorithm. And the point is, one has to have some kind of an error criterion to form an error. It's certainly conceivable if we could somehow have an evaluation criteria or some way to establish an error signal, it would be feasible.

PROF. NEWHOUSE: You do need a procedure which is adaptive and can change from instant to instant.

PROF. GORDON KINO (Stanford): We have tried a procedure with that. It's not an inverse filter, it's a correlation filter. But I merely describe it so that basically you can read a signal into a storage device, correlate the weighted signal, use one angle to calibrate the exponent. And that works quite well.

PROF. NEWHOUSE: We hope to describe a procedure using the computer to do exactly the same thing. If anybody would like to get into the subject of piezoelectric transducers versus acoustoelectric transducers, because one thing that hasn't been brought out is that the terrible problem with piezoelectric transducers is that if you change the orientation of your target by just a smidgen, your spectrum changes completely, whereas these phase insensitive transducers that Dr. Heyman talked about don't have that problem. Should we throw away our piezoelectric transducers immediately?

DR. JOSEPH HEYMAN (NASA, Langley Research Center): No.

PROF. MACK BREAZEALE (University of Tennessee): Unless we all throw them away, I would like to ask about the sensitivity of the alternatives to the piezoelectric transducer.

DR. HEYMAN: The power detector is less sensitive than, say, a quartz or even a PZT type of transducer. However, it is not a limiting factor. I'm talking of maybe two orders of magnitude less sensitive.

PROF. R. E. GREEN (Johns Hopkins University): Can you also generate sound waves with the power transducers?

DR. HEYMAN: Well, it is piezoelectric, so you certainly can generate sound waves, but it's not as efficient as some other technique. We're working on a combination of transmit and receive detector which would marry optimum conditions.

PROF. GREEN: Do you think the generated mode will be as sensitive as the receiver mode?

DR. HEYMAN: The only loss in combining the two is going to be in the relative impedance difference between the material.

DR. ROD PANOS (Air Force Systems Command, Materials Lab): I would like to have Dr. Heyman explain a little more in detail this new technique.

DR. HEYMAN: The power detector as it currently stands now is a cadmium sulphide acoustoelectric cell, and the conversion of the acoustic wave to the electrical signal is via phonon carrier coupling in the material itself. So that when an acoustic wave enters the cadmium sulphide cell, it creates an electric field in the cell which couples to the electrons. This leads to a loss of energy in the acoustic wave and a corresponding momentum transfer to the electrons in the cell. This in turn leads to a net charge flow in the cell which results in the whole picture which can be measured. At present we're trying to optimize some of the rise times associated with this phenomena and hope to be able to achieve rise times that would make it very suitable for pulse echo work. I must admit my bag is CW ultrasonics, and I have found it to be very valuable in that area.

A NON-PHASE SENSITIVE TRANSDUCER FOR ULTRASONICS

J. Heyman
NASA-Langley Research Center
Hampton, Virginia 23665

I would like to describe some of our programs at NASA, Langley Research Center, Hampton, VA, on the development and use of a new type of phase insensitive transducer we call an Acoustoelectric Converter, or an AEC. In the very short time I have here, I shall indicate why the AEC is significant and show some ultrasonic transmission results obtained from modified isometric attentuation scans of conventional NDE resolution test plates containing simple flaws.

In general ultrasonic NDE, an acoustic wave incident on a transducer is composed of many phase fronts and frequency components which are all added in a complicated way with conventional phase sensitive transducers. For example, consider the simplest use of just two phase fronts at the same frequency entering a piezoelectric transducer from the left, as shown in Fig. 1. To the right of the transducer, the electrical signal thus produced is shown.

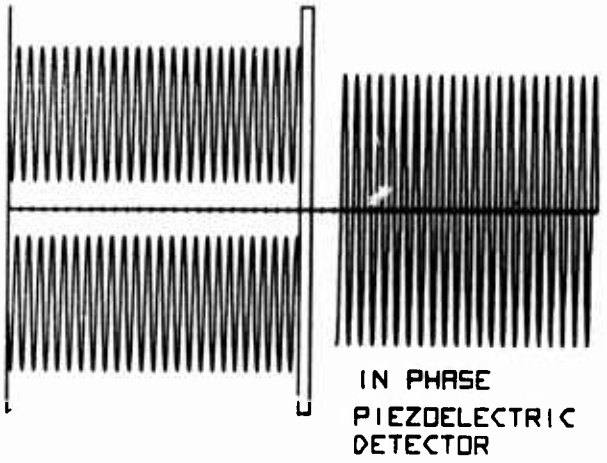

Figure 1. This figure shows two incident ultrasonic waves entering from the left and impinging on a conventional piezoelectric transducer in the center of the figure. To the right is shown the resulting electrical signal obtained from the transducer for waves of the same frequency and phase.

If the two incident waves are slightly out of phase, the resulting electrical signal is reduced as shown in Fig. 2. This occurs because a conventional transducer is phase sensitive and averages the piezoelectric voltages.

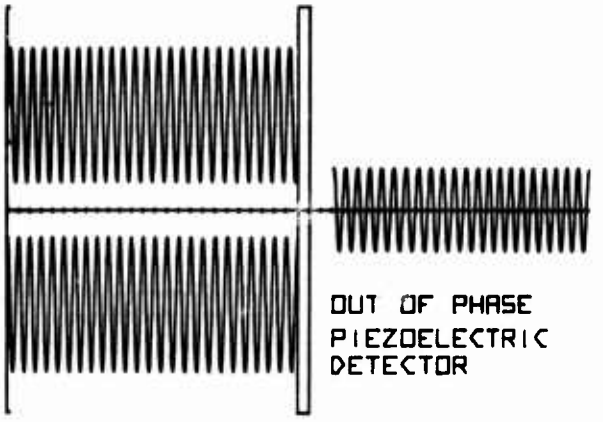

Figure 2. Same as Fig. 1, but with a phase shift between the two incident waves. Note the decreased amplitude of the electrical output as compared to Fig. 1.

If the acoustic waves are composed of two different frequencies entering the piezoelectric transducer, then severe phase modulation occurs as shown in Fig. 3. In other words, the use of piezoelectric transducers suffers, if you will, from too much information in some instances; i.e., their output is modulated due to the phase of the acoustic wave front.

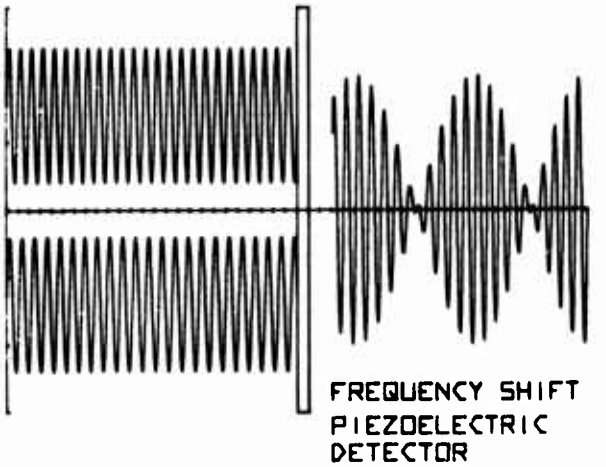

Figure 3. Same as Fig. 1, but with a frequency shift between the two incident waves. In this case note the severe modulated electrical output.

If one were able to develop a transducer truly insensitive to phase, then, regardless of the phase and the frequency of the incident waves, the resulting signal would merely be the incident power. This is shown for two incident waves of any phase or frequency in Fig. 4. Note that the output for this case is not modulated and that it is a D.C. signal consistent with the concept that the AEC is a power "monitor."

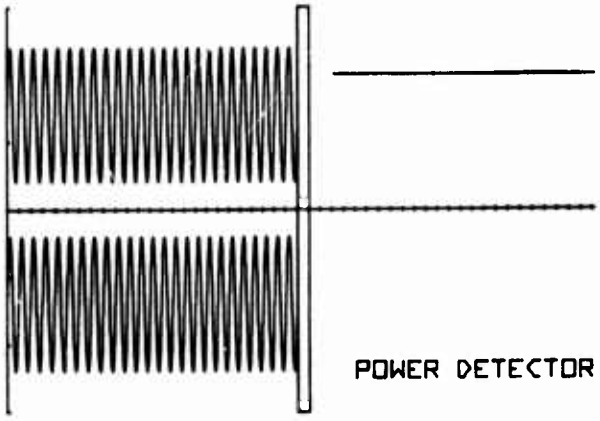

Figure 4. This figure shows the effect of a real power detector instead of a piezoelectric transducer for all cases of phase and frequency. The AEC mentioned in this article approximates a power detector. Note that the output is constant for all phase and frequency and that the signal is effectively D.C.

The characteristics of the AEC are desirable and may provide a significant improvement in NDE as well as ultrasonic imaging quality. The basis for these statements is provided by several figures obtained with the AEC and a conventional transducer. These are presented below without going into the specifics of the AEC which will be forthcoming in another paper. These data are obtained by scanning a conventional flat aluminum test plate with some milled flat bottom grooves and some rather small flat bottom holes. A photograph of the plate is shown in Fig. 5. The smaller holes are of the order of 500 microns; the larger are of the order of a millimeter in diameter. The plate is scanned in a transmission experiment, which is not necessarily the highest resolution technique for conventional detection but does demonstrate the difference between the two transducers.

Figure 5. A photograph is shown of a high resolution ultrasonic test block. The smallest flat bottomed holes are one-sixty-fourth of an inch in diameter.

In Fig. 6, one finds a very complicated signal obtained with a conventional piezoelectric detector. Looking back at Fig. 5 again, one can see that the large grooves are visible but the holes are obscured by the phase information.

Figure 6. An ultrasonic transmission scan through the test plate using conventional piezoelectric transducers presented in a modified isometric plan. The large grooves are clearly visible while the holes are obscured by phase modulation.

Replacing the receiving transducer in this transmission experiment with the new AEC transducer and repeating the scan at the same frequency, one obtains the response shown in Fig. 7, from the plate of Fig. 5. In Fig. 7, using the AEC, one clearly sees the rather small holes. There is no obvious presence of phase modulation which would produce a background signal. Furthermore, one can see in the large grooves that plate resonances are being excited, which is not so obvious from the conventional transducer data of Fig. 6.

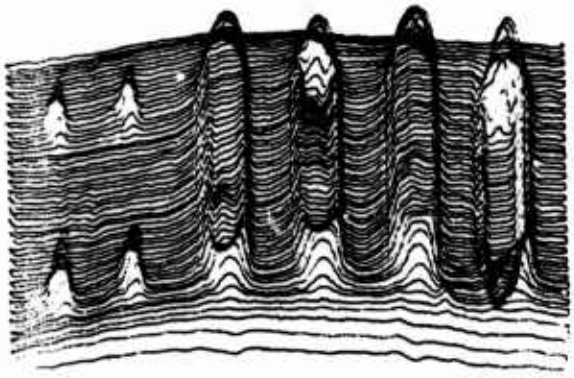

Figure 7. Same identical test as shown in Fig. 6, but with the receiving transducer replaced with an AEC. The small holes are clearly visible and plate resonances in the large grooves are easily discernable.

In conclusion, we think we have a new transducer which has very definite application to high resolution NDE. It's by no means optimized; we have by no means looked at all the parameters, but we are enthusiastic as to the future potential for the device.

Thank you.

DISCUSSION

DR. JERRY TIEMANN (General Electric): Would you please state the physical principle or the construction of that transducer?

DR. JOSEPH HEYMAN: Certainly. The transducer is a device which converts the incident acoustic wave into an electrical current through the coupling of the phonons to the free electrons in the detector. It's basically an acoustoelectric-type of detection scheme. When the acoustic wave is incident on the detector, the momentum transferred by the acoustic wave to the electrons results in an electric current which will be independent of the phase of the incident acoustic wave. Therefore, the conversion process of the AEC makes it non-phase sensitive.

PROF. VERNON NEWHOUSE (Purdue University): Was it you who gave the paper at the American Institute of Ultrasonics in Medicine conference of a few weeks ago?

DR. HEYMAN: No. No, I did not.

PROF. NEWHOUSE: Not you or one of your collaborators?

DR. HEYMAN: Dr. Miller and his group at Washington University have been applying the AEC in the medical area for tissue characterization.

PROF. NEWHOUSE: Yes.

DR. HEYMAN: I might add that some very striking figures will be presented by Dr. Miller at the IEEE Ultrasonics Symposium in October, 1976.

DR. STEPHEN HART (Naval Research Labs): What sort of frequency range are you getting at the present time?

DR. HEYMAN: The AEC has been used up to about 10 MHz although there is no practical NDE limit on the higher frequency; at the lower frequency limits, one has less conversion so that there is a poorer signal to noise ratio. With the AEC, one cannot convert the acoustic wave to an electrical signal at the lower frequency without losing some signal strength.

ADAPTIVE DECONVOLUTION TO IMPROVE RESOLUTION*

E. S. Furgason & V. L. Newhouse
School of Electrical Engineering
Purdue University
West Lafayette, Indiana

ABSTRACT

Deconvolution applied to ultrasonic flaw detection offers the possibility of greatly improved resolution through the elimination of the transducer response. Seydel has previously demonstrated that at least a modest increase in resolution is possible provided the signal-to-noise ratio of the signal being deconvolved is large enough. The random signal flaw detection system can be shown to be ideally suited to deconvolution since it provides enormous signal-to-noise ratio enhancement. Furthermore, the bandwidth compression inherent in this system allows A-D conversion of the output at a rate several orders of magnitude lower than the transmitted ultrasonic frequency.

The computer program created to implement the deconvolution procedure also utilizes elementary pattern recognition techniques to deal with the remaining signal noise and ensure a good signal-to-noise ratio for the deconvolution output. The operation of this program was discussed and some preliminary results were presented which showed that at least a ten-fold increase in resolution is possible. At present this processing technique is restricted to a special class of targets, those composed of a series of plane surfaces.

*Sponsored by Air Force Contract No. F33615-75-C-5252

REPORT ON THE SYMPOSIUM ON NONDESTRUCTIVE TESTING STANDARDS May 19-21, 1976

G. Birnbaum
National Bureau of Standards
Washington, D.C. 20234

A symposium on nondestructive testing (NDT) standards reflecting widespread current concern with this area was held at the National Bureau of Standards (NBS) May 19-21, 1976. The symposium was co-sponsored by the National Bureau of Standards (NBS), the American Society for Testing and Materials (ASTM), the American Society for Nondestructive Testing (ASNT), with the American National Standards Institute (ANSI) cooperating. The meeting provided the first general forum encompassing discussions on the processes by which NDT codes, standards, and specifications become accepted, and discussions on the status and needs that exist in all NDT methods. Major themes included standards documents, the status of standards in the major methods used in NDT and future directions.

The initial series of papers were devoted to standards documents preparation by such authoritative bodies as ASTM, ASNT, and ANSI giving recommended practices and procedures, and on the needs in this area of various society and government organizations. C. H. Hastings (Army Materials and Mechanics Research Center) outlined the problem of NDT specifications in military standards. He estimated that there are probably 0.25 megaspecs existent in the Department of Defense, a situation attributable to the relegation of NDT specifications and procedures to the low tiers of the procurement/specification pyramid and to the writing of NDT specifications by non-NDT personnel. The important matter of nondestructive testing personnel and the certification of their qualifications were discussed by F. C. Berry (Chicago Bridge and Iron) from his vantage point of ASNT personnel certification experience.

The bulk of the papers dealt with standards for the major NDT methods including radiography, ultrasonics, acoustic emission, liquid penetrants and magnetic particles, visual and optical methods, electromagnetic testing and leak testing. Because of the interest of the ARPA/AFML program in ultrasonic and acoustic methods, we will mention some contributions in these areas.

In his review of the NBS program in NDT standards, H. Berger (NBS) noted that a recent round-robin program initiated by NBS revealed unexpectedly large variations in the results obtained with different sets of aluminum reference blocks. These discrepancies were traced to variations of velocity and attenuation in the material. It was announced that there would be soon available for loan from NBS a set of certified test blocks.

The role of the transducer and ultrasonic instrumentation in obtaining reliable results was discussed respectively by J. T. McElroy (Southwest Research Institute) and C. E. Burley (Reynolds Aluminum). Efforts to improve reproducibility in acoustic emission were discussed by W. F. Hartman (Trodyne Corp.).

The final series of papers dealt with future directions and included discussions of quantitative test results. Methods for quantitative ultrasonic standards based on the theory of ultrasonic scattering from a spherical inclusion or void were described by B. R. Tittmann, D. O. Thompson and R. B. Thompson (Rockwell International Science Center). Other speakers discussed the needs for improvement in techniques, equipment and standards. As emphasized by E. T. Wessel (Westinghouse Research Labs.), such improvements are needed if fracture mechanics as a method for establishing an acceptable flaw size is to play a future role in quality control.

Among the general comments voiced at the Symposium, concern was expressed regarding the added cost of NDT testing, and that NDT standards may engender an unwarranted sense of reliability in products conforming, in fact, to inadequate standards. In discussing the economic benefits of NDT to a manufacturer, J. E. Doherty (Pratt and Whitney) pointed out that improving the yield of an acceptable product would reduce unit cost. Although some expressed the view that NDT standards are presently inadequate and the efforts are overlapping and uncoordinated, many others expressed the belief that effective and realistic NDT standards are not only possible but essential.

A question that was implicitly raised but not directly addressed was the role of the government in the generation and imposition of NDT standards. It may be expected as a result of the Alaskan pipeline problem that there will be greater awareness and greater focus on NDT inspection. As evidence of government interest in NDT are two proposed congressional bills: The Tunney-Hart bill in the Senate; and the Teague bill in the House, which recognize that NDT plays a role in material conservation.

In summary, the increasing awareness of the benefits of NDT and the need for higher confidence in its results are causing attention to be focused on code specifications, procedures, and personnel certification, and are causing standards and code generating groups and others to re-evaluate existing standards and recognize the need for new ones.

SAGAMORE, NDE TOPICS

George Mayer
U. S. Army Research Office
Durham, North Carolina

The 23rd Sagamore Army Materials Research Conference was held last week in upstate New York. The theme was Nondestructive Characterization of Materials, and the intent of this meeting was to approach the subject with a broad brush treatment, including historical aspects, the assessment of significant advances in each topic area, important new capabilities, and discussion of some exploratory techniques as contrasted with the generally more focused and in-depth studies that have been reported here at Asilomar.

Recognizing the proliferation of nondestructive meetings this year, we took care to have Don Thompson and Mike Buckley serve as part of our organizing committee. The meeting was subdivided into four sections that included x-ray or non-optical radiation based methods; sonic and ultrasonic techniques; optical methods, and a session called "other", involving both established methods, such as penetrants, and newer techniques, such as exo-electron emission.

In the brief time that I have, I would like to hit the high points as they impressed me. First, I was struck by the idea that the major advances in the nondestructive field seemed to fall into two major areas. These were instrumental advances, and secondly, application of new signal and data proccessing methods. These two are different from new phenomena which I, as a metallurgist, naturally think of as the area of opportunity.

Sometimes these two areas are connected in rather sophisticated ways, and sometimes in straightforward ways. An example was the work presented by Birks of NRL on compositional analysis by x-ray fluorescence. New techniques in this area allow rapid analysis for 20 to 30 elements at less than $10 a sample now with sensitivities in the ppm range for metals and alloys.

Similarly in the x-ray diffraction area, rotating anode instruments are able to provide up to 6 orders of magnitude enhanced intensity over what was available a few years ago, opening up new subjects for study such as kinetics of transformations, which in the past have been impractical because of the time considerations, and here we're talking about time factors which have now been reduced from hours or days to seconds.

In the extreme case, flash x-ray methods can provide detection of dynamic events on a scale of nanoseconds. And here again, there are great opportunities for looking at phenomena such as phase transformations that are diffusionless and other things of this sort.

Great advances have also been made in new solid state detectors. These were covered as well as image intensifiers. In this area, I was quite impressed by how close x-ray methods seem to be for fairly routine detection of residual stresses under field conditions using portable equipment, etc. And similarly, analysis of fatigue damage in fairly complicated hardware seems to be performed fairly routinely in Japan by x-ray methods.

Special capabilities of neutron radiography, e.g., detection of moisture and bond inspection (among other things) in composites and in honeycomb sections, were pointed out in an excellent review by one of our number here, Dr. Joseph John, of IRT.

I won't go into the sonic and ultrasonic methods at all since they're being covered in great depth and breadth at this meeting and were nicely treated at Sagamore by some of the speakers here, Bruce Thompson, Otto Buck and Tom Moran, among others, except to cite again by way of example of expanded instrumental capability, a random signal flaw detection system which provides a signal to noise ratio enhancement of 4 orders of magnitude greater than with conventional pulse echo techniques.

On the optical end of things, we heard of a new venture to optically detect acoustic emission waves. Some of you who are interested can talk to Professor Bob Green here who presented this work. Of course, this offers another attractive potential of a non-contacting detection system.

Two most interesting discussions in the optical area had to do with infrared techniques to perform such varied tasks as automated IR control of spot welding controlled to plus or minus one degree centigrade in the range of, say, 1,000° C of the meniscus of a crystal growing through the melt, and a water-cooled IR probe which measures the temperature of moving turbine blades within operating engines. I thought this was very important and highly exciting.

Advances in magnetic perturbation techniques hold promise now of providing reliable flaw signatures in cases of fatigue or fatigue-wear cracks in bearing systems, and significant progress was also reported in eddy current methods. For example, multi-frequency eddy current techniques for a simultaneous measurement of surface hardness and case depth in gears; the probing of cracks under fasteners in aircraft, and so on.

High frequency microwave techniques were posed as potentially useful for surface crack detection, again, a non-contacting method, in rotating systems such as in helicopter rotor sections.

Also, on the more speculative end of things, developments in positron annihilation and exo-electron emission were reviewed along with potential applications, the former being proposed to study such things as order/disorder phenomena and small levels of either surface or bulk damage (for example, from cold work), and the latter to study phenomena such as adsorption, oxidation, or wear, where the work function of the material is paramount.

New approaches in the penetrant area were discussed, including attempts to correlate crack detection efficiency with fluorescence absorption behavior, better ways to quantify performance and inspection specifications, for example, employing quantitative metallographic techniques and new statistical analytical methods.

Last, it was suggested that the NDI community might profit from taking a fresh look at physical phenomena from the standpoint of coupled effects; that is, if it should prove impractical to detect an event, for example, to measure a temperature optically, there may be several other ways to do so: electrically, magnetically, etc. depending upon the proportionality coefficients of various detector materials.

By and large we were worried at the beginning that the Sagamore conference would get lost in the background of all the others, but those of us who were there felt that it pretty much did accomplish what it set out to do. The proceedings volume should be out within the year, and for those of you who are interested, I can provide copies of extended abstracts.

ACOUSTICAL IMAGING AND HOLOGRAPHY
SEVENTH INTERNATIONAL SYMPOSIUM

D. E. Yuhas
Sonoscan, Incorporated
Bensenville, Il. 60106

I am going to report briefly on the Acoustical Imaging and Holography Conference that was concluded yesterday in Chicago. These conferences were started in 1967, and are concerned primarily with ultrasonics and visualization techniques as applied to medicine, nondestructive evaluation, sonar, seismic analysis and acoustic microscopy.

I think what I will do is just present some results, including some slides that various contributors were kind enough to give me. I will not be able to describe the results of all contributors since the conference lasted more than three days. In particular, I have omitted some interesting work from Stanford. Dr. Waugh and Kino's group made some important contributions, but because they are attending this conference they can describe their work much better than myself.

The first slide* is a color-coded image of a normal eye taken from the work of Jones et al. at Case Western[1]. The color-coding of this ultrasonic image shows an interesting way to display frequency domain ultrasonic information. Essentially what they have done is used a broadband pulse with frequency components in the range of 6 to 12 MHz and then color-coded different frequency regions. Components that range from 6 to 8 MHz are red, green represents a 2 MHz bandwidth around 9 MHz, and the blue colors correspond to ultrasonic signals in the range of 10 to 12 MHz.

The next slide* shows a color-coded picture of an eye with a large malignant melanoma. It is obvious from this example that there are some marked differences in the colors (ultrasonic scattering properties) of abnormal as compared with normal eye tissue.

The next slide* is a tomographic image of breast tissue. There are actually two images here which are color-coded and superimposed. The blue image is an ultrasonic index of refraction tomogram where the dark blue regions are areas of lower sound velocity. Superimposed on this image is an attenuation tomogram. The attenuation tomogram is red with the higher attenuation areas the most intense.

These color-coded tomographic images are the work of Greenleaf and colleagues at Mayo[2]. The color-coded images differ from those presented by Dr. Jones in that they are: a) Computer reconstructed ultrasonic images obtained at a single frequency. b) Color-coded according to two distinct physical acoustic properties. In red we have the attenuation properties, in blue the acoustic index of refraction properties. Like the Case Western group, the Mayo group presented some vivid examples contrasting the acoustic properties of normal and abnormal tissues.

In another study Eggleton, at the Indiana Center for Advanced Research, presented some interesting data on changes in the acoustic properties of muscle in the contracted and relaxed state[3]. His investigations were on a much finer scale. Using the scanning laser acoustic microscope he was able to measure slight changes in ultrasonic velocity in muscle tissue undergoing isometric contraction.

The next investigation I want to mention is another application of ultrasonic tomography. This is work done by Percy Hildebrand and D. E. Hufferd at Battelle Northwest[4]. The problem is the following: If you want to do tomographic imaging, normally you have to work in transmission and have access to the object from all sides. If you have a situation where you cannot obtain a 360 degree perspective, is tomography possible? For example, can one image the residual stress resulting from the butt weld of thick metal plates?

Dr. Hildebrand's investigations are involved with determining how well an object can be tomographically imaged by taking ultrasonic data in reflection over only a 90 degree sector. This geometry is illustrated in Fig. 1. Their initial investigations involved imaging test objects. Their particular test object was the finger of a glove filled with a solution which had a 2 percent velocity difference from the surrounding water coupling media. They scanned this object in a 90 degree sector and reconstructed a tomographic index of refraction image. The image they obtained is shown in Fig. 2. The peaks here correspond to the glove where the velocity of sound values are higher. There are actually two images shown. The double image results from the tomographic signal processing algorithms which produce both a real image and a mirror image. The ultimate goal is to look at ultrasonic velocity fields which result from residual stresses in welded thick metal plates. They have also imaged a 0.2 percent velocity change with the liquid model and have done work on stress fields in metal samples. The results look encouraging.

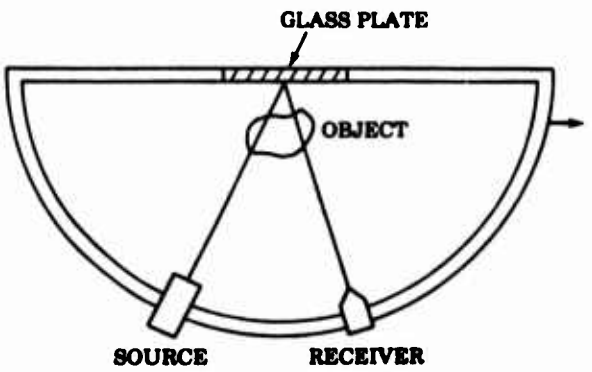

Figure 1. Experimental arrangement for reflection tomogtaphic imaging.

* Images of these slides did not reproduce due to color-coding.

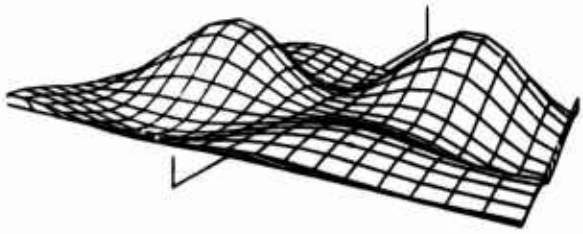

Figure 2. Reconstruction of the 2 percent liquid model profiled by reflection

Figure 3 is an interesting image. This is the work of a French group from the University of Paris, Alais and Fink[5]. It is an image of a 7 month old fetus. Their transducer configuration is a linear Fresnel zone focusing array of 160 elements. As you can see, the detail is quite good. One can visualize a number of the features, such as the lungs and the vertebrae of the fetus. The dimensions here are about 120mm across the figure.

Figure 3. Ultrasonic C-Scan image of a 7 month fetus made using a 160 element linear Fresnel zone focusing array.

I would also like to mention some work done by R. Mezrich at RCA Laboratories[6]. He employs two sets of Risley prisms to form a rapid X-Y raster scan of an ultrasonic beam. Using this technique in a C-scan, impressive, high resolution images are obtained at a frequency of 1.6 MHz. Shown in Fig. 4a is the acoustic image of a nickel resting on a metal canning. Using this system depth resolution can be obtained by time gating the echoes.

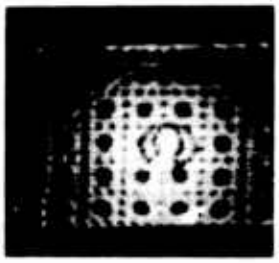

Figure 4a. Ultrasonic image (1.6 MHz) of a coin placed on a metal canning.

Figure 4b and 4c show the nickel and canning, respectively. These images were obtained by changing the detection gate delay. The time required to form each image is approximately 4 seconds.

Figure 4b. Image of canning

Figure 4c. Image of coin.
Latter two images are produced by changing the detection gate delay time

The next slides are images produced by Havlice and colleagues at the Stanford Research Institute[7]. They were trying to eliminate spurious detail in transmission acoustic images which result from the spatially and temporally coherent insonification. Figure 5a shows a transmission image of a human elbow made with coherent ultrasound. As you can

see there is considerable image clutter in the fleshy part of the arm which makes these images difficult to interpret. A second image of the elbow is shown in Fig. 5b. This image was produced by placing an acoustic "shower window" (diffuse scatter) between the transmitter and receiver and vibrating it very rapidly, thus introducing spatial and temporal incoherency. This reduces extraneous features produced by out-of-focus structures which might otherwise mask important features.

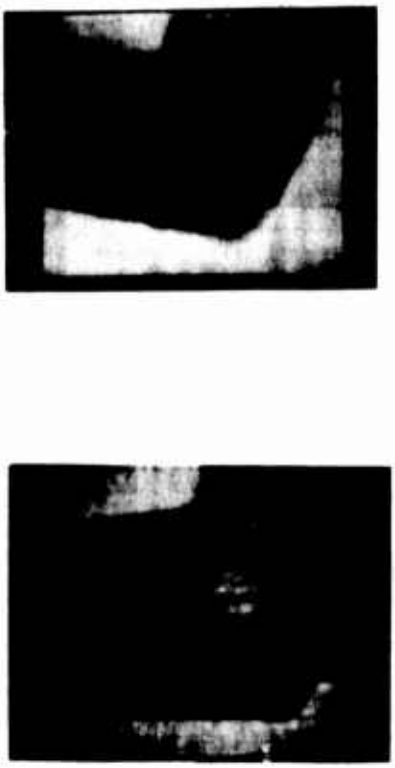

Figure 5. Comparison of ultrasonic transmission images of the elbow. Image on the left (a) was obtained with coherent insonification while that on right (b) used incoherent insonification.

References

1. J. P. Jones, E. Holasek, E. W. Purnell and A. Sokollu, A Technique for Incorporating Spectral Information into a B-scan Ultrasonic Display. In Acoustical Holography Vol. VII (ed. L. W. Kessler) in press.

2. J. F. Greenleaf, S. A. Johnson, W. F. Samayou and C. R. Hansen, Refractive Index by Reconstruction: Use to Improve Compound B-Scan Resolution. Proceedings of Seventh International Symposium on Acoustical Imaging and Holography.

3. R. C. Eggleton and F. S. Vinson, Heart Model Supported in Organ Culture and Analyzed by Acoustic Microscope. In Acoustical Holography Vol. VII (ed. L. W. Kessler) in press.

4. B. P. Hildebrand and D.E. Hufferd, Computerized Reconstruction of Ultrasonic Velocity Fields for Mapping of Residual Stress. In Acoustical Holography Vol. VII (ed. L. W. Kessler) in press.

5. P. Alais and M. Fink, Fresnel Zone Focusing of Linear Arrays Applied to B and C Echography. In Acoustical Holography Vol. VII (ed. L. W. Kessler) in press.

6. R. Mezrich, High Resolution, High Sensitivity Ultrasonic C-Scan Imaging System. In Acoustical Holography Vol. VII (ed. L. W. Kessler) in press.

7. J. F. Havlice, P. S. Green, J. C. Taenzer and W. Muller, Spatially and Temporally Varying Insonification for the Elimination of Extraneous Detail in Acoustic Transmission Imaging. In Acoustical Holography Vol. VII (ed. L. W. Kessler) in press.

INTERPRETATION OF ULTRASONIC SCATTERING MEASUREMENTS BY VARIOUS FLAWS FROM THEORETICAL STUDIES

J. A. Krumhansl
Cornell University
Ithaca, New York

Let me begin by saying that this is part of a program which is very much complementary to and is helped by the experimental program; so I'll repeat, in part, some of the overview comments that Bruce Thompson made this morning.

We've regarded our role as one of trying to plug into the overall program those aspects of the theory of elastic wave scattering which can be developed in a utilitarian way in terms of modern analytical and computational techniques, in a form which I hope can be useful in signal processing, interpretation, design of experiment, etc.

To outline our point of view, I'm going to first give a survey of what we have been doing and then give some of the results. It's rather shocking to think of the amount of money that goes into an experimental program and its interpretation, if the interpretation is done in terms of acoustic or scalar wave scattering theories, when the differences from proper elastic theory can be as great as those which Bruce Thompson pointed to this morning.

Now, there certainly has been a tremendous amount done on elastic wave scattering. There are some methods, however, which have now become practical because of the advances in our understanding of an analytical techniques and computers. The work I'm reporting on has been done primarily by Jim Gubernatis of Los Alamos, Eytan Domany and others at Cornell and myself. The experimental work we have interacted strongly with is that of Tittmann at Rockwell and Adler of Tennessee. We have received stimulus from the ARPA MRC, Materials Research Council program, and from Tony Mucciardi at Adaptronics, and from the Rockwell program in general.

As I said, our program objective is to be utilitarian, and utilitarian means not necessarily simple.

The diagnostics of ultrasonic flaw detection involve two aspects: where is the defect (the existence of a defect) and what is the defect? Perhaps the real justification of the extent to which we try to carry the theory is in this latter regard, doing everything we can to squeeze out whatever characteristic information we can from ultrasonic scattering data.

Let me briefly outline the theoretical methods. A traditional method with which most of us are familiar for problems of this sort is to use normal mode expansions. Now, in textbooks and teaching, this method is useful, but the geometries chosen are always spheres. Once you go beyond spherical harmonics you find that, if not hopeless, life is at least extremely difficult.

Programming some of the calculations is cumbersome, and non-intuitive. At least some of the training in modern theoretical physics has enriched the bag of tools which can be used, particularly with integral equation methods which have the advantage that one plugs in information which can be related rather directly to the experimental features of the situation in question. They are also subject to approximation techniques such as iteration- try something, improve it ;try it again, improve it- principle. With brute force large scale computers, one can hope to do some of these things inexpensively. Indeed, there are standard approximation methods that we use in nuclear scattering; Born approximation, variational methods, distorted wave methods and so forth, which provide a hunting license of sorts to see what one can do in the present context.

Our first year's program, 1975, was largely concerned with establishing the theoretical base; the Cornell Materials Science Center report number 2654 presents a summary of the general theory, and provides detailed computer results for the Born approximation. The Born approximation simply inserts incident field displacement and strain at appropriate points in the integral formula as needed. This really doesn't solve the integral equation, but it's a first step, and has been very useful as an exploratory device.

As the program has progressed we have tried to express the results of such a calculation concisely, and Jim Gubernatis has found that it's particularly useful to define something called an "f-vector", which will give complete scattering data. It depends directly on the changes in material parameters, $\Delta\rho$, and directly on the changes in the elastic constant, Δc. In addition, we require a knowledge of the displacement and strain fields in the flaw region . .

We are now in the process of using this approach to examine carefully exact limiting behavior for low frequency. By utilizing all the information present in the longitudinal, transverse, and mode converted scattering, material parameter changes can be determined--over and above any imaging or echo detection. Hopefully, microprocessors can eventually make the on-line analysis cheap and easy.

Now, I'd like to run through the main results we have obtained at Cornell during the past year. My colleagues have been Eytan Domany, Paul Muzikar, Steve Teitel, Dave Wood, and Jim Gubernatis, whose support came from Los Alamos.

1. General Summary of 1975-76 Research

Last year we presented an integral equation formulation of the ultrasonic scattering problem. We also compared the results of the Born approximation with exact results for spherical scatterers. From that study we learned much about the regions of applicability and validity of the Born approximation.

In this year's research we have continued the theoretical work[1], but placed special emphasis on attempts to make contact with the experimental situation for laboratory flaws prepared at Rockwell in determined geometries - (a step closer to the "real world"). In particular, we tried to identify some general features or indices that might be useful in evaluation of scattering data for NDT.

In the course of many fruitful interactions with the experimental groups at Rockwell and Tennessee we learned about the needs and the formats most convenient for them, and developed a library of computer programs for various scattering situations.

We have also investigated further approximations (static, quasi-static), which may be better in certain limits, and started to compute and compare them with exact and experimental data.

Finally, we have begun work to implement scattering theory for defects other than holes or inclusions, particularly scattering by flat cracks. We proceed with details of the studies.

II. Indices for NDT

We have considered scattering by defects of two shapes, spheroids and cylinders, to seek information that indicates the deviation of the scatterer from spherical symmetry. The geometry of both scatterers can be characterized by a ratio b/a (see Fig. 1).

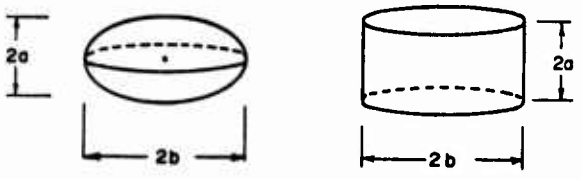

Figure 1. Cylindrical and spheroidal scatterers, characterized by b/a ratio.

Since we now know that the Born approximation (BA) is good for Al in Ti, we looked at Al inclusions in Ti. A sample of the numerous figures we generated is given in Fig. 2; in all these the incident wave is longitudinal, and along the axis of symmetry. After generating many of these, and recognizing that this abundance of information was conceptually unwieldy we looked for some features that seem general and physically plausible.

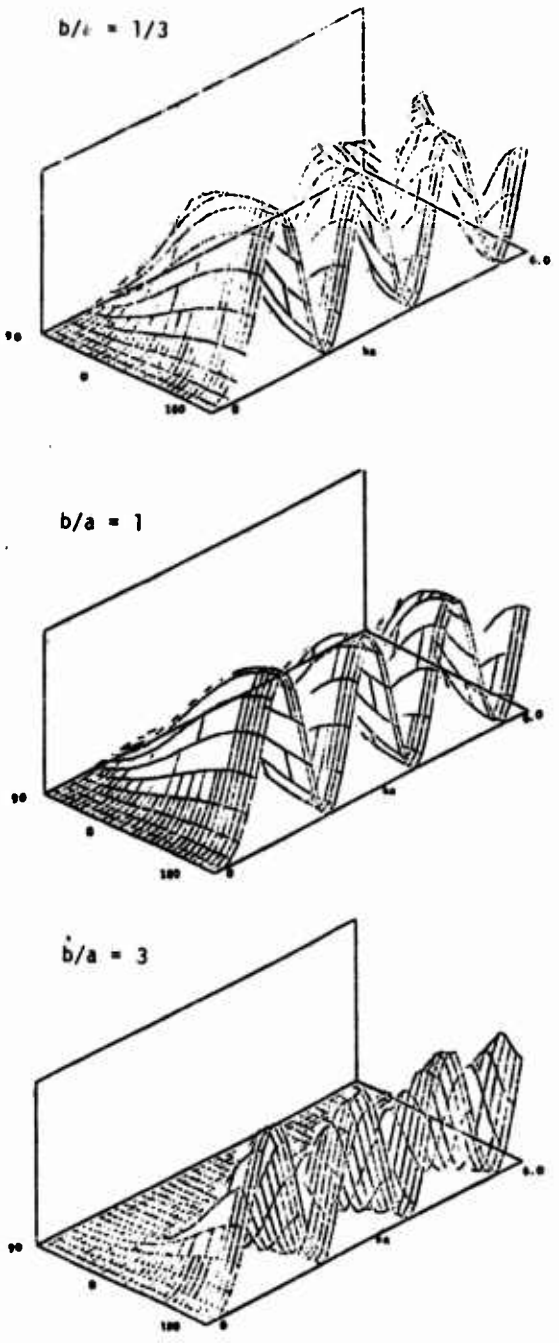

Figure 2a. Scattered (longitudinal) power for longitudinal wave incident along the symmetry axis of spheroidal scatterers (Al in Ti) of varying b/a ratio.

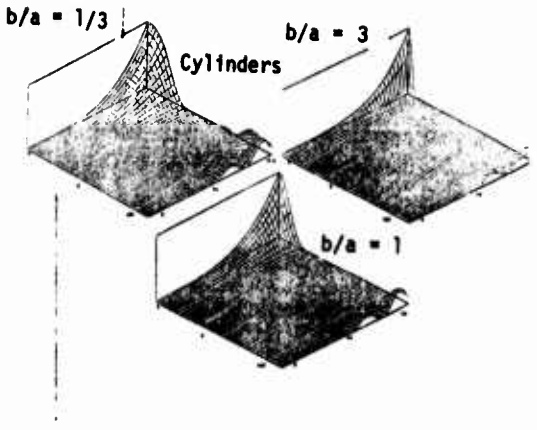

Figure 2b.. Scattered (longitudinal) power for longitudinal wave incident along the symmetry axis of cylindrical scatterers (Al in Ti) of varying b/a ratio.

II. 1) Cylinder vs Spheroid. The backscattered power vs k is shown for each in Fig. 3. These results still have to be checked experimentally.

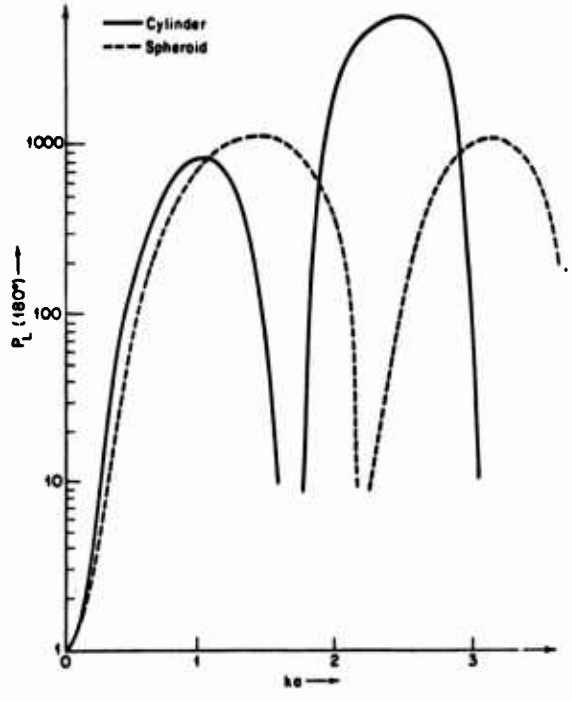

Figure 3. Back scattered longitudinal power, for longitudinal wave incident along axis of symmetry of cylindrical and spheroidal cavity.

II.2) The b/a Ratio. We found that on the average (taken over a range of k) the ratio of back to 90° scattering depends strongly on b/a, both for spheroids and cylinders. Not only is the averaging usually done experimentally in the transducer and circuitry, but also the averaging tends to wash out "accidental" computational resonances that obscure the detailed pictures. Thus, we studied the (k-averaged) back scattered power, P(180), to 90°, P(90) for Al in Ti- where BA is expected to work; and then "conjectured" it for cavities too (BA is not too bad for low ka~1 and 90 < θ < 180°). Results are shown in Fig. 4 for spheroids; we get similar results for cylinders. Thus, we conclude that given the orientation of a spheroidal/cylindrical scatterer, with longitudinal waves incident along the axis of symmetry, one can hope to determine the b/a ratio from a relatively simple measurement; the more oblate the object, the larger the ratio of averaged back/90° scattering.

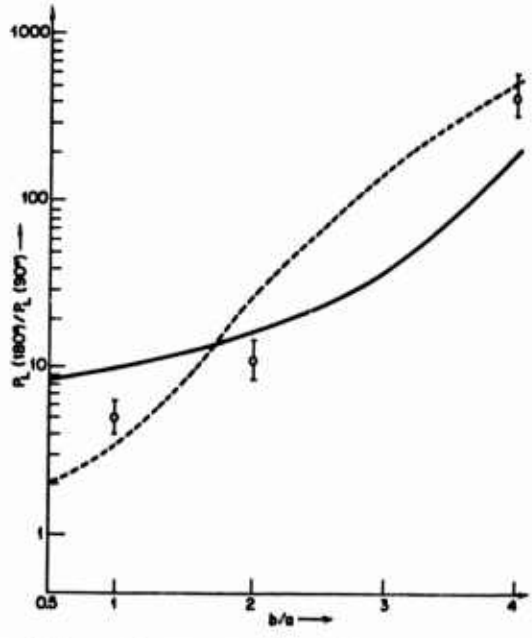

Figure 4. The ratio p (180/p (90) for longitudinal power with longitudinal wave incident along symmetry axis of spheroidal cavities in Ti, vs b/a of the scatterer. Uniform averages of 0 < ka < 1 (full lines) and 0 < ka < 2 (broken lines) were used. The circles are experimental results.

It should be emphasized that our analytical "result" is not intended to serve as a basis for quantitative comparison with experiment, but rather as a general, simple, qualitative feature which should be considered experimentally, particularly as a training criterion for computer-adaptive flaw identification procedures.

A similar investigation of similar transverse waves from longitudinal incident waves and for an incident transverse wave is planned. The experimental situation here has been looked at by Adler.

Mr. CRAIG BIDDLE (Pratt/Whitney): Is that against the side of the cylinder or against the end of the cylinder?

DR. KRUMHANSL: It's against the end of the cylinder along the axis--incident along the axis of the cylinder.

MR. BIDDLE: Flat bottom hole?

DR. KRUMHANSL: Right!

II. 3) Non-normal Incidence on Spheroid. As part of characterizing a spheroidal defect, one might want to determine its orientation. To this end, we considered the case of a longitudinal wave incident at an angle α to the axis of symmetry. See Fig. 5.

We first looked at the (experimentally) simplest situation; that of back scattering (single transducer experiment). Our results are summarized in Fig. 6.

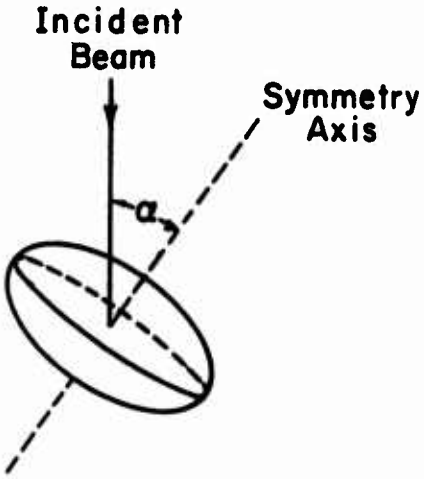

Figure 5. Scattering situation with incident beam at angle α off symmetry axis of scatterer.

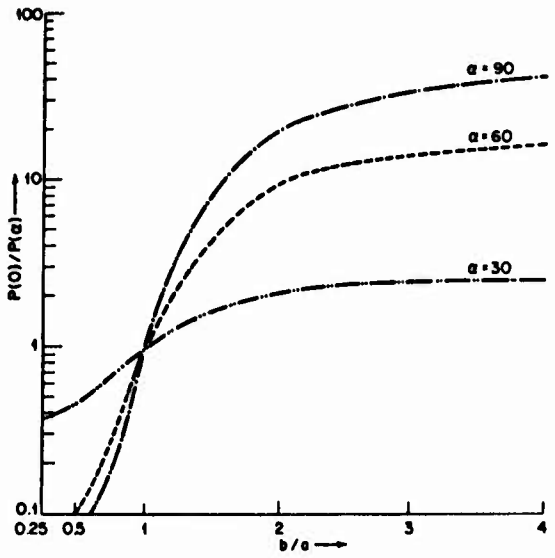

(a)

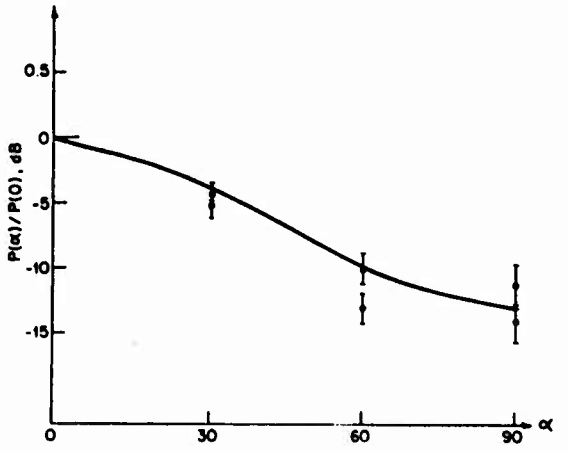

(b)

Figure 6. (a) Ratio of backscattered powers, $p(0)/p(\alpha)$ of longitudinal wave incident along axis of symmetry ($\alpha = 0$) and off axis by angle α; Rockwell transducer characteristics were used for the frequency averaging. (Spheroidal cavity in Ti).

(b) Same for spheroidal cavity of b/a= 400 μ/200μ as a function of off symmetry angle α.

The agreement (for the oblate spheroid) with experiment is surprising. In any case, it seems that again we can say that the more oblate the scatterer, the higher the ratio of back scattering powers for normal incidence/incidence at $\alpha = 0$.

II.4) A Display Format. Using the computed data from these programs we have followed D. Thompson's suggestion for an efficient visual presentation of our results. Imagine an array of transducers on a hemisphere (generalization to plane is straight forward). The one located on the pole sends in a longitudinal signal; the scattered longitudinal power is now recorded by all the array, and the relative (to the maximum) power displayed by each transducer. The power ratio, for each receiving position, is then plotted by mercator projection. Some samples of pictures one gets in various scattering situations are shown in Figs. 7. The development of asymmetrical, as well as numerical, features with orientation changes is to be noted.

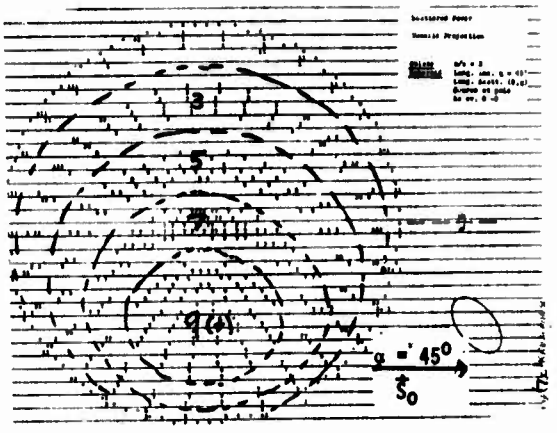

7(c) Oblate Spheroid

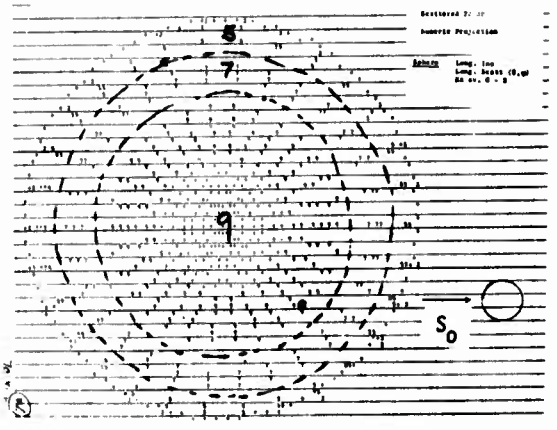

7(a) Sphere

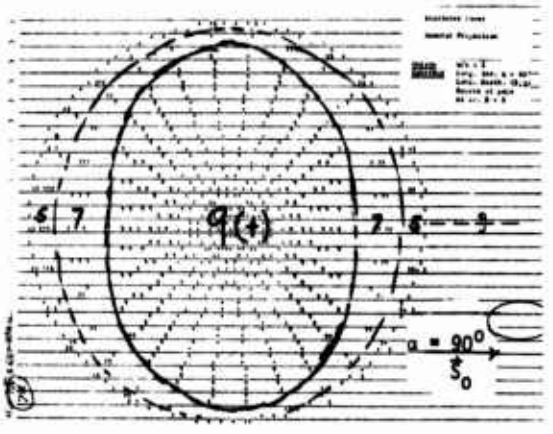

7(d) Oblate Spheroid

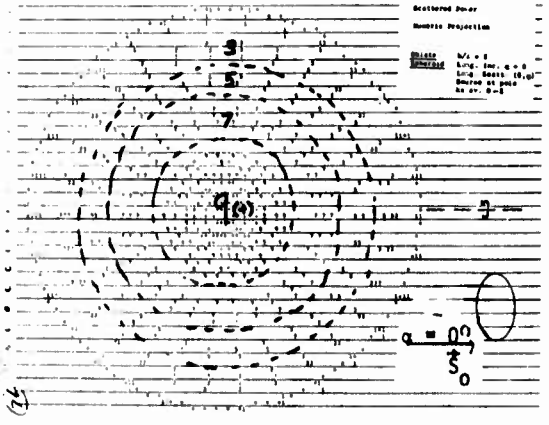

7(b) Oblate Spheroid

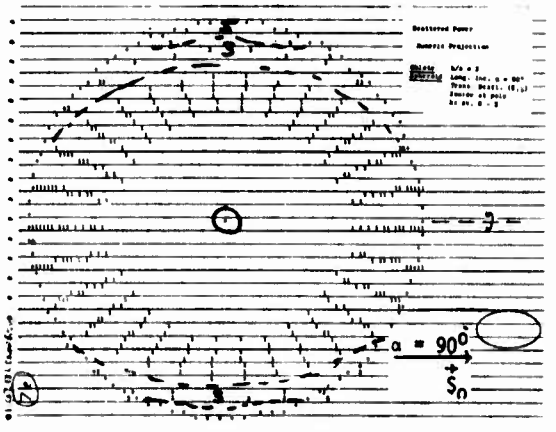

7(e) Oblate Spheroid

Figure 7. Projection display of scattering in various directions.

III. Static and Quasi-Static Approximations

The integral equation for the scattered field by an elastic inclusion is

$$u_i^s(r) = u_i^0(\xi) + \delta\rho\omega^2 \int_V d\xi'\, g_{im}(\xi-\xi')u_m(\xi') + \delta C_{ijkl} \int_V d\xi'\, g_{ij,k}(\xi-\xi')u_{l,m}(r') \quad (1)$$

In the far field limit[1] this expression has been reduced to a simple form; (with the explicit substitution of the Greens function) u_i^s is determined by volume integrals of the displacement field and the strain field in the volume of the defect. The Born approximation consists of replacing these fields by the respective incident field. In a static approximation proposed by Mal and Knopoff[2] the displacement field is approximated by the incident displacement field at the center of the defect. As to the strain field, one considers the solution of a static problem, with uniform stress at infinity equal to the incident stress, i.e.:

$$u_{m,n}(\phi) = i\left[k_n^0 u_m^0 + k_m^0 u_n^0\right]$$

The solution of the static problem, (known for ellipsoids)[3] is then used in the integral. This static (or MK) approximation is exact in the long wavelength limit.

The quasi-static approximation, proposed by one of us, consists of allowing for spatial variation of the various fields inside the scatterer. Some of the results of these approximations for scattering by a spherical cavity are compared with the exact results in Fig. 8 (a,b,c,d.)

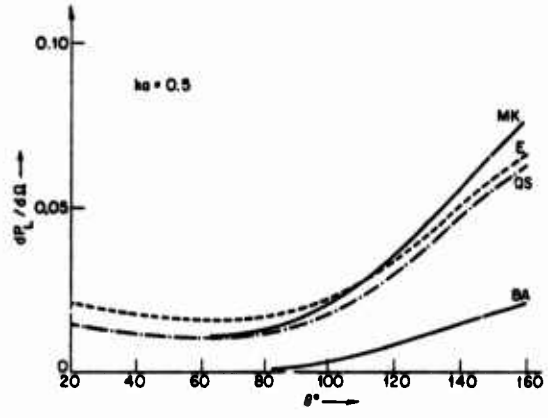

(a)

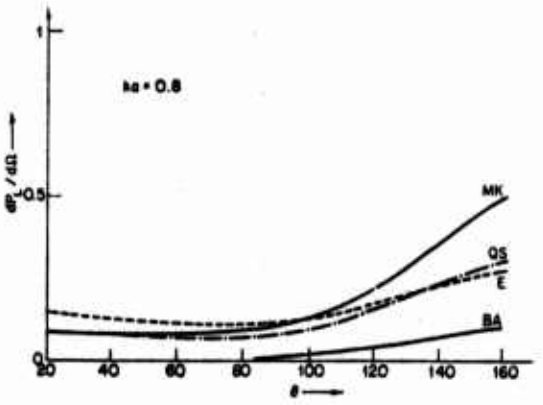

(b)

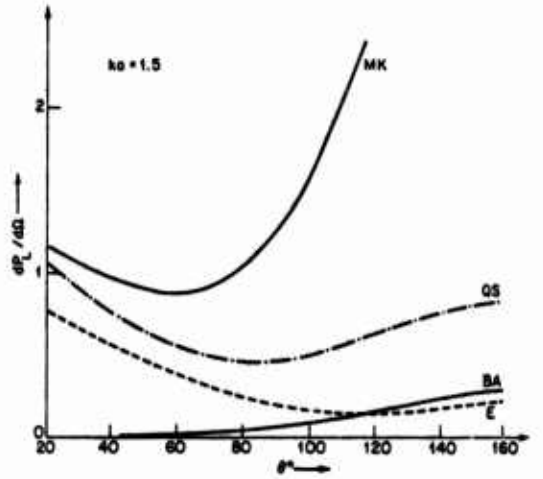

(c)

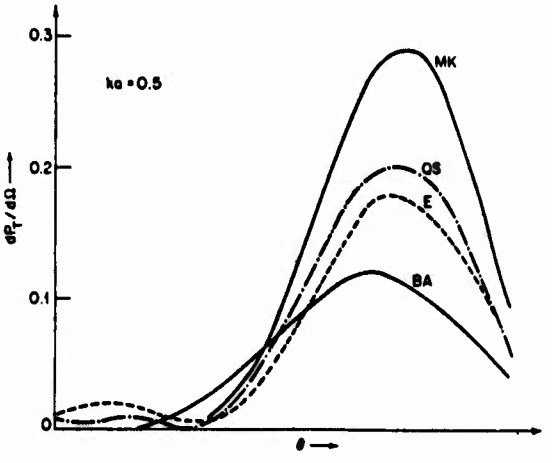

(d)

Figure 8. Comparison of exact (E), BA, Mal-Knopoff (MK) and quasi-static (QS) approximations for scattering of incident longitudinal wave by spherical cavity in Ti for various values of (ka).

The quasi-static approximation for scattering by a sphere, with some ad-hoc assumption about the variation inside the scatterer, yields an expression for u_i^s which is identical to one derived independently by E. R. Cohen[4]. However, our expressions can be easily generalized for scattering by spheroids and ellipsoids; those results will be presented elsewhere.

IV. Scattering of a Longitudinal Wave by a Stress-free Circular Crack.

While the volume integral equation turned out to be most useful in generating approximate solutions to scattering by volume defects, for "flat" cracks surface integral representations are more natural. An extensive survey of background has been given by Kraut[5].

We have considered various known approximations, and also constructed a new approximation, expected to be good in the long wavelength limit.

In all these approximations the scattered field at point $\underline{r}$ is represented in terms of an integral over a surface Σ of the displacement and stress fields.

In Fig. 9 we display the results of scattering by a circular crack, using various approximations. Our approximations are inserted in the formula[5]

$$u_m^s(\underline{r}) = C_{ijkl} \int_S ds\, n_j \left\{ g_{im} \left[u_{k,l}^s \right]^+_- - g_{km,l} \left[u_i^s \right]^+ \right. \quad (2)$$

where S is the surface of the crack, u_i^s is the scattered displacement field, and $[\ ]^+_-$ is the jump in the appropriate quantity. For a stress-free crack only the jump in the displacement field contributes to Eqn. (2). In additon to the simple Kirchoff choices, as an approximant to $[u_i^s]^+_-$ we used the solution to the problem of a circular crack under static uniform stress[6]. This approximation is "quasi-static" and is expected to be good at low k, i.e. long wavelength.

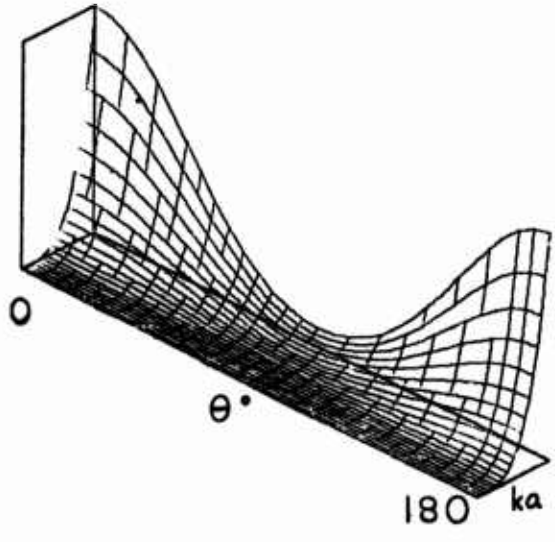

9(a)

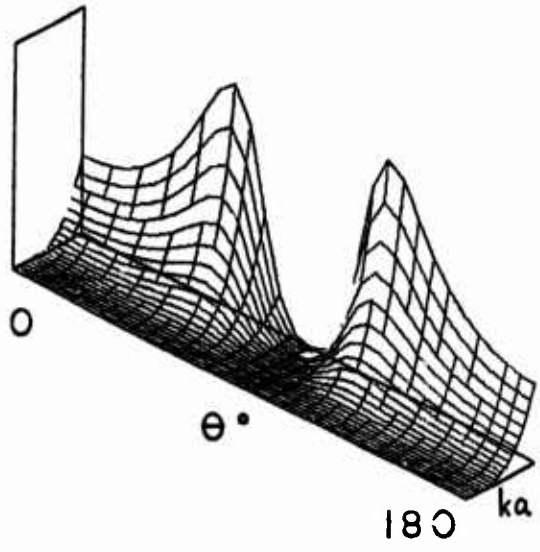

9(b)

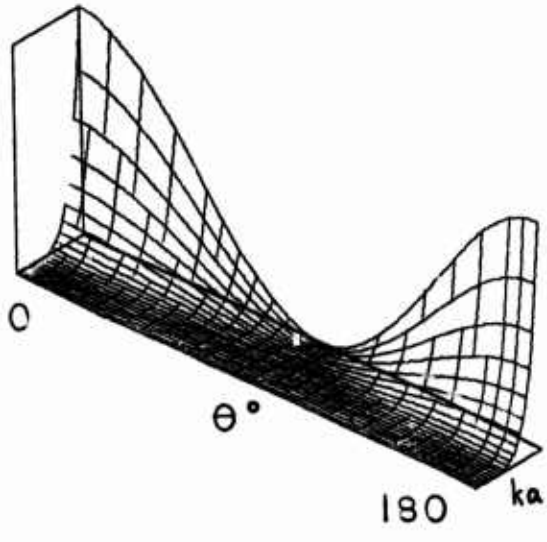

9(c)

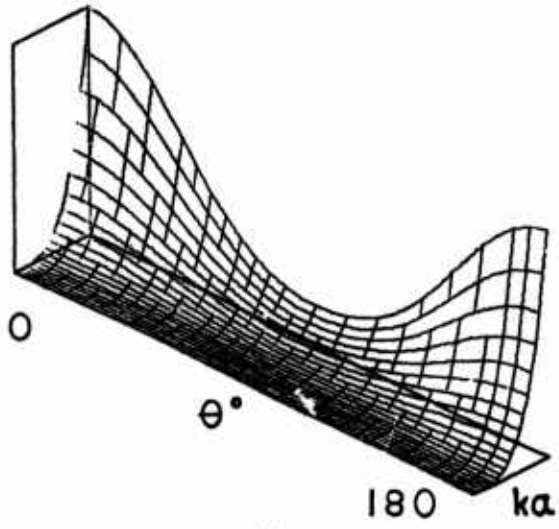

9(d)

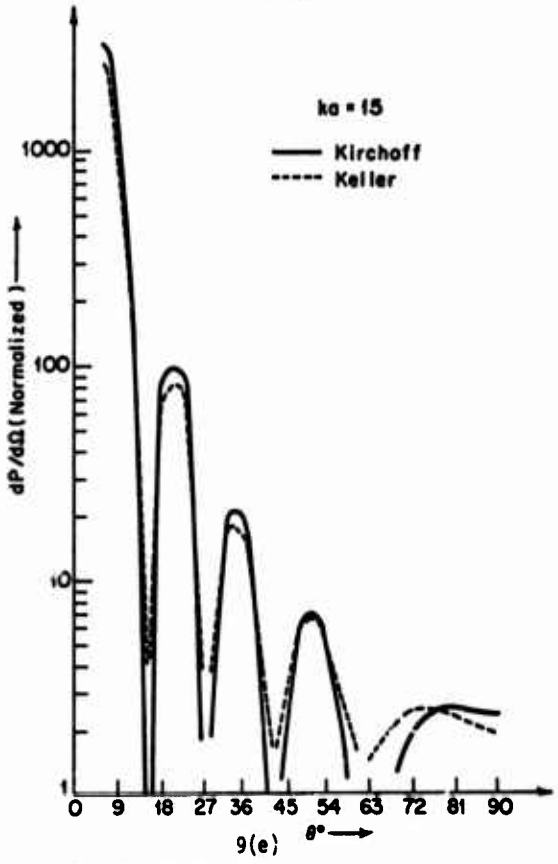

9(e)

Figure 9. Scattered longitudinal power by stress free circular crack of radius a; incident longitudinal wave along axis of crack.

a) Kirkhoff condition on displacement jump.
b) Half-plane Greens function.
c) Comparison with Filipczynski (see Review by E. Kraut[5]).
d) Quasi-static
e) Kirkhoff vs. Keller for ka = 15.

The first programming of these studies has just been carried out; we expect to devote considerable attention to cracks, corners, etc. during the coming year.

Let me summarize, when your data does not allow you to direct imaging, or when you're in a region where there is a limitation on wavelength for example, in a lossy medium whose attenuation increases rapidly with frequency, then perhaps all of this rich additional detail can be used to squeeze estimates out where you're at the limit of other methods.

Thank you.

References

1. MSC Report).

J. E. Gubernatis, E. Domany, J. A. Krumhansl, and M. Huberman, Report #2654, Materials Science Center, Cornell University 1976.

2. A. K. Mal and L. Knopoff, J. Inst. Maths. Applis, 3, 376-387.

3. J. D. Eshelby, Proc. Roy. Soc. A241, 376 (1957).

4. E. R. Cohen, May 1976, Rockwell Report SC579.31R on Contract F 44620-74-C-0057.

5. E. A. Kraut IEEE Transactions, SU-23, 162 (1976).

6. I. N. Sneddon, "Fourier Transforms," p. 490, McGraw Hill, 1951.

DR. EMMANUEL PAPADAKIS (Ford Motor Company): Good. We have three quarters of a minute. Let's have a question.

DR. LASZLO ADLER (University of Tennessee): Is it safe to say that for the back scattering region the Born approximation behavior is about the same as the exact calculations?

DR. KRUMHANSL: The Born approximation is really quite usable for the backward scattering in almost all cases, including cavities which present a complete discontinuity in elastic properties. The Born approximation is often remarkably good for all scattering angles for moderate material changes; e.g. computations cost about $5 or so, a really ridiculously cheap kind of thing compared to the cost of an experiment.

DR. PAPADAKIS: Just one, yes.

DR. GORDON KINO (Stanford University): If you now go through the electrostatic approximation which modifies the Born approximation, how does that compare for the sphere with the exact theory? Where does it begin to drop?

DR. KRUMHANSL: Well, we had one of those plots, Gordon, at ka equals unity. The "static" in MK could be called S; Mal and Knopoff where the first to use it, in a geophysics context. Our calculation gives an indication of how badly off it is for large scattering angles. The Born is quite wrong at small scattering angles, yes. That's the reason for exploring these other approximations systematically.

DR. PAPADAKIS: Thank you very much.

SCATTERING OF ULTRASOUND BY ELLIPSOIDAL CAVITIES

B. R. Tittmann
Science Center, Rockwell International
Thousand Oaks, California 91360

Before I begin I would like to emphasize that the work reported here is the result of a team effort, and was carried out in close collaboration with Neil Paton of the Science Center in the sample fabrication, Ken Lakin of USC in the characterization of the transducers, Dick Cohen of the Science Center in the theoretical calculations from "exact theory," John Richardson and Dick Elsley of the Science Center in the Fourier analysis of the ultrasonic pulses and the synthesis of the calculations over the band width of the transducers. We thank Jim Krumhansl and his group at Cornell University for the Born approximation results and Lazlo Adler of the University of Tennessee for the Keller theory results.

Objectives in this program are two-fold: firstly, to conduct those experiments that will explore and define the scattering of elastic waves from defects; in particular, to determine experimentally the scattering cross-sections of ellipsoidal defects in solids and to provide a critical data base for testing the regimes of validity of various approximate scattering theories; secondly, to explore and define the role of the scattering studies in the failure prediction processes where fracture is controlled by the slow growth of a single flaw; i.e.: to determine key failure prediction parameters, such as size, shape, and orientation of the flaw.

Now, you might ask why we are studying these simple ellipsoidal shapes when we are really interested in cracks. There are two reasons for this. First, we need to build up a data base for the simple shapes so that after understanding those we can launch into more complex geometries. Second, there are a lot of "real-world" defects that have the simpler geometries such that the results of our present studies would become useful immediately.

Figure 1 shows schematically the configurations of the samples which are made by the diffusion bonding process. The bond plane goes across the middle of the spherical dome with the defect in this case an exaggerated prolate ellipsoid.

The samples range from prolate spheroids to spheres to oblate spheroids and circular disks. For example, one of the disk shaped defects has a thickness of about 200μm and a diameter of 1200μm. The ultrasonic wave length is roughly 10 to 30 times the thickness of the disk.

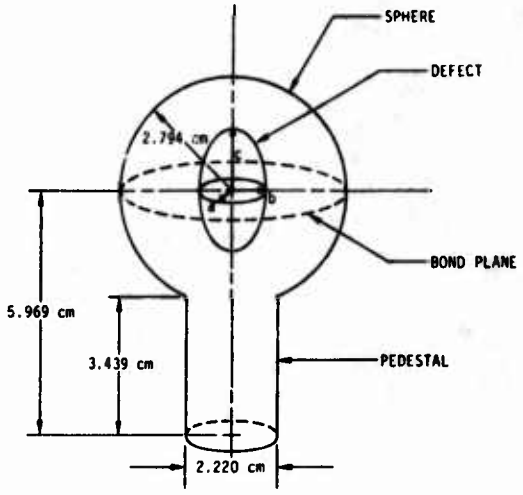

DESCRIPTION	a (μm)	b (μm)	c (μm)	STAMP NO.
PROLATE SPHEROID	200	200	800	40
PROLATE SPHEROID	400	400	800	41
SPHERE	200	200	200	35
SPHERE	400	400	400	36
SPHERE	600	600	600	37
OBLATE SPHEROID	400	400	200	39
OBLATE SPHEROID	400	400	100	38
CIRCULAR DISC	600	600	100	62
ELLIPTICAL DISC	2500	600	250	61

Figure 1. Sample configuration.

The samples are mounted in a measurement fixture, shown in Fig. 2, which allows control of the transducer location in both elevation and azimuth in a coordinate system as shown in Fig. 3.

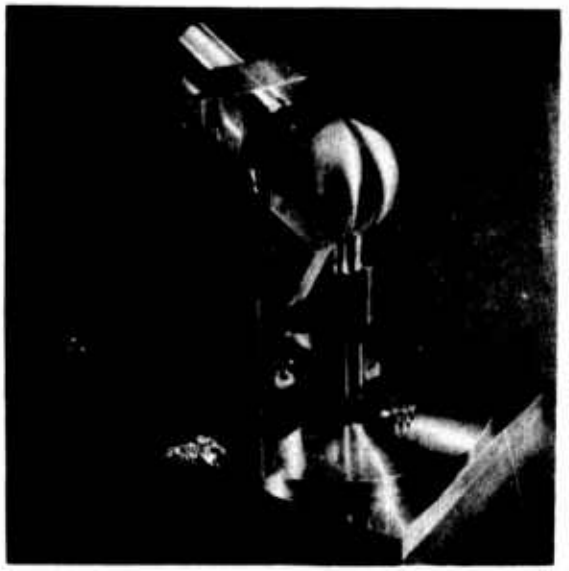

Figure 2. Photo of measurement fixture.

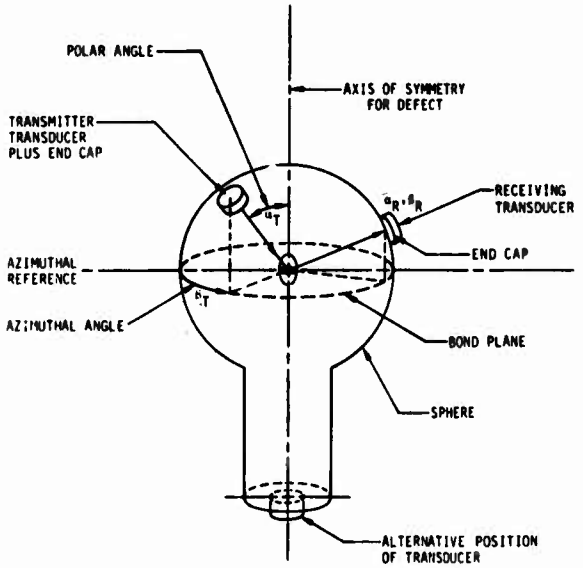

Figure 3. Measurement coordinate system.

Figure 4 summarizes results obtained with a single transducer by the pulse echo method. The graph plots the power scattered from several different defects as a function of polar angle. The polar angle is defined as the angle which the transducer makes with the axis of rotational symmetry of the defect. The data are normalized at zero polar angle. The results of Fig. 4 show that for the four different classes of defects, we get very characteristic defect signatures. As you might expect, the sphere gives us a flat response with changes in the polar angle. The prolate spheroids fall above this flat line; the oblate spheroids below that line, and if we go to the limit of the very thin disk, we get a rapid fall off to very low amplitudes. So, these results, therefore, suggest that by making a few measurements at small polar angles, we can readily distinguish the shapes of these four principal classes of objects, even though they are approximately the same size.

The second point to be made about Fig. 4 is that the main features discussed above are in good qualitative agreement with the theoretical calculations obtained from the Born approximation. In fact, the solid line is the theoretically predicted curve from the Born approximation and is shown here for a quantitative comparison. As you can see, good agreement is observed for this defect, an oblate spheroid, at a frequency of about 5 MHz. The dimensions of the spheroid are a=b=400μm and C=100μm. The results for the oblate spheroids and the disks are also in good qualitative agreement with calculations from the Keller theory.

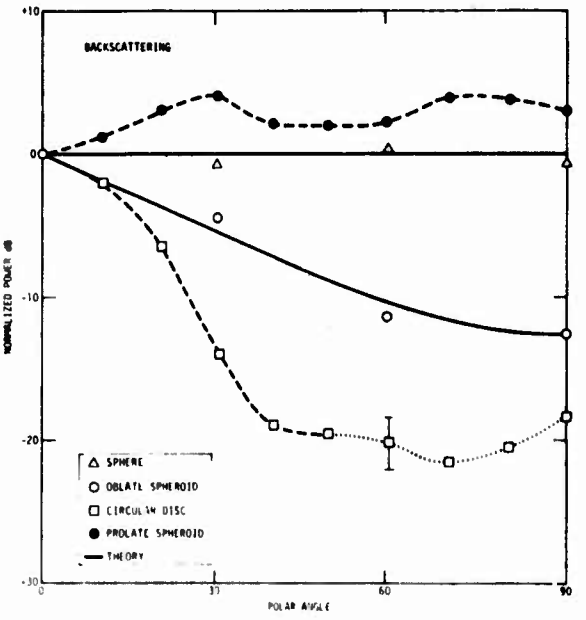

Figure 4. Angular dependence of pulse-echo intensity. (Data normalized).

If we lift the restriction of normalizing at zero polar angle, we find that the curves of Fig. 4 are displaced vertically, approximately in proportion to the product of the radii of curvature. As shown in Fig. 5, if we look at the 400μm radius and the 600μm spheres, we find the two corresponding experimental curves are separated by about 4 db. This is in agreement with physical intuition and in good quantitative agreement with geometric optics, which scales the intensity by p^2, where p is the radius of curvature - in this case p= a - and predicts a difference of 3.5 dB. This trend is qualitatively also borne out by the data on the oblate spheroid with a=b=400μm, c=200μm and by the circular disk with a=b=600μm, which gave higher back-scattered power levels at a=0 than the sphere with a=b=c=400μm, and the sphere with a=b=c=600μm respectively.

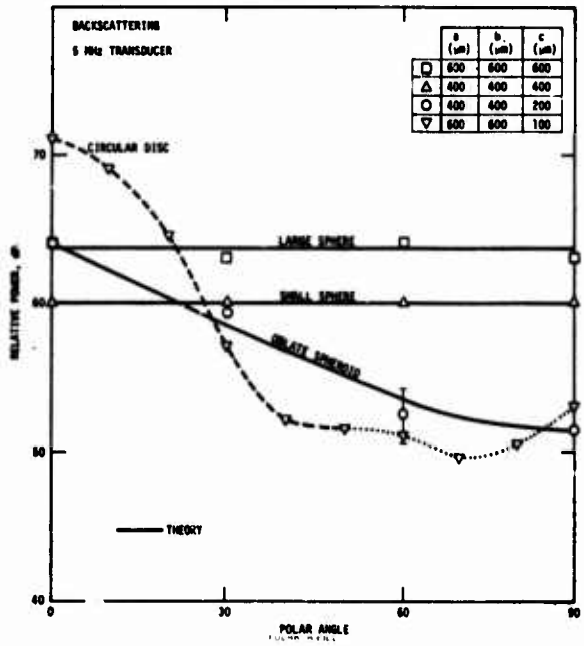

Figure 5. Angular dependence of pulse-echo intensity.

We also find that if we look at the edge of the disk, the separation in the curves of Fig. 6 is in direct proportion to the change in the cross sectional area. In this regime of angles, the curves are dotted to indicate that the main beam splits into two beams. This effect goes along with the notion that when the transducer is illuminating a disk-shaped defect at an oblique angle in the pulse echo mode, and because of specular reflection, the transducer does not see the flat portion of the disk, but only the near and far edges. If one calculates what one might expect for the splitting of the two beams on the basis of the difference in travel paths, then the calculated time delays are very close to those observed.

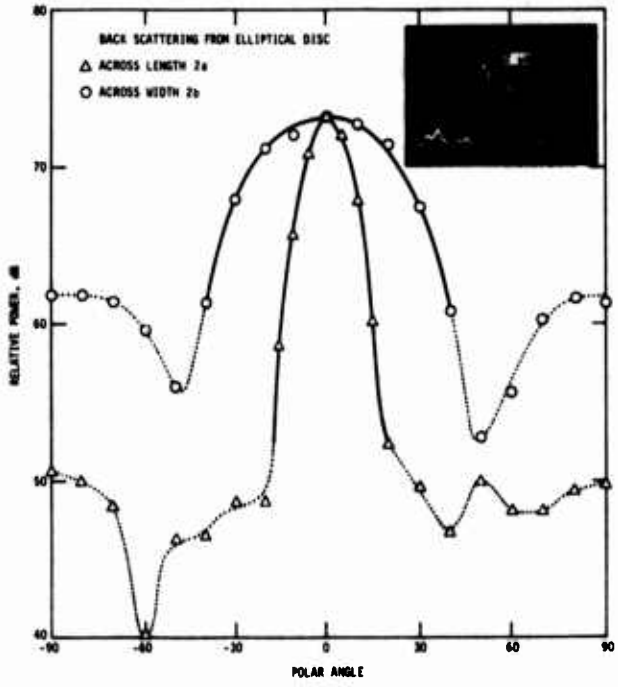

Figure 6. Angular dependence of pulse-echo intensity for disk at 2.25 MHz. The dashed lines indicate regimes where double pulse (see insert) appears.

Figure 6 presents an interesting result because it was performed on a quasi-unknown defect by virtue of the fact that the sample was mislabeled. By making measurements as a function of the polar angle we could ascertain what the principal axes of symmetry were, and that we were having an encounter with an elliptical disk. In Fig. 6, we also see that across the width (the small dimension) the fall off in power is much less rapid in angle than for the length (the large dimension) with the notion that phase cancellation would occur at smaller angles for traversals across the large dimensions.

We have also conducted measurements with two transducers in the pitch-catch mode in which one transducer is placed at the axis of symmetry for the defect, and the other one at right angles. The result of this measurement is shown in Fig. 7 (see proceedings article by J. Krumhansl), which plots the ratio of the back scattered to side scattered power as a function of the aspect ratio. The solid line is the prediction of the Born approximation and is in semi-quantitative agreement with the experimental results shown as open circles.

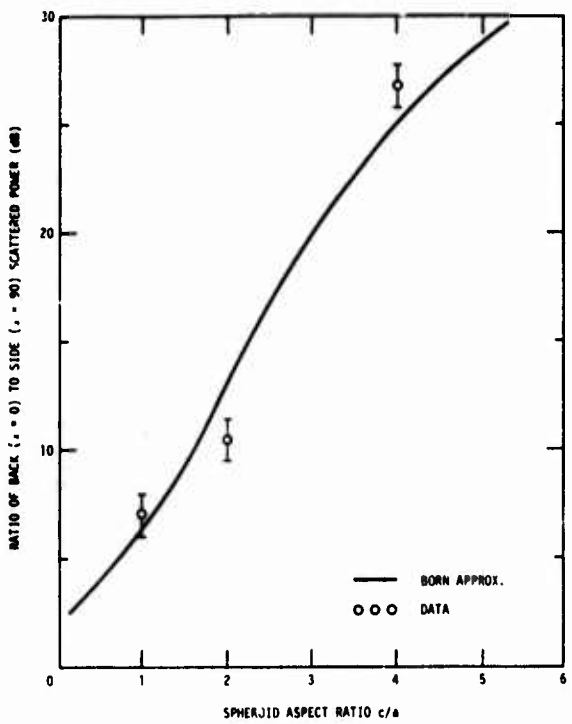

Figure 7. Ratio of back-scattered (pulse-echo) to side-scattered (pitch-catch) power.

We may conclude that both techniques, the single transducer or pulse echo technique and the two transducer or pitch-catch method, are powerful techniques for deducing the shape and orientation of geometrically shaped scattering objects. This discussion represents a brief survey of what we have been trying to do in characterizing the scattering from ellipsoids of revolution. We plan to carry out detailed measurements of the angular and frequency dependence of the scattered power and try to obtain both amplitude and phase information. We have done some very careful experiments with one category of the defects, namely, the sphere, and I will show some of those results briefly, with emphasis on the angular dependence. Comparisons will be shown between experiment and "exact theory" as developed by Lamb[1], Pao and Mow[2], Ying and Truell[3], and more recently Tittmann, Cohen and Richardson[4]. To remind you, the differential scattering cross section falls into two components for a longitudinal incident wave, i.e., the directly scattered longitudinal wave and the mode converted shear wave. The independent variable used is the scattering angle which is defined as the angle with respect to the forward direction.

Figure 8 shows theoretical and experimental results for a spherical cavity plotted in the form of a polar diagram for the case of an incident longitudinal wave. In the top portion of the graph are shown the results of "exact" theory, experimental observations as well as the Born approximation. On the bottom of the graph, similar results are presented for the mode converted shear waves, and you see that for this case where the product of the wave vector and the radius ka≈1, the results are in quite reasonable agreement.

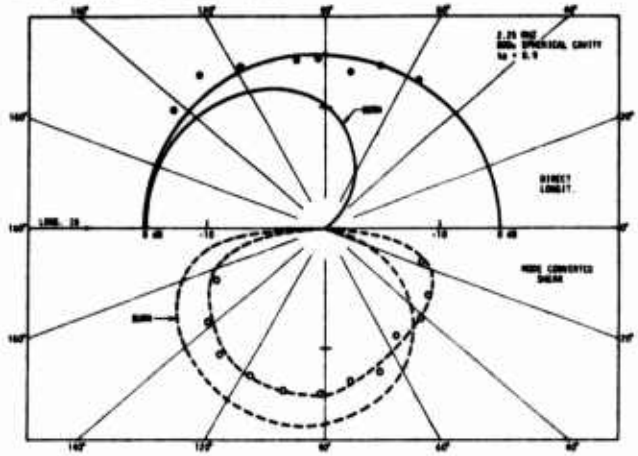

Figure 8. Scattered radiation patterns for spherical void at 2.25 MHz.

Figure 9 shows results for ka≈2 and we see deviations start to develop between the predictions of the Born approximation on one hand and "exact theory" and experiment on the other. This disagreement is expected and becomes worse as ka is increased.

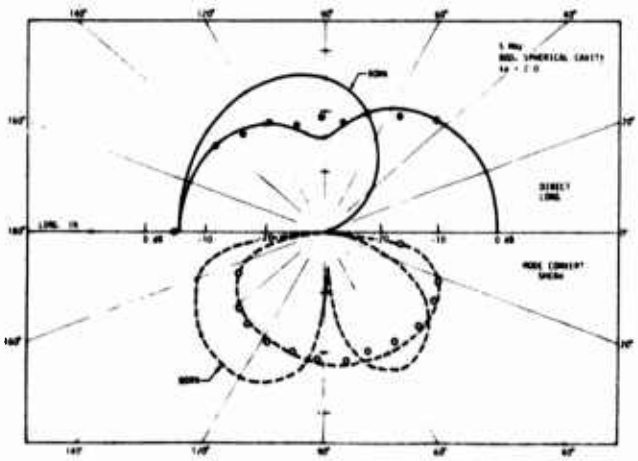

Figure 9. Scattered radiation pattern for spherical void at 5.0 MHz incident longitudinal waves.

Figure 10 is an example of our measurements with shear wave incidence and compares the data with the predictions of "exact theory." We see that considerable structure develops in the angular dependence and that the data points coincide reasonably well with theory.

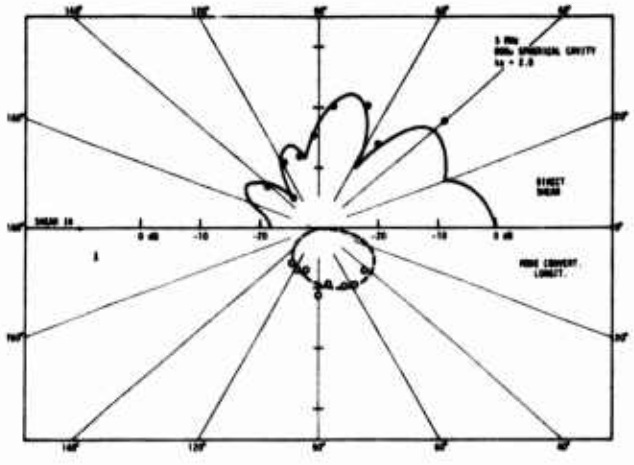

Figure 10. Scattered radiation pattern for spherical void at 5 MHz for incident shear waves.

In these studies, we come across an interesting result, namely, that the process of mode conversion is reciprocal; that is to say, if one has an incident longitudinal wave and looks at the mode converted shear wave, one gets the same angular dependence as when one sends in a shear wave and looks at the mode converted longitudinal wave. This result, shown in Fig. 11, is very useful and was originally unexpected but has now been verified theoretically, both from the Born approximation and "exact theory."

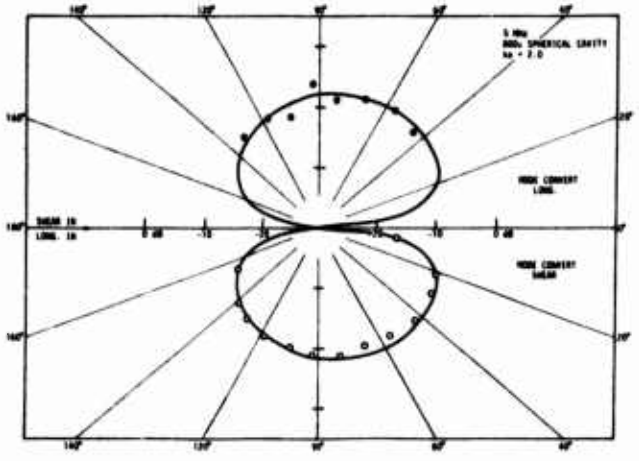

Figure 11. Reciprocity observed for spherical void.

For the Born approximation the displacement of the scattered wave in the far field can be written as[5]

$$u_j^{(s)}(\underline{r}) = \left|K_s\right|^2 \frac{e^{i\underline{K}_s \cdot \underline{r}}}{4\pi r} G_{jm} u_m^{(0)} \times$$

$$\int e^{i(\underline{K}_s - \underline{K}_o)\cdot \underline{r}'} \, d^3r' \qquad (1)$$

where u^0 is the amplitude of the displacement of the incident wave with wave vector $\underline{K}_o$, $u_j^{(s)}(\underline{r})$ is the far field amplitude of the scattered wave with wave vector $\underline{K}_s$, and the matrix G_{jm} depends only on the angle of scattering and the properties of the scatterer. The term containing the integral is essentially the Fourier transform of the shape of the scatterer. From the expression it is clear that if the roles of K_s and K_o are reversed, i.e., $K_s \rightarrow K_o$ and $-K_o \rightarrow K_s$ the expression is unchanged. The result of reciprocity is significant from several points of view, one of which is just in reducing the number of measurements and calculations in the study of mode conversion.

In conclusion, we have measured the scattering of elastic waves from a variety of defects ranging from spherical cavities to ellipsoidal cavities and to very thin elliptical disks. We have explored the validity of various theories, such as the Born approximation and the Keller theory, and have tested their regimes of validity. We have observed features which aid in the identification of size, shape, and orientation of geometrically shaped defects, which are three of the parameters important in failure prediction.

What we now need is to determine defect dimensions in an absolute sense in the regime of flaw criticality. Experimentally, we need to evaluate the use of the pulse echo versus the two transducer or pitch-catch method and pursue vigorously the obtainment of amplitude and phase information from the scattering signature with frequency and angular dependence as parameters, so that we can start to tackle the inverse problem. Finally, we should also direct our attention to crack-like defects.

Acknowledgements

The author is grateful to E. Domany, E.R. Cohen and L. Adler for making available the results of their calculations and to H. Nadler and L. Ahlberg for their assistance in the experiments.

REFERENCES

1. H. Lamb, "Problems Relating to the Impact of Waves on a Spherical Obstacle in an Elastic Medium," Proc. London Mathemat. Soc., Ser.1, Vol. 32, 1900 pp. 120-150.

2. Y.H. Pao and C.C. Mow, "The Diffraction of Elastic Waves and Dynamic Stress Concentrations," (Crane Russack and Co., New York, 1973).

3. C.F. Ying and R. Truell, "Scattering of a Plane Longitudinal Wave by a Spherical Obstacle in an Isotropically Elastic Solid," Y. Appl. Phys., Vol. 27, 1956, pp. 1086-1097.

4. B.R. Tittmann, E. Richard Cohen, and John M. Richardson, "Scattering of Longitudinal Waves Incident on a Spherical Cavity in a Solid," Y. Acoust. Soc. of America, in press.

5. E. R. Cohen, private communication.

DISCUSSION

DR. PAPADAKIS: Questions?

MR. ROY SHARPE (Harwell Labs): I still don't know how you use all this information in practice. I think it came up this morning that "real" defects are not in nice spheres. You can normally only look at them from one direction. I just don't see how you're going to tackle the inverse problem.

DR. TITTMANN: As I mentioned earlier, we have to first develop a theoretical and experimental data base with simple geometries from which we can then launch into complex shapes, which may always be approximated by combinations of the simpler shapes. I think the results for the very thin elliptical disk are a good start in the direction towards "real" cracks. We have demonstrated the ease with which you can identify the axes of symmetry, the changes in radii of curvature, and the aspect ratios. We are therefore confident that many of these features can be obtained by interrogation over a limited range of angles and frequencies, as would be required by "real world" inspections of parts.

DR. EYTAN DOMANY (Cornell University*): One of the slides that Prof. Krumhansl showed displayed results for cracks in the regime of low ka, so that we can now make available calculations for comparison with experiment in this regime.

DR. TITTMANN: Thank you. This would be very useful when well characterized samples with cracks become available.

DR. PAPADAKIS: I wanted to ask you whether you have gotten an integrated cross section to--

DR. TITTMANN: You mean the power averaging over all angles?

DR. PAPADAKIS: Yes, power averaging over all angles. Does that agree with what has been published concerning the grain scattering contribution of longitudinal to shear conversion and so on?

DR. TITTMANN: That's difficult to do experimentally because of the need to collect very thoroughly all the angular information. One of the difficulties is that in the forward scattering direction the direct beam of the transducer completely masks the scattered radiation.

DR. PAPADAKIS: How about in theory?

DR. TITTMANN: The theoretical work has been done. I think Ying and Truell[3] calculate total scattering cross sections and make these comparisons.

DR. PAPADAKIS: The same approximations that go into your theory and Dr. Krumhansl's theory?

DR. TITTMANN: I don't know about that. Would you care to comment on that, Jim?

PROF. KRUMHANSL(Cornell University): We know that in some regimes for strong scattering from a cavity, the Born approximation will not give quite the right total because it simply won't. On the other hand, the Born approximation is only a "plug-in" at a second stage in the general equation. We do have some general expressions for scattering cross sections which would provide very good approximations to the Ying-Truell calculations[3] for the sphere.

DR. DICK COHEN (Rockwell International): I think the main problem with trying to do experimentally the evaluation of the power split between longitudinally scattered and shear scattered is trying to calibrate your transducers absolutely. You have a longitudinal receiver and a shear wave receiver and then to make sure that they're really calibrated to the same standard is quite difficult.

DR. PAPADAKIS: Yes.

DR. COHEN: You can make relative measurements quite easily, of course, and get the angular distribution, but to get those cross sections evaluated on an absolute basis is very difficult.

DR. PAPADAKIS: Okay. I didn't want to belabor the point, because I know you were actually aiming at different things, that is, characterizing the shape and orientation of the flaw.

* Now at the University of Washington.

MODELS FOR THE FREQUENCY DEPENDENCE OF ULTRASONIC SCATTERING FROM REAL FLAWS

Laszlo Adler and Kent Lewis
University of Tennessee
Knoxville, Tennessee 37916

My objective is to help develop a quantitative working model for a typical nondestructive testing system. Specifically, our objective is to relate the parameters which characterize a defect such as size, orientation, and shape to the ultrasonic scattering field parameters such as amplitude, frequency, scattering angle, and polarization or mode conversion. In Fig. 1 is shown a flat surface sample immersed in liquid containing a real flaw a certain distance below the surface; i.e., in the bulk of the material. Sound waves propagate through the liquid and for the simplest case the wave front enters such that only incident longitudinal waves are present. The waves at the flaw are scattered, and also mode converted; the scattered wave, which will now be both shear and longitudinal will be reconverted back to a longitudinal wave once leaving the solid body and picked up by a receiver oriented at some angle.

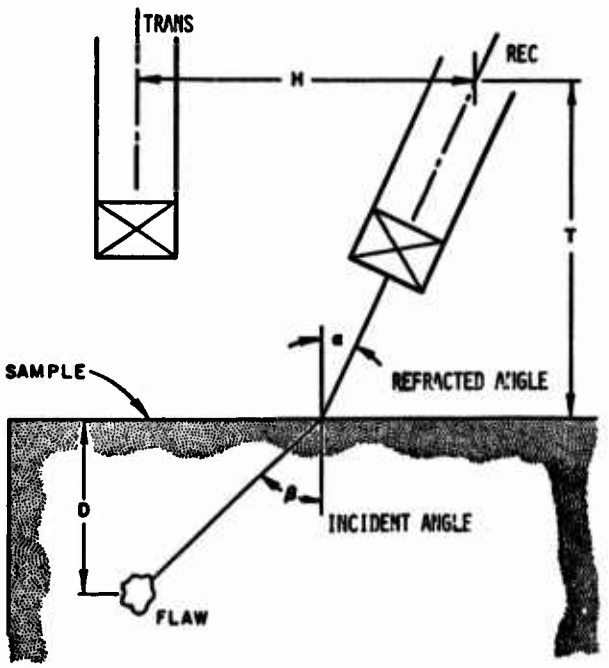

Figure 1. Typical NDE system to characterize real flaws by elastic wave scattering.

We received diffusion bonded samples from the Rockwell International Science Center for our investigation. These were titanium samples, disks 4 in. in diam. and 2 in. thick and various types of cavities were at the center. These cavities were in two basic categories: (1) circular and elliptical crack-like disks, and (2) spheroidal type of cavities. The first group models crack-like flaws and the second group would be more like a void type of flaw. The oblate spheroid, when it is smashed, will also approach the crack-like flaw.

There is another difference between the two groups of cavities. For the crack-like flaws, that is for the disks, the dimensions ranged from about 1200 μm to 5,000 μm in diam., and for the spheroidal defects, the dimensions were as small as 100 μm. So, we are dealing with problems that from a scattering point of view are ranging from something like ka = 0.1 to about ka = 20.

In order to make a quantitative evaluation we searched for existing studies to evaluate our experiments. There is not really one single theory which would cover the range from ka much less than 1 to ka much larger than 1. For ka less than 1 or equal to 1 we used the Born approximation developed at Cornell by Krumhansl, Gubernatis and Domany. For the large size defects, especially with sharp edges and for the circular and elliptical disk cavities, we used Keller's theory which originally was developed for diffraction of electromagnetic waves, and we applied it to scalar acoustic waves.

I should say a few words about this theory. As I mentioned, Keller introduces the concept of diffracted rays in his theory. When you have an edge of some sort, contrary to geometrical theory for acoustics or optics in which only incident reflected and refracted waves are considered, diffracted rays are produced any time a ray hits an edge. Figure 2 shows these diffracted rays. They describe a cone. The angle for the diffracted rays from the edge is the same as the incident.

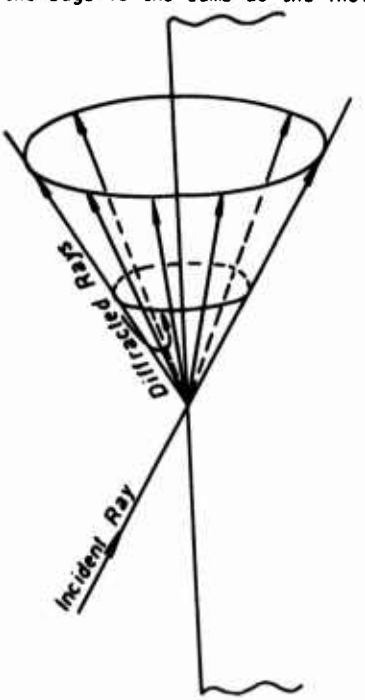

Figure 2. Schematic diagram of "Ray" diffraction from edges.

Generalizing the Fermat principle to a bonded and a discontinuous medium is another way to treat the problem.

The advantage of this theory is that in addition to having qualitative information through ray tracing, some field and phase values are assigned to the incident waves. One can actually make some quantitative calculations of the incident field. The incident field is related to the diffracted field through the diffraction coefficient. The diffraction coefficients are evaluated from the exact theory using some kind of asymptotic expansion of exact theory to get the result for the semi-infinite plane as solved by Sommerfield.

Keller points out that although the result originally was intended for ka larger than 1, it works surprisingly well for ka equal to 1. This is in the region of our interest.

Let me give you one expression here. This is for the complex amplitude of the diffracted field at any given point due to an arbitrary shaped two-dimensional scatterer. Let me point out some of these parameters. We have a summation for the number of diffracted rays. A(k) is the incident amplitude in k space. The important parameters are all geometrical.

$$U = \sum \frac{Ae^{ik(\psi+s)+\frac{i\pi}{4}}}{2(2\pi k)^{\frac{1}{2}}\sin\beta x}\left[\sec\tfrac{1}{2}(\theta-\alpha)\right] \pm \csc\tfrac{1}{2}(\theta+\alpha)\Big] x$$

$$\left[s\left(1-\frac{s\left[\cos\delta+\rho\dot{\beta}\sin\beta\right]}{\rho\sin^2\beta}\right)\right]^{-1/2}$$

In Figure 3 the symbols are explained.

β is the angle between the incident ray and the tangent to the aperture. It will depend on both the geometry of the scatterer as well as the direction of the incident ray. For normal incidence it's fairly simple, but for oblique incidence, the value of β will depend on several factors.

$\dot{\beta}$ from the previous equation is the derivative of this β with respect to the arc length. For a scatterer with complicated shape, the problem is fairly complex, but it can be handled for a two-dimensional scatterer having any shape.

For a circular scatterer, the expression we obtain for the general case of any oblique incident wave is expressed in fairly simple form

$$U = A(k)\sqrt{\frac{2}{k(\sin\theta+\sin\alpha)}}\left[\frac{\sin^2\left[ka(\sin\theta+\sin\alpha)-\frac{\pi}{4}\right]}{\sin^2\left(\frac{\theta+\alpha}{2}\right)} + \frac{\cos^2\left[ka(\sin\theta+\sin\alpha)-\frac{\pi}{4}\right]}{\cos^2\left(\frac{\theta-\alpha}{2}\right)}\right]^{1/2} \qquad (2)$$

where α is the incident angle and θ is the diffracted angle; A(k) is the amplitude distribution of the incident wave and is characteristic of the transducer. This expression can be used for both the pulse echo technique and for the pitch-catch method. The incident beam is perpendicular to the scatterer. In this case $\alpha = 0$ and the expression simplifies.

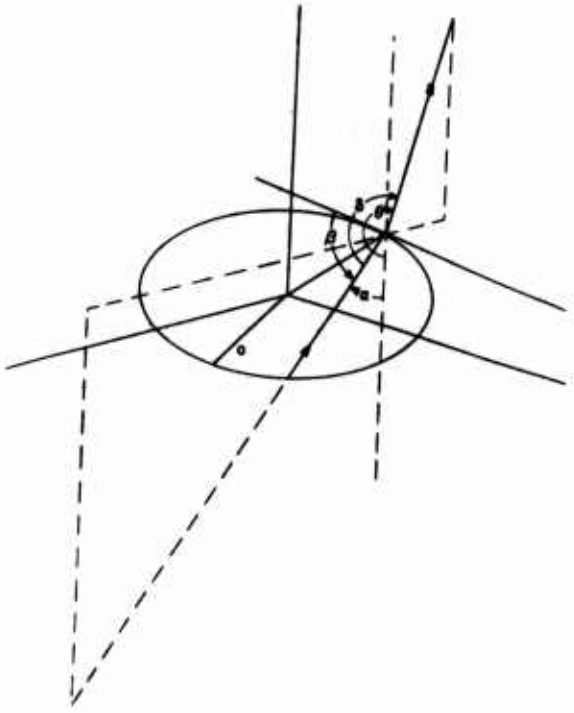

Figure 3. Diffraction of ray from aperture.

The two variables, the frequency F and the scattered angle θ, are the ones which we tried to correlate to the size of the scatterer and this is calculated from Eqn. (2) for the 1200 μm diam. penny-shaped cavity inside titanium as shown in Fig. 4. The scattered angle varies from 30° to about 70° and the frequency varies from about 2 to 6 MHz. This is the frequency range in our investigation.

We made some calculations for the case where the scattered wave mode is converted into a shear wave. The calculations for the scattered shear wave are shown in the same figure.

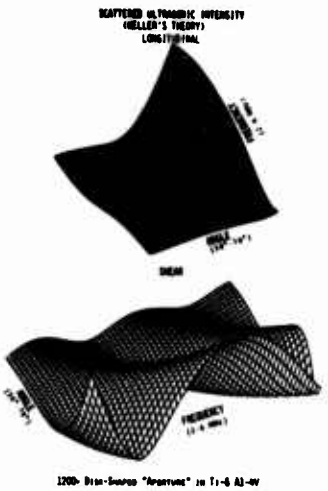

Figure 4. Calculated intensity distribution for a 1200μ disk-shaped aperture (Keller's theory).

For a 5000 μm diam. disk the result is shown in Fig. 5. The larger the size of the defect, the more detail is obtained in the frequency spectrum. In the angular dependence there is also more detail for the larger size cavity than for the smaller cavity.

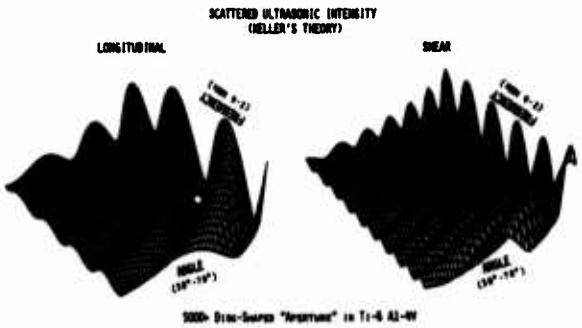

Figure 5. Calculated intensity distribution for a 5000μ disk-shaped aperture (Keller's theory).

The other type of crack-like defect was an elliptical disk inside titanium and we made calculations for the elliptical case from Keller's theory.

$$U(p) = \frac{A(k)\rho\ (\psi)}{\sin\phi}\ \frac{1-\cos\phi\sin 2(ka(\psi)\sin\phi}{k\rho\ (\psi)\sin\phi}^{1/2} \qquad (3)$$

where

$$a(\psi) = \varepsilon b[1 + (\varepsilon^2 - 1)\ (1+ \varepsilon^2\tan^2\psi)^{-1}]^{-1/2}$$

$$\rho\ (\psi) = \varepsilon^{-1}b\,[1 + (\varepsilon^2-1)(1 + \varepsilon^2\tan^2\psi)^{-1}]^{3/2}.$$

Equation (3) applies to the case of normal incidence for longitudinal waves. The basic difference between Eqn. (2) and Eqn. (3) is an additional parameter ψ, which is the angle in the plane of ellipse.

Figure 6 shows the calculated scattering pattern as a function of frequency and projection angle ψ for a fixed scattering angle for a 1200μmx 5000μm elliptical aperture in titanium. The separation of the frequency maxima along the major and minor axes are the same as the pattern for the corresponding circular aperture of the same size but there is a change in the relative intensities. The pattern change in ψ indicates that there is an asymmetrical discontinuity. No such variation is present for a circular discontinuity.

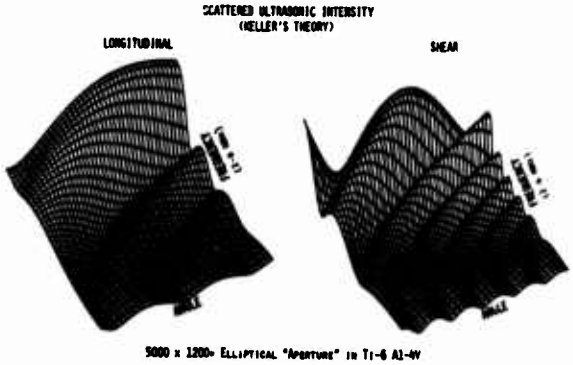

Figure 6. Calculated intensity distribution for a 5000μ x 1200μ elliptical aperture (Keller's theory) shown as a function of projection angle ψ for a fixed scattering angle of 45°.

In Fig. 7 is shown a schematic idagram of our experimental setup. A ceramic transducer is shock excited, producing a broadband spectrum. This pulse propagates through the water-titanium interface and interacts with the cavity. The scattered pulse (which is now both shear and longitudinal) through the titanium-water interface (the shear wave is mode converted in water) and is received by a second broadband transducer. The signal is amplified, gated out, and spectrum analyzed. Figure 8 is a picture of the experimental setup.

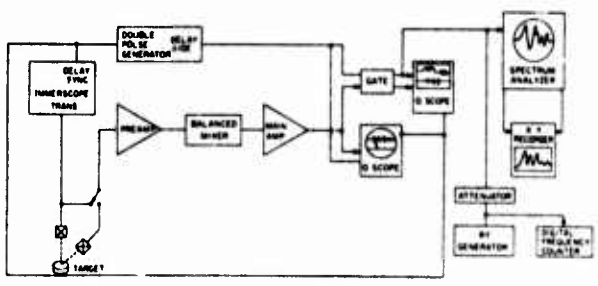

Figure 7. Experimental arrangement.

Figure 8. Mechanical System.

Since both Keller's theory and the Born approximation theory are valid for an infinitely extended solid, we had to make corrections due to the interface. We calculated the transmission curve for the shear and for the longitudinal wave coming out from a titanium sample in water (Fig.9) These corrections were applied to our data.

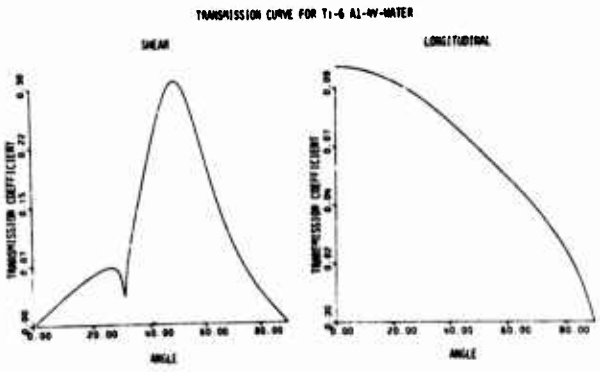

Figure 9. Transmission curve for titanium-water.

Scattering experiments were carried out for the 1200 μm and 5000 μm diameter circular shaped cavities in titanium for various scattering angles. Experiments were done also for the 1200 μm x 5000μm epplitical cavity. The condensed result is shown for the longitudinal scattering in Fig. 10 in the case of the 5000 μm cavity for four different scattering angles. The solid line is calculated from Keller's theory. The agreement is quite good. The agreement is also good for the elliptical disk shown in Fig. 11.

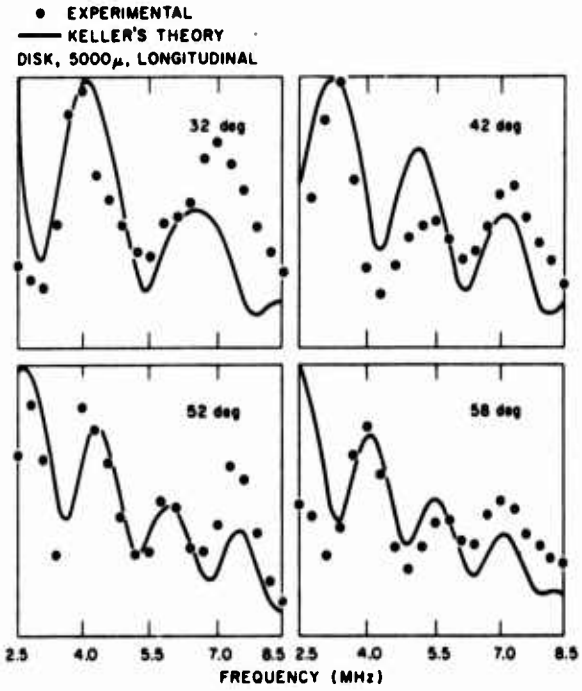

Figure 10. Comparison between experimental and Keller's theory for the intensity of longitudinal scattered wave as a function of frequency for a 5000μ thin disk-shaped cavity embedded in tianium.

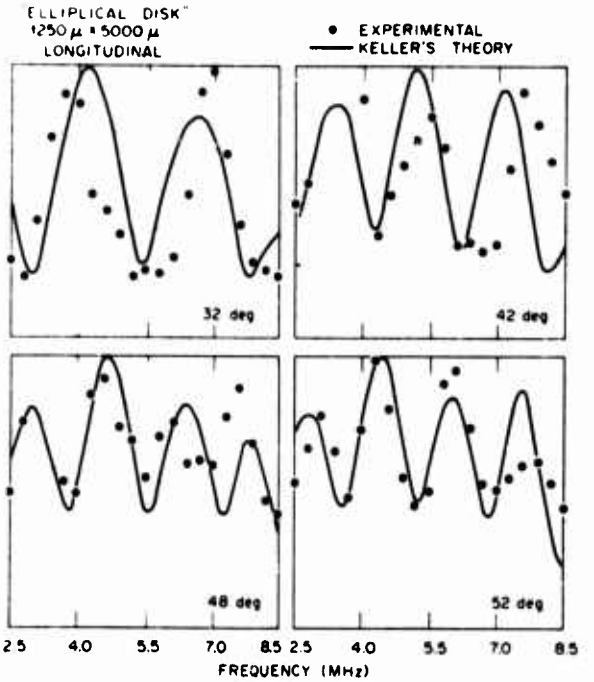

Figure 11. Comparison between experiment and Keller's theory for the intensity of longitudinal scattered wave as a function of frequency for a 1250μ x 5000μ thin elliptical disk-shaped cavity embedded in titanium.

In the next set of experiments, we investigated elastic waves scattering from spheroidal cavities in titanium. Three cavities were studied: an oblate spheroid of dimensions 400 x 800 μm (diameters), the 800 μm diam. sphere, and the 1600 μm x 800 μm prolate spheroid. For an incident longitudinal wave at normal incidence the scattered frequency spectrum was recorded for several scattered angles. The scattered shear and longitudinal waves were separately analyzed. In the theoretical analysis the Born approximation was used. Figures 12, 13, and 14 are three-dimensional plots of calculations using the Born approximation for the three cavities. The frequency and angular dependence of the scattered power is plotted for the range of our experiment. Clearly there are distinct features of both the scattered shear and longitudinal waves with cavities' shape and/or size obtainable from the Born approximation theory. The theory compares well with experiment for the oblate spheroid (Fig. 15). For the sphere (Fig. 16) and prolate spheroid (Fig. 17) the agreement is only fair. One would expect that, since the ka is about 0.1 to 0.8 for the oblate spheroid but is up to ka ≃ 10 for the prolate spheroid (for shear waves at 8 MHz) and the Born approximation really works better for small ka.

In conclusion, I would like to point out that all these experiments were carried out using normal incidence and pitch-catch techniques. We are also planning to do some work using the oblique incidence to the surface. This, of course, will introduce additional problems because both incident shear and longitudinal waves will be present.

We would like to extend Keller's theory to other than plane geometry. It seems to me that it would be somewhat useful to have the ray approach for focussed transducers and for other than flat surfaces. The theory should also be extended to elastic problems.

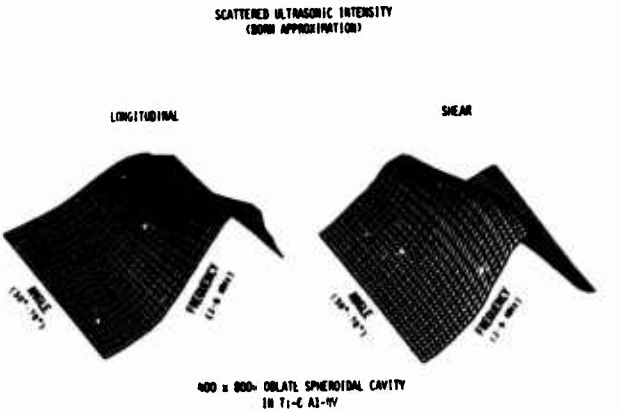

Figure 12. Calculated intensity distribution for a 400μ x 800μ oblate spheroid cavity in titanium (Born approximation).

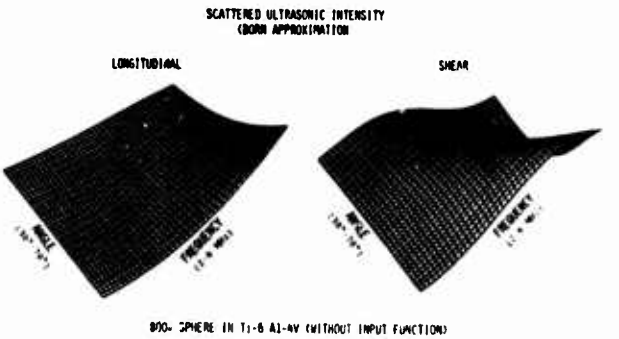

Figure 13. Calculated intensity distribution for a 800μ spherical cavity in titanium (Born approximation).

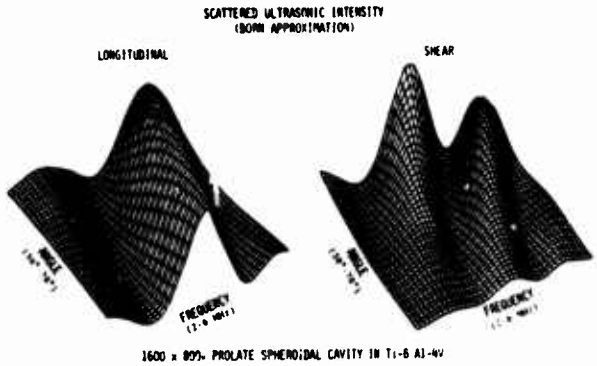

Figure 14. Calculated intensity distribution for a 1600μ x 800μ prolate spheroid cavity in titanium (Born approximation).

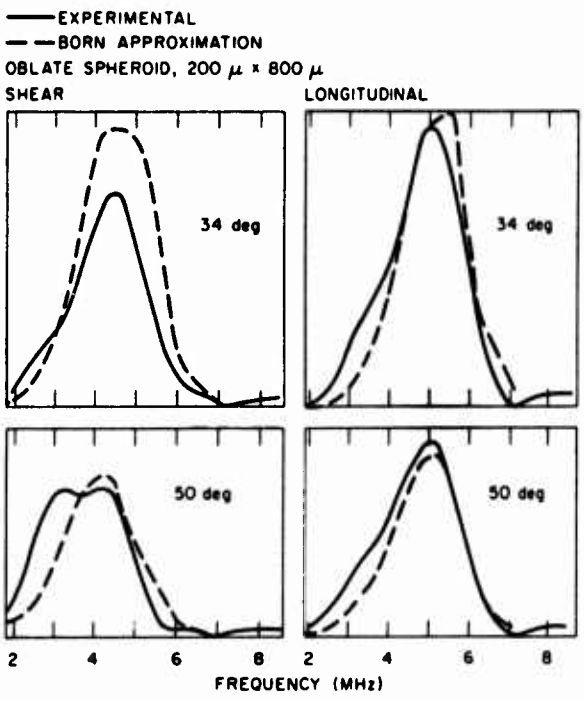

Figure 15. Comparison of experiment to Born approximation for the intensity of scattered waves spectra for a 200μ x 800μ oblate spheroid cavity embedded in titanium.

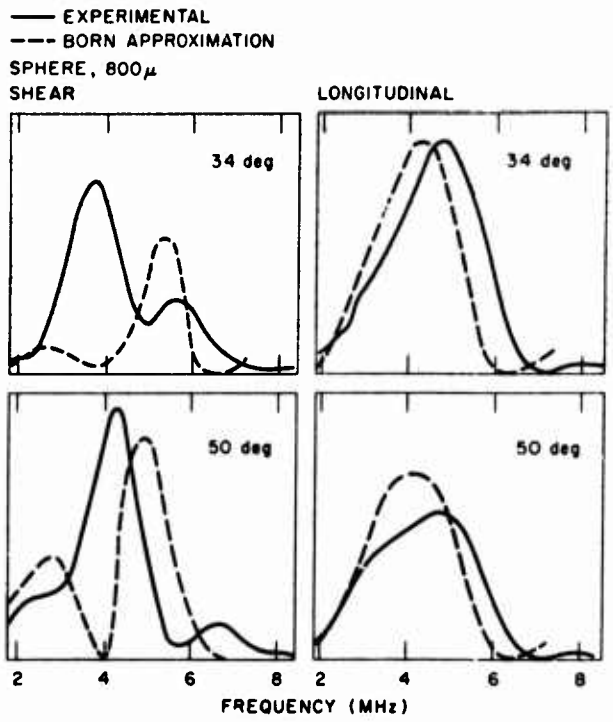

Figure 16. Comparison of Experiment to Born approximation for the intensity of scattered waves spectra for a 800μ spherical cavity embedded in titanium.

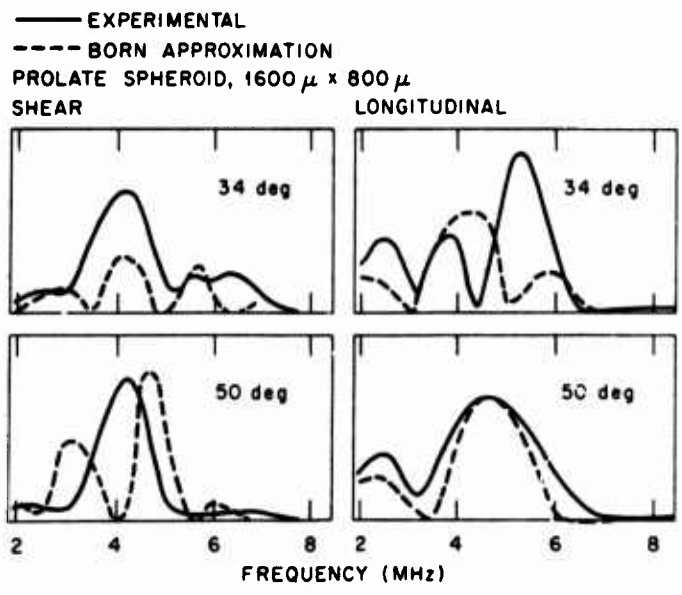

Figure 17. Comparison of experiment to Born approximation for the intensity of scattered waves spectra for a 1600μ x 800μ prolate spheroid cavity embedded in titanium.

DISCUSSION

DR. EMMANUEL PAPADAKIS (Ford Motor Company): Thank you, Laszlo. May I ask you to save your questions for him for coffee break.

NEW PROCEDURE FOR CALIBRATING ULTRASONIC SYSTEMS FOR QUANTITATIVE NDE

B. R. Tittmann
Science Center, Rockwell International
Thousand Oaks, California 91360

The presently used ultrasonic standard for calibrating ultrasonic systems is the "flat bottom hole." In view of some dissatisfaction by many, we sought to apply the results of our scattering studies to explore the possibility of coming up with an alternative. This is a proposal for a new standard, and as I go through the discussion, please keep in mind that this work is still very much in its infancy.

Our objectives in this study were, first, to develop an overall system calibration; secondly, to develop a technique that has sufficient dynamic range so that a linearity check is meaningful with no degrees of freedom; and thirdly, to develop a technique so that the system can be calibrated and compared to the theoretically known expectations.

Before we begin this discussion, I would like to make two definitions to orient the audience. We define the "calibration standard" as an ultrasonic standard solely employed to ensure equipment is functioning according to its specifications. The "reference standard," on the other hand, we define as a library of scatterers of different shapes used to aid in the identification of an unknown defect after the ultrasonic system has already been calibrated with the use of the "calibration standard."

If we look at a typical ultrasonic system and write down the characteristic equation keeping track of all the losses, we have to take into account the following items: the electrical signal available at the terminals of the receiving transducer is equal to the electrical signal fed into the terminals of the transmitting transducer times the transfer function or the loss in conversion from electrical to acoustic energy; the losses due to propagation in the medium whether they are attenuation or beam spreading; the losses upon scattering from the standard defect; again, the propagation losses in the return path and the conversion from the acoustic signal to the electric signal. This equation is presented in Fig. 1, together with a schematic identifying the terms discussed. This equation will be employed shortly, but first the scattering term $S(f,a,\theta)$ is treated in more detail. What we would like to propose is that we use a sphere as the calibration standard and use, for example, the diffusion bonding technique to build such a sphere into a solid material.

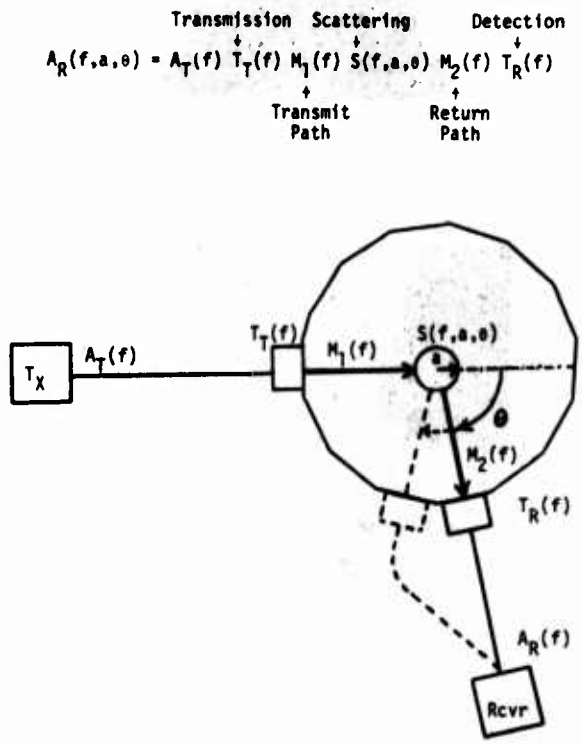

Figure 1. Characteristic ultrasonic equation.

Figure 2 is an example of what the diffusion bonding process is able to do. We see here a micrographical cross-section of a hemisphere and notice that the hemispherical shape is maintained intact and that the bond line has disappeared with grains having grown across the bond plane.

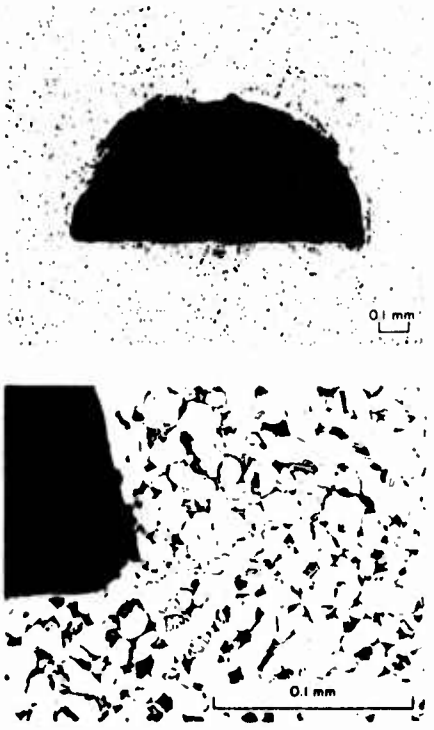

Figure 2. Micrograph of the cross-section of a hemispherical cavity produced by diffusion bonding of two machined sections of Ti-alloy. The lower figure shows an enlargement of the section where the bond was made and demonstrates the complete disappearance of the bond line by grain growth across it. The top figure is a mosaic of several micrographs.

As we know from scattering studies, the sphere is ideally suited for use as reference scatterer in the sense that it can be treated by exact theoretical calculations as exemplified in Fig. 3. Here the solid line shows the scattering term $S(f,a,\theta)$ as a function of the scattering angle for a tungsten carbide sphere, whereas the dashed line shows it for a spherical void. We see that the total variation in $S(f,a,\theta)$ is about 15 to 25 dB so that with one defect we have enough dynamic range for calibration purposes.

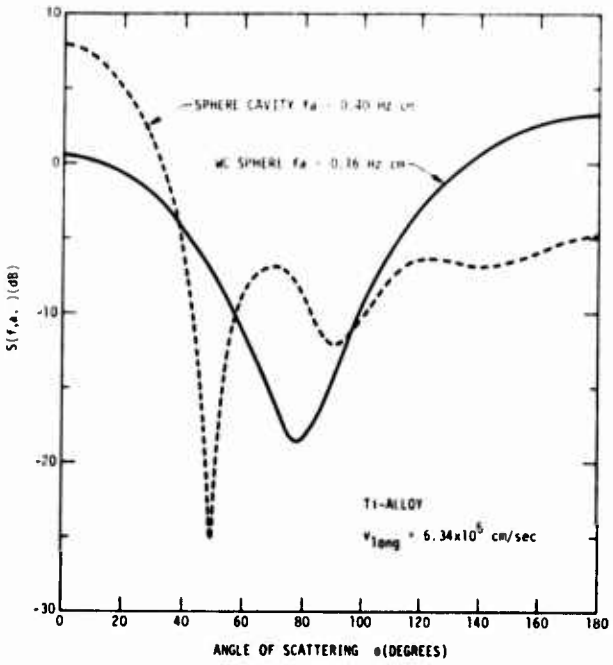

Figure 3. Master curves for the angular dependence of the theoretical scattering function for spherical cavity and a tungsten carbide circle inclusion embedded in Ti-alloy.

In Fig. 4, we have rewritten the ultrasonic characteristic equation by specifically including beam spreading, attenuation, and a new figure of merit for the transducer, namely, the G factor.

$$\frac{|A_R(f,a,\theta)|}{|A_T(f,a,\theta)|} = \frac{va}{fR^2(4\pi)^{3/2}} \; |S(f,a,\theta)| \; \sqrt{G_T(f)\,G_R(f)} \; \exp[-2R\alpha(f)]$$

Diffraction — Scattering — Attenuation — Transducers

Identification of G:

G is the gain of the transducer and is defined as the power per unit solid angle in the forward direction in terms of power delivered to the transducer terminals.

$$(A_R)_{dB} - (A_T)_{dB} = (P_t)_{dB} + (S)_{dB} + (G_T)_{dB} + (G_R)_{dB}$$

$$(A_R)_{dB} - (A_T)_{dB} = 20 \log_{10} \frac{|A_R(f,a,\theta)|}{|A_T(f,a,\theta)|}$$

$$(P_t)_{dB} = 20 \log_{10} \frac{va \exp(-2R\alpha)}{fR^2(4\pi)^{3/2}}$$

$$(S)_{dB} = 20 \log_{10} |S(f,a,\theta)|$$

$$(G_T)_{dB} = 20 \log_{10} \sqrt{G_T(f)}$$

$$(G_R)_{dB} = 20 \log_{10} \sqrt{G_R(f)}$$

Figure 4. Characteristic equation for ultrasonic system.

For the transmitter, G is defined as the power per unit solid angle in the forward direction in terms of the power delivered through the transducer terminal. For the receiver transducer, G is the maximum power delivered to the load matched to the transducer transmission line of assumed zero loss when the power per unit solid angle incident on the transducer is known.

This definition, then, is the backbone for evaluating this expression and effectively lumps into one parameter all the processes and losses involved in taking electrical energy from the input terminals into the acoustic energy of the main beam as it propagates in the medium normal to the transducer face. The G factor is analogous to the gain of an antenna in radar and becomes a figure of merit. It is unitless since it is a ratio and may be best expressed in dB.

In the lower portion of Fig. 4, all the terms of the characteristic equation are given in units of power, i.e., dB, and one may identify the difference between the received and transmitted signal in terms of the losses due to propagation, scattering, and the G factors of the two transducers.

Before I continue, I think I really should describe how one can measure the G factor shown in Fig. 5. The equipment needed is a transmitter, directional coupler, detector, coaxial short and a transducer coupled to some acoustic reflector.

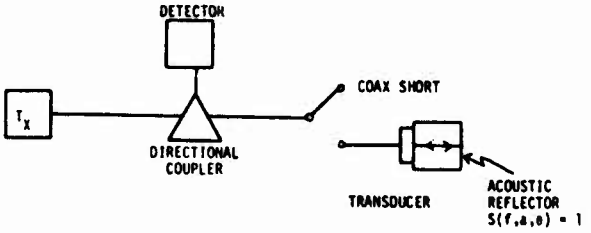

(1) Coax. short: signal detected = $(A_T)_{dB}$

(2) Transducer as load: signal detected (1st echo) = $(A_R)_{dB}$

$$2(G)_{dB} = \left[(A_R)_{dB} - (A_T)_{dB}\right] - (S)_{dB} - (P_t)_{dB}$$

where $(S)_{dB} = 0$

Figure 5. Measurement of G-factor.

The first step is to use the coaxial short as a load and then the detected signal is simply the transmitted signal $(A_T)_{dB}$. The second step is to use the transducer and acoustic reflector as a load. which gives the first echo as the measured signal. From the difference between these two measurements, the scattering function of the acoustic reflector, and the propagation loss in the material, we can derive the G factor.

One acoustic reflector that may be used is simply the back surface of the sample for which the scattering function is essentially zero dB. Another reflector could be a diffusion bonded sphere for which the scattering function is very well specified as has been shown earlier.

Figure 6 presents a number of G factors measured in the way described above for a variety of commercial transducers at various frequencies. We will be using some of these G factors in the calculations later on.

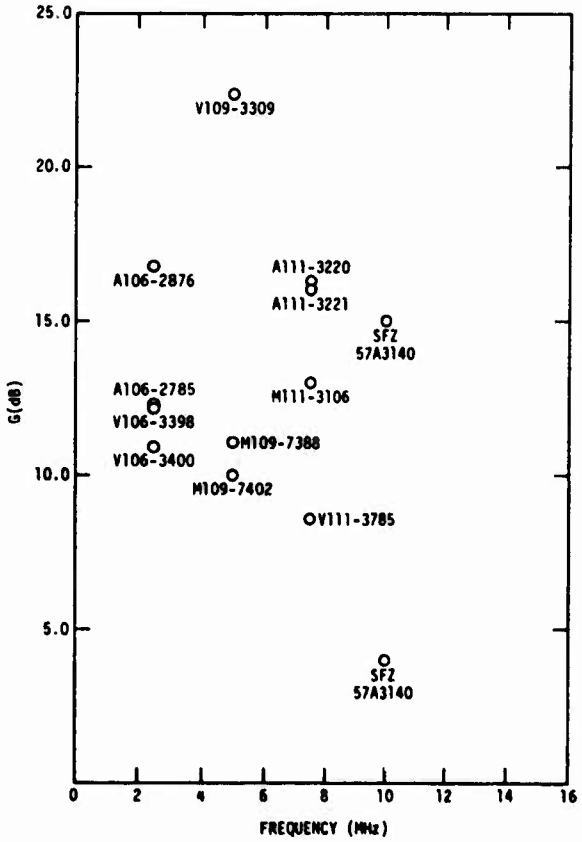

Figure 6. G-factors for a variety of commercial transducers.

Figure 7 presents the required equipment and information to carry out a calibration. First one uses a substitution bridge with a precision attenuator to measure the insertion loss of the polygon standard and transducers to obtain $(A_R)_{dB}$-$(A_T)_{dB}$.

REQUIRED EQUIPMENT AND INFORMATION

A. Substitution Bridge:

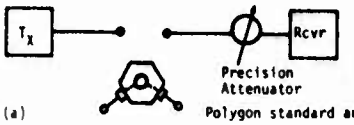

(a) Polygon standard and transducers.

(b) Short coaxial connector (negligible loss)

$(A_R)_{dB} - (A_T)_{dB}$ = Att. Rdg. (a) - Att. Rdg. (b).

B. Reference table for choice of Standard:

f (MHz)	fa=0.40 Hz cm Cavity Radius a_C (cm)	fa=0.16 Hz cm Tungsten Carbide Radius a_W (cm)
2.5	0.160	0.064
4.0	0.100	0.040
7.5	0.053	0.021
10.0	0.040	0.016

C. Data sheet for standard giving propagation loss P_ℓ(dB).

Figure 7. Required equipment and information.
A) Substitution Bridge.
B) Reference table for choice of Standard.
C. Data sheet for standard giving propagation loss P_ℓ(dB).

Now, one needs a reference table so that one can decide what standard to choose. The reference table shown in Fig. 7 is based on our scattering studies and gives a good dynamic range and a simple angular dependence for the scattered power, both for the cavity and the tungsten carbide sphere. Finally, one needs a data sheet giving the propagation loss for the particular standard.

Figure 8 is a photo of our goniometer that might be used with the standard. The goniometer allows you to vary the scattering angle by moving a receiving transducer along about 14 faces. The block is shown in cross section in Fig. 9. It is a polygon with 14 faces which are arranged in such a way that none of the faces corresponds to the same angle giving you, therefore, a maximum number of probing points in the angular dependence of the scattered radiation pattern.

Figure 10 gives a sample calibration at 4 MHz with the aid of a WC sphere of radius .04 cm. The solid line is the theoretical scattering function and the data points are those obtained by a combination of the experimental measurements and the use of the characteristic equation.

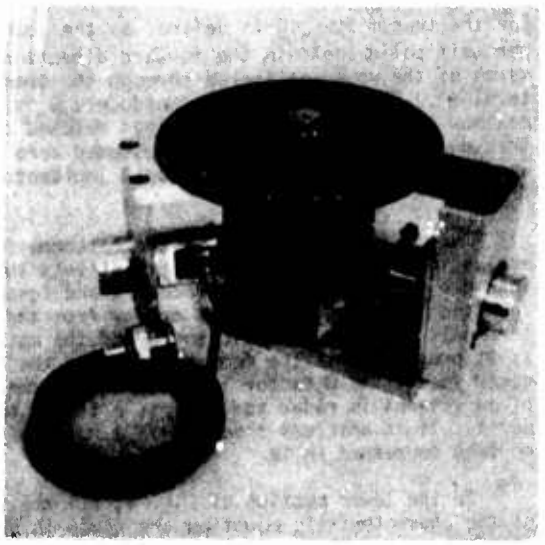

Figure 8. Photograph of measurement fixture including a polygon sample and a pair of commercial transducers.

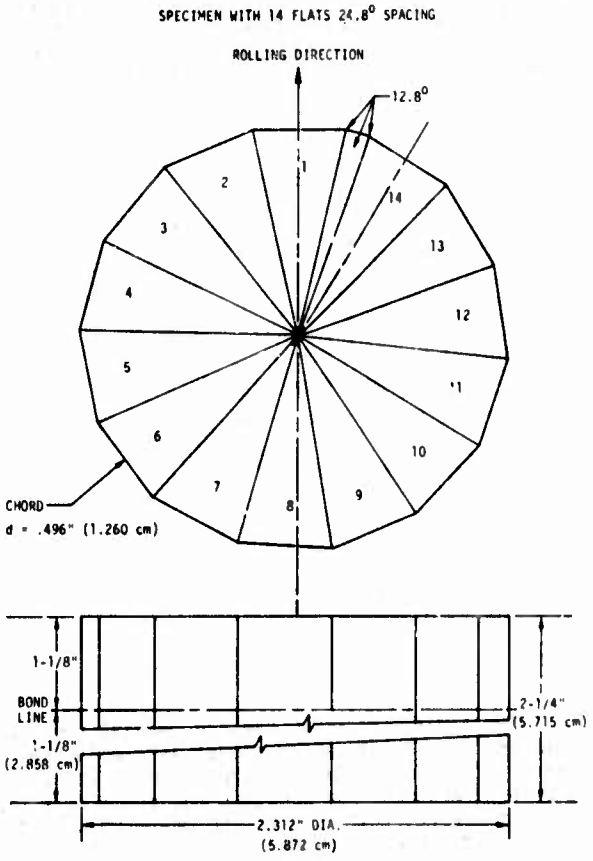

Figure 9. Cross section of diffusion bonded blocks of Ti-alloy machined into the shape of a polygon with 14 faces.

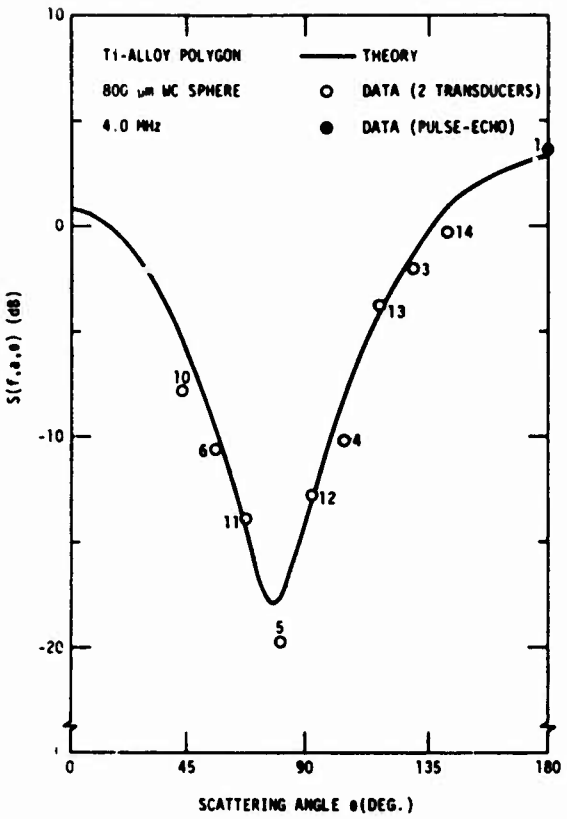

Figure 10. Graph showing S(f,a,θ), for an 800 micrometer diameter (a = 0.04 cm) tungsten carbide (WC) sphere embedded in Ti-6% Al -4% V by diffusion bonding. The theoretical curve and experimental points have been determined in an absolute way.

You see that most of the points (open circles) were obtained in the pitch-catch mode with two transducers, but one point (the solid dot) was obtained by the pulse-echo mode in the back scattering direction. The fact that both of these sets of points appear on the same graph shows that we were able to take into account the differences between the two sets of measurements and demonstrates the power of the characteristic equation.

In summary, the calibration described here involves a "kit" consisting of a guide to a choice of standards; an assortment of standards in the shape of polygons; a data sheet for each standard giving the propagation loss including attenuation, bond losses, and diffraction losses; a data sheet giving the theoretical power scattered versus scattering angle for each standard at selected frequencies; the G factor values for each transducer to be used; and a measurement fixture, such as shown before, to be used as a calibration goniometer.

What are the new features incorporated into the calibration procedure proposed here? First of all, we have a standard defect that is rather well and quantitatively characterized by an exact theory. Secondly, we have introduced a new figure-of-merit for the transducer, the G factor. Instead of having to use a number of standards for the calibration, we can - taking advantage of the angular dependence - accomplish the calibration with a single sample. We have achieved a dynamic range anywhere from 22 dB for the WC sphere to 35 dB for the spherical void.

The advantages of this system are that we have determined a method for the self-consistent calibration of an ultrasonic system. We have a way to get the required dynamic range variation independent of the gain control and using the same ultrasonic standard. We know quantitatively what the dynamic range should be so that a quantitative calibration is feasible with no additional degrees of freedom, and we have allowed for an absolute comparison of pulse echo and the through transmission mode.

There is still a lot of work to be done. For example, we have to learn to take into account broad band characteristics of transducers, i.e., operate in the pulse mode rather than the tone burst mode as was done so far. We also have to develop an analysis procedure for the calibration error. And finally, we also need some statistics on the quality of fabrication of the standards by the diffusion bonding process.

DISCUSSION

DR. EMMANUEL PAPADAKIS (Ford Motor Company): Questions?

DR. JERRY TIEMANN (General Electric): Sort of a comment. I also suggest that you consider how to take into account transducers of different focal lengths, and you should also take into account the transducer in the context of a water coupling medium instead of a direct metal contact.

DR. TITTMANN: That's a good suggestion.

DR. EYTAN DOMANY (University of Washington): If I understand you correctly, the sphere was used because the exact solution exists.

DR. TITTMANN: That's one of the reasons.

DR. DOMANY: I think that the exact solutions also exist for long elliptical cylinders if you hit them from the side, and it seems that there's a simpler geometry to use because you could drill a hole instead of diffusion bonding.

DR. TITTMANN: Yes.

DR. PAPADAKIS: Well, it isn't necessarily easy to drill a long, skinny hole.

DR. TIEMANN: It's a lot easier than making a sphere down the middle of something.

DR. PAPADAKIS: Not the way they're doing it.

PROF. R.E. GREEN (John Hopkins): How do you plan to take account the coupling loss? You have different types of couplers; are you going to make a table of all possible couplings?

DR. TITTMANN: No, before you make your measurement and calibration, you decide what coupling agent you are going to use for the rest of the experiment. And then you use that coupling agent to obtain the G factors that you need for the calibration.

DR. ALFRED BAHR (Stanford Research Institute): In all these measurements, though, you either need the G factors or the total attenuation.

DR. TITTMANN: Attenuation in the material?

DR. BAHR: Well, a total loss including all that you have lumped into P_ℓ.

DR. TITTMANN: P_ℓ does not include the transducers.

DR. BAHR: Right. But what's your feeling about the accuracy to which you can obtain P_ℓ or other quantities in the equation?

DR. TITTMANN: P_ℓ contains the bond losses, the attenuation in the material, and the diffraction losses. There is a standard way to get diffraction losses, and I think Papadakis has pioneered in that field. And the attenuation in polycrystalline media is also obtainable. It's not an easy process, but it certainly can be done, and it should be done by the individual, perhaps, or it can be done by the maker of the standard and provided to the individual if the individual feels that he doesn't have the equipment to do it.

DR. PAPADAKIS: It's probably good to a few tenths of a dB.

DR. TITTMANN: I would think so. With a dynamic range of 30 dB approximately, that's pretty good.

DR. C. C. MOW (RAND): All the papers I have heard so far have tried to look at the overall signature of the spectrum. Have you tried to correlate the peak and valleys with the normal modes of the inclusion shape? We have recently done a lot of calibrations with Prof. Pao from Cornell. We have found that the information lies in the wave number between the peak and valley. You can correlate that with the actual mode, the normal mode of the crack or sphere or cylinder, and from that you can correlate it by the shape that you are really dealing with or what kind of inclusion you have really got.

DR. TITTMANN: I'm well acquainted with that work. It's very beautiful work. I think it's a very viable technique. I haven't seen any such work for a sphere; it's mostly been done for cylinders.

DR. MOW: We did the cylinder with fluid in the cavity.

DR. TITTMANN: I see.

DR. MOW: I think the sphere cavity is also contained in a monograph that was published several years ago. If you want it, I'll send it.

DR. TITTMANN: Yes, I'd like to see it.

DR. JOSEPH HEYMAN (NASA, Langley): I'd like to make one point about this. This is a calibrator. It also calibrates the operator, for if he does not have the proper application technique, this would be easily determined by the non-agreement with the standard.

MR. CHARLES K. BERBERICH (Alcoa Tech Center): How do you intend to implement this procedure as a replacement for normal reference blocks?

DR. TITTMANN: As a replacement for what, please?

MR. BERBERICH: Normal reference blocks.

DR. TITTMANN: I guess I don't know exactly what you mean by implement. I have tried to describe the standards kit with X items and how to use each item.

MR. BERBERICH: I guess I'm referring more to the specification field. How do you intend to influence specifications to incorporate this procedure in lieu of the current procedures?

DR. TITTMANN: Oh, that's a totally different question. It is an important problem which we haven't addressed here. I think we will need a lot of help from people that are doing the implementation of the current standards to accomplish that.

DR. SY FRIEDMAN (Naval Ship R and D): How do you regard the reproducibility of this calibration standard as compared to the current standard? Now, that's a rhetorical question because prior to this talk and also earlier presentations, it was pointed out that the current standards are unreproducible. You have an 800 percent difference, I think I heard mentioned earlier today. What percent difference do you anticipate with this proposed standard?

DR. TITTMANN: Well, to answer that question takes a lot of time. Let me just say a few of the features where I think this procedure has some advantages. First of all, we're dealing here with a thoroughly theoretically characterized defect. The other standard, for example, the flat bottom hole, has not been described theoretically in terms of elastic theory. So, you don't really know what the scattering radiation pattern of that flat bottom hole should look like, even if you ideally could measure it.

DR. PAPADAKIS: And they haven't measured the attenuation in any of those blocks, although there may be 100,000 out in the field.

DR. TIEMANN: There's another problem in that your calculations essentially assume a rather good transducer, one with a uniform field pattern because you're calculating in your G factor the power transmitted per unit solid angle at zero degrees; actually, practical transducers can be very non-uniform and their beams can be skewed off in various angles, and your G factor in that case won't correspond to the actual transmission down the actual beam direction. Now, when a person tries to apply that transducer in an NDE environment, he's not really going to know which direction the beam is, he's just going to shoot it into the part and get an echo back. So, I think your G factor isn't quite adequate.

DR. TITTMANN: Yes, it is; I have taken that into account. Consider the following: suppose you are looking for a certain size of defect, a certain range of sizes. Then you pick a standard defect that is in that range of sizes of defect. Now, suppose the operator takes a poor transducer that has hot spots in it, whose beam is cocked off the normal to the transducer. When he measures that G factor, that G factor will be very, very low and would accurately reflect in his calibration the use of that transducer in his measurement with the unknown defect. I think this is an important question, and I think that's why this definition is so valuable, because it takes these problems into account explicitly. The operator quantitatively measures the quality of the transducer as a figure of merit just as he will be using it in the actual operation.

MEASUREMENT OF SUBSURFACE FATIGUE CRACK SIZE USING NONLINEAR ADAPTIVE LEARNING

A. N. Mucciardi
Adaptronics, Inc.
McLean, Virginia 22101

I would like to present some ideas regarding the current status of fatigue crack NDE, where the field could go, and then give a case example of a recently synthesized NDE (software) system for detection and sizing aluminum fatigue cracks.

Currently, NDE training protocol requires calibrated test specimens. The specimens may not be appropriate, for example, for calibrating a crack detection system, and this creates problems. Detection is accomplished via amplitude thresholds and the amplitude, of course, is often ambiguous. Defect location is usually performed by the time-of-arrival factors. Multi-paths and other spurious reflections can give create "ghosts" which permit false readings to the place. Reliance on an operator to minimize problems such as low signal-to-noise also causes variability in detection probabilities. Additionally, operator difficulties in coping with complex geometries is troublesome. So, what I am proposing consists of another NDE protocol in which test specimens are used, but they are chosen to be much more appropriate for the task. Rather than simple flat bottom holes, one may have the type that Bernie Tittmann described previously, or others more germane to the problem. This will increase the cost of fabrication and also necessitate the training of a "smart" signal processor and interpretive system.

Instead of only examining the reflected echo amplitude, the entire signal must be examined in order to exploit properly the maximum information available. This is one of the reasons why increased reliance will be placed on a germane set of specimens.

Defect location can be estimated much more accurately by using special (phase) processing techniques to mask out ghosts and other spurious reflectors. The reliance on an operator can be minimized by enhancing the kind of display the operator sees and also by providing the person with more quantitative information. In terms of comparing the two, it is our estimate that the cost to upgrade current NDE equipment, (after its development) is between 5 and 10 K; the main addition is an in-line processor that we call a "smart instrument."

The cost of the test specimens required to make the processor "smart" depends upon the application. The benefits derived are improved, enhanced echoes for signal processing, less reliance on operator interpretation, improved time-of-arrival discrimination, and better ability to separate superimposed echoes. We can eliminate the reliance on amplitude thresholds and consequently, use all other characteristics of the signal except amplitude for improved size and orientation estimates.

This proposed practice has been developed and tested in off-line software, and the software exists for creating such a smart instrument. What we need is experience in determining what a representative specimen set is, some experience with on-line hardware, and the best structural form for this processor.

I would now like to present a case example of the proposed NDE practice in terms of a project that was sponsored by the Air Force Materials Lab regarding detection of subsurface fastener hole fatigue cracks in aluminum.

The test specimens were half-inch aluminum plates, 2 3/4 inches by 5 inches long, into which a one-fourth inch "fastener hole" was drilled. A notch was made on the lower surface - this was put in a fatigue bending jig, and a crack was grown out of the bottom of the hole. Two samples had no crack at all, and 14 other samples grew cracks ranging from 11 to 279 mils (see Fig. 1).

Specimen No.	EDM Starter Notch Depth*	EDM Starter Notch Width**	Crack Length
00-000	---	---	0
01-000	---	---	0
02-011	.0026	.0022	.011
3-014	.0016	.0020	.014
4-018	.0016	.0019	.018
5-022	.0035	.0020	.022
6-027	.0020	.0020	.027
7-039	.0014	.0018	.039
8-048	.0019	.0020	.048
9-054	.0016	.0018	.054
10-073	.0019	.0021	.073
11-093	.0020	.0021	.093
12-113	.0024	.0019	.113
13-150	.0015	.0019	.150
14-192	.0017	.0018	.192
15-279	---	---	.279

*Depth along hole radius
**Width tangent to hole circumference

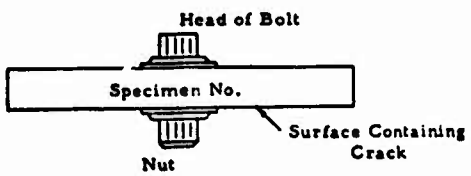

Figure 1. Crack lengths of specimens.

We wanted to not only detect cracks, but also to measure the subsurface crack length, particularly below 30 mils where detection presently is virtually nonexistent. The crack size range was logarithmically spread between 0 and 279 mils such that fifty percent of our sample cracks were less than 30 mils.

After the cracks had been grown, four more specimen cracks were grown in this range and destructively tested to verify the fact that we were dealing with quarter round cracks; that is, the surface length and the bore length were approximately equal. After the cracks were grown, a fastener was installed and torqued to the appropriate amount. Figure 2 schematically depicts the specimen plate without the fastener installed. The fastener hole and the crack are growing along the bottom surface. The crack is essentially a quarter round; the bore length and the surface length are nearly equal.

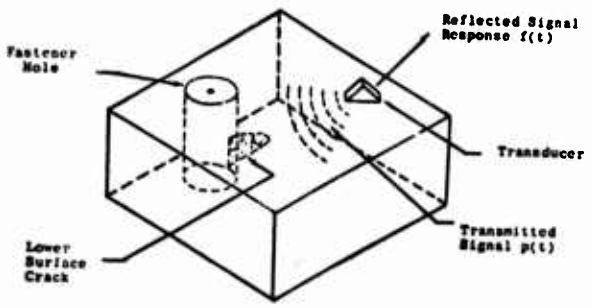

Figure 2. Simplified view of the ultrasonic test procedure.

The 10 MHz transducer is placed on a lucite wedge on top of the surface and an ultrasonic pulse is directed toward the crack at a 60° angle. The wave front interacts with a corner reflector made up of the hole, the bottom surface, and the crack. A reflection is transmitted back and recorded by the (same) transducer. The data were recorded by Bill Lawrie of Babcock & Wilcox.

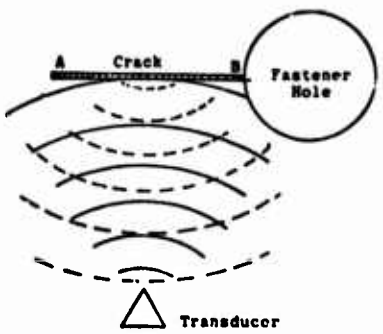

Figure 3. Illustration of interference effects as function of transducer viewing angle.
(a) wave patterns with transducer at normal incident position

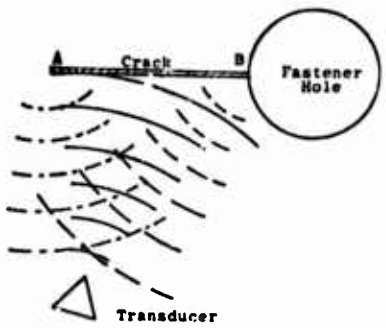

Figure 3. (b) Wave patterns with transducer at off-normal position

Figure 4 illustrates the kind of signal resulting from a corner reflector below the surface. This is an example of the base line noise level. There are really three events of interest.

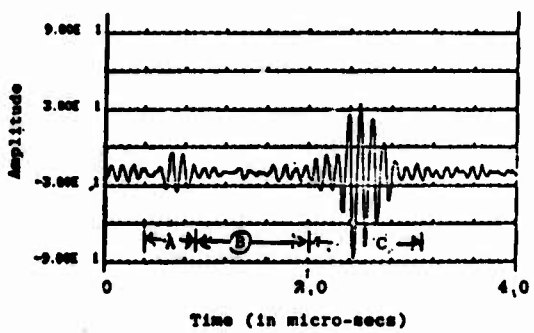

A = Response from hole.
B = Time between responses from hole and crack.
C = Response from crack.

Figure 4. Response from 14-192 specimen viewed at $\theta = 0°$.

First of all, the beam comes in and hits the side of the hole. It continues to propagate until it encounters the crack. Echoes are recorded from the hole and crack reflections as shown in Fig. 4. The hole is always there; the crack may or may not be there. So, the objective is to first find the crack and then to determine its size.

Figure 5 illustrates some of the problems encountered if only amplitude is considered. These are actual echoes from just the portion of the signal due to the crack. Notice that the echo from the 93 mil crack is larger than the 192 mil crack.

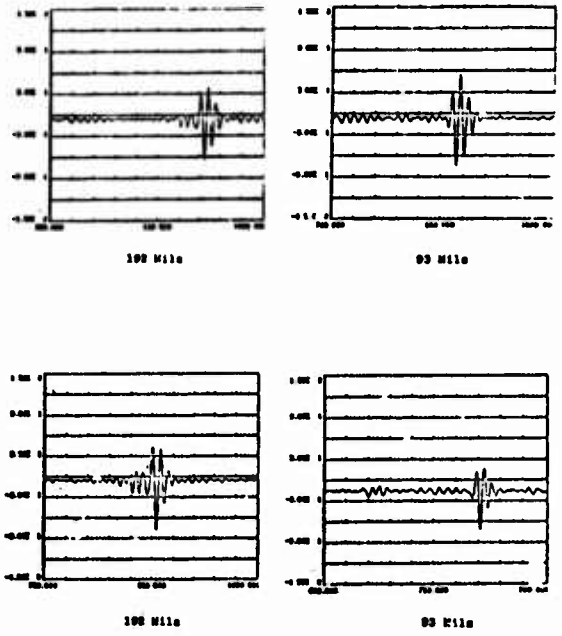

Figure 5. Ultrasonic waveforms recorded from two sample specimen cracks under different test conditions.

(a) Series 1: 192 and 93 mil crack signatures. Note the larger amplitude of the 93 mil crack. 1/

(b) Series 2: 192 and 93 mil signatures. 93 mil crack signature is considerably smaller.

1/The abscissa of each plot is time (μsec) and the ordinate is signal amplitude (arbitrary units).

It became evident that the fastener hole would have to be scanned in a circular manner to provide accurate estimates of crack size. Six viewing angles were chosen as shown in Fig. 6. The normal incident position is defined tc be $\theta = 0°$. As θ increases, the incident beam is reflected from the hole and from the two edges of the crack (as shown in Fig. 3). As expected, large cracks (i.e., greater than 100 mils) are visible at all viewing angles Cracks between 50 and 100 mils in length are mainly visible only at $\theta = 0°$; while cracks below about 30 mils are very difficult to see, and in fact, nearly impossible to detect.

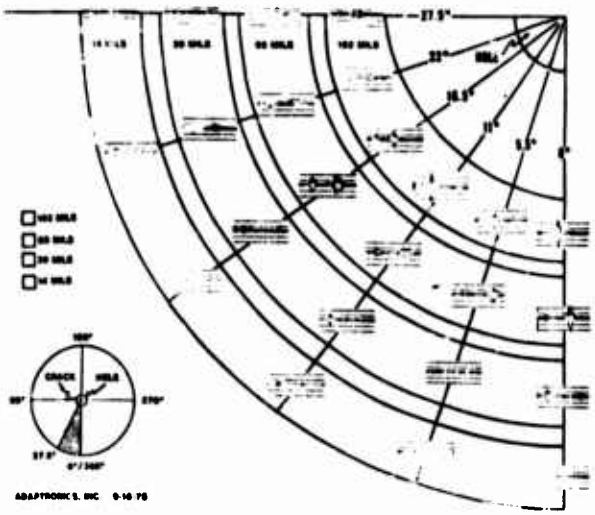

Figure 6. Ultrasonic scanning plan about hole.

We put together a (software) system to process this kind of information. Figure 7 is a scatter plot of our results showing the true vs. measured crack length, from zero to 279 mils.

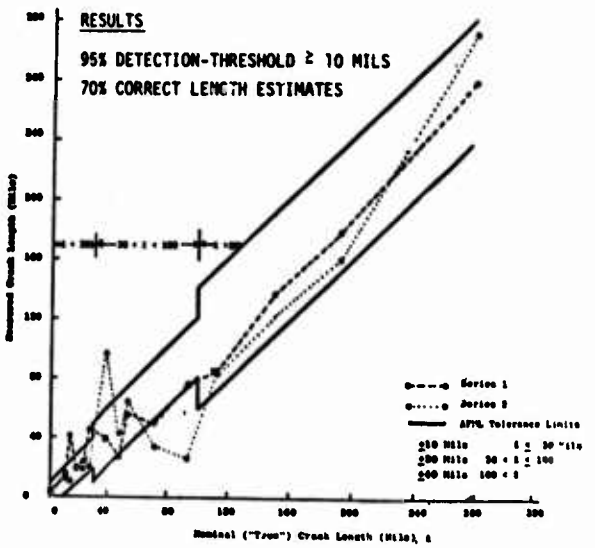

Figure 7. Performance of ALN quantitative surface/ subsurface fatigue crack length measurement system

The tolerance limits on the curve are according to AFML: if a crack is truly larger than 100 mils, a 40 mil error would be tolerable; if it is between 30 and 100 mils, a 20 mil error would be tolerable; if it is below 30 mils, a 10 mil error would be tolerable. So, as you can see, the Adaptronics system has the ability to detect cracks across this range, and also has the ability to measure cracks within 70 percent of the true crack length--even down to 11 mils. In fact, the "no" crack specimens were classified as cracks of just a few mils length. Furthermore, if these results are recast in terms of probability of detection, a threshold can be placed at any position of the abscissa, parallel to the ordinate, and a count of those cracks that were truly larger than the threshold and which were correctly classified as larger than the threshold can be made. The percentage of correct calls is an estimate of the probability of detection for this threshold setting. This threshold can be varied between 10 and 200 mils, and it is found that correct detection of cracks occurs 95 percent of the time. Not only are 95 percent of the cracks detected, but in addition, our system can size cracks to within 70 percent of the true value,on the average. So, here is a quantitative NDE system that really works in an actual environment.

The details of how the system works can be summarized in the following way. The transducer beam is directed such that it first encounters the hole and then contacts the crack (when aligned in a normal incidence portion, the main portion of the reflected energy will be directed back to the transmitter). As the transducer is swung around the hole, the beam will be reflected from the crack edges; however, most of the energy will be reflected away from the transducer. The reflection will come from the two edges of the hole, A and B, as shown in Fig. 3 and, depending upon the frequency transmitted and the length of the crack, these waves that are returning from A will return sooner than B. The A and B echoes may or may not be in phase. If they're not, they will destructively interfere; if they are, they will constructively interfere. So, these interference patterns are functions of, among other things, the size of the crack.

One can use these interference patterns as a method of inferring the size of the crack. To do this, we built a jig to mount our transducer for data recording purposes. On that jig we made a little slit and attached the transducer. The transducer was clamped down at a fixed radius from the hole so we could swing the jig around, such that the transducer was always at a fixed distance from the center of the hole (see Fig. 8).

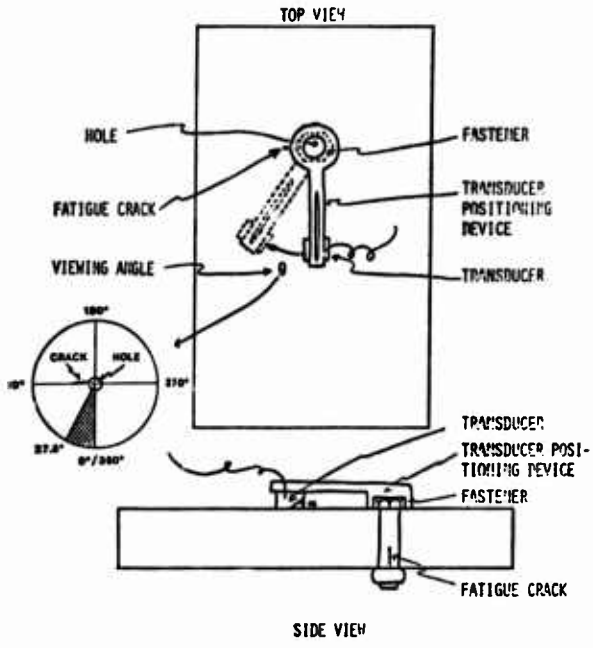

Figure 8. Fatigue crack ultrasonic recording equipment.

After a preliminary look at the data, we decided to record echoes between the normal incident position (which we defined to be $\theta = 0°$) up to 27.5 degrees away ($\theta = 27.5°$); we took 5.5 degree increments ($\Delta\theta = 5.5°$) which gave us six pulse echoes.

Signals were averaged to increase the signal-to-noise ratio. We determined that an average of 32 signals the optimum value because of the quantification level of our digital transient recorder (we were using an 8-bit, 2048-word biomation 8100 to digitize these transients). Digitizing at a rate of 50 MHz with an 8-bit transient recorder enabled us to accurately capture the 10 MHz transducer pulse echo. We determined that our usable frequency range was about plus or minus 4 MHz on either side of 10 MHz; or, 6 to 14 MHz.

The signal that is actually recorded is a composite of a number of subsytems: the pulser, the transducer that connects electrical energy to sound energy, medium, and finally, the discontinuity. Therefore, the recorded signal is sensitive not only to the defect but also to the transducer and the medium through which it propagates.

We wanted to minimize the effect of transducer and medium. To do this, the transducer was swung around to the side of the hole which had no crack. Another signal was recorded with the same transducer and medium but without the defect. Then, we deconvolved our "crack signal" with what we call our "reference signal." This was done by dividing by the reference signal in the frequency domain. Since the deconvolution process is a noise-inducing step, we had to filter the quotient signal to finally end up with a signal which was stripped somewhat of transducer and medium effects.

We then generated a number of parameters from these wave forms. Figure 9 is a plot of one of the parameters--total power--versus crack length the trend can hardly be called monotonic. This parameter was maximally correlated with crack size. This shows that no single parameter in a real environment is every going to be clearly correlated with crack size. However, even though there is no monotonic relationship with defect size, there is a general trend of increasing power with increasing defect size.

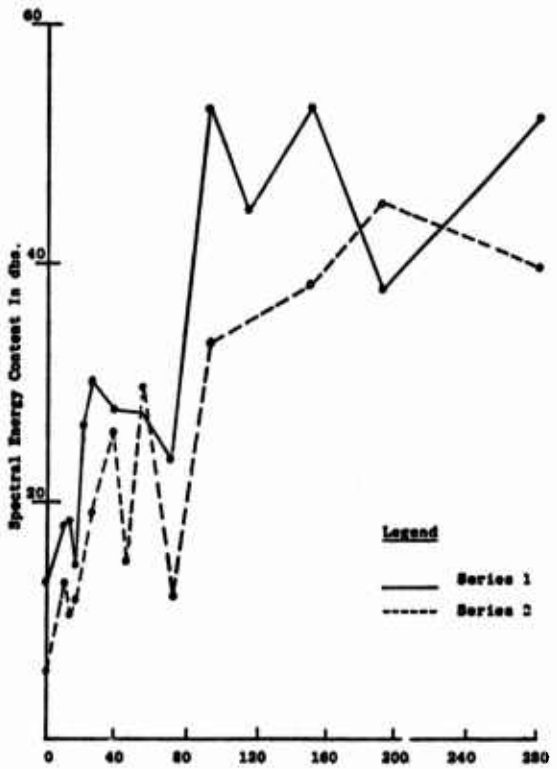

Figure 9. Plot of deconvolved total spectral energy versus crack length.

We generated a number of parameters from the power spectrum by dividing it into 1 MHz bands, and computing the percentage power in each band between 6 and 14 MHz. Small cracks ought to have more high frequency energy, whereas larger cracks should be more broad band. Other transformations were performed to look for echoes contained within the signal. A set of 31 descriptors or each echo were generated. A nonlinear polyramid model--called an Adaptive Learning Network--was synthesized. This ALN function mapped echo descriptors into a predicted defect size. The parameters are given in Table 1.

TABLE I. ALN Input Parameters

WAVEFORM	NUMBER	DESCRIPTION
POWER SPECTRUM	9	FRACTIONAL POWER IN 1 MHz BANDS IN RANGE 6 TO 14 MHz; TOTAL POWER
SPATIAL POWER	1	TOTAL POWER DIVIDED BY WIDTH OF SPATIAL RANGE
CEPSTRUM	20	NUMBER OF T's OBSERVED IN 10 EQUALLY SPACED BANDS BETWEEN 0 - 2, 700 NANOSECONDS; TOTAL CEPSTRAL VALUES IN THE 10 BANDS
TRANSDUCER ORIENTATION	1	SIN 9

TOTAL: 31

Since we wanted to be proportionately more accurate for below 30 mils, we modeled the logorithm of the crack length rather than the crack length itself. This spread the small values intended to bring in the larger values of crack size. What happens is that in synthesizing our model we forced it to be very sensitive to small errors in crack lengths below 30 mils and less sensitive about crack lengths above 30 mils (see Fig. 10.).

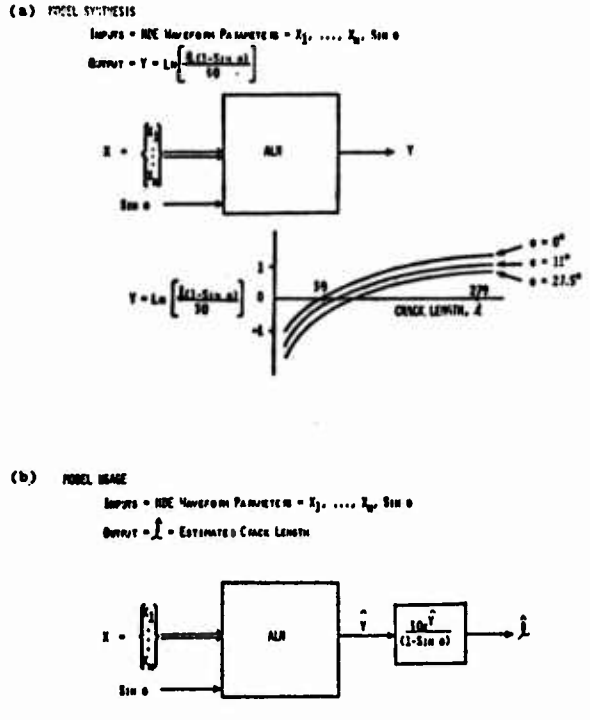

Figure 10. Quantitative surface/subsurface fatigue crack length measurement system.

In the usage phase we record an echo, generate the necessary parameters, make an estimate of the crack size logarithm, and take the antilog to produce the length estimate. The results were tested on new data as well as some of the data that were used to synthesize the ALN model (see Fig. 7.).

You can also recast these results into a probability-of-correct acceptance curve. In current practice, very little detection capability exists below about 40 or 50 mils, so our system is very accurate indeed.

In terms of placing this NDE system into the field, a "teething ring" transducer array would be best for rapid inspection of fastener holes. The transducers would be electronically fired and computer processing such as that described above would be used to establish the most nearly normal incident beam as well as the remainder of the parameter generation and crack size estimation steps.

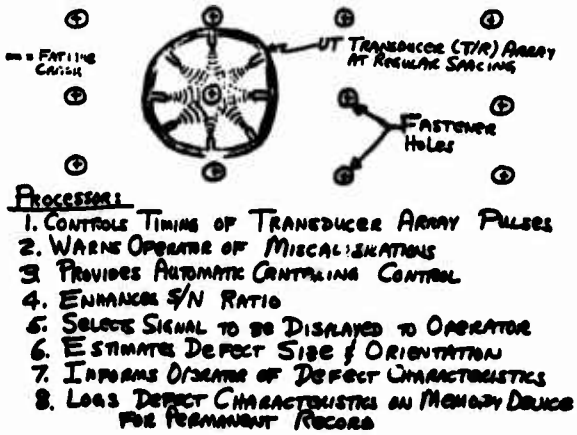

Figure 11. Schematic for "Teething ring" transducer array.

In summary, we have demonstrated the first quantitative system (at least in this kind of environment) that can detect and measure cracks in this size range. It is also the first quantitative system to show high insensitivity to different transducers and materials. We can process a pulse echo all the way to a crack size estimate within a few milliseconds in software per fastener hole.

DISCUSSION

DR. PAPADAKIS: Thank you. This looks as if we are getting new solution packages which are beyond the things we have been taught to expect in the past.

Since we're running behind, I'm going to ask you to question privately.

DEFECT CHARACTERIZATION-FUNDAMENTAL FLAW CLASSIFICATION SOLUTION POTENTIAL

Joseph L. Rose, Bruce Eisenstein, John Fehlauer, & Michael Avioli
Drexel University
Philadelphia, Pennsylvania 19104

Pattern recognition techniques are currently being applied to many signal interpretation problems in nondestructive testing. Simulearning technology combines various aspects of wave propagation analysis, pattern recognition philosophy, and signal processing theory in such a way as to outline procedures and establish guidelines for solving many problems in flaw classification. A portion of this paper will be used to present flaw classification problem statements and potential solution techniques along with simple data and analysis techniques.

Emphasis in the paper will be placed on a work description and analysis associated with a flaw classification problem of discriminating between ultrasonic signals that have been reflected from elliptical and circular side drilled electro discharge machined slots in a steel block. The flaw types used in this experiment are several elliptical holes with eccentricities, ϵ, from 0.15 to 1.0. The signals are sampled at a 100 MHz rate and quantized with an 8 bit word length. The signal processing is performed on a PDP 11/05 minicomputer.

Items discussed in this paper also include aspects of computational efficiency, waveform averaging, adaptive quantization, and Wiener filtering to suppress the effects of measurement and quantization noise. A novel deconvolution procedure was considered for removing the effects of the transmission medium and transducers and to enhance the discrimination between the flaw types. Feature extraction and pattern classification techniques that were used include the Fischer linear discriminant function, a declustering algorithm, and nearest neighbor classifiers.

Results obtained thus far indicate that for minor diameter to major diameter ratios ϵ in excess of 0.7, discrimination between elliptical and circular flaws is very difficult. For ϵ less than 0.3, discrimination is easy. Consequently, the feature extraction and pattern classification techniques have been concentrated on ϵ in the range 0.3 to 0.7 in order to establish the efficiency of the research protocol.

With the increasing importance of nuclear power plant inspection, pressure vessel inspection for the energy industry, and rail inspection for the transportation industry, there has become an urgent need for the development of reliable and precise flaw classification techniques. Emphasis has recently been placed on studying ultrasonic response variations as a function of flaw type, shape, size and orientation. Considerable attention is currently being placed on quantitative aspects of NDE, as illustrated by many of the research programs on scattering theories and flaw characterization work carried out by Rockwell International and the various sub-contractors in the ARPA/AFML NDE research program. Emphasis is being placed on obtaining an improved understanding of the physics and mechanics of wave interaction with a flaw.

The purpose of this paper is to review aspects of flaw classification work, but with the emphasis being placed on pattern recognition and signal processing, rather than detailed physics and mechanics. Physics and mechanics is used in a qualitative sense to improve data acquisition systems and to gain insight into potential signal processing and feature extraction techniques for solving critical problems in flaw classification. Frequency analysis has demonstrated some potential for solving problems of this type. The state of the art on this subject, however, is progressing very slowly because of the large number of parameters generally associated with flaw characteristics. Other transform signature techniques are also being studied, but it is becoming quite evident that computer search and analytical techniques are required because of the signature complexities and computational efficiency required to obtain satisfactory correlations and/or solution paths.

A brief review of two research papers is presented in the following paragraphs, followed by a sample problem of side drilled elliptical hole eccentricity classification. Concepts presented in the first two papers serve as background information in the development of the elliptical hole classification problem. The two papers are:

1) "Disk and Spherical Inclusion Classification Concepts" by J. Rose, Drexel University; Phil Mast, Naval Research Laboratory; and Phil Walker, Krautkramer-Branson, Inc. This paper was presented at the fall meeting of ASNT in Atlanta, Georgia, in 1975 and has been submitted to Materials Evaluation for publication.

2) "Flaw Classification Techniques in Ultrasonic Inspection" by J. Rose, Drexel University; L. Niklas, Krautkramer GMBH; P. Mast, Naval Research Laboratory. This paper is included in proceedings of the Eighth World Conference on Nondestructive Testing held in Cannes, France, September 1976.

The subject of simulearning is outlined next and is presented in references (1) and (2) above. Many signal interpretation procedures have been studied to date that rely on such simple data reduction techniques as peak amplitude analysis or arrival time analysis, or more sophisticated transform "signature" analysis. For many complex problems in ultrasonic inspection and flaw characterization, however, these simplified approaches to signal interpretation and classification are not adequate. The simulearning technique presented in this paper provides us with a procedure for obtaining complete experiences associated with data acquisition along with methods of complete analysis through signal processing in a computationally efficient fashion. Techniques are presented that

enable us to obtain a reasonable solution technique for material or flaw characterization, provided a solution is possible at all. The technique of simulearning is a hybrid concept integrating various aspects of analytical mechanics, wave propagation analysis, learning machine philosophies, various mathematical pattern recognition and signal processing techniques, and finally, human judgment. A simulearner can best be described as a logic system activated by a parametric input that searches for classifier parameters for solving specific flaw, material, or system classification problems in a computationally efficient fashion. Parameters related to this technique are fed into a numerical computation scheme or model that generates data representative of many real world flaw characterization problems. Large numbers of data sets are obtained either analytically, experimentally, or generated by some combined analytical-experimental technique. The amplitude-time signatures of the simulated flaw situations are then subjected to a class of fast linear (tensor) transforms, such as Fourier, Mellin, etc. This set of data forms the domain of definition for non-linear maps, the range being a pattern space. For example, amplitudes at N specified frequency coordinates of the Fourier spectrum may be used to generate a column vector or pattern with N entries. The simulearner will generate patterns of this nature using a class of known useful characteristics, such as 6dB down points, the maximum amplitude over an interval, etc. The simulearner will sequence through these "pure" patterns and evaluate each derived set as to its separability into classes and the relevancy of these class divisions to the particular problem at hand. The simulearner will then investigate the utility of hybrid patterns, that is, column vectors whose entries are disjoint in the sense that each is obtained from a different linear transform, followed by the non-linear feature extraction process mentioned above.

A proposed simulearning computation procedure is shown in Table I. Variations on the proposed scheme certainly exist. Discussions, definitions, and interpretations of the various items contained in the chart could be carried out with both enthusiasm and controversy. The chart does, however, provide us with one logical approach of solving many complex problems in flaw classification. Only portions of the chart are required for obtaining solutions to some problems. On the other hand, careful attention to every block may not solve some of the more complex problems in flaw classification.

TABLE I - A PROPOSED SIMULEARNING COMPUTATION PROCEDURE

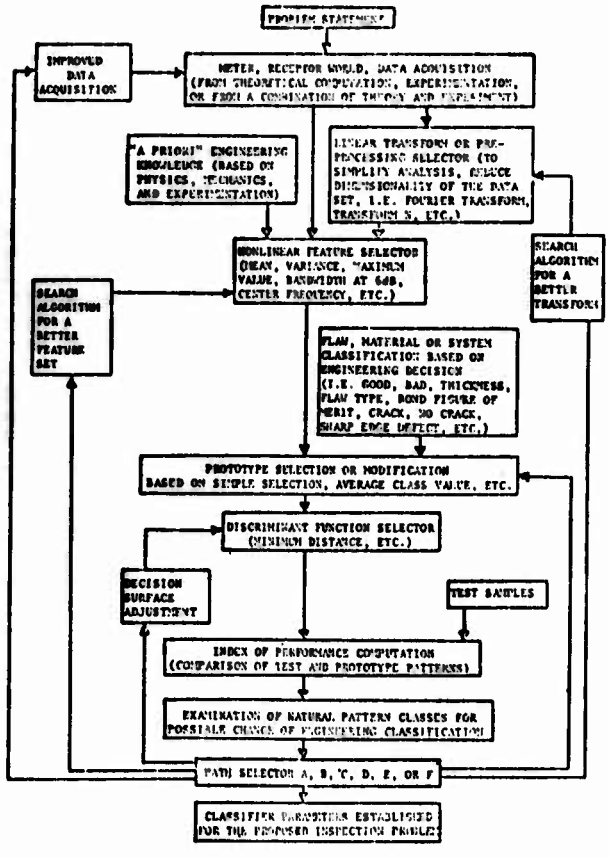

Disk and Spherical Inclusion Classification Concepts

Potential applications of pattern recognition and simulearning in flaw classification and ultrasonic inspection analysis are reviewed in (1). The sample problem of disk and spherical inclusion classification is reviewed. Analytical procedures for generating ultrasonic response function data sets for the spherical and disk inclusion in a fluid are presented along with amplitude time profiles, selected transform signatures, and finally the resulting index of performance values for the simulearning computation.

A computer program is reviewed in (1) to calculate the ultrasonic field pressure variations in a fluid resulting from ultrasonic wave interactions with arbitrarily shaped air type flaws in the fluid. The flaw is divided into segments of approximately equal surface area from which a spherical wave is propagated from each segment on the surface of the flaw. Although the problem of studying ultrasonic wave reflections from an air-filled inclusion in a fluid is not totally realistic, the data sets generated from this kind of problem allows us to evaluate qualitatively the concepts of simulearning, feature extraction from a data set, pattern recognition details, etc.

Data sets considered in the study consisted of two amplitude-time profiles, one for normal wave scattering at the sending transducer and one for normal wave scattering received at the receiving transducer located at a position x_2.

Ultrasonic pulse echo signals representing response echoes from either spherical or disk type flaws were generated as a series of sample data sets. Certain features of the ultrasonic response functions were chosen to be stored in the simulearner. Then, test data representing spherical and disk flaws of unknown size were compared with the prototypes in the simulearner in order to make a flaw classification prediction. Features selected for this comparison were Fourier transform amplitude C, phase angle phi, Laplace transform magnitude, and Mellin transform magnitude. The comparison of test data with the prototype data was based on the minimum distance classification technique.

In the first problem of sphere and disk classification, all sphere training points clustered nicely and were separated easily from the disk training points, regardless of the transform selected for the study. In this particular problem, there was no need for more sophisticated analysis utilizing either decision surface adjustment techniques that force the data into the correct class or the selection of some other transform. The straightforward procedure of transform selection and prototype selection based on average training data produces for us an index of performance in all cases of 100%.

Let us now consider the problem of disk size classification. This problem illustrates the values of transform selection in that a 100% index of performance value is obtained for only 2 of the 4 transforms studied. The Fourier phase angle and Laplace transform approaches produce index of performance values which were not acceptable.

Let us consider, for example, the problem of sphere size classification, a summary of which is outlined in Table 2. In this particular case, no index of performance value was 100%. The values shown, however, do indicate the best possible values for the case of the transform selected in combination with the minimum distance classifier since of 4 training sets considered in the study, 4 prototype points were considered, therefore forcing all of the training set information to appear in the proper class. The index of performance results shown in the table could perhaps be improved by considering some other transform or discriminant function type, or possibly by classification adjustment if engineering knowledge of the subject permits such action. As an example, if we were to combine classes 1 and 2 in Table 2, as a result of some engineering study, the index of performance would be 100% for the Fourier transform amplitude situations.

Table 2 - Index of Performance Results for the Simulearner Sample Problem of Sphere Size Classification

Engineering Classification	Prototype Used	Test Set Classification Using the Following Transform: Fourier Amplitude	Fourier Phase	Laplace	Mellin
Class 1 .005 to .02 spheres	.0[illegible]	.0[illegible], .0[illegible](na)	.0[illegible], .0[illegible], .05, .07, .09 (all na)	-	.0[illegible]
Class 2 .02 to .05 spheres	.04	.0[illegible]	-	.0[illegible], .0[illegible]	-
Class 3 .05 to .07 spheres	.06	.0[illegible]	.0[illegible](na)	.0[illegible](na), .0[illegible]	.0[illegible](na), .0[illegible](na), .05, .07, .0[illegible](na)
Class 4 .07 to .09 spheres	.08	.07, .09	-	.07, .09	-
Index of Performance →		[illegible]	[illegible]	[illegible]	[illegible]

(na) = not acceptable classification based on the specified engineering classifications

Although specific details of the complete simulearning computation procedure have not been carried out in (1), the subject of transform selection and its utility in varying the index of performance has been illustrated quite well. The concept of classification selection and adjustment is also illustrated quite well.

Flaw Classification Techniques in Ultrasonic Inspection

The work reported in Ref. (1) is theoretical in nature. In order to consider the more realistic experimental problem with such parameters as "noise" components, instrumentation variations, transducer effects, etc., it was decided to conduct a 10 flaw sorting study, the goal of the study being to separate the 10 test flaws into as many groups as possible. Flaw types considered in the study are presented in Table 3. The flaws were all manufactured by electrode discharge machining in steel blocks. Characteristics of the various flaws are presented in Table 4. The data acquisition technique considered in this study is illustrated in Fig. 1. Transducer 1 was considered as the sending transducer to the flaw machined in the test specimen approximately 25mm from the sending transducer. An angle beam transducer was used in position 2 to receive scattered normal and shear waves. The transducers used in this study were of 5 MHz center frequency with a 6dB down bandwidth of 3 MHz. The angle beam receiving transducer was rated at 45° in steel. The data was recorded with a Biomation 8100 analog to digital converter and stored in a PDP 11/05 minicomputer. The data points were stored along with the corresponding Fourier transform and phase angle.

TABLE 3 - ELECTRO-DISCHARGE MACHINED SIDE DRILLED FLAW TYPES

Type 1		Normal Sharp Edge Defect
Type 2		Inclined Sharp Edge Defect
Type 3		Cylindrical Defect
Type 4	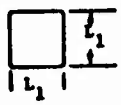	Rectangular Edge Defect
Type 5	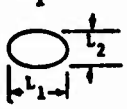	Elliptical Defect

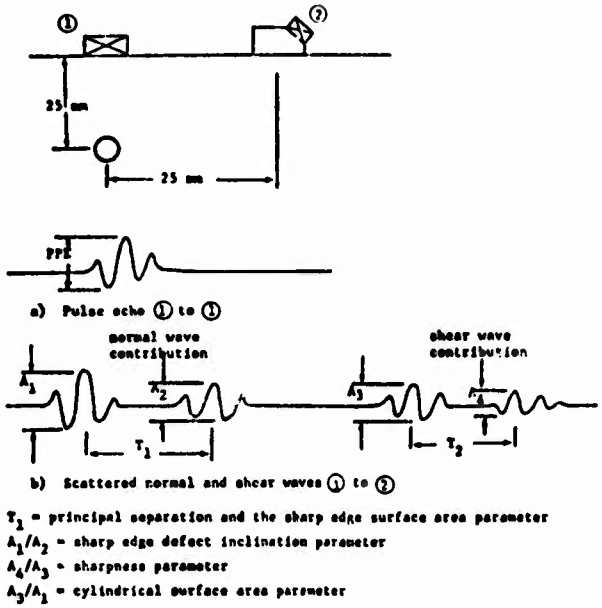

Figure 1. Data acquisition technique.

TABLE 4 - TEST SPECIMEN FLAW CHARACTERISTICS

FLAW NO.	TYPE	L_1(mm.)	L_2(mm.)	θ
1.	1	4.76	-	0°
2.	1	3.18	-	0°
3.	4	3.18	-	-
4.	1	2.38	-	0°
5.	2	3.18	-	30°
6.	2	3.18	-	45°
7.	3	4.76	-	-
8.	3	3.18	-	-
9.	3	1.59	-	-
10.	5	3.18	2.38	-

Combinations of the parameters A_1, A_2, T_1, A_3, A_4, and T_2 were studied in detail. After several attempts at classification, it was found that the 10 flaws could be separated nicely by considering the parameters defined below.

- T_1 = principal separation and the sharp edge surface area parameter
- A_1/A_2 = sharp edge defect inclination parameter
- A_4/A_3 = sharpness parameter
- A_3/A_1 = cylindrical surface area parameter

The final sorting procedure for this problem is illustrated in Table 5.

TABLE 5 - A SORTING PROCEDURE FOR THE 10 FLAW FEASIBILITY STUDY

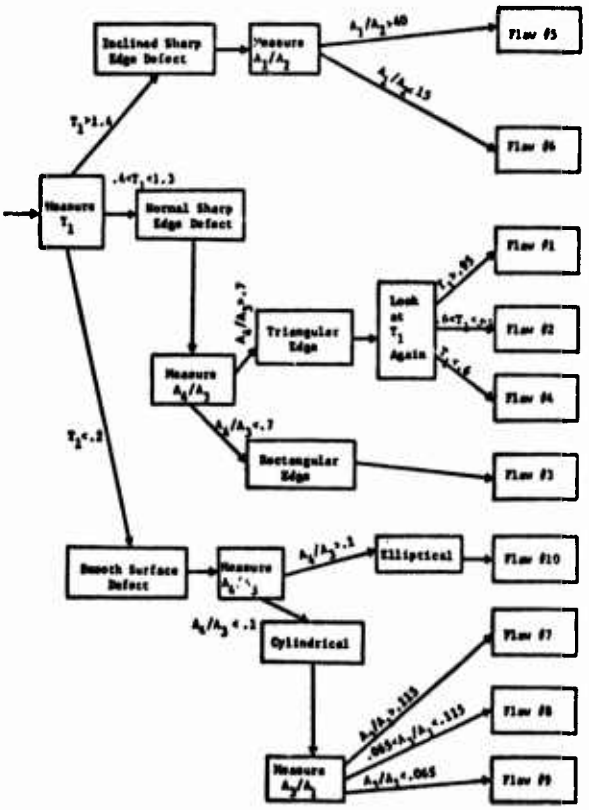

Additional work is currently being carried out that examines various flaw cluster groups, etc. A problem encountered quite early, however, in the new work was that of classifying various elliptical shapes. The purpose of the sample problem, therefore, presented in the next section, is to study the elliptical eccentricity classification problem in detail.

Elliptical Eccentricity Classification Study

The subject of elliptical cavity eccentricity classification is reviewed in this section. As indicated earlier, emphasis will be placed on noise aspects of the classification problem.

The signal processing techniques described below were employed to reduce random variations, or noise in the received ultrasonic signal. Although these techniques are necessary for complex operations such as deconvolution, they can also greatly improve the performance of simple classification algorithms. In preliminary studies, the discrimination between signals reflected from circular flaws versus those reflected from elliptical flaws has been poor, especially for elliptical flaws with eccentricities greater than 0.5. Three elliptical flaws and a circular flaw, all with the same major axis diameter, were assembled as shown in Fig. 2. Typical signals arising from each flaw type are shown in Fig. 3, utilizing data acquisition pro-

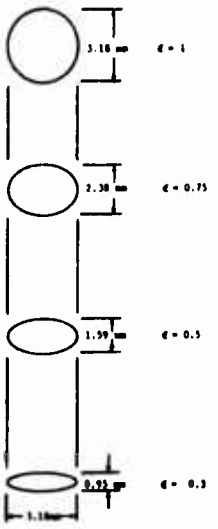

Figure 2. Elliptical test flaws.

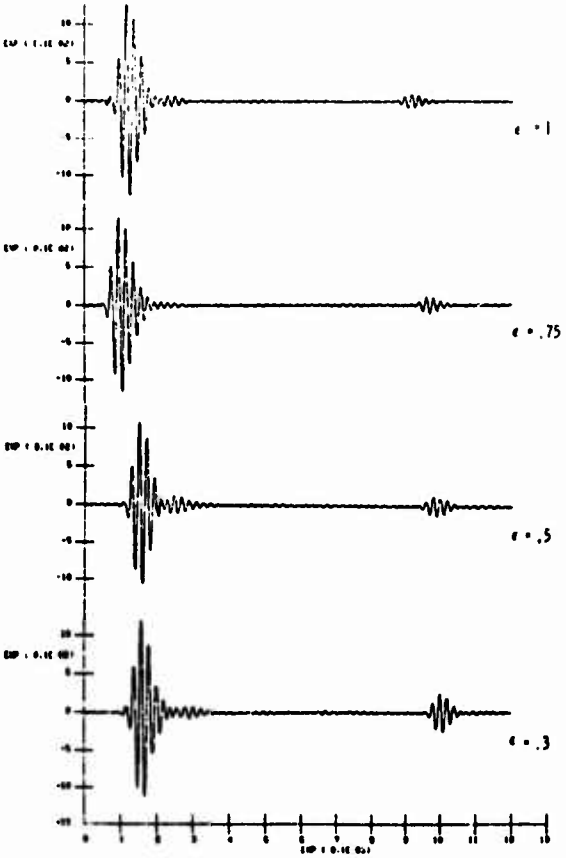

Figure 3. Signals from test flaw types.

cedures illustrated in Fig. 1. The shear wave amplitude, normalized by the longitudinal wave amplitude, appears to increase with decreasing eccentricity. This feature, termed the shear strength, performed unsatisfactorily as evidenced by the overlapping probability density functions in Fig. 4. The density function estimates are based on approximately 120 points for both $\epsilon = 1$ and $\epsilon = 0.75$, and approximately 50 points for each of the other two classes. The probability of error in discriminating between $\epsilon = 1$ and $\epsilon = 0.75$ is approximately 30%, between $\epsilon = 0.75$ and $\epsilon = 0.5$ approximately 3%, and negligible between $\epsilon = 0.5$ and $\epsilon = 0.3$. By employing noise reduction procedures, this performance can be greatly improved as indicated in the following sections.

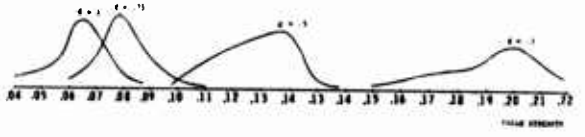

Figure 4. Probability density functions of shear strength before signal processing.

The primary sources of noise contaminating the ultrasonic return pulse are the placement noise, the measurement noise, and the quantization noise, as shown in Fig. 5. The placement noise includes the effects of the material, the coupling, and varying transducer placement. This noise term affects the signal in a complex manner, and was minimized by positioning both the sending and receiving transducers to maximize the energy in the reflected acoustic signal.

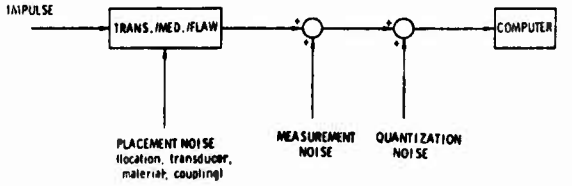

Figure 5. Primary sources of noise.

Measurement noise, sometimes called thermal noise, arises mainly from the wideband amplifiers used to amplify the ultrasonic signals. One way to suppress measurement noise effects is to increase the signal energy. Since the received signal is repetitive, a simple averaging procedure is also possible. The variance of the measurement noise term using the latter method is reduced by a factor inversely proportional to the number of waveforms averaged.

However, in this problem the signal plus measurement noise is quantitized by an 8 bit analog to digital (A/D) converter. At each sampling instant the signal is assigned to one of 28 or 256 quantum levels. This step can be modeled as the addition of a quantization noise term whose probability density function is uniform. With the biomation 8100 A/D converter used in this project, the quantization noise has a mean of +Q/2 for positive signals and -Q/2 for negative signals, where Q is the quantum step size. The variance is proportional to Q^2. The effect of the quantization can be neglected when the signal is large compared to Q.

However, normally the range of the A/D converter is set to accommodate the largest signal encountered in the received signal. The low level signals therefore are severely degraded by the quantization. In particular, the shear signal may only reach the 8th or 10th quantum levels. The result is that the shear strength can only be measured approximately due to the quantization noise.

The obvious way to decrease the quantization effects is to increase the number of quantum levels. However, since this option wasn't available, an alternate scheme, termed adaptive quantization, was implemented. The signal is stored in the computer in the usual manner. The ultrasonic signal's amplitude is next increased by a fixed amount. Some portions of the signal are now clipped, but these can be detected since they reside in either the lowest or highest quantum levels. The remaining sample values, which now span a greater number of quantum levels, can be rescaled to their correct values in the computer. Thus the quantum step size is effectively reduced for the lower amplitude signals, improving the signal to quantization noise ratio.

To test these signal processing procedures, each signal was stored in the computer, amplified by 20 dB and rescaled. This process was repeated 6 times, and the results averaged. An example of a signal before and after processing is shown in Fig. 6.

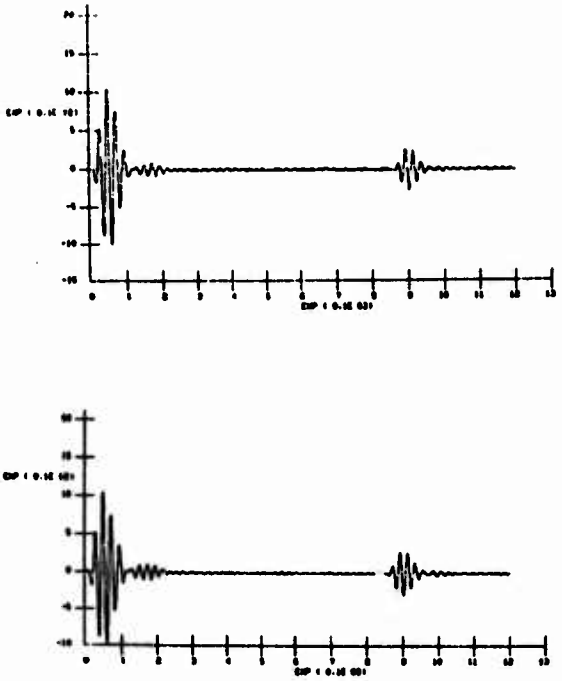

Figure 6. Typical signal before and after processing.

The shear strength parameter measured from the processed waveform now discriminates between the various flaw classes as shown in Fig. 7. The estimated probability of error for approximately 20 points per class is about 5% for discriminating between the circle and the ellipse with ϵ =0.75, 2% between ϵ =0.75 and ϵ =0.5, and negligible between ϵ =0.5 and ϵ =0.3. The main source of error is due to careless transducer placement and not quantization or measurement noise.

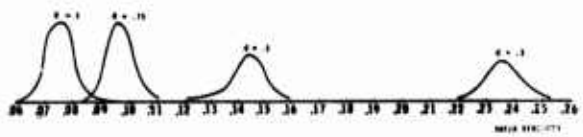

Figure 7. Probability density functions of shear strength <u>after</u> signal processing.

Further signal processing may be necessary for more complex feature extraction. For example, the averaged and adaptively quantized signal still contains high frequency components due to noise. Some type of low pass filtering is required, for example, if deconvolution is attempted, since this emphasizes the high frequencies. Preliminary tests indicate that the waveform averaging and adaptive quantization described in this paper, followed by filtering out all frequency components above 15 MHz, provides a signal whose major variation is due solely to placement noise. The low pass filtering had little effect on simple features such as shear strength, and, hence, wasn't incorporated into the present test.

Further improvements in performance can be effected by improving the classification algorithm. For example, additional features can be used to increase the reliability of the classifier, or to permit the assignment of waveforms into classes other than circular or elliptical.

One approach to incorporate additional features is to implement a Bayes decision rule. The Bayes rule is the optimal decision strategy in the sense of minimizing the probability of error. Also, the Bayes classifier can be used to evaluate feature sets to determine which features are needed for discrimination and which can be discarded. Although the Bayes approach requires knowledge of the multivariate probability density functions for each pattern class, these can be estimated from test waveforms.

In conclusion, it has been shown how a simple signal processing scheme comprised of waveform averaging and adaptive quantization can improve the performance of a pattern classification system.

Acknowledgement

We would like to thank Krautkramer Branson Inc. for their motivation and minicomputer support of various phases of this program of study.

DISCUSSION

DR. PAPADAKIS: Are there any questions?

MR. PAT RYAN (DOT): Could you select the quantizationized problem with logarithmic compression before quantizing or would that louse something else up?

DR. CARSON: I don't know for sure.

DR. TIEMANN (General Electric): I know the answer to that. The problem is that the wave form crosses zero and so you can't really, and it goes negative; so, you can't take logarithms.

DR. PAPADAKIS: Any others?

DR. SY FRIEDMAN (Naval Ship R and D Center): The word shear strength in the presentation - I'm just wondering how your measurement related to shear strength?

DR. CARSON: This is the shear wave--reflected shear wave.

DR. FRIEDMAN: Oh, not shear strength but reflected shear wave. Thank you.

DR. PAPADAKIS: Good. Thank you very much.

THE NDT PROGRAM AT STANFORD UNIVERSITY

G. S. Kino
Ginzton Laboratory
Stanford University
Stanford, California

Jerry Tiemann talked this morning about various ways of giving a paper. I was undecided what to talk about, so I thought I would tell you a little about a lot instead of a lot about a little.

Some of the things that are going on at Stanford include my own, Shaw's, Auld's and Quate's work. In particular, one of the things that was mentioned this morning which I think is very exciting, is Shaw's work on PVF_2 plastic transducers. He is obtaining very broad bandwidths of the order of 10 MHz with absolutely flat responses. These are very impressive transducers, and I think they are going to be very important in the future.

We are also carrying out a great deal of research on acoustic imaging in various frequency ranges. Some examples are the Fresnel lens of Auld, the acoustic microscope with 1 micron definition of Quate, and the electronically scanned acoustic imaging arrays by Shaw, Waugh, and Kino. In this work, we have, perforce, been very much involved in how to make transducers for imaging systems. So, I will spend the first part of my talk discussing transducers, and try to relate this to some of the things we have heard in other talks on aircraft materials.

We are basically concerned with various kinds of signal processing techniques. These are the kinds of things that an electrical engineer, when he first meets NDT, says, "Oh, this looks interesting, why aren't they doing more signal processing?" So, we come along and we try to do more signal processing. Some of the signal processing is aimed at imaging, and using some of it for improving the signal to noise ratio and some for pattern recognition.

One obvious approach is to say, "Phased arrays ought to be good; we ought to be able to use, instead of one transducer, a large number of transducers. If we can do that we can gather information much more quickly." Mucciardi talked about one aspect of this. He usually moves one transducer to several places; but he ultimately talks about using several transducers, and then use signal processing to essentially deal with that information at a relatively high speed. Here we shall talk about other techniques.

If one wants to make a transducer array, one must have a large number of separate elements. Some of the problems and structure are illustrated in Fig. 1. Typically, they are put on a backing medium which is, in our case, tungsten powder in epoxy. They may have matching on the front with matching layers and so on, and they have to have slots cut between them to separate them, so that there is not too much coupling between them. The immediate problem is to learn to make one transducer correctly, because, with an array, one needs N identical transducers. If one cannot make single transducers correctly and reproducibly, then the problem of making N transducers in an array is insuperable.

ACOUSTIC TRANSDUCER ARRAY DESIGN

Theoretical Problems	Technological Problems
Description of extensional mode of transducer element of near square cross-section	Fabrication of high loss high impedance acoustic backing
Description of effective backing impedance seen by slotted element	Selection of $\lambda/4$ matching materials
Effect of finite bond thickness on response of element	Slotting composite material
Design of acoustic matching layers into load medium	Structure to create acoustically matched elements
Description of cross coupling between array elements	Thin bonds for matching layers
Effect of cross-coupling between elements on element response	Fabrication of strong thin face plate with low acoustic cross-coupling

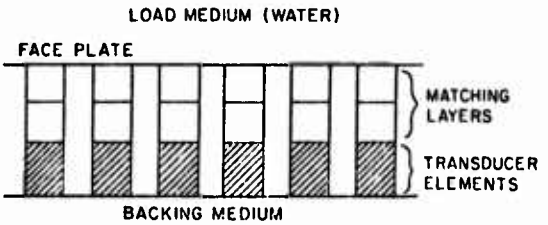

Figure 1. Acoustic transducer array design.

So, we have been dealing with that problem and it was very interesting to me to listen to the people talking about composites yesterday, because the story is much the same with our tungsten epoxy backing. In our case, we want a tungsten epoxy backing, because it is about the only material that one can use which has a high impedance and a high loss to match the impedance of the ceramics typically used in a transducer. When we first started in this field, we tested a number of commercial transducers. They vary, one from another, quite rapidly. The reason is that it is very difficult to make the tungsten epoxy uniform. So it was very interesting to hear what the composite people were saying, for they use just the same tricks as we do. We are very careful about sputter cleaning the back of the PZT that we use; we sputter down nickel on it; we then put the tungsten powder on the back of the PZT in a press so that it is pressed uniformly; we vary the pressure to vary the packing density of the tungsten powder, and then we vacuum impregnate the epoxy. In this way, we get very uniform characteristics.

Figure 2 shows the calculated impedance of a slotted transducer element, and you can see that the calculated and the experimental results are in excellent agreement. There are some slight differences, but most of them are explainable. It will be seen that one can get the order of an octave bandwidth with these devices. We can also predict their frequency, which can be a problem with rectangular resonators. But they are very inefficient for exciting an acoustic wave in water. One of the things that would be desirable is an efficient transducer: for this one wants matching on the front rather than on the back, so that most of the power goes into the water rather than into the backing.

Now, Jerry Tiemann will differ with me, obviously on this, but we ar -t interested in looking at objects 1/8" away. We are interested in imaging systems where we might get 10 cm or more away, so our problems are different.

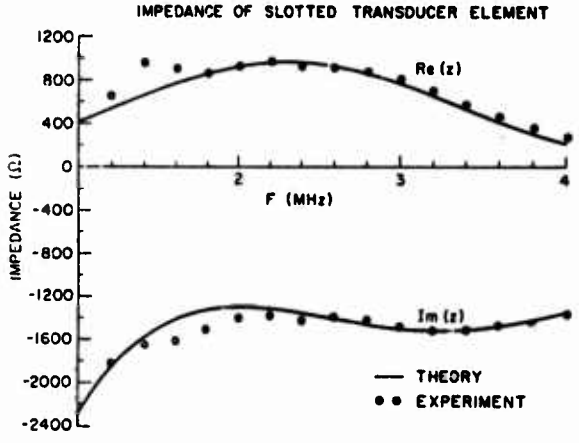

Figure 2. Impedance of slotted transducer element.

We have been working to get the bonding technology right for the λ/4 matching layers we require. We have been successful and have used multiple layers to match from water to PZT. And, again, we think the technology is in pretty good shape, although we have only done this so far with half inch diameter transducers. A result for a PZT5A transducer with two λ/4 matching layers of glass and epoxy is shown in Fig. 3. We have obtained about an octave bandwith with a net return loss from transmit to receive and back again of about 3½ dB's. The theory, in fact, predicts about 1½ dB's, but we haven't taken losses in the transformer and the matching network into account. Otherwise, theory and experiment are in very good agreement.

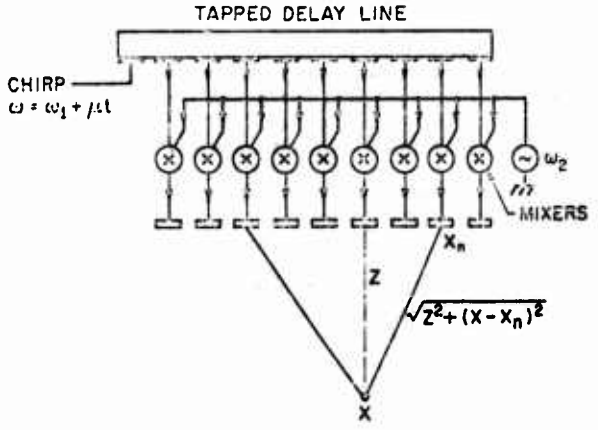

Figure 3. Illustration of the arrangement transducers-delay line.

Now, what do we use these transducer arrays for? Last year and the year before I described the basic imaging system that we have been working with, which, of course, uses an acoustic array. So, I am not going to give a long description of this imaging system. I will just refresh your memories slightly.

In Fig. 4 is shown a transducer array used as a receiver. Each element of the transducer is connected to a mixer which mixes a signal from an element with a signal from a tap on an acoustic surface wave delay line. The whole point of this operation is to synthesize the action of a lens by signal processing. The wave front emitted from a single point is spherical; this implies that it will have a parabolic variation of phase along the transducer array. When a signal from an element of the array of frequency ω_s is mixed with a signal of frequency ω from the corresponding tap on the ASW delay line, a product of the two is formed. The output at the sum frequency $\omega + \omega_s$ will also be the sum of their phases. And, if you now sum all the phases from all the mixers, you can cancel out the parabolic variation of phase by using a signal on the delay line with the correct parabolic phase variation. But from a different point source the phase variation will be different, and so the system will not respond in the same way. Thus, we have made a matched filter for a particular point source in space.

The way we do this is very simple. You put in a signal that has a linear variation of frequency along the delay line. In other words, a linear variation of frequency going in that becomes a linear variation of frequency spatially, becomes a parabolic variation of phase.

The basic signal needed on the delay line is just a so-called linear fm chirp. This produces a parabolic variation of phase along the delay line which matches the parabolic variation of phase from the array; the sum of the two is a constant. When we insert this signal in to the delay line, it travels along it and gives a linear scan along a

line parallel to the array automatically. In addition, by varying the so-called chirp rate, the rate at which the frequency varies in time, you can, in fact, vary the focal length. So, it is an electronically variable focusing system.

In a reflection mode, one can use this system as a transmitter or receiver. In essence, the chirp system acts like a lens which is moving along, and it moves fast. It moves at essentially acoustic wave velocity on the acoustic surface wave delay line, which is comparable to the acoustic wave velocity, say, in water.

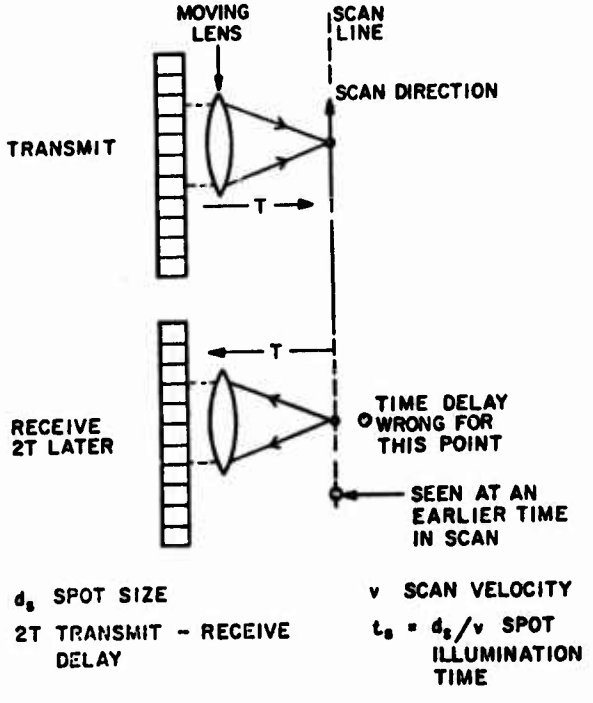

Figure 4. Transducer array used as a receiver.

In a B mode reflector imaging system, as illustrated in Fig. 5, we send out a transmitted signal which is focused on a particular point and then, as the lens moves, the point scans along a line. After the appropriate time delay, we turn the array into a receiver, and pick up a signal from the same point. Thus, the lens is opposite the point at the appropriate moment and picks up a signal from it. We obtain a definition appropriate to the transverse definition of the lens, but we also get a good range definition, because if a signal from the wrong range reaches the array, the lens has moved past by the time the signal reaches the array.

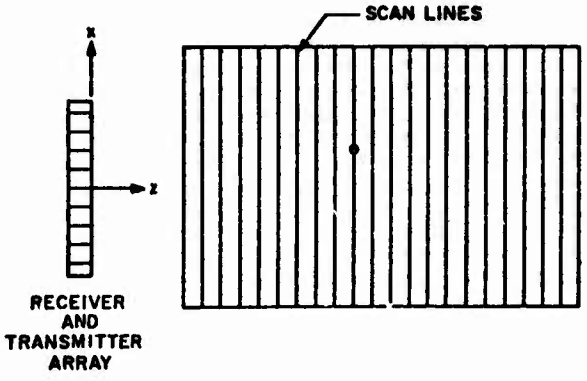

Figure 5. B-scan - scan lines parallel to array.

In practice, we focus on one line, and scan along it with the appropriate time delay between transmit and receive. Then we change the time delays and the focal length of the lens to the next line and scan out a raster, as shown in Fig. 6, perpendicular to the array. We display images in the usual way by using the amplitudes of the received signal to modulate the intensity of the cathode ray tube which is being scanned in synchronism with the acoustic scan.

Last year I talked about the reflection we obtained in water. I also talked about transmission images in bonded epoxy samples and boron fiber reinforced epoxy samples. This year I will show you some of the kinds of things we have done in metals; this is basically an illustration of what real time imaging systems can do.

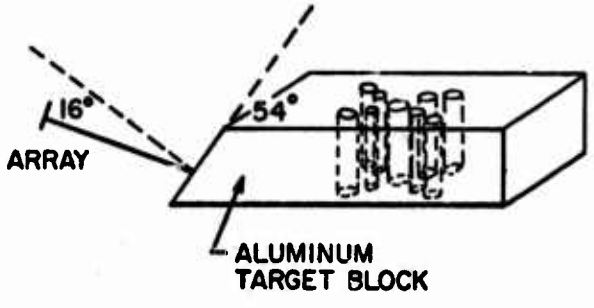

Figure 6. 2.0 MHz shear wave B-scan imaging in aluminum.

Now, to obtain images from the interior of a metal sample, we have been using shear waves. We have cut a block in the appropriate way, as shown in Fig. 7, and insert the beam at the right angle to excite a shear wave propagating along the metal parallel to its surface. If the beam is properly focused in water, it will focus and scan, in fact, in the metal.

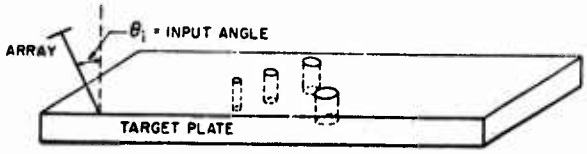

Figure 7. Schematic of setup to excite Rayleigh waves and Lamb waves in target plates. For Rayleigh waves in aluminum $\theta_i = 28°$.

Two sets of results from a series of holes drilled in a piece of metal are shown in Fig. 8. The top set is taken at 1.7 MHz; the bottom set at 2.75 MHz. You can see that we can delineate very closely both the transverse position and the distance away from the array of the holes.

Now, we can use the same system to excite surface waves or Lamb waves by coming in at the appropriate angle, as shown in Fig. 9, and we can get focused surface waves, Rayleigh waves, or Lamb waves, as the case may be.

If you want to look at cracks, the problem is more difficult, because they are specular reflectors. So, the problem with an imaging system in the present form is that the return signal only comes from a limited range of angles. So, unless the crack is normal or essentially parallel to the surface of the transducer array, one really has trouble obtaining a good image of the crack. However, one might expect that the ends of the cracks, according to the Keller theory, would, in fact, radiate. We have been able to illustrate this effect by showing that, as the crack is rotated, an image of the end of the crack is still seen. The point about such a result is that one does see the ends of a crack with this kind of technique. But, I don't know really how reliable it is, because the basic problem is that small nicks also show up the same way, at least with surface waves, and this experiment was carried out with surface waves. But it is an indication that you do, in fact, see the direct scattering from the ends of the cracks.

Now, I want to talk about another signal processing technique. Some people have been talking about correlation; I want to show you another type of device that carries out that kind of operation. I won't go into the details of how this device works other than to say it is a surface wave delay line in which there is interaction of the waves with silicon. By reading a signal into

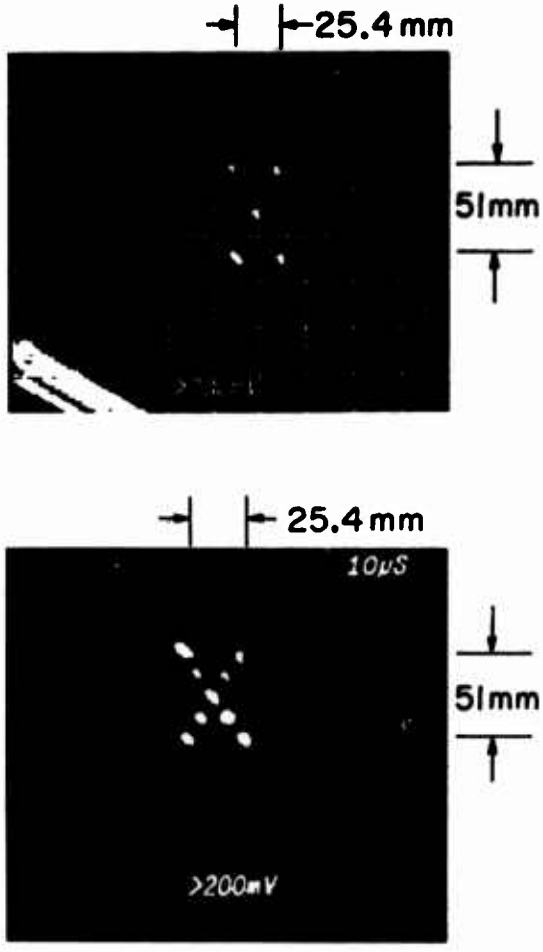

Figure 8. B-mode shear wave images of 2 mm diameter holes in aluminum block.

A. f_0 = 1.7 MHz; scan velocity =2.54mm/μsec

B. f_0 = 2.75 MHz; scan velocity= 2.0mm/μsec; central hole is 150 mm from input end of target block.

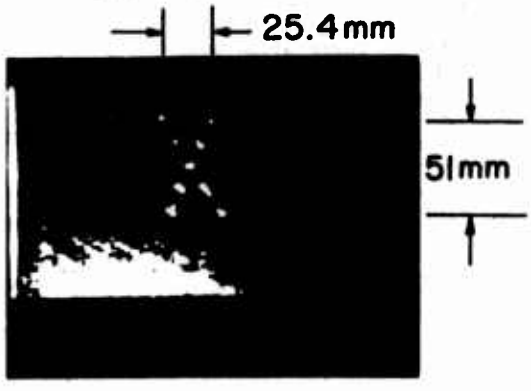

Figure 9. B-mode surface wave image of 2 mm dia. holes shown in Fig. # 6.

f_0 = 1.3 MHz; scan velocity = 2.54 mm/μsec.

this delay line, in an appropriate way, it can be stored in PN diodes laid down in the silicon. Later, another signal can be read into the device; the output is then the correlation between the original signal and the later signal. This, we believe, will become a very powerful tool for this kind of work. A schematic diagram is shown in Fig. 10.

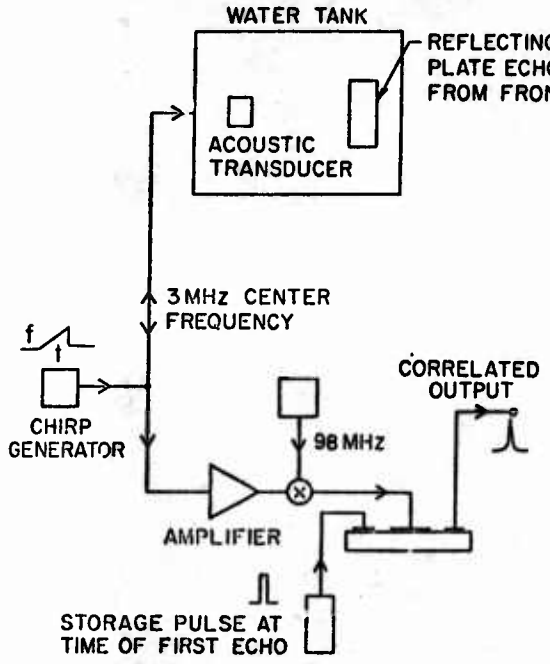

Figure 10. Schematic of the acoustical pulse echo system.

We carried out an experiment to demonstrate how to use this surface wave correlation device in an A scan system. We took an acoustic transducer and read read it into storage, as shown in Fig. 11. The whole point about this operation is that we can store such a reference echo on the device then correlate it with a later echo. If the acoustic transducer distorts these echoes, the reference and a later echo will both be distorted the same way. If the distortion is basically phase distortion, the correlation output will eliminate the phase distortion and a short pulse obtained. Alternatively, if one of the references echoes is a known defect, we can correlate it with the signal from an unknown defect to see if they are the same. The experiment here was to compensate for a poor transducer, somewhat like White's experiment carried out earlier in a different way.

We took a good transducer with a good impulse response; we read an FM chirp into it, about 6 μsec long, and the first echo stored on the storage devices. We then correlated it with a later echo and we obtained a correlation peak which, in fact, is a bit wider than the original good impulse response of the transducer, as shown in Fig. 11a and b. But then we took a poor transducer with a bad impulse response and did the same thing. You can see that, essentially, by using this adaptive device we obtained a correlation peak which is much narrower than the response of the transducer, Fig. 11c, d and e.

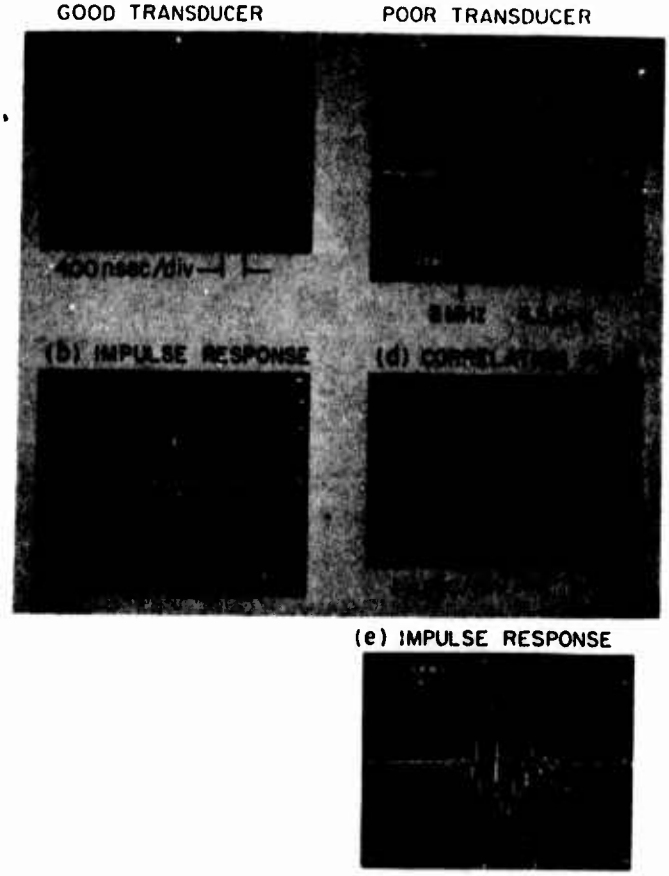

Figure 11. Pulse echo experiment results with both good and bad transducers.

This is an adaptive system; a very crude system, as yet. But the basic idea here is to use signal processing to clean up the response of a transducer or to use it for pattern recognition by using correlation techniques. Such devices, we believe, can make a great deal of difference to this field and, in particular, to pattern recognition. Thus, we have demonstrated that by using various kinds of signal processing techniques, it is possible to do something about speed recognition of flaws and location and determine the size, and so on, of flaws.

Thank you.

DR. EMMANUEL PAPADAKIS (Ford Motor Company): Good. Questions?

DR. JERRY TIEMANN (General Electric Company): Gordon, why does an almost periodic impulse response give a single peak and a correlation function? On the last slide, the right-hand side. I just think your student had the knobs turned wrong.

DR. KINO: No way. First of all he's transferring it up to a carrier and you are always taking the product. A minus times a minus really gives you a plus, and a plus times a plus gives you a plus also, and so you tend to get a positive--

DR. TIEMANN: But then, when you shift it by one half wavelength, you get a minus, and an almost periodic function has an almost periodic correlation function.

DR. KINO: But what we're using is a long chirp, in fact, so we're getting some more averaging.

DR. TIEMANN: -- you get the impulse response of the transducer back?

DR. KINO: No, not if you're correlating chirps.

DR. TIEMANN: Oh, yes.

DR. KINO: Only if you were inserting the chirp through the transducer and the correct matched filter for the chirp itself. Then you get the response of the transducer. That's not what we're doing; we are using the response of the transducer as a calibration, and by correlating two echoes we are removing all phase distortion.

NEAR REAL TIME ULTRASONIC PULSE ECHO HOLOGRAPHIC IMAGING SYSTEM

G. J. Posakony
Battelle-Northwest
Richland, WA 99352

Nondestructive flaw characterization has keen research interests throughout industry. The nuclear industry is no exception. Identifying the size, shape, orientation, type and position of material flaws in nuclear reactor pressure vessels has a top priority. Under a contract with the Electric Power Research Institute of Palo Alto, California, Battelle-Northwest is developing a demonstration model of a sequentially pulsed phased linear array system for ultrasonic inspection of reactor vessels.[1] This program employs the linear array in both pulse echo and holographic modes and provides near real time images of the weld zone volume. The objectives of the program are to develop a rapid and accurate means for sizing subsurface defects in heavy section steel members. This article outlines the first six months effort on the two year program.

The first objective of this program is to design, develop and evaluate a breadboard ultrasonic imaging system which can provide a rapid and accurate means for evaluating ultrasonic reflectors in nuclear reactor pressure vessels.

To meet this objective, Battelle-Northwest will use a multielement linear ultrasonic array which, in conjunction with appropriate electronic, ultrasonic, computer, mechanical and display subsystems, can provide either pulse echo or holographic mode evaluations. The pulse echo mode operation will be designed for high speed scanning to detect and locate subsurface indications. The holographic mode operation will be designed to characterize and record the detail of subsurface defects.

ASME Section XI Codes are the control documents for inservice inspection of nuclear reactor pressure vessels. Present inservice inspection requirements are written around pulse echo ultrasonic techniques which employ discrete transducers operating within specific operating conditions. Use of advanced concepts such as ultrasonic arrays or holography are allowed under present codes, provided equivalence of performance can be established. Holographic techniques are not as yet recognized under the code requirements; however, research and laboratory experimentation has shown the potential that this approach can provide the characterization desired.

A second objective of the program, therefore, is to establish the capability of the high speed scanning and evaluations using the multielement linear array and demonstrate that the concept can meet and exceed the ability of present inspection techniques. As presently envisioned, one goal is to show that the ultrasonic array pulse echo system can provide a much faster inspection. A second goal is to demonstrate the capability of the ultrasonic array used in holographic imaging, thus potentially providing the basis for incorporating holographic interpretations into future appropriate ASME Code requirements.

A final objective of the program is to build an operating demonstration model of the advanced imaging system that can be used to establish the potential for multielement ultrasonic arrays in the examination of reactor pressure vessel welds. The program is aimed at developing a system for inspection of welds in reactor vessels from the outside surface.

Background

Ultrasonic inspection of welds in accordance with 1974 ASME Section XI BPVC Codes requires examination of 0°, 45° and 60° sound beam viewing from both sides of the weld. Current testing systems used to inspect pressure vessels from the outside surface employ quasi-contact techniques to couple the ultrasonic energy from a multiple transducer head into the surface of the part. These transducer heads are moved across the weld and the data are recorded on magnetic tape, CRT display, pen recorder or a combination of displays. The systems are relatively slow and require several minutes to cover a 1 ft section of weld. Interpretation of recorded data requires detailed examination and is subject to human interpretation to develop dimensional size information.

Acoustic holography has been successfully used to characterize known defects; however, present single surface holographic techniques are quite slow (typically 5-10 minutes per 1/sq ft) and many holograms are required to develop an accurate interpretation of the ultrasonic reflector.

Ultrasonic arrays are being used with great success in the medical ultrasonic diagnostic field (pulse echo techniques). The use of arrays has been proposed for industrial applications, but while several concepts have been researched and validated, no system has been developed. The use of ultrasonic arrays for holographic imaging has also been researched and validated, but technology has not been carried to demonstration instrumentation. The system proposed by Battelle-Northwest has high versatility and should be capable of clearly demonstrating the ability of the ultrasonic arrays. Using the combined technology of pulse echo and holographic imaging and incorporating the latest advances in multielement ultrasonic arrays can provide a substantial improvement in the speed of inspection and the accuracy of detailing the characteristics of subsurface defects.

SYSTEM CONCEPT

Basic System

An artist's concept of the demonstrated model to be developed under Phase II of the program is shown in Fig. 1. The system components include the computer, ultrasonic array, pulse echo and holographic electronics, pulse echo and holographic

displays,[2] and the transducer scanning bridge. The key element in the system is the ultrasonic transducer array which, under control from the computer and electronic steering circuitry, will produce a steerable ultrasonic sound beam that can cover various angles from -70° through zero to +70°. The array itself is approximately 7 in. long and is made up of 240 individual transducer elements. The mechanical scanning bridge will move the array over the weld zone in a pattern designed to give full coverage to both sides of the weld.

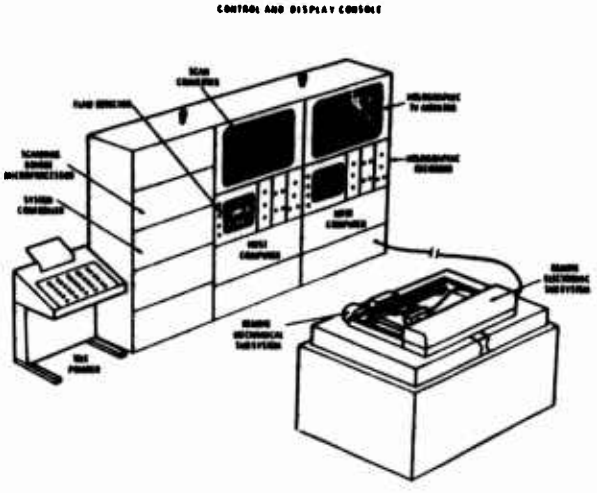

Figure 1. Artist's concept of the ultrasonic imaging system

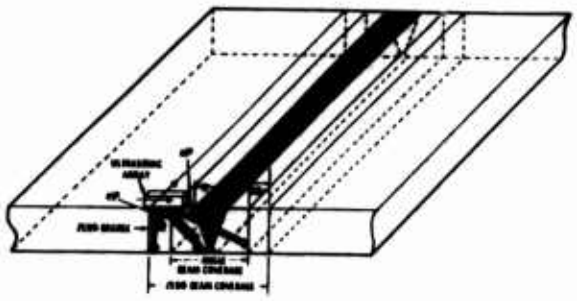

Figure 2. Volume of weld to be examined

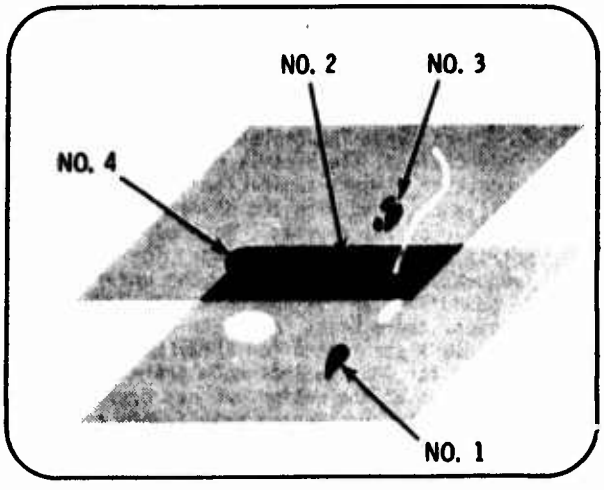

Figure 3. B-scan isometric presentation on scan converter display

For developing the pulse echo images the ultrasonic sound beam will scan the volume under inspection at discrete angles in accordance with code requirements. Each traverse of the array will provide a 6 in. wide inspection path and, since only a few seconds are needed for each traverse, a high speed inspection of the volume of the weld can be accomplished (e.g., 12 in. lineal distance per minute). Figure 2 shows the volume of the weld that is evaluated with the array for the pulse echo inspection. Figure 3 shows the projection of the image that is planned for the high speed pulse echo B-scan isometric display. Approximately 2 ft of the weld will appear on the display at one time, and each of the ultrasonic reflectors which exceed the established threshold will be displayed. The pulse echo data will be displayed both on the conventional A-scan monitor used in standard ultrasonic flaw detectors and on A-scan converter used as the B-scan isometric display monitor. Ultrasonic reflectors which show on the monitors will be further evaluated with the holographic system.

To develop the hologram the electronic system is switched to the holographic mode of operation. While the computer controls both the pulse echo and the holographic operations, the computer performs more functions in holographic mode. Once the suspect zone has been identified and the transducer is positioned over the zone, the computer is used to control the sound beam angle and the protocol followed during the development of the hologram. The hologram aperture is about 6 in. x 6 in. Approximately five seconds are required to complete each scan. The 'viewing' angle can be adjusted to obtain multiple views of the ultrasonic reflector under investigation.

System Operation

The host computer (PDP 11-34) has sufficient memory to handle the command functions, the pulse echo functions, the holographic mode and correction functions, and all future interface requirements projected for the program.

On computer command the mechanical scanning bridge initiates its scan. The scanning bridge microcomputer defines all standard X and Y movements of the array, selects the speed of travel and maintains exact position information for locking the transducer coordinates to the image display. The scanning bridge may be controlled by the microcomputer, the host computer, or manually by joystick control. Under pulse echo search scan conditions the array will travel across the carriage in approximately ten seconds and index to the next scan position in approximately five seconds. An entire 2 x 4 ft area can be covered in about two minutes.

Ultrasonic Array

The array consists of 120 transmitter and 120 receiver elements. The piezoelectric material is PZT 5, which has been acoustically damped with a moderate backing to achieve an intermediate Q. As a range resolution is not a major factor and since it is desirable to have both holographic and pulse echo operation from a single array, the damping characteristics are of secondary consideration. The center-to-center spacing of the individual elements is 0.058 in. with an element-to-element separation of 0.008 in. The unit is designed with the positive electrode on the rear of the crystal. An epoxy-aluminum oxide matrix is used as the backing. The operating frequency is 2.3 MHz. Since the shear velocity of sound in steel is approximately 1.25×10^5 in./sec, the element center-to-center spacing provides λ separation for shear mode and $\lambda/2$ spacing for longitudinal mode operation. Final evaluation of the design has not been completed; however, the zero degree experiments have shown the desired gaussian beam pattern.

Transmit Electronics

The transmit steering electronics, as controlled by the host computer, selects the mode of operation (pulse echo or holographic), the array elements to be used, the beam angle, and the sequence of pulsing. Each element in the 120 element array has a separate pulser. The time delay established between elements determines the propagation angle of the sound beam. In the present system a 37 MHz oscillator is used as the reference clock. The basic time period between clock pulses is 1/f or 27 nanoseconds. Thus the transmit delay periods between elements are a function of $f(t) = n \times 27$ nanoseconds as established by the N divide counter. The 16 bit shift register provides the delay time inputs to the switching matrix which in turn selects the pulsers that will be used to launch the ultrasonic beam. The basic frequency of the waveform driving the pulsers is 2.3 MHz as determined by the clock frequency divided by 16 through a counter. The number of cycles applied to the pulsers (or elements) is determined by the divide "m" counter. For pulse echo mode the pulser is excited for 2-4 cycles. For holographic mode the pulser is excited for longer periods ranging from ten to two-hundred-fifty cycles.

The switching matrix can establish either positive or negative beam angles in either the pulse echo or holographic modes. The available delays provide a total of 49 selectable angles, including 15 shear mode, 9 longitudinal mode, in both positive and negative directions, plus the zero mode.

Sixteen elements are used for the pulse echo mode providing a sound beam that is about the same as obtained from a 1 in. square crystal.[3] The scan across the array is achieved by sequencing successive blocks of sixteen elements. Under normal operation the zero degree beam sequences through its series followed by the 45 degree beam and then the 60 degree beam (see Fig. 4). Upon completion of the sequence the cycle is repeated over and over. The pulse rate of the system is based on the longest path length (60° shear beam) while the speed of the travel of the array is established to maintain a minimum of 50% indexing of the sound beam in both the X and Y scan directions. Elements 1-16 are used to generate the sound beam for the first pulse. The second pulse utilizes elements 8-24, and so forth, until the entire 120 element array is scanned.

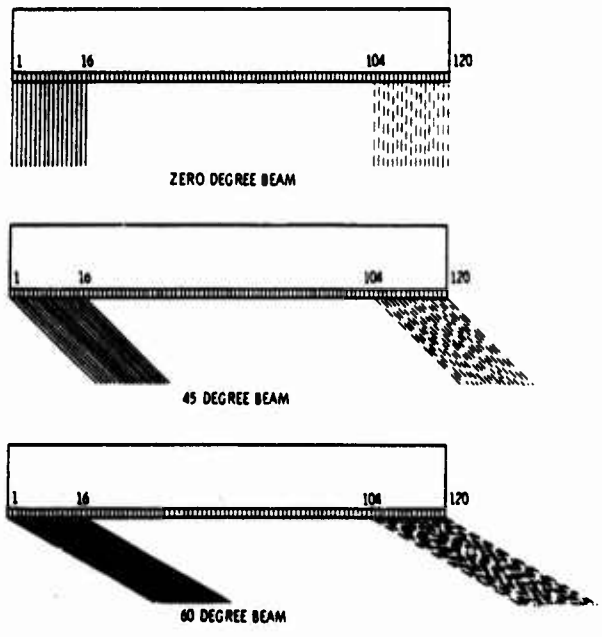

Figure 4. Sequentially pulsed phased linear array

For the holographic mode an analogous sequencing scan is made; however, the number of elements is reduced to develop a divergent sound beam. Our present research indicates that three to five elements can project an adequate beam. To develop a beam that is symmetrical in the X and Y directions involves selection of an appropriate number of transmitter elements and the use of a mechanical shutter which is placed over the face of the array to develop a square configuration. Beam steering (as required) is again developed by selecting the time delay

triggering the individual pulsers. The array sequencing is different from the pulse echo case in that the index is advanced by a single element for each pulse (e.g., 1-2-3, 2-3-4, 3-4-5, etc.). Other functions of the transmit circuitry are common for the two operational modes.

Receiver Electronics

For the pulse echo operation, eight receiver elements are used for each sixteen block of transmitter elements. As an example, receiver elements 1, 3, 5, 7, 9, 11, 13, and 15 are used when transmitter elements 1-16 are pulsed. Since the receiver delays are the reciprocal of those of the transmitter, the electronic circuitry must handle the received signals in a different manner. For zero degree beam naturally there are no delays. For any angle beam operation the signals impressed on the receiver elements are amplified and input to an A to D converter. The digitized signals are then delayed by an appropriate amount, reconverted to analog waveforms and summed to reconstruct the signal. The response speed of the electronic switching, delay circuitry, and the A to D and D to A converters controls the number of receiver elements that can be conveniently used. Our present design uses eight receiver elements for the pulse echo mode. Once the signals are summed, the signal is input to the display system for further processing and imaging.

In the holographic mode, only a single receiver element is used. The switching electronics selects the center element adjacent to the transmitter group as the receiver. The sequence is a simple progression - 2, 3, 4, 5, etc. across the array. As the complete sequence requires 150-200 milliseconds, the entire 6 in. x 6 in. aperture area can be covered in a few seconds. The holographic signal is amplified and input to the holographic electronic circuit.

Display Electronics and Monitor

Four monitors are planned for the demonstration system; two for pulse echo and two for holographic.

The A-scan display is a commercial flaw detector used as a calibration, setup and single trace monitor. The electronic gates and distance amplitude compensator (DAC) of this instrument will be used as part of the operating system. Additional electronics are being developed to convert the ultrasonic signals for display on the scan converter monitor. The image displayed on the scan converter is an isometric projection buildup of the multiple B-scan signals from the ultrasonic reflectors. The front and back surfaces of the reflections (zero degree beam) are electronically suppressed to show as a light shade of gray. The signals from internal reflectors are brightness enhanced and displayed in their correct positions.

The computer maintains coordinate position information to accurately trace the 0.45 degree and 60 degree sound beams so that the B-scan overlays are correctly positioned on the monitor. The isometric display is a buildup of all reflector information in the electronic gates and the picture is developed as the weld zone is scanned. Since the scan converter displays the peak signal from any ultrasonic reflector, the brightness of the signal is indicative of the amplitude of the echo. The scan converter is designed to hold the image until erased allowing time for visual interpretation of the signals displayed. When the mechanical scan is complete a two-foot length of the volume of the weld will be displayed.

Recall that the pulse echo system is designed as a high speed search and locate scan. Reflectors which exceed the established threshold are to be evaluated using holographic techniques to provide more accurate archival records which detail the suspected flaw.

In the holographic mode the signals from the ultrasonic reflector are input through amplifiers and gates in the A-scan flaw detector to the holographic electronics. Here the phase of the ultrasonic signals is compared to the reference oscillator and the quadrature components (real and imaging) are developed. These quadrature signals are input to the host computer for compensation of distortions which result from the holographic process and from geometrical boundary conditions. Signal distortions due to aberrations (spherical, astigmatism, field curvature, etc.) and from the curvature of the entry surface must be corrected before accurate holograms can be generated. Many of these distortions can be predicted and computer corrections can be input to the quadrature components before the signals are presented to the holographic display section.

The holographic display is being developed by the Holosonics Corporation under separate contract with the Electric Power Research Institute. Their system consists of a 128 x 128 element solid state memory, a hologram recording monitor and a real time image display monitor which incorporates a Ruticon(TM) solid state device developed by the Xerox Corporation. The solid state memory stores the hologram data output from the computer. The data stored in the memory is displayed continually on the hologram monitor. The image on this monitor provides a continuous updated hologram which can be photographed for future use. The image from the hologram monitor is imaged onto the Ruticon to provide a means for real time reconstruction of the hologram thus replacing the holographic film used in present scan holographic systems. The Ruticon devices[4] will temporarily store an input image as a surface deformation pattern on an elastomer layer. These devices consist of a transparent conductive substrate, a photoconductive layer, an elastomer

layer and a means for applying voltages across the two layers. A light image impressed on the photoconductor layer changes the voltage distribution across the layer which in turn changes the electric field across the elastomer layer. The resulting forces cause a surface deformation on the electromer layer which corresponds to the light image. By scanning the surface with a laser and optically reconstructing the ordered diffractions, the hologram image can be displayed on an image plane. The vidicon used to view the image plane develops the image for display on a TV monitor. The Ruticon display provides real time images of the hologram stored in the memory and displayed on the hologram monitor.

Summary

Flaw characterization is a most critical requirement for developing a means for evaluating the severity of defects in structural or fracture critical components. Ultrasonic imaging techniques offer promise of providing detail of subsurface defects that is difficult to obtain by conventional means. The versatility of the sequentially pulsed phase linear arrays indicated that isometric projections of the volume of material surrounding the weld in a nuclear reactor pressure vessel can provide a detailed image which can accurately describe subsurface defects. The aim of Battelle-Northwest's program is to establish the capability of the linear array and demonstrate the practicality of imaging subsurface defects. While only limited performance data has been generated to date, no technological limits have developed which pose a limit to the system. Initial results from both pulse echo and holographic results look most promising.

REFERENCES

1. F.L. Becker, V.L. Crow, T.J. Davis, B.P. Hildebrand, G.J. Posakony, "Development of an Ultrasonic Imaging System for the Inspection of Nuclear Reactor Pressure Vessels", First Progress Report - July, 1976.

2. The holographic data developed by the ultrasonic array and electronic systems being developed by Battelle is to be interfaced to a digital memory device and display system being designed by the Holosonics Corporation of Richland, Washington, under a separate contract from EPRI.

3. Typical systems in use today operate at 2.25 MHz and use transducers with crystal elements from 3/4 in. to 1 1/2 in.

4. N.K. Sheridon, "The Ruticon Family of Erasable Image Recording Devices", IEEE Transactions on Electron Devices, Sept., 1972.

DISCUSSION

DR. EMANUEL PAPADAKIS (Ford Motor Company): Any questions? Yes?

DR. ROBERT SANDERS (Acoustic Emission Corporation): First, I'd like to mention that I think we're overseeking small flaws in a rather large structure, so I'd like to ask how you're comparing this with probes in space and as to its positional accuracy and also, do you have a positional error feedback signal since, obviously, the scanning area is of a critical nature on that large of a structure?

MR. POSAKONY: To answer your last question first, yes, we do have the corrections--we have a very accurate location within plus or minus 0.001 of an inch recall on the position of the array with respect to the structure. This gives us a positive position for the start of the ultrasonic beam. We've also provided corrections for the geometrical distortions on the surface of the structure so we can correct those in time.

Your other question had to do with--would you restate it, please?

DR. SANDERS: I think it's probably covered. I started to bring out the point that our company is working with a similar system that G.E. has, which is on the market, in which a rather unique use of acoustical emission occurs in that we pulse at the ultrasonic carriage, and by acoustical triangulation attain a continuous error signal as to the location of the ultrasonic scanning carriage. Is your carriage magnetically attached to the---

MR. POSAKONY: No, sir, it is not. It is mechanically placed on the surface of the structure and scanned from there. The G.E. development is a magnetic crawler. We could apply the very same technique, but essentially what we're doing is saying we have an array contained in a very sophisticated mechanical scanning bridge. The mechanical scanning bridge has a tolerance of plus or minus 0.002 inches over a distance of (vibration tolerance) one foot, giving us pretty good assurance that we're not going to get phase distortion from our holographic reconstruction. We are only requiring a 6 inch span. We do have very accuracte recall as to the position of the array. So, we think we've covered most of the problems one way or another. We also can put back into the computer a correction function for anything that we need to have before it is displayed. Our concern, of course, is not necessarily in pulse echo. We can have distortion there and not be overly concerned because that's the search and locate device. But the hologram itself has to be very carefully controlled.

MR. ROY S. SHARPE (Harwell Labs): Can you comment on how the variability in the cladding is going to degrade your image?

MR. POSAKONY: Yes, it certainly will. If you notice, I avoided the use of the inside system. We are going to the outside to prove in principle that the concept is valid. We do not know what we would do for I.D. inspection through the clad. The clad is a very rough, undulating surface; it is not smooth. Sometimes you'll have as much as 1/16 of an inch variation peak to valley, and its going to be a real bearcat to do holographic reconstruction in that aspect, but many, many of the new reactors going on plan now are inspectable from the O.D., and, of course, BWR's are only inspectable from the O.D.

USAF NDE PROGRAM - REQUIREMENTS FOR TECHNOLOGY TRANSITION

D. M. Forney, Jr.
Air Force Materials Laboratory
WPAFB, Ohio 45433

The final session of our meeting is intended to be a change of pace with the express purpose of better focusing on the realistic aspects of the application of NDE in the field; practical problems and limitations, the requirements, potential and opportunities. Actually, Gerry Posakony did a good job of kicking off this end of the meeting subject last night with a discussion of his problem with the rather complex looking structures for which he has to develop operational inspection techniques.

Assuring that the R and D community has a better understanding of the realities and range of field conditions, requirements and limitations, we feel is both helpful and important because it is this future market place into which new technology must be transitioned if the research is going to be profitable at all.

Technology transfer is not an automatic, self-sustaining process nor is it a process where responsibilities are obvious or even accepted for that matter. On the one hand the scientific R and D community is involved, rightly so, in advancing the state of the art, worrying about fundamentals, bridging the gap between phenomena and the understanding of the nature and physics of things. They are a rather conservative group whose scope is usually limited, necessarily, to fundamental aspects and details of the problem, and their understanding or concern for field application requirements may not be brought into the picture or may not exist.

On the other hand are the systems developers and users. They have schedules to keep, they have costs to keep down; they are not really interested in incurring risks that can go with the introduction of new technology. As a matter of fact, to hear them say it, new technology initially has a pretty poor track record. To sum it up they are suspicious, basically, of new technology and very conservative in its application.

The question is: who is in the middle with the job of making transition occur? Generally speaking, the systems people just don't have the time or the inclination to reach backward very far and draw new technology in. Therefore, like it or not, the R and D community carries the bulk of the job of technology transfer if it is to occur. Consequently, it is important that this group have a constantly updated view of the realities of field application; they must take the initiative to get the user interested in and supportive of the R and D program early, and eventually make plans to demonstrate new technology on real situation problems in order to interest the user market, which paradoxically, needs the new technology.

Current USAF NDI Program

Until about ten years ago, NDI* activities in the USAF were still somewhat narrow in scope, being concerned mainly with remedial diagnostic inspection of parts as necessary during the maintenance of aircraft at the local base level. Many NDI shops were operating somewhat independently with periodic support coming from individual aircraft manufacturers, all of which resulted in considerable variation in practice, accuracy and effectiveness. Major inspection and overhaul programs on aircraft were conducted at several major depots in the U.S. only as necessitated by specific repair requirements. Thus, these programs were called Inspection and Repair as Necessary (IRAN). In 1964, as part of an effort to improve and standardize maintenance engineering procedures and significantly reduce cost, a major decision was made to place all USAF NDI activities under central management control and to incorporate the NDI function as a critical step in a new controlled maintenance process. This new role for NDI, and the details of its implementation, were formalized in 1966 in USAF Regulation 66-38 entitled, "Nondestruction Inspection Program," which established new NDI policies, including:

---

*The terms "Nondestructive Testing" (NDT), "Nondestructive Inspection" (NDI) and "Nondestructive Evaluation" (NDE) are frequently used interchangeably and have sometimes been the cause of confusion. While no consensus has been reached, there is, in fact, increasing agreement that

NDT should refer to the development and application of the nondestructive test methods themselves ...("tools").

NDI should refer to the performance of inspections to established specifications or procedures using the NDT methods to detect anomalies ...("functions").

NDE should refer to the broad examination of materials, components, or assemblies to define, classify and make qualitative, and eventually, quantitative measurements of anomalies in terms of size, shape, type, orientation, and hopefully materials strength and stress levels. The term NDI was initially chosen to describe the USAF inspection task within the maintenance function as established by AFR 66-38. The term NDE as used by the USAF, and in this paper, encompasses the entire subject including the research and development activities.

a) NDI will be used as an integral part of all activities.

b) Accessability of critical components for NDI will be a design consideration.

c) NDI skills and equipment required by new aircraft systems will be identified and made available before system delivery.

d) USAF - approved NDI techniques will be incorporated by manufacturers in qualification of first articles.

This official document also established the authority and assigned responsibilities to specific commands to:

a) Maintain NDI field laboratories at most major air bases worldwide to conduct field NDI using standardized procedures, equipment and specifications.

b) Develop and implement NDI procedures which will reduce life cycle costs.

c) Identify aircraft systems and components requiring NDI.

d) Establish aircraft inspection intervals.

e) Verify and approve new NDI methods and equipment for field use.

f) Develop standards and specifications for NDI procedures.

g) Conduct NDI technician training and certification programs.

h) Perform research and development on new and improved NDI techniques and equipment.

In the nine years since implementation, the NDI program has moved rapidly toward procedural maturity and is now an integral part of the overall task of maintaining operational readiness of USAF equipment. Today the USAF aircraft maintenance program is supported by NDI field laboratories at over 190 air bases worldwide and at five major USAF maintenance depots (Air Logistics Centers or ALC's). The Air Force Logistics Command (AFLC) is responsible for program implementation. The present USAF inventory includes 58 different aircraft, missile and engine systems, and their associated ancillary supporting equipment, and each is monitored through its own periodic maintenance cycle geared to specific design features, operational environments and usage rates, and feedback from service experience.

The current inspection and maintenance program in the USAF is designed to emphasize field maintenance procedures which cause a minimum disruption of flight-ready status of aircraft (termed "on-condition" maintenance) and to anticipate and avoid problems before they occur. A particular version of this program is established for each aircraft system in which all critical locations or possible failure points which must be monitored are identified during system designs and full scale tests. Additional information is derived from initial service experience, and past engineering experience in general. In addition, specific NDI procedures for each inspection point are worked out and verified on the full-scale test article as well as on other experimental set-ups. Finally, the frequency of the field inspections is chosen, as illustrated in Table 1, so as to be consistent with those found to be necessary during the system design, development and full scale test programs, and occasionally modified by service experience (see Ref. 1 for additional discussion).

TABLE 1

PROGRAMMED INSPECTION AND MAINTENANCE PROCESS

INSPECTION TASK	INTERVAL
1. ORGANIZATIONAL AND INTERMEDIATE (BASE LEVEL) MAINTENANCE (O&I)	
PREFLIGHT	BEFORE FIRST FLIGHT OF THE DAY
BASIC POSTFLIGHT	AFTER EACH FLIGHT
SPECIAL INSPECTION	AS NECESSARY
PERIODIC INSPECTION	
● AIRFRAME	FLIGHT HOUR BLOCKS
● ENGINE	FLIGHT HOUR BLOCKS
● FUNCTIONAL SUBSYSTEMS	FLIGHT HOUR BLOCKS
● CORROSION	CALENDAR TIME BLOCKS
2. PHASED/ISOCHRONAL INSPECTION	AFTER SEVERAL PERIODIC INSP.
3. PROGRAMMED DEPOT MAINTENANCE (PDM)	TYPICALLY 20 TO 40 MONTHS
4. ANALYTICAL CONDITION INSPECTION (ACI)	AS APPROPRIATE
5. LEAD THE FORCE (LTF) AIRCRAFT INSPECTION	AS APPROPRIATE

An official NDI technical application manual entitled "Nondestructive Inspection Procedures" is prepared for each system detailing all of the NDI procedures required by the maintenance schedule. These manuals are published as Technical Orders (TO's) with designations such as TO-1F-111A-36 for the F-111A aircraft, TO-1C-5A-36 for the C-5A transport, TO-1J-57-9 for the J-57 turbojet engine, and so on. The manual for each aircraft system is referred to as its "dash 36" manual; for each engine system, its "dash 9" manual; and for each missile system, its "dash 26" manual. A TO entitled "Periodic Inspection Requirements" and referred to as the "dash 6" manual, is also issued for each system to establish the specific timing of each inspection action. The manuals for each system are distributed to all base and depot NDI laboratories where the system is expected to be located. A comprehensively prepared general manual, TO33B, which documents uniform procedures for conducting the five basic NDI methods, as well as certain specialized procedures, is also available at every laboratory as a technician level manual and NDI technicians are required to have full knowledge of the skills involved.

To date, approximately $30 million has been invested in the preparation and distribution of this series of manuals. In addition, the USAF has provided specialized NDI training for over 2,000 inspection personnel. Moreover, an inventory of over 8,500 NDI equipment and component items, along with over 10,000 ancillary items, has been established by AFLC to perform the NDI program at a cost in excess of $24 million.

The Air Force has sponsored NDE research and development projects, although initially at relatively modest levels, since the early 1950's. Emphasis was placed on:

- methods and equipment improvement

- assistance in solving field problems
- development of new approaches.

Funding levels for NDE R&D efforts were about as shown in Fig. 1. Some funding increase resulted from the introduction of AFR 66-38 which brought new management attention to the area.

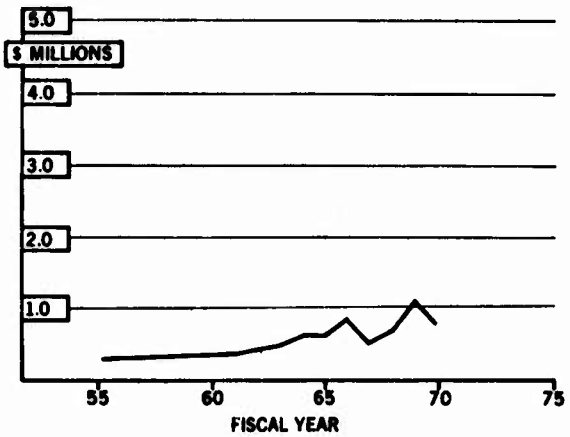

Figure 1. Air Force NDE R&D funding trend.

New Factors Expand Importance of NDE

The continuing program to increase the strength and effectiveness of the USAF at minimum cost is applying considerable pressure to improve supporting NDE capabilities. Behind this pressure are several significant new factors affecting aircraft systems which have increased in importance since 1970:

A. Adoption of new airplane damage tolerant design requirements.

B. Trend toward aircraft life extension rather than replacement.

C. Efforts to reduce operational and support (O&S) costs (cost of ownership).

D. Emergence of new structural concepts and materials.

A. New Design Requirements

Since 1961, USAF aircraft have been designed, manufactured and operated in accordance with the technical requirements of an Aircraft Structural Integrity Program (ASIP) established to assure that they have adequate integrity and service life[2] Flight critical structural elements also had to meet damage-tolerant design requirements such that if a fracture or crack initiated, the structure remaining or a portion of the same structure could sustain a percentage of its design load without catastrophic failure. The inadequacy of these ASIP requirements and guidelines was revealed in 1969 with the crash of a USAF F-111A fighter bomber when, even though operating well below design limits, a wing separated in flight during a practice run over a target area. An investigation revealed that the loss was caused by the failure of a wing pivot fitting and this failure emanated from a one-inch flaw generated during the manufacturing process which remained undetected by all subsequent NDE.

The F-111 incident, together with various deficiencies experienced with other aircraft systems, led to the assurance of a new set of ASIP requirements in 1972, now contained in Military Standard MIL-STD-1530,[3] which set forth a new structural integrity and durability design philosophy for USAF aircraft. The designer must generate data required to manage fleet operations in terms of inspections, modifications and damage assessments. This in turn, led to the development of a new Military Specification MIL-A-83444 "Airplane Damage Tolerance Requirements", dated 2 July 1974. A critical feature of this philosophy is that a designer must now assume that aircraft structures unavoidably contain small flaws and defects at delivery whose assumed presence must be taken into consideration in the initial design and in setting up NDI intervals,[4] as well as technique selection, sensitivity levels and inspection zones in parts. MIL-A-83444 allows, under prescribed conditions, a choice between a fail-safe approach which prevents catastrophic failure by using multiple load paths or crack-stoppers, and a slow growth approach in which growth rates are kept too low for cracks to reach critical sizes within the inspection interval. In addition, the required initial flaw size assumptions and required levels of inspectability for both design approaches are prescribed. The introduction of these requirements focused considerable new attention on NDE capabilities, and limitations, and indirectly set new and stiff goals for achievement of improved detection sensitivity and reliability levels.

B. Trend Toward Life Extension

As a natural consequence of the rising costs of manufacturing replacement aircraft and the greater initial cost of new advanced designs of increased sophistication, management motivation exists to consider the alternative of extending the useful life of as much hardware already on hand as possible while still maintaining fleet strength. The useful service lives of several aircraft systems, such as the B-52 bomber and KC-135 tanker, have in fact been extended through engineering modifications, selected structural replacements, and increased inspection coverage. An important step was also taken, with the institution of MIL-STD-1530 in 1972, to establish significantly longer service lives for aircraft in the future as an initial design requirement. Since 1972, engineering evaluations conducted on several in-service aircraft have established structural changes necessary to meet the new life requirements, although existing aircraft were essentially exempt from the requirements. Many first line aircraft systems will eventually undergo this structural integrity and durability reassessment. It is anticipated that upgraded NDE procedures will play a vital role in assuring the required safety and economic levels.

C. Efforts to Reduce O&S Costs

The operation and support (O&S) of USAF airplanes is a major category of expenditure, and the time consumed in maintenance and NDE is an important limitation on the number of aircraft available

to meet mission requirements at any given time. Serious efforts are underway to improve and reduce the costs of these functions in two important ways:

- Streamline the maintenance cycle
- Make NDE more economical

The USAF is presently conducting an extensive Maintenance Posture Improvement Program to parameterize the total maintenance process, to develop alternative analytically-based scheduling models, and to present new options for a cheaper and more efficient inspection and maintenance program flexible enough to accommodate changing conditions, economics and fleet management schemes. The interface between NDE and corrosion control requirements is an example of the factors being considered.

There are, as can be imagined, many instances where the cost of NDE methods and procedures applied to aircraft inspection must be reduced, and many opportunities to do so are available. An important objective in many of the current USAF research and engineering development efforts is to learn more about so called "high cost centers" in the many NDE functions, and to devise alternative techniques, technique modifications, simpler procedures or cheaper inspection materials.

D. New Structural Concepts and Materials

An aggressive research and development program is conducted by the USAF to investigate and develop new airframe and engine structural concepts, construction materials, and fabrication processes. The achievement of significant weight and cost reductions as well as improvements in damage tolerance and performance are the principal motivating objectives. From a performance point of view, a few important opportunities are becoming realities; however, marginal NDE capabilities in some of the cases will be a limiting factor unless major improvements are brought about. Among the significant challenges to the NDE field are or will be:

- advanced composite structures
- primary adhesive bonded structures
- laminated components
- processed-to-near-net shapes
- special engine materials: ceramics, directionally solidified (DS) eutectics, single crystals, metal matrix composites.
- highly complex shapes (such as hollow air-cooled turbine blades).

The level of funding devoted to NDE research and development since the 1970 time period has been influenced upward significantly, as shown in Fig.2, by the factors just discussed. It is principally the trend of this chart that is important in illustrating the magnitude of the increased attention to NDE. The specific dollar amounts should be considered approximate since they are estimated by combining several NDE funding sources, including, for example, ARPA funding for the Science Center program being reviewed at this conference.

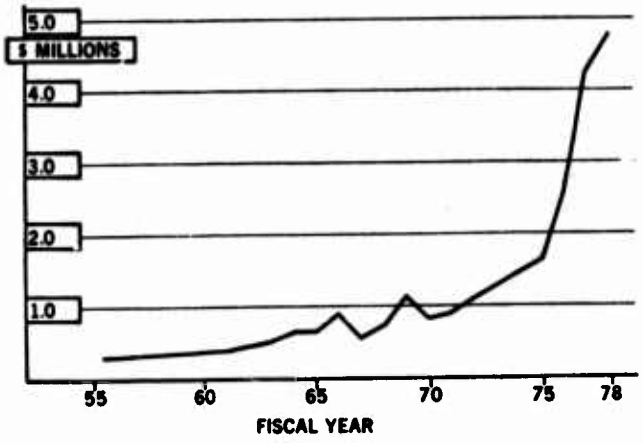

Figure 2. Air Force NDE funding trend.

User's Requirements for Improvement

NDE user requirements for improved capabilities and practice provide the basis of the Air Force NDE R&D program plan. The success of technology transfer, no matter how sensational the technology, depends ultimately on its utility in meeting some of these requirements and within the limitations of the user's application environment. Thus, an appreciation of these becomes quite important to the researcher. Some of the more important needs and requirements are to:

- Improve sensitivity and resolution under field conditions
- Reduce operator dependency of NDE techniques
- Lower cost of NDE
  - Production
  - Maintenance
- Reduce inspection technique variables without sacrificing equipment versatility
- Develop simple quantitative readouts
- Establish new, simple capabilities where absent
- Solve specific field inspection problems

One can conclude from this list that the emphasis is on increasing accuracy with reduced variability while lowering cost. A point must also be made that the cost-effectiveness and cost reduction opportunities related to production NDE and maintenance NDE functions are usually quite different and may involve different approaches.

Another standing user need is reflected in the fact that the "old, standard" techniques still require improvements. For example, despite the fact that x-ray radiography was initially introduced in 1934 and has seen wide, routine application, numerous use variables are still not resolved:

- Optimum kilovoltage
- Beam to crack alignment range
- Non-uniform developing solution characteristics
  (Time-Temp. - Density - Thickness Relations)

- Radiography viewing techniques
- Deterioration criteria/rates for unexposed film
- Penetrameters - Hole vs Wire vs Mesh vs? (not useful in maintenance - what is?)

The fact that approximately 2,000 radiographs are made in the course of the periodic inspection of the USAF C-5A transport exemplifies the importance of and cost reduction potential in technique improvement and optimization. Other "classical" techniques - ultrasonics, eddy current, floures-cent liquid penetrant and magnetic particle - need similar improvement.

The Air Force field NDE program, performed as an integral part of the maintenance function, has numerous limiting characteristics, due in great part to its large scope. Some of these are intrinsic in nature while others can offer opportunity for R&D improvement efforts. Either way, they are important to recognize and take into consideration when deciding on the pctential for development and transition of new technology. They include the following:

- Air Force inventory involves multitude of dissimilar items to inspect
- Reference standards are generally inadequate, ill-defined
- Commercial equipment designs/capabilities are frequently outdated
- Sensitivity/reliability factors are hard to pinpoint, control
- No certification-recertification (MIL-STD-410D) required for AF personnel
- Resistance to change or adopt new technology at field level
- Pressure to keep costs down

It would be fair to summarize this list as follows with respect to the Air Force NDE field environment:

1) techniques and equipment must be versatile-can't afford many specialized, limited application items.

2) large variable scope of inspection requirements makes standardization, generalization difficult.

3) techniques and new technology must be easy to apply by routinely trained technicians.

4) Field technicians are reluctant to change, are suspicious of new concepts, equipment or procedures.

NDE Research and Development Planning

The responsibility for planning and conduct of the USAF NDE R&D program, authorized in Air Force Regulation 66-38 described above, is assigned to the Air Force Systems Command (AFSC) and further delegated to the Air Force Materials Laboratory (AFML) as depicted in Figure 3.

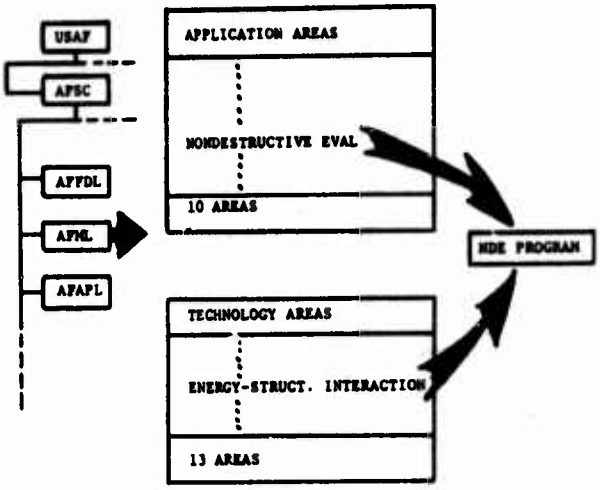

Figure 3. NDE R&D program evolution.

The AFML conducts a full spectrum materials technology program consisting of basic research, exploratory development, advanced development and manufacturing technology. The program is organized for planning, implementation and management purposes into the 13 "technology" base subjects or areas and 10 technology "application" areas shown in Fig. 4. The total AFML NDE program consists of a technology base program (entitled "Energy-Structure Interaction") incorporating all basic and some exploratory development and manufacturing technology work. The planning process is a broadbase team effort involving participation of or input from:

- AFML and other AFSC laboratories
- Aeronautical systems division (ASD) engineering
- AFLC NDI program office
- AF major commands, other DoD and Government agencies
- Aerospace and related industries

The total R&D program is organized as long range "roadmaps" which provide

- coordinated elements: R&D to transition
- consistent funding committment
- specific application or customer "windows"

Through this method of program planning, it is possible to assure that all essential R&D projects or subelements of an overall development thrust are brought along at the required time. Consistent funding of all subelements is assured as a single decision. Finally, the integrated thrusts are designed to meet identified end requirements, generally a systems requirement. The program thrusts, established as of the Fiscal Year 1977 planning cycle, are prioritized as shown:

Applications Area

1. Fastened Joint NDE
2. NDE Method, Process and Equipment Optimization
3. Advanced Composite NDE
4. Adhesive Bond Evaluation
5. NDE of Complex (Engine and Airframe) Shapes
6. In-flight Structural Monitoring

Technology Area

1. Quantitative Flaw Characterization
2. Measurement of Adhesive Bond Strength
3. Characterization of Failure Related Materials Properties

A roadmap (current in FY77) from thrust No. 5 is illustrated in Figure 4. (It is beyond the scope of this paper to discuss the content of specific roadmaps).

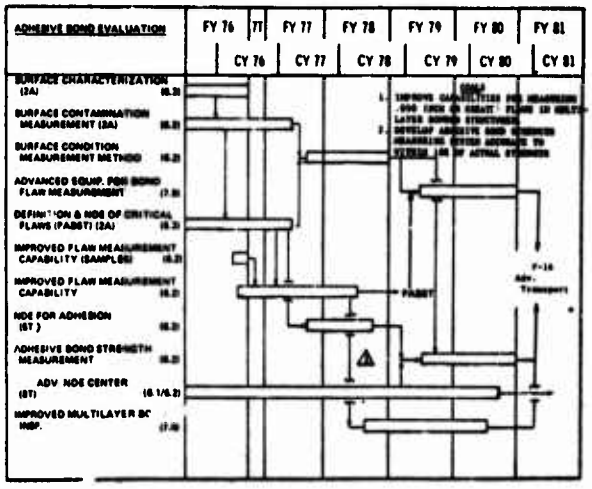

Figure 4. Typical program roadmap

Factors Controlling Technology Transition

While much can be said about the difficulties that can be encountered in the introduction of new or improved technology into use, one major obstacle worth noting is the significant length of time required for the R&D - Implementation cycle itself. Figure 5 illustrates the time needed for a typical R&D project on an inspection device (using a recent case history).

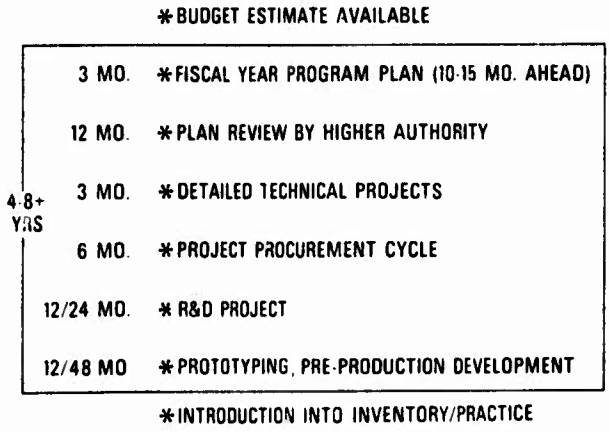

Figure 5. Typical R&D/implementation cycle

Following pre-production development and a successful field demonstration, and a requirement for inventorying has been established, a procurement cycle, such as shown in Fig. 6, may follow:

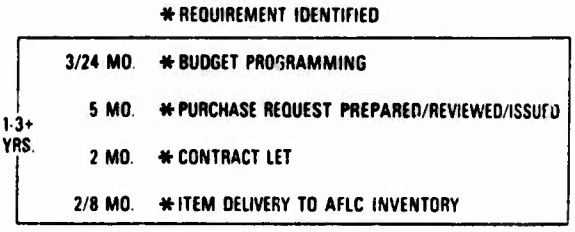

Figure 6. Typical procurement cycle AFLC NDI equipment

Thus, as this illustrates, it can take ten or more years to transition a new device to inventory (and that is if all goes well).

With few exceptions, new technology must transition into a conservative user's market where change usually raises concerns about increased risk, cost additions, lost time, new training requirements and general uncertainty as to benefits. The best chance to overcome these concerns is to show that benefits outweigh the other factors. In the Air Force NDE application environment, the essential questions which govern acceptability of new NDE procedures, methods or equipments include:

- Does it directly solve a current inspection problem?
- Is it faster?
- Is it more reliable?
- Is it more cost-effective?
- Does it provide more essential information?
- Is it usable in the inspection environment?

To generate enough justification or motivation to successfully introduce new technology usually requires at least several of these benefits in combination. The first and last features are usually required. To make new methods, instruments, or equipments functional and marketable, even though technologically acceptable, it then becomes essential to produce designs to

- Optimize simplicity
- Maximize versatility
- Optimize compatibility with existing equipment
- Minimize ownership cost
  - -Acquisition
  - -Operation
  - -Maintenance
- Make rugged as possible
- Maximize operational stability (reproducibility)
- Minimize operator dependency
- Minimize required operator training

The criticality of the user environment factors such as outlined in this section cannot be overemphasized. Outstanding technical innovations have been known to die because of failure to satisfy such requirements.

References

1. Forney, D. M., "NDI in the United States Air Force," British Journal of NDT, pp 72-81, May 1976.

2. Wells, H. M., Jr., and King, T. T., "Air Force Aircraft Structural Integrity Program: Airplane Requirements," ASD-TR-66-57, May 1970.

3. Military Standard MIL-STD-1530 (USAF), "Aircraft Structural Integrity Program, Airplane Requirements," 1 September 1972.

4. Haviland, G. P. and Tiffany, C., "Understanding the USAF Structural Integrity Program," Astronautics, pp. 67-70, July 1973.

DISCUSSION

DR. C. C. MOW (Rand Corporation): We have time for one or two questions.

COMDR. JIM ANDERSON (ONR): The question of certification and recertification, once your military people go to a school or learn the NDI inspection techniques, do they then acquire some sort of a designator that identifies them as skilled NDI operators?

MR. FORNEY: Yes, they are assigned an Air Force Specialty Code, or AFSC. All Air Force career fields are identified by AFSC as described in Air Force Manual (AFM 39-1. The AFSC assigned to military NDI inspectors is 531X5 where 531 is the Metal Working career field, X represents skill level and 5 identifies the NDI specialty. The entry skill level value of X (just out of NDI school) is 3, 5 represents six or more months on the job training plus a written proficiency test. Finally, 7 is the fully qualified senior level obtained after extensive experience (usually the senior non-commissioned officer level). Civilian NDI personnel are not included in the AFSC system and are governed by Civil Service regulations. The point to be made is that there is no automatic scheme and authority to require certification/recertification of these NDI personnel periodically as in the commercial sector. Opportunity for promotion/advancement must provide the motivation and retraining opportunity provides the means.

CRITERIA FOR NONDESTRUCTIVE TESTING R&D

C. S. Smith
Office of Assistant Secretary of Defense
(Installations and Logistics)
The Pentagon
Washington, D.C.

Gentlemen, I'm probably more out of place than any of your other speakers. Some have noted that they're chemists; some have noted that they're metallurgists. I have no research results to report; I'm a bureaucrat, one of those hopefully nice, gray, faceless, beings from the Pentagon. I must ask your forebearance this morning if I seem a bit obtuse; where I work a square corner has 108 degrees.

Unfortunately, listening to your meeting I quickly concluded that my initial topic for this talk was unsuitable for this occasion. What follows is a different talk. My apologies for the misleading abstract.

Now, the office I work in is charged with a rather odd problem: that of somehow arranging that the necessary resources: dollars, people, spare parts, whatever, are programmed and actually delivered to make all of the various equipments which DoD buys ready to satisfactorily accomplish their purpose when they're called upon. This can be somewhat challenging at times.

In Genesis we are told that God took six days to make the Heavens and the Earth, and apparently quality assurance was satisfactory because "behold, it was very good". As Secretary Brownman pointed out on Tuesday, it takes the Army considerably more than six years to buy a tank, and there is strong reason to doubt that the resulting product is very good at all, especially when you have to persuade someone to pry enough money out of a tightly constrained defense budget to maintain the beasts. Digging up the funds becomes more difficult every year, probably because it costs so much. This year DoD is spending somewhere between $15 and $20 billion just to maintain airplanes, ships, tanks and those other primary equipments which we buy.

The point is that I'm one of the guys who are going to need all of those cute black boxes which you want to produce. Frankly, those devices are needed very badly. Let me talk a little about our problems. Perhaps these difficulties can serve as a challenge to some of the research managers here in thinking about their own programs and how to move them forwards.

Several presentations about such topics as x-ray diffraction methods have mentioned potential benefits. They started me thinking about the time about ten years ago when a gentleman from MIT, who shall remain nameless, was convinced that aircraft operators should apply x-ray diffraction to the turbine blades in aircraft gas turbine engines. The Air Force and several airlines sent some of their best maintenance people to talk to him, as he explained that he could save millions of dollars. After several days of meetings, it was revealed that there were only two prerequisites to using this methodology: one of them was that all turbine blades be made out of a single crystal of metal, and the second was that each single crystal turbine blade be reinspected in the identically same place on a daily basis. He was confident that operators should start observing reproducible results after taking some 800 to 1,000 sample observations on a given turbine blade.

This process was very hard to justify to the maintainers. For some reason, DoD has not yet invested in x-ray diffraction of turbine blades. Unfortunately, this example is not untypical of the problems of bringing NDE to the field.

I got into this whole NDE business indirectly Mike Buckley, whom I don't see this morning--there he is. You made it up, Mike. Congratulations!--got his name into an Aviation Week article which claimed near-miraculous savings as a result of his efforts. These were dangerous words. If you claim savings, somebody is going to try to subtract them from the already scarce dollars which my office is paid to care about. For this reason, I promptly picked up the telephone, called Dr. Buckley, and said, "Michael, wouldn't you like to come to Washington and explain how you calculated those savings?"

Well, Mike came. And, we found that perhaps there were some serious questions as to whether such savings would be realized. This disconnect resulted from assumptions being made which might seem perfectly reasonable to a laboratory scientist, but which don't match operating and financial realities.

For example, Mike pointed out how many disassemblies and inspections he was going to get rid of. Well, my office has recently been engaged in a very small exercise to apply what the airlines call MSG-2--it stands for the Maintenance Steering Group 2--methodology to aircraft maintenance. There is, in fact, a textbook in preparation; I have here Volume III, our "cookbook" in manuscript form. Applying MSG-2 has reduced the preventive maintenance on a typical military airframe by 50 percent and the total depot maintenance on aircraft engines to which it has been applied by more than 50 percent. Thus, MSG-2 eliminated many of the tasks Mike's improved NDE was going to do more efficiently.

How was this done? MSG-2 does only three things. It asks the questions: (1) Will doing this task improve safety? (2) If it won't improve safety, is there an economic benefit? (3) If there is neither a safety nor an economic benefit, why do it all?

Well, this seems a very simple form of discipline to apply. However, it took a certain amount of formalization--if we could show the first viewgraph, please. (Figure 1) I'll see if I can get over there without tripping over myself.--This example is that for the formal evaluation of aircraft structures. All the discipline that was

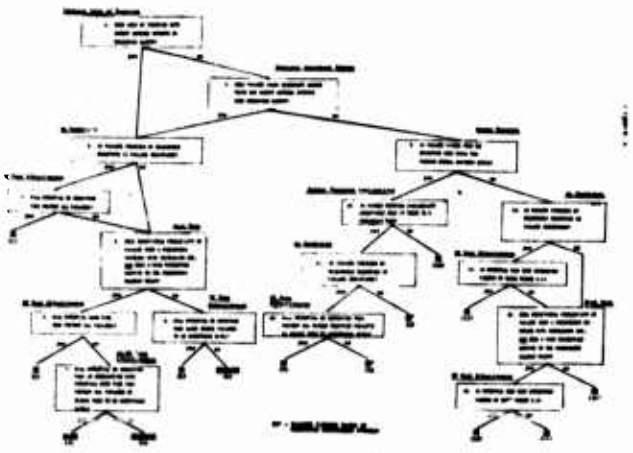

Figure 1. Reliability centered maintenance - Decision diagram

applied was to ask maintenance planners to ask themselves these questions in an organized manner. As you look at them you say, "You've got to be more quantitative than that." I wish we could be; I'd be very happy if we were. Perhaps you gentlemen can help us in becoming more quantitative.

More importantly, an analogy to this simple discipline should be applied to NDE development. One of the things that has been much reduced as a result of MSG-2 has been "on-condition" maintenance tasks, that is, tasks related to tests for reduced resistance to failure. Why has on-condition maintenance suffered? For one reason. It couldn't pass the test of simple questions.

First question, can the test detect reduced resistance to failure for some specific failure mode? Simple, but a very strong implication. You've not only got to detect something but you should also be able to relate what you detect to some failure mode. Many of the tasks didn't meet this criterion. They might detect something, but no one had any idea how to interpret or act upon the results.

Second question, can the test anticipate that failure far enough in advance to permit effective response to correct the problem before actual failure? This is an important question. For example, there is the, perhaps apocryphal, proposal for an acoustic emission nondestructive test to warn the pilots of one well-known aircraft when the wings start cracking. Its only serious drawback was that the warning would occur only 8 to 20 seconds before the pilot had to bail out. Fortunately, that device has been removed from modification planning.

We are still suffering from another device, somewhat the opposite, which is known as the helicopter chip light. This marvelous nondestructive evaluator is installed in helicopter transmissions to measure whether metallic particles are being accumulated. There are only two problems with the helicopter chip light. First, its frequency of Type II error (false accusal) is approximately 20 times greater than its actual identification of real problems. Second, it gives you a minimum of ten hours warning before you should take corrective action.

Giving so much notice is fine except that some pilots, God bless them, get all kinds of distraught the moment that light goes on. They ground their airplanes immediately wherever they are. Sometimes in the middle of South or North Viet Nam. Some have crashed, killed themselves. The chip light has cost DoD at least 10 times as much damage as it has averted according to the best analysis I've seen. And, so far as can be determined, it has little or no safety benefit.

Now, it was good of the nondestructive evaluation community to provide such a device. However, it would have been better if someone had thought enough to locate the readout someplace off the instrument panel so as to preclude accidents because the pilot had an unreliable ten hour warning that someone should inspect his transmission for possible problems.

After that digression, we get to the last question about on-condition tests. Does the task have a greater likelihood of doing good than harm? This was certainly a problem with the chip light. Let me give you another example.

For the C5A, the Air Force decided to do all kinds of performance trend analysis. To this end they installed a monitoring system called MADARS-GPS on every C5. At Dover, where the greatest number of C5s are based, the principal cause of aircraft being "down" was failure of the monitoring system. Now, for every hour of tapes of the numerous variables which this monitoring system records on the airplane, it takes 16 hours of computer analysis time on a rather large machine. But, there is no evidence that anyone has ever taken an effective action as a result. The fact that this expensive airplane is now being grounded because an unproductive monitoring system isn't working well frightens me a little.

Okay. Those are the prerequisites to get monitoring which works satisfactorily or, at least, is such that someone should be willing to pay for it. Those prerequisites are, as the gentleman who preceded me pointed out, going to be applied in an environment quite hostile to any device requiring sophisticated operators. As a result, I have gotten rather fatalistic. Dearly as I would like to see the daily maintenance burden reduced, most of the benefits of your work are going to be seen (and hopefully should be seen) in applications before the equipment is ever accepted.

Now, we DoD logisticians have another small problem. Materials quality assurance is black magic to many, if not most, managers. Perhaps enough of us are not technically qualified to understand the answer when we ask the question, "Will it do any good?" before spending money for NDI or NDE. We often are forced to act through mist or mystification.

However, I for one, am still curious why dye penetrant inspection, which detects flaws less than 1/16" deep, is performed on billets before a half inch is shaved off each side. I'm equally unclear as to why, of the numerous metallurgical tests required by MILSPEC, almost none seems to be relatable to any of the specific failures that we experience. Frankly, we need not only tests, but we need tests that we can soundly and tightly relate to something that is failing or that will cause a failure.

To be direct: Please, before you go out and design a 35-pound black box that will do acoustic holography of titanium parts, think about how to relate the resulting acoustic holograms to something, anything. If you can't, don't really count on a market. Even DoD isn't dumb all of the time.

Unfortunately, I'm not sure a disciplined answer to the questions I've raised is at all easy to arrive at. I think that it involves a lot of work; and it's going to take people in a number of fields talking to each other to get those answers.

In essence, that's my message. Before quitting, I would like to tell another horror story, because I think it says something important.

I was approached recently by a gentleman with a marvelous inspection technique that eliminated all disassemblies in inspecting the outer skin panel of a wing. There is only one problem with this application. One still has to inspect the inner skin panel; thus, disassembly is still required anyway, and the new technique saves nothing. It would probably cost an additional $10,000 per airplane. If, like DoD, you have a 25,000 airplane fleet, 10,000 of which are potential users, that would get expensive fairly fast.

In spite of all these horror stories, DoD needs nondestructive evaluation. In proposing NDE applications, however, you should bear in mind that the armed forces are not run by engineers, they are run by people who have been oepratorS. Operators usually do not understand the technologies embodied in their weapons systems and, as a result, are often very much afraid of technological change. In a number of studies, we have clearly documented their great hesitation to engage in anything that looks like it might be riskier. For example, even though, on an engineering basis, it was clear that the Navy should overhaul an F-4 aircraft at 48 month intervals rather than every 24 months, it took 14 years from the time the engineers reached that conclusion to the time pilot managers were willing to accept it and permit it to happen. In short, your case had better be good, and you may need a bit of patience.

I have had one other difficulty with what I have heard here. Everyone has talked about costs; everyone talks about savings; occasionally, we talk about reliability. Reliability needs to be discussed.

We're buying new weapons. We have to buy new weapons. Unfortunately, it's a competitive world, and in a society which seems to find it very difficult to produce non-military work, the Soviets are beginning to produce very good weapons these days.

Building those new weapons has all kinds of interesting implications. For example, to build a really effective VTOL aircraft, we will need gas turbine hot stages which operate 500 to 600 degrees Fahrenheit hotter than present designs. I don't think anyone understands enough about how the materials that work at those temperatures fail. We're going to need means of testing new materials just to find out what their characteristics are and how they fail. Then we're going to need means of evaluating production materials to be sure they are within meaningful quality standards.

Again and again when considering use of a material we must think not merely of its cost, but also of its reliability and how that reliability impacts on design capability. The real benefits from NDE, I'm convinced, will often not be cost savings; in fact, almost never cost savings. But, hopefully, NDE will benefit effectiveness, the ability to make the equipments we have work. As has been frankly discussed, they don't always work well now. And, NDE is clearly pre-requisite to the ability to design and manufacture equipments with new capabilities that really do work. That's a very different set of benefits than people have been talking about.

Thinking about the likely pay-offs suggests that some variation in present development plans might be helpful. For example, much as it may be painful, researchers should start looking at titanium instead of just aluminum. I was fascinated with the number of papers about aluminum. I have asked several speakers afterwards, "Why don't you look at titanium?" Their uniform reply was, "Well, it's difficult." It's difficult, but that's where the problem is.

DR. GEORGE MARTIN (UCLA): You mentioned the Russian equipment as being rather superior. How do the Russians handle their equipment inspection problems?

DR. SMITH: Sir, I did not mention it as superior; I mentioned it as improving rapidly, as becoming competitive. The Department of Defense would be loathe to admit that the Russian equipment was superior, and if I were to make such a statement I should promptly and deservedly be shot by my bosses.

The problem of poor quality assurance in the Soviet Union has been well publicized. It is very clear that in certain of their newer weapons systems they are addressing the issue much more effectively than they ever have in the past. One can see this in the fact that we now actually worry about the counterforce effectiveness of their strategic missiles which suggests that they have met a very tight assurance equipment. And, one sees it in the fact that we begin to think the armor plate on their tanks might be good, which implies they have solved another quality assurance problem.

The question is a different one. I think, than your rephrasing, and one would not wish to be quoted otherwise. I was noting that we find ourselves in a competitive environment. I would not want to evaluate, but certainly we are feeling the hot breadth of competition much more strongly. We are feeling it for a number of reasons. One of them is that you are now defended by an all volunteer force. In 1962 with many more men in uniform, the U.S. could devote more than 70 percent of its defense monies to new procurement, R and D, etc. Defense now devotes over 55 percent of its monies to personnel. That leaves less than 45 percent for procurement, R and D, etc.

DR. GEORGE MAYER (Army Research Office): I guess I don't understand your objection to the chip detector. The question, number one, is: does it work?

DR. SMITH: Very serious questions on that. The work I'm quoting, in fact, was done by and for Army's Air Mobility Research and Development Lab at Fort Eustis.

DR. MAYER: Yes, but the point is, if it does work, then the factor of your warning light making your pilots crash--

DR. SMITH: Okay, but let's go the other way.

DR. MAYER: --is simply a psychological one.

DR. SMITH: That psychology may be lovely. It's a lovely black box, but if that psychology does me harm, sir, I don't want it. New York Airways took on this same problem and solved it very nicely. They took the chip detector off of the instrument panel, put it on a servicing panel that had to be checked every time the helicopter landed. Helicopters don't have 10-hour flights so they had plenty of warning. By making this change, they produced a situation where chip detectors stopped frightening the pilots, without preventing action from being taken where it needed to be, by the maintenance personnel.

DR. MAYER: I think that's fine, but this community here is mainly composed of R and E engineers and they're not going to determine where you put your warning lights.

DR. SMITH: Sir, with all due respect, the real problem is that nobody seems to determine those things. If the instrument designer doesn't think about the user of his product, who else should?

DR. KIRK RUMMEL (Boeing, Vertol): You threw some rather interesting challenges out to this group of engineers and scientists. I guess more than most of these I'm one of those people who try to make the system evaluations for those systems. Let me throw a challenge back to you. Given that we've done our homework, and maybe in many cases we haven't, and we've tried to do those evaluations rigorously, once we've reached that point and have great factors missing in our equation such as the cost of a maintenance man hour or where the problem is, there's many things that we certainly can't come up with that the operator can. Perhaps you could give us some advice of how we've run that system, and we've got a course of action which we feel we've done the right way and come up with the right answer, how do we tackle that red tape, that bureaucracy whose, I guess, inaction can best be described as inertia parading as caution?

DR. SMITH: Fair question. Two answers. You're from Boeing, Vertol; you know Tom House?

DR. RUMMEL: I'm giving his paper.

DR. SMITH: That's what I thought. Okay. One way to get action is to find an effective and interested agent in the bureaucracy and work through that office. Many of us bureaucrats really do care.

In the helicopter business in the Army, the USAAMRDL at Fort Eustis, especially the group that Tom is associated with, probably has done a better job of looking systematically at the relationship of design to operating and support costs than anyone else in DoD. In fact, I think the results coming out of that shop do tell us things like where the failure modes really are, where costs are, what we can do about them. That's where you get some of the answers you need to change your designs. In fact, some of those answers are reflected in your new designs, for example, the UTTAS which is really a remarkable aircraft from a support point of view, as is SIKORSKY's.

Where I work, many people are trying very hard to put it in rather clear and stringent criteria on how to select a maintenance program. I've talked about some of these. It's a very simple set of criteria, and we are trying to take a number of steps to see that these are carried out and that the theoretical improvement will be realized.

Fort Eustis, for example, is being listened to more now. Secretary Brownman, in fact, has had one briefing from Tom House and is due for more. We are making some headway there.

I think the AF will have some dollars for emergent problems in its FY 78 budget. They even have a little bit of this kind of money in FY 1977. The revolution that is implied in that statement probably seems very small to you gentlemen; however, I am wearing a suit partially because I have to cover the scars. Believe me, it is a very hard thing to do and the battle is only begun. At least, we're trying.

If there is no friendly pocket of bureaucrats, you try to educate one. The Air Force now has a focused place for a man with a solution to contact, the PRAM SPO. Similarly, for Navy ships, the "RED/E" effort has a charter to change things. The Army is moving in a very positive direction right now. They are starting to apply some of the research results which we had all wondered if anybody ever read. Your best bet there is probably USAAMRDL.

Maybe that's part of an answer. You asked a tough question. With an organization as big as DoD, you don't try to control very many details. I don't even think that approach is possible. Management of such a large organization has to be thought of in terms of entropy and thermodynamics. -- I'm not sure I want to be quoted and I wish the tape recorder weren't running, but -- when you need to do something quickly in an organization like DoD you start by asking, "Well, where are we falling on our faces and what's going to make a difference?" Then you try to design short circuits around the system so as to do what needs to be done until the system catches up several years downstream.

The Russians have a worse problem than we do on this. I have occasionally muttered that we should look at Lieberman's writings on putting incentives into the Soviet economy. Perhaps we could find something useful to DoD there.

It is a problem; it's often not going to be solvable. If all else fails, give me a ring. My telephone number is (202) 697-6079. If you've got a case, I'll be happy to hear from you; maybe I'll know someone who can help.

DR. C. MOW: I'm sorry I have to cut the interesting discussion off. You can continue during the coffee break. Thank you, Dr. Smith.

DR. SMITH: Thank you.

NONDESTRUCTIVE EVALUATION UNCERTAINTY AND INSPECTION OPTIMIZATION*

Duane P. Johnson
Failure Analysis Associates
Palo Alto, California 94304

NDE decisions differ from most other engineering decisions in that the NDE response or responses used in making a decision with regard to the serviceability of a part are often only weakly correlated with the serviceability of the part. The impact of of this weak correlation or inspection uncertainty on inspection errors and the effectiveness of the inspection is discussed. A quantitative methodology for selecting the optimum NDI accept/reject decision thresholds in the face of the inspection uncertainty is outlined. Also discussed briefly is how inspection uncertainty analysis can be used to estimate the inspection reliability from field or production inspection data without the use of a flawed specimen program.

What I will discuss with you today is a quantitative approach for selecting the accept/reject levels in nondestructive inspections such that the expected life cycle costs of a part are at a minimum. In the process I hope to illuminate some of the critical factors external to the inspection process itself that influence the cost effectiveness of inspection and how these external factors influence the optimum accept/reject level or the optimum inspection sensitivity. In addition, I hope to identify what it is about the inspection that is critical to its potential to be a cost effective inspection.

Our discussion will apply to the use of nondestructive inspection as a tool for segregating defective parts from sound parts, and will not consider, per se, the other function of NDI which is its use as part of the feedback to the quality control or design functions.

The justification for an inspection is that the additional expenditures for inspection will reduce the total expectant life cycle costs. Here, cost is used in a broad sense, and includes the cost of personal injuries and fatalities. An improved inspection process is not necessarily a more sophisticated process, but is a process which results in a reduction in the total life cycle costs of the product. The cost of the inspection itself is often a very small fraction of the total cost surrounding and associated with an inspection.

Lack of Traceability between Cost and Benefits

The time delay and the lack of traceability between the application of an inspection and the benefits that accrue from the inspection are major barriers to more effective utilization of NDE. Normally, the real downstream benefits in terms of increased product reliability that accrue from an inspection are neither specifically predicted at the time the inspection is instituted, nor evaluated later in the product life.

Normally, a new inspection procedure is introduced because management is convinced that the procedure will decrease the total life cycle costs of the product or increase sales because of the higher reliability of the product. The first thing that occurs is not a cost reduction, but a cost increase because of the additional cost of this new inspection. The next thing that occurs is not a cost reduction, but an increased manufacturing cost because now the parts have to pass the new inspection. This latter cost may be many times the specific inspection cost. Two, five, ten years later, the benefits of the inspection in terms of more reliable operation occurs, if there are any benefits. It is unlikely that the benefits in dollars of this increased reliability are actually identified; it is even more unlikely that the increase in profitability attributable to the new inspection is identified.

In general, management gives greater weight to the immediate and identifiable costs than the vague and unidentified later date benefits. More accurate estimates of cost trade-offs would result in greater acceptance of inspections that would in fact significantly improve the part reliability and would eliminate many ineffective inspections.

Probabilistic Economic/Engineering Analysis Methodology

Failure Analysis Associates has developed under Electric Power Research Institute funding, the general methodology required to handle this cost interchange between in-service costs, manufacturing costs and inspections costs. A number of practical means of attaining the required input functions have been established. The methodology has been applied or is being applied to a number of engineering systems including: steam turbines, bearings, nuclear reactors, and railroad track. Failure Analysis Associates has applied aspects of the methodology to one of the world's largest supertankers, a major freeway bridge here in the state, a major radio tower complex and a number of automobile components.

In the following outline of the methodology, mathematical details will be avoided. These details are given in (1 - 5). Hopefully, a better understanding of the effects of inspection on the life cycle costs will be obtained. Particular consideration is given to the role of inspection sensitivity, inspection uncertainty, the conditional failure probability (that is, the probability of failure if the part contains a flaw), the pre-inspection material quality, the failure costs and inspection costs. Furthermore, the specific functions required to quantitatively describe the total life cycle costs are identified.

The first thing that must be appreciated about a nondestructive inspection is that the accept/reject decision is based on a nondestructive inspection signal response and is not based on the severity of the imperfection. As much as one would like to know, for example, how large the imperfection

is, all one really knows is how large some NDE signal response or combination of responses are.

The second thing that must be appreciated is that given the NDI signal response, there usually exists a significant variation or uncertainty in the actual severity of the imperfection. Because of this inspection uncertainty, a nondestructive inspection decision on accepting or rejecting a part is subject to two types of errors:

1) A defective part may be accepted because the response signal from a significant defect is smaller than our acceptance criteria.

2) A sound part may be rejected because a benign indication gives a response to the probing agent that exceeds the rejection criteria.

If the acceptance criteria is too sensitive, then an excessive number of sound parts will be rejected by the inspection; if the acceptance criteria are too insensitive, an excessive number of defective parts will be passed by the inspection. The optimum accept/reject criteria has a balance between these two types of errors. In order to establish this balance, some weight must be given to how serious a defective part in the field is versus rejecting a sound part.

Our approach to establishing the optimum accept/reject level and the cost effectiveness of the inspection is summarized in Fig. 1. An average cost is established for a failed part (C_F), for a rejected part (C_R), and for inspecting a part (C_I). These three cost factors are combined with the failure probability and the rejection probability, both as a function of the accept/reject level, to arrive at an estimate of the expectant total life cycle cost of a part as a function of the accept/reject level.

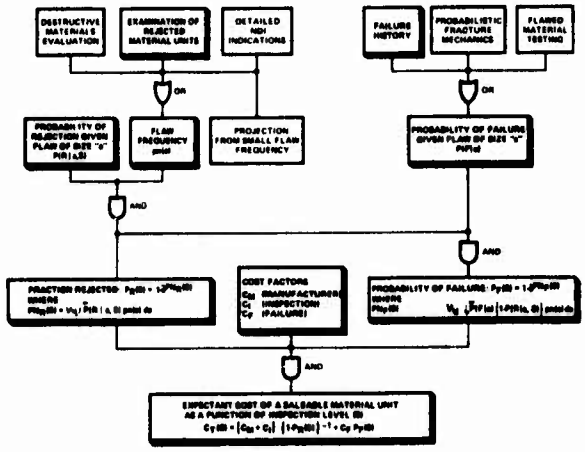

Figure 1. Flow chart summarizing the Engineering/ Economic Analysis Methodology

As indicated in Fig. 1, there are three basic engineering functions that are determined in order to predict the dependence of the failure and rejection probability upon the accept/reject levels. One of these functions describes the inspection performance, the second function describes the material quality before inspection, and the third function describes the structural performance of material containing defects.

The imperfection rejection probability ($P(R \mid a,S)$) gives the probability of rejection of a part, given that the part contains an imperfection of size a and the inspection level is S. This function describes the inspection performance and is the only term that is dependent upon the accept/reject level S. Three techniques have been identified for determining the inspection performance. Two techniques involve defective specimen inspection programs and the third involves the use of results from field or production inspections. In the most common approach, specimens containing known defects are inspected at various imperfection levels and the number of rejected and nonrejected imperfections are counted.[6] More detailed information on the inspection performance can be obtained from a defective specimen program if an uncertainty analysis of the results is conducted to determine the correlation between the imperfection size and the NDI response parameters used to make the accept/reject decision.[3] The advantage of inspection uncertainty analysis over conventional counting analysis of defective specimen inspection programs are illustrated in detail in (4). The third approach is to record the NDI responses obtained in production or field inspection and remove a sampling of the parts for metallurgical evaluation in order to establish the correlation between the imperfection size and the NDI response parameters used to make NDI accept/reject decisions. This inspection uncertainty analysis of field or production data is discussed in detail in (3).

The material quality in this case is described by the flaw frequency pn(a). Here pn(a)da is the probable number of imperfections per unit volume with size between a and a+da, prior to inspection of the part. Four techniques have been identified for determining the flaw frequency. One is simply to metallurgically examine a sufficient amount of material to establish the frequency of imperfection at the size of interest. A second approach is to metallurgically examine a sufficient number of rejected parts, and knowing the imperfection rejection probability, the flaw frequency can be determined. The third approach is to keep track of the frequency and strength of the NDI indications. If the inspection uncertainty (correlation between the indication strength and imperfection size) is known, the flaw frequency can be determined. A final technique that is used is to project the large-flaw frequency from the more easily determined small-flaw frequency using an assumed log normal distribution.

The conditional failure probability $P(F \mid a)$ describes the probability a part will fail given that it contains an imperfection of size a. Three technologies have been identified for determining these functions. One simply uses failure history and will be illustrated later. The second approach uses probabilistic fracture mechanics[7] and the final approach involves defective material testing. A

combined analysis using failure history and fracture mechanics analysis has been particularly successful in situations where only limited data are available.[8]

The imperfection rejection probability, the flaw frequency and the conditional failure probability are combined to give the probability of failure and rejection as follows:

$$P_R = 1-e^{-PN_R(S)}$$

where

$$PN_R(S) = V_u \int_0^\infty P(R|a,S)\, pn(a)\, da.$$

$$P_F = 1-e^{-PN_F(S)}$$

where

$$PN_F(S) = V_u \int_0^\infty P(F|a) \left[1-P(R|a,S)\right] pn(a)\, da.$$

Here, V_u is the material volume of the part.

Illustrative Example: Turbine Blades

Consider a hypothetical situation that is representative of quality assurance questions that may be encountered with certain turbine blades. This example shows:

A. The use of failure history and the result of examining rejected blades to select the inspection level that will minimize the expectant cost to the turbine manufacturer.

B. The effect of a significant increase in failure cost on the optimum inspection level.

C. The use of the methodology to select the best of three inspection methods and to optimize the inspection level.

First, consider the failure history. Assume that 10^5 blades have been used for their design life and 100 of the blades have failed prematurely. The fraction failed is then $F_F = 10^{-3}$. The total cost of these 100 failures to the manufacturer, including indirect costs such as bad will with certain customers, is estimated to be 10 million dollars. This gives an average cost per failure C_F = \$100,000. The 100 failed blades were analyzed to determine the size of defect which initiated the failure, and the results are summarized in Table 1.

Table 1 - Number of Failure Initiating Flaws per 0.1 cm Interval in 100 Failed Blades

Flaw Size Interval in cm	Number of Flaws	$pn_0(F,a,S_0)$ in cm^{-4}	Flaw Size "a" in cm
0.00 - 0.10	0	0×10^{-6}	0.05
0.10 - 0.20	0	0×10^{-6}	0.15
0.20 - 0.30	0	0×10^{-6}	0.25
0.30 - 0.40	0	0×10^{-6}	0.35
0.40 - 0.50	1	2×10^{-6}	0.45
0.50 - 0.60	7	14×10^{-6}	0.55
0.60 - 0.70	25	50×10^{-6}	0.65
0.70 - 0.80	36	72×10^{-6}	0.75
0.80 - 0.90	22	44×10^{-6}	0.85
0.90 - 1.00	7	14×10^{-6}	0.95
1.00 - 1.10	2	4×10^{-6}	1.05
1.10 - 1.20	0	0×10^{-6}	1.15

The turbine blades before being admitted to service had to pass an inspection** in which the inspection uncertainty $\delta = (0.2S + 0.1)$ cm, and the inspection size $S = S_0 = 3/4$ cm. The rejection rate has historically been $F_{R0} = 4.5\%$. A sample of 100 rejected blades was destructively examined, and the imperfections in these blades which caused rejectable indications are summarized in Table 2.

Table 2 - Number of Rejectable Indications per 0.1 cm Interval in 100 Rejected Blades

Flaw Size Interval in cm	Number of Rejectable Indications	$pn_0((a,S_0)\|R)$ in cm^{-4}	Flaw Size "a" in cm
0.00 - 0.10	16	32×10^{-3}	0.05
0.10 - 0.20	19	38×10^{-3}	0.15
0.20 - 0.30	19	38×10^{-3}	0.25
0.30 - 0.40	17	34×10^{-3}	0.35
0.40 - 0.50	13	26×10^{-3}	0.45
0.50 - 0.60	9	18×10^{-3}	0.55
0.60 - 0.70	5	10×10^{-3}	0.65
0.70 - 0.80	3	6×10^{-3}	0.75
0.80 - 0.90	1	2×10^{-3}	0.85
0.90 - 1.00	1	2×10^{-3}	0.95

The cost of manufacturing a blade is \$100 plus an additional \$10 to inspect the blade. The question arises as to whether the total cost to the manufacturer could be reduced by selecting a different inspection size. Using the data above as input into the methodology, the dependence of the expectant cost of a saleable blade upon inspection size can be determined. The expectant cost to manufacture a turbine blade that passes the historical inspection method as a function of inspection size is summarized by Fig. 2, along with the expectant failure cost.

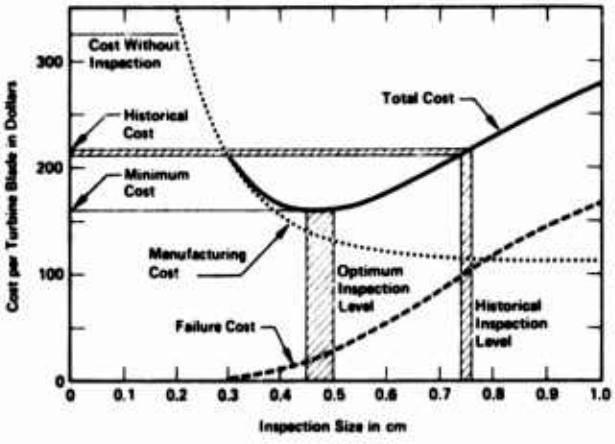

Figure 2. Cost per turbine blade as function of inspection size.

The total expectant cost of an acceptable turbine blade is the sum of expectant cost to manufacture a turbine blade that passes the inspection and the expectant cost due to the finite probability that the blade will fail. The total expectant cost per saleable blade is also illustrated in Fig. 2. The total expectant cost of a turbine blade if no inspection is conducted is $328. It is evident from Fig. 6 that the historical inspection reduces the total cost of a saleable blade to $215, which represents a total savings of over 11 million dollars for the 10^5 blades. The total expectant cost of a blade can be further reduced from the present cost of $215 per blade to $159 per blade by reducing the inspection size from the historical 0.75 cm to an optimum 0.45 cm. Over 10^5 blades, this represents a potential additional savings of approximately 6 million dollars.

Now assume that there is an additional loss, on the average, of $900,000 that results from the fact that a blade failure forces the unit to be out of service for an extended period of time and, due to a new contract with the users, these consequential costs are also passed on to the manufacturer. Hence, under the new contract, the average failure cost to the manufacturer will increase from $100,000 to $1,000,000. Figure 3 illustrates the new expectant costs of a saleable blade as a function of inspection size. If the inspection size is left at the historical level, the expectant cost of saleable blade will increase from $215 to $1,115 per blade. A change in inspection size from the historical level to the level of 0.35 cm will reduce the cost impact of the contractual change to a $19 increase per blade ($234).

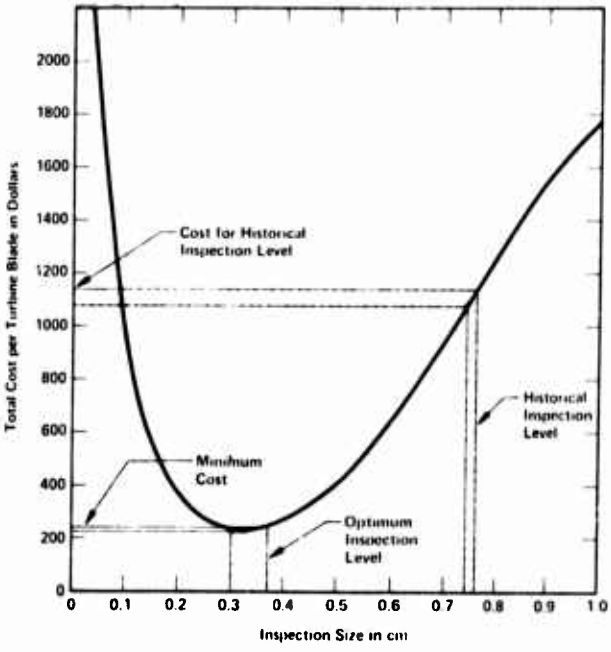

Figure 3. Total cost of a saleable blade as a function of inspection size when the average cost of a failure is a million dollars.

Even at the optimum inspection level the cost of failure and blade rejection ($234 per blade) still represents a major increase over the base manufacturing and inspection costs of $110 per blade. Let us suppose that two alternative inspection methods, A and B, are available, which are reported to be better than the historical inspection method. The direct inspection cost for each of these methods is projected to be essentially the same as the historical inspection method. Both inspection A and B have been used to inspect material specimens that are somewhat similar to the blade material. The results of examining 100 material units rejected by inspection method A and method B, along with the results given in Table 2 for the historical inspection, are summarized in Fig. 4. Inspection method A rejected a significantly greater fraction of the material units than did inspection B. Inspection method A has an inspection uncertainty (width of the correlation function between the imperfection size and the NDI response amplitude) which is twice as large as that characteristic of the historical inspection, while method B has an inspection uncertainty which is half the historical method.

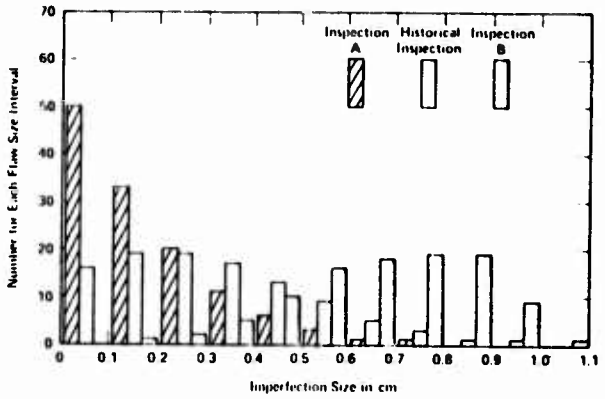

Figure 4. Number of rejectable indications for each flaw size interval for 100 rejected material units observed for inspection A, the historical inspection and inspection B.

Although Fig. 4 shows that inspection method A is more sensitive than either the historical inspection or inspection B, this does not necessarily mean that A is the better of the three methods. Which inspection method should be introduced to produce the minimum total cost blade and at what level the inspection size should be set requires a cost-risk analysis. Figure 5 summarizes the expectant total cost of a saleable turbine blade utilizing the historical inspection method, inspection method A and inspection method B. It is evident from Fig. 5 that the introduction of inspection method A, which appeared most sensitive in Fig. 4, would result in a minimum cost of $494 per turbine blade, or $160 more than minimum cost possible with the historical inspection. With inspection method B, a saleable turbine blade can be manufactured with a total expectant cost of $146 per blade. The introduction of inspection method B with an inspection size S = 0.35 cm would result in a potential savings of 9 million dollars over the minimum cost blade if the historical inspection method is used.

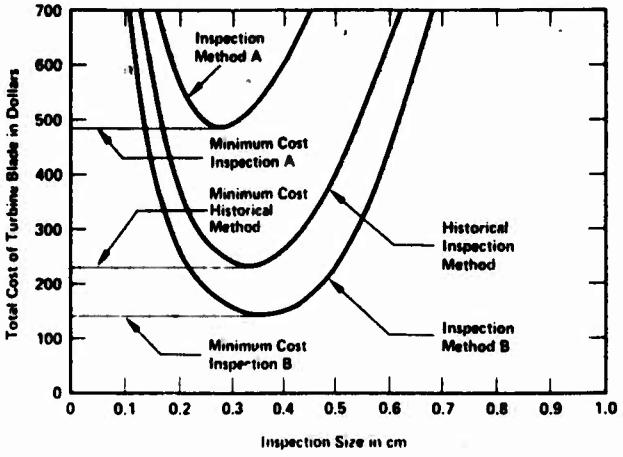

Figure 5. Comparison of turbine blades total costs for three inspection methods.

This example clearly shows the potential impact of this inspection optimization methodology. In situations involving a number of inspections and failure modes, Monte Carlo computer algorithms are used to predict the expected life cycle cost.

In summary, the better the correlation between the signal parameter that is used in the decision and the actual severity of the imperfection; that is, the smaller the inspection uncertainty, the greater the potential cost effectiveness of that inspection.

Secondly, having selected an inspection and having determined what the inspection uncertainty is, there exists an optimum accept/reject criteria or inspection sensitivity which is dependent upon pre-inspection material quality, the inspection uncertainty, the stress and environment the part is subjected to, the cost of failure and the cost of rejecting the part. These factors can be quantitatively determined and combined to establish the cost effectiveness of the inspection and to select the optimum accept/reject level or levels.

---

* This work was supported by the Electric Power Research Institute under contracts Nos. RP217-1 and RP700-1.

** Here the inperfection rejection probability is taken to be a normal cumulative distribution function with standard deviation δ and mean S.

REFERENCES

1. D.P. Johnson, "Inspection Uncertainty: The Key Element in Nondestructive Inspection," Materials Evaluation 34, 129 (June 1976).

2. D.P. Johnson, "Cost-Rist Optimization of Nondestructive Inspection Levels," EPRI 217-1 Technical Report 5 (September 1975).

3. D.P. Johnson, "Determination of Nondestructive Inspection Reliability Using Field or Production Data," EPRI, Technical Report, NP-315 (October 1976).

4. D.P. Johnson and T.L. Toomay, "In-Service Inspection Detection Probability for Thick Section Steels," (to be published).

5. C.A. Rau, et al, "Failure Analysis and Failure Prevention in Electric Power Systems," EPRI Final Report, NP-280, November 1976.

6. P.F. Packman, et al, "Reliability of Flaw Detection by Nondestructive Inspection," Metals Handbook 11, p. 414 (1976).

7. P.M. Besuner and A.S. Tetelman, "Probabilistic Fracture Mechanics," EPRI 217-1, Technical Report 4 (July 1975).

8. P.M. Besuner, et al, "The Combined Use of Engineering and Reliability Analysis in Risk Assessment of Mechanical and Structural Systems," Proceedings of Risk-Benefit Methodology and Application Conference, Asilomar, California, UCLA-ENG-7598 (edited by David Okrent), December 1975.

DISCUSSION

DR. RICHARD CHANCE (Grumman Aerospace Corp.): How would you propose to utilize a system like this where the manufacturer is not charged with the failure cost by the user?

DR. JOHNSON: In most cases, there is some expectant failure cost assigned to the manufacturer, even if it is only lost profits due to loss of future sales. If a manufacturer is interested in maximizing profits and there are no possibilities of failure cost being charged to him, then he should not conduct an inspection. Seldom are all the failure costs charged to the manufacturer, hence, based on this analysis, the optimum inspection for the manufacturer will be less restrictive than the optimum inspection as seen by the user. As can be seen by comparing Figs. 2 and 3, the optimum inspection size is not strongly dependent upon the perceived failure costs.

MR. JACK NICHOLAS (Naval Ship Engr. Center): Does the total cost of failure include the cost of lost revenues, or is that the cost to repair the failure?

DR. JOHNSON: The total cost of failure depends upon whose point of view you are taking. Certainly from a user's point of view, possible loss of revenue is part of the total expectant cost associated with failure. Possible fatalities or personal injury must also be included in the total expectant cost.

DISCUSSION OF FACTORS CONTROLLING ARMY HELICOPTER RELIABILITY

K. Rummel
Boeing Vertol Company
Philadelphia, Pennsylvania
and
T. House
Eustis Directorate
U.S. Army Materials Research and Development Laboratory

I'm Kirk Rummel from Boeing Vertol. Tom House, from the Eustis Directorate of USAAMROL, had intended to present this paper and was looking forward to this very fine group. He apologizes for not coming.

What we would like to do is try to show the Army's program in the diagnostics area; specifically, I hope I can respond to some of the challenges that Charlie Smith threw out about having a logical approach to research planning.

The Army's interest in significant aviation improvements actually started, or at least gained steam, in the 1960's during the extended combat we had in southeast Asia where a lot of problems in the utilization of the rotary wing aircraft came to a head, and I'll talk about those in more detail. What I would like to do is go through how the Army has responded to those problems that were revealed, through R&D and even more specifically in the diagnostics area. When I say diagnostics, what I'm talking about is the second category of NDI that I see, the first category being the one I think that most people here have a prime interest in and that is the one time, static inspection during manufacture, a verification of quality control. The other type is the repetitive in-service inspection.

I think there's a lot of differences in those two categories. The first is very obvious: there are high levels of funding, and secondly, there appears to be a good deal of technology interchange which, quite seriously, draws my envy. I think that's one of the messages that you have given me from this symposium; that we need to do a much better job of technology transfer in this latter area of in-service diagnostics.

I do want to diverge just for a moment to express my appreciation of what I observe is the high caliber of the work being performed. The scientific progress that you're making is obviously quite considerable. Perhaps this paper addresses more of the engineering rather than the scientific aspects of NDI.

I would like to become more specific and talk about the approach that some like to call "deficiency oriented." It starts with problems rather than solutions, and on Fig. 1 is a simple outline of what I think is the generic approach to problem solution. I don't want to insult your intelligence but rather remind you of this fundamental aspect of good engineering application. I want to show it because I think all too frequently we start at step 6 and go to 8 or at least try to get to 8 and have to return eventually to 1 through 5. It's very important that we move on down that order in a very sequential manner, attempting to be as quantitative as possible, particularly in steps 2 and 3. I think quantitative assignments there can be either in a delta expression or in an absolute value. The material I'm going to show you, I hope, will adhere to that requirement that all of our goals are quantitative.

1. DEFINE REQUIREMENTS.
2. ESTABLISH WORKABLE GOALS.
3. ASSESS CURRENT POSITION.
4. REVIEW ALL POSSIBLE SOLUTIONS.
5. PERFORM PRELIMINARY EVALUATIONS.
6. DETAILED RESEARCH.
7. EVALUATE BEST CANDIDATES.
8. INCORPORATE.

Figure 1. Process for problem solution.

Figure 2 is a distribution of maintenance costs. This does not include fuel and crew. It happens to be on our CH-47. A thousand dollars an hour for any helicopter and I think there's where we start with the problem.

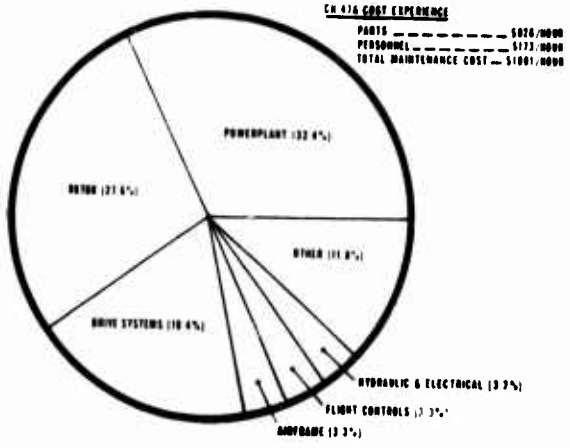

Figure 2. Distribution of CH-47A parts cost by subsystem.

The distribution of subsystems may be of some surprise to some of you. I have seen a great deal of emphasis on the airframe structures here; it's a small segment of that pie: the engine, the rotors, the drive system are the big contributors. Another display of the problem is Fig. 3 which is of in-flight aborts on the UH-1. Here we see a slightly different subsystem distribution, the hydraulics there is a little bigger because of the single hydraulic boost system that the UH-1 has which makes the operator a bit more sensitive to hydraulic indications. Those are both false and real indications, I might remind you.

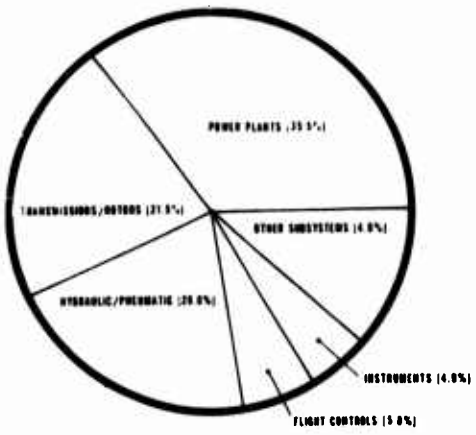

Figure 3. Subsystem causes of UH-1H Mission Aborts.

Figure 4 displays maintenance man hours per flight hour. Here I think you begin to realize some of the impact of scheduled inspections. Now, remember, that's organizational level maintenance man hours per flight hour. We're doing an awful lot of inspection.

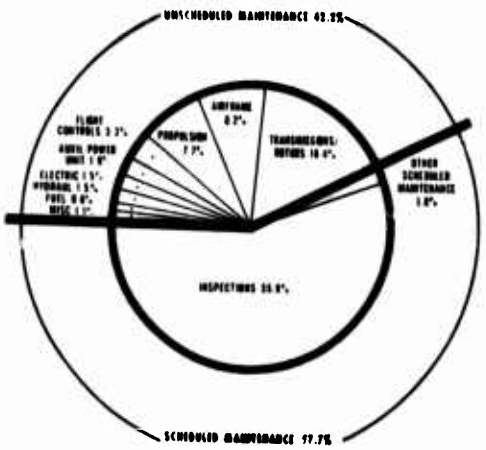

Figure 4. Distribution of MMH/FH for CH-47A by subsystem.

I don't have a chart, unfortunately, of accidents. The chart I had in mind to present had the simple message that rotary wing aircraft are considerably higher than fixed wing aircraft. Our goal is to bring it down to the fixed wing level and we think we can, at least on a realistic basis of accidents per landings.

In Army aviation, we're generally talking about goals, showing a factor of two improvement. In other words, we want to cut that experience by half. Now, that's rather optimistic, but I think you'll see in some of the later presentations that it's achievable.

Moving on from aircraft level display, let's follow the thread down through the transmission that we saw as a rather large contribution to aborts and maintenance man hours. In Fig. 5, you see a distribution of TBO (Time Between Overhaul) or scheduled removals, component failure deterioration, and false removals due to inadequate diagnostics.

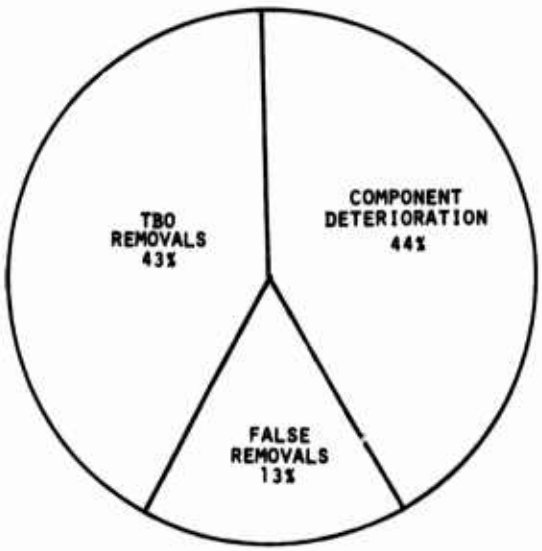

TRANSMISSION REMOVALS (CH-47 EXPERIENCE)

Figure 5. Drive system major constraints.

Now, Charlie Smith alluded a little bit in the previous presentation to some of the work the Army is trying to do, which I'm proud to say I was a part of, in applying more rigorous analytical criteria for determining when and if we should have TBO removals. I don't want to explore that now, but just to throw one, perhaps controversial, thought out; our analysis has concluded that, in general, we do not have to have any additional diagnostics to allow our transmissions to go on-condition. If you want to pursue that with me later, I'll be glad to. It's a rather fundamental concept and some have had a hard time accepting it.

The inherent reliability of component deterioration is being addressed by many Army programs both in terms of material capabilities and, in fact, nondestructive inspection techniques that would improve reliability.

I want to concentrate on our efforts to reduce false removals through improved diagnostics. Before I do that, let me turn to a tabular list of accidents caused by transmissions. Figure 6 represents all Army rotary wing aircraft. It's a composite of many different aircraft. The top level causes are the lubrication starvation induced failures which we have addressed through many design improvements-redundant jets and last chance screens, etc., in new aircraft.

Component	Failure Mechanism
	Lubrication starvation induced
Scavenge Line	Box spewed oil; inhaled by engine causing turbine failure
Input Pinion Bearing	Seizure - Lube starvation (local)
Input Pinion Bearing	Seizure - Lube starvation (local) residual contamination
Input Pinion Gear	Locknut backed off - Lube starvation of bearing-blocked oil jet
Input Pinion Bearing	Seizure - Lube starvation; filter stude pulled out
Filter Leak	Improperly reused gaskets leak badly
Input Pinion Bearing	Seizure and subsequent oil-fed fire - Lube starvation from quick disconnect failure
Gear Tooth	Possibly gear failure due to low lube - Possibly stained sight glass led to maintenance misreading level
Gear Scuffing	Tooth failures due to lube problems (common)
Gear Pitting	First stage bevel gear pitting clogs pump
	Isolated Causes
Quill Shaft	Cracking through improperly machined hole in shaft
Bevel Gear	Crack through mounting flange due to material inclusion
Bevel Gear Retent	Failures of bevel gear retention cap screw
Stud Failure	Stud fatigue failure due to bending on hard landings
Control Yoke	Gross rotor imbalance or blade loss caused yoke failures
Mounting Studs	Transmission left aircraft - Mounting studs failed
	Repetitive Causes
Clutch	Slippage and resultant rpm loss

Figure 6. Transmission/gearbox accident history.

The isolated causes are the one time events that are experienced, and down at the bottom is one of the few repetitive causes we see that create accidents, that is, clutch slippage. It's a particular insidious mode that so far has resisted any diagnostic technique to determine when the clutch is going to slip. Any sudden loss of power in a rotary wing aircraft is disturbing, particularly if it occurs as you are coming in for a landing. One of the things I want you to notice are the cracks we have had in shafting and bevel gears, and these are of concern to us, although, as you can see, they are isolated cases. They have not heretofore been detectable through debris monitoring because they simply don't generate debris until it's too late.

The next consideration that we ran into in looking at accidents, and this is what Charlie Smith was alluding to when he talked about the impact of precautionary landings, are the accidents which are simply due to misexecuted precautionary landings. The potential for these accidents is shown on Fig. 7.

Landing Mode	(≈ Rvn)	(≈ Conus)
P(Accident/ loss of structural integrity)	1/3	1/3
P(Accident/ power loss)	1/10	1/100
P(Accident/ controlled pre-cautionary landing)	1/2,000	1/4,000
P(Accident/ normal landing)	1/60,000	1/120,000

Figure 7. Accident probabilities.

The third category in Fig. 7 is the accidents due to the controlled precautionary landings which occur in one in 2,000 landings to one in 4,000 landings. Now, that simply says the world is not a pool table and you're going to land on a stump once in a while, but your criteria for an adequate diagnostic system depends on your recognition of this.

In Fig. 8 is illustrated the methodology we have been developing to determine how the probability of an accident, given a precautionary landing, could affect the requirements for a reliability objective on your diagnostic system. What we show is that the accident rate can go up as the reliability of your diagnostic system goes down, and indeed, in certain kinds of conditions, you can actually cause more accidents than you would have had if you simply didn't detect it and let the inherent failure progression of the mode take its natural course.

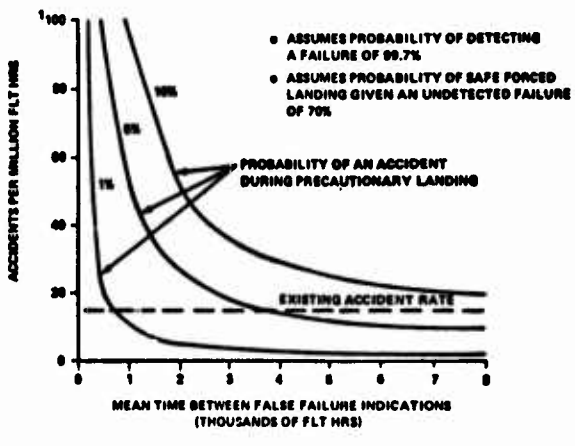

Figure 8. Accidents rate as a function of diagnostic system unreliability.

The important message here is that in trying to utilize a rigorous approach in looking at the problem, we end up defining some of the criteria that you then later apply to an adequate diagnostic system. In summary, after looking at all of the aircraft systems, the major needs that emerged were, 1) improved detection of the shaft and gear cracks in transmission for accident reduction 2) the reduction of erroneous removals of transmissions and 3) the reduction of in-flight aborts, both necessary and unnecessary.

Now, improved detection can be accomplished in two basic approaches, as shown on Fig. 9. You can invent a new technique or you try to improve the old one. Improvement of old techniques can be done in three ways: you can change the threshold, the logic, or you can change the use intervals, inspect more frequently or less frequently as the case may be.

- INVENT NEW TECHNIQUE (DIFFERENT SENSING PROCESS)
- IMPROVE EXISTING SYSTEMS THRU:
  - DETECTION THRESHOLD
  - LOGIC
  - USE INTERVAL

Figure 9. Methods of improving detection systems.

What I would like to do is run through some of the things that the Army has tried to do in these kinds of categories. For instance, in the new technique area, in addressing the shaft and gear crack problems, some of the research we're doing is with a vibration detection technique using a very high frequency carrier, like 200 to 300 KHz. Figure 10 shows the result of a test for gear tooth cracking. What we did here is put a saw cut through the root of the tooth in a bevel gear, ran it about 270 percent load to try to get the crack to progress. What you see there are nice spikes that occurred as the crack progressed. So, there is some hope that we perhaps have a technique for detecting this heretofore undetectable mode. Of course, it still has to pass the test of some rigorous cost effectiveness analysis.

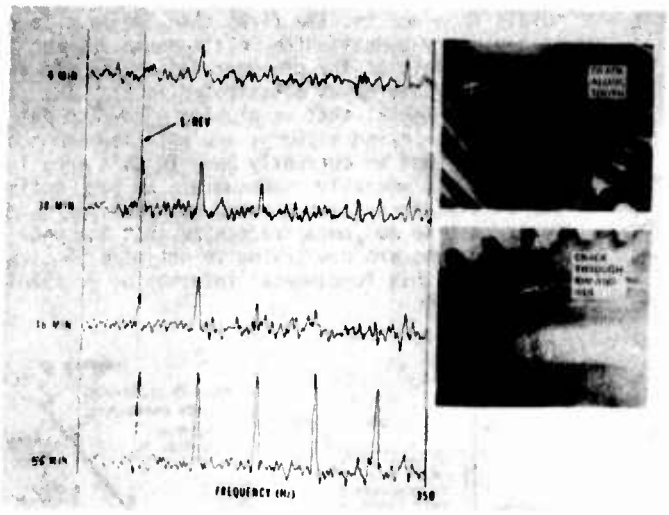

Figure 10. Spiral bevel gear crack progression test.

In terms of improving the existing techniques, the first thing we have to do is recognize that the primary diagnostic technique for helicopter transmissions is oil borne debris. Figure 11 indicates that 55 percent of the removals are caused by some sort of oil contamination, whether it be through a filter examination, soap analysis, or the notorious chip detector. Noise and vibration, that is, personally observed noise and vibration, is the next major cause. It is a large source of our false removals, just as in the oil contamination area. The miscellaneous visual observations such as oil pressure indicator fluctuations are the last group of symptoms.

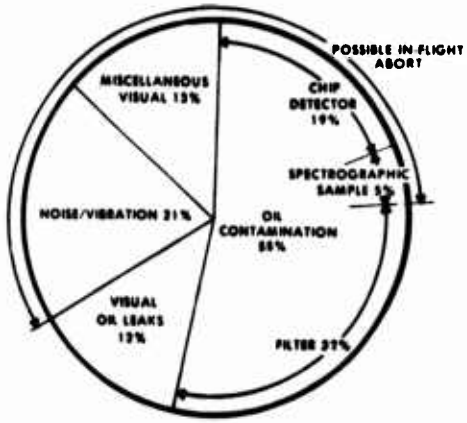

Figure 11. Debris in oil causes 55% of failure warnings. (Data from 193 CH-47 and 56 CH-46 transmission).

Before we can start to improve the false removals from debris, the first thing we have to do is basically quantify the relationship between the various levels of failure degradation and the detection signature, as illustrated in Fig. 12. It is so fundamental that we shouldn't have to put a chart up to remind anybody, and yet the amount of knowledge that we currently have in this area is disgraceful, woefully inadequate. We have optimized our diagnostic systems through gut feel for so many years that we no longer recognize that the poor engineers who are now trying to optimize it simply don't have this fundamental information available.

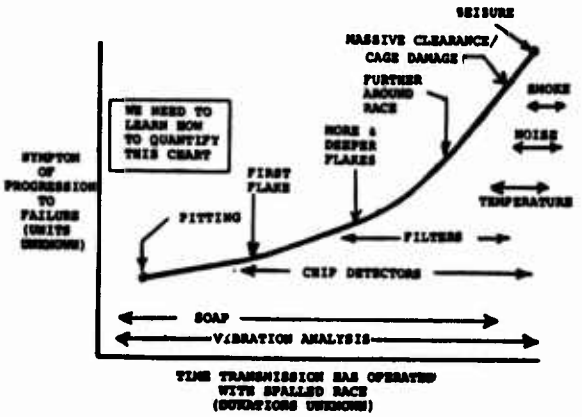

Figure 12. Crucial failure relationships.

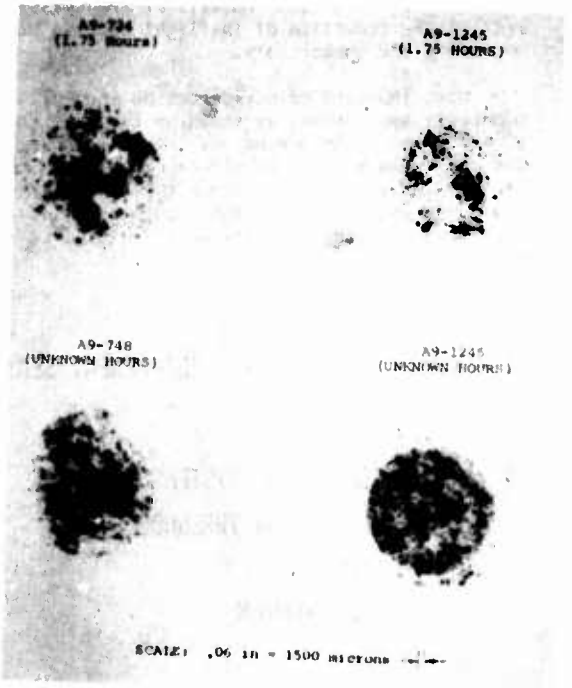

Figure 13. Examples of debris from failed transmissions.

Some of the work the Army is funding in this area, recognizing this problem, are research programs where we're examining the filters that have captured most of the debris in the oil and trying to quantify the various particle distributions of good and bad transmissions so we can begin to draw that distinction and understand where that threshold might be.

Figure 13 shows slides of some debris from failed transmissions. You can see the lower left one has some bronze from the cage and the upper left one has some rather large particles. There are obviously some 4,000 micron boulders floating around in the oil system. There is a certain reality here to the particle sizes floating around in a complex helicopter transmission that is not recognized by many people. Certainly engine lubrication systems run a little bit cleaner than these do, and this has got to be recognized in trying to optimize the diagnostic system.

We can convert these debris samples to some distributions. Figure 14 is an example of some work we just recently finished. This is a failed transmission particle size distribution. If you overlay the good transmissions on it you will begin to see that there is an awful tight overlap, and you conclude that you only begin to get some real distinction out at around 1500 microns. That's the kind of information that we need to change thresholds to improve our existing detection systems.

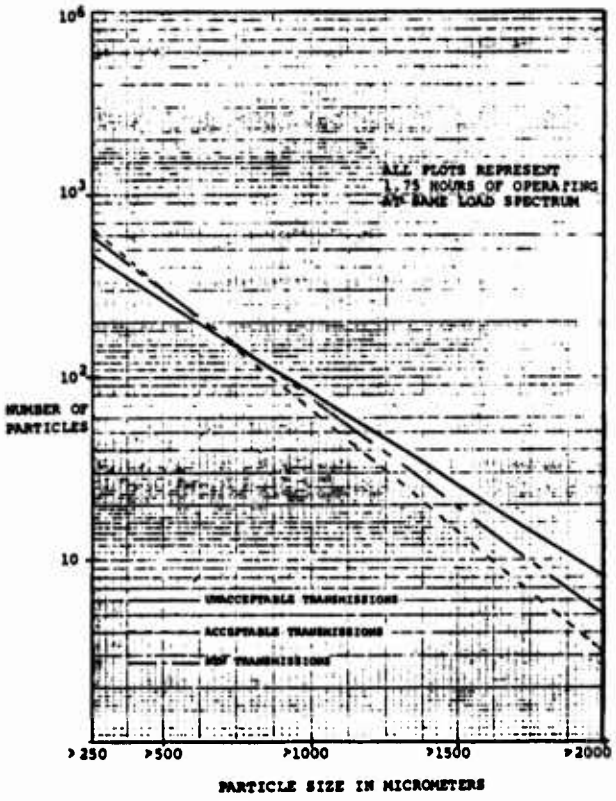

Figure 14. Large particle size distributions on CH-47 transmissions.

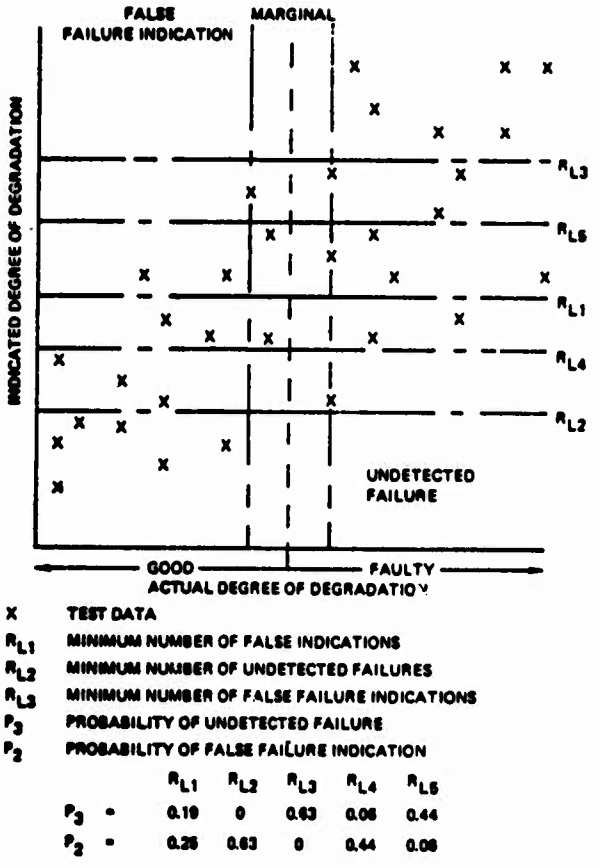

	R_{L1}	R_{L2}	R_{L3}	R_{L4}	R_{L5}
P_3 =	0.19	0	0.63	0.06	0.44
P_2 =	0.26	0.63	0	0.44	0.06

Figure 15. Sensitivity of false indication to reject limits (R_L).

Once the signature to failure relationships are known, you can pick any threshold you want. We're trying to indicate on Fig. 15 that with any threshold of degradation level you end up getting different probability of false indications as well as the probability of missing a failure.

Other things we're doing is exploring with "and/or" logic. To illustrate, Fig. 16 displays how we could get different cumulative probabilities of false indications given some inherent reliabilities of an individual sensor.

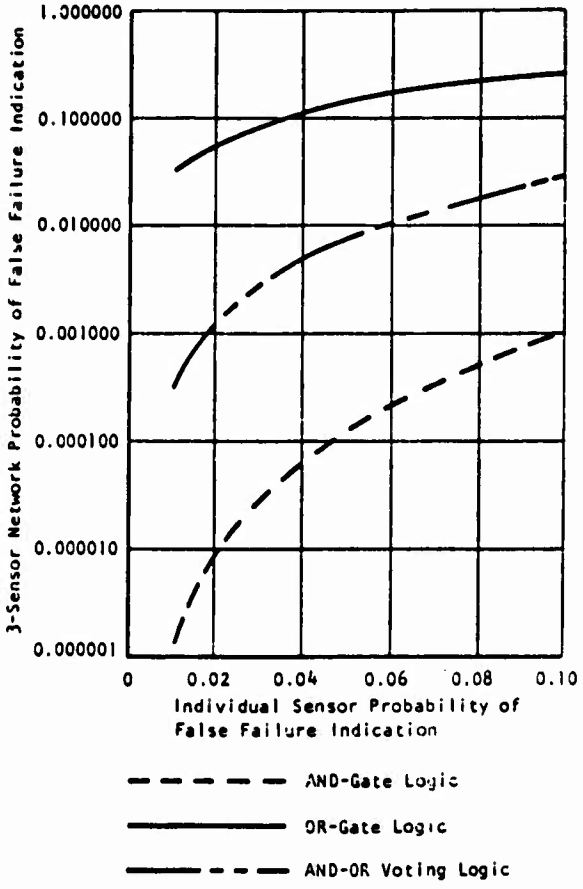

Figure 16. Three basic types of fault isolation logic on the probability of undetected failure.

The last area of improvement is inspection interval. Figure 17 is a plot of cumulative probability of detection versus the frequency at which you do an inspection with different progression intervals. I think what you see there is the problem we face of having to understand what is the failure progression interval of the failure modes we're trying to detect. Obviously, if it's 10 hours it's one thing; if it's 300 you would optimize it in an entirely different inspection interval. And again, here I must admit that our information is woefully inadequate. Utilizing in-service experience, information is simply truncated by whenever the diagnostic system took the failure out. Since we don't run our military systems for analysts, we don't let failures go all the way through to some catastrophic nature; we have to rely on R and D funding and limited test programs to fill the information gap in that area. They are obviously very critical to our understanding of failure progression levels.

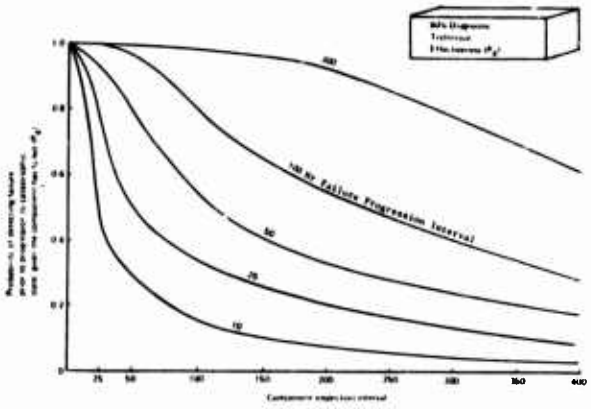

Figure 17. Detection probability as a function of progression interval and inspection interval.

Charlie Smith has previously alluded to our caution in moving the chip detectors out of the cockpit. It arises from our lack of understanding of failure progression intervals from all the common failure modes that we might see in the transmission, and research only can fill this gap. Certainly, the traditional bearing spalling due to subservice fatigue is definitely 200 to 300 hours in our low speed transmission application, but there may be other failure modes which we must detect that may be considerably less than that.

I want to move on now to give you an example of some of the system evaluations we have been attempting to do recently. Figure 18 illustrates the results from a recent study where various diagnostic systems were examined. We tried to evaluate these different configurations in a given situation This happens to be a low utilization situation of only 10 hours a month (we did others at higher utilizations, such as 60 or 80 hours a month which would represent a combat situation) and tried to quantify the accidents, for instance, due to both missed failures as well as those aborts, those accidents caused by precautionary landings that I noted before. The number of in-flight aborts (in their own right as a mission abort parameter), the removals, both valid, false and the scheduled removals and the availability were all quantified. The next table (Fig. 19) simply takes all those parameters and converts them to a standard measure of life cycle costs.

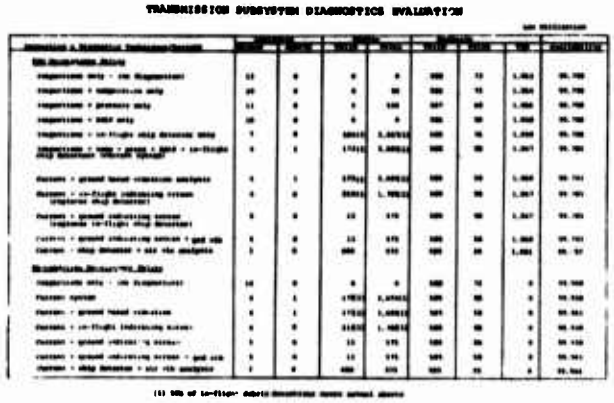

Figure 18. Transmission subsystem diagnostics evaluation.

Rather startling results emerged. It is a fact of life that in the current usage of helicopter systems, basically, the wholesale delivery of goods, it is extremely difficult to justify high cost airborne diagnostic systems. There are simply not enough benefits to be achieved to amortize, if you will, both the acquisition and the development cost, let alone the O and M cost of the diagnostic system.

Those are some examples of the Army's R and D approach in the diagnostics area. I think they reflect the methods I have earlier defined and produced a rigorous evaluation process. They first identify the problem and then try to fit some solutions to the problem. I would really encourage this group to look at the Army's problems and see if they don't have some solutions to these problems. I would encourage you to maintain a vigilance on the problems that you are trying to address. Consider the cost effectiveness of them.

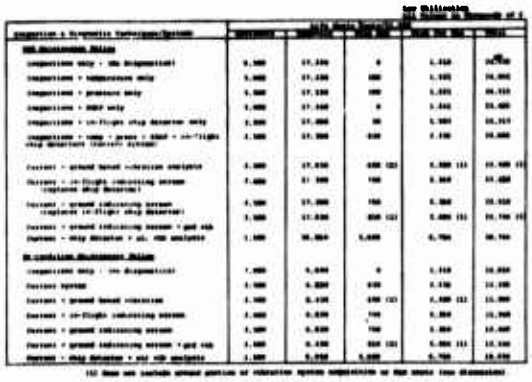

Figure 19. Transmission subsystem life cycle costs.

DISCUSSION

DR. MOW: We can take one or two questions.

DR. JOSEPH JOHN (IRT): I want to focus attention on the failed transmissions. I have heard a similar remark made several times now on the EPRI analysis.

DR. RUMMEL: What analysis?

DR. JOHN: EPRI analysis of the oil. Are there statistically meaningful data that exist now after analyzing some failed transmissions as to what you find in the oil, the particle size and elements?

DR. RUMMEL: The data you saw here, I must say with some regret, is about the best particle size distribution work that I've seen in complex transmissions. We're not very satisfied with it; it's a limited number of samples. There are a lot of problems in doing the data analysis whether you want to do metal or all particles, whether you're looking at just ferrous metals, whether you want to talk about shapes, whether you want to talk about particles that have been machined or pressed together going through gears. I'm not sure I'm answering your question. Yes, there is some quantitative display and distribution of particle sizes that are in the oil all the way from the smallest one micron soap type sample up to the largest 5,000 micron size.

DR. JOHN: Is that available on other transmissions or only for-----

DR. RUMMEL: I really don't know. I don't know how generic those distributions are. We just recently, honestly, started to do that work. We've done it on our new UTTAS, and on some CH-47 transmissions. I don't know whether the differences are due to the complexity of the transmission, the filtration levels which are different in those two transmissions, or what.

DR. JOSEPH HEYMAN (NASA, Langley): Kirk, would you care to mention something about the fact that a number of people have set different criteria on particle size as to relative predictability of failures, especially in oil lubricated systems?

DR. RUMMEL: I'm not sure I understand your question, Joe. Certainly the lower particle sizes are represented by the traditional spectrographic oil analysis program that is in use in the Air Force, Navy and Army programs, and that is a very viable tool, an important tool, for detecting many failure modes, particularly those failure modes which generate only the small debris. I'm thinking of spline wear and gear fretting. We're very concerned that perhaps we're going to infringe on the soap reliability with the fine filtrations that we're now going to.

Larger particle sizes, in our mind, seem to be where the action is. We can pick up later stages of failure and we feel we can let the transmissions run into those stages of failure and eliminate a lot of false removal that comes through wear and tear and the high quantities of particles that are generated at lower particle sizes. Did I answer your question, Joe?

I'm not sure how much difference of opinion there is in the technical community. I think most people accept the importance of soap. I think there are a lot of people who feel that its false removal rate is a bit too high and, indeed, there are programs going, particularly in the Navy; the Navy is doing some nice work in the soap area trying to improve their thresholds for soap detection. The Army has done some fine work in trying to evaluate how to take the sample, where to take it, how long to let the oil settle, etc. I don't think there's any disagreement on that. I think the disagreement may lie in how big the particle size is where the area of discrimination is. If this is what you're alluding to, and I do think there's a lot of open questions, what can I say, send money. Then we might be able to answer that question.

See you next year.

EXPERIENCES OF NDT TECHNOLOGY TRANSFER AT HARWELL

R. S. Sharpe
NDT Centre, AERE, Harwell
England

I very much appreciate the opportunity of being able to come over to this meeting. I was a bit surprised when Don Thompson phoned me up and said, "Come and talk about technology transfer to a meeting on quantitative NDT," but having sat attentively during the past day and a half here, I think I can now appreciate the need for urgent discussion and debate on the subject.

Now, when you are scheduled to speak on the last day like this, you usually find that you have got to completely rewrite your talk the evening before to fit in with what's been said before, and this is certainly the case in my situation. Having listened to some of those who talked last evening, I thought indeed that it might be as well to go right back to the beginning and tell you a little bit about how the whole project at Harwell started.

I should perhaps say at the outset that I have interpreted technology transfer to mean: How does one bridge the gap between, on the one hand, the high technology end of the NDT spectrum that we have been discussing at this Conference (and most of which I gather is funded on DoD contracts for advanced defense programmes) and, on the other hand, the large spectrum of engineering and manufacturing industries where the general quality of products could undoubtedly be improved, given the efficient transfer and the effective application of this knowledge and know-how?

Our experience at Harwell is, I am sure, relevant here, although the detailed pattern of evolution and development of the technology transfer process obviously relates in our case to the particular requirements of the UK scene.

The formal motivation for diversification from nuclear to non-nuclear activity within the UKAEA arose from Parliamentary legislation embodied in the Science and Technology Act dated 23rd March, 1965. This Act resulted in the setting up of a number of non-nuclear Projects (the majority at Harwell) based on areas of scientific expertise which were clearly translatable to technological needs in Industry. This statement itself of course embodies one of the prime requirements for technology transfer to be successful, since without the industrial 'pull' based on current need, no amount of hard 'pushing' by the scientist is likely to have any noticeable effect - except perhaps a hardening of the resistance!

Perhaps not surprisingly (bearing in mind the 'clearly translatable' criterion), one of the two Projects initially set up in this way at Harwell was the NDT Centre. Since that date a wide range of industrially orientated Projects has been established (Fig. 1) and these now absorb about 400 UKAEA professional staff (involving incidentally approximately 1/3 of the current Harwell scientific complement) and have a total operating expenditure of around £10M. At the present time the NDT Centre is the largest of these industrial projects, constituting about 10% of the total effort deployed on Authority non-nuclear work.

- NDT Centre
- Ceramics Centre
- High Temperature Chemical Technology
- Heat Transfer & Fluid Flow Service
- Industrial Electro-Technology
- Tribology
- Systems Design & Computer Optimisation
- Systems Reliability Service
- Laser Applications
- Carbon Fibres
- Advanced Metal Forming
- Macro-Molecular Separation Processes
- Sodium Sulphur Batteries
- Analytical R & D Unit
- Physico-Chemical Measurements Unit
- Separation Processes
- Reverse Osmosis
- Computer Optimisation

(In descending order of complement (1975/76) from 40 to 5)

Figure 1. Projects forming Harwell's industrial programme.

Recruitment into these projects has been achieved almost entirely by internal movements of staff to match the overall changes in programme priorities. Staff mobility has been aided by a matrix management structure at Harwell based on the co-existence of Divisions which control staff and careers, and maintain scientific standards, and Projects which manage and operate the inter-divisional programmes (Fig. 2).

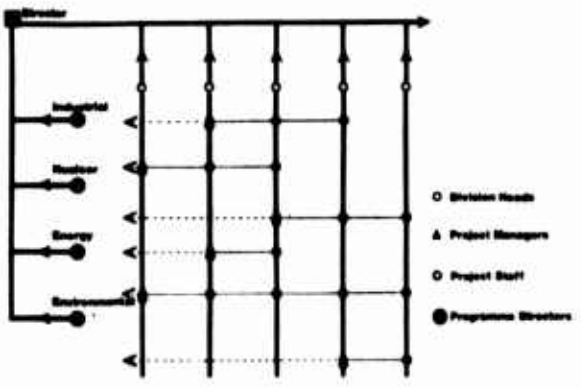

Figure 2. The Matrix management structure at Harwell.

So much for motivation, statistics and management. Let us now look at the objectives of the NDT Centre and the operation that has been set up to achieve them. The four objectives originally defined (Fig. 3) are still the basis on which the programme is built up and the criteria on which its success, or otherwise, is judged. The operating pattern that has evolved to achieve these objectives revolves around the central funding role of the Department of Industry's Mechanical Engineering and Machine Tools Requirements Board (MEMTRB) to which the Centre reports.

(a) to offer advisory, consultancy and information services to industry as a whole

(b) to carry out and encourage applied research and development so as to improve and extend NDT techniques within industry

(c) to undertake investigations into problems of a more general nature and to examine techniques which can be applied to a wide range of industries

(d) to carry out research and development programmes in co-operation with industry aimed at solving specific industrial problems

Figure 3. Objectives of the Harwell NDT Centre.

Over the years the Centre's programme has shown a healthy expansion as seen in Fig. 4 (although the rate of expansion, using 'historical' prices as I have done, gives a somewhat exaggerated picture, in view of the fortunes - or misfortunes - of the UK economy in recent years!). In addition to the overall expansion there has also been a significant increase in the amount of work carried out under contract compared with that funded directly from the Department of Industry itself (65% at present) and this is perhaps the best measure of any of the success of the technology transfer process.

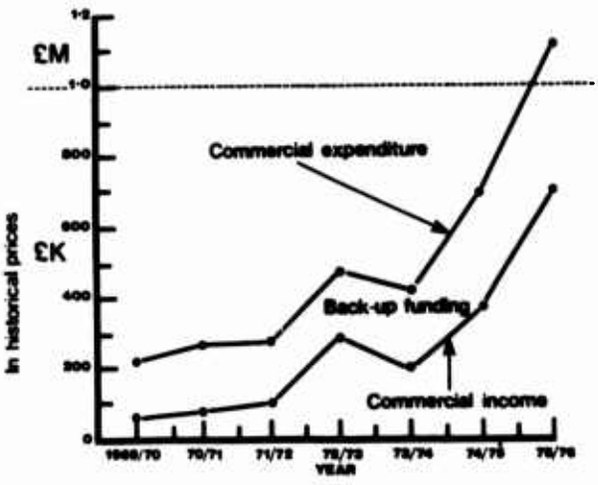

Figure 4. The growth in activity of the Harwell NDT Centre.

Another factor that has served to provide some additional credibility and realism to our activity was the setting up at the outset by Harwell of an independent Advisory Committee for the NDT Centre, with its members drawn largely from industry. This has provided us with a helpful two-way communication: problems and ideas being fed in by members from their own industrial experience and members acting in an ambassadorial role, disseminating information about our activities and programmes to their own circles of industrial contacts.

The Centre, with its primary objective of assisting UK manufacturing industry, has tried to build up both formal and personal links with all of the various organizations contributing to the 'NDT scene' and this perhaps, as much as anything, has engendered confidence in the Centre, its staff and its programmes. It has also allowed and encouraged staff to play an active and constructive role in a wide range of associated activity and, in so doing, this has helped to improve our commercial interaction and strengthen our business connections with industry. Creating active interaction and identifying a complementary role is indeed an essential requisite in ensuring the success of any technology transfer exercise.

The 'NDT Industry' in the UK is by and large made up of a large number of specialist instrument firms, with somewhat limited development potential, plus a broad spread of NDT service firms with staff complements ranging all the way from 200-300 down to 2-3. Expenditure on NDT in the UK was estimated to lie somewhere between £30M and £45M when two surveys were carried out in 1972. This expenditure included the output of the NDT Industry (services and instrumentation firms) and additional in-house spend on NDT within 'user' firms. The total NDT work-force in the UK was estimated then to be between 8000 and 10,000 persons.

One of the constraints put on the NDT Centre from the outset was that it should not 'compete' with the UK NDT Industry in the provision of NDT services or in the manufacture of instrumentation. This pattern of the NDT industry, coupled with this constraint, has meant that apart from our primary role in supplying R & D support (as our terms of reference demand) we have augmented this with 'specialist services', and the provision and introduction of 'prototype' systems in situations where commercially available instruments are unsuitable or in some way inadequate. This seems to have worked satisfactorily and the encouraging links and cross-links shown in Fig. 5 now exist. Another pointer to our success in technology transfer in NDT we feel lies in this conscious attempt over the years to provide a 'total NDT capacity' with abilities and skills available to industry spanning consultancy, applications, systems design, technique evaluation and research. Indeed we think it goes further and we are slowly moving towards the broader umbrella of 'quality technology' which links the 'nuts and bolts' of NDT technology to an understanding of materials properties on the one hand and an appreciation of defect significance and fracture modelling on the other.

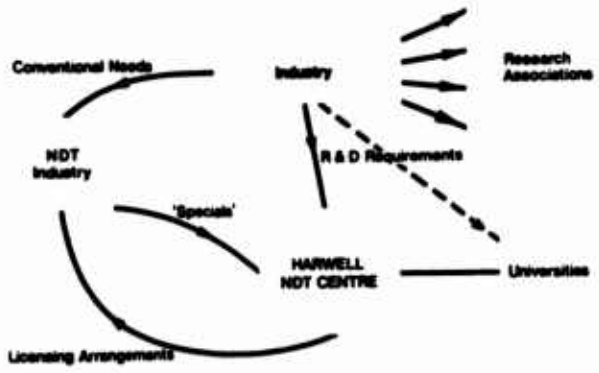

Figure 5. Cross-links between Harwell and industry.

I am conscious that in my talk so far there has been a conspicuous absence of any mention of interaction with NDT in MOD establishments. The situation is that this area of NDT development has, by policy decision, tended to limit itself to its own in-house requirements and not 'spill over' in any significant way to support industrial requirements. Our own nuclear NDT support group within Harwell was of comparable size pre-1967, to these various in-house groups, and it was only the conscious political decision to diversify Harwell into industrial research (rather than any of the MOD establishments) that has led to the present situation.

Given comparable opportunity and encouragement, one or other of the MOD teams could undoubtedly have accepted the challenge and provided an adequate base for similar expansion to a national Centre. As it is we are now being called in from time-to-time to provide some support to the MOD establishments on a contract basis, although the volume of this activity is quite small (only about 2% by value of our total contracts last year). The only formal link to MOD at present is through membership of the Centre's Advisory Committee.

If we now look in more detail at the two parts of our programme, you will see that that part of our programme which is funded directly from MEMTRB is a useful spring-board for providing a scientific 'push' into new NDT fields and, at the same time, providing better scientific understanding of existing techniques (Fig. 6).

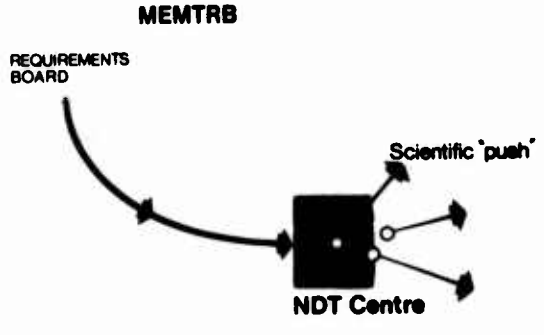

Figure 6. Interaction between the NDT Centre and the Dept. of Industry Requirements Board

Actually, this is by no means a forward push in a vacuum, and much of the progress is in fact provided 'catalytically' by diverting scientific progress in response to an anticipated inspection need as identified through the industrial communciations framework in which we operate (Fig. 7).

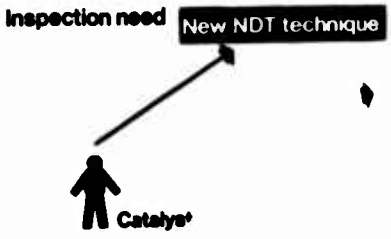

Figure 7. The catalytic function of the NDT Centre.

Our present underlying research programme built up in this way (Fig. 8) is strongly orientated to acoustic and ultrasonic techniques at the present time, but this we feel reflects current interests and requirements.

- Defect Size Assessment
- Ultrasonic Holography
- Sonic Vibration Studies
- Ultrasonic Transducers & Transducer Evaluation
- Acoustic Emission Studies
- Acoustic Impact Testing
- Polymeric Foil Transducers
- Infrared Techniques for Surface Inspection
- Optical Techniques in NDT
- Adhesive Bond Studies
- Concrete Testing
- Positron Annihilation
- High Definition Radiography
- Dynamic Radiography
- Image Analysis

Figure 8. Current underlying research programmes in NDT at Harwell.

The end product of these programmes is often 'hardware' and we are encouraged to develop licensing arrangements with UK firms in order to assist the industry and at the same time ensure the development of full market potential. High definition radiographic equipment developed under this programme has recently been licensed and ultrasonic defect sizing and laser interferometry are techniques where licenses for developed equipment are currently being negotiated. Positron annihilation studies aimed at fatigue monitoring is at a much earlier stage of development and evaluation.

In our contract work with industry we can identify two basic types of technology transfer:

(a) We act in some of our contracts quite deliberately as a 'research jobbing shop' carrying out sponsored work, offering an applications service or providing hardware under contract to individual customers (Fig. 9). This we regard as true 'technology

transfer'. We have tight time and cost specifications to work to and the knowledge of the process to which it is to be applied really need only be minimal. To be successful at this work one requires adaptable staff willing to apply themselves single-mindedly to the solution of a customer's problem. Normally, the outcome is very specific and our contribution is really towards general industrial innovation by helping to improve a manufacturing process or the quality of a product. The direct and consequential benefits unfortunately are often not disclosed to us and attempts at wider exploitation are indeed often positively discouraged. In this category, hardware systems are designed and supplied to meet particular industrial problems. In this context I would say that our decision early-on to develop a modular range of NDT instrumentation in order to provide a flexible signal processing capability and a means to assemble systems speedily and efficiently, has proved very beneficial in the long run in helping us exploit our technology transfer capability.

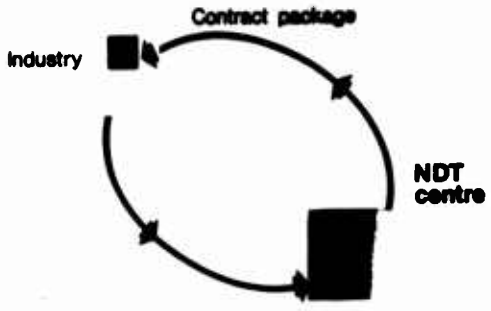

Figure 9. Research 'jobbing shop' activities for industry.

(b) In other contracts we play a much more collaborative role in helping industry develop a new inspection procedure, in many cases quite specifically from ideas which originate from within Harwell (Fig. 10). These contracts require the closest technical interaction with appropriate technical staff in the sponsoring organization. They also require that the NDT Centre staff themselves develop a very detailed knowledge of the problem and its context. This arguably is more 'technology innovation' than 'technology transfer' since our involvement tends to be with large high-technology organizations, rather than with the broad spread of small and medium-sized manufacturing industries. These contracts, because of their size and often somewhat less-urgent time scales, can be tackled more fundamentally and scientifically, and technology can be pushed forward more aggressively and there is a greater chance of more 'fall out' and more opportunities in related fields or related industries where similar opportunities or problems may present themselves. Commercial sensitivity, however, varies a good deal in these contracts, depending very much on the exploitation potential that results from a technological 'breakthrough'.

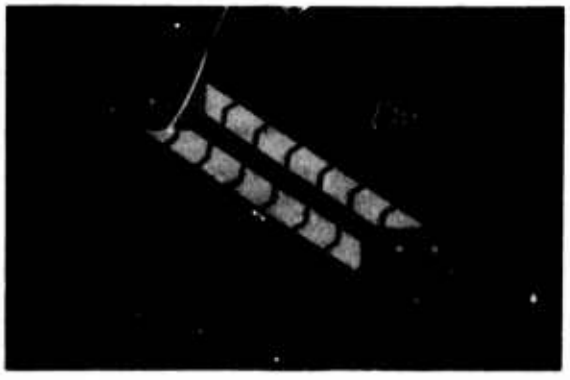

Figure 10. Collaborative innovation with industry.

In support of the programme as a whole, the Centre has been encouraged to set up and operate a computerized NDT information store. This now includes 20,000 documents. Access to this store is freely available to UK industrial enquirers as part of a general advisory service which is encouraged and sponsored by MEMTRB. Overseas organizations can have access to the literature through an annual subscription service.

In providing a strong technological thrust in many NDT techniques, we are continually conscious of the historical trend that consistently seems to send new NDT technology into orbit and produce an unstable 'oversell' situation (Fig. 11). This not only has a very damaging effect on the progress of the particular technique but also on the credibility of NDT as a whole.

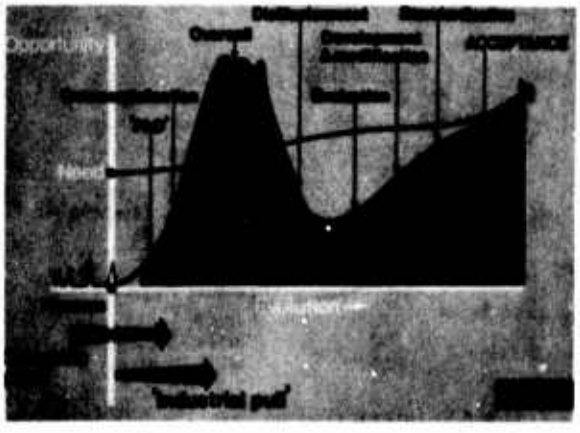

Figure 11. Progress towards innovation in NDT.

In summary, I would say that our experience at Harwell is, we believe, an encouraging example of what can be achieved in stimulating industry to improve its NDT technology by injecting science and transferring know-how - and even persuading it to pay for the privilege of doing so! Figure 12 lists the primary needs that we would identify as important in carrying through such an enterprise and which, with varying degrees of priority depending on the particular context, would be relevant to any similar exercise elsewhere.

In conclusion, I would simply say thank you and good luck with your own technology transfer activities.

- Good links into the NDT infrastructure
- Broad base of existing knowledge and experience
- Staff motivated to industrial interaction
- Close links between underlying and commercial programmes
- Links to a broader materials context
- Good scientific stimulation to generate new ideas
- Credibility with industry
  (technical and commercial)
- Broad capability across the board
  (advice, information, applications, systems & research)

Figure 12. Requirements of effective technology transfer in NDT.

DISCUSSION

DR. JOHN WALLACE (Westinghouse Research & Development): How far along is your positron work at Harwell?

DR. SHARPE: The positron work in the NDT area has been going for about a year and we haven't written any papers on the work yet. We are linking it with a fatigue program and hopefully in about three months' time we shall be able to publish some initial results.

DR. JOSEPH JOHN (IRT): I have a question about technology transfer. I guess technology transfer means different things to different people.

DR. SHARPE: Yes, it certainly does.

DR. JOHN: I specifically am asking about the attempt you are making, if any, to transfer the technology into private industry at a fairly early stage, to encourage the establishment of both engineering and scientific capability within the private industry. Is that being addressed at all?

DR. SHARPE: There are problems here and we are finding, in fact, that the easiest interaction is still with the larger organizations like British Rail, CEGB, Rolls Royce. Where you have got people in industry who speak the same language, it's much easier to get the technology transfer process moving. We are being encouraged by the Department of Industry to transfer technology to smaller engineering firms, but this is quite a problem and I don't think we have completely found the answer to this problem yet.

DR. JOHN: I have one more comment to that. One of the things that I have heard here the last couple of days talking to different people, is the general feeling of the lack of engineering and scientific capability in the smaller NDT companies, and therefore they are unable to tackle some of the NDT problems.

DR. SHARPE: Well, I certainly don't want to make derogatory comments about the NDT industry. I think it's an historical fact that these firms have developed largely by a process of fragmentation. At one time we did have one fairly large organization covering all of NDT in the UK. Now the industry has got rather split up. So, you do now have these rather small firms whose interest and capability is more in selling specific developed systems rather than in actual development work. We feel that we are helping that part of industry by doing some of this initial hardware development work and then getting it out into their companies for exploitation.

DR. DON THOMPSON (Science Center): I am in total agreement with your comment, Roy, about the necessity of linking materials science to NDT. I think I understood you to indicate that we were in contradiction on that.

DR. SHARPE: No. You showed a slide which identified quantitative NDT as a new science, and I am merely saying that I don't think of it in quite the same way. I think it's more properly an extension of some of the existing and established disciplines.

DR. THOMPSON: It has to extend in some way.

DR. SHARPE: Yes, I accept that, and I'm sure we're not in any real disagreement. I think, however, that we already have a pre-existing framework in which it can expand.

MR. PAT RYAN (DOT, Cambridge): Do you have any comment on the problem of getting acceptance of a new technique in industry? It depends ultimately on the industry buying new instrumentation or introducing new procedures, which is going to cost them money. They are reluctant to buy until somebody proves it works, and the only way you can prove it works is in industry, so you're in a chicken and egg situation.

DR. SHARPE: Well, this is true. The way we involve ourselves with these firms is to build our interaction up fairly slowly. In other words, we often start with the equivalent of a small 1,000 dollar contract, mainly to see whether a technique has got any promise in that area, and then if it does, we attempt to go into the next stage. We will then probably do some evaluation work on typical samples and if it still looks promising, we work towards the development of a system. So we tend to go in slowly and build up confidence to see whether the idea works or not. I think this may be one way of solving this problem of getting acceptance. I should point out, of course, that there is a fundamental difference between your technology transfer problems and mine. You are, I gather, basically talking about transfer of technology into Department of Defense contractors, whereas everything that we're concerned with is getting it into industry at large and, obviously, the problems and solutions are somewhat different.

DR. R. J. WASLEWSKI (National Science Foundation): To what extent, if any, when you identify a problem do you assign it to a group of people or split it into individual tasks managed overall?

DR. SHARPE: Well, I can't really give you a categoric answer on this. It depends very much on the problem. For some of the large, what I have called industrial innovation research programmes, we do, in fact, bring together quite large teams. We do, for example, have one involvement on gas pipeline inspection, which I am afraid I can't talk to you about in detail, where we have physically brought together a large, multi-disciplinary team to tackle the problem. The method of attack depends really on the amount of scientific effort that is required to match the problem.

DR. MOW: Thank you, Dr. Sharpe.

TECHNOLOGY TRANSITION-OPPORTUNITIES AND PROGRESS

H. M. Burte
Air Force Materials Laboratory
Wright-Patterson Air Force Base, Ohio 45433

Don Thompson in his introductory remarks, and many other speakers since then, have talked to the needs for NDE. These fall into three major categories: reliability of the complex constructs that seem increasingly to pervade our civilization; the role of NDE as an important factor in what I might call a rational approach to a "conservation ethic" or a "total life cycle cost" approach to systems; and the use of NDE as a tool for lower cost production. If we accept the validity of these and other needs let us consider the challenge posed by our keynote speaker.

Our keynote speaker scolded us for our apparent, to him, inability to "get things into the field." Knowledge in reports or even scholarly journals does not necessarily satisfy the needs. This is something that has concerned many of us particularly during the last five years in which there has been a significant increase in the science base underlying NDE (including the work we are reviewing here.) How well, then, is it "getting into the field?" Those of us producing the new knowledge have a normal desire for the satisfaction of seeing it used; those of us who have the practical needs want new approaches to meet them. Are there any ponies in that pile that one of our earlier speakers talked about? Have we found any yet? At the same time, do we have procedures to prevent the oversell in Dr. Sharpe's push-pull slide. Let me briefly review some of the things we've done to try to transition technology intelligently and effectively.

First, of course, is to generate extensive communication between the "scientists" who are generating the possibilities and the "engineers" who will be doing the application engineering or using the new methods. Such "coupling" should be continuous, and include early stages of someone's research to enable the science to vector itself more effectively. Such general communication increases the likelihood that research will not only produce good work, but that it will soon be useful. Beyond this obvious approach, which usually considers generic needs (to an Air Force man an airplane which flies higher, faster and further; to an NDE engineer a more sensitive, more reliable method) we have found it useful to create forums, e.g., a workshop, in which possibilities and needs can be interacted under the stimulus of specific "windows." For example, instead of merely citing the need for more reliable, more sensitive NDE methods for engine components, present a requirement to determine 99.9 percent of 15 mil flaws or larger (99 percent of the time) in the bolt holes or blade slots of nickle base superalloy disks if one is to develop a maintenance philosophy based upon the retirement for cause of engine parts rather than the current retirement after a fixed arbitrary life. This is a window; citing technical goals and specific opportunities for their use. Bringing "possibilities" and "needs" people together in a workshop environment has not only defined approaches towards known windows, it may lead to the definition of unrecognized windows to profitably exploit a new possibility. Workshops like this have been very useful, but remember, they take extensive preparation, and concentrated (to the point of physically exhausting) attention by the participants.

Defining such windows for our possibilities can take a lot of effort, but offers several advantages. First, it obviously gives us a first potential use for our new possibilities. This also helps to sell the effort and get the resources together for an adequate reduction to practice program. Most important, however, it helps us focus our attention. It gives us a baseline against which to measure if we are really doing something useful and effective, and this is important even if the window which provides this baseline is not the specific way in which the new technology is eventually used.

In my experience, one of the keys to accomplishing the coupling I have been talking about is for some of us to become not only horizontally interdisciplinary (able to help combine the classic disciplines such as solid state physics, chemistry, mechanics and metallurgy) but also vertically interdisciplinary. Some of us must be able to understand, effect combinations between, and even contribute to work at the fundamental end, in engineering development, at the initial application stage, and on service engineering problems. Vertical interdisciplinary people are the facilitators who make communication and rapid technology transition work. I have been encouraging some of you to take on this difficult responsibility, and I am pleased at how well some of you have been doing.

Given possibilities, given the knowledge of what we can or cannot do in a specific area of science, given clear-cut windows, given motivated scientists and application engineers with some interdisciplinary facilitators, we should be able to: establish clear cut reduction to practice goals; define program options; select and obtain resources for some of them and get the major reduction to practice programs under way (Fig. 1). The road maps which Don Forney showed you earlier are then a useful tool for outlining what it takes to get from where we are to the eventual objective. They help organize our thinking and allow everybody to be aware of their roles and responsibilities. Equally important, they help other people, not directly involved in the specific efforts on the road map, but who may be working in associated areas, see how they might "plug in" to make a contribution or to derive some benefit. As with any plan, road maps must be subject to change as our knowledge develops. Optimistic and aggressive time lines and predictions are permissable only if we do not let them become straight jackets or delusions.

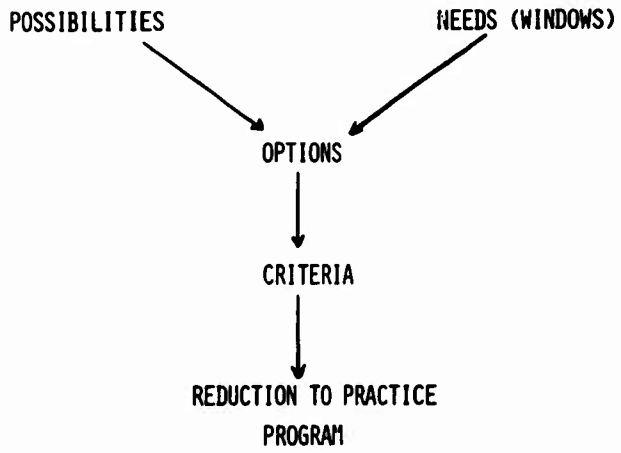

Figure 1. Requirements for technology transition.

Now then, given some tools for stimulating technology transition (communication, windows, roadmaps, workshops, interdisciplinary couplers, etc.), how well have we been doing? The philosophy of the ARPA/AFML program is to work at the fundamental and more speculative end of the R&D spectrum, to identify possibilities for reduction to practice, to spin them off into separately funded efforts (perhaps with some of the same investigators, but with resources from the agencies, etc., which will use the results) while the efforts can be reinvested into the next generation of understanding and new approaches. How many pieces have we been able to spin off, and what are some of the possibilities for the future. I will give you a very brief progress report and I think you will be surprised at how much you have accomplished in a very few years. (We should temper our pride just a little since a few products came early, either because there had already been background work which the ARPA/AFML effort capped off, or there were opportunities to transfer concepts and work from other areas such as medical technology.) You have already heard details of many of these.

In the area of adaptive signal processing the ARPA/AFML program expanded work that had already been underway. Spin-offs now include:

- a small effort in EPRI for corrosion detection
- an AFML activity to develop adaptive signal processing for inspecting adhesive bonds (using separate applied research money)
- plans for separate work to expand the use of adaptive signal processing for inspection of turbine disks

At the same time, there is work going on in the A.F. Avionics Laboratory to provide the chips that will be used in the microprocessers which will be necessary. All of these things, hopefully, can be brought together in manufacturing technology type programs with hardware manufacturers who can produce the complete systems that can, for example, be delivered to our logistics center people at the right point in time to support a new retirement for cause approach to maintenance. In addition, research under the ARPA/AFML program is continuing to provide a new generation of capability: for example, to combine adaptive signal processing with available theoretical models from scattering analysis.

The acoustic imaging work you have heard about is borrowed from medical technology. It has yielded a first generation spin-off which will be pursued in a large manufacturing technology program which will exploit this and other approaches to produce a whole new generation of NDE equipment which we want to provide to Air Force repair and maintenance people over the next five to ten years.

Another example of the equipment the Air Force will try to develop using manufacturing technology funds will be a new generation of advanced pulse echo systems. In addition to a major redesign of the electronics, this program will address the question of the variability of transducers using two "competitive" approaches spun off the fundamental program. One will use surface acoustic wave filters to compensate for variability. The other will build upon some work done under the ARPA/AFML program as well as independent work at places such as G.E. which has resulted in significantly improved transducer performance in terms of reduced ringing and consequently improved signal to noise ratios.

The random signal technique, although explored under a separate ARPA program, provides another example of a spin-off to a reduction to practice program. Here too, it is planned to exploit this approach next year, a manufacturing technology program to provide an alternative to normal pulse echo methods where much improved sensitivity is needed, such as for thick section titanium.

The electromagnetic transducer work leads even this early in the game, to a wide range of possible applications:

- the American Gas Association for pipeline inspection
- the Army for projectile inspection
- EPRI for reactor steam leaks
- Rockwell International to inspect truck axles.

In most cases, these are funded or "hard planning" spin-off programs.

The early work on measuring moisture content of epoxy matrix resins will also be pursued as a spin-off this year using separate applied research money, permitting the ARPA/AFML program to go back and look into further new possibilities.

The preceding are existing programs or fairly firm plans for spin-offs (although we can expect some change in even "hard" plans) that I am aware of. Some of you may know of others.

Let me now mention two possibilities that appear ready but for which there appear to be no spin-off plans. The first combines our ability to make well defined flaws or discrepancies (for example, by diffusion bonding) with our improved ability to analytically describe scattering from them. It should be possible to use this to provide a wide variety of improved standard defects for calibration. There are no firm funded plans to exploit this, yet. It seems like something some of us should consider doing. The second example involves the recent work which suggests that a real ability to measure surface residual stress in ferrous alloys can be developed. There are other possibilities I'm sure, and perhaps some of you would like to make suggestions.

I would like to encourage all of you to enter into discussions with me, or my colleagues in the Air Force such as Mike Buckley or Don Forney; (and I'm sure my colleagues in the other agencies feel the same) to tell us about additional possibilities which may be ready for transitioning to use. What windows do any of you know about against which we can vector these new possibilities? I'm impressed by what we've done so far, but that's no reason we should rest on our laurels. Are there some particularly pregnant topics where it would be useful to convene a small group of people who know the possibilities, with people who might be possible users, to suggest road maps for spinoff programs?

Finally, let me emphasize the importance of the fundamental scientists who have deep insight into what their work really means (into what we know and what we don't know) keeping some connection with many of these spin-off programs even if they're not a funded, direct part of them, but have gone on to new topics. I'm well aware that subtleties and fine points can be ignored in large, enthusiastic - I think the words often used are "success oriented" - programs. If any of you, particularly in the fundamental community, feel that particular spin-off programs are on thin ice for any reason, I ask you to tell the program monitors about it. If you think they're giving you the idiot treatment, which can happen in a large bureaucracy, come and tell me or some of my senior counterparts in the other agencies about it. After all, the success of technology transition requires that the communication and the cooperation between the fundamental scientists, the application engineers and the eventual users be a total life cycle activity.

DISCUSSION

DR. C. C. MOW (RAND): We have some time to take questions.

DR. BURTE: Or suggestions.

DR. GEORGE MARTIN (UCLA): Your summary and indeed most of the papers here are mainly concerned with finding defects after they have occurred, and sometimes that is necessary. But a thing like weld porosity is something that occurs in the production process. There has been no suggestion so far about bringing the NDT process back to the production stage, using it as a feedback message to control the production process immediately so that you don't make porosity, you don't make the holes in the initial stage.

DR. BURTE: I quite agree with your suggestion. You remember at the beginning I suggested three major categories of need, one of which was for more efficient production. In fact, this whole area of need is going to increase because of increasing activity in computer aided manufacturing. We will need sensors of various sorts to feed into this; it's going to be a big requirement.

DR. DAVID KAELBLE (Science Center): If I can address a point to that comment. Last summer at the ARPA La Jolla meeting there came out identification of a whole class of NDE which is called premanufacturing NDE and that was tied into the very thing that came out here.

DR. BURTE: Some of our more productive windows may well be in that sort of work, but it's going to take some effort on all our part to define these, and then focus work into meeting them.

MR. TOM DeLACY (Ford, Aeronutronics): I guess my remarks would be that I think that in the transfer of the technology we're missing the boat in that we seem to be driven to these boxes. We seem to feel that if you're going to be productive we have to result in a box. I think there should be an office, an area of responsibility within the AFML or ARPA, which guarantees that technology be filtered into the manufacturing community, more particularly into the material sciences community, so that you will eliminate the need for a lot of these boxes. I'll give an example.

I was involved with work in radioactive lighting. The studies were associated with coating development and fused slurry coatings and were especially revealing of problems in the formulations of certain coatings. Techniques such as Mössbauer spectroscopy and others which might evolve from programs such as the ARPA/AFML program would help us to study the oxidation mechanisms in our materials. I think that technology transfer should include as a necessary, important and a very credible product the feeding information into the material sciences community, credible information that will enable us to learn a lot more about the materials and the behavior of materials.

A lot of work that I've seen reported here has been addressing models which I do feel (at least in the short run) will not provide solutions to measure things such as adhesive bond strength. The model will have such limited application (even if we can do it) that it will be impossible to compete with the inconsistency of processing, of variables as they exist and as they will continue to exist. But I think a good part of the technology has applications to the problems of the analysis of fabrication technology that may perhaps eliminate the need for that box. Maybe it will be downstream that we will develop the capability to monitor the adhesive bond strength as well, but in the meantime a good part of the information could serve the material science world and we should accept that charter as credible. However, it seems that at least the general platform here is that if you're not going to generate a black box we're not justified. I think that many of the problems that can be solved are really engineering problems. The problems that have to be solved to eliminate the need for the box, of course, are the materials science problems.

DR. BURTE: Let me comment. I don't disagree with much of what you say. This, remember, is a program to develop inspection capability in areas where it is felt to be needed. However, (and these are words which many of us have said several times) if done well, some of these capabilities can be useful as research tools as well as for actual production line or receiving or maintenance inspection tools. This is well known; it has always been the case for NDE. I don't know if there need be any pressurizing (perhaps I'm wrong) by AFML or ARPA to get the scientific community to pick up the new research tools as they are made aware of them. In addition, I think good NDE research (of the sort we're talking about here which is predicated upon models of what's going on) should have as an "expected byproduct," a considerable amount of feedback to the materials community as to how to make the materials better. For example, some of the work reported by Dave Kaelble has, as a byproduct, directions for how to make less moisture sensitive epoxy resins. In fact, I say an "expected byproduct" because if such information doesn't come out perhaps we have not been doing the research in the right way - perhaps it has been too empirical.

DR. PAUL FLYNN (General Dynamics): I'm rather interested in the technology transfer aspect of this, but in some of the RFPs that have come out in the manufacturing technology area, there are, from the NDE standpoint, demands made to define size, shape and orientation of flaws in structures as complicated as laminar composites and fiber reinforced composites. From the things that were discussed here this is a very tentative ability, even on a laboratory basis--in Dr. Mucciardi's paper, he did reasonably well in looking at size when shape and orientation were constant. I just wonder about the payoff of putting NDE requirements like that in a manufacturing technology program that is supposed to be the application of something that already exists.

DR. BURTE: All I can say is if you think there were unreasonable requirements put in a specific request for proposal, let me know about it or let Don Forney know about it. If the shoe fits, we'll wear it. Tell us about specific cases. That's the request that I made earlier.

DR. FLYNN: Okay, thank you.

MR. PAT RYAN (DOT): There is a funding gap in the intermediate stage of proving feasibility at the lab level and developing for an application. The man who is responsible for solving the practical problem cannot take a risk on something that he can't be pretty sure is going to pay off. There is a need for a venture capital approach in this area, and I wonder if you mean, when you tell us of your windows, that you are in a position to supply some of that venture capital.

DR. BURTE: Yes. Most of the reduction to practice spin-offs I mentioned involve such "venture capital." Even for venture capital areas, though, where you needn't justify the program on the basis of solving the problem involved in a specific window, I believe you need a window so you can measure what you're doing, so you can evaluate your progress.

DR. MOW: I'm sorry I have to cut the discussion off. Don Thompson would like to make a few concluding remarks.

CONCLUSION

DR. DON THOMPSON (Science Center): Thank you very much. That was a very good description of work done to date in this program and by other participants who have attended our meeting.

To conclude the meeting I would like to make only a few comments. As you know, our proceedings have been transcribed by Mr. Voigtsberger. Our procedure after the meeting will be to transmit to the authors the transcripts of their talk for editing and inclusion of the artwork, and then prepare them for publication as the proceedings of the meeting. They will be published as an Air Force Materials Lab report. The attendees at this meeting will receive a copy of the report, and so if there is some reason that that doesn't happen in the future, let me know. This procedure may take on the order of five to six months, depending upon the schedules, times and so forth of both the printing shop and in the workloads of the people who have to edit their work.

I want to thank you all for coming to this meeting; it's been a pleasure to have you here. In concluding, I'd like to make several acknowledgements which I feel are very important. First of all, I wish to acknowledge the support of our ARPA/AFML hosts, Dr. Mike Buckley, Dr. Ed van Reuth, Mr. Don Forney, Dr. Harris Burte; our advisory committee who have always provided guidance for the program; the participants in the program; and our other invited speakers and our session chairmen. Especially, I'd like to thank Roy Sharpe for coming over from England and giving us a very fine summary of the Harwell work and our keynote speaker, the Honorable Harold Brownman. I'd also like to acknowledge with thanks the work of our chief organizer, Mrs. Diane Harris and her staff, Miss Shirley Dutton and Mr. Paul Occor. This group has done an excellent job in organizing and managing so many aspects of this meeting.

ATTENDEE LIST

REVIEW OF PROGRESS
IN
QUANTITATIVE NDE

ASILOMAR CONFERENCE GROUNDS

AUGUST 31-SEPTEMBER 3, 1976

Dr. Laszlo Adler
Dept. of Physics
University of Tennessee
Knoxville, Tennessee 37916

Dr. George Alers
Rockwell International Science Center
1049 Camino Dos Rios
Thousand Oaks, Calif. 91360

Dr. Wm. F. Andersen
Nuclear Regulatory Commission
Washington, D.C. 20555

Commander James Anderson
Office of Naval Research
Pasadena, Calif.

Dr. Harry Anderton
Textronix
P.O. Box 500
Mail Stop 39/308
Beaverton, Oregon 97077

Dr. Danelle Andrade
Manufacturing Research
Lockheed Missiles & Space
P.O. Box 504
Sunnyvale, Calif. 94088

Dr. Bert A. Auld
Microwave Laboratory
Stanford University
Stanford, Calif. 94305

Dr. Michael Avioli
Drexel University
Philadelphia, Pa. 19104

Dr. Alfred Bahr
Stanford Research Institute
333 Ravenswood Avenue
Menlo Park, Calif. 94025

Dr. Willard Bascom
Navy Research Lab.-Code 6170
455 Overlook Avenue
Washington, D.C. 20375

Dr. Arden L. Bement
Director, Matl. Sciences Offices
Advanced Research Projects Agency
1400 Wilson Blvd.
Arlington, Va. 22209

Dr. Charles K. Berberich
Alcoa Technical Center
Alcoa Center, Pa. 15069

Dr. Craig Biddle
Pratt & Whitney Aircraft
Florida Research & Development Center
P.O. Box 2691
West Palm Beach, Fla. 33402

Dr. George Birnbaum
National Science Foundation
Institute of Materials Sciences
Reactor A-106
Washington, D.C. 20234

Prof. Mack Breazeale
Physics Dept.
University of Tennessee
Knoxville, Tenn. 37916

Dr. John Brinkman
Deputy Director, RD&E
U.S. Army Armament Command
Rock Island, Ill. 61201

Dr. Thomas W. Bristol
Hughes Aircraft Company
1901 Malvern, Box 3310
Bldg. 600, M.S. E-248
Fullerton, Ca. 92634

Dr. Stephen D. Brown
Battelle
Columbus Laboratories
505 King Avenue
Columbus, Oh 43201

Honorable Harold L. Brownman
Assistant Secretary of Army (I&L)
The Pentagon
Room 3E606
Washington, D.C. 20310

Dr. Kent Bryan
Elec. & Computer Engr. Dept.
Clemson University
Clemson, So. Carolina 29631

Dr. Otto Buck
Rockwell International Science Center
1049 Camino Dos Rios
Thousand Oaks, Calif. 91360

Dr. Michael J. Buckley
Air Force Systems Command
AFML/LLP
Wright-Patterson AFT
Dayton, OH. 45433

Mr. Roy Buckrop
Commander, U.S. Army Armament Command
Attn: DRSAR-RDS
Rock Island, Il. 61201

Dr. O. J. Burchett
Sandia Labs.
Box 5800
Albuquerque, NM. 87115

Dr. Harris Burte
AFML
Wright-Patterson AFB
Dayton, Oh. 45433

Dr. R. Ronald R. Cahall
Dept. of the Navy
Naval Air Engr. Ctr. -92724
Lakehurst, NJ. 08733

Dr. Peter Cannon
Vice, President, Rockwell Intl. Science Center
1049 Camino Dos Rios
Thousand Oaks, Calif. 91360

Prof. Steve Carpenter
Dept. of Metallurgy & Matls. Science
University of Denver
Denver, Colo. 80112

Dr. James Carson
Drexel University
Philadelphia, Pa. 19104

Dr. David Carver
Lockheel Missiles & Space
Bldg. 102, Org. 7574
Sunnyvale, Ca. 94088

Dr. R. E. Chance
Grumman Aerospace Corp.
Bethpage, NY.

Dr. Francis Chang
Applied Research Lab.
General Dynamics
Fort Worth, Tx 76101

Mr. Keith E. Claxton
Lewis Associates
165 University Ave., Suite 205
Palo Alto, Ca. 94301

Dr. R. Clough
National Bureau of Standards
Reactor A-106
Washington, C.D. 20234

Dr. E. Richard Cohen
Rockwell Int. Science Center
1049 Camino Dos Rios
Thousand Oaks, Ca. 91360

Dr. Dorothy Comassar
General Electric Co.
3-45 - AEG
Cincinnati, Oh. 45215

Dr. Don Conn
Armco Steel Corporation
Research Center
Middletown, Oh 45053

Dr. Harry E. Cook
University of Illinois
Dept. of Physics
Urbana, Il. 61801

Mr. Ernest Cooper
Chief, ASD/PPMRA
Wright-Patterson AFB
Dayton, Oh 45433

Dr. W. L. Crawford
Alcoa
1501 Alcoa Bldg.
Pittsburgh, Pa. 15219

Dr. John Crocker
Lockheed Calif. Company
P.O. Box 551
Dept. 5713, Bldg. 85A
Burbank, Ca.

Dr. Ben Cross
Atomics International
Rocky Flats Plant
P.O. Box 464
Golden, Colo. 80401

Mr. George Darcy, Jr.
Chief, Nondestructive Testing
Industrialized Appl. Branch
AMMRC
Watertown, Mass.

Dr. Thomas J. DeLacy
Sr. Staff Scientist
Aeronutronics - Ford
Mail Station G97
3939 Fabian Way
Palo Alto, Ca. 94303

Dr. Eugene J. Del Grosso
Hamilton Standard Division
United Technologies Corp.
Windsor Locks, Ct. 06096

Dr. Steve Doctor
Battelle-Northwest
P.O. Box 997
Richland, Wash. 99352

Dr. J. E. Doherty
Bldg. 140
Materials Eng. & Res. Lab.
Pratt/Whitney Aircraft
Middletown, Conn. 06457

Dr. Eytan Domanv
University of Washington
Physics Department
Seattle, Wash.

Prof. Davis M. Egle
Aerospace & Mechanical Engr.
University of Oklahoma
Norman, Okla. 74069

Dr. Wm. Al. Ellingson
Argonne National Labs.
1401 Palmer
Downers Grove, Ill. 60515

Dr. Foster Ellis
Institute for Defense Analysis
Washington, D.C.

Dr. Richard Elsley
Rockwell Intl. Science Center
1049 Camino Dos Rios
Thousand Oaks, Ca. 91360

Dr. D. Erwin
Northrop Aircraft Division
3109 W. Broadway
Mail Stop 76-20/84
Hawthorne, Ca. 90260

Dr. Tony Evans
Rockwell Intl. Science Center
1049 Camino Dos Rios
Thousand Oaks, Ca. 91360

Dr. John Fehlauer
Drexel University
Philadelphia, Pa. 19104

Dr. Paul Flynn
Applied Research Lab.
General Dynamics
Ft. Worth, Tx. 76101

Mr. Don M. Forney
AFML/LLP
Wright-Patterson AFB
Dayton, Oh 45433

Dr. Chris Fortunko
Rockwell Intl. Science Center
1049 Camino Dos Rios
Thousand Oaks, Ca. 91360

Dr. Seymour Friedman
Naval Ship Systems
Annapolis, Md.

Dr. C. Gerald Gardner
University of Houston
Dept. Electrical Engr.
University of Houston
Houston, Tx 77004

Dr. Glenn Geithman
The Boeing Company
B-6620 73-05
P.O. Box 3707
Seattle, Wash. 98124

Mr. John H. Gleim
Naval Ship Engr. Ctr.
Hyattsville, Md. 20782

Dr. Lloyd Graham
Rockwell Intl. Science Center
1049 Camino Dos Rios
Thousand Oaks, Ca. 91360

Dr. Robert S. Graham
Automotive Operations
Rockwell Intl.
2135 W. Maple Road
Troy, Mich. 48084

Prof. R. E. Green
John Hopkins University
Mech. & Matls. Dept.
Charles & 34th Street
Baltimore, Md. 21218

Dr. Jim Gubernatis
University of California
Los Alamos Scientific Lab.
Mail Stop 244 T-DOT
P. O. Box 1663
Los Alamos, N.M. 87544

Dr. Steve Gustafson
AFML/UDRI
Wright-Patterson AFB
Dayton, Oh 45433

Dr. Stephen D. Hart
Naval Research Lab.
4555 Overlook Avenue
Washington, DC 20375

Dr. Edmund Henneke
Dpt. of Science & Mechanics
Virginia Polytechnic Inst. & State University
Blackburg, Va. 24061

Dr. Joseph Heyman
NASA-Langley Research Center
MS-5499
Hampton, Va. 23665

Mr. Phil Hodgetts
B-1 Div., Rockwell Intl.
5701 W. Imperial Highway
Los Angeles, Ca. 90009

Dr. Edward L. Hoffman
NASA-Langley Research Center
Hampton, Va. 23665

Mr. Tom House
U.S. Army Air Mobility R&D Lab.
Fort Eustis, Va. 23604

Dr. N.H. Hsu
Dept. of Engr. Mechanics
College of Engr.
University of Kentucky
Lexington, Ken. 40506

Dr. John Irwin
Sandia Labs.
Div. 1323
Box 5800
Albuquerque, N.M. 87115

Dr. Marvin Jacoby
Lockheed Palo Alto Research Lab
3251 Hanover Street
Palo Alto, Ca. 94304

Dr. Michael James
Northwestern University
Technological Institute
Dept. of Materials Science
Evanston, Ill. 60202

Dr. Joseph John
Intelcom Rad Tech.
San Diego, Ca.

Dr. Dwayne Johnson
Failure Analysis Associates
750 Welch Road
Palo Alto, Ca. 94304

Dr. Wm. Jones
Hughes Aircraft Company
1901 Malvern, Box 3310
Bldg. 600, M.S. E-248
Fullerton, Ca. 92634

Dr. David Kaelble
Rockwell Intl. Science Center
1049 Camino Dos Rios
Thousand Oaks, Ca. 91360

Prof. Gordon Kino
Dept. Electrical Engr.
W.W. Hanson Lab of Physics
Stanford University
Stanford, Ca. 94305

Dr. Howard J. Klug
Naval Weapons Engr. Support
Code ESA 113
Washington, D.C.

Dr. Donald Y. Konishi
Los Angeles Aircraft Division
Rockwell International
5701 W. Imperial Highway
Los Angeles, Ca. 90009

Mr. Robert G. Kreider
Dept. of the Navy
Naval Ship Engr. Center
Prince George's Center
Hyattsville, Md. 20782

Prof. James A. Krumhansl
Cornell University
Dept. of Physics
Cornell University, Clark Hall
Ithaca, NY 14850

Dr. John Laister
Lockheed
Dept. 7574
P.O. Box 551
Burbank, Ca.

Dr. Ken Lakin
Dept. of Elec. Engr.
Univ. of Southern Calif.
University Park
Los Angeles, Ca. 90007

Dr. Joseph R. Lane
National Matls. Advisory Board
National Research Council
2101 Constitution Avenue
Washington, D.C. 20418

Dr. James F. Lovelace
Materials Processes Lab.
General Electric Co.
Schenectady, N.Y.

Dr. Keith C. MacMillan
Lawrence Livermore Lab
Univ. of Calif.
Livermore, Ca. 94305

Mr. B.G. Martin
McDonnell-Douglas
Long Beach Facility
3855 Lakewood Blvd.
Long Beach, Ca. 90846

Dr. George Martin
1660-9th Street
Santa MOnica, Ca.

Mr. C.W. Marvin
Director, Research Texas Eastern
Transmission Corp.
P.O. Box 1612
Shreveport, La. 71130

Dr. George Matzkanin
Southwest Research Institute
P.O. Drawer 28510
San Antonio, Tex. 78284

Dr. George Mayer
Dept. of the Army
U.S. Army Research Office
Box CM, Duke Station
P.O. Box 1211
Durham, N.C. 27709

Dr. Jerry McElroy
Southwest Research Institute
8500 Culebra Road
San Antonio, Tex. 78206

Dr. Bruce Maxfield
Lawrence Livermore Labs
Mail Code L415
Livermore, Ca. 94550

Dr. William McKinley
Lawrence-Livermore Lab
Univ. of California
Livermore, Ca. 94305

Prof. Jim Meindl
Dept. of Elec. Eng.
Stanford University
Palo Alto, Ca. 94305

Dr. Roger Melen
Stanford University
W.W. Hansen Lab of Physics
Stanford, Ca. 94305

Dr. Frank Moore
Div. of Conservation, Res. & Tech.
Mail St. 2221C
20 Mass Ave., NW
Washington, D.C. 20545

Mr. James A. Moore
Vought Corporation
Unit 2-42211
P.O. Box 907
Dallas, Tex.

Dr. Tom Moran
AFSC
AFML/LLP
Wright-Patterson AFB
Dayton, Ohio 45433

Mr. Parker E. Moreland, Jr.
Sperry Division
Automation Industries, Inc.
1000 Shelton Rock Road
Danbury, Conn. 06810

Dr. C. C. Mow
The RAND Corp.
1700 Main Street
Santa Monica, Ca. 90406

Dr. Anthony Mucciardi
Adaptronics, Inc.
7700 Old Springhouse Road
McLean, Va. 22101

Dr. Bill J. Munn
Rockwell Intl.-Tulsa Div.
P.O. Box 51308
Tulsa, Okla. 74151

Dr. S.K. Nash
Commander, Frankford Arsenal
Attn: SARFA-PDM-E
Philadelphia, Pa. 19137

Prof. Vernon Newhouse
Medical Engr. Office
Purdue University
LaFayette, Ind.

Mr. Nicholas
Commander, Naval Ship Engr. Center
Center Bldg. Code 6107C
Hyattsville, Md. 20782

Dr. William A. Owczarski
Pratt/Whitney Aircraft
Main Street
East Hartford, Conn. 06108

Dr. Rod Panos
Air Force Systems Command
AFML/LLP
Dayton, Ohio 45433

Dr. Emmanuel Papadakis
Ford Motor Company
Manufacturing Processing Lab
24500 Glendale Road
Detroit, Mich. 48239

Dr. William Pardee
Rockwell Intl. Science Center
1049 Camino Dos Rios
Thousand Oaks, Ca. 91360

Dr. Neil Paton
Rockwell Intl. Science Center
1049 Camino Dos Rios
Thousand Oaks, Ca. 91360

Dr. R. Bryon Pipes
Associate Professor
Mech. & Aero. Engr.
Univ. of Delaware
Evans Hall
Neward, De. 19711

Dr. W.M. Pless
Lockheed Georgia Co.
Dept. 7262, Zone 319
86 South Cobb Drive
Marietta, Ga. 30063

Dr. Herbert G. Popp
General Electric Co.
Mail Stop M-87
Cincinnati, Ohio 45215

Mr. Jerry Posakony
Battelle Northwest
P.O. Box 999
Richland, Mash. 99352

Dr. Noel Proctor
AFM, Tuboscope - P.O. Box 809
Houston, Tex 70001

Mr. Joe Provens
ASD/PPMRA
Wright-Patterson AFB
Dayton, Ohio 45433

Dr. John Raney
AFSC
AFML/LLP
Wright-Patterson AFB
Dayton, Ohio 45433

Dr. John Richardson
Rockwell Intl. Science Center
1049 Camino Dos Rios
Thousand Oaks, Ca. 91360

Dr. J. H. Rose
Physics Dept.
University of Calif.-San Diego
San Diego, Ca.

Dr. Kirk Rummel
Boeing-Vertol
Philadelphia, Pa.

Dr. Ward D. Rummel
Martin-Marietta Aerospace
Denver, Colo. 80210

Dr. Robert P. Ryan
Dept. of Transportation
Code 611
Transportation Sys. Ctr-Kendall Sq.
Cambridge, Mass. 02142

Dr. Robert V. Salkin
Chief, R&D - Metallurgy
SA Cokerill
Seraing-Belgium

Dr. Robert Sanders
Acoustic Emission Technology
1828A Tribute Road
Sacramento, Ca. 96815

Dr. George Sandoz
Office of Naval Research
536 So. Clark Street
Chicago, Ill. 60605

Dr. Donald G. Schindler
U.S. Steel Research
Murraysville, Pa.

Dr. John Shott
Stanford University
W.W. Hansen Hall
Stanford, Calif.

Dr. William R. Scott
Naval Air Development Center
Code 30233
Warminster, Pa. 18974

Dr. William J. Shack
Argonne Natl. Lab.
1401 Palmer
Downers Grove, Ill. 60615

Dr. Roy S. Sharpe
Harwell Laboratory
England
United Kingdom

Dr. H.J. Shaw
Microwave Lab
Stanford University
Stanford, Ca. 94305

Dr. W. Sheldon
Northrop Corp. Aircraft Div.
3901 W. Broadway
Hawthorne, Ca. 90250

Mr. Bill Shelton
Air Force Systems Command
AFDL/FBA
Wright-Patterson AFB
Dayton, Ohio 45433

Major Wilbur Simmons
AFOSR/NE
1400 Wilson Blvd.
Arlington, Va. 22209

Dr. Richard Skulski
Rockwell Intl.-Rocky Flats Plant
P.O.Box 464
Golden, Colo. 80401

Dr. Charles Smith
Undersecretary of Defense-INL
(P&A)
Room 2D311, The Pentagon
Washington, D.C.

Dr. Kempton Smith
General Electric
Corporate R&D
1 River Road
Schenectady, N.Y.

Dr. Richard T. Smith
Southwest Research Institute
Director, NTIAC
8500 Culebra Road
San Antonio, Tex 78206

Dr. Tennyson Smith
Rockwell Intl. Science Center
1049 Camino Dos Rios
Thousand Oaks, Ca. 91360

Dr. Karl Stahlkopf
Electric Power Research Institute
Stanford Industrial Park
3412 Hillview
Palo Alto, Ca. 94304

Lt. Col. H. Staubs
SAMSO/WAPC
Worldway Postal Center
Los Angeles, Ca.

Dr. Michael L. Stellabotte
Naval Air Development Center
384 Westfield Drive
Broomall, Pa. 19008

Dr. Gordon E. Stewart
The Aerospace Corporation
El Segundo, Cal.

Mr. Wayne Stump
Atomics Intl-Rockwell Intl.
Rocky Flats Plant
P.O. Box 464
Golden, Colo. 80401

Mr. Bill Sturrock
Northrop Aircraft Div.
3109 W. Broadway
Mail Stop 3882/84
Hawthorne, Ca. 90250

Mr. Warren Swanson
North American Operations
Rockwell Intl.
2300 E. Imperial Highway
El Segundo, Ca. 90245

Dr. Lydon J. Swartzenruber
National Bureau of Standards
Bldg. 223
Washington, D.C. 20234

Dr. Thomas Szabo
AF Cambridge REsearch Lab
Hanscom Field
Bedford, Mass. 01730

Dr. Graham Thomas
Drexel University
Philadelphia, Pa.

Dr. Robert L. Thomas
Wayne State University
Dept. of Physics
Detroit, Mich. 48202

Dr. R.B. Thompson
Rockwell Intl. Science Center
1049 Camino Dos Rios
Thousand Oaks, Ca. 91360

Dr. Donald O. Thompson
Rockwell Intl. Science Center
1049 Camino Dos Rios
Thousand Oaks, Ca. 91360

Dr. Robb Thomson
Senior Research Scientist
Institute of Matls. Research
Room B354
National Bureau of Standards
Washington, D.C. 20234

Dr. Jerry Tiemann
General Electric
Schenectady, N.Y.

Prof. John Tien
Henry Crumb School of Mines
Columbia University
New York, N.Y. 10027

Dr. Bernie Tittmann
Rockwell Intl. Science Center
1049 Camino Dos Rios
Thousand Oaks, Ca. 91360

Dr. Edward van Reuth
Advanced Research Projects Agency
1400 Wilson Blvd.
Arlington, Va. 22209

Dr. Carmine Vasile
Rockwell Intl. Science Center
1049 Camino Dos Rios
Thousand Oaks, Ca. 91360

Mr. John Viertl
General Electric Co.
Bldg. 37, Room 663
Schenectady, N.Y. 12345

Dr. Richard F. Vyhnal
Bulsa Div.-Rockwell Intl.
20000 N. Memorial Drive
Tulsa, Okla.

Dr. Shirley L. Wakefield
General Electric Co.
Cincinnati, Ohio

Dr. John Wallace
Westinghouse Research & Dev.
1310 Beulah Rd., Churchill Boro
Pittsburgh, Pa. 15235

Dr. R. J. Waselewski
Section Head, Matls. Research
National Science Foundation
1800 "G" Street, N.W.
Washington, DC 20550

Mr. Tom Waugh
Dept. of Elec. Engr.
W.W. Hansen Lab of Physics
Stanford University
Stanford, Ca.

Dr. Francis Wells
Vanderbilt University
School of Engr.
Nashville, Tenn. 37203

Mr. H.L. Whaley
Babcock Wilcox
Lynchburgh Research Center
P.O. Box 1260
Lynchburgh, Va. 24505

Dr. W.J. Whelan
The RAND Corp
1700 Main Street
Santa Monica, Ca. 90406

Prof. Henry White
Dept. of Physics
University of Missouri
Columbus, Mo.

Prof. R.M. White
University of Calif.-Berkeley
Elec. Engr. Dept.
479 Cory Hall
Berkeley, Ca.

Prof. Max L. Williams
Dean, School of Engr.
University of Pittsburgh
Pittsburgh, Pa. 16260

Prof. Thomas Wolfram
University of Missouri
223 Physics Bldg.
Columbia, Missouri 65201

Prof. Benjamin Yen
Stanford University
Dept. of Matls. Science
Stanford, Ca.

Prof. Donald Yuhas
Sonoscan, Inc.
720 Foster Avenue
Bensonville, Ill. 60106

Dr. John Zurbrick
General Electric Co.
Schenectady, N.Y.

*U.S.Government Printing Office: 1977 — 757-001/132